INSTITUT FÜR INFORMATIK

Conformal Geometric Algebra in Stochastic Optimization Problems of 3D-Vision Applications

Christian Gebken

Bericht Nr. 1001
Februar 2010

CHRISTIAN-ALBRECHTS-UNIVERSITÄT

ZU KIEL

Institut für Informatik der
Christian-Albrechts-Universität zu Kiel
Olshausenstr. 40
D – 24098 Kiel

Conformal Geometric Algebra in Stochastic Optimization Problems of 3D-Vision Applications

Christian Gebken

Bericht Nr. 1001
Februar 2010

e-mail: C.Gebken@gmx.net

Dieser Bericht gibt den Inhalt der Dissertation wieder, die der Verfasser im April 2009 bei der Technischen Fakultät der Christian-Albrechts-Universität zu Kiel eingereicht hat.
Datum der Disputation: 21. Oktober 2009.

Conformal Geometric Algebra in Stochastic Optimization Problems of 3D-Vision Applications

D i s s e r t a t i o n

zur Erlangung des akademischen Grades

Doktor der Ingenieurwissenschaften

(Dr.-Ing.)

im Fach Informatik

eingereicht an
der Technischen Fakultät
der Christian-Albrechts-Universität zu Kiel

von
Dipl.-Inf. Christian Gebken

Kiel

2009

1. Gutachter: Prof. Dr. Gerald Sommer (Kiel)

2. Gutachter: Prof. Dr. Wolfgang Förstner (Bonn)

3. Gutachter: Prof. Dr. Reinhard Koch (Kiel)

Datum der mündlichen Prüfung: 21. Oktober 2009

Dedicated to my beloved wife, Stephanie,

and my beloved son, Loven.

Abstract

In the present work, the modeling capabilities of conformal geometric algebra (CGA) are harnessed to approach typical problems from the research field of 3D-vision. This increasingly popular methodology is then extended in a new fashion by the integration of a least squares technique into the framework of CGA. Specifically, choosing the linear Gauss-Helmert model as the basis, the most general variant of least squares adjustment can be brought into operation. The result is a new versatile parameter estimation, termed *GH-method*, that reconciles two different mathematical areas, that is algebra and stochastics, under the umbrella of geometry. The main concern of the thesis is to show up the advantages inhering with this combination.

Monocular pose estimation, from the subject 3D-vision, is the applicational focus of this thesis; given a picture of a scene, position and orientation of the image capturing vision system with respect to an external coordinate system define the pose. The developed parameter estimation technique is applied to different variants of this problem. Parameters are encoded by the algebra elements, called multivectors. They can be geometric objects as a circle, geometric operators as a rotation or likewise the pose. In the conducted pose experiments, observations are image pixels with associated uncertainties. The high accuracy achieved throughout all experiments confirms the competitiveness of the proposed estimation technique.

Central to this work is also the consideration of omnidirectional vision using a para-catadioptric imaging sensor. It is demonstrated that CGA provides the ideal framework to model the related image formation. Two variants of the perspective pose estimation problem are adapted to the omnidirectional case. A new formalization of the epipolar geometry of two images in terms of CGA is developed, from which new insights into the structures behind the essential and the fundamental matrix, respectively, are drawn. Renowned standard approaches are shown to implicitly make use of CGA. Finally, an invocation of the GH-method for estimating epipoles is presented. Experimental results substantiate the goodness of this approach.

Next to the detailed elucidations on parameter estimation, this text also gives a comprehensive introduction to geometric algebra, its tensor representation, the conformal space and the respective conformal geometric algebra. A valuable contribution is especially the analytic investigation into the geometric capabilities of CGA.

ACKNOWLEDGMENT

This thesis as is cannot be considered as the work of one person alone. Many people have contributed in different ways. Here I like to appreciate these people.

I begin with my supervisors Prof. Gerald Sommer and Dr. habil. Christian Perwass who were always there for me. In numerous discussions I received valuable advice from Prof. Sommer. Whenever asked for, Prof. Sommer knew related contemporary or vintage scientific papers. It was him who gave me the chance to do a doctorate, who formed my way at the university and who encouraged me to participate in conferences from which I gained a lot. Also, in tutoring the students who attended his lecture I had the chance to be up on signal theory, stochastic and topology.
From Christian Perwass I learned the most. In countless discussions we derived the early ideas and overcame many problems. He often 'infected' me with his verve. I am thankful for his program `CLUCalc` [94] that often helped me to find an intuitive access to many problems.

I further acknowledge Antti Tolvanen for our joint work on catadioptric imaging. I am thankful for the good cooperation, his patience and all the discussions we had. I am grateful for the discussions I had with Dr. Bodo Rosenhahn and Dr. Norbert Krüger who also attended me during my student research projects. I thank my (former) colleagues and friends Dr. Sven Buchholz, Marco Chavarria, Oliver Granert, Dr. Florian Hoppe, Dr. Yohannes Kassahun, Herward Prehn, Lennart Wietzke and Dr. Stephan Zeitschel for the nice time we had.

Furthermore, I appreciate our technicians Hendrick Schmidt and Gerd Diesner who helped my very often. My gratitude also goes to our former secretary Francoise Maillard and to our secretary Armgard Wichmann who supported me in administrative matters.

Last, but by no means least, I thank my family for their encouragement (and pressure): my parents Johanna Elisabeth and Wilhlem Gebken, my parents-in-law Vera and Manfred Eilers, my brother-in-law Oliver Eilers, Ela and my beloved family - Steffi and Loven.

Contents

Chapter 1

Introduction

The main concern of this thesis is to establish an amalgamation of three different subjects: conformal geometric algebra, computer vision and stochastics - a demanding task since the computer vision community tends to adopt a 'stepmotherly' attitude towards geometric algebra. The subjects are not brought together because it is possible, but rather because it is suggesting and, retrospectively, worth while. This is affirmed, for instance, by the recent work of Rosenhahn [102] and Perwass [93], who did a great job in their endeavor to advance the acceptance of geometric algebra in computer vision. It is one of the aims of this thesis to carry on their work from an engineer's standpoint. For this purpose, many practical applications of geometric algebra from the field of computer vision, including experimental results, are proposed. The description of geometric algebra was rendered as complete as possible so that it can additionally be used as a reference book. Likewise, a comprehensive introduction to the theory of parameter estimation is given. For the subject specific related work refer to the respective sections. Subsequently, each of the three major disciplines is motivated in a few words. Thereafter, a synopsis of the individual chapters is given.

1.1 Motivation Geometric Algebra

It shall be mentioned in advance that it is not the aim to proselytize readers of this work to employ geometric algebra (GA), rather the aim is to convince them to thoroughly occupy themselves with GA for a while.
Geometric algebra can be viewed as a set of elements which are closed under a certain product. The elements are linear combinations from the algebra basis, which in turn consists of ordered combinations, or rather concatenations, of orthogonal basis elements from a vector space. Each of these may occur at most once per combination. The number of participating basis vectors specify the dimensionality of the algebra basis element and is referred to as its *grade*.

One cannot ignore that established constructs as the complex numbers ($\mathbb{R}_{0,1}$), the quaternions ($\mathbb{R}_{0,2}$), the algebra of the Pauli matrices ($\mathbb{R}_{3,0}$), or the Minkowski space (space-time algebra $\mathbb{R}_{1,3}$), to mention the best known, all of whom can be identified

with a simple, i.e. low dimensional, geometric algebra (indicated in brackets). Each of the quoted constructs possesses its own specific notation even though all of them can be treated in a unified manner by means of GA. A similar situation holds for the 3D-space with its scalar product and the vector cross product: in GA a single operation encompasses both of the 'constructs'. These then arise naturally insofar as they reflect the symmetric and anti-symmetric part, respectively, of this only product. And it does so irrespective of the dimension, i.e. it generalizes to algebras built on spaces with dimension different from three. The portrayed product is of course the algebra product - the *geometric product*. By the excess of information, it follows that, not least from a sheerly geometrical point of view, the geometric product must be reversible if one of its operands is still known. It is hence the accomplishment of the geometric product that virtually all elements of the algebra have a multiplicative inverse. As the algebra always comprises the vector space it is built on, it can in particular be 'divided' by a vector.
Clearly, every task may likewise be accomplished, in a way, by means of the standard vector algebra. It may be permitted to say: 'this is comparable to a pipe fitter who incessantly utilizes hammer and screwdriver, although, for example, the pipe wrench in his toolkit beside him would be much more practicable.' Since GA can be regarded as a universal framework, problems should be modeled with it from the beginning on. It is then still possible to make the transition to a suitable matrix representation if a numerical evaluation is due. This is exactly the way chosen in this work - no modeling option is abandoned before the time.

1.1.1 GA - General Things

The term $\mathbb{R}_{p,q}$ denotes the geometric algebra over an n-dimensional vector space $\mathbb{R}^n$, $n = p + q$, equipped with signature $(p, q) \in \mathbb{N}^2$. The latter will, however, become of importance not before the next chapter. The dimension of the algebra is then 2^n. Its elements are termed *multivectors*, where it is fully sufficient to treat a multivector as a vector from $\mathbb{R}^{2^n}$ as long as its respective algebra is known. The components of a multivector comprise $n+1$ different grades, each with a multiplicity according to the $n + 1$th row of Pascal's triangle. By convention, the components of a multivector are ordered according to their grade: one scalar (grade zero), n vectors (grade one) and the higher grades. Note that this one-to-one corresponds to the quadruplet representation of the quaternions with basis $1 = (1, 0, 0, 0)$, $i = (0, 1, 0, 0)$, $j = (0, 0, 1, 0)$ and $k = (0, 0, 0, 1)$. Hence, imposing the common order $1, i, j, k$, multivector k, for instance, correctly reflects the element of grade two. Moreover, observe that just like for the complex numbers, e.g. $z = a + i\,b$, a number a can be added to a vector $i\,b$ in a meaningful way. The simple relationships can be looked up in many textbooks. Important for this work is as well that for every GA there exists at least one matrix representation with real square matrices representing multivectors. Building the geometric product simply amounts to the matrix product. An illustrative example are the Pauli matrices (of size 4×4 in the real case): the identity matrix holds the scalar component. The Pauli matrices themselves can be identified with the three vector valued basis elements of the eight-dimensional Pauli algebra. The existence of the isomorphism between GA and its matrix representation easily reveals one of the most important and necessary features of the geometric product - associativity. As a further feature its bilinearity is to mention: consider the geometric product of two multivectors. Each component of the resultant multivector can be expressed by means of a quadratic form being linear in every operand. Hence numerically the geometric product can be given by 2^n $2^n \times 2^n$ matrices. This is from now on being referred to as the *tensor notation* of geometric algebra. It is essential for the invocation of GA-external numerical methods.

One of the most outstanding capabilities of GA is the possibility to do calculations on linear subspaces. These are embodied by a special kind of multivector, so-called *blades*. These elements will clearly go on being linear subspaces, yet it is remarkable that they can be used to represent non-linear geometric objects like spheres, circles or the higher-dimensional generalizations of which. The inherent advantage of blades is their nature as undistinguished elements of the geometric algebra. Thus while doing calculations, for example in an algorithm, no workaround or special treatment is necessary as it would be if these elements were to be parameterized artificially. Consequently, through the existence of the multiplicative inverse it may be divided by subspaces in an uncomplicated manner, which on the other hand enables a projection of subspaces onto subspaces.

Blades can be built by applying the *outer product* to (linearly independent) vectors. The outer product is briefly speaking the anti-symmetric part of the geometric product. Irrespective of the dimension of the surrounding space, the magnitude of a blade yields the area, the volume, etc. spanned by its forming vectors - hence a generalization of the cross product. Furthermore, an orientation can be attributed to each blade such that, given some point in space, it can be discriminated between the inside or the outside of a sphere, to mention an example. The significance of the outer product may further be justified by the fact that it can be used to intersect subspaces.

1.1.2 Conformal Geometric Algebra

One of the most important chapters in this thesis deals with the conformal geometric algebra (CGA). This is basically the algebra of the five-dimensional Minkowski space. Nonetheless, CGA amounts to more than the mere algebraic frame. Its particularity is a non-linear embedding of Euclidean vectors from $\mathbb{R}^3$ into the *projective conformal space* $\mathbb{R}^{4,1}$ - in principle something that takes places even before the actual algebra is built. The algebra over this space, in which $\mathbb{R}^3$ constitutes a 3-manifold, is astonishing closed and consistent in respect to the possible interactions between the immanent geometric entities. The central element in CGA is the sphere and its degenerate descendants, the plane and the point. Circles, lines and point pairs, just to mention the known major objects, can then be obtained with the help of intersections. But the outer product can equally by used to directly create these elements from points: three (four) points yield a circle (sphere) unless they are collinear (coplanar). In the latter case a line (plane) emerges. This is remarkable compared to the effort necessary if a circle was to be determined from three points by means of generic techniques. Note that parameters such as radius or center can effortlessly be retrieved using CGA expressions.

Even more than with the algebra of the projective space, CGA permits to effectively work with 'infinity'. That is because it exists a distinguished element which behaves as and which can be associated with the point at infinity. The best example that can already be given arises on replacing one of the points that define a sphere with 'infinity' - it results the unique plane incident with the three unchanged points.

In CGA geometric objects are equally geometric operators[1]. Multiplying object A from both sides with object B corresponds to a reflection of A in B. With the sphere as most general object in CGA, it can be inferred that the spherical reflection - the *inversion* - is the most basic operation in CGA. Note that by nesting reflections in planes, for instance, any arbitrary rigid body motion (RBM) can be carried out. The multivector appertaining to the geometric product of the respective planes then represents the compound operation. It is noteworthy that all objects can be transformed in the same, above mentioned, manner. Especially, building the outer product of transformed points amounts to the same as applying the transformation to the outer product of the points, i.e. the object. The underlying vital aspect is called *outermorphism*. It describes an inherent quality of GA, pursuant to which a linear transformation of the whole indeed coincides with the linear transformation of its parts - in contradiction to Aristotle.
It can finally be deduced that CGA gives access to the conformal group, with the Euclidean group as subgroup. This circumstance is vastly exploited in the present work.

1.1.3 A Vivid Entry into Geometric Algebra

Much was already said about the possibilities of geometric algebra. Thus the idea is to render the so far vague and abstract notions somewhat tangible. But at the same time it is intended to enlighten an aspect of particular importance. It relates to another facet of geometric algebra, namely *geometric computing* or *geometric reasoning*. In [64], for instance, some classical theorems in projective geometry are proven. For the subsequent phenomenological considerations a pared-down framework (of CGA), with bounded capabilities, is introduced.

In order to not obscure the reader some assumptions have to be made explicit[2] by the following axioms

- Geometric objects, as points, spheres, planes, lines and circles exist and are denoted by capital letters like $\boldsymbol{X}$, $\boldsymbol{P}$, etc.
- Each geometric object, say $\boldsymbol{A}$, defines its own equivalence class formed by all scalar multiples, i.e. $\boldsymbol{A} \equiv \lambda\, \boldsymbol{A}$, $\lambda \in \mathbb{R}\backslash\{0\}$.

[1] But not vice versa

[2] It follows an informal trimmed to fit paraphrase of the geometric algebra of the conformal space. This algebra is the subject of chapter 3.3.

- Let the juxtaposition, e.g. $\boldsymbol{PQ}$, be a placeholder for a bilinear, associative and non-commutative 'geometric product' between the involved elements.
- Suppose the elements considered here square to real numbers, typically ± 1. Spheres, in particular, are assumed to square to $\boldsymbol{S}^2 = r^2$, where r denotes the radius of the respective sphere $\boldsymbol{S}$.
- If $\boldsymbol{P}$ denotes a plane, then a reflection $\boldsymbol{A}'$ of any object $\boldsymbol{A}$ in the plane can be expressed via the sandwich product
$$\boldsymbol{A}' = \boldsymbol{PAP}\,.$$

Intersection from Reflection

One strength of geometric algebra is the ability to intersect geometric objects. It was refrained from putting the intersection to the above axioms. Instead a (weaker) concept of intersection is deduced in an informal but descriptive way.

Suppose the two planes $\boldsymbol{P}_1$ and $\boldsymbol{P}_2$ are perpendicular. The reflection of $\boldsymbol{P}_2$ in $\boldsymbol{P}_1$ must then result in $\boldsymbol{P}_2$ again

$$\boldsymbol{P}_1\boldsymbol{P}_2\boldsymbol{P}_1 \equiv \boldsymbol{P}_2 \qquad \Longleftrightarrow \qquad \boldsymbol{P}_1\boldsymbol{P}_2\boldsymbol{P}_1 \propto \boldsymbol{P}_2\,.$$

According to the above axioms, the multiplication with $\boldsymbol{P}_1$ from the right results in

$$\Big[(\boldsymbol{P}_1\boldsymbol{P}_2\boldsymbol{P}_1)\boldsymbol{P}_1 = \boldsymbol{P}_1\boldsymbol{P}_2\boldsymbol{P}_1\boldsymbol{P}_1 = \boldsymbol{P}_1\boldsymbol{P}_2(\boldsymbol{P}_1\boldsymbol{P}_1) \propto \boldsymbol{P}_1\boldsymbol{P}_2\Big] \propto \boldsymbol{P}_2\boldsymbol{P}_1$$

and hence

$$\boldsymbol{P}_1\boldsymbol{P}_2 \propto \boldsymbol{P}_2\boldsymbol{P}_1\,. \tag{1.1}$$

Let $\boldsymbol{L} = \boldsymbol{P}_2\boldsymbol{P}_1$, then the effect of $\boldsymbol{P}_1$ and $\boldsymbol{P}_2$ on $\boldsymbol{L}$ is

$$\begin{aligned} \boldsymbol{P}_1\boldsymbol{L}\boldsymbol{P}_1 &= \boldsymbol{P}_1(\boldsymbol{P}_2\boldsymbol{P}_1)\boldsymbol{P}_1 & \qquad \boldsymbol{P}_2\boldsymbol{L}\boldsymbol{P}_2 &= \boldsymbol{P}_2(\boldsymbol{P}_2\boldsymbol{P}_1)\boldsymbol{P}_2 \\ &= \boldsymbol{P}_1\boldsymbol{P}_2\boldsymbol{P}_1^2 & &= \boldsymbol{P}_2^2\boldsymbol{P}_1\boldsymbol{P}_2 \\ &\propto \boldsymbol{P}_1\boldsymbol{P}_2 & &\propto \boldsymbol{P}_1\boldsymbol{P}_2 \\ &\equiv \boldsymbol{L} & &\equiv \boldsymbol{L} \end{aligned}$$

with equation (1.1). $\boldsymbol{L}$ is invariant to reflections in $\boldsymbol{P}_1$ and $\boldsymbol{P}_2$ and can therefore be regarded as the line of intersection between $\boldsymbol{P}_1$ and $\boldsymbol{P}_2$.

Note that $\boldsymbol{L}$ is an operator at the same time since it describes two consecutive reflections. The operator $\boldsymbol{L}$ applied to any point $\boldsymbol{X}$ on $\boldsymbol{L}$ will give $\boldsymbol{X}$ again

$$\boldsymbol{LXL} \propto \boldsymbol{X}\,.$$

In general, a point $\boldsymbol{X}$ is located on a geometric object $\boldsymbol{A}$ *iff* the point is invariant to the sandwich product, i.e. $\boldsymbol{AXA} \equiv \boldsymbol{X}$. This will become evident in chapter 3.

The derivation of the intersection of two planes can be done for different geometric objects in the same way. Hence another axiom is

- The intersection of two perpendicular geometric objects, $\boldsymbol{A}$ and $\boldsymbol{B}$, is given by the product $\boldsymbol{AB}$.

The prerequisite of perpendicularity will be abolished later on in this chapter.

Spherical Reflection

This example demonstrates that a spherical reflection is possible, yet its main message is the simplicity of reasoning; some elementary calculations and assumptions lead to a profound result.

Consider a circle $\boldsymbol{C}$ in 3D - it can clearly be thought of as an intersection of two spheres. Given one sphere, which coincides with the circle, the set of suitable spheres to reconstruct the circle is endlessly big. The set also comprises a plane, that is a special sphere with infinite radius, which actually is the circle's plane $\boldsymbol{P}_C$. Let $\mathcal{S}$ denote a different set that contains pairs of spheres such that the intersection between the respective spheres of each pair yields the circle. Each pair in $\mathcal{S}$ for which the constituting spheres locally intersect at right angles can now be taken to build the (infinitely big) subset $\mathcal{S}_\perp \subset \mathcal{S}$. There are at least two special cases in $\mathcal{S}_\perp$.

- One sphere is of minimal size the other one is of maximum size: the circle plane $\boldsymbol{P}_C$ intersected with the sphere $\boldsymbol{S}_C$ whose center lies on $\boldsymbol{P}_C$ yields $\boldsymbol{C}$, see figure 1.1. The radius of $\boldsymbol{S}_C$ equals the circle's radius.
- Symmetrical case: both spheres, $\boldsymbol{S}_I$ and $\boldsymbol{S}_J$, have equal radius, see figure 1.2.

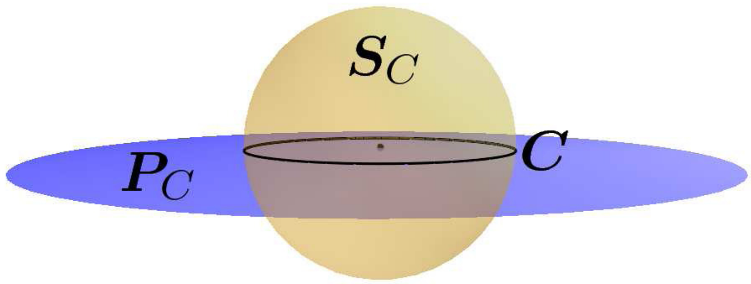

Fig. 1.1: Construction of the circle $\boldsymbol{C}$ from sphere and plane.

Because both cases fulfill the requirement of perpendicularity, the results of section 1.1.3 can be used and the circle $\boldsymbol{C}$ can be built in two ways

$$\boldsymbol{C}_{SP} = \boldsymbol{S}_C \boldsymbol{P}_C \qquad \text{and} \qquad \boldsymbol{C}_{SS} = \boldsymbol{S}_I \boldsymbol{S}_J\,.$$

Note that, in the symmetrical case, each sphere can be replaced by the reflection of the opposite sphere in the circle's plane, for example $\boldsymbol{S}_J \equiv \boldsymbol{P}_C \boldsymbol{S}_I \boldsymbol{P}_C$. The following calculation makes use of this fact. It starts from $\boldsymbol{C} \equiv [\boldsymbol{C}_{SP} \propto \boldsymbol{C}_{SS}]$.

$$\begin{array}{rcll} \boldsymbol{S}_C \boldsymbol{P}_C & \propto & \boldsymbol{S}_I \boldsymbol{S}_J & \text{employ } \boldsymbol{S}_J \propto \boldsymbol{P}_C \boldsymbol{S}_I \boldsymbol{P}_C \\ \boldsymbol{S}_C \boldsymbol{P}_C & \propto & \boldsymbol{S}_I (\boldsymbol{P}_C \boldsymbol{S}_I \boldsymbol{P}_C) & \text{multiply by } \boldsymbol{P}_C \\ \boldsymbol{S}_C \boldsymbol{P}_C^2 & \propto & \boldsymbol{S}_I \boldsymbol{P}_C \boldsymbol{S}_I \boldsymbol{P}_C^2 & \\ \boldsymbol{S}_C & \propto & \boldsymbol{S}_I \boldsymbol{P}_C \boldsymbol{S}_I & \text{since } \boldsymbol{P}_C^2 \in \mathbb{R} \text{ by axiom} \end{array} \tag{1.2}$$

Besides, with $\boldsymbol{S}_I^2 \in \mathbb{R}$, $\boldsymbol{P}_C \propto \boldsymbol{S}_I \boldsymbol{S}_C \boldsymbol{S}_I$ is implied. The feasibility of a spherical reflection has hereby been shown, though solely for the special setup in which the center of $\boldsymbol{S}_I$ is located on $\boldsymbol{S}_C$.

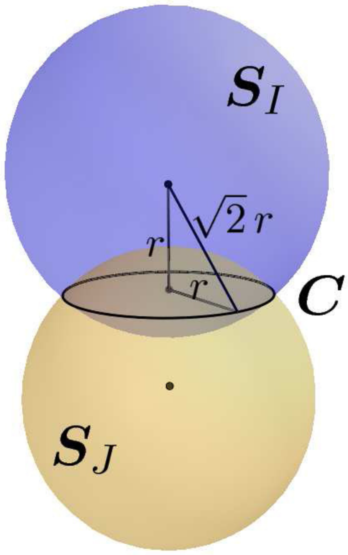

Fig. 1.2: Construction of the circle $\boldsymbol{C}$ from two spheres.

Inversion

By the previous section it is known that the reflection in a sphere can map a plane to a certain sphere, and vice versa. It remains to show what happens to each single point on the plane or on the sphere under spherical reflection.

Consider two arbitrary lines $\boldsymbol{L}_1$ and $\boldsymbol{L}_2$ passing through the center $\boldsymbol{N}$ of the sphere $\boldsymbol{S}_I$ (naming as in section 1.1.3), compare figure 1.4. The new axiom of section 1.1.3 applies to the expressions $\boldsymbol{Q}_1 = \boldsymbol{L}_1\boldsymbol{S}_I$ and $\boldsymbol{Q}_2 = \boldsymbol{L}_2\boldsymbol{S}_I$ because the lines are perpendicular to the sphere $\boldsymbol{S}_I$. The $\boldsymbol{Q}$s are the geometric objects, in this case point pairs, which represent the intersection. For each point pair $\boldsymbol{Q} = \boldsymbol{L}\boldsymbol{S}_I$ it follows

$$\begin{aligned}
\boldsymbol{Q}^2 &\propto 1 && \text{by the axioms} \\
\boldsymbol{L}\boldsymbol{S}_I\boldsymbol{L}\boldsymbol{S}_I &\propto 1 && \text{multiply with}\boldsymbol{L} \\
\boldsymbol{L}^2\boldsymbol{S}_I\boldsymbol{L}\boldsymbol{S}_I &\propto \boldsymbol{L} && \text{and consequently, with } \boldsymbol{L}^2 \in \mathbb{R}\,, \\
\boldsymbol{S}_I\boldsymbol{L}\boldsymbol{S}_I &\equiv \boldsymbol{L}\,.
\end{aligned} \tag{1.3}$$

The meaning of equation (1.3) is clear: the spherical reflection in $\boldsymbol{S}_I$ has no effect on the lines $\boldsymbol{L}_1$ and $\boldsymbol{L}_2$, nor on any line perpendicular to $\boldsymbol{S}_I$. In conclusion, there are two main observations regarding the spherical reflection.

i) Each point on the sphere $\boldsymbol{S}_C$ is mapped somewhere onto the plane $\boldsymbol{P}_C$, and vice versa.

ii) Each point on a line perpendicular to $\boldsymbol{S}_I$ is mapped somewhere onto that line again.

As a result, a point on the sphere *and* on the line maps to a point on the plane *and* on the line. The fact that every intersecting line pierces $\boldsymbol{S}_C$ two times complicates

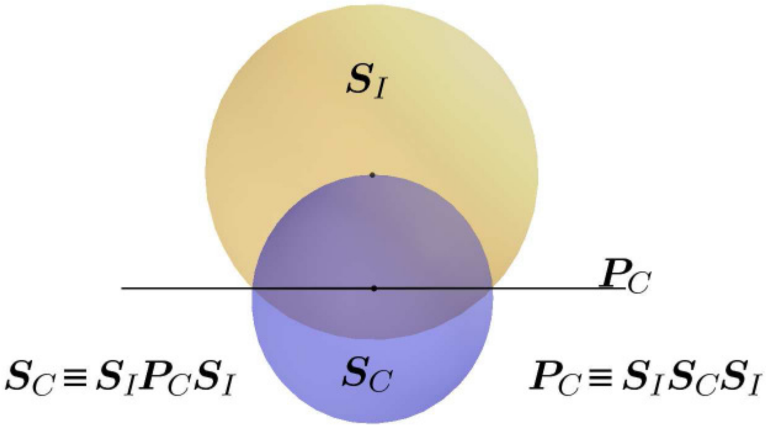

Fig. 1.3: View along the plane $\boldsymbol{P}_C$: the reflection in the sphere $\boldsymbol{S}_I$ maps $\boldsymbol{P}_C$ to $\boldsymbol{S}_C$, and vice versa.

matters. Nevertheless, all lines under consideration share a common point of intersection - the center $\boldsymbol{N}$ of $\boldsymbol{S}_I$. In conjunction with figure 1.4 it is apparent that the spherical reflection maps $\boldsymbol{A}_i$ to $\boldsymbol{B}_i$, $i \in \{1, 2\}$, and vice versa. In order to see this, assume that $\boldsymbol{N}$ is mapped to $\boldsymbol{B}_1$: $\boldsymbol{S}_I\boldsymbol{N}\boldsymbol{S}_I \equiv \boldsymbol{B}_1$. This would violate observation ii) since $\boldsymbol{N}$ is an element of $\boldsymbol{L}_2$ at the same time and must therefore map to $\boldsymbol{L}_2$ - a contradiction.
It seems that $\boldsymbol{N}$ is mapped to itself, i.e. $\boldsymbol{S}_I\boldsymbol{N}\boldsymbol{S}_I \equiv \boldsymbol{N}$. But this would, as described in section 1.1.3, imply that $\boldsymbol{N}$ is located on $\boldsymbol{S}_I$ - a contradiction again. Observing that the distance from $\boldsymbol{M}$ to the points $\boldsymbol{B}$ increases while the corresponding points $\boldsymbol{A}$ approach $\boldsymbol{N}$ leads to the hypothesis that $\boldsymbol{N}$ is mapped to a point at infinity. This effortless result is confirmed in chapter 3.2 where the point at infinity '$\mathbf{e}_\infty$' is formally introduced.
It is noteworthy that the spherical reflection of points, as discussed here, resembles a stereographic projection. This fact is vastly exploited in chapter 8.

The spherical reflection with the above properties is an *inversion* operation. The inversion $\boldsymbol{S}_I\boldsymbol{A}\boldsymbol{S}_I$ of a point $\boldsymbol{A}$ in a sphere $\boldsymbol{S}_I$, called the inversion sphere, is always defined. This is evident because a scenario similar to the one in figure 1.4 can always be constructed. The inversion is the generating operation for the group of conformal mappings, cf. chapter 3.3. Next, a reflection in a plane simply is the inversion in a particular sphere with infinite radius. By further noting that the group of Euclidean transformations can be constructed from (successive) reflections it follows that every Euclidean transformation is a conformal mapping as well. The inversion can therefore be considered the most important operation for this work, for rigid body motions herein play a central role.

Finally, there are two more things worth noting

- The inversion operation is an *involution* with respect to the equivalence classes of geometric objects. The involution-property, commonly expressed as identity $f(f(x)) = x$, is easily verified by exploiting associativity

$$\boldsymbol{B} \;=\; \boldsymbol{S}_I(\boldsymbol{S}_I\boldsymbol{A}\boldsymbol{S}_I)\boldsymbol{S}_I \;=\; (\boldsymbol{S}_I\boldsymbol{S}_I)\boldsymbol{A}(\boldsymbol{S}_I\boldsymbol{S}_I) \;\propto\; \boldsymbol{A} \qquad \text{with } \boldsymbol{S}_I^2 \in \mathbb{R}\,.$$

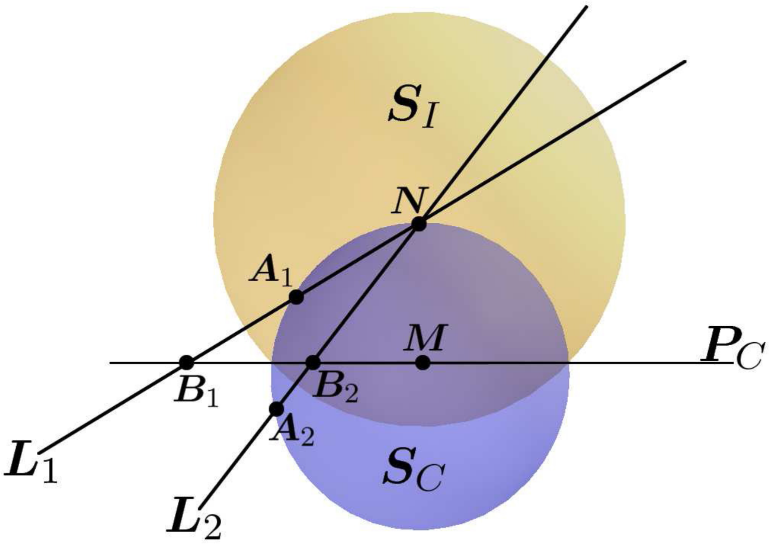

Fig. 1.4: To the issue of how points behave under spherical reflection. The illustration suggests a mapping from $\boldsymbol{A}_i$ to $\boldsymbol{B}_i$, $i \in \{1, 2\}$, and vice versa.

Hence $\boldsymbol{A}$ doubly subjected to the inversion in the sphere $\boldsymbol{S}_I$ results in the point $\boldsymbol{B}$ representing the same point as $\boldsymbol{A}$, i.e. $\boldsymbol{B} \equiv \boldsymbol{A}$.

- The successive application of basic operations, like inversion or reflection, leads to more complex operators. Self-evidently, these must equally be applied via the sandwich product.

In conclusion, it has been shown that the limited framework utilized is already comprehensive, closed and meaningful. Profound and useful results have been deduced from a handful of axioms in a descriptive manner.

1.2 Motivation Stochastics

Uncertain data occurs almost invariably, especially in computer vision applications. It is hence a necessity to develop and use methods, which account for the errors in observational data. Here the main aspects of and foundations for the parameter estimation from uncertain data within the unified mathematical framework of geometric algebra are outlined.

In general, the aim is to estimate a multivector representing a geometric entity from a set of uncertain measurements. In the present case only point measurements, mostly image points, are considered. Clearly, in order to approach the problem, a mathematical formulation has to be found that relates the sought geometric entity, which can equally be an object or an operator, and the observations to each other. That is both have to satisfy a particular condition equation, which is referred to as the functional model. Its impact on the actual estimation is decisive [73], whence it should well reflect the problem at hand. So one motivation for coupling parameter estimation with geometric algebra is CGA. Its strength to express distances or incidence relations makes it possible to derive simple yet eligible condition equations. This does certainly not hold for all problems encountered in everyday life but CGA smoothly integrates into many computer vision tasks as those addressed in this thesis. Practical issues give rise to a further motivation: a suitable numerical interface between GA and the estimation method, whichever one is chosen, has to be found. This is where the tensor representation of CGA comes into play. It gives numerical access to each component of any product or multivector. At first a parameter vector encoding the multivector which is to be estimated can be built up. Likewise, each observation yields one vector. Second the tensor representation allows for the handling of uncertainties, i.e. covariance matrices can be attributed to the vectors. Next certain structural constraints on the multivector components can be exploited which finally gives lean condition equations. The bilinearity of the geometric product is advantageous in that it alleviates error propagation.

Because linear relationships, or rather linear condition equations, often arise in GA, a parameter estimation method which particularly benefits from this behavior is employed. For the classical linear model the well-known technique of least squares adjustment is proven to provide what is called the best linear unbiased estimator. It is usually described by unbiasedness, minimal variance, consistency, efficiency, sufficiency and robustness. Least squares, also known as fitting, is generally characterized by minimizing the sum of the squared residuals; these are the deviations of the observations from the model. The term 'adjustment' relates to the redundancy in observational data in that it emphasizes that the parameter estimation should exhibit compensatory qualities, i.e. the impact of each measurement must be weighted according to its respective uncertainty. Since the residuals can be considered corrections to the observations, adjustment equally means finding the most likely observations. Least squares on the original observations, rather than incorrectly on derived quantities, is what the Gauss-Helmert (GH) model was designed for. This linear model rounds the classical model out because it can additionally account for conditions among the original observations. As a consequence of this, it becomes possible to appropriately integrate uncertainty information into the estimation process. As in many photogrammetric areas of application, the Gauss-Helmert based least squares method is used throughout this work.

1.3 Motivation Pose Estimation

Self-localization definitely is an important aspect for a moving robot. But it is to no avail if the robot knows that it stands next to an abyss without having an idea of the direction of the abyss. This explains why the *pose* comprises information about position and orientation. These quantities relate to some coordinate system which is, of course, different from the one of the robot. Hence the pose corresponds to a rigid body motion consisting of a rotational and a translational part. A robot can infer its pose from many different sources, that is types of sensory data: visual (images, laser scan), audio (ultrasound), haptic, odometric (observing own movements, e.g. by tracking the revolution of wheels), etc.

Almost all the vision applications proposed in this thesis do involve estimating a pose/RBM. In all cases input data is drawn from images. Two strategies can be distinguished because of their principle methodology: first, the holistic approach in which the global features of images are considered, for instance by a fourier analysis, a principle component analysis or a radon transform. In this way, the complete image information can be reduced, worked up and finally rearranged so as to have a small-sized, uniform and thus comparable image representation. Sampling the environment gives a topology map, which can afterwards, at navigation, be used to estimate the pose. Second, the analytic approach where local image features are used. These are typically points with a non-zero intrinsic dimension, i.e. places where areas form noticeable edges, corners or junctions. Likewise, lines, line segments, possibly disconnected curves, image patches, point sets, histograms or more generally probability density functions, and so forth can be taken as features. Here the second approach is pursued using point or line features.

Doing pose estimation implies to be aware of the environment. Hence the robot must have a map with suitable landmarks which it can recognize in the images. If the perception focusses on points and lines, the landmarks must equally be point- and line-like, respectively, otherwise it becomes difficult to establish the connection between the 3D-world and the retrieved image features. Hereafter, it is referred to the 'map' as the *object model* so that pose estimation can be condensed into one sentence: rigidly moving an object in 3D such that it comes into agreement with 2D-sensory data from a vision system, is called 2D-3D pose estimation.

Note that pose estimation is not restricted to the customary pinhole camera model. In this thesis, special attention is payed to omnidirectional vision, where the role of the inversion is substantial. It turns out that CGA is particularly useful for modeling imaging independent of which kind of vision system is used. This is because its elements ideally match the needed components.

1.4 The Thesis

At the beginning geometric algebra is derived from scratch by considering only three axioms. Studying products involving more and more operands the computational abilities of GA disclose stepwise. This first part is strongly connected to multilinear algebra; the fundamental part of determinants is elaborated. Knowing the foundations, the tools of the trade for effectively working with GA are made available. These 'basic concepts' and relationships are most important for understanding. The last part of chapter 2 deals with more sophisticated aspects of geometric algebra and should not be regarded as optional because some vital ideas, like those connected to the dual operation, are explained.

The next chapter represents an investigation into conformal geometric algebra. It unveils in particular the geometrical streaks of CGA, and it clearly gives the answer to the question 'Why geometric algebra?'. It is eligible to say that the CGA chapter makes up the effective core of this work.
It starts with constructing CGA, thereby elucidating the notion behind the conformal space. After that, the algebra basis and the products over which are listed in

tabular form. Then a wide selection of geometric entities, which are at the same time the here most often used CGA elements, are presented. For each entity, be it an object or a pure operator, the defining CGA expressions, geometrical issues and interrelations with other entities are detailed. This comprehensive repertoire has proven itself most helpful many times.

The principle of pose estimation as used in this work is introduced in chapter 4. Thales' theorem is made use of to model a pose estimation based on three feature points. This purely geometric problem is formalized employing CGA in a very illustrative manner. Touched are important issues like fitting, outermorphism, constructing rigid body motions by composing reflections, subjecting a circle to an RBM and the multivector valued differentiation so as to apply the Newton-Raphson method to a CGA expression. Besides the fact is exploited that both, the conformal group and the related Lie algebra, are elements of the conformal geometric algebra. Moreover, the connection between group and algebra can simply be modeled by invoking the `exp/log` map of the corresponding multivectors.

Parameter estimation in general and the technique of least squares adjustment assuming the linear Gauss-Helmert model in particular is the subject of chapter 5. In the beginning there is a survey of the different parameter estimation approaches. It shows the connections between Bayesian estimation, specifically the maximum a posteriori estimation and the maximum likelihood estimation, and the method of least squares. The latter is then formally and intelligibly derived, including concerns as linearization. After reporting the basic varieties of observations that may occur, the Gauss-Helmert method, which simultaneously allows for different kinds of observations, is described in detail. The chapter ends with a presentation of the GH-method as is underlain the parameter estimation of the subsequent chapters.

In chapter 6 it is delved into several vital aspects of geometric algebra. It is about the matrix representation and the tensor representation of GA. The latter is used to derive a concept of error propagation specially tailored to the geometric product. It allows for the possibility to propagate uncertainty information in the form of covariance matrices for every thinkable GA expression. Likewise, expectation values can be treated. This is vastly exploited in chapter 8, where pixel observations with initially independently and identically distributed error are subjected to a transformation that somehow mimics the inverse omnidirectional imaging process. The uncertainties belonging to the new 'pseudo' observations have to be evaluated using error propagation so as to comply with the least squares principle.

The next chapter is essential in more than one sense: it shows in three main sections the necessary basics for coupling conformal geometric algebra and the numerical back-end - the GH-parameter estimation - via the tensor representation of GA. Next, it provides the key ideas for realizing pose estimation in this joint framework. By means of three examples, i.e. fitting a circle to a 3D-point-set, estimating the RBM between two 3D-point-sets and eventually the perspective pose estimation, the foundations for chapter 8, which takes the pose estimation to the omnidirectional case, are laid. Particularly, it can be seen how uncertainty information, initially attributed to the observations, integrates into the estimation and eventually influences the outcome. The overall approach proposed in this thesis is finally justified for each of the three examples through experimental results.

Omnidirectional vision has recently become very popular, but regrettably primarily on account of surveillance. However, robot navigation has profited similarly strong. The related image formation can often be modeled using a parabolic mirror. After a while it became obvious that imaging is comparable to the one in the pinhole camera model, albeit an inversion has additionally to be introduced. Combining projective geometry with an inversion operation seems to prescribe the usage of conformal geometric algebra. Hence three of such problems are addressed in chapter 8. First, omnidirectional imaging is formalized using the expressiveness of CGA. Special attention is also given to images of world lines. Pose estimation from the previous chapter is then adapted to omnidirectional vision systems. Specifically, a variant with point features and a variant with line features is studied. Experimental results are presented for each of the two scenarios. The last area of application deals with the epipolar geometry in omnidirectional vision. It emerges considering two vision sensors ($\sim$ cameras) at the same time, or equally one moving sensor, by inquiring into the pixel-wise relationships between two images taken at different positions. In short, an epipole is the (theoretical) image of the optical center of another camera. The 'stochastic epipole estimation' focusses on this aspect: CGA is used to set up conditions relating two pixels from two images to one another. The resultant parameter estimation is again a pose estimation, but in an indirect manner. Elaborate experiments were conducted to provide evidence of the accuracy of the estimation.

Chapter 9 gives the conclusion.

Appendix A contains several definitions of the most important terms from linear algebra, a number of rules, identities and remarks that apply to the as well important commutator formalism, some proofs separated from the main text and a collection of useful formulae relating to conformal geometric algebra.

Parts of this work have been published in [41, 42, 43, 44, 45, 95, 96, 109].

Chapter 2

Geometric Algebra

The beginning is a tale of a mathematical success story ...

Historical note

> *The quest for a mathematical language suitable to express geometrical relationships in an algebraic way can be traced back to the ancient Greeks: it was Euclid with his seminal work 'Elements' in the 3rd century B.C. who first wrote down geometrical laws for a world as he perceived it. It took a long time, until the eighteenth century, that mathematicians caused a furor by discovering geometries distinct from the Euclidian one. The predominant task was then to find an algebraic framework which would unify all different geometries...*
>
> *Inspired by the algebra of complex numbers, which allows the division by a vector, William Rowan Hamilton (1805-1865) was preoccupied with a generalization to three dimensions: he had been trying to find a reasonable way to multiply three-dimensional points for a couple of years, in such a way as to allow division. Finally, on 16th of October 1843 Hamilton discovered the numbers later called Quaternions. Considering an anti-commutative multiplication and the idea of using four dimensions instead of three were the crucial factors making his finding possible.*
>
> *At that time, another pivotal question was how best to represent rotations in 3D. Here Quaternions emerged as a very clear to handle and very efficient way for carrying out rotations and are still in use today. Despite the then positive impact the role of Quaternions diminished with the introduction of the more straightforward vector algebra of Josiah Willard Gibbs (1839-1903) in the 1880s. The framework promoted by Gibbs is basically the classical vector algebra being taught high school students nowadays; it distinguishes between the scalar product and the vector cross product. The Quaternion product, in contrast, combines both of them. Eventually, the Quaternions were, due to Gibbs's established reputation, displaced by his hybrid vector algebra.*
>
> *The probably most important step towards geometric algebra was taken by the German mathematician and schoolteacher Hermann Günther*

Grassmann (1809-1877). In 1844 he composed his Ph.D. thesis 'Die Lineare Ausdehnungslehre', in which he introduced an outer product between vectors as a generalization of the idea of the cross product. His product is anti-commutative, too, but it is associative and its result is neither a scalar nor a vector, it is a new mathematical entity encoding an oriented linear subspace of arbitrary dimension (bounded by the number of involved vectors or by the dimension of the superordinate space). In this way Grassmann was able to overcome the limitations of the cross product, which only exists in three dimensions. His work, however, was rejected as it was too innovative for its time.

Neither less important than Grassmann and the driving force behind the development of geometric algebra was the English mathematician William Kingdon Clifford (1845-1879). He was one among the few who had understood Grassmann and it was his stroke of genius to realize the potential within it. Recognizing significant overlaps between the concepts of Grassmann and Hamilton it was henceforth his ambition to unite the two frameworks into a single structure. In the 1870s, Clifford established his algebra later to be known as Clifford algebra. He originally used the name geometric algebra since he understood geometry to be inherent in that algebra. His naming partly was a concession to Grassmann, too, attributed to significant parallels between their products. Clifford's geometric product extends Grassmann's outer product by an inner product. Just like the outer product the inner product can be applied to elements of any dimension. Both products can be considered antagonists as the outer product raises the dimensionality of the result, whereas the inner product reduces it. In Clifford's algebra elements of any type, i.e. scalar, vector and higher-dimensional elements, can be added or multiplied together. Much of its power arises from the possibility to divide by a vector. Moreover, it exists a certain meaningful class of higher-dimensional elements by which can be divided as well.
Regrettably, Clifford algebra had to suffer the same fate as Quaternions. In the follow-up time the geometric strength of Clifford algebra was lost sight of and it was at best utilized as formal algebra, e.g. in physics.

In the 1960s a rediscovery of geometric algebra was initiated by the American physicist and mathematician David Hestenes (born 1933). During his study of quantum mechanics he found what had been completely overlooked all along: physicists had implicitly been dealing with Clifford algebras in the guise of matrix algebras over the Dirac and Pauli matrices. Hestenes then showed that Pauli and Dirac algebras have a geometric meaning which had notable consequences for the physical interpretation of quantum mechanics. After observing that the common but patchwork-like cousage of Gibbs's vector algebra with the matrix algebras is unintelligible and redundant, Hestenes was able to reformulate quantum mechanics expressions in terms of the coherent language of geometric algebra. He finally came to the insight that Clifford algebra is nothing less than a universal language for mathematics, physics and *engineering.*

Today geometric algebra is interdisciplinarily acknowledged and being used in a multiplicity of applications over a wide range of fields.

Note that the term 'geometric algebra' is to be preferred to 'Clifford algebra' whenever the geometrical facets of the algebra come to the fore. The term 'Clifford algebra' is advisable whenever the focus is on the formal character or use of the algebra. Although this applies to section 2.1, Clifford's original choice of name - 'geometric algebra' - is adopted throughout this work.

As indicated in the historical note before geometric algebra is a powerful and unifying language being used in many mathematically influenced areas of research or application. A clue what geometric algebra can render was already given in section 'A Vivid Motivation for Geometric Algebra'. Compared to the whole range of applications, for example, in physics, the contents of this work is virtually minuscule. Anyway, by the following sections is intended to convey the adequate understanding of GA. It is begun with an axiomatic derivation. Next the key aspects of geometric algebra are enlightened. This mainly includes the relationships between the products of GA. The section thereafter seeks to enlarge upon this basis. It is supplementary and contains several interesting identities and definitions which sometimes go somewhat beyond the prerequisite of this work.

2.1 An Axiomatic Derivation

Here a comprehensive discussion of geometric algebra is given. At first, some basic concepts as the algebra basis and the geometric (algebra) product are gradually and not that much formally introduced along with the respective notation. Readers who are not new to geometric algebra should at least skim over the introductory part in order to get the notations. Some of the underlying algebraic basics can be found in the appendix A.1 at page 235. The picture given of the algebra is then to be refined with the help of the algebra formally defining axioms. Next, the approach of Hestenes and Sobczyk [63] can be followed in that the two most important products, that is the *inner* and the *outer product*, are derived from the *geometric product*. Starting from this level the full geometric algebra is constructed.

For a complete understanding of GA the vintage book of Hestenes and Sobczyk [63] or the cutting-edge book of Dorst [23] is recommended. While the setting of the former is more physical, the latter approaches engineers and programmers.

Consider the *canonical basis* $\mathbb{B}^{p,q}$ of the *quadratic space*[1] $\mathbb{R}^{p,q}$ consisting of the $n = p + q$ basis vectors

$$\mathbb{B}^{p,q} = \{\mathbf{e}_1, \mathbf{e}_2, \ldots, \mathbf{e}_p, \mathbf{e}_{p+1}, \ldots, \mathbf{e}_n\}$$

with the scalar products

$$\mathbf{e}_1 * \mathbf{e}_1 = \mathbf{e}_2 * \mathbf{e}_2 = \ldots = \mathbf{e}_p * \mathbf{e}_p = 1$$

[1]The quadratic space $\mathbb{R}^{p,q}$ may henceforth be referred to as vector space $\mathbb{R}^{p,q}$.

and

$$\mathbf{e}_{p+1} * \mathbf{e}_{p+1} \;=\; \mathbf{e}_{p+2} * \mathbf{e}_{p+2} = \ldots = \mathbf{e}_n * \mathbf{e}_n \;=\; -1\,.$$

The pair (p, q) is called *signature* and specifies that $p\ \ (q)$ basis vectors square to $+1\ \ (-1)$. Beyond that it is possible to include basis vectors that square to zero, which would result in a *degenerate algebra*. The number of basis vectors squaring to zero is typically denoted with r, and the corresponding signature would be the triple (p, q, r), cf. $\mathbb{R}^{p,q,r}$. However, a degenerate algebra can always be embedded into a non-degenerate but larger algebra such that all basis vectors are mutually orthogonal. Luckily, the problems dealt with in this thesis lead to non-degenerate algebras only.

Note that in the remainder of this text, only finite-dimensional non-degenerate algebras over the reals $\mathbb{R}$ are taken into account.

By the next couple of pages it will become apparent that $\mathbb{B}^{p,q}$ can be used to construct the algebra basis, denoted by $\mathbb{B}_{p,q}$, of the respective geometric algebra $\mathbb{R}_{p,q}$. Roughly speaking, any possible combination of elements $\mathbf{e}_i \in \mathbb{B}$ yields one basis vector in $\mathbb{B}_{p,q}$. The 'empty' combination, in analogy to the element $\emptyset$ denoting the empty set in a power set, has no vector parts and the corresponding algebra basis element therefore represents the scalars. It is commonly introduced as $\mathbf{e}_0 := 1$. An intelligible way to state the algebra basis is

$$\mathbb{B}_{p,q} \;=\; \big\{\mathbf{e}_0\big\} \;\cup\; \Big\{\; \mathbf{e}_{i_1}\mathbf{e}_{i_2}\ldots\mathbf{e}_{i_r} \;\;\Big|\;\; {\scriptstyle 1 \le i_1 < i_2 < \ldots < i_r \le n, \quad 1 \le r \le n} \;\Big\}\,. \tag{2.1}$$

The cardinality of $\mathbb{B}_{p,q}$ and so the dimension $\dim(\mathbb{R}_{p,q})$ of the algebra is $|\mathbb{B}_{p,q}| = 2^n$ because the sum over all $n+1$ possible r-combinations results in

$$\dim\left(\mathbb{R}_{p,q}\right) \;=\; \sum_{r=1}^{n} \binom{n}{r} \;=\; 2^n\,.$$

The definition of $\mathbb{B}_{p,q}$ reveals that

$$\mathbb{B}_{p,q} \;\supset\; \mathbb{B}^{p,q}\,.$$

A case in point is the basis of the geometric algebra $\mathbb{R}_3$ (trailing zeros, e.g. $q = 0$ in $\mathbb{R}^{p,q}$, will be omitted from now on) of the 3D-Euclidean vector space $\mathbb{R}^3$ with basis $\mathbb{B}^3 = \{\mathbf{e}_1, \mathbf{e}_2, \mathbf{e}_3\}$

$$\mathbb{B}_3 \;=\; \{1,\; \mathbf{e}_1, \mathbf{e}_2, \mathbf{e}_3,\; \mathbf{e}_1\mathbf{e}_2, \mathbf{e}_1\mathbf{e}_3, \mathbf{e}_2\mathbf{e}_3,\; \mathbf{e}_1\mathbf{e}_2\mathbf{e}_3\}\,. \tag{2.2}$$

The elements of $\mathbb{B}_{p,q}$ are called *ordered basis blades*. In order to work with basis blades a set notation with small characters is introduced. Symbols like $\mathbb{u}, \mathbb{v}, \ldots, \mathbb{z}$ are meant to represent subsets of $\mathcal{N} := \{1, 2, \ldots, n = p + q\}$ and are designated to appear in the index, for example $\mathbf{e}_{\mathbb{u}}, \mathbf{e}_{\mathbb{v}}, \ldots, \mathbf{e}_{\mathbb{z}}$. The usual set based operations apply to these index sets, e.g. $\mathbb{w} = \mathbb{u} \cap \mathbb{v}$. Let $\mathbb{u} = \{i_1, i_2, \ldots, i_r\} \subseteq \mathcal{N}$, then the ordered basis blade

$$\mathbf{e}_{\mathbb{u}} := \mathbf{e}_{i_1}\mathbf{e}_{i_2}\ldots\mathbf{e}_{i_r} \qquad \text{with} \qquad i_1 < i_2 < \ldots < i_r$$

is defined. The notation $|\mathbb{u}|$ denotes the *grade* of $\mathbf{e}_{\mathbb{u}}$ and yields the number of basis vectors incorporated in $\mathbf{e}_{\mathbb{u}}$. Clearly, the grade of $\mathbf{e}_{\mathbb{u}} = \mathbf{e}_1\mathbf{e}_2$ is 2. Expressions like $\mathbf{e}_{i_1}\mathbf{e}_{i_2}\ldots\mathbf{e}_{i_r}$ may henceforth be abbreviated to $\mathbf{e}_{i_1 i_2 \ldots i_r}$.

Consider the arrangement of the basis in equation (2.1) or equation (2.2). In the first place, the elements are sorted according to their grade. Within groups of equal grade the ordered basis blades are in a lexicographical order with respect to the indices. This enables the identification of basis blades by means of a consecutive numbering. The i^{th} element, $1 \leq i \leq 2^n$, of $\mathbb{B}_{p,q}$ is referred to as $\mathbf{E}_i$, so

$$\mathbb{B}_{p,q} \;=\; \{\mathbf{E}_1, \mathbf{E}_2, \ldots, \mathbf{E}_{2^n}\}\,.$$

The elements of $\mathbb{R}_{p,q}$ are called *multivectors*. They are linear combinations of basis blades. Multivectors[2] will be symbolized using bold capital letters

$$\boldsymbol{A} \;=\; \sum_{\mathbb{u}\subseteq\mathcal{N}} \lambda_{\mathbb{u}}\, \mathbf{e}_{\mathbb{u}}\,, \qquad \lambda_{\mathbb{u}} \in \mathbb{R}$$

or expressed in the *numbered basis*

$$\boldsymbol{A} \;=\; \sum_{i=1}^{2^n} \lambda_i\, \mathbf{E}_i\,, \qquad \lambda_i \in \mathbb{R}\,.$$

More special elements are κ-vectors. They are linear combinations of basis blades of a particular grade, say of grade k. The κ-vector $\boldsymbol{A}_{[k]}$ can thus be written

$$\boldsymbol{A}_{[k]} \;=\; \sum_{\substack{\mathbb{u}\subseteq\mathcal{N},\\ |\mathbb{u}|=k}} \lambda_{\mathbb{u}}\, \mathbf{e}_{\mathbb{u}}\,, \qquad \lambda_{\mathbb{u}} \in \mathbb{R}\,. \tag{2.3}$$

A naming convention distinguishes κ-vectors according to their grades, viz. *scalar*, *vector*, *bivector*, *trivector* and *quadvector*. For $\mathbb{R}_3$ the basis can be subdivided into

$$\mathbb{B}_3 \;=\; \{\underbrace{1}_{scalar}\,,\ \underbrace{\mathbf{e}_1, \mathbf{e}_2, \mathbf{e}_3}_{vectors}\,,\ \underbrace{\mathbf{e}_1\mathbf{e}_2, \mathbf{e}_1\mathbf{e}_3, \mathbf{e}_2\mathbf{e}_3}_{bivectors}\,,\ \underbrace{\mathbf{e}_1\mathbf{e}_2\mathbf{e}_3}_{trivectors}\}\,.$$

The basis blade of highest order is called *unit pseudoscalar* and is denoted by $\boldsymbol{I}$. It is of specific importance in algebraic reasoning comparable to $\mathbf{e}_0$, the representative of the scalars. The unit pseudoscalar of $\mathbb{R}_3$, for instance, is $\boldsymbol{I} = \mathbf{e}_{123}$. The common notation and notion of a vector, symbolized by small bold letters, is kept

$$\boldsymbol{a} \;=\; \sum_{i=1}^{n} \alpha_i\, \mathbf{e}_i\,.$$

Note that $\boldsymbol{a} \;\in\; \mathbb{R}^{p,q} \;\subset\; \mathbb{R}_{p,q}$.

In the following it will be enlightened why basis vectors can be 'lined up' to form basis blades. It is, as probably expected, the tacitly used geometric product that ties the vectors together.

[2]In some publications multivectors are termed 'Clifford numbers'.

2.1.1 Deriving Geometric Algebra

The algebra product is the already in the historical note at page 16 mentioned Clifford product and is named geometric product. It will now be used to axiomatically develop the entire geometric algebra as indicated above from a vector space $\mathbb{R}^{p,q}$.

The geometric product is declared in terms of only three axioms. A juxtaposition of elements, i.e. the omission of any operator symbol, denotes the use of the geometric product. Let $\boldsymbol{a}, \boldsymbol{b}$ and $\boldsymbol{c}$ be three vectors of $\mathbb{R}^{p,q}$. The axioms are

1. **Associativity**
$$\boldsymbol{a}(\boldsymbol{bc}) = (\boldsymbol{ab})\boldsymbol{c} \tag{2.4}$$

2. **Distributivity**
$$\boldsymbol{a}(\boldsymbol{b}+\boldsymbol{c}) = \boldsymbol{ab}+\boldsymbol{ac} \tag{2.5}$$

3. **Quadrature**
$$\boldsymbol{a}^2 \in \mathbb{R} \tag{2.6}$$

The third axiom has to be given the most attention since it accounts for the differences between a general associative algebra and a Clifford algebra; it makes up the geometric algebra. However, a certain amendment to this axiom will have to be done in order to comply with the characteristics of the underlying vector space $\mathbb{R}^{p,q}$.

Consider the square of a vector $\boldsymbol{a}+\boldsymbol{b}$

$$(\boldsymbol{a}+\boldsymbol{b})^2 = (\boldsymbol{a}+\boldsymbol{b})(\boldsymbol{a}+\boldsymbol{b}) = \boldsymbol{a}^2+\boldsymbol{ab}+\boldsymbol{ba}+\boldsymbol{b}^2\,. \tag{2.7}$$

By the third axiom it can be deduced that the expression $\boldsymbol{ab}+\boldsymbol{ba}$ must be a scalar because

$$\boldsymbol{ab}+\boldsymbol{ba} = (\boldsymbol{a}+\boldsymbol{b})^2-\boldsymbol{a}^2-\boldsymbol{b}^2 \in \mathbb{R}\,.$$

Such class of symmetric expressions lends itself to a decomposition into the two parts

$$\boldsymbol{ab} = \underbrace{\tfrac{1}{2}(\boldsymbol{ab}+\boldsymbol{ba})}_{\boldsymbol{a}\,\overline{\times}\,\boldsymbol{b}} + \underbrace{\tfrac{1}{2}(\boldsymbol{ab}-\boldsymbol{ba})}_{\boldsymbol{a}\,\underline{\times}\,\boldsymbol{b}}\,,$$

which is nothing but the common splitting $\boldsymbol{ab} = \boldsymbol{a}\,\overline{\times}\,\boldsymbol{b}+\boldsymbol{a}\,\underline{\times}\,\boldsymbol{b}$ of a product into the *anti-commutator* product (denoted by $\overline{\times}$) and the *commutator* product (denoted by $\underline{\times}$), respectively. Section A.2 in the appendix details the rules and usage of these important products.

At this point the symmetric *inner product*, denoted by '$\cdot$',

$$\boldsymbol{a}\cdot\boldsymbol{b} = \tfrac{1}{2}(\boldsymbol{ab}+\boldsymbol{ba}) \tag{2.8}$$

and the anti-symmetric *outer product*, denoted by '$\wedge$',

$$\boldsymbol{a}\wedge\boldsymbol{b} = \tfrac{1}{2}(\boldsymbol{ab}-\boldsymbol{ba}) \tag{2.9}$$

are defined. The symbol '$\wedge$' for the outer product is called 'wedge'. Hence the geometric product of vectors can be written as

$$\boldsymbol{ab} = \boldsymbol{a} \cdot \boldsymbol{b} + \boldsymbol{a} \wedge \boldsymbol{b} \,. \tag{2.10}$$

Inner and outer product are distributive with respect to addition. This property is inherited from the geometric product and can be shown with the help of the commutator notation. Another obvious result is

$$\boldsymbol{a} \cdot \boldsymbol{b} \;=\; \boldsymbol{b} \cdot \boldsymbol{a} \quad \text{and} \quad \boldsymbol{a} \wedge \boldsymbol{b} \;=\; -\,\boldsymbol{b} \wedge \boldsymbol{a} \quad \Longrightarrow \quad \boldsymbol{a} \wedge \boldsymbol{a} \;=\; 0 \,.$$

The inner product bears its name well: it is symmetric, distributive (bilinear) and it maps to the scalars. But it must be considered that it might be indefinite. Equation (2.8) is closely related to the third axiom as it can be followed that

$$\boldsymbol{a}^2 \;=\; \boldsymbol{a} \cdot \boldsymbol{a} \,.$$

In conjunction with the approach of equation (2.7) the consistency of the inner product with the geometric product can be shown

$$\begin{aligned} (\boldsymbol{a}+\boldsymbol{b}) \cdot (\boldsymbol{a}+\boldsymbol{b}) \;&=\; (\boldsymbol{a}+\boldsymbol{b})^2 \\ \Longleftrightarrow \quad \boldsymbol{a}\cdot\boldsymbol{a} + 2\boldsymbol{a}\cdot\boldsymbol{b} + \boldsymbol{b}\cdot\boldsymbol{b} \;&=\; \boldsymbol{a}^2 + \boldsymbol{ab} + \boldsymbol{ba} + \boldsymbol{b}^2 \;. \\ \Longleftrightarrow \quad \boldsymbol{a}\cdot\boldsymbol{b} \;&=\; \tfrac{1}{2}\big(\boldsymbol{ab}+\boldsymbol{ba}\big) \end{aligned} \tag{2.11}$$

Nevertheless, any symmetric bilinear form would fulfill the above equations. At the same time, the geometric product and likewise the geometric algebra are yet in an undifferentiated state due to the lacking connection to the underlying vector space $\mathbb{R}^{p,q}$. This begs the question whether identifying the scalar product with the inner product is possible. Consider the inner product of two vectors $\boldsymbol{a}$ and $\boldsymbol{b}$, this time in terms of their basis $\mathbb{B}^{p,q}$. Using the anti-commutator and the axioms of the geometric product it is

$$\begin{aligned} \boldsymbol{a}\cdot\boldsymbol{b} \;&=\; (a_1\mathbf{e}_1 + a_2\mathbf{e}_2 + \ldots + a_n\mathbf{e}_n) \cdot (b_1\mathbf{e}_1 + b_2\mathbf{e}_2 + \ldots + b_n\mathbf{e}_n) \\ &=\; a_1b_1(\mathbf{e}_1\cdot\mathbf{e}_1) + a_2b_2(\mathbf{e}_2\cdot\mathbf{e}_2) + \ldots + a_nb_n(\mathbf{e}_n\cdot\mathbf{e}_n) \end{aligned}$$

which is much the same as for the scalar product

$$\begin{aligned} \boldsymbol{a}*\boldsymbol{b} \;&=\; (a_1\mathbf{e}_1 + a_2\mathbf{e}_2 + \ldots + a_n\mathbf{e}_n) * (b_1\mathbf{e}_1 + b_2\mathbf{e}_2 + \ldots + b_n\mathbf{e}_n) \\ &=\; a_1b_1(\mathbf{e}_1*\mathbf{e}_1) + a_2b_2(\mathbf{e}_2*\mathbf{e}_2) + \ldots + a_nb_n(\mathbf{e}_n*\mathbf{e}_n) \,. \end{aligned}$$

The characteristics of $\mathbb{R}^{p,q}$, especially the signature of which, can now be passed on to the geometric algebra by means of a reformulation of the third axiom

3. **Quadrature**

$$\boldsymbol{a}^2 \;=\; \boldsymbol{a}*\boldsymbol{a} \tag{2.12}$$

Notice that just like in equation (2.11) it follows that $\boldsymbol{a}\bar{\times}\boldsymbol{b} = \boldsymbol{a}*\boldsymbol{b}$, which is, in concordance with the definition in equation (2.8), equal to $\boldsymbol{a}\cdot\boldsymbol{b} \;=\; \boldsymbol{a}*\boldsymbol{b}$. It is further important to bear in mind that the inner product and the scalar product only coincide whenever the product of pure vectors is considered. Later on in this text the inner product will be defined for general multivectors, too.

The geometric product is still not completely defined since the outer product in equation (2.10) remained undefined. Regarding this issue the inner product $\mathbf{e}_i \cdot \mathbf{e}_j$, $i \neq j$, is analyzed in detail

$$\mathbf{e}_i \neq \mathbf{e}_j \quad \Longrightarrow \quad \tfrac{1}{2}\big(\mathbf{e}_i\mathbf{e}_j + \mathbf{e}_j\mathbf{e}_i\big) \;=\; \mathbf{e}_i \cdot \mathbf{e}_j \;=\; \mathbf{e}_i * \mathbf{e}_j \;=\; 0\,.$$

There are principally two distinct solutions to the above equation

1. $\mathbf{e}_i\mathbf{e}_j = \mathbf{e}_j\mathbf{e}_i = 0$
2. $\mathbf{e}_i\mathbf{e}_j = -\,\mathbf{e}_j\mathbf{e}_i \neq 0\,.$

The first case implies $\mathbf{e}_i \wedge \mathbf{e}_j = \mathbf{e}_j \wedge \mathbf{e}_i = 0$ and would therefore lead back to the (trivial) standard vector algebra of $\mathbb{R}^{p,q}$, in which no elements of higher grade could be built. Moreover, the first axiom of associativity would be violated[3], for example

$$0 = \mathbf{e}_1\underbrace{\big(\mathbf{e}_1\mathbf{e}_2\big)}_{0} = \underbrace{\big(\mathbf{e}_1\mathbf{e}_1\big)}_{\pm 1}\mathbf{e}_2 = \pm\mathbf{e}_2 \quad \text{(violates associative law).}$$

The second case implies $\mathbf{e}_i\mathbf{e}_j = \mathbf{e}_i \wedge \mathbf{e}_j$, $i \neq j$, and $\mathbf{e}_i \wedge \mathbf{e}_j = -\,\mathbf{e}_j \wedge \mathbf{e}_i$. The far-reaching consequence is that $\mathbf{e}_i\mathbf{e}_j$ denotes a new and irreducible element that does not belong to $\mathbb{R}^{p,q}$ any more. Hence in selecting the second (non-trivial) option the geometric product of two basis vectors becomes

$$\mathbf{e}_i\mathbf{e}_j = \begin{cases} +1, & 1 \leq \;\; i = j \;\; \leq p \\ -1, & p < \;\; i = j \;\; \leq n \\ -\mathbf{e}_j\mathbf{e}_i, & \qquad i \neq j \end{cases} . \tag{2.13}$$

It splits into outer product and inner product, respectively, in the following way

$$\mathbf{e}_i \wedge \mathbf{e}_j = \begin{cases} 0, & i = j \\ \mathbf{e}_i\mathbf{e}_j, & \text{else} \end{cases} \qquad \text{and} \qquad \mathbf{e}_i \cdot \mathbf{e}_j = \begin{cases} \mathbf{e}_i^2, & i = j \\ 0, & \text{else} \end{cases} .$$

By multiplying together the basis vectors of $\mathbb{R}^{p,q}$ a set of exactly 2^n linear independent algebra elements can be found. With the help of the 'swapping rule' $\mathbf{e}_i\mathbf{e}_j = -\,\mathbf{e}_j\mathbf{e}_i$ from equation (2.13) the set can be arranged in concordance with the definition given in equation (2.1). In this way the entire algebra basis $\mathbb{B}_{p,q}$ is generated from $\mathbb{B}^{p,q}$.

Note that basis of $\mathbb{R}_{p,q}$ is certainly not comparable to a customary vector space basis since its elements can not be chosen to be mutually *orthogonal*, especially not in case of the geometric product: the product of $\mathbf{e}_1$ and $\mathbf{e}_{123}$, for example, is

[3] The same argument prohibits that $\mathbf{e}_i\mathbf{e}_j \in \mathbb{R}\backslash\{0\}$, $i \neq j$.

$\mathbf{e}_1\mathbf{e}_{123} = (\mathbf{e}_1\mathbf{e}_1)\mathbf{e}_{23} = \mathbf{e}_{23}$. The elements in $\mathbb{B}^{p,q}$ and $\mathbb{B}_{p,q}$ share at least one common property - they square to ± 1:

$$\mathbf{e}_{123}^2 \;=\; (\mathbf{e}_1\mathbf{e}_2\mathbf{e}_3)(\mathbf{e}_1\mathbf{e}_2\mathbf{e}_3) \;=\; \mathbf{e}_1\mathbf{e}_2\mathbf{e}_3\mathbf{e}_1\mathbf{e}_2\mathbf{e}_3 \;=\; -\,\mathbf{e}_1^2\mathbf{e}_2^2\mathbf{e}_3^2 \;\in\; \{+1,-1\}$$

In summary, the entire geometric algebra has been derived from the three axioms (2.4), (2.5) and (2.12) in conjunction with the quadratic space $\mathbb{R}^{p,q}$. In some constructions of geometric algebra it is additionally required to have a linear map (inclusion map) $i\,:\,\mathbb{R}^{p,q} \longrightarrow \mathbb{R}_{p,q}$ for the embedding of $\mathbb{R}^{p,q}$ into $\mathbb{R}_{p,q}$. Here the existence of i is implicitly assumed and not made explicit because $\mathbb{R}^{p,q}$ can be considered a linear subspace of $\mathbb{R}_{p,q}$. A vector $\boldsymbol{a} \in \mathbb{R}^{p,q}$ is therefore embedded into $\mathbb{R}_{p,q}$ the moment it gets involved in a calculation that makes its embedding necessary. The usage of lower case letters for vectors is, in a manner of speaking, a notation to indicate that the grade of the element equals one - higher order basis blades are zero.

2.1.2 On and beyond the Products

Here the aim is to work with the currently known products in order to gain insights into their functioning and about their meaning. At first, the outer product of two vectors is examined in some detail.

Let $\boldsymbol{a}$ and $\boldsymbol{b}$ be two arbitrary but linearly independent vectors. By exploiting the bilinearity of the geometric product it can be seen that

$$\left.\begin{array}{ccc} \boldsymbol{a} & \wedge & (\alpha\boldsymbol{a}+\beta\boldsymbol{b}) \\ \boldsymbol{b} & \wedge & (\alpha\boldsymbol{a}+\beta\boldsymbol{b}) \end{array}\right\} \propto \; \boldsymbol{a}\wedge\boldsymbol{b} \qquad\qquad \alpha,\beta \in \mathbb{R}\setminus\{0\}$$

is still, up to a scalar factor only, $\boldsymbol{a}\wedge\boldsymbol{b}$. Hence moving the operands $\boldsymbol{a}$ and $\boldsymbol{b}$ within the plane spanned by them leaves the outer product basically unchanged, which is why $\boldsymbol{a}\wedge\boldsymbol{b}$ reflects the *linear subspace* (plane) $\{\boldsymbol{p} = \alpha\boldsymbol{a}+\beta\boldsymbol{b}\,|\,\alpha,\beta \in \mathbb{R}\}$. Self-evidently, this idea will be reinforced later on in section 2.2, when the necessary concepts that are to be developed here will be available.

The subspace stays the same as long as the linear transformation of the constituent vectors is regular (invertible). Consider, for instance, a transformation with matrix $\mathsf{A} \in \mathbb{R}^{2\times 2}$

$$\begin{array}{ccc} \boldsymbol{a}' & = & (\mathsf{A}_{11}\boldsymbol{a}+\mathsf{A}_{21}\boldsymbol{b}) \\ \boldsymbol{b}' & = & (\mathsf{A}_{12}\boldsymbol{a}+\mathsf{A}_{22}\boldsymbol{b}) \end{array}, \qquad \text{with} \quad \mathsf{A} = \begin{bmatrix} \mathsf{A}_{11} & \mathsf{A}_{12} \\ \mathsf{A}_{21} & \mathsf{A}_{22} \end{bmatrix}.$$

According to equation (2.39), on page 46, it is

$$\boldsymbol{a}'\wedge\boldsymbol{b}' \;=\; \det(\mathsf{A})\,\boldsymbol{a}\wedge\boldsymbol{b}. \tag{2.14}$$

Thus the outer product remains exactly unchanged iff the determinant of the transformation matrix is one. The set of real $k\times k$-matrices satisfying this criterion forms

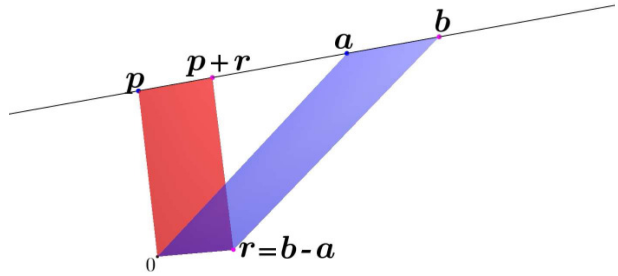

Fig. 2.1: Preservation of the outer product: it is $\boldsymbol{a} \wedge \boldsymbol{b} = \boldsymbol{p} \wedge (\boldsymbol{p} + \boldsymbol{r})$. Note that the shear is area preserving.

a *Lie group*, the *special linear group* $SL(k)$. Figure 2.1 may serve as an example; The equality of $\boldsymbol{a} \wedge \boldsymbol{b}$ and $\boldsymbol{p} \wedge \boldsymbol{r}$ can be seen with

$$\begin{aligned} \boldsymbol{p} \wedge (\boldsymbol{p} + \boldsymbol{r}) = \boldsymbol{p} \wedge \boldsymbol{r} &= \big(\boldsymbol{a} + \lambda(\boldsymbol{b} - \boldsymbol{a})\big) \wedge (\boldsymbol{b} - \boldsymbol{a}), \qquad \lambda \in \mathbb{R} \\ &= \boldsymbol{a} \wedge \boldsymbol{b} - \lambda \boldsymbol{b} \wedge \boldsymbol{a} - \lambda \boldsymbol{a} \wedge \boldsymbol{b} \\ &= \boldsymbol{a} \wedge \boldsymbol{b}. \end{aligned} \tag{2.15}$$

The respective transformation matrix A for $\boldsymbol{p}$ and $\boldsymbol{r}$ reads

$$\mathsf{A} = \begin{bmatrix} 1 - \lambda & -1 \\ \lambda & 1 \end{bmatrix}, \qquad \text{and} \quad \det(\mathsf{A}) = 1.$$

It will shortly be shown that $\boldsymbol{a} \wedge \boldsymbol{b}$ may also be regarded as an *area element*.

Note that the subspace representation is independent of the inner product, that is the result of an outer product is invariable regardless of the signature chosen for the algebra.

It is also helpful to look at the outer product in terms of its coordinate representation. Let $\boldsymbol{a} = a_1\mathbf{e}_1 + a_2\mathbf{e}_2 + \ldots + a_n\mathbf{e}_n$ and $\boldsymbol{b} = b_1\mathbf{e}_1 + b_2\mathbf{e}_2 + \ldots + b_n\mathbf{e}_n$. Then

$$\begin{aligned} \boldsymbol{a} \wedge \boldsymbol{b} &= (a_1\mathbf{e}_1 + a_2\mathbf{e}_2 + \ldots + a_n\mathbf{e}_n) \wedge (b_1\mathbf{e}_1 + b_2\mathbf{e}_2 + \ldots + b_n\mathbf{e}_n) \\ &= (a_1b_2 - a_2b_1)\mathbf{e}_1\mathbf{e}_2 + (a_1b_3 - a_3b_1)\mathbf{e}_1\mathbf{e}_3 + \ldots \\ &\quad + (a_2b_3 - a_3b_2)\mathbf{e}_2\mathbf{e}_3 + \ldots + (a_{n-1}b_n - a_nb_{n-1})\mathbf{e}_{n-1}\mathbf{e}_n \,. \end{aligned}$$

The coefficients exhibit the same structure as those ones that appear in the vector cross product[4] for $n = 3$ or in the determinant of a 3×3-matrix, respectively. Following the notion that there is no predominant orientation in $\mathbb{R}^n$, it will now be shown that the Euclidean norm of the coefficients is invariant under coordinate rotations. *Lagrange's identity*[5]

$$\sum_{i=1}^{n-1} \sum_{j=i+1}^{n} (a_ib_j - a_jb_i)^2 = \left(\sum_{k=1}^{n} a_k^2\right)\left(\sum_{k=1}^{n} b_k^2\right) - \left(\sum_{k=1}^{n} a_kb_k\right)^2 \tag{2.16}$$

[4]Indeed, in $\mathbb{R}_3$ the expression $(\boldsymbol{a} \wedge \boldsymbol{b})\mathbf{e}_3\mathbf{e}_2\mathbf{e}_1$ is equal to the vector cross product.

[5]Lagrange's identity is a special case of the Binet-Cauchy identity (2.45).

perfectly suits to this task. Let $\mathsf{a} = [a_1 a_2 \ldots a_n]^\mathsf{T}$ and $\mathsf{b} = [b_1 b_2 \ldots b_n]^\mathsf{T}$ denote the vector representation of $\boldsymbol{a}$ and $\boldsymbol{b}$, respectively. The right side of equation (2.16) then reads $(\mathsf{a}^\mathsf{T}\mathsf{a})(\mathsf{b}^\mathsf{T}\mathsf{b}) - (\mathsf{a}^\mathsf{T}\mathsf{b})^2$. Also, let $\mathsf{R} \in \mathbb{R}^{n \times n}$ be an appropriate rotation matrix with $\mathsf{R}^\mathsf{T}\mathsf{R} = \mathsf{I}_n$ (I_n denotes the $n \times n$-identity matrix). Hence substituting the rotated versions 'Ra' and 'Rb' into Lagrange's identity (2.16)

$$(\mathsf{a}^\mathsf{T}\mathsf{R}^\mathsf{T}\mathsf{R}\mathsf{a})(\mathsf{b}^\mathsf{T}\mathsf{R}^\mathsf{T}\mathsf{R}\mathsf{b}) - (\mathsf{a}^\mathsf{T}\mathsf{R}^\mathsf{T}\mathsf{R}\mathsf{b})^2 \;=\; \mathsf{a}^\mathsf{T}\mathsf{a}\;\mathsf{b}^\mathsf{T}\mathsf{b} - (\mathsf{a}^\mathsf{T}\mathsf{b})^2$$

demonstrates that the choice of the coordinate system does not affect the Euclidean norm of the coefficients in the outer product $\boldsymbol{a} \wedge \boldsymbol{b}$. This result is well known to hold for the vector cross product as well.

Example 2.1 (Magnitude of an area element in $\mathbb{R}_n$):
Along the above lines it is possible, in $\mathbb{R}_n$, to align the coordinate system with respect to the problem at hand: let $\boldsymbol{a} = a\mathbf{e}_1$ and $\boldsymbol{b} = b\cos\theta\mathbf{e}_1 + b\sin\theta\mathbf{e}_2$ so that $\theta \in [0, \pi]$ is the angle between $\boldsymbol{a}$ and $\boldsymbol{b}$. Computing the outer product yields

$$\boldsymbol{a} \wedge \boldsymbol{b} \;=\; a\mathbf{e}_1 \wedge (b\cos\theta\,\mathbf{e}_1 + b\sin\theta\,\mathbf{e}_2) \;=\; ab\sin\theta\;\mathbf{e}_{12}\,, \qquad a, b > 0.$$

Since $\mathbf{e}_{12}$ is a (unit) basis blade in that it squares to -1, the only coefficient $ab\sin\theta$ must be considered the magnitude of the outer product. Consequently, the magnitude of $\boldsymbol{a} \wedge \boldsymbol{b}$ reflects the area inside the parallelogram spanned by $\boldsymbol{a}$ and $\boldsymbol{b}$.

A more formal way to derive the expression for the magnitude is worth mentioning. Let $a = \sqrt{\mathsf{a}^\mathsf{T}\mathsf{a}}$ and $b = \sqrt{\mathsf{b}^\mathsf{T}\mathsf{b}}$. Using the familiar formula $\mathsf{a}^\mathsf{T}\mathsf{b} = ab\cos\theta$ from Euclidean geometry the term $(\mathsf{a}^\mathsf{T}\mathsf{b})^2$ in the matrix notation of equation (2.16) can be replaced with $a^2b^2\cos^2\theta$, whence it follows

$$a^2b^2 - a^2b^2\cos^2\theta \;=\; a^2b^2(1-\cos^2\theta) \;=\; a^2b^2\sin^2\theta\,.$$

This again suggests the term $ab\sin\theta$ for the magnitude of $\boldsymbol{a} \wedge \boldsymbol{b}$.

Notice that the previous result does in general not hold for non-Euclidean spaces, i.e. spaces with mixed signature, as the inner product does not any more reflect the concepts of distance and angle. The aspect of the magnitude appears again in section 2.3.2.

Although the magnitudes of $\boldsymbol{a} \wedge \boldsymbol{b}$ and $\boldsymbol{b} \wedge \boldsymbol{a}$ are identical it is $\boldsymbol{b} \wedge \boldsymbol{a} = -\boldsymbol{a} \wedge \boldsymbol{b}$. In analogy to vectors, where $\boldsymbol{a}$ is no way the same as $-\boldsymbol{a}$, $\boldsymbol{b} \wedge \boldsymbol{a}$ is called the oppositely oriented element to $\boldsymbol{a} \wedge \boldsymbol{b}$. Hence an *orientation* is additionally attributed to the outer product. Even though in principle arbitrary the orientation is typically introduced as depicted in figure 2.2: it arises from extending vector $\boldsymbol{a}$ along vector $\boldsymbol{b}$. Hence it complies with the right-handed vector cross product.

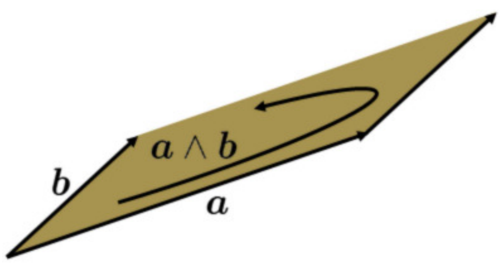

Fig. 2.2: The area of the parallelogram reflects the magnitude of the outer product $\boldsymbol{a} \wedge \boldsymbol{b}$. Its orientation is indicated by the counterclockwise arc.

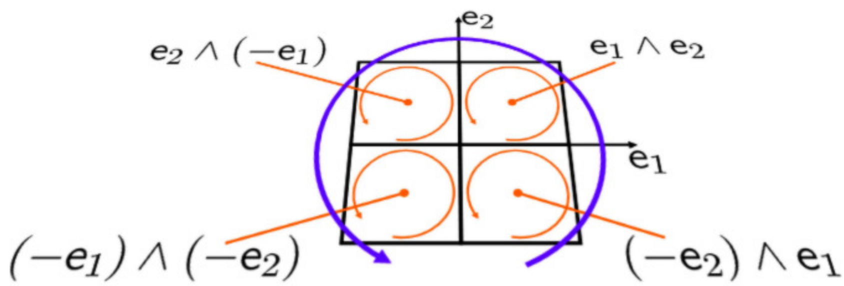

Fig. 2.3: Four identically oriented unit cells. The notion of orientation complies with the outer product since $\mathbf{e}_1 \wedge \mathbf{e}_2$ is identical to $\mathbf{e}_2 \wedge -\mathbf{e}_1$, $-\mathbf{e}_1 \wedge -\mathbf{e}_2$ and $-\mathbf{e}_2 \wedge \mathbf{e}_1$. All cells exhibit the same orientation.

Figure 2.3 illustrates that the chosen rule to determine the orientation is sound in that it is consistent with the bilinearity and anti-symmetry of the outer product. The (thought) extension of $-\mathbf{e}_2$ along $\mathbf{e}_1$, for example, induces the same orientation as all remaining unit cells that are equal to $\mathbf{e}_1 \wedge \mathbf{e}_2$. This notion of orientation can be generalized to higher dimensions. Interestingly, orientations are identical if their respective 'constructions', which arise from successively extending the elements along each other, are congruent.

Recall now that the geometric product is associative. The respective axiom is succinct and unobtrusive but it has profound implications: consider the product $\boldsymbol{ab}$ of two vectors. A right-multiplication with $\boldsymbol{b}$ results in $\boldsymbol{abb} = \boldsymbol{ab}^2 = \lambda \boldsymbol{a}$, with $\lambda = \boldsymbol{b}^2 \in \mathbb{R}$. Whenever $\boldsymbol{b}$ is not a *null vector*, i.e. $\boldsymbol{b}^2 = 0$, it is possible to define the *inverse of a vector* by setting

$$\boldsymbol{b}^{-1} \; = \; \frac{\boldsymbol{b}}{\boldsymbol{b}^2}\,, \qquad \boldsymbol{b}^2 \neq 0\,.$$

As a consequence, the multiplication of $\boldsymbol{a}$ with $\boldsymbol{b}$ can be undone and $\boldsymbol{a}$ is reobtained with

$$(\boldsymbol{ab})\boldsymbol{b}^{-1} \; = \; \boldsymbol{a}(\boldsymbol{bb}^{-1}) \; = \; \boldsymbol{a}\,.$$

The above result is now being used. Let, at first, $\boldsymbol{x}$ and $\boldsymbol{n}$ be two linearly independent vectors of the Euclidean geometric algebra $\mathbb{R}_n$. Without loss of generality it can be assumed that $\boldsymbol{n}^2 = 1$. From the identity $\boldsymbol{x} = \boldsymbol{xnn}$ the following decomposition of $\boldsymbol{x}$ arises

$$\boldsymbol{x} \; = \; \underbrace{(\boldsymbol{x} \cdot \boldsymbol{n})\boldsymbol{n}}_{\boldsymbol{x}_\parallel} + (\boldsymbol{x} \wedge \boldsymbol{n})\boldsymbol{n}\,. \tag{2.17}$$

Since, in the case of vectors, the inner product is identical to the scalar product, it is known from Euclidean geometry that the first term $(\boldsymbol{x} \cdot \boldsymbol{n})\boldsymbol{n}$ must be the projection $\boldsymbol{x}_\parallel$ of $\boldsymbol{x}$ onto $\boldsymbol{n}$. Therefore

$$(\boldsymbol{x} \wedge \boldsymbol{n})\boldsymbol{n} \; = \; \boldsymbol{x} - \boldsymbol{x}_\parallel \; = \; \boldsymbol{x}_\perp \tag{2.18}$$

represents the part of $\boldsymbol{x}$ *perpendicular* to $\boldsymbol{n}$. Since $\boldsymbol{x}_\parallel$ resides in the plane $\boldsymbol{x} \wedge \boldsymbol{n}$, spanned by $\boldsymbol{x}$ and $\boldsymbol{n}$, $\boldsymbol{x}_\perp$ does so as well. This may also be verified by right-multiplying equation (2.18) with $\boldsymbol{n}$

$$\boldsymbol{x} \wedge \boldsymbol{n} \; = \; \boldsymbol{x}_\perp \boldsymbol{n} \; = \; \boldsymbol{x}_\perp \wedge \boldsymbol{n} \quad \text{with } \boldsymbol{x}_\perp \cdot \boldsymbol{n} \; = \; 0\,.$$

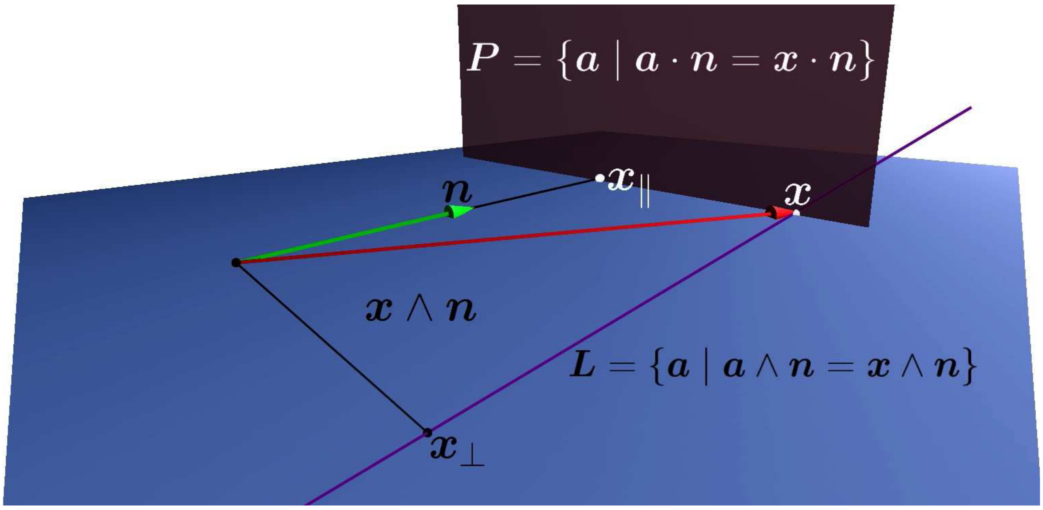

Fig. 2.4: Invertibility of the geometric product in $\mathbb{R}_n$: the function $\boldsymbol{F}(\boldsymbol{x}) = \boldsymbol{x}\boldsymbol{n}$ is a bijection. Possible preimages of $\boldsymbol{x} \cdot \boldsymbol{n}$ and $\boldsymbol{x} \wedge \boldsymbol{n}$ alone would be the plane $\boldsymbol{P}$ and the line $\boldsymbol{L}$, respectively. Hence, on their own, inner and outer product are not injective and therefore not invertible.

Equation (2.17) shows that $\boldsymbol{x}_{\perp}$ can be retrieved from $\boldsymbol{x} \wedge \boldsymbol{n}$ for given $\boldsymbol{n}$. Besides, the remaining part $\boldsymbol{x}_{\|}$ of $\boldsymbol{x}$ is encoded in the inner product $\boldsymbol{x} \cdot \boldsymbol{n}$ so that the geometric product $\boldsymbol{x}\boldsymbol{n}$, in contrast to the scalar product or the vector cross product, does not discard any information contained in $\boldsymbol{x}$. Figure 2.4 illustrates the connection to the invertibility of the geometric product.

Remark (null vector)

Regarding a non-null vector there are two distinct directions: parallel to the vector and orthogonal to the vector. This is different for a null vector. Consider the two-dimensional subspace spanned by the null vector $\boldsymbol{n}$ and another vector $\boldsymbol{x}$. For simplicity, let $\boldsymbol{x} = \mathbf{e}_1$ and $\boldsymbol{n} = \mathbf{e}_1 + \mathbf{e}_2$ with $\mathbf{e}_1^2 = +1$ and $\mathbf{e}_2^2 = -1$. It can be shown that $\boldsymbol{d} = \alpha_1\mathbf{e}_1 + \alpha_2\mathbf{e}_2$, $\alpha_1, \alpha_2 \in \mathbb{R}$, must be a scalar multiple of $\boldsymbol{n}$ in order to have $(\boldsymbol{x} + \boldsymbol{d}) \cdot \boldsymbol{n} = \boldsymbol{x} \cdot \boldsymbol{n}$. So

$$(\boldsymbol{x} + \lambda\boldsymbol{n}) \wedge \boldsymbol{n} \;=\; \boldsymbol{x} \wedge \boldsymbol{n} \qquad \textbf{and} \qquad (\boldsymbol{x} + \lambda\boldsymbol{n}) \cdot \boldsymbol{n} \;=\; \boldsymbol{x} \cdot \boldsymbol{n},$$

for some $\lambda \in \mathbb{R}$. Hence algebraically, the direction parallel to the null vector is the orthogonal direction at the same time.

Example 2.2 (Reflecting in $\mathbb{R}_n$):

In the vector space $\mathbb{R}^n$ a reflection of a (column) vector x in the $(n-1)$-dimensional hyperplane defined by the unit vector $\hat{\mathsf{n}}$ may be expressed in terms of a multiplication with the Householder matrix $\mathsf{H} = \mathsf{I}_n - 2\hat{\mathsf{n}}\hat{\mathsf{n}}^\mathsf{T}$, where I_n denotes the $n \times n$-identity matrix. The underlying principle is to subtract twice the parallel part $\mathsf{x}_{\|} = \hat{\mathsf{n}}\hat{\mathsf{n}}^\mathsf{T}\mathsf{x}$.

Return to the $\boldsymbol{x}$ and $\boldsymbol{n}$ in $\mathbb{R}_n$: using equation (2.17) a reflection of $\boldsymbol{x}$ in $\boldsymbol{n}$ therefore amounts to

$$\begin{aligned}\boldsymbol{x}-2\boldsymbol{x}_{\parallel} &= -(\boldsymbol{x}\cdot\boldsymbol{n})\boldsymbol{n}+(\boldsymbol{x}\wedge\boldsymbol{n})\boldsymbol{n}\\ &= -(\boldsymbol{n}\cdot\boldsymbol{x})\boldsymbol{n}-(\boldsymbol{n}\wedge\boldsymbol{x})\boldsymbol{n}\\ &= -\boldsymbol{nxn}\,,\end{aligned}$$

where the distributive law as well as the commutator properties of the inner and outer product were used. Observing that

$$\boldsymbol{nxn} \;=\; -(\boldsymbol{x}-2\boldsymbol{x}_{\parallel}) \;=\; -(\boldsymbol{x}_{\parallel}+\boldsymbol{x}_{\perp}-2\boldsymbol{x}_{\parallel}) \;=\; \boldsymbol{x}_{\parallel}-\boldsymbol{x}_{\perp} \;=\; \boldsymbol{x}-2\boldsymbol{x}_{\perp}$$

reveals that $\boldsymbol{nxn}$ corresponds to a reflection in the vector $\boldsymbol{n}$ itself.

Aside: *It should not be overlooked that the reflection, as introduced in the motivating section 1.1.3, can in effect be expressed in terms of a sandwich product.*

Under the assumption of being in a Euclidean algebra $\mathbb{R}_n$ it was previously supposed that $\boldsymbol{x}_{\parallel}=(\boldsymbol{x}\cdot\boldsymbol{n})\boldsymbol{n}$ is orthogonal to $\boldsymbol{x}_{\perp}=(\boldsymbol{x}\wedge\boldsymbol{n})\boldsymbol{n}$. It is now being verified that this holds in algebras $\mathbb{R}_{p,q}$ with mixed signature as well. It can be assumed that $\boldsymbol{n}^2=\eta$, $\eta\in\{+1,-1\}$, unless $\boldsymbol{n}$ is null (or zero). Let, as before, $\boldsymbol{x}$ and $\boldsymbol{n}$ be linearly independent. Subsequently, the orthogonality of $\boldsymbol{x}_{\parallel}$ and $\boldsymbol{x}_{\perp}$ is checked by means of the inner product.

$$\begin{aligned}\boldsymbol{x}_{\parallel}\cdot\boldsymbol{x}_{\perp} &= (\boldsymbol{x}\cdot\boldsymbol{n})\boldsymbol{n}\cdot(\boldsymbol{x}\wedge\boldsymbol{n})\boldsymbol{n}\,, \qquad\qquad \text{Let } \gamma:=(\boldsymbol{x}\cdot\boldsymbol{n})\in\mathbb{R}\\ &= \tfrac{1}{2}\Big(\gamma\boldsymbol{n}(\boldsymbol{x}\wedge\boldsymbol{n})\boldsymbol{n}+(\boldsymbol{x}\wedge\boldsymbol{n})\boldsymbol{n}\,\gamma\boldsymbol{n}\Big)\\ &= \gamma\tfrac{1}{2}\Big(\boldsymbol{n}\,\tfrac{1}{2}(\boldsymbol{xn}-\boldsymbol{nx})\boldsymbol{n}+\eta\,\tfrac{1}{2}(\boldsymbol{xn}-\boldsymbol{nx})\Big)\\ &= \frac{\gamma}{4}\Big(\boldsymbol{nx}\,\eta-\eta\,\boldsymbol{xn}+\eta\,\boldsymbol{xn}-\eta\,\boldsymbol{nx}\Big)\\ &= \frac{\gamma\eta}{4}\Big(\boldsymbol{nx}-\boldsymbol{xn}+\boldsymbol{xn}-\boldsymbol{nx}\Big)\\ &= 0\end{aligned}$$

Later on, it can be shown that $(\boldsymbol{n}\wedge\boldsymbol{x})\boldsymbol{n}$ equals $(\boldsymbol{n}\cdot\boldsymbol{x})\boldsymbol{n}$ if $\boldsymbol{n}$ is a null vector. It demonstrates that in such cases no reasonable decomposition of a vector exists and that a reflection in a null vector via $\boldsymbol{nxn}$ is not possible - the result would be linearly dependent on $\boldsymbol{n}$: $\boldsymbol{nxn}=2(\boldsymbol{n}\cdot\boldsymbol{x})\boldsymbol{n}$

2.1.3 Generalizing to higher Dimensions

Here the focus will remain on the inner and outer product. Previously, many properties of these products have been derived, mainly based on vectors. The question to be answered now is how inner and outer product have to be generalized such that more complex expressions, which comprise a couple of vectors, can be built. Clearly, this will immediately require to lay down precedence rules for the operations. In terms of the axiomatic derivation the aim is to accomplish the generalization by postulating as few as possible. So, in other words, the aim is to logically deduce the generalization from a minimal number of requirements. Necessarily, these requirements must be downwards compatible with the product properties derived in the preceding part of section 2.1. The rules for the outer product of $k > 2$ vectors, for example, must comply with the already stated rules for the outer product of only two vectors. The subsequent text gives a first clue as to the principle that might underly the generalization.

Extending the Products to three Vectors

Let a third vector $\boldsymbol{c}$ come into play. It is always allowed to split a geometric product into a commutator and anti-commutator product. Thus

$$\begin{aligned}
(\boldsymbol{a} \wedge \boldsymbol{b})\boldsymbol{c} \quad &= \quad (\boldsymbol{a} \,\underline{\times}\, \boldsymbol{b}) \,\underline{\times}\, \boldsymbol{c} \quad + \quad (\boldsymbol{a} \,\underline{\times}\, \boldsymbol{b}) \,\overline{\times}\, \boldsymbol{c} \\
&\overset{(A.2,A.3)}{=} \quad \boldsymbol{a} \,\overline{\times}\, (\boldsymbol{b} \,\overline{\times}\, \boldsymbol{c}) - (\boldsymbol{a} \,\overline{\times}\, \boldsymbol{c}) \,\overline{\times}\, \boldsymbol{b} \quad + \quad \boldsymbol{a} \,\overline{\times}\, (\boldsymbol{b} \,\underline{\times}\, \boldsymbol{c}) - (\boldsymbol{a} \,\overline{\times}\, \boldsymbol{c}) \,\underline{\times}\, \boldsymbol{b} \\
&= \quad \boldsymbol{a} \,\overline{\times}\, (\boldsymbol{b} \cdot \boldsymbol{c}) - (\boldsymbol{a} \cdot \boldsymbol{c}) \,\overline{\times}\, \boldsymbol{b} \quad + \quad \boldsymbol{a} \,\overline{\times}\, (\boldsymbol{b} \wedge \boldsymbol{c}) - (\boldsymbol{a} \cdot \boldsymbol{c}) \,\underline{\times}\, \boldsymbol{b} \\
&= \quad \underbrace{(\boldsymbol{b} \cdot \boldsymbol{c})\boldsymbol{a} - (\boldsymbol{a} \cdot \boldsymbol{c})\boldsymbol{b}}_{\in \mathbb{R}^{p,q}} \quad + \quad \underbrace{\boldsymbol{a} \,\overline{\times}\, (\boldsymbol{b} \wedge \boldsymbol{c})}_{\text{new}} - \underbrace{(\boldsymbol{a} \cdot \boldsymbol{c}) \,\underline{\times}\, \boldsymbol{b}}_{0} \,.
\end{aligned}$$

The new element $\boldsymbol{a} \,\overline{\times}\, (\boldsymbol{b} \wedge \boldsymbol{c})$ is obviously a 3-vector. This follows from linearity and the coordinate representation of the vectors. Each component $\mathbf{e}_i \,\overline{\times}\, (\mathbf{e}_k \wedge \mathbf{e}_l)$ of $\boldsymbol{a} \,\overline{\times}\, (\boldsymbol{b} \wedge \boldsymbol{c})$ vanishes unless the three indices i, j and k are mutually different[6]. Due to the constructive character of the outer product it is reasonable to define

$$(\boldsymbol{a} \wedge \boldsymbol{b}) \wedge \boldsymbol{c} \;:=\; (\boldsymbol{a} \wedge \boldsymbol{b}) \,\overline{\times}\, \boldsymbol{c} \,, \qquad \boldsymbol{a}, \boldsymbol{b}, \boldsymbol{c} \in \mathbb{R}^{p,q} \,, \tag{2.19}$$

and conversely $\boldsymbol{c} \wedge (\boldsymbol{a} \wedge \boldsymbol{b}) \;:=\; \boldsymbol{c} \,\overline{\times}\, (\boldsymbol{a} \wedge \boldsymbol{b})$. Consequently, the outer product is associative

$$(\boldsymbol{a} \wedge \boldsymbol{b}) \wedge \boldsymbol{c} = (\boldsymbol{a} \,\underline{\times}\, \boldsymbol{b}) \,\overline{\times}\, \boldsymbol{c} \overset{(A.3)}{=} \boldsymbol{a} \,\overline{\times}\, (\boldsymbol{b} \,\underline{\times}\, \boldsymbol{c}) = \boldsymbol{a} \wedge (\boldsymbol{b} \wedge \boldsymbol{c}) \,, \tag{2.20}$$

for vectors $\boldsymbol{a}, \boldsymbol{b}, \boldsymbol{c} \in \mathbb{R}^{p,q}$ and the brackets may be discarded. The definition of the inner product may also be extended to the case of three vectors. The choice

$$(\boldsymbol{a} \wedge \boldsymbol{b}) \cdot \boldsymbol{c} \;:=\; (\boldsymbol{a} \wedge \boldsymbol{b}) \,\underline{\times}\, \boldsymbol{c} \tag{2.21}$$

is sensible for the inner product not only because the inner product is considered the counterpart of the outer product but also due to the grade decreasing property of equation (2.21) - recall that the result of $(\boldsymbol{a} \wedge \boldsymbol{b}) \,\underline{\times}\, \boldsymbol{c}$ is vector valued.

Note that if not otherwise indicated by brackets, then the geometric product takes precedence over inner and outer product (and the commutators products). The predominance among inner and outer product is basically arbitrary but in case of

[6]This reflects the action of the *Levi-Civita tensor* ϵ_{ikl}, i.e. $\mathbf{e}_i \,\overline{\times}\, (\mathbf{e}_k \wedge \mathbf{e}_l) = \epsilon_{ikl}\, \mathbf{e}_i \mathbf{e}_k \mathbf{e}_l$.

doubt, i.e. in the absence of brackets, the inner product is assumed to bind stronger than the outer product. The order of evaluation is

$$\begin{array}{c}\text{Geometric}\\\text{Product}\end{array} \quad \text{before} \quad \begin{array}{c}\text{Inner}\\\text{Product}\end{array} \quad \text{before} \quad \begin{array}{c}\text{Outer}\\\text{Product}\,.\end{array}$$

In conclusion, inner and outer product were generalized such that mixed expressions of the form $(\boldsymbol{a}\wedge\boldsymbol{b})\wedge\boldsymbol{c}$ or $(\boldsymbol{a}\wedge\boldsymbol{b})\cdot\boldsymbol{c}$ can be dealt with. Accordingly, equation (2.10) $\boldsymbol{ab} = \boldsymbol{a}\cdot\boldsymbol{b} + \boldsymbol{a}\wedge\boldsymbol{b}$ can be extended to

$$(\boldsymbol{a}\wedge\boldsymbol{b})\boldsymbol{c} \;=\; (\boldsymbol{a}\wedge\boldsymbol{b})\wedge\boldsymbol{c} \;+\; (\boldsymbol{a}\wedge\boldsymbol{b})\cdot\boldsymbol{c}\,.$$

For the coming section it should be remembered that equation (2.3) defines the κ-vector $\boldsymbol{A}_{[k]}$ - a linear combination of basis blades of grade k. Shortly a special version of a κ-vector, the so-called blade will be introduced. A blade of grade k ('k-blade') denotes a κ-vector of equal grade and has an outer product representation in terms of k vectors. However, blades are strongly related to one of the key results that is to be derived in the following

$$\boldsymbol{a}\boldsymbol{A}_{[r]} \;=\; \boldsymbol{a}\cdot\boldsymbol{A}_{[r]} \;+\; \boldsymbol{a}\wedge\boldsymbol{A}_{[r]}\,. \tag{2.22}$$

This is the analogue of the famous equation (2.10)[7]. Next, the first part $\boldsymbol{a}\cdot\boldsymbol{A}_{[r]}$ will be examined on the basis of $\boldsymbol{a}\cdot\boldsymbol{b} = \boldsymbol{a}\barwedge\boldsymbol{b}$.

Extension to κ-Vectors

The aim is now to derive inner and outer product of a vector with a κ-vector. For this purpose the multiple geometric product $\boldsymbol{b}\,\boldsymbol{a}_1\boldsymbol{a}_2\ldots\boldsymbol{a}_k$ is to be expanded by means of the repeated application of the identity $\boldsymbol{ba} = 2(\boldsymbol{a}\cdot\boldsymbol{b}) - \boldsymbol{ab}$ from equation (2.8). The trick is that the first term $2(\boldsymbol{a}\cdot\boldsymbol{b})$ may always be factored out as it is scalar valued. Let $\boldsymbol{a}_1\boldsymbol{a}_2\ldots\check{\boldsymbol{a}}_i\ldots\boldsymbol{a}_k$ denote the term $\boldsymbol{a}_1\boldsymbol{a}_2\ldots\boldsymbol{a}_{i-1}\boldsymbol{a}_{i+1}\ldots\boldsymbol{a}_k$ that $\boldsymbol{a}_i$ was removed from then

$$\begin{aligned}
\boldsymbol{b}\,\boldsymbol{a}_1\boldsymbol{a}_2\ldots\boldsymbol{a}_k &= \Big(2(\boldsymbol{a}_1\cdot\boldsymbol{b}) - \boldsymbol{a}_1\boldsymbol{b}\Big)\boldsymbol{a}_2\ldots\boldsymbol{a}_k\\
&= 2(\boldsymbol{a}_1\cdot\boldsymbol{b})\boldsymbol{a}_2\ldots\boldsymbol{a}_k \;-\; \boldsymbol{a}_1\boldsymbol{b}\,\boldsymbol{a}_2\ldots\boldsymbol{a}_k\\
&= 2\sum_{i=1}^{k}(-1)^{i-1}\,(\boldsymbol{a}_i\cdot\boldsymbol{b})\,\boldsymbol{a}_1\boldsymbol{a}_2\ldots\check{\boldsymbol{a}}_i\ldots\boldsymbol{a}_k\\
&\quad +\; (-1)^k\,\boldsymbol{a}_1\boldsymbol{a}_2\ldots\boldsymbol{a}_k\boldsymbol{b}\,.
\end{aligned}$$

The expansion in particular holds for basis blades of grade k, but then, by linearity, also for κ-vectors. For a basis blade $\mathbf{e}_{\mathbb{u}} = \mathbf{e}_{j_1}\mathbf{e}_{j_2}\ldots\mathbf{e}_{j_k}$ it may be written

$$\tfrac{1}{2}\Big(\boldsymbol{b}\mathbf{e}_{\mathbb{u}} - (-1)^k\mathbf{e}_{\mathbb{u}}\boldsymbol{b}\Big) = \sum_{i=1}^{k}(-1)^{i-1}\,(\mathbf{e}_{j_i}\cdot\boldsymbol{b})\,\mathbf{e}_{\mathbb{u}\setminus j_i}\,.$$

[7] The equation only holds if at least one operand represents a vector.

Hence the operation has decreased the grade of $\mathbf{e}_{\mathbb{u}}$ by one such that the resulting κ-vector is of grade $k-1$. Since it is the inner product that is supposed to have such a characteristic and since the expansion is also compliant with the inner product for the cases $k = 1$ (vector) and $k = 2$ (bivector), one is free to define

$$\boldsymbol{a} \cdot \boldsymbol{A}_{[k]} \;:=\; \tfrac{1}{2}\Big(\boldsymbol{a}\boldsymbol{A}_{[k]} \;-\; (-1)^k \boldsymbol{A}_{[k]}\boldsymbol{a}\Big)\,. \tag{2.23}$$

By symmetry considerations this would suggest to use the remaining part $\boldsymbol{a}\boldsymbol{A}_{[k]} - \boldsymbol{a}\cdot\boldsymbol{A}_{[k]}$ of the geometric product for the counterpart of the inner product - the outer product. Indeed, it will be shown in the following section that

$$\boldsymbol{a} \wedge \boldsymbol{A}_{[k]} \;:=\; \tfrac{1}{2}\Big(\boldsymbol{a}\boldsymbol{A}_{[k]} \;+\; (-1)^k \boldsymbol{A}_{[k]}\boldsymbol{a}\Big)\,. \tag{2.24}$$

The summary of the previous two equations reads

k even	k odd
$\boldsymbol{A}_{[k]} \underline{\times} \boldsymbol{a} = \boldsymbol{A}_{[k]} \cdot \boldsymbol{a}$	$\boldsymbol{A}_{[k]} \overline{\times} \boldsymbol{a} = \boldsymbol{A}_{[k]} \cdot \boldsymbol{a}$
$\boldsymbol{A}_{[k]} \overline{\times} \boldsymbol{a} = \boldsymbol{A}_{[k]} \wedge \boldsymbol{a}$	$\boldsymbol{A}_{[k]} \underline{\times} \boldsymbol{a} = \boldsymbol{A}_{[k]} \wedge \boldsymbol{a}.$

Generalization of the Outer Product

There is a multiplicity of interesting properties that are known so far about the outer product $\boldsymbol{a} \wedge \boldsymbol{b}$. It is bilinear and anti-symmetric because of its commutator definition, it represents a linear subspace, the coefficients of the components are determinants, it is invariant under orthogonal transformations, it is metric independent, it coincides with the geometric product in case of orthogonal vectors and an oriented area may be associated with it. From $\boldsymbol{a} \wedge \boldsymbol{b} \wedge \boldsymbol{c}$ it has additionally been deduced that the outer product must be associative. Clearly, in the end the generalization is a matter of definition, but if the preceding properties are changed into requirements, it is easy to verify that two particular of them would imply the remaining ones. The minimal requisites for the generalization of the outer product are

- Multilinearity
- Associativity

As a result, the outer product is *alternating*, that is the outer product of vectors takes on zero if at least two vectors are equal. Say, the vector $\boldsymbol{x}$ appears twice in an outer product

$$\ldots \wedge \boldsymbol{x} \wedge \boldsymbol{a}_r \wedge \boldsymbol{a}_{r+1} \wedge \ldots \wedge \boldsymbol{a}_{r+s} \wedge \boldsymbol{x} \wedge \ldots\,.$$

Due to associativity it is

$$\boldsymbol{x} \wedge \boldsymbol{a}_r \wedge \boldsymbol{a}_{r+1} = (\boldsymbol{x} \wedge \boldsymbol{a}_r) \wedge \boldsymbol{a}_{r+1} = (-\,\boldsymbol{a}_r \wedge \boldsymbol{x}) \wedge \boldsymbol{a}_{r+1} = -\boldsymbol{a}_r \wedge \boldsymbol{x} \wedge \boldsymbol{a}_{r+1}\,,$$

whence

$$\begin{aligned}
& \ldots \wedge \boldsymbol{x} \wedge \boldsymbol{a}_r \wedge \boldsymbol{a}_{r+1} \wedge \ldots \wedge \boldsymbol{a}_{r+s} \wedge \boldsymbol{x} \wedge \ldots \\
= \; & (-1)^{s+1} \ldots \boldsymbol{a}_r \wedge \boldsymbol{a}_{r+1} \wedge \ldots \wedge \boldsymbol{a}_{r+s} \wedge (\boldsymbol{x} \wedge \boldsymbol{x}) \wedge \ldots \\
= \; & 0 \,.
\end{aligned}$$

Bear in mind that the *outer product of linearly dependent vectors is zero* as well. This is not difficult to see: simply replace one vector by its respective linear combination of the remaining vectors. Then, by the distributivity of the outer product, every summand of the expansion attains zero.

A further implication is the *total anti-symmetry* of the outer product: exchanging two vectors in an outer product will introduce a minus sign. Consider, as an example, an arbitrary but multilinear and alternating function f, the image of which not necessarily has to be scalar valued. Without loss of generality it is

$$\begin{aligned}
f(a+b, a+b, \ldots) &= 0 \\
&= f(a, a, \ldots) + f(a, b, \ldots) + f(b, a, \ldots) + f(b, b, \ldots) \\
&= f(a, b, \ldots) + f(b, a, \ldots) \,,
\end{aligned}$$

thus $f(a, b, \ldots) = -f(b, a, \ldots)$. Note that anti-symmetry likewise implies associativity. In the above generalization the requisites multilinearity and associativity can equally be replaced with multilinearity and total anti-symmetry.

In the following it is being examined whether the requirements multilinearity and associativity lead to a unique definition for the outer product. This time, let $\boldsymbol{f}$ denote a candidate function for the outer product of k vectors $\boldsymbol{a}_1, \boldsymbol{a}_2, \ldots, \boldsymbol{a}_k$. The vectors have a coordinate representation $\boldsymbol{a}_r = \mathsf{A}^{i_r}{}_r \mathbf{e}_{i_r}$, $1 \leq i_r \leq n$, $\;1 \leq r \leq k$, where the *Einstein summation convention* is made use of, see page 256. Besides, $\mathsf{A} \in \mathbb{R}^{n \times k}$ symbolizes the coefficient matrix for the linear combinations of all vectors $\boldsymbol{a}_r$. Now equation (2.26) below is being elucidated. First, the summation over the $\mathbf{e}_i$ can be factored out by the multilinearity of $\boldsymbol{f}$. Notice that the summation in the second row is taken over all n^k combinations of indices i_1, i_2, …, i_k. Clearly, $\boldsymbol{f}(\mathbf{e}_{i_1}, \mathbf{e}_{i_2}, \ldots, \mathbf{e}_{i_k})$ attains zero whenever at least two indices are equal. The respective summands can be discarded, and the summation can be reformulated with the help of the set of k-tuples

$$I_{k/n} := \{(v_1, v_2, \ldots, v_k) \mid 1 \leq v_1 < v_2 < \ldots < v_k \leq n\} \,, \quad |I_{k/n}| = \binom{n}{k} \,. \tag{2.25}$$

Accordingly, for each combination of pairwise different indices v provided from $I_{k/n}$, the inner sum in the third row is intended to be taken over all $k!$ permutations of the indices in v. The term $\mathcal{S}(k)$ denotes the space of all permutations of indices $\{1, 2, \ldots, k\}$. In order to avoid double subscripts, the i^{th} element v_i of v is symbolized by $\mathsf{v}(i)$. Because of the alternating property of $\boldsymbol{f}$ it must be that $\boldsymbol{f}(\mathbf{e}_{\mathsf{v}(\sigma(1))}, \mathbf{e}_{\mathsf{v}(\sigma(2))}, \ldots, \mathbf{e}_{\mathsf{v}(\sigma(k))})$ equals $\operatorname{sgn}(\sigma)\; \boldsymbol{f}(\mathbf{e}_{\mathsf{v}(1)}, \mathbf{e}_{\mathsf{v}(2)}, \ldots, \mathbf{e}_{\mathsf{v}(k)})$, where

$$\operatorname{sgn}(\sigma) \;:=\; \begin{cases} +1, & \sigma \text{ is an even permutation of } \{1, 2, \ldots, k\} \\ -1, & \sigma \text{ is an odd permutation of } \{1, 2, \ldots, k\} \,. \end{cases}$$

This leads to the fourth row of equation (2.26). As the arguments of $\boldsymbol{f}$ do not depend any more on σ, $\boldsymbol{f}$ is factored out. Let $A|_{\mathsf{v}}$ denote the matrix A restricted to the rows given in the tuple/vector v. Thus $A|_{\mathsf{v}}$ is a quadratic $k \times k$ matrix. Observe now that the inner sum in the fifth row is nothing but the *Leibniz formula* for determinants. Using the expression $\det(\mathsf{A}|_{\mathsf{v}})$ finally yields equation (2.26).

$$
\begin{aligned}
\boldsymbol{f}(\boldsymbol{a}_1, \boldsymbol{a}_2, \ldots, \boldsymbol{a}_k) \;&=\; \boldsymbol{f}(\mathsf{A}^{i_1}{}_1\mathbf{e}_{i_1}, \mathsf{A}^{i_2}{}_2\mathbf{e}_{i_2}, \ldots, \mathsf{A}^{i_k}{}_k\mathbf{e}_{i_k})\,, \qquad 1 \le i \le n \\
&= \mathsf{A}^{i_1}{}_1\mathsf{A}^{i_2}{}_2 \ldots \mathsf{A}^{i_k}{}_k \;\; \boldsymbol{f}(\mathbf{e}_{i_1}, \mathbf{e}_{i_2}, \ldots, \mathbf{e}_{i_k}) \\
&= \sum_{\mathsf{v}\in I_{k/n}} \sum_{\sigma\in\mathcal{S}(k)} \mathsf{A}_{\mathsf{v}(\sigma(1)),1}\mathsf{A}_{\mathsf{v}(\sigma(2)),2} \ldots \mathsf{A}_{\mathsf{v}(\sigma(k)),k}\; \boldsymbol{f}(\mathbf{e}_{\mathsf{v}(\sigma(1))}, \mathbf{e}_{\mathsf{v}(\sigma(2))}, \ldots, \mathbf{e}_{\mathsf{v}(\sigma(k))}) \\
&= \sum_{\mathsf{v}\in I_{k/n}} \sum_{\sigma\in\mathcal{S}(k)} \prod_{j=1}^{k} \mathsf{A}_{\mathsf{v}(\sigma(j)),j} \;\; \operatorname{sgn}(\sigma)\, \boldsymbol{f}(\mathbf{e}_{\mathsf{v}(1)}, \mathbf{e}_{\mathsf{v}(2)}, \ldots, \mathbf{e}_{\mathsf{v}(k)}) \\
&= \sum_{\mathsf{v}\in I_{k/n}} \boldsymbol{f}(\mathbf{e}_{\mathsf{v}(1)}, \mathbf{e}_{\mathsf{v}(2)}, \ldots, \mathbf{e}_{\mathsf{v}(k)}) \sum_{\sigma\in\mathcal{S}(k)} \operatorname{sgn}(\sigma) \prod_{j=1}^{k} \mathsf{A}_{\mathsf{v}(\sigma(j)),j} \\
&= \sum_{\mathsf{v}\in I_{k/n}} \det(\mathsf{A}|_{\mathsf{v}})\; \boldsymbol{f}(\mathbf{e}_{\mathsf{v}(1)}, \mathbf{e}_{\mathsf{v}(2)}, \ldots, \mathbf{e}_{\mathsf{v}(k)})
\end{aligned}
\tag{2.26}
$$

Before it can be continued it is necessary to think about $\boldsymbol{f}$'s structure. It is worth mentioning that the outer product of geometric algebra is multilinear with respect to the algebra product, but it must be taken into account that the geometric product is not commutative. It can therefore be inferred that the most general form $\boldsymbol{f}$ may take on is

$$
\boldsymbol{f}(\boldsymbol{a}_1, \boldsymbol{a}_2, \ldots, \boldsymbol{a}_k) \;=\; \sum_{\sigma\in\mathcal{S}(k)} \theta_\sigma\, \boldsymbol{a}_{\sigma(1)}\boldsymbol{a}_{\sigma(2)} \ldots \boldsymbol{a}_{\sigma(k)}\,, \qquad \theta_\sigma \in \mathbb{R}\,. \tag{2.27}
$$

Each summand has to include all vectors; an expression $\boldsymbol{f}(\boldsymbol{a}, \boldsymbol{b}) = \boldsymbol{ab} + \boldsymbol{a}$, for example, would not be linear in $\boldsymbol{b}$ any more, compare $\boldsymbol{f}(\boldsymbol{a}, \beta\boldsymbol{b}) = \beta\boldsymbol{ab} + \boldsymbol{a}$ with $\beta\boldsymbol{f}(\boldsymbol{a}, \boldsymbol{b}) = \beta\boldsymbol{ab} + \beta\boldsymbol{a}$ for some scalar $\beta \in \mathbb{R}$.

Besides, the alternating property of $\boldsymbol{f}$ can be exploited to analyze the coefficients θ_σ. This is done in section A.3.2: using equation (A.14) equation (2.27) may be reformulated as

$$
\boldsymbol{f}(\boldsymbol{a}_1, \boldsymbol{a}_2, \ldots, \boldsymbol{a}_k) \;=\; c \sum_{\sigma\in\mathcal{S}(k)} \operatorname{sgn}(\sigma)\, \boldsymbol{a}_{\sigma(1)}\boldsymbol{a}_{\sigma(2)} \ldots \boldsymbol{a}_{\sigma(k)}\,, \qquad c > 0\,. \tag{2.28}
$$

In carrying over the previous result to the case $\boldsymbol{f}(\mathbf{e}_{\mathsf{v}(1)}, \mathbf{e}_{\mathsf{v}(2)}, \ldots, \mathbf{e}_{\mathsf{v}(k)})$ one obtains

$$\begin{aligned}
\boldsymbol{f}(\mathbf{e}_{\mathsf{v}(1)}, \mathbf{e}_{\mathsf{v}(2)}, \ldots, \mathbf{e}_{\mathsf{v}(k)}) &= c \sum_{\sigma \in \mathcal{S}(k)} \operatorname{sgn}(\sigma)\, \mathbf{e}_{\mathsf{v}(\sigma(1))} \mathbf{e}_{\mathsf{v}(\sigma(2))} \ldots \mathbf{e}_{\mathsf{v}(\sigma(k))} \\
&= c \sum_{\sigma \in \mathcal{S}(k)} \operatorname{sgn}(\sigma) \Big(\operatorname{sgn}(\sigma)\, \mathbf{e}_{\mathsf{v}(1)} \mathbf{e}_{\mathsf{v}(2)} \ldots \mathbf{e}_{\mathsf{v}(k)} \Big) \\
&= \left(c \sum_{\sigma \in \mathcal{S}(k)} \operatorname{sgn}(\sigma)^2 \right) \mathbf{e}_{\mathsf{v}(1)} \mathbf{e}_{\mathsf{v}(2)} \ldots \mathbf{e}_{\mathsf{v}(k)} \\
&= \big(c\, k! \big)\, \mathbf{e}_{\mathsf{v}(1)} \mathbf{e}_{\mathsf{v}(2)} \ldots \mathbf{e}_{\mathsf{v}(k)}\,, \quad c > 0\,.
\end{aligned} \tag{2.29}$$

Notice that $\mathbf{e}_{\mathsf{v}(1)} \mathbf{e}_{\mathsf{v}(2)} \ldots \mathbf{e}_{\mathsf{v}(k)}$ represents an ordered basis blade due to the definition (2.25) of v. The expression for $\boldsymbol{f}$ ultimately becomes

$$\boldsymbol{f}(\boldsymbol{a}_1, \boldsymbol{a}_2, \ldots, \boldsymbol{a}_k) = \big(c\, k! \big) \sum_{\mathsf{v} \in I_{k/n}} \det(\mathsf{A}|_{\mathsf{v}})\, \mathbf{e}_{\mathsf{v}(1)} \mathbf{e}_{\mathsf{v}(2)} \ldots \mathbf{e}_{\mathsf{v}(k)}\,, \quad c > 0\,.$$

Consequently, the outer product is uniquely defined up to a positive constant $c \in \mathbb{R}$. Regarding the outer product of basis vectors in equation (2.29) it is sensible to set the factor c to $c := 1/k!$. The function $\boldsymbol{f}$ can now be replaced with the fully determined outer product, symbolized by $\bigwedge$. Let

$$\bigwedge(\boldsymbol{a}_1, \boldsymbol{a}_2, \ldots, \boldsymbol{a}_k) := \boldsymbol{a}_1 \wedge \boldsymbol{a}_2 \wedge \ldots \wedge \boldsymbol{a}_k =: \bigwedge_{j=1}^{k} \boldsymbol{a}_j\,.$$

Then the **definitions for the outer product** of k vectors $\boldsymbol{a}_1$, $\boldsymbol{a}_2$, …, $\boldsymbol{a}_k$ are

$$\bigwedge(\boldsymbol{a}_1, \boldsymbol{a}_2, \ldots, \boldsymbol{a}_k) := \frac{1}{k!} \sum_{\sigma \in \mathcal{S}(k)} \operatorname{sgn}(\sigma)\, \boldsymbol{a}_{\sigma(1)} \boldsymbol{a}_{\sigma(2)} \ldots \boldsymbol{a}_{\sigma(k)} \tag{2.30}$$

and

$$\bigwedge(\boldsymbol{a}_1, \boldsymbol{a}_2, \ldots, \boldsymbol{a}_k) := \sum_{\mathsf{v} \in I_{k/n}} \det(\mathsf{A}|_{\mathsf{v}})\, \mathbf{e}_{\mathsf{v}(1)} \mathbf{e}_{\mathsf{v}(2)} \ldots \mathbf{e}_{\mathsf{v}(k)}\,, \tag{2.31}$$

with

$$I_{k/n} := \{ (v_1, v_2, \ldots, v_k) \mid 1 \le v_1 < v_2 < \ldots < v_k \le n \}\,.$$

Note that the application of equation (2.30) to the outer product of mutually different basis vectors, say $\mathbf{e}_{i_1} \wedge \mathbf{e}_{i_2} \wedge \ldots \wedge \mathbf{e}_{i_r}$, in conjunction with the rule $\mathbf{e}_i \mathbf{e}_j = -\mathbf{e}_j \mathbf{e}_i$, $i \neq j$, immediately yields

$$\mathbf{e}_{i_1} \wedge \mathbf{e}_{i_2} \wedge \ldots \wedge \mathbf{e}_{i_r} = \mathbf{e}_{i_1} \mathbf{e}_{i_2} \ldots \mathbf{e}_{i_r}\,. \tag{2.32}$$

Besides, by means of the associativity of the outer product it is

$$\begin{aligned}
&(\mathbf{e}_{i_1} \mathbf{e}_{i_2} \ldots \mathbf{e}_{i_r}) \wedge (\mathbf{e}_{j_1} \mathbf{e}_{j_2} \ldots \mathbf{e}_{j_s}) &= \\
&\qquad (\mathbf{e}_{i_1} \wedge \mathbf{e}_{i_2} \wedge \ldots \wedge \mathbf{e}_{i_r}) \wedge (\mathbf{e}_{j_1} \wedge \mathbf{e}_{j_2} \wedge \ldots \wedge \mathbf{e}_{j_s}) &= \\
&\qquad \mathbf{e}_{i_1} \wedge \mathbf{e}_{i_2} \wedge \ldots \wedge \mathbf{e}_{i_r} \wedge \mathbf{e}_{j_1} \wedge \mathbf{e}_{j_2} \wedge \ldots \wedge \mathbf{e}_{j_s} &= \\
&\qquad \mathbf{e}_{i_1} \mathbf{e}_{i_2} \ldots \mathbf{e}_{i_r} \mathbf{e}_{j_1} \mathbf{e}_{j_2} \ldots \mathbf{e}_{j_s}\,,
\end{aligned}$$

if all basis vectors are pairwise different. It can therefore be inferred that whenever the index sets $\mathbb{u}$ and $\mathbb{v}$ of two basis blades $\mathbf{e}_{\mathbb{u}}$ and $\mathbf{e}_{\mathbb{v}}$ are disjoint, geometric product $\mathbf{e}_{\mathbb{u}}\mathbf{e}_{\mathbb{v}}$ and outer product $\mathbf{e}_{\mathbb{u}} \wedge \mathbf{e}_{\mathbb{v}}$ are the same. Otherwise, say $\mathbf{e}_{\mathbb{u}}$ and $\mathbf{e}_{\mathbb{v}}$ share at least one common basis vector, the total anti-symmetry, cf. equation (2.30), will force the outer product to vanish. Hence,

$$\mathbf{e}_{\mathbb{u}} \wedge \mathbf{e}_{\mathbb{v}} := \begin{cases} \mathbf{e}_{\mathbb{u}}\mathbf{e}_{\mathbb{v}}, & \mathbb{u} \cap \mathbb{v} = \emptyset \\ 0, & \text{else} \end{cases} \tag{2.33}$$

A further and quite useful representation for the outer product is its commutator representation

$$\bigwedge_{j=1}^{k} \boldsymbol{a}_j = \begin{cases} (...((\boldsymbol{a}_1 \mathbin{\underline{\times}} \boldsymbol{a}_2) \mathbin{\overline{\times}} \boldsymbol{a}_3) \mathbin{\underline{\times}} \;\ldots\; \mathbin{\overline{\times}} \boldsymbol{a}_{k-1}) \mathbin{\underline{\times}} \boldsymbol{a}_k, & k \text{ even} \\ (...((\boldsymbol{a}_1 \mathbin{\underline{\times}} \boldsymbol{a}_2) \mathbin{\overline{\times}} \boldsymbol{a}_3) \mathbin{\underline{\times}} \;\ldots\; \mathbin{\underline{\times}} \boldsymbol{a}_{k-1}) \mathbin{\overline{\times}} \boldsymbol{a}_k, & k \text{ odd,} \end{cases} \tag{2.34}$$

where commutator and anti-commutator alternate with each other. These commutator expressions comply with the respective expressions found for $\boldsymbol{a}_1 \wedge \boldsymbol{a}_2$ and $\boldsymbol{a}_1 \wedge \boldsymbol{a}_2 \wedge \boldsymbol{a}_3$. In order to be reckoned a general expression for the outer product, equation (2.34) must be multilinear and anti-symmetric. Solely the latter condition is being checked next as commutator products are known to be linear. Consider the i^{th} position in equation (2.34) - if i is even, it may be written

$$(((\underbrace{\boldsymbol{a}_1 \wedge \boldsymbol{a}_2 \wedge \ldots \wedge \boldsymbol{a}_{i-1})}_{\boldsymbol{A}} \mathbin{\underline{\times}} \underbrace{\boldsymbol{a}_i}_{\boldsymbol{b}}) \mathbin{\overline{\times}} \underbrace{\boldsymbol{a}_{i+1}}_{\boldsymbol{c}}) \wedge \underbrace{\boldsymbol{a}_{i+2} \wedge \ldots \wedge \boldsymbol{a}_k}_{\boldsymbol{D}} .$$

For simplicity, the commutator expressions of $\boldsymbol{A}$ and $\boldsymbol{D}$ were changed back into the respective wedge expressions. The $\boldsymbol{D}$-term may be discarded. Then the situation is as follows

$$(\boldsymbol{A} \mathbin{\underline{\times}} \boldsymbol{b}) \mathbin{\overline{\times}} \boldsymbol{c} \qquad \text{must be} \qquad -(\boldsymbol{A} \mathbin{\underline{\times}} \boldsymbol{c}) \mathbin{\overline{\times}} \boldsymbol{b} .$$

The equality can easily be verified with the help of equation (A.4), in which the term $\boldsymbol{A} \mathbin{\underline{\times}} (\boldsymbol{b} \mathbin{\overline{\times}} \boldsymbol{c})$ attains zero. If i is odd, equation (A.5) applies.

The commutator representation (2.34) can be further expanded by means of equation (A.11), page 244. It must be given special importance to that equation as it gets along with only 2^k summands to evaluate the outer product of k vectors whereas equation (2.30) requires $k!$ summands to eventually do the same thing.

Note that by distributivity over the basis blades, equation (2.34) is the sought substantiation of equation (2.24).

In conclusion, three different representations of the outer product have been derived merely from the requisites multilinearity and associativity. The next section includes an introduction to blades - the probably most important concept of geometric algebra - although a blade is simply an outer product of vectors, i.e. what has been dealt with before. It follows a discussion on calculation rules and other extended concepts of geometric algebra.

2.2 Basic Concepts of GA

This section is more formal than the preceding one. It is dominated by the term 'blade' because this class of multivectors has meaningful properties. Accordingly, several calculation rules for manipulating expressions that involve blades are given. The section starts with the introduction of an important tool - the grade-projection operator. Besides, some elementary identities regarding basis blades are given.

At first it is caught up on some simple identities that rely on the definition of the geometric product of basis vectors, cf. equation (2.13).

Proposition 2.1
Given a basis vector $\mathbf{e}_i$, $i \in \mathcal{N}$, *and a basis blade* $\mathbf{e}_{\mathbb{u}}$, $\mathbb{u} \subseteq \mathcal{N}$, *then*

$$\mathbf{e}_i \mathbf{e}_{\mathbb{u}} \;=\; (-1)^{|\mathbb{u}| - \mathbf{1}_{\mathbb{u}}(i)} \, \mathbf{e}_{\mathbb{u}} \mathbf{e}_i \,,$$

where $\mathbf{1}_{\mathbb{u}}(i)$ *denotes the characteristic/indicator function*[8] *of the set* $\mathbb{u}$.

The proof of the proposition is left out as it follows directly from the properties of the geometric product. As an example, consider $\boldsymbol{a} = \mathbf{e}_2$ and $\boldsymbol{b} = \mathbf{e}_1 \mathbf{e}_2$. It is

$$\boldsymbol{ab} \;=\; \mathbf{e}_2\, \mathbf{e}_1 \mathbf{e}_2 \;=\; -\mathbf{e}_1 \mathbf{e}_2\, \mathbf{e}_2 \;=\; -\boldsymbol{ba} \,.$$

The repeated application of proposition 2.1 to each of the basis vectors of a basis blade $\mathbf{e}_{\mathbb{u}}$ shows whether $\mathbf{e}_{\mathbb{u}}$ and $\mathbf{e}_{\mathbb{v}}$ commute or not

$$\mathbf{e}_{\mathbb{u}} \mathbf{e}_{\mathbb{v}} \;=\; (-1)^{|\mathbb{u}|\,|\mathbb{v}| - |\mathbb{u} \cap \mathbb{v}|} \, \mathbf{e}_{\mathbb{v}} \mathbf{e}_{\mathbb{u}} \,. \tag{2.35}$$

Corollary 2.1
Let $\mathbf{e}_{\mathbb{u}}$ *and* $\mathbf{e}_{\mathbb{v}}$ *be two basis blades. Then the outer product satisfies*

$$\mathbf{e}_{\mathbb{u}} \wedge \mathbf{e}_{\mathbb{v}} \;=\; (-1)^{|\mathbb{u}|\,|\mathbb{v}|} \, \mathbf{e}_{\mathbb{v}} \wedge \mathbf{e}_{\mathbb{u}} \,.$$

Similarly, for two κ*-vectors* $\boldsymbol{A}_{[k]}$ *and* $\boldsymbol{B}_{[l]}$ *is follows from the linearity of the outer product*

$$\boldsymbol{A}_{[k]} \wedge \boldsymbol{B}_{[l]} \;=\; (-1)^{k\,l} \, \boldsymbol{B}_{[l]} \wedge \boldsymbol{A}_{[k]} \,.$$

Proof: *According to equation (2.33), it is required that* $\mathbb{u} \cap \mathbb{v} = \emptyset$ *in order to have that* $\mathbf{e}_{\mathbb{u}} \wedge \mathbf{e}_{\mathbb{v}}$ *is non-zero. But then it is* $\mathbf{e}_{\mathbb{u}} \wedge \mathbf{e}_{\mathbb{v}} = \mathbf{e}_{\mathbb{u}} \mathbf{e}_{\mathbb{v}}$ *so that equation (2.35) applies:* $\mathbf{e}_{\mathbb{u}} \wedge \mathbf{e}_{\mathbb{v}} = (-1)^{|\mathbb{u}|\,|\mathbb{v}|} \, \mathbf{e}_{\mathbb{v}} \mathbf{e}_{\mathbb{u}}$ *and after all* $\mathbf{e}_{\mathbb{u}} \wedge \mathbf{e}_{\mathbb{v}} = (-1)^{|\mathbb{u}|\,|\mathbb{v}|} \, \mathbf{e}_{\mathbb{v}} \wedge \mathbf{e}_{\mathbb{u}}$. ∎

The next proposition is about the grade of a product of two basis blades.

[8] The indicator function of a set $\mathbb{A} \subseteq \mathbb{Z}$ is defined as

$$\mathbf{1}_{\mathbb{A}}(x \in \mathbb{Z}) \;=\; \begin{cases} 1 & \text{if } x \in \mathbb{A} \\ 0 & \text{if } x \notin \mathbb{A}. \end{cases}$$

Proposition 2.2
Let $\mathbf{e}_{\mathbb{u}}, \mathbf{e}_{\mathbb{v}} \in \mathbb{R}_{p,q}$. *Then the geometric product* $\mathbf{e}_{\mathbb{u}}\mathbf{e}_{\mathbb{v}}$ *yields a signed basis blade* $\pm\mathbf{e}_{\mathbb{w}}$ *with*

$$\mathbb{w} \;=\; (\mathbb{u} \cup \mathbb{v}) \backslash (\mathbb{u} \cap \mathbb{v}) \,.$$

The sign of $\mathbf{e}_{\mathbb{w}}$ *depends on the signature of the algebra and especially on the specific basis blades* $\mathbf{e}_{\mathbb{u}}$ *and* $\mathbf{e}_{\mathbb{v}}$. *The grade of* $\mathbf{e}_{\mathbb{w}}$ *can be determined via*

$$|\mathbb{w}| \;=\; |\mathbb{u}| + |\mathbb{v}| - 2|\mathbb{u} \cap \mathbb{v}| \,.$$

Proof: *Basis vectors that are shared by both basis blades will cancel out by squaring to* ± 1. *This explains the first identity.*
One has $(\mathbb{u} \cup \mathbb{v}) \backslash (\mathbb{u} \cap \mathbb{v}) = (\mathbb{u} \backslash \mathbb{v}) \cup (\mathbb{v} \backslash \mathbb{u}) = (\mathbb{u} \backslash (\mathbb{u} \cap \mathbb{v})) \cup (\mathbb{v} \backslash (\mathbb{u} \cap \mathbb{v}))$. *Since* $\mathbb{u} \backslash \mathbb{v}$ *is disjoint from* $\mathbb{v} \backslash \mathbb{u}$ *and since* $\mathbb{u} \cap \mathbb{v}$ *is part of* $\mathbb{u}$ *and* $\mathbb{v}$, *respectively, it may be written* $(\mathbb{u} - (\mathbb{u} \cap \mathbb{v})) + (\mathbb{v} - (\mathbb{u} \cap \mathbb{v}))$. *Moreover,* $|\mathbb{w}| = |\mathbb{u}| - |\mathbb{u} \cap \mathbb{v}| + |\mathbb{v}| - |\mathbb{u} \cap \mathbb{v}|$, *whence the proposition follows.* ■

Recall that a general multivector can be composed of a mixture of basis blades of different grade. In order to have access to elements of a given grade the grade-projection operator is introduced. With its help a couple of important relations can be formulated.

Definition 2.1 (Grade-projection operator):
The grade-projection of the basis blade $\mathbf{e}_{\mathbb{u}} \in \mathbb{B}_{p,q}$ *onto the grade-*r *component (if exists) is indicated by* $\langle \mathbf{e}_{\mathbb{u}} \rangle_r$. *It is defined as*

$$\langle \mathbf{e}_{\mathbb{u}} \rangle_r = \begin{cases} \mathbf{e}_{\mathbb{u}} & \textit{if } \; |\mathbb{u}| = r \leq n \\ 0 & \textit{otherwise.} \end{cases}$$

The grade-projection operator is linear w.r.t. its arguments. A scalar projection $\langle \boldsymbol{A} \rangle_0$ *is usually abbreviated to* $\langle \boldsymbol{A} \rangle$. *Note that* $r > n \Rightarrow \langle \boldsymbol{A} \rangle_r = 0$. ■

Doubtlessly, using Kronecker's delta it is

$$\langle \boldsymbol{A}_{[k]} \rangle_r = \delta_{kr}\, \boldsymbol{A}_{[k]} \,.$$

The distributivity enables the extension to general multivectors as well

$$\boldsymbol{A} \;=\; \langle \boldsymbol{A} \rangle_0 + \langle \boldsymbol{A} \rangle_1 + \ldots + \langle \boldsymbol{A} \rangle_n \,. \tag{2.36}$$

It is now possible to combine proposition 2.2 with the grade-projection operator.

Corollary 2.2
Let $\boldsymbol{A}_{[k]} = \sum\limits_i a_i \mathbf{e}_{\mathbb{a}_i}$ *and* $\boldsymbol{B}_{[l]} = \sum\limits_i b_i \mathbf{e}_{\mathbb{b}_i}$ *with* $|\mathbb{a}_i| = k$ *and* $|\mathbb{b}_i| = l$. *Consider the*

geometric product $\boldsymbol{C} = \boldsymbol{A}_{[k]}\boldsymbol{B}_{[l]} = \sum_{i,j} a_i b_j \mathbf{e}_{\mathbb{a}_i}\mathbf{e}_{\mathbb{b}_j}$ *of the two* κ*-vectors* $\boldsymbol{A}_{[k]}$ *and* $\boldsymbol{B}_{[l]}$*, then*

$$\boldsymbol{C} \;=\; \langle \boldsymbol{A}_{[k]}\boldsymbol{B}_{[l]}\rangle_{|k-l|} \;+\; \langle \boldsymbol{A}_{[k]}\boldsymbol{B}_{[l]}\rangle_{|k-l|+2} \;+\; \ldots \;+\; \langle \boldsymbol{A}_{[k]}\boldsymbol{B}_{[l]}\rangle_{k+l}\,.$$

Proof: *Let* $c_k\mathbf{e}_{\mathbb{c}_k} = a_i b_j \mathbf{e}_{\mathbb{a}_i}\mathbf{e}_{\mathbb{b}_j}$ *be an arbitrary component from the product* $\boldsymbol{C} = \boldsymbol{A}_{[k]}\boldsymbol{B}_{[l]}$*. There are three cases: first, if* $\mathbb{a}_i \subseteq \mathbb{b}_j$ *or* $\mathbb{b}_j \subseteq \mathbb{a}_i$*, then, by proposition 2.2,* $|\mathbb{c}_k| = |\mathbb{b}_j| - |\mathbb{a}_i| = l - k$ *or* $|\mathbb{c}_k| = |\mathbb{a}_i| - |\mathbb{b}_j| = k - l$*, respectively. The component therefore contributes to the* $\boldsymbol{C}$*-term with lowest grade* $|\mathbb{c}_k| = |k-l|$*. Second, if* $\mathbb{a}_i \cap \mathbb{b}_j = \emptyset$*, a term with highest grade* $|\mathbb{c}_k| = k + l$ *is obtained. Finally, the remaining intermediate grades have to increase in steps of two as* $|\mathbb{a}_i| = k$ *and* $|\mathbb{b}_j| = l$ *are constant in* $|\mathbb{c}_k| = |\mathbb{a}_i| + |\mathbb{b}_j| - 2|\mathbb{a}_i \cap \mathbb{b}_j|$*.* ■

Corollary 2.3

The geometric product of k *vectors* $\{\boldsymbol{a}_{1\ldots k}\}$ *can be decomposed into summands of particular grades as*

$$\boldsymbol{a}_1\boldsymbol{a}_2\ldots\boldsymbol{a}_k \;=\; \sum_{i=0}^{\lfloor k/2\rfloor} \langle \boldsymbol{a}_1\boldsymbol{a}_2\ldots\boldsymbol{a}_k\rangle_{k-2i}$$

The corollary comes without a proof. Instead an example is given. With its help it becomes clear that a successive application of equation (2.22), i.e. splitting the geometric product into the inner and outer product, like

$$\boldsymbol{a}_1\boldsymbol{a}_2\ldots\boldsymbol{a}_k \;=\; (\ldots((\boldsymbol{a}_1\cdot\boldsymbol{a}_2 + \boldsymbol{a}_1\wedge\boldsymbol{a}_2)\cdot\boldsymbol{a}_3 + (\boldsymbol{a}_1\cdot\boldsymbol{a}_2 + \boldsymbol{a}_1\wedge\boldsymbol{a}_2)\wedge\boldsymbol{a}_3)\ldots,$$

reveals a grade structure as stated in the corollary.

Example 2.3 (Grade structure):

The table below demonstrates which grades emerge from which products. An algebra over a 5-dimensional space is assumed, that is $n := 5$*.*

Grade:	*0*	*1*	*2*	*3*	*4*	*5*
$\boldsymbol{a}_1\boldsymbol{a}_2$	*		*			
$\boldsymbol{a}_1\boldsymbol{a}_2\boldsymbol{a}_3$		*		*		
$\boldsymbol{a}_1\boldsymbol{a}_2\boldsymbol{a}_3\boldsymbol{a}_4$	*		*		*	
$\boldsymbol{a}_1\boldsymbol{a}_2\boldsymbol{a}_3\boldsymbol{a}_4\boldsymbol{a}_5$		*		*		*
$\boldsymbol{a}_1\boldsymbol{a}_2\boldsymbol{a}_3\boldsymbol{a}_4\boldsymbol{a}_5\boldsymbol{a}_6$	*		*		*	
$\boldsymbol{a}_1\boldsymbol{a}_2\boldsymbol{a}_3\boldsymbol{a}_4\boldsymbol{a}_5\boldsymbol{a}_6\boldsymbol{a}_7$		*		*		*

By means of corollary 2.3, it can be shown that equation (2.24) and equation (2.23) can be extended to multivectors of the form $\boldsymbol{A} = \boldsymbol{a}_1\boldsymbol{a}_2\ldots\boldsymbol{a}_k$.

Corollary 2.4
Let $\boldsymbol{B} = \boldsymbol{b}_1 \boldsymbol{b}_2 \ldots \boldsymbol{b}_l$ the geometric product of the vectors $\{\boldsymbol{b}_{1\ldots l}\}$. Inner and outer product with a vector $\boldsymbol{a} \in \mathbb{R}^{p,q}$ can then be calculated via

$$\boldsymbol{B} = \boldsymbol{b}_1 \boldsymbol{b}_2 \ldots \boldsymbol{b}_l \qquad \Longrightarrow \qquad \begin{array}{rcl} \boldsymbol{a} \cdot \boldsymbol{B} & = & \frac{1}{2}\Big(\boldsymbol{aB} \; - \; (-1)^l \boldsymbol{Ba}\Big) \\ \boldsymbol{a} \wedge \boldsymbol{B} & = & \frac{1}{2}\Big(\boldsymbol{aB} \; + \; (-1)^l \boldsymbol{Ba}\Big). \end{array}$$

Proof: *The proof is given for the case addressing the inner product, the analogous proof regarding the outer product is skipped. Using corollary 2.3 the term*

$$\boldsymbol{a} \cdot \boldsymbol{B} \; = \; \tfrac{1}{2}\Big(\boldsymbol{a}\, \boldsymbol{b}_1 \boldsymbol{b}_2 \ldots \boldsymbol{b}_l \; - \; (-1)^l \, \boldsymbol{b}_1 \boldsymbol{b}_2 \ldots \boldsymbol{b}_l \boldsymbol{a}\Big).$$

may be rewritten as

$$\tfrac{1}{2}\Big(\boldsymbol{a} \sum_{i=0}^{\lfloor l/2 \rfloor} \langle \boldsymbol{B} \rangle_{l-2i} \; - \; (-1)^l \sum_{i=0}^{\lfloor l/2 \rfloor} \langle \boldsymbol{B} \rangle_{l-2i} \, \boldsymbol{a}\Big).$$

Since $(-1)^l$ is the same as $(-1)^{l-2i}$ one obtains

$$\begin{aligned} \sum_{i=0}^{\lfloor l/2 \rfloor} \tfrac{1}{2}\Big(\boldsymbol{a}\, \langle \boldsymbol{B} \rangle_{l-2i} \; - \; (-1)^{l-2i} \langle \boldsymbol{B} \rangle_{l-2i} \, \boldsymbol{a}\Big) \quad &= \quad \sum_{i=0}^{\lfloor l/2 \rfloor} \boldsymbol{a} \cdot \langle \boldsymbol{B} \rangle_{l-2i} \\ &= \quad \boldsymbol{a} \cdot \sum_{i=0}^{\lfloor l/2 \rfloor} \langle \boldsymbol{B} \rangle_{l-2i} \; = \; \boldsymbol{a} \cdot \boldsymbol{B}\,. \end{aligned}$$

■

Note that although $\boldsymbol{a} \cdot \boldsymbol{B}_{[l]} = \langle \boldsymbol{a}\, \boldsymbol{B}_{[l]} \rangle_{l-1}$, it is in general $\boldsymbol{a} \cdot \langle \boldsymbol{B} \rangle_l \neq \langle \boldsymbol{aB} \rangle_{l-1}$ for some $\boldsymbol{B} = \boldsymbol{b}_1 \boldsymbol{b}_2 \ldots \boldsymbol{b}_l$ or any other multivector $\boldsymbol{B}$ that is not at least a κ-vector. The reason is that $\langle \boldsymbol{aB} \rangle_{l-1} = \boldsymbol{a} \cdot \langle \boldsymbol{B} \rangle_l + \boldsymbol{a} \wedge \langle \boldsymbol{B} \rangle_{l-2}$.

From equation (2.33), in the context of corollary 2.2, it can be inferred that the components of highest grade in $\boldsymbol{A}_{[k]} \boldsymbol{B}_{[l]}$, i.e. $\langle \boldsymbol{A}_{[k]} \boldsymbol{B}_{[l]} \rangle_{k+l}$, must be identified with the outer product $\boldsymbol{A}_{[k]} \wedge \boldsymbol{B}_{[l]}$.

Definition 2.2 (Outer product):
Let $\boldsymbol{A}_{[k]}$ and $\boldsymbol{B}_{[l]}$ be two κ-vectors in $\mathbb{R}_{p,q}$. Their outer product may be defined as

$$\boldsymbol{A}_{[k]} \wedge \boldsymbol{B}_{[l]} \; = \; \langle \boldsymbol{A}_{[k]} \boldsymbol{B}_{[l]} \rangle_{k+l}\,.$$

■

Note that for the special case of basis blades, $\mathbf{e}_{\mathbb{u}}$ and $\mathbf{e}_{\mathbb{v}}$, definition 2.2 reads $\mathbf{e}_{\mathbb{u}} \wedge \mathbf{e}_{\mathbb{v}} := \langle \mathbf{e}_{\mathbb{u}} \mathbf{e}_{\mathbb{v}} \rangle_{|\mathbb{u}|+|\mathbb{v}|}$. It is easily verified that the above definition exhibits the fundamental properties multilinearity and associativity, see page 31. The linearity follows from the linearity of the geometric product and from the linearity of the grade-projection operator. The associativity can be shown in this way:

$$\begin{aligned}(\boldsymbol{A}_{[r]} \wedge \boldsymbol{B}_{[s]}) \wedge \boldsymbol{C}_{[t]} &= \langle \boldsymbol{A}_{[r]} \boldsymbol{B}_{[s]} \rangle_{r+s} \wedge \boldsymbol{C}_{[t]} &&= \langle (\boldsymbol{A}_{[r]} \boldsymbol{B}_{[s]}) \boldsymbol{C}_{[t]} \rangle_{r+s+t} \\ &= \langle \boldsymbol{A}_{[r]} (\boldsymbol{B}_{[s]} \boldsymbol{C}_{[t]}) \rangle_{r+s+t} &&= \boldsymbol{A}_{[r]} \wedge \langle \boldsymbol{B}_{[s]} \boldsymbol{C}_{[t]} \rangle_{s+t} \\ &= \boldsymbol{A}_{[r]} \wedge (\boldsymbol{B}_{[s]} \wedge \boldsymbol{C}_{[t]})\end{aligned}$$

Regarding equation (2.22), it seems as if inner and outer product reflect the lower and upper limit of the spread of grades. Following this notion the generalized inner product may be defined.

Definition 2.3 (Inner product):
Let $\boldsymbol{A}_{[k]}$ and $\boldsymbol{B}_{[l]}$ be two κ-vectors in $\mathbb{R}_{p,q}$. Their inner product may be defined as

$$\boldsymbol{A}_{[k]} \cdot \boldsymbol{B}_{[l]} = \delta_{(kl)} \langle \boldsymbol{A}_{[k]} \boldsymbol{B}_{[l]} \rangle_{|k-l|} \,.$$

■

A scalar component $\langle \boldsymbol{A}_{[k]} \boldsymbol{B}_{[l]} \rangle$ can therefore only be obtained if the grades are equal ($k = l$). The scalar component of a geometric product always corresponds to the result of the inner product.

The striking term '$\delta_{(kl)}$' in the above definition has the purpose to prevent the problematic special case in which the grade of one of the operands is zero. Given a κ-vector of grade zero, for example $\boldsymbol{A}_{[0]} \in \mathbb{R}$, and some κ-vector $\boldsymbol{B}_{[l]}$, the application of definition 2.2 and definition 2.3, respectively, would - if the term was not there - inconsistently result in

$$\boldsymbol{A}_{[0]} \wedge \boldsymbol{B}_{[l]} \overset{\text{Def.2.2}}{=} \langle \boldsymbol{A}_{[0]} \boldsymbol{B}_{[l]} \rangle_{0+l} \overset{\lightning}{=} \langle \boldsymbol{A}_{[0]} \boldsymbol{B}_{[l]} \rangle_{|0-l|} \overset{\text{Def.2.3}}{=} \boldsymbol{A}_{[0]} \cdot \boldsymbol{B}_{[l]} \,.$$

The commutator expressions in equation (2.23) and equation (2.24), respectively, allow a sensible specialization on scalars. However, the next definition aims to re-emphasize the role of grade zero elements in geometric algebra.

Definition 2.4 (Treatment of scalars):
Let $\boldsymbol{A} \in \mathbb{R}_{p,q}$ be a multivector, then for every scalar $\alpha \in \mathbb{R}$

$$\alpha \cdot \boldsymbol{A} = 0 \qquad \textit{and} \qquad \alpha \wedge \boldsymbol{A} = \alpha \boldsymbol{A}.$$

■

In terms of basis blades definition 2.3 would take on the form $\mathbf{e}_{\mathbb{u}} \cdot \mathbf{e}_{\mathbb{v}} := \delta_{(|\mathbb{u}|\,|\mathbb{v}|)}$ $\langle \mathbf{e}_{\mathbb{u}} \mathbf{e}_{\mathbb{v}} \rangle_{||\mathbb{u}|-|\mathbb{v}||}$. This case corresponds to the first case in the proof of corollary 2.2; it is either $\mathbb{u} \subseteq \mathbb{v}$ or $\mathbb{v} \subseteq \mathbb{u}$. An equivalent but more intuitive definition for the inner product is thus

$$\mathbf{e}_{\mathbb{u}} \cdot \mathbf{e}_{\mathbb{v}} := \begin{cases} \delta_{(|\mathbb{u}|\,|\mathbb{v}|)}\, \mathbf{e}_{\mathbb{u}} \mathbf{e}_{\mathbb{v}}, & \mathbb{u} \subseteq \mathbb{v} \;\text{ or }\; \mathbb{v} \subseteq \mathbb{u} \\ 0, & \text{else.} \end{cases} \tag{2.37}$$

The analogue regarding the outer product, i.e. $\mathbf{e}_{\mathbb{u}} \wedge \mathbf{e}_{\mathbb{v}}$, is defined in equation (2.33).

Now inner and outer product can be expressed for general multivectors $\boldsymbol{A} = \sum_i a_i \mathbf{e}_{\mathbb{a}_i}$ and $\boldsymbol{B} = \sum_i b_i \mathbf{e}_{\mathbb{b}_i}$

$$\begin{aligned} \boldsymbol{A} \cdot \boldsymbol{B} &= \sum_{i,j} a_i b_j \;\mathbf{e}_{\mathbb{a}_i} \cdot \mathbf{e}_{\mathbb{b}_j} \\ \boldsymbol{A} \wedge \boldsymbol{B} &= \sum_{i,j} a_i b_j \;\mathbf{e}_{\mathbb{a}_i} \wedge \mathbf{e}_{\mathbb{b}_j}. \end{aligned}$$

Corollary 2.5

Let $\mathbf{e}_{\mathbb{u}}$ and $\mathbf{e}_{\mathbb{v}}$ be two basis blades such that $\mathbb{u} \subseteq \mathbb{v}$. Then the inner product satisfies

$$\mathbf{e}_{\mathbb{u}} \cdot \mathbf{e}_{\mathbb{v}} \;=\; (-1)^{|\mathbb{u}|\,|\mathbb{v}|-|\mathbb{u}|}\; \mathbf{e}_{\mathbb{v}} \cdot \mathbf{e}_{\mathbb{u}}, \qquad \mathbb{u} \subseteq \mathbb{v}.$$

Similarly, for two κ-vectors $\boldsymbol{A}_{[k]}$ and $\boldsymbol{B}_{[l]}$, $k \leq l$, is follows from the linearity of the inner product

$$\boldsymbol{A}_{[k]} \cdot \boldsymbol{B}_{[l]} \;=\; (-1)^{k\,l-k}\, \boldsymbol{B}_{[l]} \cdot \boldsymbol{A}_{[k]}, \qquad k \leq l.$$

Proof: *First it is to mention that the conditions of equation (2.37) are met. Hence the statement of the corollary follows directly from equation (2.35) by noting that $\mathbb{u} \cap \mathbb{v} = \mathbb{u}$.*
Regarding the second part of the statement let $\boldsymbol{A}_{[k]} = \sum_i a_i \mathbf{e}_{\mathbb{a}_i}$ and $\boldsymbol{B}_{[l]} = \sum_i b_i \mathbf{e}_{\mathbb{b}_i}$ with $|\mathbb{a}_i| = k$ and $|\mathbb{b}_i| = l$, so $\boldsymbol{A}_{[k]} \cdot \boldsymbol{B}_{[l]} = \sum_{i,j} a_i\, b_j\, \mathbf{e}_{\mathbb{a}_i} \cdot \mathbf{e}_{\mathbb{b}_j}$. It must be taken into account that for some of the summands $a_i\, b_j\, \mathbf{e}_{\mathbb{a}_i} \cdot \mathbf{e}_{\mathbb{b}_j}$ neither $\mathbb{a}_i \subseteq \mathbb{b}_j$ nor $\mathbb{b}_j \subseteq \mathbb{a}_i$ is fulfilled. The respective summands are therefore zero with the result that $\mathbf{e}_{\mathbb{a}_i} \cdot \mathbf{e}_{\mathbb{b}_j} = 0 = (-1)^{|\mathbb{a}_i|\,|\mathbb{b}_j|-|\mathbb{a}_i|}\, \mathbf{e}_{\mathbb{b}_j} \cdot \mathbf{e}_{\mathbb{a}_i}$ does not contradict the second statement of the corollary.

■

Corollary 2.6

The inner product of two κ-vectors $\boldsymbol{A}_{[k]}$ and $\boldsymbol{B}_{[l]}$ is commutative if they both have the same grade $k = l$, or equally if the outcome is scalar valued. Then

$$\boldsymbol{A}_{[k]} \cdot \boldsymbol{B}_{[l]} \;=\; \langle \boldsymbol{A}_{[k]} \boldsymbol{B}_{[l]} \rangle \;=\; \boldsymbol{B}_{[l]} \cdot \boldsymbol{A}_{[k]}, \qquad k \;=\; l.$$

Proof: *With respect to corollary 2.5 it must be shown that $(-1)^{k\,l-k} \overset{k=l}{=} (-1)^{k^2-k}$ equals one. Thus $z := k^2 - k$ has to be an even number. Assume at first that k is odd: $k := 2m+1$, $m \in \mathbb{Z}$. Then $z = (2m+1)^2 - 2m - 1 = 4m^2 + 2m$ is even. In case $k := 2m$, $m \in \mathbb{Z}$, the expression evaluates to $z = (2m)^2 - 2m = 4m^2 - 2m$, which is even as well.*

■

Definition 2.5 (Blade):
The outer product of a set of $0 \leq k \leq n$ linearly independent vectors $\{\boldsymbol{a}_{1\ldots k}\} \subset \mathbb{R}^{p,q}$ is called a blade of grade k or simply k-blade. It is denoted by $\boldsymbol{A}_{\langle k\rangle}$.

$$\boldsymbol{A}_{\langle k\rangle} \;=\; \boldsymbol{a}_1 \wedge \boldsymbol{a}_2 \wedge \ldots \wedge \boldsymbol{a}_k$$

A scalar is considered as a blade of grade 0. ■

Subsequently, every appearance of blades $\boldsymbol{A}_{\langle k\rangle}$, $\boldsymbol{B}_{\langle l\rangle}$, etc will implicitly stand for $\bigwedge_{i=1}^{k} \boldsymbol{a}_i$, $\bigwedge_{i=1}^{l} \boldsymbol{b}_i$, etc if no deviant declaration is given.
As a matter of course, every blade is a certain κ-vector, which is why every computation rule for κ-vectors is applicable to blades as well. Likewise, any κ-vector $\boldsymbol{A}_{[k]}$ is a k-blade $\boldsymbol{A}_{\langle k\rangle}$ *iff* it has an outer product representation $\boldsymbol{a}_1 \wedge \boldsymbol{a}_2 \wedge \ldots \wedge \boldsymbol{a}_k$.

Example 2.4 (κ-vector vs. blade):

$$\begin{array}{ccccc} (\mathbf{e}_1 + \mathbf{e}_2) \wedge (\mathbf{e}_2 + \mathbf{e}_3) & \Longleftrightarrow & \mathbf{e}_1\mathbf{e}_2 + \mathbf{e}_1\mathbf{e}_3 + \mathbf{e}_2\mathbf{e}_3 & & \textit{blade} \\ ?? & \Longleftarrow & \mathbf{e}_1\mathbf{e}_2 + \mathbf{e}_1\mathbf{e}_3 + \mathbf{e}_2\mathbf{e}_4 & & \kappa\textit{-vector}\,. \end{array}$$

On page 23 it is stated that the outer product $\boldsymbol{a} \wedge \boldsymbol{b}$, $n > 2$, represents a linear 2D-subspace, i.e. a plane. In addition, it is shown on page 32 that the outer product of vectors is zero if the vectors are linearly dependent. Hence the outer product of a vector $\boldsymbol{x}$ with a blade $\boldsymbol{A}_{\langle k\rangle} = \bigwedge_{i=1}^{k} \boldsymbol{a}_i$ is zero if the vectors $\{\boldsymbol{x}, \boldsymbol{a}_1, \boldsymbol{a}_2, \ldots, \boldsymbol{a}_k\}$ are linearly dependent, or rather if $\boldsymbol{x}$ lies in the k-dimensional subspace spanned by the $\{\boldsymbol{a}_{1\ldots k}\}$. The spanning vectors are of course termed the basis or the *frame* of the subspace.

Corollary 2.7
A blade $\boldsymbol{A}_{\langle k\rangle} = \bigwedge_{i=1}^{k} \boldsymbol{a}_i$ represents a linear k-dimensional subspace in that

$$\boldsymbol{x} \wedge \boldsymbol{A}_{\langle k\rangle} \;=\; 0 \qquad \Longleftrightarrow \qquad \boldsymbol{x} \textit{ lies in the span of the } \{\boldsymbol{a}_{1\ldots k}\}$$

for every vector $\boldsymbol{x} \in \mathbb{R}^{p,q}$

Proof: *An outline for a direct proof of the 'only-if' direction is given on page 32. The 'if' direction can be deduced from equation (2.31): let $\mathsf{x} \in \mathbb{R}^n$ and $\mathsf{A} \in \mathbb{R}^{n\times k}$ be the matrices, the columns of which hold the coefficients of $\boldsymbol{x} \in \mathbb{R}^{p,q}$ and $\boldsymbol{A}_{\langle k\rangle} \in \mathbb{R}_{p,q}$, respectively. Then $\boldsymbol{x} \wedge \boldsymbol{A}_{\langle k\rangle}$ may be expressed as*

$$\boldsymbol{x} \wedge \boldsymbol{A}_{\langle k\rangle} \;=\; \sum_{\mathsf{v} \in I_{k+1/n}} \det([\mathsf{x}, \mathsf{A}]|_{\mathsf{v}})\; \mathbf{e}_{\mathsf{v}_1}\mathbf{e}_{\mathsf{v}_2}\ldots\mathbf{e}_{\mathsf{v}_{k+1}},$$

where $[\mathsf{x}, \mathsf{A}] \in \mathbb{R}^{n\times k+1}$ symbolizes the horizontal concatenation of the matrices x and A. If at least one $k+1$-minor $\det([\mathsf{x}, \mathsf{A}]|_{\mathsf{v}})$ was non-zero, the matrix $[\mathsf{x}, \mathsf{A}]$ would *have its full column rank $k+1$. Hence the condition $\boldsymbol{x} \wedge \boldsymbol{A}_{\langle k \rangle} = 0$ implies that the columns in* $[\mathsf{x}, \mathsf{A}]$ *are linearly dependent, whence the proposition follows.* ■

As a blade $\boldsymbol{A}_{\langle k \rangle}$ can be identified with a vector space, it can be treated as such, i.e. the statements known from linear algebra hold as well. For example, it will shortly be shown that a blade always possesses an orthogonal basis. Rather, the outer product of any set of linearly independent vectors that span the same subspace as $\boldsymbol{A}_{\langle k \rangle}$ yields, up to a scalar factor, $\boldsymbol{A}_{\langle k \rangle}$ again. It can therefore already be inferred that the outer product of two blades must be zero *iff* they share a common subspace (except the trivial 0-dimensional vector space $\{\mathbf{0}\}$). Specifically,

$$\boldsymbol{A}_{\langle k \rangle} \wedge \boldsymbol{A}_{\langle k \rangle} \;=\; 0.$$

The proof of the following special case, relating bivectors and 2-blades, is given in section A.3.1.

Proposition 2.3
Given a bivector $\boldsymbol{A}_{[2]}$ from $\mathbb{R}_{p,q}$ the following relationship holds

$$\boldsymbol{A}_{[2]} \wedge \boldsymbol{A}_{[2]} = 0 \qquad \Longleftrightarrow \qquad \boldsymbol{A}_{[2]} \textit{ is a 2-blade } \boldsymbol{A}_{\langle 2 \rangle}.$$

The next proposition states two very useful calculation rules - one of which is a pseudo associative law for the inner product.

Proposition 2.4
Let $\mathbf{e}_{\mathbb{u}}$, $\mathbf{e}_{\mathbb{v}}$ and $\mathbf{e}_{\mathbb{w}}$ denote three basis blades. Then the following identities can be found

$$\begin{aligned}
(\mathbf{e}_{\mathbb{u}} \cdot \mathbf{e}_{\mathbb{v}}) \cdot \mathbf{e}_{\mathbb{w}} &= \mathbf{e}_{\mathbb{u}} \cdot (\mathbf{e}_{\mathbb{v}} \cdot \mathbf{e}_{\mathbb{w}}), \qquad |\mathbb{v}| \geq |\mathbb{u}| + |\mathbb{w}| \\
(\mathbf{e}_{\mathbb{u}} \wedge \mathbf{e}_{\mathbb{w}}) \cdot \mathbf{e}_{\mathbb{v}} &= \mathbf{e}_{\mathbb{u}} \cdot (\mathbf{e}_{\mathbb{w}} \cdot \mathbf{e}_{\mathbb{v}}), \qquad |\mathbb{v}| \geq |\mathbb{u}| + |\mathbb{w}|.
\end{aligned}$$

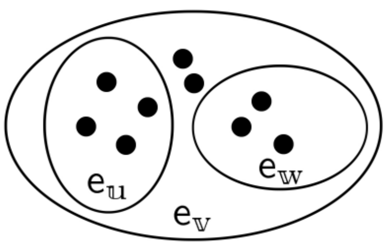

Fig. 2.5: Example partitioning of basis vectors that reflects the condition $|\mathbb{v}| \geq |\mathbb{u}| + |\mathbb{w}|$ imposed in proposition 2.4: each black dot symbolizes a different basis vector.

The arrangement in figure 2.5 shows a setup in which the condition $|\mathbb{v}| \geq |\mathbb{u}| + |\mathbb{w}|$ of proposition 2.4 is fulfilled. It certainly is possible to give a geometrical proof as suggested in [21] or to analyze all cases in a proof by exhaustion. However, here a common but elegant proof is favored that bases on the grade-projection operator.

Proof: *Let the grades of* $\mathbf{e}_{\mathbb{u}}$, $\mathbf{e}_{\mathbb{v}}$ *and* $\mathbf{e}_{\mathbb{w}}$ *be denoted with* u, v *and* w, *respectively. Assume that* $|\mathbb{v}| \geq |\mathbb{u}| + |\mathbb{w}|$ *is fulfilled, then*

$$\begin{aligned}
(\mathbf{e}_{\mathbb{u}} \cdot \mathbf{e}_{\mathbb{v}}) \cdot \mathbf{e}_{\mathbb{w}} &= \langle \mathbf{e}_{\mathbb{u}} \mathbf{e}_{\mathbb{v}} \rangle_{|u-v|} \cdot \mathbf{e}_{\mathbb{w}} & |u-v| &= v-u \\
&= \langle \mathbf{e}_{\mathbb{u}} \mathbf{e}_{\mathbb{v}} \mathbf{e}_{\mathbb{w}} \rangle_{|(v-u)-w|} & |(v-u)-w| &= |u-(v-w)| \\
&= \langle \mathbf{e}_{\mathbb{u}} \mathbf{e}_{\mathbb{v}} \mathbf{e}_{\mathbb{w}} \rangle_{|u-(v-w)|} \\
&= \mathbf{e}_{\mathbb{u}} \cdot \langle \mathbf{e}_{\mathbb{v}} \mathbf{e}_{\mathbb{w}} \rangle_{|v-w|} \\
&= \mathbf{e}_{\mathbb{u}} \cdot (\mathbf{e}_{\mathbb{v}} \cdot \mathbf{e}_{\mathbb{w}}).
\end{aligned}$$

Similarly, it is

$$\begin{aligned}
(\mathbf{e}_{\mathbb{u}} \wedge \mathbf{e}_{\mathbb{w}}) \cdot \mathbf{e}_{\mathbb{v}} &= \langle \mathbf{e}_{\mathbb{u}} \mathbf{e}_{\mathbb{w}} \rangle_{u+w} \cdot \mathbf{e}_{\mathbb{v}} \\
&= \langle \mathbf{e}_{\mathbb{u}} \mathbf{e}_{\mathbb{w}} \mathbf{e}_{\mathbb{v}} \rangle_{|(u+w)-v|} & |(u+w)-v| &= |(v-w)-u| \\
&= \langle \mathbf{e}_{\mathbb{u}} \mathbf{e}_{\mathbb{w}} \mathbf{e}_{\mathbb{v}} \rangle_{|u-|v-w||} & &= |u-|v-w|| \\
&= \mathbf{e}_{\mathbb{u}} \cdot \langle \mathbf{e}_{\mathbb{w}} \mathbf{e}_{\mathbb{v}} \rangle_{|w-v|} \\
&= \mathbf{e}_{\mathbb{u}} \cdot (\mathbf{e}_{\mathbb{w}} \cdot \mathbf{e}_{\mathbb{v}}).
\end{aligned}$$

■

By employing the distributive law, the preceding proposition can easily be extended to κ-vectors.

Corollary 2.8

Given three κ*-vectors* $\boldsymbol{A}_{[k]}$, $\boldsymbol{B}_{[l]}$ and $\boldsymbol{C}_{[t]}$, *it holds that*

$$\begin{aligned}
(\boldsymbol{A}_{[r]} \cdot \boldsymbol{B}_{[s]}) \cdot \boldsymbol{C}_{[t]} &= \boldsymbol{A}_{[r]} \cdot (\boldsymbol{B}_{[s]} \cdot \boldsymbol{C}_{[t]}) \qquad \textit{if } s \geq r+t \\
(\boldsymbol{A}_{[r]} \wedge \boldsymbol{B}_{[s]}) \cdot \boldsymbol{C}_{[t]} &= \boldsymbol{A}_{[r]} \cdot (\boldsymbol{B}_{[s]} \cdot \boldsymbol{C}_{[t]}) \qquad \textit{if } t \geq r+s
\end{aligned}$$

By writing $\boldsymbol{A}_{\langle k \rangle} = \boldsymbol{A}_{\langle k-1 \rangle} \wedge \boldsymbol{a}_k$, the value of the second identity is disclosed

$$\boldsymbol{A}_{\langle k \rangle} \cdot \boldsymbol{B}_{\langle l \rangle} = (\boldsymbol{A}_{\langle k-1 \rangle} \wedge \boldsymbol{a}_k) \cdot \boldsymbol{B}_{\langle l \rangle} = \boldsymbol{A}_{\langle k-1 \rangle} \cdot (\boldsymbol{a}_k \cdot \boldsymbol{B}_{\langle l \rangle}), \qquad k \leq l.$$

Furthermore

$$\boldsymbol{A}_{\langle k \rangle} \cdot \boldsymbol{B}_{\langle l \rangle} = \boldsymbol{a}_1 \cdot (\boldsymbol{a}_2 \cdot \ \ldots \ (\boldsymbol{a}_{k-1} \cdot (\boldsymbol{a}_k \cdot \boldsymbol{B}_{\langle l \rangle}))...), \qquad k \leq l. \tag{2.38}$$

According to corollary 2.4 the inner product $\boldsymbol{a} \cdot \boldsymbol{B}_{\langle l \rangle}$ of a vector with a blade $\boldsymbol{B}_{\langle l \rangle}$ is defined by the commutator (anti-commutator) if the grade l is even (odd). In this way equation (2.38) may be expressed in a new manner.

Corollary 2.9
The inner product of two blades $\boldsymbol{A}_{\langle k\rangle}$ and $\boldsymbol{B}_{\langle l\rangle}$ can be expressed by means of the commutator formalism, that is

$$\boldsymbol{A}_{\langle k\rangle}\cdot\boldsymbol{B}_{\langle l\rangle} \;=\; \begin{cases} \ldots\;\overline{\times}\;(\boldsymbol{a}_{k-2}\underline{\times}\;(\boldsymbol{a}_{k-1}\overline{\times}\;(\boldsymbol{a}_k\;\underline{\times}\;\boldsymbol{B}_{\langle l\rangle})))..., & l \;\; even\\ \ldots\;\underline{\times}\;(\boldsymbol{a}_{k-2}\overline{\times}\;(\boldsymbol{a}_{k-1}\underline{\times}\;(\boldsymbol{a}_k\;\overline{\times}\;\boldsymbol{B}_{\langle l\rangle})))..., & l \;\; odd\,. \end{cases}$$

The commutator expressions can be further expanded with the help of equation (A.11) and equation (A.12): if the grade l of $\boldsymbol{B}_{\langle l\rangle}$ is even (odd), the former (latter) equation has to be used.

Example 2.5 (Expanded inner product):
The inner product $(\boldsymbol{a}_1\wedge\boldsymbol{a}_2\wedge\boldsymbol{a}_3)\cdot\boldsymbol{B}_{\langle 5\rangle}$ may be expanded as

$$\begin{aligned}\boldsymbol{a}_1\overline{\times}(\boldsymbol{a}_2\underline{\times}(\boldsymbol{a}_3\overline{\times}\boldsymbol{B}_{\langle 5\rangle})) \;\overset{(A.12)}{=}\;\; & +\boldsymbol{a}_1\boldsymbol{a}_2\boldsymbol{a}_3\boldsymbol{B}_{\langle 5\rangle}+\underline{\boldsymbol{a}_1\boldsymbol{a}_2\boldsymbol{B}_{\langle 5\rangle}\boldsymbol{a}_3}-\underline{\boldsymbol{a}_1\boldsymbol{a}_3\boldsymbol{B}_{\langle 5\rangle}\boldsymbol{a}_2}\\ & -\boldsymbol{a}_1\boldsymbol{B}_{\langle 5\rangle}\boldsymbol{a}_3\boldsymbol{a}_2+\underline{\boldsymbol{a}_2\boldsymbol{a}_3\boldsymbol{B}_{\langle 5\rangle}\boldsymbol{a}_1}+\boldsymbol{a}_2\boldsymbol{B}_{\langle 5\rangle}\boldsymbol{a}_3\boldsymbol{a}_1\\ & -\boldsymbol{a}_3\boldsymbol{B}_{\langle 5\rangle}\boldsymbol{a}_2\boldsymbol{a}_1-\underline{\boldsymbol{B}_{\langle 5\rangle}\boldsymbol{a}_3\boldsymbol{a}_2\boldsymbol{a}_1}.\end{aligned}$$

Note that changing the sign of the underlined summands (with an odd number of trailing vectors) yields the outer product, see equation (A.11).

Proposition 2.5
Let $\boldsymbol{A}$ and $\boldsymbol{B}$ denote two general multivectors of $\mathbb{R}_{p,q}$. It then holds that

$$\langle\boldsymbol{AB}\rangle \;=\; \langle\boldsymbol{BA}\rangle.$$

Proof: *Let $\boldsymbol{A}=\sum_{i=0}^{n}\langle\boldsymbol{A}\rangle_i$ and $\boldsymbol{B}=\sum_{j=0}^{n}\langle\boldsymbol{B}\rangle_j$. It follows that*

$$\langle\boldsymbol{AB}\rangle = \left\langle\sum_{i,j=0}^{n}\langle\boldsymbol{A}\rangle_i\langle\boldsymbol{B}\rangle_j\right\rangle \;=\; \sum_{i,j=0}^{n}\Big\langle\langle\boldsymbol{A}\rangle_i\langle\boldsymbol{B}\rangle_j\Big\rangle$$

and further by the definition 2.3 of the inner product

$$\langle\boldsymbol{AB}\rangle \;=\; \sum_{i,j=0}^{n}\delta_{ij}\Big\langle\langle\boldsymbol{A}\rangle_i\langle\boldsymbol{B}\rangle_j\Big\rangle \;=\; \langle\boldsymbol{A}\rangle\langle\boldsymbol{B}\rangle \;+\; \sum_{i=1}^{n}\langle\boldsymbol{A}\rangle_i\cdot\langle\boldsymbol{B}\rangle_i.$$

According to corollary 2.6, it is $\langle\boldsymbol{A}\rangle_i\cdot\langle\boldsymbol{B}\rangle_i=\langle\boldsymbol{B}\rangle_i\cdot\langle\boldsymbol{A}\rangle_i$. Hence

$$\langle\boldsymbol{AB}\rangle \;=\; \langle\boldsymbol{B}\rangle\langle\boldsymbol{A}\rangle \;+\; \sum_{i=1}^{n}\langle\boldsymbol{B}\rangle_i\cdot\langle\boldsymbol{A}\rangle_i \;=\; \ldots \;=\; \langle\boldsymbol{BA}\rangle.$$

■

In this way the so-called *cyclic reordering property* is obtained

$$\langle \boldsymbol{A}_1 \boldsymbol{A}_2 \ldots \boldsymbol{A}_{k-1} \boldsymbol{A}_k \rangle \;=\; \langle \boldsymbol{A}_k\, \boldsymbol{A}_1 \boldsymbol{A}_2 \ldots \boldsymbol{A}_{k-1} \rangle.$$

Particular attention should be paid to next proposition. Its existential statement seems to be obvious with regard to the insights of linear algebra, cf. page 238, but it has to be kept in mind that the underlying algebra might be non-Euclidean. Besides, the given proof is a constructive one, i.e. it also reveals the way to orthogonalize a frame.

Proposition 2.6
For every blade $\boldsymbol{A}_{\langle k \rangle} = \bigwedge_{i=1}^{k} \boldsymbol{a}_i$ it exists a set of $k \leq n$ orthogonal (anti-commuting) vectors $\{\boldsymbol{z}_{1 \ldots k}\} \subset \mathbb{R}^{p,q}$ such that

$$\boldsymbol{A}_{\langle k \rangle} \;=\; \boldsymbol{z}_1\, \boldsymbol{z}_2 \ldots \boldsymbol{z}_k\,.$$

<u>Proof</u>: *Let $\mathsf{P} \in \mathbb{R}^{k \times k}$ denote the $k \times k$ symmetric matrix with entries $\mathsf{P}_{ij} = \boldsymbol{a}_i \cdot \boldsymbol{a}_j$, $\boldsymbol{a}_i \in \{\boldsymbol{a}_{1 \ldots k}\}$. It is known from matrix calculus that P is diagonalizable by means of an Eigenvalue decomposition*

$$\mathsf{P} \;=\; \mathsf{U}\mathsf{D}\mathsf{U}^\mathsf{T} \qquad \overset{\mathsf{U}\mathsf{U}^\mathsf{T} = \mathsf{I}_k}{\Longleftrightarrow} \qquad \mathsf{U}^\mathsf{T}\mathsf{P}\mathsf{U} \;=\; \mathsf{D}\,,$$

where $\mathsf{D} \in \mathbb{R}^{k \times k}$ symbolizes the diagonal matrix of Eigenvalues. The matrix of Eigenvectors $\mathsf{U} \in \mathbb{R}^{k \times k}$ is orthonormal, i.e. $\mathsf{U}\mathsf{U}^\mathsf{T} = \mathsf{I}_k$.
Note that P may be written as $\mathsf{P} = \mathsf{A}\mathsf{Q}\mathsf{A}^\mathsf{T}$, where the i^{th} row of matrix $\mathsf{A} \in \mathbb{R}^{k \times n}$ is assumed to hold the coefficients of vector $\boldsymbol{a}_i$, ${\scriptstyle 1 \leq i \leq k}$. The diagonal matrix $\mathsf{Q} \in \mathbb{R}^{n \times n}$ stands for the inner product as it realizes the quadratic form Q of the quadratic space $\mathbb{R}^{p,q}$, see page 239. It is $\mathsf{Q}_{ij} = \delta_{ij} \mathbf{e}_i^2$. Consequently,

$$\underbrace{\mathsf{U}^\mathsf{T}\mathsf{A}}_{=:\mathsf{Z}}\,\mathsf{Q}\,\underbrace{\mathsf{A}^\mathsf{T}\mathsf{U}}_{\mathsf{Z}^\mathsf{T}} \;=\; \mathsf{D}\,.$$

Now the rows of matrix $\mathsf{Z} \in \mathbb{R}^{k \times n}$ hold the coefficients of the orthogonal vectors $\{\boldsymbol{z}_{1 \ldots k}\} \subset \mathbb{R}^{p,q}$ (linear combinations of the $\{\boldsymbol{a}_{1 \ldots k}\}$) because $\mathsf{Z}\mathsf{Q}\mathsf{Z}^\mathsf{T} = \mathsf{D}$ corresponds to $\mathsf{Z}_{ij} = \boldsymbol{z}_i \cdot \boldsymbol{z}_j = \mathsf{D}_{ij}\, \delta_{ij}$. Due to associativity one has $\boldsymbol{z}_1 \boldsymbol{z}_2 \ldots \boldsymbol{z}_k = \boldsymbol{z}_1 \wedge \boldsymbol{z}_2 \wedge \ldots \wedge \boldsymbol{z}_k$ and eventually with $\boldsymbol{z}_j = \sum_{i=1}^{k} (\mathsf{U}^\mathsf{T})_{ji} \boldsymbol{a}_i = \mathsf{U}^i{}_j \boldsymbol{a}_i$

$$\begin{aligned}
\boldsymbol{z}_1 \boldsymbol{z}_2 \ldots \boldsymbol{z}_k \quad &= \quad \boldsymbol{z}_1 \wedge \boldsymbol{z}_2 \wedge \ldots \wedge \boldsymbol{z}_k \\
&= \quad (\mathsf{U}^{i_1}{}_1 \boldsymbol{a}_{i_1}) \wedge (\mathsf{U}^{i_2}{}_2 \boldsymbol{a}_{i_2}) \wedge \ldots \wedge (\mathsf{U}^{i_k}{}_k \boldsymbol{a}_{i_k}) \\
&= \quad \mathsf{U}^{i_1}{}_1\, \mathsf{U}^{i_2}{}_2 \,\ldots\, \mathsf{U}^{i_k}{}_k \;\; \boldsymbol{a}_{i_1} \wedge \boldsymbol{a}_{i_2} \wedge \ldots \wedge \boldsymbol{a}_{i_k} \\
&\overset{(2.26)}{=} \quad \sum_{\sigma \in \mathcal{S}(k)} \prod_{j=1}^{k} \mathsf{U}_{\sigma(j),j} \;\; sgn(\sigma) \; \bigwedge_{i=1}^{k} \boldsymbol{a}_i \qquad (2.39) \\
&= \quad \det(\mathsf{U})\; \boldsymbol{a}_1 \wedge \boldsymbol{a}_2 \wedge \ldots \wedge \boldsymbol{a}_k \\
&\overset{(*)}{=} \quad \boldsymbol{A}_{\langle k \rangle}.
\end{aligned}$$

(*) A determinant $\det(\mathsf{U})$ *of* -1 *can easily be remedied by exchanging two of the vectors* $\{\boldsymbol{z}_{1\ldots k}\}$ *or by switching the sign of an odd number of vectors.* ■

It is worth mentioning that the above orthogonalization of the frame $\{\boldsymbol{a}_{1\ldots k}\}$ can equally be done with any signature (specified by the matrix Q). By using, for example, the *Euclidean scalar product* $\mathsf{P}_{ij} = \boldsymbol{a}_i *_{\boldsymbol{\varepsilon}} \boldsymbol{a}_j$ a basis with perpendicular vectors $\{\boldsymbol{z}_{1\ldots k}\} \subset \mathbb{R}^{p,q}$ is obtained, so $\boldsymbol{z}_i *_{\boldsymbol{\varepsilon}} \boldsymbol{z}_j = 0$, but mostly $\boldsymbol{z}_i \cdot \boldsymbol{z}_j \neq 0$, $i \neq j$. However, pursuant to the previous proof the spanned vector space $\boldsymbol{A}_{\langle k\rangle}$ stays the same. This substantiates the statement on page 24 according to which the subspace representation by means of the outer product is independent of the inner product and the signature, respectively.

Note that the decomposition of a blade into orthogonal vectors is not unique. By rotating the vectors $\boldsymbol{z}_1 := \mathbf{e}_1$ and $\boldsymbol{z}_2 := \mathbf{e}_2$ by 45°, for example, the vectors $\boldsymbol{z}_1' = (\mathbf{e}_1 + \mathbf{e}_2)/\sqrt{(2)}$ and $\boldsymbol{z}_2' = (\mathbf{e}_2 - \mathbf{e}_1)/\sqrt{(2)}$ are obtained, with

$$\boldsymbol{z}_1\boldsymbol{z}_2 \;=\; \mathbf{e}_1 \wedge \mathbf{e}_2 \;=\; \boldsymbol{z}_1'\boldsymbol{z}_2', \qquad \boldsymbol{z}_1, \boldsymbol{z}_2 \in \mathbb{R}^2.$$

But however the decomposition comes off, the signature of an orthogonal frame, i.e. the number of basis vectors that square to positive values, negative values or to zero, respectively, stays the same as stated by *Sylvester's law of inertia*.

It is now being shown that a certain type of transformation of the spanning vectors inside the spanned subspace (the vectors in the example stay in the $\mathbf{e}_1$-$\mathbf{e}_2$-plane) do not alter the blade. As a consequence, the vectors may be assumed to be aligned as desired, i.e. as advantageously as possible for the problem under consideration. Assume that $\boldsymbol{n}$ is a vector in $\boldsymbol{A}_{\langle k\rangle}$ with $\boldsymbol{n}^2 = 1$. By exploiting that $\boldsymbol{n} \wedge \boldsymbol{A}_{\langle k\rangle} = 0$ and $\boldsymbol{n} \cdot (\boldsymbol{n} \cdot \boldsymbol{A}_{\langle k\rangle}) = (\boldsymbol{n} \wedge \boldsymbol{n}) \cdot \boldsymbol{A}_{\langle k\rangle} = 0$, the expansion of the expression $\boldsymbol{n}\boldsymbol{A}_{\langle k\rangle}\boldsymbol{n}$ is

$$\boldsymbol{n}\boldsymbol{A}_{\langle k\rangle}\boldsymbol{n} \;=\; (\boldsymbol{n} \cdot \boldsymbol{A}_{\langle k\rangle}) \wedge \boldsymbol{n} \;=\; \begin{cases} (\boldsymbol{n} \veebar \boldsymbol{A}_{\langle k\rangle}) \veebar \boldsymbol{n}, & k \text{ even}, \\ (\boldsymbol{n} \barwedge \boldsymbol{A}_{\langle k\rangle}) \barwedge \boldsymbol{n}, & k \text{ odd}. \end{cases}$$

By means of equation (A.2) (k is even) and equation (A.8) (k is odd), respectively, it can be shown that

$$\boldsymbol{n}\boldsymbol{A}_{\langle k\rangle}\boldsymbol{n} \;=\; \boldsymbol{n} \cdot (\boldsymbol{A}_{\langle k\rangle} \wedge \boldsymbol{n}) + (-1)^{k-1}\boldsymbol{A}_{\langle k\rangle} \;=\; (-1)^{k-1}\boldsymbol{A}_{\langle k\rangle}.$$

Thus the subspace does not change. By considering the representation of $\boldsymbol{A}_{\langle k\rangle}$ in terms of an orthogonal frame $\{\boldsymbol{z}_{1\ldots k}\}$ it may further be written[9]

$$\begin{aligned}
-\boldsymbol{n}\boldsymbol{A}_{\langle k\rangle}\boldsymbol{n} \;&=\; -\boldsymbol{n}\boldsymbol{z}_1\boldsymbol{z}_2\ldots\boldsymbol{z}_k\boldsymbol{n} \\
&=\; -\boldsymbol{n}\boldsymbol{z}_1\,1\,\boldsymbol{z}_2\,1\,\ldots\,1\,\boldsymbol{z}_k\boldsymbol{n} \\
&=\; -\boldsymbol{n}\boldsymbol{z}_1\,\boldsymbol{n}\boldsymbol{n}\,\boldsymbol{z}_2\,\boldsymbol{n}\boldsymbol{n}\,\ldots\,\boldsymbol{n}\boldsymbol{n}\,\boldsymbol{z}_k\boldsymbol{n} \\
&=\; (-\boldsymbol{n}\boldsymbol{z}_1\boldsymbol{n})\,(-\boldsymbol{n}\boldsymbol{z}_2\boldsymbol{n})\ldots(-\boldsymbol{n}\boldsymbol{z}_k\boldsymbol{n}) \\
&=\; \boldsymbol{z}_1'\boldsymbol{z}_2'\ldots\boldsymbol{z}_k' \;=\; (-1)^k\boldsymbol{A}_{\langle k\rangle}
\end{aligned}$$

[9] The minus sign in front of the terms $-\boldsymbol{n}\boldsymbol{z}_i\boldsymbol{n}$, $1 \le i \le k$, indicates the reflection in the $n-1$–dimensional subspace of $\boldsymbol{n} \in \mathbb{R}^{p,q}$, cf. example 2.2.

due to the associativity of the geometric product. The set $\{\boldsymbol{z'}_{1\ldots k}\}$ is a new frame for $\boldsymbol{A}_{\langle k\rangle}$ built of the reflected versions (see page 27) of the vectors $\{\boldsymbol{z}_{1\ldots k}\}$. The orthogonality is retained as can be seen by

$$\begin{aligned}
\boldsymbol{z}'_i \cdot \boldsymbol{z}'_j &= (-\boldsymbol{n}\boldsymbol{z}_i\boldsymbol{n}) \cdot (-\boldsymbol{n}\boldsymbol{z}_j\boldsymbol{n}) \\
&= \tfrac{1}{2}\Big(\boldsymbol{n}\boldsymbol{z}_i\boldsymbol{n}\boldsymbol{n}\boldsymbol{z}_j\boldsymbol{n} + \boldsymbol{n}\boldsymbol{z}_j\boldsymbol{n}\boldsymbol{n}\boldsymbol{z}_i\boldsymbol{n}\Big) \\
&= \boldsymbol{n}(\boldsymbol{z}_i \cdot \boldsymbol{z}_j)\boldsymbol{n} \;=\; \delta_{ij}.
\end{aligned}$$

In conclusion, the operation $\boldsymbol{n}\boldsymbol{A}_{\langle k\rangle}\boldsymbol{n}$, where $\boldsymbol{n}$ is contained in $\boldsymbol{A}_{\langle k\rangle}$, amounts to the reflection of the entire basis, thereby letting the subspace invariant. Also in general, if $\boldsymbol{n}$ is not or partly contained in $\boldsymbol{A}_{\langle k\rangle}$, the operation $\boldsymbol{n}\boldsymbol{A}_{\langle k\rangle}\boldsymbol{n}$ represents the reflection of $\boldsymbol{A}_{\langle k\rangle}$ in $\boldsymbol{n}$. The specific property of blades that particular operations as the reflection affect the basis is called *outermorphism* and is the subject of section 2.3.4.

Technically speaking, a vector is in fact a 1-blade. It is interesting that in this regard a certain property of vectors can be attributed to blades as well - blades square to scalars. The proof employs the previous proposition.

Corollary 2.10
For every blade $\boldsymbol{A}_{\langle k\rangle}$ it holds that

$$\boldsymbol{A}^2_{\langle k\rangle} \;\in\; \mathbb{R}.$$

<u>Proof</u>: *According to proposition 2.6, it exist k orthogonal vectors $\{\boldsymbol{z}_{1\ldots k}\}$ so that $\boldsymbol{A}_{\langle k\rangle} = \boldsymbol{z}_1\boldsymbol{z}_2\ldots\boldsymbol{z}_k$. Hence it may be written*

$$\begin{aligned}
\boldsymbol{A}_{\langle k\rangle}\boldsymbol{A}_{\langle k\rangle} &= \boldsymbol{z}_1\boldsymbol{z}_2\ldots\boldsymbol{z}_k\;\boldsymbol{z}_1\boldsymbol{z}_2\ldots\boldsymbol{z}_k \\
&= (-1)^{\frac{k\,(k-1)}{2}}\quad \boldsymbol{z}_1^2\,\boldsymbol{z}_2^2\,\ldots\,\boldsymbol{z}_k^2 \quad \in \mathbb{R}.
\end{aligned}$$

■

This shows that all possible grades $0, 2, 4, \ldots, 2k$ of the geometric product $\boldsymbol{A}^2_{\langle k\rangle}$ vanish except the scalar part. This gives rise to the next corollary.

Corollary 2.11
The geometric product of a blade $\boldsymbol{A}_{\langle k\rangle}$ with itself coincides with the inner product, i.e.

$$\boldsymbol{A}^2_{\langle k\rangle} \;=\; \langle\boldsymbol{A}_{\langle k\rangle}\boldsymbol{A}_{\langle k\rangle}\rangle \;=\; \boldsymbol{A}_{\langle k\rangle}\cdot\boldsymbol{A}_{\langle k\rangle}.$$

The example

$$(\boldsymbol{a}\wedge\boldsymbol{b})^2 \;=\; (\boldsymbol{a}\cdot\boldsymbol{b})^2 - \boldsymbol{a}^2\boldsymbol{b}^2$$

demonstrates that it is possible that a blade squares to zero as well:

Definition 2.6 (Null blades):
A blade $\boldsymbol{A}_{\langle k\rangle}$ is called a null blade if it squares to zero, or rather

$$\boldsymbol{A}_{\langle k\rangle} \cdot \boldsymbol{A}_{\langle k\rangle} \;=\; 0.$$

■

Null blades can only occur in algebras of mixed signature. Since every blade has a representation in terms of mutually orthogonal vectors, at least one of these vectors must at the same time be a null vector in order to have a null blade.

Example 2.6 (Null blades):
Consider the mutually orthogonal vectors $\boldsymbol{z}_1 = \mathbf{e}_1$, $\boldsymbol{z}_2 = \mathbf{e}_2$ and $\boldsymbol{z}_3 = \mathbf{e}_3 + \mathbf{e}_4$ from $\mathbb{R}^{3,1}$. Their outer product is $\boldsymbol{A}_{\langle k\rangle} = \mathbf{e}_1\mathbf{e}_2\mathbf{e}_3 + \mathbf{e}_1\mathbf{e}_2\mathbf{e}_4$. The square of $\boldsymbol{A}_{\langle k\rangle}$ is

$$\boldsymbol{A}^2_{\langle k\rangle} \;=\; -(\boldsymbol{z}_1\boldsymbol{z}_2\boldsymbol{z}_3)(\boldsymbol{z}_3\boldsymbol{z}_2\boldsymbol{z}_1) \;=\; -\boldsymbol{z}_1^2\boldsymbol{z}_2^2\boldsymbol{z}_3^2 \;=\; -(1)(1)(0) \;=\; 0$$

due to $\boldsymbol{z}_3^2 = 0$.

Next to blades it exists another important class of multivectors in $\mathbb{R}_{p,q}$.

Definition 2.7 (Versor):
A multivector is called a versor iff *it can be expressed as the geometric product of (invertible) non-null vectors.*

■

Note that with this definition any non-null blade is a versor at the same time. Furthermore, bear in mind that

$$\boldsymbol{V} \in \mathbb{R}_{p,q} \;\text{ versor} \qquad \not\Rightarrow \qquad \boldsymbol{V}^2 \in \mathbb{R}.$$

Another neat application of proposition 2.6 effortlessly shows that

$$\begin{aligned}
\boldsymbol{A}_{\langle k\rangle}\boldsymbol{b}\boldsymbol{A}_{\langle k\rangle} &= \boldsymbol{z}_1\boldsymbol{z}_2\ldots\boldsymbol{z}_k\;\boldsymbol{b}\;\boldsymbol{z}_1\boldsymbol{z}_2\ldots\boldsymbol{z}_k \\
&= (-1)^{\frac{k\,(k-1)}{2}}\quad \boldsymbol{z}_1\boldsymbol{z}_2\ldots\boldsymbol{z}_k\;\boldsymbol{b}\;\boldsymbol{z}_k\boldsymbol{z}_{k-1}\ldots\boldsymbol{z}_1 \\
&= (-1)^{\frac{k\,(k-1)}{2}}\quad \boldsymbol{z}_1(\boldsymbol{z}_2(\ldots(\boldsymbol{z}_{k-1}(\boldsymbol{z}_k\;\boldsymbol{b}\;\boldsymbol{z}_k)\boldsymbol{z}_{k-1})\ldots)\boldsymbol{z}_2)\boldsymbol{z}_1
\end{aligned}$$

is (apart from a scalar factor since $\boldsymbol{z}_i^2 \neq 1$, $i \in [1,k]_{\mathbb{Z}}$) nothing but a series of reflections of $\boldsymbol{b}$ in the vectors $\{\boldsymbol{z}_{1\ldots k}\}$. The result of $\boldsymbol{A}_{\langle k\rangle}\boldsymbol{b}\boldsymbol{A}_{\langle k\rangle}$ is therefore a vector as well, i.e.

$$\boldsymbol{A}_{\langle k\rangle}\boldsymbol{b}\boldsymbol{A}_{\langle k\rangle} \;\in\; \mathbb{R}^{p,q}. \tag{2.40}$$

It is known from linear algebra that a vector $\boldsymbol{a}$ can be decomposed with respect to its component $\boldsymbol{a}_{\|}$ inside and the component $\boldsymbol{a}_{\perp}$ outside a certain subspace $\boldsymbol{B}_{\langle l\rangle}$, i.e. $\boldsymbol{a} = \boldsymbol{a}_{\|} + \boldsymbol{a}_{\perp}$. A decomposition with respect to a vector - a 1-blade - is the subject of the considerations starting at page 26. In analogy to that 1-blade case as given by equation (2.17), it may be conjectured that $\boldsymbol{a}_{\|} = (\boldsymbol{a} \cdot \boldsymbol{B}_{\langle l \rangle})\boldsymbol{B}_{\langle l \rangle}$ and $\boldsymbol{a}_{\perp} = (\boldsymbol{a} \wedge \boldsymbol{B}_{\langle l \rangle})\boldsymbol{B}_{\langle l \rangle}$ is the decomposition of $\boldsymbol{a}$ with respect to $\boldsymbol{B}_{\langle l \rangle}$, whenever $\boldsymbol{B}_{\langle l \rangle}^2 = 1$. At first, it has to be verified that $(\boldsymbol{a} \cdot \boldsymbol{B}_{\langle l \rangle})\boldsymbol{B}_{\langle l \rangle}$ and $(\boldsymbol{a} \wedge \boldsymbol{B}_{\langle l \rangle})\boldsymbol{B}_{\langle l \rangle}$ are indeed vector valued. For this purpose the recent equation (2.40) is suitable. Naturally, it is sufficient to check that one of the terms is vector valued:

$$(\boldsymbol{a} \cdot \boldsymbol{B}_{\langle l \rangle})\boldsymbol{B}_{\langle l \rangle} \;=\; \tfrac{1}{2}\Big(\underbrace{\boldsymbol{a}\boldsymbol{B}_{\langle l \rangle}\boldsymbol{B}_{\langle l \rangle}}_{\in\, \mathbb{R}^{p,q}} - (-1)^l \underbrace{\boldsymbol{B}_{\langle l \rangle}\boldsymbol{a}\boldsymbol{B}_{\langle l \rangle}}_{\in\, \mathbb{R}^{p,q} \text{ by } (2.40)}\Big) \in \mathbb{R}^{p,q}$$

Second, building the anti-commutator of $(\boldsymbol{a} \cdot \boldsymbol{B}_{\langle l \rangle})\boldsymbol{B}_{\langle l \rangle}$ and $(\boldsymbol{a} \wedge \boldsymbol{B}_{\langle l \rangle})\boldsymbol{B}_{\langle l \rangle}$ demonstrates that, regardless of $\boldsymbol{B}_{\langle l \rangle}$, $\boldsymbol{a}_{\|}$ and $\boldsymbol{a}_{\perp}$ are orthogonal with respect to the inner product as assumed. This is denoted by writing $\boldsymbol{a}_{\|} \perp \boldsymbol{a}_{\perp}$. Third, it must be analyzed whether $\boldsymbol{a}_{\|}$ lies in $\boldsymbol{B}_{\langle l \rangle}$ and whether $\boldsymbol{a}_{\perp}$ is orthogonal to $\boldsymbol{B}_{\langle l \rangle}$. Reusing the previous expansion of $\boldsymbol{a}_{\|} = (\boldsymbol{a} \cdot \boldsymbol{B}_{\langle l \rangle})\boldsymbol{B}_{\langle l \rangle}$ it is

$$\begin{aligned}
\boldsymbol{a}_{\|} \wedge \boldsymbol{B}_{\langle l \rangle} \;=&\; \\
&\frac{1}{4}\boldsymbol{B}_{\langle l \rangle}^2\Big[\boldsymbol{a}\boldsymbol{B}_{\langle l \rangle} - (-1)^l\boldsymbol{B}_{\langle l \rangle}\boldsymbol{a} + (-1)^l\boldsymbol{B}_{\langle l \rangle}\boldsymbol{a} - (-1)^{2l}\boldsymbol{a}\boldsymbol{B}_{\langle l \rangle}\Big] \;=\; 0.
\end{aligned}$$

In the same way the orthogonality of $\boldsymbol{a}_{\perp}$ and $\boldsymbol{B}_{\langle l \rangle}$ can be proven, i.e. $\boldsymbol{a}_{\perp} \cdot \boldsymbol{B}_{\langle l \rangle} = 0$. Thus the generalization of equation (2.17) reads

$$\begin{aligned}
\boldsymbol{B}_{\langle l \rangle}^2 \;=\; 1 \quad \Longrightarrow \quad \boldsymbol{a} \;&=\; \boldsymbol{a}\boldsymbol{B}_{\langle l \rangle}\boldsymbol{B}_{\langle l \rangle} \\
&=\; (\underbrace{\boldsymbol{a} \cdot \boldsymbol{B}_{\langle l \rangle}}_{\boldsymbol{a}_{\|}\cdot\boldsymbol{B}_{\langle l \rangle}})\boldsymbol{B}_{\langle l \rangle} \;+\; (\underbrace{\boldsymbol{a} \wedge \boldsymbol{B}_{\langle l \rangle}}_{\boldsymbol{a}_{\perp}\wedge\boldsymbol{B}_{\langle l \rangle}})\boldsymbol{B}_{\langle l \rangle} \\
&=\; \underbrace{(\boldsymbol{a}_{\|} \cdot \boldsymbol{B}_{\langle l \rangle})\boldsymbol{B}_{\langle l \rangle}}_{\boldsymbol{a}_{\|}} \;+\; \underbrace{(\boldsymbol{a}_{\perp} \wedge \boldsymbol{B}_{\langle l \rangle})\boldsymbol{B}_{\langle l \rangle}}_{\boldsymbol{a}_{\perp}}. \qquad (2.41)
\end{aligned}$$

Note that the decomposition of a vector with respect to a general blade $\boldsymbol{B}_{\langle l \rangle}$, that means subject to the weaker condition $\boldsymbol{B}_{\langle l \rangle}^2 \neq 0$, is explained in section 2.3.5.
Self-evidently, $\boldsymbol{a}_{\|}$ and $\boldsymbol{a}_{\perp}$ are, in general, only orthogonal for the currently chosen signature of the inner product. This shall be illustrated by an example.

Example 2.7 (Orthogonality vs. perpendicularity):
Consider the algebra $\mathbb{R}_{1,2}$ *with* $\mathbf{e}_1^2 = +1$ *and* $\mathbf{e}_2^2 = \mathbf{e}_3^2 = -1$*. The three vectors*

$$\begin{aligned}
\boldsymbol{a} \;&=\; 2\mathbf{e}_1 + \mathbf{e}_2 + \mathbf{e}_3 \\
\boldsymbol{b}_1 \;&=\; \mathbf{e}_1 + 4\mathbf{e}_2 - 2\mathbf{e}_3 \\
\boldsymbol{b}_2 \;&=\; 2\mathbf{e}_1 + \mathbf{e}_2 + 3\mathbf{e}_3
\end{aligned}$$

are related to each other by

$$\boldsymbol{b}_1 *_{\boldsymbol{\varepsilon}} \boldsymbol{b}_2 \;=\; 0 \qquad \begin{aligned} \boldsymbol{a} \cdot \boldsymbol{b}_1 \;&=\; 0 \\ \boldsymbol{a} \cdot \boldsymbol{b}_2 \;&=\; 0 \end{aligned} \qquad \begin{aligned} \boldsymbol{a} *_{\boldsymbol{\varepsilon}} \boldsymbol{b}_1 \;&=\; 4 \\ \boldsymbol{a} *_{\boldsymbol{\varepsilon}} \boldsymbol{b}_2 \;&=\; 8 \end{aligned} \;,$$

where '$*_\varepsilon$' denotes the Euclidean scalar product. If, as in the example, a Euclidean vector space is taken as a basis, then $\boldsymbol{a}$ still has components in $\boldsymbol{b}_1 \wedge \boldsymbol{b}_2 = 7(\mathbf{e}_1\mathbf{e}_3 - \mathbf{e}_1\mathbf{e}_2 + 2\mathbf{e}_2\mathbf{e}_3)$ although it is orthogonal to $\{\boldsymbol{b}_1, \boldsymbol{b}_2\}$ regarding the inner product.

Corollary 2.12

Let $\boldsymbol{a} = \boldsymbol{x} + \boldsymbol{y}$ be the decomposition of the vector $\boldsymbol{a} \in \mathbb{R}^{p,q}$ w.r.t the subspace $\boldsymbol{B}_{\langle l\rangle} \in \mathbb{R}_{p,q}$ such that $\boldsymbol{x} \wedge \boldsymbol{B}_{\langle l\rangle} = 0$, $\boldsymbol{x}^2 \neq 0$ and $\boldsymbol{y} \cdot \boldsymbol{B}_{\langle l\rangle} = 0$. If $\boldsymbol{B}^2_{\langle l\rangle} \neq 0$, then the inner product of $\boldsymbol{a}$ and $\boldsymbol{B}_{\langle l\rangle}$ is a blade of grade $l-1$.

Proof: *Recall that an orthogonal basis of $\boldsymbol{B}_{\langle l\rangle}$ can be determined such that $\boldsymbol{x}$ is part of it. Hence let $\{\boldsymbol{x}, \boldsymbol{z}_1, \boldsymbol{z}_2, \ldots, \boldsymbol{z}_{l-1}\}$ be an adequate basis of $\boldsymbol{B}_{\langle l\rangle}$, i.e. $\boldsymbol{B}_{\langle l\rangle} = \boldsymbol{x}\boldsymbol{z}_1\boldsymbol{z}_2 \ldots \boldsymbol{z}_{l-1}$. Then*

$$
\begin{aligned}
\boldsymbol{a} \cdot \boldsymbol{B}_{\langle l\rangle} &= \boldsymbol{a} \cdot (\boldsymbol{x}\boldsymbol{z}_1\boldsymbol{z}_2 \ldots \boldsymbol{z}_{l-1}) \\
&= \boldsymbol{x} \cdot (\boldsymbol{x}\boldsymbol{z}_1\boldsymbol{z}_2 \ldots \boldsymbol{z}_{l-1}) \\
&= \tfrac{1}{2}\Big(\boldsymbol{x}\boldsymbol{x}\boldsymbol{z}_1\boldsymbol{z}_2 \ldots \boldsymbol{z}_{l-1} - (-1)^l \boldsymbol{x}\boldsymbol{z}_1\boldsymbol{z}_2 \ldots \boldsymbol{z}_{l-1}\boldsymbol{x}\Big) \\
&= \tfrac{1}{2}\Big(\boldsymbol{x}\boldsymbol{x}\boldsymbol{z}_1\boldsymbol{z}_2 \ldots \boldsymbol{z}_{l-1} - (-1)^l\,(-1)^{l-1} \boldsymbol{x}\boldsymbol{x}\boldsymbol{z}_1\boldsymbol{z}_2 \ldots \boldsymbol{z}_{l-1}\Big) \\
&= \boldsymbol{x}^2\ \underbrace{\boldsymbol{z}_1\boldsymbol{z}_2 \ldots \boldsymbol{z}_{l-1}}_{l\text{–}1\text{ - blade}}.
\end{aligned}
$$

■

Because $\boldsymbol{y}$ is orthogonal to $\boldsymbol{B}_{\langle l\rangle}$ and since $\boldsymbol{x}$ is assumed to be orthogonal to the frame $\{\boldsymbol{z}_1, \boldsymbol{z}_2, \ldots, \boldsymbol{z}_{l-1}\}$ as well, $\boldsymbol{a}$ must altogether be orthogonal to $\boldsymbol{a} \cdot \boldsymbol{B}_{\langle l\rangle}$. This is easily ascertained by observing that $\boldsymbol{a} \cdot (\boldsymbol{a} \cdot \boldsymbol{B}_{\langle l\rangle}) = (\boldsymbol{a} \wedge \boldsymbol{a}) \cdot \boldsymbol{B}_{\langle l\rangle}$. The blade $\boldsymbol{a} \cdot \boldsymbol{B}_{\langle l\rangle}$ is said to be the orthogonal complement of $\boldsymbol{a}$ in $\boldsymbol{B}_{\langle l\rangle}$. By observing that $(\boldsymbol{a}_1 \wedge \boldsymbol{a}_2) \cdot \boldsymbol{B}_{\langle l\rangle} = \boldsymbol{a}_1 \cdot (\boldsymbol{a}_2 \cdot \boldsymbol{B}_{\langle l\rangle})$, or generally by equation (2.38), it must be deduced that $(\bigwedge_{i=1}^k \boldsymbol{a}_i) \cdot \boldsymbol{B}_{\langle l\rangle}$ represents the part of $\boldsymbol{B}_{\langle l\rangle}$ orthogonal to each vector in $\{\boldsymbol{a}_{1\ldots k}\}$. The inner product $\boldsymbol{A}_{\langle k\rangle} \cdot \boldsymbol{B}_{\langle l\rangle}$, $k < l$, is therefore the orthogonal complement of $\boldsymbol{A}_{\langle k\rangle}$ in $\boldsymbol{B}_{\langle l\rangle}$, i.e.

$$\boldsymbol{A}_{\langle k\rangle} \cdot (\boldsymbol{A}_{\langle k\rangle} \cdot \boldsymbol{B}_{\langle l\rangle}) \ = \ 0, \qquad k < l. \tag{2.42}$$

Substituting $\boldsymbol{A}_{\langle k\rangle} \cdot \boldsymbol{B}_{\langle l\rangle}$ for $\boldsymbol{A}_{\langle k\rangle}$ immediately leads to

$$(\boldsymbol{A}_{\langle k\rangle} \cdot \boldsymbol{B}_{\langle l\rangle}) \cdot \Big[(\boldsymbol{A}_{\langle k\rangle} \cdot \boldsymbol{B}_{\langle l\rangle}) \cdot \boldsymbol{B}_{\langle l\rangle}\Big] \ = \ 0. \tag{2.43}$$

Corollary 2.13

The inner product of a vector $\boldsymbol{a}$ and a blade $\boldsymbol{B}_{\langle l\rangle}$, $\boldsymbol{B}^2_{\langle l\rangle} \neq 0$, is zero, iff *$\boldsymbol{a}$ lies entirely in the orthogonal complement of $\boldsymbol{B}_{\langle l\rangle}$ in $\mathbb{R}^{p,q}$. This may be expressed by*

$$\boldsymbol{a} \cdot \boldsymbol{B}_{\langle l\rangle} \ = \ 0 \quad \overset{\boldsymbol{B}^2_{\langle l\rangle} \neq 0}{\Longleftrightarrow} \quad \boldsymbol{a} \ \perp \ \boldsymbol{B}_{\langle l\rangle}.$$

Corollary 2.14

If one blade $\boldsymbol{A}_{\langle k\rangle}$, $\boldsymbol{A}^2_{\langle k\rangle} \neq 0$, is contained in the space of another blade $\boldsymbol{B}_{\langle l\rangle}$, $\boldsymbol{B}^2_{\langle l\rangle} \neq 0$ and $l \geq k$, the blades satisfy the right side of the following relation

$$\forall \boldsymbol{x} \in \mathbb{R}^{p,q} :$$

$$\boldsymbol{x} \wedge \boldsymbol{A}_{\langle k\rangle} = 0 \Rightarrow \boldsymbol{x} \wedge \boldsymbol{B}_{\langle l\rangle} = 0 \qquad \Longrightarrow \qquad \boldsymbol{A}_{\langle k\rangle}\boldsymbol{B}_{\langle l\rangle} \;=\; \boldsymbol{A}_{\langle k\rangle} \cdot \boldsymbol{B}_{\langle l\rangle}$$

Proof: *Let $\{\boldsymbol{a}_1, \boldsymbol{a}_2, \ldots, \boldsymbol{a}_k, \boldsymbol{b}_{k+1}, \boldsymbol{b}_{k+2}, \ldots, \boldsymbol{b}_l\}$ be an orthogonal basis of $\boldsymbol{B}_{\langle l\rangle}$ such that $\{\boldsymbol{a}_{1\ldots k}\}$ is a frame for $\boldsymbol{A}_{\langle k\rangle}$ at the same time. Hence $\boldsymbol{B}_{\langle l\rangle} = \boldsymbol{a}_1\boldsymbol{a}_2 \ldots \boldsymbol{a}_k\boldsymbol{b}_{k+1}\boldsymbol{b}_{k+2} \ldots \boldsymbol{b}_l$ and*

$$\begin{aligned} \boldsymbol{A}_{\langle k\rangle}\boldsymbol{B}_{\langle l\rangle} &= \boldsymbol{a}_1\boldsymbol{a}_2 \ldots \boldsymbol{a}_k \; \boldsymbol{a}_1\boldsymbol{a}_2 \ldots \boldsymbol{a}_k\boldsymbol{b}_{k+1}\boldsymbol{b}_{k+2} \ldots \boldsymbol{b}_l \\ &= (-1)^{\frac{k(k-1)}{2}} \; \boldsymbol{a}_1^2\boldsymbol{a}_2^2 \ldots \boldsymbol{a}_k^2 \;\; \boldsymbol{b}_{k+1}\boldsymbol{b}_{k+2} \ldots \boldsymbol{b}_l. \end{aligned}$$

The resultant element is a blade of grade $l - k$. Thus

$$\boldsymbol{A}_{\langle k\rangle}\boldsymbol{B}_{\langle l\rangle} \;=\; \left\langle \boldsymbol{A}_{\langle k\rangle}\boldsymbol{B}_{\langle l\rangle} \right\rangle_{l-k} \;=\; \boldsymbol{A}_{\langle k\rangle} \cdot \boldsymbol{B}_{\langle l\rangle}.$$

■

Regarding the recent considerations in terms of a vector $\boldsymbol{a}$ and a blade $\boldsymbol{B}_{\langle l\rangle}$, $l \geq 2$, it can be inferred that

$$\begin{aligned} (\boldsymbol{a} \cdot \boldsymbol{B}_{\langle l\rangle})\boldsymbol{B}_{\langle l\rangle} &= (\boldsymbol{a} \cdot \boldsymbol{B}_{\langle l\rangle}) \cdot \boldsymbol{B}_{\langle l\rangle} \\ (\boldsymbol{a} \wedge \boldsymbol{B}_{\langle l\rangle})\boldsymbol{B}_{\langle l\rangle} &= (\boldsymbol{a} \wedge \boldsymbol{B}_{\langle l\rangle}) \cdot \boldsymbol{B}_{\langle l\rangle}. \end{aligned}$$

For the remainder of this text let

$$[\boldsymbol{A}_{\langle k\rangle} \backslash \boldsymbol{a}_i] \;:=\; 1 \wedge \boldsymbol{a}_1 \wedge \boldsymbol{a}_2 \wedge \ldots \boldsymbol{a}_{i-1} \wedge \boldsymbol{a}_{i+1} \wedge \ldots \wedge \boldsymbol{a}_k$$

be a blade of grade $k - 1$. In addition, the canonical generalization of $[\boldsymbol{A}_{\langle k\rangle} \backslash \boldsymbol{a}_i]$ regarding a set of vectors reads

$$\Big[\boldsymbol{A}_{\langle k\rangle} \backslash \bigcup_{j=1}^{m} \boldsymbol{a}_j\Big].$$

Example 2.8 (Basis orthogonalization):
Here the orthogonal complement of $[\boldsymbol{A}_{\langle k\rangle}\backslash\boldsymbol{a}_i]$ *in* $\boldsymbol{A}_{\langle k\rangle}$ *is to be analyzed. Let* $\boldsymbol{A}_{\langle k\rangle}$ *be a non-null blade, i.e.* $\boldsymbol{A}^2_{\langle k\rangle} \neq 0$*, with basis* $\{\boldsymbol{a}_{1\ldots k}\}$*. Then*

$$\begin{aligned}
[\boldsymbol{A}_{\langle k\rangle}\backslash\boldsymbol{a}_i]\ \boldsymbol{A}_{\langle k\rangle} &= [\boldsymbol{A}_{\langle k\rangle}\backslash\boldsymbol{a}_i]\Big([\boldsymbol{A}_{\langle k\rangle}\backslash\boldsymbol{a}_i] \wedge (-1)^{k-i}\ \boldsymbol{a}_i\Big) \\
&= (-1)^{k-i}\ [\boldsymbol{A}_{\langle k\rangle}\backslash\boldsymbol{a}_i]^2\ \ \boldsymbol{a}_{i\perp}.
\end{aligned}$$

Hence with

$$\boldsymbol{b}_i\ :=\ (-1)^{k-i}\ \frac{[\boldsymbol{A}_{\langle k\rangle}\backslash\boldsymbol{a}_i]\ \boldsymbol{A}_{\langle k\rangle}}{[\boldsymbol{A}_{\langle k\rangle}\backslash\boldsymbol{a}_i]^2},$$

it follows $\forall i,j \in [1,k]_{\mathbb{Z}}$:

$$i \neq j \quad\Longleftrightarrow\quad \boldsymbol{b}_i \cdot \boldsymbol{a}_j = 0$$

Starting from the expansion of $\boldsymbol{a}\cdot\boldsymbol{A}_{[k]}$, given in equation (2.23), it is now being focused on the expansion of $\boldsymbol{a}\cdot\boldsymbol{A}_{\langle k\rangle}$: proposition 2.7 is of fundamental significance as it, for example, expresses a kind of distributive law for the inner product over the outer product.

Proposition 2.7
Given a vector $\boldsymbol{a}$ *and a blade* $\boldsymbol{B}_{\langle l\rangle} = \bigwedge_{i=1}^{l}\boldsymbol{b}_i$ *the following expansion can be used*

$$\boldsymbol{a}\cdot\boldsymbol{B}_{\langle l\rangle}\ =\ \sum_{i=1}^{l}(-1)^{i-1}(\boldsymbol{a}\cdot\boldsymbol{b}_i)\ [\boldsymbol{B}_{\langle l\rangle}\backslash\boldsymbol{b}_i]$$

Proof: *Let* $\boldsymbol{B} = \boldsymbol{b}_1\boldsymbol{b}_2\ldots\boldsymbol{b}_l$ *the geometric product of the vectors* $\{\boldsymbol{b}_{1\ldots l}\}$ *such that* $\boldsymbol{a}\cdot\boldsymbol{B}_{\langle l\rangle} = \boldsymbol{a}\cdot\langle\boldsymbol{B}\rangle_l = \langle\boldsymbol{a}\cdot\boldsymbol{B}\rangle_{l-1}$*. Consequently, it is*

$$\begin{aligned}
\boldsymbol{a}\cdot\boldsymbol{B}_{\langle l\rangle} &= \tfrac{1}{2}\Big(\boldsymbol{a}\,\langle\boldsymbol{B}\rangle_l\ -\ (-1)^l\langle\boldsymbol{B}\rangle_l\boldsymbol{a}\Big) \\
&= \Big\langle\ \tfrac{1}{2}\big(\boldsymbol{a}\boldsymbol{B}\ -\ (-1)^l\boldsymbol{B}\boldsymbol{a}\big)\ \Big\rangle_{l-1}.
\end{aligned}$$

According to the derivations on page 30, the inner term can be replaced as

$$\begin{aligned}
\boldsymbol{a}\cdot\boldsymbol{B}_{\langle l\rangle} &= \Big\langle\sum_{i=1}^{l}(-1)^{i-1}\,(\boldsymbol{a}\cdot\boldsymbol{b}_i)\,\boldsymbol{b}_1\boldsymbol{b}_2\ldots\check{\boldsymbol{b}}_i\ldots\boldsymbol{b}_l\Big\rangle_{l-1} \\
&= \sum_{i=1}^{l}(-1)^{i-1}\,(\boldsymbol{a}\cdot\boldsymbol{b}_i)\,\langle\boldsymbol{b}_1\boldsymbol{b}_2\ldots\check{\boldsymbol{b}}_i\ldots\boldsymbol{b}_l\rangle_{l-1} \\
&= \sum_{i=1}^{l}(-1)^{i-1}\,(\boldsymbol{a}\cdot\boldsymbol{b}_i)\ \underbrace{\langle\boldsymbol{b}_1\boldsymbol{b}_2\ldots\check{\boldsymbol{b}}_i\ldots\boldsymbol{b}_l\rangle_{l-1}}_{[\boldsymbol{B}_{\langle l\rangle}\backslash\boldsymbol{b}_i]}
\end{aligned}$$

■

Pursuant to corollary 2.12, the linear combination of blades $[\boldsymbol{B}_{\langle l\rangle}\backslash \boldsymbol{b}_i]$ obtained from $\boldsymbol{a}\cdot\boldsymbol{B}_{\langle l\rangle}$ still represents a blade.

The eight commutator identities (A.1) - (A.8) stated on page 243 are of value as many interesting geometric algebra identities can be derived from them, especially when working with vectors. Four of them have already been used in section 2.1.3. The expression $(A\overline{\times}B)\underline{\times}C$, for example, will attain zero whenever vectors are substituted for A and B. Also, if two variables stand for a blade, say $A = C = \boldsymbol{A}_{\langle k\rangle}$, then a scalar is obtained for $\boldsymbol{A}_{\langle k\rangle}\overline{\times}\boldsymbol{A}_{\langle k\rangle} = \boldsymbol{A}^2_{\langle k\rangle}$. By looking for these special cases, the following rules can additionally be derived.

$$
\begin{array}{rrclcl}
1. & (\boldsymbol{a}\wedge\boldsymbol{b})\cdot\boldsymbol{c} & \overset{(A.1)}{=} & \boldsymbol{a}\cdot(\boldsymbol{b}\wedge\boldsymbol{c}) & + & (\boldsymbol{a}\wedge\boldsymbol{c})\cdot\boldsymbol{b} \\
2. & \boldsymbol{A}_{\langle k\rangle}\underline{\times}(\boldsymbol{b}\wedge\boldsymbol{c}) & \overset{(A.1,A.8)}{=} & (\boldsymbol{A}_{\langle k\rangle}\cdot\boldsymbol{b})\wedge\boldsymbol{c} & - & (\boldsymbol{A}_{\langle k\rangle}\cdot\boldsymbol{c})\wedge\boldsymbol{b} \\
3. & \boldsymbol{A}_{\langle k\rangle}\underline{\times}(\boldsymbol{b}\wedge\boldsymbol{c}) & \overset{(A.1,A.8)}{=} & (\boldsymbol{A}_{\langle k\rangle}\wedge\boldsymbol{b})\cdot\boldsymbol{c} & - & (\boldsymbol{A}_{\langle k\rangle}\wedge\boldsymbol{c})\cdot\boldsymbol{b} \\
4. & \boldsymbol{A}_{\langle k\rangle}\overline{\times}(\boldsymbol{b}\wedge\boldsymbol{c}) & \overset{(A.3,A.6)}{=} & (\boldsymbol{A}_{\langle k\rangle}\cdot\boldsymbol{b})\cdot\boldsymbol{c} & - & (\boldsymbol{A}_{\langle k\rangle}\wedge\boldsymbol{c})\wedge\boldsymbol{b} \\
5. & \boldsymbol{A}_{\langle k\rangle}(\boldsymbol{b}\cdot\boldsymbol{c}) & \overset{(A.2,A.7)}{=} & (\boldsymbol{A}_{\langle k\rangle}\cdot\boldsymbol{b})\wedge\boldsymbol{c} & + & (\boldsymbol{A}_{\langle k\rangle}\wedge\boldsymbol{c})\cdot\boldsymbol{b} \\
6. & (\boldsymbol{A}_{\langle k\rangle}\underline{\times}\boldsymbol{b})\overline{\times}\boldsymbol{A}_{\langle k\rangle} & \overset{(A.3)}{=} & 0 & & \\
7. & (\boldsymbol{A}_{\langle k\rangle}\overline{\times}\boldsymbol{b})\underline{\times}\boldsymbol{A}_{\langle k\rangle} & \overset{(A.5)}{=} & 0 & &
\end{array}
\tag{2.44}
$$

The two last identities are helpful if, for example, the expression $\boldsymbol{A}_{\langle k\rangle}\boldsymbol{b}\boldsymbol{A}_{\langle k\rangle}$ is to be expanded. The fifth identity can be used to prove, by induction on the grade, that $\boldsymbol{a}\cdot\boldsymbol{B}_{\langle l\rangle}$ is generally a blade of grade $l-1$. The inductive step $s-1\mapsto s$ would be

$$
([\boldsymbol{B}_{\langle s\rangle}\backslash\boldsymbol{b}_s]\wedge\boldsymbol{b}_s)\cdot\boldsymbol{a} \;=\; \underbrace{[\boldsymbol{B}_{\langle s\rangle}\backslash\boldsymbol{b}_s]\;(\boldsymbol{b}_s\cdot\boldsymbol{a})}_{s-1\text{-blade}} \;-\; \overbrace{\underbrace{([\boldsymbol{B}_{\langle s\rangle}\backslash\boldsymbol{b}_s]\cdot\boldsymbol{a})}_{\substack{s-2\text{- blade by}\\ \text{ind. hypothesis}}}\wedge\boldsymbol{b}_s}^{s-1\text{-blade}}.
$$

For the next fundamental proposition the following definition is needed.

Definition 2.8 ((u,v)-shuffle):
Let $l = u+v$. A (u,v)-shuffle is a special permutation from the set

$$
\mathcal{S}(u,v) = \left\{ \sigma\in\mathcal{S}(l) \;\middle|\; \begin{array}{l} 1\le \sigma(1) < \sigma(2) < \ldots < \sigma(u)\le l \\ 1\le\sigma(u+1) < \sigma(u+2) < \ldots < \sigma(l) \le l \end{array} \right\}.
$$

It is $\mathcal{S}(u,v)\subseteq\mathcal{S}(u+v)$. ■

Some $(3,4)$-shuffles $\sigma\in\mathcal{S}(3,4)$ of $(1,2,\ldots,7)$ are for example

$$
\begin{aligned}
\big(\sigma(1),\sigma(2),\ldots,\sigma(7)\big) = \;& (1,2,3,\ 4,5,6,7), \\
& (5,6,7,\ 1,2,3,4), \\
& (1,4,7,\ 2,3,5,6),\ \ \ldots
\end{aligned}
$$

As a (u,v)-shuffle is uniquely defined by the first u elements it follows that the cardinality of $\mathcal{S}(u,v)$ is $\binom{u+v}{u}$ or $\binom{u+v}{v}$, respectively.

Proposition 2.8

The inner product of two blades $\boldsymbol{A}_{\langle k\rangle}$ and $\boldsymbol{B}_{\langle l\rangle}$, $k \leq l$, can be expanded as follows

$$\boldsymbol{A}_{\langle k\rangle} \cdot \boldsymbol{B}_{\langle l\rangle} = \sum_{\sigma \in \mathcal{S}(k,l-k)} sgn(\sigma) \; \Big(\boldsymbol{A}_{\langle k\rangle} \cdot (\boldsymbol{b}_{\sigma_1} \wedge \boldsymbol{b}_{\sigma_2} \wedge ... \wedge \boldsymbol{b}_{\sigma_k})\Big)\Big[\boldsymbol{B}_{\langle l\rangle} \backslash \bigcup_{r=1}^{k} \boldsymbol{b}_{\sigma_r}\Big],$$

with the abbreviation $\sigma_i := \sigma(i)$, $1 \leq i \leq l$.

The *proof* of proposition 2.8 is somewhat extensive and can be found in section A.3.3 on page 247.

Example 2.9 (Inner product of blades):

Consider the blades $\boldsymbol{A}_{\langle 2\rangle} = \boldsymbol{a}_1 \wedge \boldsymbol{a}_2$ and $\boldsymbol{B}_{\langle 4\rangle} = \boldsymbol{b}_1 \wedge \boldsymbol{b}_2 \wedge \boldsymbol{b}_3 \wedge \boldsymbol{b}_4$. According to proposition 2.8, their inner product can be evaluated via

$$\begin{aligned} \boldsymbol{A}_{\langle 2\rangle} \cdot \boldsymbol{B}_{\langle 4\rangle} = &+ \big[\boldsymbol{A}_{\langle 2\rangle} \cdot (\boldsymbol{b}_1 \wedge \boldsymbol{b}_2)\big]\,(\boldsymbol{b}_3 \wedge \boldsymbol{b}_4) - \big[\boldsymbol{A}_{\langle 2\rangle} \cdot (\boldsymbol{b}_1 \wedge \boldsymbol{b}_3)\big]\,(\boldsymbol{b}_2 \wedge \boldsymbol{b}_4) \\ &+ \big[\boldsymbol{A}_{\langle 2\rangle} \cdot (\boldsymbol{b}_1 \wedge \boldsymbol{b}_4)\big]\,(\boldsymbol{b}_2 \wedge \boldsymbol{b}_3) + \big[\boldsymbol{A}_{\langle 2\rangle} \cdot (\boldsymbol{b}_2 \wedge \boldsymbol{b}_3)\big]\,(\boldsymbol{b}_1 \wedge \boldsymbol{b}_4) \\ &- \big[\boldsymbol{A}_{\langle 2\rangle} \cdot (\boldsymbol{b}_2 \wedge \boldsymbol{b}_4)\big]\,(\boldsymbol{b}_1 \wedge \boldsymbol{b}_3) + \big[\boldsymbol{A}_{\langle 2\rangle} \cdot (\boldsymbol{b}_3 \wedge \boldsymbol{b}_4)\big]\,(\boldsymbol{b}_1 \wedge \boldsymbol{b}_2) \end{aligned}$$

It remains to specify how the inner part $\boldsymbol{A}_{\langle k\rangle} \cdot (\boldsymbol{b}_{\mathsf{v}_1} \wedge \boldsymbol{b}_{\mathsf{v}_2} \wedge ... \wedge \boldsymbol{b}_{\mathsf{v}_k})$ of the equation in the previous proposition can be calculated[10]. This can be achieved by combining corollary 2.8, stating that $\boldsymbol{A}_{\langle k\rangle} \cdot \boldsymbol{B}_{\langle k\rangle} = [\boldsymbol{A}_{\langle k\rangle} \backslash \boldsymbol{a}_k] \cdot (\boldsymbol{a}_k \cdot \boldsymbol{B}_{\langle k\rangle})$, with proposition 2.7 in a distributive manner.

Corollary 2.15

The inner product of two blades $\boldsymbol{A}_{\langle k\rangle}$ and $\boldsymbol{B}_{\langle k\rangle}$ of equal grade can be calculated by means of the repetitive application of

$$\boldsymbol{A}_{\langle k\rangle} \cdot \boldsymbol{B}_{\langle k\rangle} = \sum_{i=1}^{k} (-1)^{i-1}\,(\boldsymbol{a}_k \cdot \boldsymbol{b}_i)\,[\boldsymbol{A}_{\langle k\rangle} \backslash \boldsymbol{a}_k] \cdot [\boldsymbol{B}_{\langle k\rangle} \backslash \boldsymbol{b}_i].$$

This can, however, be generalized a little more.

[10] The exactly matching expression and the proof are stated on page 250.

Proposition 2.9

The inner product of two blades $\boldsymbol{A}_{\langle k \rangle}$ and $\boldsymbol{B}_{\langle k \rangle}$ of equal grade can be calculated via

$$\boldsymbol{A}_{\langle k \rangle} \cdot \boldsymbol{B}_{\langle k \rangle} \;=\; \sum_{\sigma \in \mathcal{S}(k)} sgn(\sigma) \prod_{j=1}^{k} \left(\boldsymbol{a}_{k-(j-1)} \cdot \boldsymbol{b}_{\sigma(j)} \right).$$

Example 2.10 (Inner product of blades of equal grade):

Let $\boldsymbol{A}_{\langle 3 \rangle} = \boldsymbol{a}_1 \wedge \boldsymbol{a}_2 \wedge \boldsymbol{a}_3$ and $\boldsymbol{B}_{\langle 3 \rangle} = \boldsymbol{b}_1 \wedge \boldsymbol{b}_2 \wedge \boldsymbol{b}_3$.

$$\begin{aligned}
\boldsymbol{A}_{\langle 3 \rangle} \cdot \boldsymbol{B}_{\langle 3 \rangle} \;=\; & + \; (\boldsymbol{a}_3 \cdot \boldsymbol{b}_1)\,(\boldsymbol{a}_2 \cdot \boldsymbol{b}_2)\,(\boldsymbol{a}_1 \cdot \boldsymbol{b}_3), && \sigma = (1,2,3)\\
& - \; (\boldsymbol{a}_3 \cdot \boldsymbol{b}_1)\,(\boldsymbol{a}_2 \cdot \boldsymbol{b}_3)\,(\boldsymbol{a}_1 \cdot \boldsymbol{b}_2), && \sigma = (1,3,2)\\
& - \; (\boldsymbol{a}_3 \cdot \boldsymbol{b}_2)\,(\boldsymbol{a}_2 \cdot \boldsymbol{b}_1)\,(\boldsymbol{a}_1 \cdot \boldsymbol{b}_3), && \sigma = (2,1,3)\\
& + \; (\boldsymbol{a}_3 \cdot \boldsymbol{b}_2)\,(\boldsymbol{a}_2 \cdot \boldsymbol{b}_3)\,(\boldsymbol{a}_1 \cdot \boldsymbol{b}_1), && \sigma = (2,3,1)\\
& + \; (\boldsymbol{a}_3 \cdot \boldsymbol{b}_3)\,(\boldsymbol{a}_2 \cdot \boldsymbol{b}_1)\,(\boldsymbol{a}_1 \cdot \boldsymbol{b}_2), && \sigma = (3,1,2)\\
& - \; (\boldsymbol{a}_3 \cdot \boldsymbol{b}_3)\,(\boldsymbol{a}_2 \cdot \boldsymbol{b}_2)\,(\boldsymbol{a}_1 \cdot \boldsymbol{b}_1), && \sigma = (3,2,1)
\end{aligned}$$

The special case $\boldsymbol{A}_{\langle 2 \rangle} = \boldsymbol{a}_1 \wedge \boldsymbol{a}_2$ and $\boldsymbol{B}_{\langle 2 \rangle} = \boldsymbol{b}_1 \wedge \boldsymbol{b}_2$ results in

$$(\boldsymbol{a}_1 \wedge \boldsymbol{a}_2) \cdot (\boldsymbol{b}_1 \wedge \boldsymbol{b}_2) \;=\; (\boldsymbol{a}_2 \cdot \boldsymbol{b}_1)\,(\boldsymbol{a}_1 \cdot \boldsymbol{b}_2) \;-\; (\boldsymbol{a}_2 \cdot \boldsymbol{b}_2)\,(\boldsymbol{a}_1 \cdot \boldsymbol{b}_1), \tag{2.45}$$

which is known as the *Binet-Cauchy identity*.

Now let $I_{k/n}$ be defined as on page 32. Then, a more general version of the identity, expressed in matrix notation, reads

$$\det(\mathsf{A}^{\mathsf{T}}\mathsf{B}) \;=\; \sum_{\mathsf{v} \in I_{k/n}} \det(\mathsf{A}^{\mathsf{T}}|^{\mathsf{v}}) \det(\mathsf{B}|_{\mathsf{v}}), \qquad \mathsf{A}, \mathsf{B} \;\in \mathbb{R}^{n \times k},\; k < n. \tag{2.46}$$

From the definition (2.31) of the outer product it follows

$$\begin{aligned}
(\bigwedge_{i=1}^{k} \boldsymbol{a}_i) \cdot (\bigwedge_{i=1}^{k} \boldsymbol{b}_i) \;&=\; \sum_{\mathsf{v} \in I_{k/n}} \det(\mathsf{A}|_{\mathsf{v}}) \det(\mathsf{B}|_{\mathsf{v}})\; (\mathbf{e}_{\mathsf{v}(1)}\mathbf{e}_{\mathsf{v}(2)} \ldots \mathbf{e}_{\mathsf{v}(k)})^2\\
&=\; \sum_{\mathsf{v} \in I_{k/n}} \det(\mathsf{A}^{\mathsf{T}}|^{\mathsf{v}}) \det(\mathsf{B}|_{\mathsf{v}})\; (\mathbf{e}_{\mathsf{v}(1)}\mathbf{e}_{\mathsf{v}(2)} \ldots \mathbf{e}_{\mathsf{v}(k)})^2,
\end{aligned} \tag{2.47}$$

where the columns of the matrices $\mathsf{A} \in \mathbb{R}^{n \times k}$ and $\mathsf{B} \in \mathbb{R}^{n \times k}$ hold the coefficients of the vectors, e.g. $\boldsymbol{a}_i = \mathsf{A}_i{}^j \mathbf{e}_j,\; i \in [1,k]_{\mathbb{Z}}$. This shows that proposition 2.9 is in fact the Binet-Cauchy identity[11].

[11] Since the term $(\mathbf{e}_{\mathsf{v}(1)}\mathbf{e}_{\mathsf{v}(2)} \ldots \mathbf{e}_{\mathsf{v}(k)})^2$ in equation (2.47) might square to minus one, equation (2.46) is reliably obtained by employing the *conjugate* $\boldsymbol{A}_{\langle k \rangle} \cdot \boldsymbol{B}^{\dagger}_{\langle k \rangle}$, see section 2.3.2.

2.3 Extended Concepts of GA

In this section several ideas are to be introduced by means of which important GA operations can be carried out. These ideas are related to special constructs as the reverse, the inverse or meet and join. Also, the concept of duality, the practical role of outermorphisms and the mechanisms behind transformations like rotations are to be dealt with.

Null blades

> *Note that many relations presented in the first part of this section are not universally valid in that the existence of null blades is not taken into account. In such cases hints are given at the respective passages or equations.*
> *Adaptations to null blades are subject of section 2.3.5.*

At first it is focused on one of the most important involutions of geometric algebra - the reverse.

2.3.1 Reverse

Indirectly, the reverse has already been used in the context of corollary 2.10. There the order of anti-commuting vectors in $\boldsymbol{A}_{\langle k \rangle}$ has been switched from $\boldsymbol{z}_1\boldsymbol{z}_2\ldots\boldsymbol{z}_k$ to $\boldsymbol{z}_k\boldsymbol{z}_{k-1}\ldots\boldsymbol{z}_1$ in order to determine the square of $\boldsymbol{A}_{\langle k \rangle}$. Informally spoken, the reverse applied to an operand is the operand itself unless the operand contains a multiplication. In this case the order of multiplication is (recursively) reversed. Hence scalars and vectors are per se invariant under reversion. With this properties the reverse is an involutive anti-automorphism.

Definition 2.9 (Reverse):
Let $\mathbf{e}_{\mathbb{u}} = \mathbf{e}_{i_1}\mathbf{e}_{i_2}\ldots\mathbf{e}_{i_k}$, $\mathbb{u} = \{i_{1\ldots k}\}$, *be a basis blade of grade* $k = |\mathbb{u}|$. *Then the reverse of* $\mathbf{e}_{\mathbb{u}}$ *is denoted by* $\widetilde{\mathbf{e}}_{\mathbb{u}}$ *and defined as*

$$\widetilde{\mathbf{e}}_{\mathbb{u}} \;=\; \mathbf{e}_{i_k}\mathbf{e}_{i_{k-1}}\ldots\mathbf{e}_{i_1}.$$

The reverse is distributive w.r.t the addition of elements of $\mathbb{R}_{p,q}$

$$\boldsymbol{A},\boldsymbol{B} \in \mathbb{R}_{p,q} \qquad \Longrightarrow \qquad (\boldsymbol{A}+\boldsymbol{B})^{\sim} \;=\; \widetilde{\boldsymbol{A}} + \widetilde{\boldsymbol{B}}.$$

■

Given a basis blade $\mathbf{e}_{\mathbb{u}} = \mathbf{e}_i\mathbf{e}_{\mathbb{v}}$, the reverse can equally be defined in a recursive manner by $\widetilde{\mathbf{e}}_{\mathbb{u}} := \widetilde{\mathbf{e}}_{\mathbb{v}}\mathbf{e}_i$.

For vectors $\{\boldsymbol{a}_{1\ldots k}\}$ the reverse satisfies

$$\begin{aligned}(\boldsymbol{a}_1\boldsymbol{a}_2\ldots\boldsymbol{a}_k)^{\sim} &= \boldsymbol{a}_k\boldsymbol{a}_{k-1}\ldots\boldsymbol{a}_1\\ (\boldsymbol{a}_1\wedge\boldsymbol{a}_2\wedge\ldots\wedge\boldsymbol{a}_k)^{\sim} &= \boldsymbol{a}_k\wedge\boldsymbol{a}_{k-1}\wedge\ldots\wedge\boldsymbol{a}_1.\end{aligned}$$

According to the above definition it is

$$\widetilde{\mathbf{e}}_{\mathbb{u}} \;=\; (-1)^{\frac{|\mathbb{u}|\,(|\mathbb{u}|-1)}{2}}\,\mathbf{e}_{\mathbb{u}} \tag{2.48}$$

and especially

$$\begin{aligned} \langle \widetilde{\boldsymbol{A}} \rangle_i &= (-1)^{\frac{i\,(i-1)}{2}}\,\langle \boldsymbol{A} \rangle_i, \qquad 0 \le i \le n \\ \widetilde{\boldsymbol{A}_{[k]}} &= (-1)^{\frac{k\,(k-1)}{2}}\,\boldsymbol{A}_{[k]}. \end{aligned}$$

The next proposition should not be taken for granted since two basis blades $\mathbf{e}_{\mathbb{u}}$ and $\mathbf{e}_{\mathbb{v}}$ could have several basis vectors in common.

Proposition 2.10
Let $\mathbf{e}_{\mathbb{u}}$ and $\mathbf{e}_{\mathbb{v}}$ two basis blades of $\mathbb{R}_{p,q}$. Then the reverse $(\mathbf{e}_{\mathbb{u}}\mathbf{e}_{\mathbb{v}})^{\sim}$ of the geometric product $\mathbf{e}_{\mathbb{u}}\mathbf{e}_{\mathbb{v}}$ is

$$(\mathbf{e}_{\mathbb{u}}\mathbf{e}_{\mathbb{v}})^{\sim} \;=\; \widetilde{\mathbf{e}}_{\mathbb{v}}\,\widetilde{\mathbf{e}}_{\mathbb{u}}.$$

Proof: *Let $\mathbf{e}_{\mathbb{w}} = \mathbf{e}_{\mathbb{u}}\mathbf{e}_{\mathbb{v}}$ with $u := |\mathbb{u}|$, $v := |\mathbb{v}|$ and $w := |\mathbb{w}|$. Furthermore, let $\mathbb{z} = \mathbb{u} \cap \mathbb{v}$ with $z = |\mathbb{z}|$. It then must be shown that*

$$\begin{aligned} \widetilde{\mathbf{e}}_{\mathbb{w}} \overset{(2.48)}{=} (-1)^{\frac{w\,(w-1)}{2}}\,\mathbf{e}_{\mathbb{w}} &\overset{(*)}{=} (-1)^{\frac{u\,(u-1)}{2}}\,(-1)^{\frac{v\,(v-1)}{2}}\,(-1)^{u\,v-z}\,\mathbf{e}_{\mathbb{u}}\mathbf{e}_{\mathbb{v}} \\ &\overset{(2.35)}{=} (-1)^{\frac{u\,(u-1)}{2}}\,(-1)^{\frac{v\,(v-1)}{2}}\,\mathbf{e}_{\mathbb{v}}\mathbf{e}_{\mathbb{u}} \\ &\overset{(2.48)}{=} \widetilde{\mathbf{e}}_{\mathbb{v}}\,\widetilde{\mathbf{e}}_{\mathbb{u}}. \end{aligned}$$

To show the $(*)$-equality, the signs to the left and right of $(*)$ must be equal, thus

$$\begin{aligned} & w\,(w-1) &\equiv_2\;& u\,(u-1) + v\,(v-1) + 2u\,v - 2z \\ \Longleftrightarrow\quad & w^2 - w &\equiv_2\;& (u+v)^2 - u - v - 2z, \end{aligned}$$

where the $\equiv_2$-sign is meant to indicate a congruence modulo two. By means of proposition 2.2, it is known that $w = u + v - 2z$:

$$\begin{aligned} & (u+v)^2 - 4(u+v)z + 4z^2 - u - v + 2z &\equiv_2\;& (u+v)^2 - u - v - 2z \\ \Longleftrightarrow\quad & -4(u+v)z + 4z^2 &\equiv_2\;& -4z. \end{aligned}$$

Both sides are obviously even - even if the division by two is reintroduced - with the result that the above $(*)$-equality is true. ■

By the distributivity of the reverse the following computation rules hold

$$\begin{aligned} (\boldsymbol{A}\,\boldsymbol{B})^{\sim} &= \widetilde{\boldsymbol{B}}\,\widetilde{\boldsymbol{A}} \\ (\boldsymbol{A} \wedge \boldsymbol{B})^{\sim} &= \widetilde{\boldsymbol{B}} \wedge \widetilde{\boldsymbol{A}} \\ (\boldsymbol{A} \cdot \boldsymbol{B})^{\sim} &= \widetilde{\boldsymbol{B}} \cdot \widetilde{\boldsymbol{A}}. \end{aligned}$$

Finally, consider a versor $\boldsymbol{V} = \boldsymbol{v}_1\boldsymbol{v}_2 \dots \boldsymbol{v}_k \in \mathbb{R}_{p,q}$. By noting that

$$\boldsymbol{V}\widetilde{\boldsymbol{V}} \;=\; \boldsymbol{v}_1\boldsymbol{v}_2 \dots \boldsymbol{v}_k\;\boldsymbol{v}_k\boldsymbol{v}_{k-1} \dots \boldsymbol{v}_1$$

it can be seen that $\boldsymbol{V}\widetilde{\boldsymbol{V}} \in \mathbb{R}$.

2.3.2 Magnitude, Conjugate and Inverse

One of the biggest advantages and likewise one the biggest disadvantages of the quadratic space $\mathbb{R}^{p,q}$ is that it is not a metric space, that is no norm is available. This might get a numerical problem because it is often beneficial to scale data in such a way that the mean of all values gets close to one. The use of the inner product is not advisable for this task. Consider for example the vector $\boldsymbol{a} = 6\mathbf{e}_1 + 3\mathbf{e}_2 - 5\mathbf{e}_3 \in \mathbb{R}^{1,2}$. It squares to two and would therefore be already very close to the target of one. However, evaluating $6^2 + 3^2 + 5^2$ gives 70 rather than two, which shows the inappropriateness of possibly indefinite products like the inner product. Another issue arises when working with null vectors: what would happen if a vector is to be projected on a null vector $\boldsymbol{n}$ - irrespective of whether it would make sense or not? It would be necessary to scale $\boldsymbol{n}$ to unit norm in the manner of $\boldsymbol{n}/\sqrt{\boldsymbol{n}^2}$. In order to meet such requirements the *conjugate* is introduced by which a *magnitude* for general multivectors can be declared.

Similar to complex conjugation, the conjugate negates those basis blades of a multivector that would square to minus one. Like the reverse, the conjugate is an involution.

Definition 2.10 (Conjugate):
Let $\mathbf{e}_{\mathbb{u}} \in \mathbb{R}^{p,q}$ be a basis blade. Then the conjugate of $\mathbf{e}_{\mathbb{u}}$, denoted by $\mathbf{e}_{\mathbb{u}}^{\dagger}$, is defined as

$$\mathbf{e}_{\mathbb{u}}^{\dagger} \;=\; (\mathbf{e}_{\mathbb{u}}^2)\, \mathbf{e}_{\mathbb{u}}$$

■

If c denotes the number of basis vectors in $\mathbf{e}_{\mathbb{u}}$ with negative signature, i.e. $c := |\{u \in \mathbb{u} \,|\, \mathbf{e}_u^2 = -1\}|$ and thus $(-1)^c = \mathbf{e}_{\mathbb{u}}\widetilde{\mathbf{e}}_{\mathbb{u}}$, a slightly more intuitive representation for the conjugate can be specified

$$\begin{aligned}
\mathbf{e}_{\mathbb{u}}^{\dagger} &= \mathbf{e}_{\mathbb{u}}\,(\mathbf{e}_{\mathbb{u}}^2) \\
&= \mathbf{e}_{\mathbb{u}}\widetilde{\mathbf{e}}_{\mathbb{u}}\,\widetilde{\mathbf{e}}_{\mathbb{u}} \qquad \text{due to } \widetilde{\mathbf{e}}_{\mathbb{u}}^2 = \mathbf{e}_{\mathbb{u}}^2 \\
&= (-1)^c\,\widetilde{\mathbf{e}}_{\mathbb{u}}.
\end{aligned}$$

The involutive character of the conjugate is revealed by

$$\mathbf{e}_{\mathbb{u}}^{\dagger\dagger} \;=\; ((-1)^c\,\widetilde{\mathbf{e}}_{\mathbb{u}})^{\dagger} \;=\; (-1)^{2c}\,\widetilde{\widetilde{\mathbf{e}}}_{\mathbb{u}} \;=\; \mathbf{e}_{\mathbb{u}}.$$

Just like in complex conjugation an odd (imaginary) and an even (real) part of a vector may be calculated by

$$\boldsymbol{a}_{\text{even}} = \tfrac{1}{2}(\boldsymbol{a} + \boldsymbol{a}^{\dagger}) \qquad \text{and} \qquad \boldsymbol{a}_{\text{odd}} = \tfrac{1}{2}(\boldsymbol{a} - \boldsymbol{a}^{\dagger}),$$

with

$$\boldsymbol{a}_{\text{even}} \cdot \boldsymbol{a}_{\text{odd}} = 0 \qquad \text{and} \qquad \boldsymbol{a}_{\text{even}} \wedge \boldsymbol{a}_{\text{odd}} = \tfrac{1}{2}\,\boldsymbol{a}^{\dagger} \wedge \boldsymbol{a}.$$

Proposition 2.11
Let $\mathbf{e}_{\mathbb{u}}$ *and* $\mathbf{e}_{\mathbb{v}}$ *two basis blades of* $\mathbb{R}_{p,q}$. *Then the conjugate* $(\mathbf{e}_{\mathbb{u}}\mathbf{e}_{\mathbb{v}})^\dagger$ *of the geometric product* $\mathbf{e}_{\mathbb{u}}\mathbf{e}_{\mathbb{v}}$ *is*

$$(\mathbf{e}_{\mathbb{u}}\mathbf{e}_{\mathbb{v}})^\dagger \;=\; \mathbf{e}_{\mathbb{v}}^\dagger\mathbf{e}_{\mathbb{u}}^\dagger.$$

Proof: *By means of equation (2.35) a scalar* x *can be determined such that* $\mathbf{e}_{\mathbb{u}}\mathbf{e}_{\mathbb{v}} = (-1)^x\mathbf{e}_{\mathbb{v}}\mathbf{e}_{\mathbb{u}}$. *However, exchanging the basis blades twice, as in the last line, introduces no sign.*

$$\begin{aligned}
(\mathbf{e}_{\mathbb{u}}\mathbf{e}_{\mathbb{v}})^\dagger &= \mathbf{e}_{\mathbb{v}}^\dagger\mathbf{e}_{\mathbb{u}}^\dagger \\
(\mathbf{e}_{\mathbb{u}}\mathbf{e}_{\mathbb{v}})^2\,(\mathbf{e}_{\mathbb{u}}\mathbf{e}_{\mathbb{v}}) &= \mathbf{e}_{\mathbb{v}}^2\,\mathbf{e}_{\mathbb{u}}^2\,\mathbf{e}_{\mathbb{v}}\mathbf{e}_{\mathbb{u}} \\
\underbrace{\mathbf{e}_{\mathbb{u}}\mathbf{e}_{\mathbb{v}}}_{swap}\,\mathbf{e}_{\mathbb{u}}\mathbf{e}_{\mathbb{v}}\,\underbrace{\mathbf{e}_{\mathbb{u}}\mathbf{e}_{\mathbb{v}}}_{swap} &= \mathbf{e}_{\mathbb{v}}\mathbf{e}_{\mathbb{v}}\,\mathbf{e}_{\mathbb{u}}\mathbf{e}_{\mathbb{u}}\,\mathbf{e}_{\mathbb{v}}\mathbf{e}_{\mathbb{u}}
\end{aligned}$$

■

By the distributivity of the geometric product, and since inner and outer product are also defined in terms of the geometric product, these rules apply

$$\begin{aligned}
(\boldsymbol{A}\,\boldsymbol{B})^\dagger &= \boldsymbol{B}^\dagger\,\boldsymbol{A}^\dagger \\
(\boldsymbol{A}\wedge\boldsymbol{B})^\dagger &= \boldsymbol{B}^\dagger\wedge\boldsymbol{A}^\dagger \\
(\boldsymbol{A}\cdot\boldsymbol{B})^\dagger &= \boldsymbol{B}^\dagger\cdot\boldsymbol{A}^\dagger
\end{aligned}$$

and especially

$$\boldsymbol{A}_{\langle k\rangle}^\dagger \;=\; \boldsymbol{a}_k^\dagger\wedge\boldsymbol{a}_{k-1}^\dagger\wedge\ldots\wedge\boldsymbol{a}_1^\dagger.$$

In this respect, it is important that generally

$$\boldsymbol{a}^\dagger \;\neq\; \pm\boldsymbol{a} \qquad \text{and thus} \qquad \boldsymbol{A}_{\langle k\rangle}^\dagger \;\neq\; \pm\boldsymbol{A}_{\langle k\rangle}$$

because the number of basis vectors with negative signature may vary between the basis blades of $\boldsymbol{A}_{\langle k\rangle}$. Let $\boldsymbol{x} = \mathbf{e}_1 + \mathbf{e}_2 \in \mathbb{R}^{1,1}$. Then, the result of $\boldsymbol{x}\wedge\boldsymbol{x}^\dagger = -2\,\mathbf{e}_{12}$ shows that for general $\boldsymbol{x}\in\mathbb{R}^{p,q}$

$$\boldsymbol{x}\wedge\boldsymbol{A}_{\langle k\rangle} = 0 \qquad \not\Longrightarrow \qquad \boldsymbol{x}\wedge\boldsymbol{A}_{\langle k\rangle}^\dagger = 0.$$

Note that the conjugate and reverse operation commute as their result ultimately differs by a sign.

By means of the conjugate the signature independent Euclidean inner product and the likewise signature independent Euclidean scalar product may be defined.

Definition 2.11 (Euclidean inner product):
Given two basis blades $\mathbf{e}_{\mathbb{u}}$ *and* $\mathbf{e}_{\mathbb{v}}$ *of* $\mathbb{R}_{p,q}$ *their Euclidean inner product, denoted by* $\mathbf{e}_{\mathbb{u}}\cdot_{\boldsymbol{\varepsilon}}\mathbf{e}_{\mathbb{v}}$, *is defined by*

$$\mathbf{e}_{\mathbb{u}}\cdot_{\boldsymbol{\varepsilon}}\mathbf{e}_{\mathbb{v}} \;=\; \begin{cases} \mathbf{e}_{\mathbb{u}}^\dagger\cdot\mathbf{e}_{\mathbb{v}}, & |\mathbb{u}|\leq|\mathbb{v}| \\ \mathbf{e}_{\mathbb{u}}\cdot\mathbf{e}_{\mathbb{v}}^\dagger, & \textit{else}. \end{cases}$$

■

The Euclidean inner product computes the inner product as if the underlying algebra was a Euclidean one. Thus in $\mathbb{R}_n$ the Euclidean inner product coincides with the normal inner product. For basis blades of equal grade the Euclidean inner product coincides with the Euclidean scalar product.

Definition 2.12 (Euclidean scalar product):
Given two basis blades $\mathbf{e}_{\mathbb{u}}$ *and* $\mathbf{e}_{\mathbb{v}}$ *of* $\mathbb{R}_{p,q}$ *their Euclidean scalar product, denoted by* $\mathbf{e}_{\mathbb{u}} *_{\boldsymbol{\varepsilon}} \mathbf{e}_{\mathbb{v}}$, *is defined by*

$$\mathbf{e}_{\mathbb{u}} *_{\boldsymbol{\varepsilon}} \mathbf{e}_{\mathbb{v}} \;=\; \langle \mathbf{e}_{\mathbb{u}} \mathbf{e}_{\mathbb{v}}^{\dagger} \rangle \;=\; \langle \mathbf{e}_{\mathbb{v}} \mathbf{e}_{\mathbb{u}}^{\dagger} \rangle \;=\; \begin{cases} 1, & \textit{if } \mathbb{u} = \mathbb{v} \\ 0, & \textit{else.} \end{cases}$$

■

Hence in the numbered basis introduced on page 19

$$\forall\, i, j \in \mathcal{N}: \qquad \mathbf{E}_i *_{\boldsymbol{\varepsilon}} \mathbf{E}_j \;=\; \delta_{ij}.$$

The linearity of the grade projection operator allows

$$\langle \boldsymbol{A}\boldsymbol{B}^{\dagger} \rangle \;=\; \left\langle \sum_{i,j} a_i\, b_j \mathbf{E}_i \mathbf{E}_j^{\dagger} \right\rangle \;=\; \sum_{i,j} a_i\, b_j \left\langle \mathbf{E}_i \mathbf{E}_j^{\dagger} \right\rangle$$

for two general multivectors $\boldsymbol{A} = \sum_i a_i \mathbf{E}_i$ and $\boldsymbol{B} = \sum_i b_i \mathbf{E}_i$. As a consequence, their Euclidean scalar product

$$\boldsymbol{A} *_{\boldsymbol{\varepsilon}} \boldsymbol{B} \;=\; \sum_{i,j} a_i\, b_j \mathbf{E}_i *_{\boldsymbol{\varepsilon}} \mathbf{E}_j \;=\; \sum_i a_i\, b_i$$

resembles, as intended, the scalar product declared in vector spaces. In particular, the product $\boldsymbol{A} *_{\boldsymbol{\varepsilon}} \boldsymbol{A}$ is of importance as it is positive definite

$$\boldsymbol{A} *_{\boldsymbol{\varepsilon}} \boldsymbol{A} \;=\; \sum_i a_i^2.$$

Regarding the preceding equation it is a mere formality to define the magnitude.

Definition 2.13 (Magnitude):
The magnitude of an arbitrary multivector $\boldsymbol{A} \in \mathbb{R}_{p,q}$, *denoted by* $\|\boldsymbol{A}\|$, *is defined as*

$$\|\boldsymbol{A}\| \;=\; \sqrt{\boldsymbol{A} *_{\boldsymbol{\varepsilon}} \boldsymbol{A}} \quad \in\; \mathbb{R}.$$

■

Hence the expression $\boldsymbol{A}_{\langle k \rangle}^2$ mentioned in corollary 2.10 is already pretty close to the magnitude of a blade $\boldsymbol{A}_{\langle k \rangle}$, but it lacks the positive definiteness. By observing that

$$\boldsymbol{A}_{\langle k \rangle} *_{\boldsymbol{\varepsilon}} \boldsymbol{B}_{\langle l \rangle} \;=\; \left\langle \boldsymbol{A}_{\langle k \rangle} \boldsymbol{B}_{\langle l \rangle}^{\dagger} \right\rangle \;=\; \left\langle \boldsymbol{A}_{\langle k \rangle} \cdot \boldsymbol{B}_{\langle l \rangle}^{\dagger} \right\rangle \;=\; \delta_{kl}\; \boldsymbol{A}_{\langle k \rangle} \cdot \boldsymbol{B}_{\langle l \rangle}^{\dagger},$$

it can be deduced that

$$\boldsymbol{A}_{\langle k\rangle} *_{\boldsymbol{\varepsilon}} \boldsymbol{A}_{\langle k\rangle} \;=\; \boldsymbol{A}_{\langle k\rangle} \cdot \boldsymbol{A}^{\dagger}_{\langle k\rangle}.$$

In contrast to the inner product of a blade with itself, the inner product of a blade with its conjugate cannot be expressed in terms of the geometric product. Compare, for example for $\boldsymbol{a} = \mathbf{e}_1 + 2\mathbf{e}_2 \in \mathbb{R}^{1,1}$,

$$\boldsymbol{a} \cdot \boldsymbol{a}^{\dagger} \;=\; 1 + 4 \qquad \text{and} \qquad \boldsymbol{a}\boldsymbol{a}^{\dagger} \;=\; 1 + 4 \,-\, 4\mathbf{e}_{12}.$$

Finally, notice that a null vector $\boldsymbol{n}$ is perpendicular to its conjugate $\boldsymbol{n}^{\dagger}$ since

$$\boldsymbol{n} *_{\boldsymbol{\varepsilon}} \boldsymbol{n}^{\dagger} \;=\; \boldsymbol{n} \cdot \boldsymbol{n}^{\dagger\dagger} \;=\; \boldsymbol{n} \cdot \boldsymbol{n} = 0.$$

Inverse

The principle of building the inverse in geometric algebra is simply

$$\boldsymbol{ab} \quad \underbrace{\frac{\boldsymbol{ba}}{\boldsymbol{ab}\ \boldsymbol{ba}}}_{(\boldsymbol{ab})^{-1}} \;=\; 1.$$

The equation clarifies that such an inverse can only exist for versors, i.e. geometric products of invertible vectors, cf. definition 2.7.

Definition 2.14 (Inverse):
Let $\boldsymbol{V} \in \mathbb{R}_{p,q}$ denote a versor. Then its inverse can be calculated by

$$\boldsymbol{V}^{-1} \;=\; \frac{\widetilde{\boldsymbol{V}}}{\boldsymbol{V}\widetilde{\boldsymbol{V}}}.$$

■

Hence given a versor $\boldsymbol{V} = \boldsymbol{v}_1\boldsymbol{v}_2 \ldots \boldsymbol{v}_k$, the inverse can equally be stated as

$$\boldsymbol{V}^{-1} \;=\; \boldsymbol{v}_k^{-1}\boldsymbol{v}_{k-1}^{-1} \ldots \boldsymbol{v}_2^{-1}\boldsymbol{v}_1^{-1}.$$

The term $\boldsymbol{V}^{-1}$ is both the right- and the left inverse of $\boldsymbol{V}$ as $\boldsymbol{V}\widetilde{\boldsymbol{V}} = \widetilde{\boldsymbol{V}}\boldsymbol{V}$.

The inverse of a basis blade $\mathbf{e}_{\mathbb{u}}$ coincides with the conjugate because of $\mathbf{e}_{\mathbb{u}}\widetilde{\mathbf{e}}_{\mathbb{u}} = 1/(\mathbf{e}_{\mathbb{u}}\widetilde{\mathbf{e}}_{\mathbb{u}})$

$$\begin{aligned}
\mathbf{e}^{\dagger}_{\mathbb{u}} \;&=\; \mathbf{e}_{\mathbb{u}}\widetilde{\mathbf{e}}_{\mathbb{u}}\ \widetilde{\mathbf{e}}_{\mathbb{u}} \\
&=\; \frac{\widetilde{\mathbf{e}}_{\mathbb{u}}}{\mathbf{e}_{\mathbb{u}}\widetilde{\mathbf{e}}_{\mathbb{u}}} \\
&=\; {\mathbf{e}_{\mathbb{u}}}^{-1}.
\end{aligned}$$

2.3.3 Duality and the Pseudoscalar

It can almost be guessed from the expression itself that the dual operation is an automorphism and almost (up to a sign) an involution.

Definition 2.15 (Dual):
Let $\boldsymbol{A}$ be an element of $\mathbb{R}_{p,q}$. The dual of multivector $\boldsymbol{A}$ is denoted by $\boldsymbol{A}^*$ and is defined as

$$\boldsymbol{A}^* \;=\; \boldsymbol{A}\boldsymbol{I}^{-1}.$$

■

Hence in spaces where $\boldsymbol{I}^2 = +1$ the dual operation is an involution as well.

The behavior of the pseudoscalar depending on the signature (p,q) of an algebra $\mathbb{R}_{p,q}$ is depicted in figure 2.6. The figure as well shows whether $\boldsymbol{I}$ commutes with all multivectors of $\mathbb{R}_{p,q}$. It may easily be verified that

$$\boldsymbol{A}_{[k]}\boldsymbol{I} \;=\; (-1)^{k(n-1)}\,\boldsymbol{I}\boldsymbol{A}_{[k]} \qquad \text{and} \qquad \boldsymbol{I}^2 \;=\; (-1)^{\frac{n(n-1)}{2}}\,(-1)^q. \tag{2.49}$$

Self-evidently, $\boldsymbol{I}^{-1}$ behaves in the same manner as $\boldsymbol{I}$, i.e. it squares to the same values and only commutes if $\boldsymbol{I}$ commutes. From the result of the previous section that the inverse of a basis blade is its conjugate follows

$$\boldsymbol{I}^{-1} \;=\; \boldsymbol{I}^{\dagger} \;=\; (\boldsymbol{I}^2)\,\boldsymbol{I}.$$

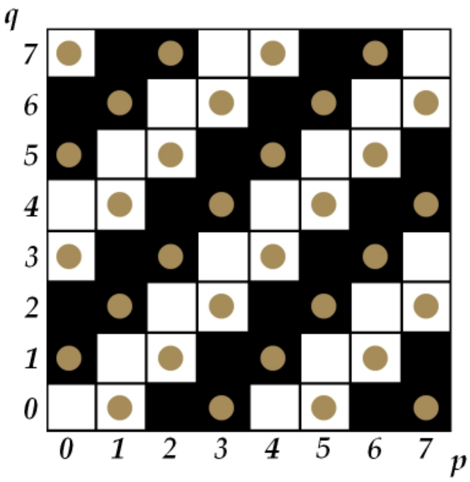

Fig. 2.6: Pseudoscalar: a white square denotes an algebra $\mathbb{R}_{p,q}$ where $\boldsymbol{I} \in \mathbb{R}_{p,q}$ squares to plus one, so that $\boldsymbol{I}^{-1} = \boldsymbol{I}$. A disc indicates that the pseudoscalar $\boldsymbol{I}$ commutes with all elements of that algebra.

It is known by equation (2.31) that the outer product of n vectors is

$$\boldsymbol{a}_1 \wedge \boldsymbol{a}_2 \wedge \ldots \wedge \boldsymbol{a}_n \;=\; \det(\mathsf{A})\;\mathbf{e}_1\mathbf{e}_2\ldots\mathbf{e}_n \;=\; \det(\mathsf{A})\boldsymbol{I},$$

where the matrix A holds the coefficients of the vectors $\{\boldsymbol{a}_{1\ldots n}\}$. As the pseudoscalar $\boldsymbol{I}$ is proportional to the outer product of n linearly independent vectors, the pseudoscalar spans the whole space $\mathbb{R}^{p,q}$. This has profound ramifications: the geometric product of a multivector $\boldsymbol{A}$ and $\boldsymbol{I}$, and so $\boldsymbol{I}^{-1}$, is always identical to the inner product of the two elements because $\boldsymbol{I}$ comprises all n basis vectors such that equation (2.37) applies. Thus for every $\boldsymbol{A} \in \mathbb{R}_{p,q}$

$$\boldsymbol{A}^* \;=\; \boldsymbol{A}\boldsymbol{I}^{-1} \;=\; \boldsymbol{A} \cdot \boldsymbol{I}^{-1}.$$

Recall from corollary 2.8 that $(\boldsymbol{A}_{[r]} \wedge \boldsymbol{B}_{[s]}) \cdot \boldsymbol{C}_{[t]} = \boldsymbol{A}_{[r]} \cdot (\boldsymbol{B}_{[s]} \cdot \boldsymbol{C}_{[t]})$ *iff* $t \geq r+s$, which now reads

$$(\boldsymbol{A}_{[r]} \wedge \boldsymbol{B}_{[s]})\boldsymbol{I}^{-1} \;=\; \boldsymbol{A}_{[r]} \cdot (\boldsymbol{B}_{[s]}\boldsymbol{I}^{-1}), \qquad \text{if } n \geq r+s,$$

or simply

$$(\boldsymbol{A}_{[r]} \wedge \boldsymbol{B}_{[s]})^* \;=\; \boldsymbol{A}_{[r]} \cdot \boldsymbol{B}^*_{[s]}. \tag{2.50}$$

$$(\boldsymbol{A}_{[r]} \cdot \boldsymbol{B}_{[s]})^* \;=\; \boldsymbol{A}_{[r]} \wedge \boldsymbol{B}^*_{[s]}, \qquad s \geq r, \tag{2.51}$$

The second very similar identity can be derived from equation (2.50) by

$$\begin{aligned} \boldsymbol{A}_{[r]} \wedge \boldsymbol{B}^*_{[s]} \;&=\; \boldsymbol{A}_{[r]} \wedge (\boldsymbol{B}_{[s]}\boldsymbol{I}^{-1}) \;=\; \left[\left(\boldsymbol{A}_{[r]} \wedge (\boldsymbol{B}_{[s]}\boldsymbol{I}^{-1})\right)\boldsymbol{I}\right]\boldsymbol{I}^{-1} \\ &\overset{(2.50)}{=}\; \left[\boldsymbol{A}_{[r]} \cdot (\boldsymbol{B}_{[s]}\boldsymbol{I}^{-1}\boldsymbol{I})\right]\boldsymbol{I}^{-1} \\ &=\; (\boldsymbol{A}_{[r]} \cdot \boldsymbol{B}_{[s]})^*. \end{aligned}$$

The second line follows if $n \geq r + (n-s)$ hence if $s \geq r$.

In case of a vector and a general multivector the following rules apply:

$$(\boldsymbol{a} \wedge \boldsymbol{B})^* \;=\; \boldsymbol{a} \cdot \boldsymbol{B}^* \tag{2.52}$$

$$(\boldsymbol{a} \cdot \boldsymbol{B})^* \;=\; \boldsymbol{a} \wedge \boldsymbol{B}^*. \tag{2.53}$$

Again, the second identity arises from the first one[12] via

$$\begin{aligned} \boldsymbol{a} \wedge \boldsymbol{B}^* \;&=\; \boldsymbol{a} \wedge (\boldsymbol{B}\boldsymbol{I}^{-1}) \;=\; \left[\left(\boldsymbol{a} \wedge (\boldsymbol{B}\boldsymbol{I}^{-1})\right)\boldsymbol{I}\right]\boldsymbol{I}^{-1} \\ &\overset{(2.52)}{=}\; \left[\boldsymbol{a} \cdot (\boldsymbol{B}\boldsymbol{I}^{-1}\boldsymbol{I})\right]\boldsymbol{I}^{-1} \\ &=\; (\boldsymbol{a} \cdot \boldsymbol{B})^*. \end{aligned}$$

With the help of the dual, a relation between corollary 2.7 and corollary 2.13 can be established. Given a vector $\boldsymbol{x}$ and a blade $\boldsymbol{A}_{\langle k\rangle}$ it is known from the corollaries that

$$\boldsymbol{x} \wedge \boldsymbol{A}_{\langle k\rangle} \;=\; 0 \quad \text{iff} \quad \boldsymbol{x} \in \boldsymbol{A}_{\langle k\rangle} \qquad \text{and} \qquad \boldsymbol{x} \cdot \boldsymbol{A}_{\langle k\rangle} \;=\; 0 \quad \text{iff} \quad \boldsymbol{x} \perp \boldsymbol{A}_{\langle k\rangle}.$$

[12] Note that the first identity $(\boldsymbol{a} \wedge \boldsymbol{B}_{[l]})^* = \boldsymbol{a} \cdot \boldsymbol{B}^*_{[l]}$ also holds for $l = n$ as both sides take on the value zero.

But equation (2.52) implies that

$$\begin{aligned} \boldsymbol{x} \wedge \boldsymbol{A}_{\langle k \rangle} = 0 \quad &\Longleftrightarrow \quad (\boldsymbol{x} \wedge \boldsymbol{A}_{\langle k \rangle})^* = 0 \\ &\Longleftrightarrow \quad \boldsymbol{x} \cdot \boldsymbol{A}^*_{\langle k \rangle} = 0 \quad \Longleftrightarrow \quad \boldsymbol{x} \perp \boldsymbol{A}^*_{\langle k \rangle}. \end{aligned} \tag{2.54}$$

Hint: *if $\boldsymbol{A}_{\langle k \rangle}$ is a null blade then $\boldsymbol{x} \cdot \boldsymbol{A}_{\langle k \rangle} = 0$ does not imply $\boldsymbol{x} \perp \boldsymbol{A}_{\langle k \rangle}$, because $\boldsymbol{x}$ might be a null vector that is part of $\boldsymbol{A}_{\langle k \rangle}$. If $\boldsymbol{x}$, however, is a null vector but $\boldsymbol{A}_{\langle k \rangle}$ not a null blade, equation (2.54) holds.*

Therefore $\boldsymbol{x}$ lies in $\boldsymbol{A}_{\langle k \rangle}$ *iff* $\boldsymbol{x}$ lies in the orthogonal complement of $\boldsymbol{A}^*_{\langle k \rangle}$, from which it can be inferred that $\boldsymbol{A}_{\langle k \rangle}$ must be the orthogonal complement of $\boldsymbol{A}^*_{\langle k \rangle}$, i.e. $\boldsymbol{A}_{\langle k \rangle} \perp \boldsymbol{A}^*_{\langle k \rangle}$. Moreover, equation (2.50) shows that $\boldsymbol{A}^*_{\langle k \rangle}$ completes $\boldsymbol{A}_{\langle k \rangle}$ to the whole space $\boldsymbol{I}$:

$$\boldsymbol{A}_{\langle k \rangle} \wedge \boldsymbol{A}^*_{\langle k \rangle} = (\boldsymbol{A}_{\langle k \rangle} \cdot \boldsymbol{A}^{**}_{\langle k \rangle})\boldsymbol{I} \quad \propto \quad \boldsymbol{I} \tag{2.55}$$

since blades square to scalars.

Hint: *if $\boldsymbol{A}_{\langle k \rangle}$ is a null blade then $\boldsymbol{A}_{\langle k \rangle} \cdot \boldsymbol{A}^{**}_{\langle k \rangle} = 0$ and hence $\boldsymbol{A}_{\langle k \rangle} \wedge \boldsymbol{A}^*_{\langle k \rangle} = 0$. The answer to what the orthogonal complement of a null blade looks like is given on page 72.*

The question remains whether the dual operation maintains the blade property, that is, is the dual of an element a blade *iff* the element itself is a blade? According to proposition 2.6, there is at least one simple way to check that the dual of a blade is a blade again: given the vectors $\{\boldsymbol{a}_{1\ldots k}\}$ a set of orthogonal vectors $\{\boldsymbol{z}_{1\ldots k}\}$ can be found such that $\bigwedge_{i=1}^{k} \boldsymbol{a}_i = \boldsymbol{z}_1 \boldsymbol{z}_2 \ldots \boldsymbol{z}_k$. In the context of the proof of proposition 2.6, the matrix multiplication $\mathsf{Z}\,\mathsf{Q}\,\mathsf{w}$ of a vector $\mathsf{w} \in \mathbb{R}^n$ with $\mathsf{Z}\,\mathsf{Q} \in \mathbb{R}^{k \times n}$ would be zero *iff* the algebra vector $\boldsymbol{w} \in \mathbb{R}^{p,q}$ corresponding to w is orthogonal to each of the vectors in $\{\boldsymbol{z}_{1\ldots k}\}$, i.e. $\boldsymbol{w} \cdot \boldsymbol{z}_i = 0$, $1 \le i \le k$. Thus the right null space of the matrix $\mathsf{Z}\,\mathsf{Q}$ consists of the coefficients of the $n-k$ vectors that span the orthogonal complement of $\boldsymbol{A}_{\langle k \rangle} = \bigwedge_{i=1}^{k} \boldsymbol{a}_i$.
The dual of a blade therefore is a blade again. Similarly, the dual of a non-blade $\boldsymbol{X}$ cannot be a blade since the dual of that blade (the dual of the dual) $\boldsymbol{X}^{**} = \pm \boldsymbol{X}$ would have to be a blade - a contradiction to the assumption.

The dual of a null blade is still a null blade, i.e.

$$\boldsymbol{A}^2_{\langle k \rangle} = 0 \qquad \Longleftrightarrow \qquad (\boldsymbol{A}^*_{\langle k \rangle})^2 = 0,$$

because of

$$(\boldsymbol{A}^*_{\langle k \rangle})^2 = \boldsymbol{A}_{\langle k \rangle} \boldsymbol{I}^{-1} \boldsymbol{A}_{\langle k \rangle} \boldsymbol{I}^{-1} = (-1)^{k(n-1)} \boldsymbol{A}_{\langle k \rangle} \boldsymbol{A}_{\langle k \rangle} (\boldsymbol{I}^{-1})^2.$$

2.3.4 Outermorphism

The subject of this section is about the fact that and the way in which linear transformations on $\mathbb{R}^n$ can be extended to the geometric algebra $\mathbb{R}_{p,q}$.

Let f be the linear map on $\mathbb{R}^n$. Setting

$$f(\boldsymbol{a}_1 \wedge \boldsymbol{a}_2 \wedge \ldots \wedge \boldsymbol{a}_k) \;:=\; f(\boldsymbol{a}_1) \wedge f(\boldsymbol{a}_2) \wedge \ldots \wedge f(\boldsymbol{a}_k) \tag{2.56}$$

extends f to the elements of $\mathbb{R}_{p,q}$ in a unique way. By linearity the basis blades $\mathbf{e}_{\mathbb{u}} \in \mathbb{R}_{p,q}$ of an arbitrary multivector are mapped according to

$$f(\mathbf{e}_{\mathbb{u}}) \;=\; f(\mathbf{e}_{\mathbb{u}_1}) \wedge f(\mathbf{e}_{\mathbb{u}_2}) \wedge \ldots \wedge f(\mathbf{e}_{\mathbb{u}_k}), \qquad k := |\mathbb{u}|.$$

It can be seen that the linear transformation ($\sim$ morphism) preserves the grade of an outer product - this is where the name *outermorphism* comes from.

Now an insight into the effects of a linear transformation on the outer product is to be given. As a byproduct, it is demonstrated that the induced generalization is compatible with the definition of the outer product.
Let the columns of the matrix $\mathsf{A}' \in \mathbb{R}^{n \times k}$ hold the coefficients of the vectors $\{\boldsymbol{a}'_{1\ldots k}\}$, e.g. $\boldsymbol{a}'_i = \mathsf{A}'^j{}_i \mathbf{e}_j$, $i \in [1,k]_{\mathbb{Z}}$. Recall that corresponding to definition (2.31) and the definition (page 32)

$$I_{k/n} := \{(v_1, v_2, \ldots, v_k) \mid 1 \leq v_1 < v_2 < \ldots < v_k \leq n\},$$

respectively, the outer product of the k vectors $\{\boldsymbol{a}'_{1\ldots k}\}$ is

$$\boldsymbol{a}'_1 \wedge \boldsymbol{a}'_2 \wedge \ldots \wedge \boldsymbol{a}'_k \;=\; \sum_{\mathsf{v} \in I_{k/n}} \det(\mathsf{A}'|_{\mathsf{v}})\, \mathbf{e}_{\mathsf{v}_1} \mathbf{e}_{\mathsf{v}_2} \ldots \mathbf{e}_{\mathsf{v}_k}.$$

Assume that $\boldsymbol{a}'_i = f(\boldsymbol{a}_i)$, $i \in [1,k]_{\mathbb{Z}}$. As f is a map $\mathbb{R}^n \longrightarrow \mathbb{R}^n$, it has a matrix representation $\mathsf{F} \in \mathbb{R}^{n \times n}$. Moreover, let A denote the matrix of the vectors $\{\boldsymbol{a}_{1\ldots k}\}$ such that $\mathsf{FA} = \mathsf{A}'$. As the columns of F are the images of the (canonical) basis $\{\mathbf{e}_{1\ldots n}\}$, let $\mathbf{f}_i := f(\mathbf{e}_i)$, $i \in [1,n]_{\mathbb{Z}}$. Hence

$$\begin{aligned}
\boldsymbol{a}'_1 \wedge \boldsymbol{a}'_2 \wedge \ldots \wedge \boldsymbol{a}'_k \;&=\; \sum_{\mathsf{v} \in I_{k/n}} \det((\mathsf{FA})|_{\mathsf{v}})\, \mathbf{e}_{\mathsf{v}_1} \mathbf{e}_{\mathsf{v}_2} \ldots \mathbf{e}_{\mathsf{v}_k} \\
&\overset{(*)}{=} \sum_{\mathsf{v} \in I_{k/n}} \sum_{\mathsf{w} \in I_{k/n}} \det(\mathsf{F}|^{\mathsf{w}}_{\mathsf{v}}) \det(\mathsf{A}|_{\mathsf{w}})\, \mathbf{e}_{\mathsf{v}_1} \mathbf{e}_{\mathsf{v}_2} \ldots \mathbf{e}_{\mathsf{v}_k} \\
&= \sum_{\mathsf{w} \in I_{k/n}} \det(\mathsf{A}|_{\mathsf{w}}) \sum_{\mathsf{v} \in I_{k/n}} \det(\mathsf{F}|^{\mathsf{w}}_{\mathsf{v}})\, \mathbf{e}_{\mathsf{v}_1} \mathbf{e}_{\mathsf{v}_2} \ldots \mathbf{e}_{\mathsf{v}_k} \\
&= \sum_{\mathsf{v} \in I_{k/n}} \det(\mathsf{A}|_{\mathsf{v}})\, \mathbf{f}_{\mathsf{v}_1} \wedge \mathbf{f}_{\mathsf{v}_2} \wedge \ldots \wedge \mathbf{f}_{\mathsf{v}_k} \\
&= \sum_{\mathsf{v} \in I_{k/n}} \det(\mathsf{A}|_{\mathsf{v}})\, f(\mathbf{e}_{\mathsf{v}_1} \mathbf{e}_{\mathsf{v}_2} \ldots \mathbf{e}_{\mathsf{v}_k}) \\
&= f(\boldsymbol{a}_1 \wedge \boldsymbol{a}_2 \wedge \ldots \wedge \boldsymbol{a}_k)
\end{aligned}$$

where in $(*)$ the *Binet-Cauchy identity*, as given in equation (2.46), is used.

Note that combining a linear transformation with the conjugate has to be taken care of. For example, if $f(\mathbf{e}_1) = \mathbf{e}_2$ in $\mathbb{R}^{1,1}$, it follows $f(\mathbf{e}_1)^\dagger = \mathbf{e}_2^\dagger = -f(\mathbf{e}_1)$, but

$f(\mathbf{e}_1^\dagger) = f(\mathbf{e}_1)$. Hence building the conjugate and doing a linear transformation do not commute.

Example 2.11 (Linearity of the Reflection):
Let $\boldsymbol{a}$ and $\boldsymbol{x}$ be two vectors from $\mathbb{R}^{p,q}$. Then, by the bilinearity of the geometric product, the reflection $\boldsymbol{b} := \boldsymbol{xax}$ of $\boldsymbol{a}$ in $\boldsymbol{x}$ is supposed to be linear in $\boldsymbol{a}$. This is to be ascertained here. First equation (A.24) is used giving

$$\boldsymbol{b} \;=\; \boldsymbol{xax} \;=\; 2(\boldsymbol{x}\cdot\boldsymbol{a})\boldsymbol{x} \;-\; \boldsymbol{x}^2\boldsymbol{a}.$$

For simplicity it is now assumed that $q = 0$, i.e. $\boldsymbol{a}, \boldsymbol{x} \in \mathbb{R}^n$. With $\boldsymbol{x} = x^i\mathbf{e}_i$ and $\boldsymbol{a} = a^i\mathbf{e}_j$ the k^{th} component b_k, $k \in [1,n]_{\mathbb{Z}}$, of $\boldsymbol{b}$ is

$$\begin{aligned} b_k &= 2(x_1a_1 + x_2a_2 + \ldots + x_na_n)x_k - \boldsymbol{x}^2a_k \\ &= 2x_1x_ka_1 + 2x_2x_ka_2 + \ldots + (2x_k^2 - \boldsymbol{x}^2)a_k + \ldots + 2x_nx_ka_n, \end{aligned}$$

so that explicitly

$$\begin{bmatrix} b_1 \\ b_2 \\ \vdots \\ b_n \end{bmatrix} = \begin{bmatrix} (2x_1^2 - \boldsymbol{x}^2) & 2x_2x_1 & \ldots & 2x_nx_1 \\ 2x_1x_2 & (2x_2^2 - \boldsymbol{x}^2) & \ldots & 2x_nx_2 \\ \vdots & \vdots & \ddots & \vdots \\ 2x_1x_n & 2x_2x_n & \ldots & (2x_n^2 - \boldsymbol{x}^2) \end{bmatrix} \begin{bmatrix} a_1 \\ a_2 \\ \vdots \\ a_n \end{bmatrix}.$$

The Role of Versors

A versor, the geometric product of non-null vectors, has always an inverse according to definition 2.14. The importance of versors arises from the importance of the reflection, which embodies the most fundamental transformation of geometric algebra: as already mentioned in the scope of equation (2.40), for the case of blades, a versor represents successive reflections in the constituent vectors. The practical use of the reflection operation comes to the fore especially in chapter 3, where it is dealt with versors $\boldsymbol{V}$ satisfying $\boldsymbol{V}\widetilde{\boldsymbol{V}} = 1$. Given a versor $\boldsymbol{V}' = \boldsymbol{v}_1'\boldsymbol{v}_2'\ldots\boldsymbol{v}_k'$, this can be achieved defining

$$\boldsymbol{V} \;=\; \frac{\boldsymbol{V}'}{\sqrt{|\boldsymbol{V}'\widetilde{\boldsymbol{V}'}|}} \;=\; \frac{\boldsymbol{v}_1'}{\sqrt{|\boldsymbol{v}_1'^2|}}\frac{\boldsymbol{v}_2'}{\sqrt{|\boldsymbol{v}_2'^2|}}\cdots\frac{\boldsymbol{v}_k'}{\sqrt{|\boldsymbol{v}_k'^2|}} \;=\; \boldsymbol{v}_1\boldsymbol{v}_2\ldots\boldsymbol{v}_k,$$

where, self-evidently, $\boldsymbol{v}_i := \boldsymbol{v}_i'/\sqrt{|\boldsymbol{v}_i'\boldsymbol{v}_i'|}$, $i \in [1,k]_{\mathbb{Z}}$. The following product illustrates the transformation of a vector $\boldsymbol{a}$ by $\boldsymbol{V}$, $\boldsymbol{V}\widetilde{\boldsymbol{V}} = 1$.

$$\boldsymbol{b} \;=\; \boldsymbol{Va}\widetilde{\boldsymbol{V}} \;=\; \boldsymbol{v}_1\boldsymbol{v}_2\ldots\boldsymbol{v}_{k-1}\boldsymbol{v}_k\boldsymbol{a}\boldsymbol{v}_k\boldsymbol{v}_{k-1}\ldots\boldsymbol{v}_2\boldsymbol{v}_1$$

Note that

$$\boldsymbol{b}^2 \;=\; \boldsymbol{Va}\widetilde{\boldsymbol{V}}\boldsymbol{Va}\widetilde{\boldsymbol{V}} \;=\; \boldsymbol{Va}^2\widetilde{\boldsymbol{V}} \;=\; \boldsymbol{a}^2.$$

Since each reflection is a linear transformation, a series of reflections is equally a linear transformation, i.e. the composition of the linear transformations. Consequently, the action of a versor can be extended, by means of the outermorphism definition (2.56), from vectors to all elements of geometric algebra. Below it is to be shown that this extension is particularly simple.

The property $\boldsymbol{V}\widetilde{\boldsymbol{V}} = 1$ is now being used. Let $\boldsymbol{C} = \boldsymbol{AB}$ be the geometric product of arbitrary multivectors $\boldsymbol{A}, \boldsymbol{B} \in \mathbb{R}_{p,q}$. The versor, applied as a sandwich product to $\boldsymbol{C}$, acts on all constituent parts in the same way it acts on the whole

$$\boldsymbol{V}\boldsymbol{C}\widetilde{\boldsymbol{V}} \;=\; \boldsymbol{V}\boldsymbol{A}\boldsymbol{B}\widetilde{\boldsymbol{V}} \;=\; \boldsymbol{V}\boldsymbol{A}\widetilde{\boldsymbol{V}}\boldsymbol{V}\boldsymbol{B}\widetilde{\boldsymbol{V}} \;=\; (\boldsymbol{V}\boldsymbol{A}\widetilde{\boldsymbol{V}})(\boldsymbol{V}\boldsymbol{B}\widetilde{\boldsymbol{V}}).$$

This may be exploited in respect of the commutator and anti-commutator product. Consider, for instance, the outer product of two transformed vectors $\boldsymbol{a}$ and $\boldsymbol{b}$, respectively.

$$\begin{aligned}
(\boldsymbol{V}\,\boldsymbol{a}\,\widetilde{\boldsymbol{V}}) \wedge (\boldsymbol{V}\,\boldsymbol{b}\,\widetilde{\boldsymbol{V}}) \;&=\; (\boldsymbol{V}\,\boldsymbol{a}\,\widetilde{\boldsymbol{V}}) \,\underline{\times}\, (\boldsymbol{V}\,\boldsymbol{b}\,\widetilde{\boldsymbol{V}}) \\
&=\; \frac{1}{2}\big(\boldsymbol{V}\boldsymbol{a}\widetilde{\boldsymbol{V}}\,\boldsymbol{V}\boldsymbol{b}\widetilde{\boldsymbol{V}} \;-\; \boldsymbol{V}\boldsymbol{b}\widetilde{\boldsymbol{V}}\,\boldsymbol{V}\boldsymbol{a}\widetilde{\boldsymbol{V}}\big) \\
&=\; \frac{1}{2}\big(\boldsymbol{V}\,\boldsymbol{ab}\,\widetilde{\boldsymbol{V}} \;-\; \boldsymbol{V}\,\boldsymbol{ba}\,\widetilde{\boldsymbol{V}}\big) \\
&=\; \boldsymbol{V}\,\Big(\,\frac{1}{2}\,(\boldsymbol{ab} \;-\; \boldsymbol{ba})\,\Big)\,\widetilde{\boldsymbol{V}} \\
&=\; \boldsymbol{V}\,\Big(\boldsymbol{a} \,\underline{\times}\, \boldsymbol{b}\Big)\,\widetilde{\boldsymbol{V}}.
\end{aligned}$$

This has ramifications. Recall that, pursuant to equation (2.34), the outer product can be expressed by means of an alternating sequence of commutators and anti-commutators between the involved vectors. A similar relation holds for the inner product of two blades, see corollary 2.9. Likewise any other combination of commutators and anti-commutators between vectors and/or blades gives either zero or an in-between product, different from the inner or the outer product. By the above relationship, recursively applied, it is shown that the extension of a (linear) versor transformation to these products simply differs in nothing from the application to a single vector – it just consists of building the sandwich structured product.

The recursive application in case of an expression involving an inner and an outer product, for example, amounts to

$$\begin{aligned}
(\boldsymbol{V}\boldsymbol{a}\widetilde{\boldsymbol{V}}) \cdot ((\boldsymbol{V}\boldsymbol{b}_1\widetilde{\boldsymbol{V}}) \wedge (\boldsymbol{V}\boldsymbol{b}_2\widetilde{\boldsymbol{V}})) \;&=\; (\boldsymbol{V}\boldsymbol{a}\widetilde{\boldsymbol{V}})\underline{\times}((\boldsymbol{V}\boldsymbol{b}_1\widetilde{\boldsymbol{V}})\underline{\times}(\boldsymbol{V}\boldsymbol{b}_2\widetilde{\boldsymbol{V}})) \\
&=\; (\boldsymbol{V}\boldsymbol{a}\widetilde{\boldsymbol{V}})\underline{\times}(\boldsymbol{V}(\boldsymbol{b}_1 \wedge \boldsymbol{b}_2)\widetilde{\boldsymbol{V}}) \\
&=\; \boldsymbol{V}(\boldsymbol{a}\underline{\times}(\boldsymbol{b}_1 \wedge \boldsymbol{b}_2))\widetilde{\boldsymbol{V}} \\
&=\; \boldsymbol{V}\Big(\;\boldsymbol{a} \cdot (\boldsymbol{b}_1 \wedge \boldsymbol{b}_2)\;\Big)\widetilde{\boldsymbol{V}}.
\end{aligned}$$

Of special importance is the fact that versors, with $\boldsymbol{V}\widetilde{\boldsymbol{V}} = 1$, do not alter the inner product

$$(\boldsymbol{V}\boldsymbol{a}\widetilde{\boldsymbol{V}}) \cdot (\boldsymbol{V}\boldsymbol{b}\widetilde{\boldsymbol{V}}) \;=\; \boldsymbol{V}(\boldsymbol{a} \cdot \boldsymbol{b})\widetilde{\boldsymbol{V}} \;=\; \boldsymbol{a} \cdot \boldsymbol{b}.$$

Hence the transformation of the whole is actually the transformation of its parts.

What makes these properties so beneficial is, for instance, that equations or rules may first be established in a simple coordinate system and do then also hold in their reflected, rotated or translated versions. A case in point is the conformal geometric algebra, which is the subject of chapter 3.

Make yourself aware of the possibility of versors acting on versors. Let $\boldsymbol{nVn}$ be the reflection of the versor $\boldsymbol{V}$ in the unit vector $\boldsymbol{n}$, $\boldsymbol{n}^2 = 1$. The effect of the transformation ensemble may easily be inferred writing

$$(\boldsymbol{nVn})\boldsymbol{x}(\boldsymbol{n}\widetilde{\boldsymbol{V}}\boldsymbol{n}) \;=\; \boldsymbol{n}(\boldsymbol{V}(\boldsymbol{nxn})\widetilde{\boldsymbol{V}})\boldsymbol{n}.$$

So the action of $\boldsymbol{V}$ eventually takes place, but in a temporally different frame. It amounts to the same, but $\boldsymbol{nVn}$ can as well be interpreted as the new modified versor $\boldsymbol{V}'$. Let, for instance $\boldsymbol{V} = \boldsymbol{v}_1\boldsymbol{v}_2\ldots\boldsymbol{v}_k$, such that

$$\boldsymbol{nVn} \;=\; \boldsymbol{nv}_1\boldsymbol{v}_2\ldots\boldsymbol{v}_k\boldsymbol{n} \;=\; (\boldsymbol{nv}_1\overbrace{\boldsymbol{n})(\boldsymbol{n}}^{1}\boldsymbol{v}_2\boldsymbol{n})\ldots(\boldsymbol{nv}_k\boldsymbol{n}) \;=\; \boldsymbol{v}_1'\boldsymbol{v}_2'\ldots\boldsymbol{v}_k' \;=\; \boldsymbol{V}'.$$

Last but not least, when applied to a k-blade, the versor likewise transforms the dual of that blade

$$\begin{aligned}
\boldsymbol{V}\boldsymbol{A}_{\langle k\rangle}\widetilde{\boldsymbol{V}} &= \boldsymbol{V}(\boldsymbol{a}_1\wedge\boldsymbol{a}_2\wedge\ldots\wedge\boldsymbol{a}_k)\widetilde{\boldsymbol{V}}\\
&= \boldsymbol{V}(\boldsymbol{x}_1\wedge\boldsymbol{x}_2\wedge\ldots\wedge\boldsymbol{x}_{n-k})\boldsymbol{I}\widetilde{\boldsymbol{V}}\\
&\overset{(2.49)}{=} (-1)^{k(n-1)}\,\boldsymbol{V}(\boldsymbol{x}_1\wedge\boldsymbol{x}_2\wedge\ldots\wedge\boldsymbol{x}_{n-k})\widetilde{\boldsymbol{V}}\boldsymbol{I}\\
&= (-1)^{k(n-1)}\,\boldsymbol{V}\boldsymbol{A}^*_{\langle k\rangle}\widetilde{\boldsymbol{V}}\boldsymbol{I},
\end{aligned} \tag{2.57}$$

where it was assumed that $\boldsymbol{a}_1\wedge\boldsymbol{a}_2\wedge\ldots\wedge\boldsymbol{a}_k = (\boldsymbol{x}_1\wedge\boldsymbol{x}_2\wedge\ldots\boldsymbol{x}_{n-k})\boldsymbol{I}$.

2.3.5 Subspace Considerations

By the next couple of definitions a phrase like '... $\boldsymbol{x}$ lies in $\boldsymbol{A}_{\langle k\rangle}$ ' can be stated more precisely.

Definition 2.16 (Outer product null space):
Given a blade $\boldsymbol{A}_{\langle k\rangle}\in\mathbb{R}_{p,q}$, its outer product null space (OPNS) comprises all points from $\mathbb{R}^{p,q}$ that lie in the subspace represented by $\boldsymbol{A}_{\langle k\rangle}$. The OPNS of $\boldsymbol{A}_{\langle k\rangle}$, denoted by $\mathbb{k}\mathrm{er}(\boldsymbol{A}_{\langle k\rangle})$, is defined as

$$\mathbb{k}\mathrm{er}(\boldsymbol{A}_{\langle k\rangle}) \;=\; \{\boldsymbol{x}\in\mathbb{R}^{p,q}\,|\,\boldsymbol{x}\wedge\boldsymbol{A}_{\langle k\rangle}=0\}.$$

■

Strictly speaking, the OPNS is supposed to be defined independently of the signature. It should, however, be clear that $\boldsymbol{x}\in\mathbb{k}\mathrm{er}(\boldsymbol{A}_{\langle k\rangle})$, with $\boldsymbol{x}=\sum_{i=1}^n x_i\mathbf{e}_i\in\mathbb{R}^{p,q}$, is equivalent to $\boldsymbol{x}'\in\mathbb{k}\mathrm{er}(\boldsymbol{A}_{\langle k\rangle})$, where $\boldsymbol{x}'=\sum_{i=1}^n x_i\mathbf{e}_i'\in\mathbb{R}^{a,b}$, as long as $a+b=n$.

Definition 2.17 (Inner product null space):
Given a blade $\boldsymbol{A}_{\langle k\rangle} \in \mathbb{R}_{p,q}$*, its inner product null space (IPNS), denoted by* $\mathbb{k}\mathrm{er}^*(\boldsymbol{A}_{\langle k\rangle})$*, consists of all points* $\boldsymbol{x} \in \mathbb{R}^{p,q}$ *that satisfy* $\boldsymbol{x} \cdot \boldsymbol{A}_{\langle k\rangle} = 0$*. Therefore its definition is*

$$\mathbb{k}\mathrm{er}^*(\boldsymbol{A}_{\langle k\rangle}) \;=\; \{\boldsymbol{x} \in \mathbb{R}^{p,q} \,|\, \boldsymbol{x} \cdot \boldsymbol{A}_{\langle k\rangle} = 0\}.$$

■

According to the last two definitions it follows

$$\mathbb{k}\mathrm{er}(\mathbf{0}) \;=\; \mathbb{R}^{p,q} \qquad \mathbb{k}\mathrm{er}(\alpha \in \mathbb{R}) \stackrel{\alpha\neq 0}{=} \{\mathbf{0}\}$$

$$\mathbb{k}\mathrm{er}^*(\mathbf{0}) \;=\; \mathbb{R}^{p,q} \qquad \mathbb{k}\mathrm{er}^*(\alpha \in \mathbb{R}) \;=\; \mathbb{R}^{p,q}$$

and

$$\boldsymbol{A}_{\langle k\rangle} \wedge \boldsymbol{B}_{\langle l\rangle} \;=\; 0 \qquad \Longleftrightarrow \qquad \dim\Big(\,\mathbb{k}\mathrm{er}(\boldsymbol{A}_{\langle k\rangle}) \cap \mathbb{k}\mathrm{er}(\boldsymbol{B}_{\langle l\rangle})\Big) \;>\; 0.$$

Subsequently, two new expressions are to be introduced - the *outer sum* and the *inner difference*. These expressions are chosen to reflect the belonging to the outer product and to the inner product, respectively. The corresponding definitions are given in terms of sets, but they are intended to be used with subspaces.

In the scope of this thesis the outer sum amounts to the *internal direct sum* and is solely formally not the same. Besides, the outer sum can be associated with the *Minkowski addition*. The inner difference $\mathbb{A} \ominus \mathbb{B}$ of the two point sets $\mathbb{A}, \mathbb{B} \subseteq \mathbb{R}^{p,q}$ retains only those points of $\mathbb{A}$ that can be considered completely orthogonal to $\mathbb{B}$. The inner difference is therefore dependent on the inner product.

Definition 2.18 (Outer sum):
Let $\mathbb{A}, \mathbb{B} \subseteq \mathbb{R}^{p,q}$*. Then their (outer) sum, denoted by* $\mathbb{A} \oplus \mathbb{B}$*, is defined as*

$$\mathbb{A} \oplus \mathbb{B} \;=\; \{\boldsymbol{a} + \boldsymbol{b} \,|\, \boldsymbol{a} \in \mathbb{A}, \boldsymbol{b} \in \mathbb{B}\}.$$

■

Note that if $\mathbb{A}$ and $\mathbb{B}$ represent vector spaces, their outer sum yields the joint vector space

$$\mathbb{A} \oplus \mathbb{B} \;=\; \mathrm{span}\{\{\boldsymbol{a}_{1\ldots r}\} \cup \{\boldsymbol{b}_{1\ldots s}\} \cup \{\boldsymbol{c}_{1\ldots t}\}\}\,,$$

such that $\{\boldsymbol{a}_{1\ldots r}\} \cup \{\boldsymbol{b}_{1\ldots s}\} \cup \{\boldsymbol{c}_{1\ldots t}\}$ is a basis of the new vector space, and where $\mathbb{A} = \mathrm{span}\{\{\boldsymbol{a}_{1\ldots r}\} \cup \{\boldsymbol{c}_{1\ldots t}\}\}$ and $\mathbb{B} = \mathrm{span}\{\{\boldsymbol{b}_{1\ldots s}\} \cup \{\boldsymbol{c}_{1\ldots t}\}\}$, respectively. Hence $\{\boldsymbol{c}_{1\ldots t}\}$ denotes the basis of a common subspace of $\mathbb{A}$ and $\mathbb{B}$.

By this definition, the OPNS of the outer product of two blades $\boldsymbol{A}_{\langle k\rangle}$ and $\boldsymbol{B}_{\langle l\rangle}$ can be evaluated by

$$\boldsymbol{A}_{\langle k\rangle} \wedge \boldsymbol{B}_{\langle l\rangle} \neq 0 \qquad \Longrightarrow \qquad \mathbb{k}\mathrm{er}(\boldsymbol{A}_{\langle k\rangle} \wedge \boldsymbol{B}_{\langle l\rangle}) \;=\; \mathbb{k}\mathrm{er}(\boldsymbol{A}_{\langle k\rangle}) \oplus \mathbb{k}\mathrm{er}(\boldsymbol{B}_{\langle l\rangle}),$$

where each element $\boldsymbol{c} \in \mathbb{k}\mathrm{er}(\boldsymbol{A}_{\langle k\rangle} \wedge \boldsymbol{B}_{\langle l\rangle})$ corresponds to a uniquely defined pair $(\boldsymbol{a}, \boldsymbol{b}) \in \mathbb{k}\mathrm{er}(\boldsymbol{A}_{\langle k\rangle}) \times \mathbb{k}\mathrm{er}(\boldsymbol{B}_{\langle l\rangle})$ such that $\boldsymbol{c} = \boldsymbol{a} + \boldsymbol{b}$. Regarding the outer sum of the vector spaces $\mathbb{A}$ and $\mathbb{B}$, as above, $\{\boldsymbol{c}_{1\ldots t}\} = \{\}$ is required.

From section 2.3.3, and especially from equation (2.54), it can be deduced that

$$\mathbb{k}\mathrm{er}(\boldsymbol{A}_{\langle k\rangle}) = \mathbb{k}\mathrm{er}^*(\boldsymbol{A}^*_{\langle k\rangle}) \qquad \mathbb{k}\mathrm{er}(\boldsymbol{A}^*_{\langle k\rangle}) = \mathbb{k}\mathrm{er}^*(\boldsymbol{A}_{\langle k\rangle})$$

$$\mathbb{k}\mathrm{er}(\boldsymbol{A}_{\langle k\rangle}) \oplus \mathbb{k}\mathrm{er}^*(\boldsymbol{A}_{\langle k\rangle}) = \mathbb{k}\mathrm{er}(\boldsymbol{A}_{\langle k\rangle}) \oplus \mathbb{k}\mathrm{er}(\boldsymbol{A}^*_{\langle k\rangle}) = \mathbb{R}^{p,q},$$

where in case of a null blade $\boldsymbol{A}_{\langle k\rangle}$, the outer sum is not a direct sum any more because it exists a common subspace, i.e. $\dim\!\big(\,\mathbb{k}\mathrm{er}(\boldsymbol{A}_{\langle k\rangle}) \cap \mathbb{k}\mathrm{er}(\boldsymbol{A}^*_{\langle k\rangle})\,\big)$ is greater than zero. This is detailed in the section starting at page 72.

Definition 2.19 (Inner difference):
Let $\mathbb{A}, \mathbb{B} \subseteq \mathbb{R}^{p,q}$. Then their (inner) difference, denoted by $\mathbb{A} \ominus \mathbb{B}$, is defined as

$$\mathbb{A} \ominus \mathbb{B} = \{\boldsymbol{a} \in \mathbb{A} \,|\, \forall \boldsymbol{b} \in \mathbb{B} : \ \boldsymbol{a} \cdot \boldsymbol{b} = 0\,\}.$$

Especially, let

$$\mathbb{A} \ominus_{\boldsymbol{\varepsilon}} \mathbb{B} = \{\boldsymbol{a} \in \mathbb{A} \,|\, \forall \boldsymbol{b} \in \mathbb{B} : \ \boldsymbol{a} *_{\boldsymbol{\varepsilon}} \boldsymbol{b} = 0\,\}$$

denote the Euclidean inner difference. ■

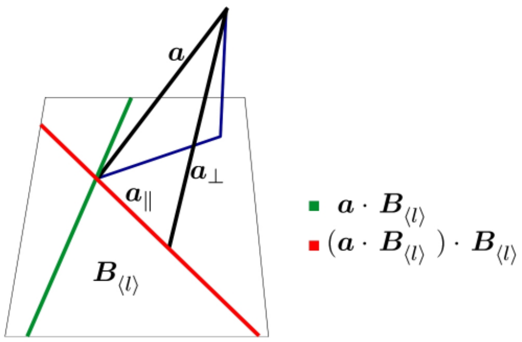

Fig. 2.7: Orthogonal complements: the spaces indicated by the blue and the red line are orthogonal. Similarly, $\boldsymbol{a}_{||}$ and $\boldsymbol{a}_\perp$ are assumed to be orthogonal. The blue 'decomposition' of $\boldsymbol{a}$ is meant to be perpendicular.

Just as the outer product is related to the outer sum, the inner product is related to the inner difference: by the considerations on page 51, it is known that $\boldsymbol{a} \cdot \boldsymbol{B}_{\langle l\rangle}$ is the orthogonal complement of $\boldsymbol{a}$ in $\boldsymbol{B}_{\langle l\rangle}$ if $\boldsymbol{B}^2_{\langle l\rangle} \neq 0$. This exactly matches the definition of the inner difference if $\boldsymbol{a} \cdot \boldsymbol{B}_{\langle l\rangle} \neq 0$

$$\mathbb{k}\mathrm{er}(\boldsymbol{a} \cdot \boldsymbol{B}_{\langle l\rangle}) = \mathbb{k}\mathrm{er}(\boldsymbol{B}_{\langle l\rangle}) \ominus \mathbb{k}\mathrm{er}(\boldsymbol{a}).$$

Hence if $\boldsymbol{B}^2_{\langle l\rangle} \neq 0$ and $\boldsymbol{a} \cdot \boldsymbol{B}_{\langle l\rangle} \neq 0$, it may be written

$$\mathbb{k}\mathrm{er}((\boldsymbol{a} \cdot \boldsymbol{B}_{\langle l\rangle}) \cdot \boldsymbol{B}_{\langle l\rangle}) = \mathbb{k}\mathrm{er}(\boldsymbol{B}_{\langle l\rangle}) \ominus \Big(\mathbb{k}\mathrm{er}(\boldsymbol{B}_{\langle l\rangle}) \ominus \mathbb{k}\mathrm{er}(\boldsymbol{a})\Big), \qquad l \geq 2.$$

These relations are of special importance as the orthogonal complement of the orthogonal complement of $\boldsymbol{a}$ in $\boldsymbol{B}_{\langle l \rangle}$ in $\boldsymbol{B}_{\langle l \rangle}$, that is $(\boldsymbol{a} \cdot \boldsymbol{B}_{\langle l \rangle}) \cdot \boldsymbol{B}_{\langle l \rangle}$, must[13] be the *projection* of $\boldsymbol{a}$ onto $\boldsymbol{B}_{\langle l \rangle}$, cf. figure 2.7. Recall that this has already been figured out on page 50, although under the condition that $\boldsymbol{B}_{\langle l \rangle}^2 = 1$.

Aside: *It is always a problem if the argument 'E' of* $\mathbb{k}\mathrm{er}(E)$ *attains a scalar, which is why several conditions, e.g. like* $\boldsymbol{a} \cdot \boldsymbol{B}_{\langle l \rangle} \neq 0$ *or* $l \geq 2$*, have to be stated. Omitting these conditions would, however, require to put an upper limit to the OPNS, i.e. to write* $\mathbb{k}\mathrm{er}(\boldsymbol{B}_{\langle l \rangle}) \cap \mathbb{k}\mathrm{er}(\boldsymbol{a} \cdot \boldsymbol{B}_{\langle l \rangle}) = \mathbb{k}\mathrm{er}(\boldsymbol{B}_{\langle l \rangle}) \ominus \mathbb{k}\mathrm{er}(\boldsymbol{a})$ *rather than* $\mathbb{k}\mathrm{er}(\boldsymbol{a} \cdot \boldsymbol{B}_{\langle l \rangle}) = \mathbb{k}\mathrm{er}(\boldsymbol{B}_{\langle l \rangle}) \ominus \mathbb{k}\mathrm{er}(\boldsymbol{a})$.

Example 2.12 (Projection of a vector):
The orthogonality of $\boldsymbol{a} \cdot \boldsymbol{B}_{\langle l \rangle}$ *and* $(\boldsymbol{a} \cdot \boldsymbol{B}_{\langle l \rangle}) \cdot \boldsymbol{B}_{\langle l \rangle}$ *can be shown via*

$$
\begin{aligned}
&(\boldsymbol{a} \cdot \boldsymbol{B}_{\langle l \rangle}) \cdot \Big((\boldsymbol{a} \cdot \boldsymbol{B}_{\langle l \rangle}) \cdot \boldsymbol{B}_{\langle l \rangle}\Big) \\
&\quad = \tfrac{1}{2}\Big\langle (\boldsymbol{a} \cdot \boldsymbol{B}_{\langle l \rangle})(\boldsymbol{a} \cdot \boldsymbol{B}_{\langle l \rangle})\boldsymbol{B}_{\langle l \rangle} - (-1)^{l-1}\, (\boldsymbol{a} \cdot \boldsymbol{B}_{\langle l \rangle})\boldsymbol{B}_{\langle l \rangle}(\boldsymbol{a} \cdot \boldsymbol{B}_{\langle l \rangle})\Big\rangle_{l-2} \\
&\quad = \tfrac{1}{2}(\boldsymbol{a} \cdot \boldsymbol{B}_{\langle l \rangle})^2 \left\langle \boldsymbol{B}_{\langle l \rangle}\right\rangle_{l-2} - (-1)^{2(l-1)}\, \tfrac{1}{2}\left\langle \boldsymbol{B}_{\langle l \rangle}(\boldsymbol{a} \cdot \boldsymbol{B}_{\langle l \rangle})(\boldsymbol{a} \cdot \boldsymbol{B}_{\langle l \rangle})\right\rangle_{l-2} \\
&\quad\quad = \tfrac{1}{2}(\boldsymbol{a} \cdot \boldsymbol{B}_{\langle l \rangle})^2 \left\langle \boldsymbol{B}_{\langle l \rangle}\right\rangle_{l-2} - \tfrac{1}{2}(\boldsymbol{a} \cdot \boldsymbol{B}_{\langle l \rangle})^2 \left\langle \boldsymbol{B}_{\langle l \rangle}\right\rangle_{l-2} \;=\; 0.
\end{aligned}
$$

Equation (2.42), that is $\boldsymbol{A}_{\langle k \rangle} \cdot (\boldsymbol{A}_{\langle k \rangle} \cdot \boldsymbol{B}_{\langle l \rangle}) = 0$ if $k < l$, immediately implies that if $\boldsymbol{A}_{\langle k \rangle} \cdot \boldsymbol{B}_{\langle l \rangle} \neq 0$

$$
\mathbb{k}\mathrm{er}(\boldsymbol{A}_{\langle k \rangle} \cdot \boldsymbol{B}_{\langle l \rangle}) \;=\; \mathbb{k}\mathrm{er}(\boldsymbol{B}_{\langle l \rangle}) \ominus \mathbb{k}\mathrm{er}(\boldsymbol{A}_{\langle k \rangle}), \qquad k < l,
$$

and in concordance with equation (2.43)

$$
\mathbb{k}\mathrm{er}((\boldsymbol{A}_{\langle k \rangle} \cdot \boldsymbol{B}_{\langle l \rangle}) \cdot \boldsymbol{B}_{\langle l \rangle}) \;=\; \mathbb{k}\mathrm{er}(\boldsymbol{B}_{\langle l \rangle}) \ominus \Big(\mathbb{k}\mathrm{er}(\boldsymbol{B}_{\langle l \rangle}) \ominus \mathbb{k}\mathrm{er}(\boldsymbol{A}_{\langle k \rangle})\Big), \qquad k < l.
$$

The previous identity describes a projection of $\boldsymbol{A}_{\langle k \rangle}$ onto $\boldsymbol{B}_{\langle l \rangle}$. Regrettably, it is only valid for non-null blades. For a better handling and understanding of null blades, it is now being dealt with frames of such. Then the discussion of how a blade can be projected onto another blade can be continued; see page 76.

The Issue of Null Blades

Consider the mutually orthogonal vectors $\mathbb{A} = \{\boldsymbol{n}\} \cup \{\boldsymbol{z}_{1\ldots k}\}$, where $\boldsymbol{n}$ is assumed to be the only null vector, i.e. $\boldsymbol{n}^2 = 0$. The vectors $\mathbb{A}' = \{\boldsymbol{n}\} \cup \{\boldsymbol{z}'_{1\ldots k}\}$ with $\boldsymbol{z}'_i = \boldsymbol{z}_i + \lambda_i \boldsymbol{n}$, $\lambda_i \in \mathbb{R}$ and $i \in [1,k]_{\mathbb{Z}}$, are still orthogonal. Let $\boldsymbol{Z}_{\langle k \rangle} = \bigwedge_{i=1}^{k} \boldsymbol{z}_i$ and

[13] Up to a scalar factor

$\boldsymbol{Z'}_{\langle k \rangle} = \bigwedge_{i=1}^{k} \boldsymbol{z}'_i$, respectively. It follows $\boldsymbol{n} \wedge \boldsymbol{Z}_{\langle k \rangle} = \boldsymbol{n} \wedge \boldsymbol{Z'}_{\langle k \rangle}$ and even $\boldsymbol{Z}^2_{\langle k \rangle} = \boldsymbol{Z'}^2_{\langle k \rangle}$. But $\boldsymbol{Z'}_{\langle k \rangle}$ has a certain offset $\boldsymbol{n} \wedge \boldsymbol{O}_{\langle k-1 \rangle}$

$$\boldsymbol{Z'}_{\langle k \rangle} = \bigwedge_{i=1}^{k} (\boldsymbol{z}_i + \lambda_i \boldsymbol{n}) \;=\; \boldsymbol{Z}_{\langle k \rangle} \;+\; \boldsymbol{n} \wedge \boldsymbol{O}_{\langle k-1 \rangle},$$

$$\text{where} \qquad \boldsymbol{O}_{\langle k-1 \rangle} \;=\; \sum_{j=1}^{k} (-1)^{j-1}\, \lambda_j \; [\boldsymbol{Z}_{\langle k \rangle} \backslash \boldsymbol{z}_j].$$

It is therefore not desirable to work in the primed basis $\mathbb{A}'$. In order to fully remove the ambiguousness the following operation, which will later on be called *rejection*, can be used

$$\boldsymbol{z} := \boldsymbol{z}' \;-\; \frac{\boldsymbol{n}^\dagger \cdot \boldsymbol{z}'}{\boldsymbol{n}^\dagger \cdot \boldsymbol{n}}\, \boldsymbol{n}, \qquad\qquad \boldsymbol{z} \in \{\boldsymbol{z'}_{1\ldots k}\}.$$

As a result it is obtained that $\boldsymbol{n}^\dagger \cdot \boldsymbol{z} = \boldsymbol{n} *_{\boldsymbol{\varepsilon}} \boldsymbol{z} = 0$ in addition to $\boldsymbol{n} \cdot \boldsymbol{z} = \boldsymbol{n}^\dagger *_{\boldsymbol{\varepsilon}} \boldsymbol{z} = 0$. The definition generalizes this concept.

Definition 2.20 (Sound basis):
Let $\mathbb{A}' = \{\boldsymbol{n'}_{1\ldots r}\} \cup \{\boldsymbol{z'}_{1\ldots s}\}$ *denote an orthogonal basis such that additionally* $\boldsymbol{n'}^2_i = 0$, $i \in [1,r]_{\mathbb{Z}}$. *Then the sound basis is defined as* $\mathbb{A} = \{\boldsymbol{n}_{1\ldots r}\} \cup \{\boldsymbol{z}_{1\ldots s}\}$, *such that* $\forall \boldsymbol{x}, \boldsymbol{y} \in \mathbb{A} : \boldsymbol{x} \neq \boldsymbol{y} \Leftrightarrow \boldsymbol{x} \cdot \boldsymbol{y} = 0$, *and moreover,* $\forall \boldsymbol{x} \in \mathbb{A},\ \forall \boldsymbol{y} \in \{\boldsymbol{n}_{1\ldots r}\} : \boldsymbol{x} \neq \boldsymbol{y} \Leftrightarrow \boldsymbol{x} *_{\boldsymbol{\varepsilon}} \boldsymbol{y} = 0$. ■

Hence all elements of a sound basis are mutually orthogonal. In addition, the null vectors are mutually perpendicular. Finally, the space span$\{\boldsymbol{z}_{1\ldots s}\}$ is perpendicular to the space span$\{\boldsymbol{n}_{1\ldots r}\}$. Recalling that $\boldsymbol{a} *_{\boldsymbol{\varepsilon}} \boldsymbol{b} = \boldsymbol{a}^\dagger \cdot \boldsymbol{b}$ demonstrates that the conjugate of each vector in $\{\boldsymbol{n}_{1\ldots r}\}$ is orthogonal to the remaining ones.

In order to achieve that the null vectors become mutually perpendicular as well, a *Gram-Schmidt orthogonalization* of $\{\boldsymbol{n'}_{1\ldots r}\}$, carried out in the Euclidean space $\mathbb{R}^n$, can be used. The i^{th} vector $\boldsymbol{n}_i$ can then be represented by the linear transformation $\boldsymbol{n}_i = \boldsymbol{n}'_i - \sum_{j<i} \lambda_{ij} \boldsymbol{n}'_j$ with suitable factors $\lambda_{ij} \in \mathbb{R}$. This transformation corresponds to a lower triangular matrix with determinant one such that the linear independence of the vectors is preserved. Besides, the orthogonality regarding $\mathbb{R}^{p,q}$ is preserved as well. In practical applications, the magnitude of the blade that might be associated with the basis could make it necessary to apply a scaling to the new basis.

The concept of the sound basis extends in a natural way to a basis of $\mathbb{R}^{p,q}$. Let $\mathbb{A} = \{\boldsymbol{n}_{1\ldots r}\} \cup \{\boldsymbol{z}_{1\ldots s}\}$ be a sound basis. Observing that $\boldsymbol{n}^\dagger_i *_{\boldsymbol{\varepsilon}} \boldsymbol{n}_j = \boldsymbol{n}^{\dagger\dagger}_i \cdot \boldsymbol{n}_j = \boldsymbol{n}_i \cdot \boldsymbol{n}_j$ demonstrates that

$$\forall \boldsymbol{n} \in \{\boldsymbol{n}_{1\ldots r}\}, \forall \boldsymbol{x} \in \mathbb{A} : \quad \boldsymbol{n}^\dagger *_{\boldsymbol{\varepsilon}} \boldsymbol{x} \;=\; 0.$$

Consequently, the space spanned by the conjugates $\{\boldsymbol{n}^\dagger_{1\ldots r}\}$ is perpendicular to span$\mathbb{A}$. Further, the blade $\boldsymbol{Z'}_{\langle 2r \rangle} = (\bigwedge_{i=1}^{r} \boldsymbol{n}^\dagger_i) \wedge (\bigwedge_{i=1}^{r} \boldsymbol{n}_i)$ is not a null blade as $(\boldsymbol{n}^\dagger \wedge \boldsymbol{n})^2 = \|\boldsymbol{n}\|^2$. Hence an orthogonal basis $\{\overline{\boldsymbol{z}}_{1\ldots t}\}$ can be determined from the dual $(\boldsymbol{Z'}_{\langle 2r\rangle} \wedge \bigwedge_{i=1}^{s} \boldsymbol{z}_i)^*$ such that $(\bigwedge_{j=1}^{t} \overline{\boldsymbol{z}}_j) \wedge \boldsymbol{Z'}_{\langle 2r\rangle} \wedge (\bigwedge_{i=1}^{s} \boldsymbol{z}_i) \propto \boldsymbol{I}$. In analogy with $\mathbb{A}$, the frame $\{\overline{\boldsymbol{z}}_{1\ldots t}\}$ can be chosen to be perpendicular to $\{\boldsymbol{n}^\dagger{}_{1\ldots r}\}$. Hence $\overline{\mathbb{A}} = \{\overline{\boldsymbol{z}}_{1\ldots t}\} \cup \{\boldsymbol{n}^\dagger{}_{1\ldots r}\}$ is a sound basis as well that completes $\mathbb{A}$ to an overall basis of $\mathbb{R}^{p,q}$. Note, however, that $\mathbb{A} \cup \overline{\mathbb{A}}$ is neither a pure perpendicular nor a pure orthogonal basis since, for example, for any null vector $\boldsymbol{n}^\dagger \cdot \boldsymbol{n} \neq 0$. So eventually, null blades induce a partitioning of $\mathbb{R}^{p,q}$ into the two complementary sound frames $\mathbb{A}$ and $\overline{\mathbb{A}}$.

Equation (2.55) brings up a problem: the outer product of a null blade with its dual is zero rather than the pseudoscalar $\boldsymbol{I}$.

$$\boldsymbol{A}_{\langle k\rangle}^2 = 0 \quad \Longleftrightarrow \quad (\boldsymbol{A}_{\langle k\rangle}^*)^2 = 0 \quad \Longleftrightarrow \quad \boldsymbol{A}_{\langle k\rangle} \wedge \boldsymbol{A}_{\langle k\rangle}^* = 0$$

This implies that a null blade $\boldsymbol{A}_{\langle k\rangle}$ and its dual $\boldsymbol{A}_{\langle k\rangle}^*$ share a common subspace. In the case of $\boldsymbol{A}_{\langle k\rangle} = \boldsymbol{n}$, $\boldsymbol{n}^2 = 0$, the only space that can be shared is $\boldsymbol{n}$ itself. It is therefore suggesting that the common subspace is spanned by those basis vectors of $\boldsymbol{A}_{\langle k\rangle}$ that square to zero. This is now to be analyzed.

Example 2.13 (Null blade):

Let $\boldsymbol{A}_{\langle k\rangle} = (\mathbf{e}_3 + \mathbf{e}_4) \wedge \mathbf{e}_1 \in \mathbb{R}_{3,1}$ *with* $\boldsymbol{n} = \mathbf{e}_3 + \mathbf{e}_4$. *Hence the pseudoscalar is* $\boldsymbol{I} = \mathbf{e}_{1234}$ *with* $\boldsymbol{I}^{-1} = -\boldsymbol{I}$. *Then, at first,*

$$\boldsymbol{n}^* = (\mathbf{e}_3 + \mathbf{e}_4)^* = -\mathbf{e}_1\mathbf{e}_2(\mathbf{e}_3 + \mathbf{e}_4) = -\mathbf{e}_1\mathbf{e}_2 \wedge \boldsymbol{n}.$$

Now consider the dual of $\boldsymbol{A}_{\langle k\rangle}$

$$\boldsymbol{A}_{\langle k\rangle}^* = \boldsymbol{A}_{\langle k\rangle}\boldsymbol{I}^{-1} = \mathbf{e}_2\mathbf{e}_3 + \mathbf{e}_2\mathbf{e}_4 = \mathbf{e}_2 \wedge \boldsymbol{n}.$$

Moreover

$$\boldsymbol{n} \cdot [\boldsymbol{A}_{\langle k\rangle} \backslash \boldsymbol{n}]^* = \boldsymbol{n} \cdot \mathbf{e}_1^* = \mathbf{e}_2\mathbf{e}_3 + \mathbf{e}_2\mathbf{e}_4 = \mathbf{e}_2 \wedge \boldsymbol{n} = \boldsymbol{A}_{\langle k\rangle}^*.$$

Let, at first, $\{\boldsymbol{n}_1, \boldsymbol{z}_2, \boldsymbol{z}_3, \ldots, \boldsymbol{z}_k\}$ be a *sound* orthogonal frame of $\boldsymbol{A}_{\langle k\rangle}$ such that only $\boldsymbol{n}_1^2 = 0$ and thus $\boldsymbol{A}_{\langle k\rangle}^2 = 0$. Then the dual of $\boldsymbol{A}_{\langle k\rangle}$ can be expressed as

$$\boldsymbol{A}_{\langle k\rangle}^* = (\boldsymbol{n}_1 \wedge (\boldsymbol{z}_2\boldsymbol{z}_3 \ldots \boldsymbol{z}_k))\boldsymbol{I}^{-1} = \boldsymbol{n}_1 \cdot (\boldsymbol{z}_2\boldsymbol{z}_3 \ldots \boldsymbol{z}_k)\boldsymbol{I}^{-1} = \boldsymbol{n}_1 \cdot [\boldsymbol{A}_{\langle k\rangle} \backslash \boldsymbol{n}_1]^*.$$

Note that $([\boldsymbol{A}_{\langle k\rangle} \backslash \boldsymbol{n}_1]^*)^2 \neq 0$ and thus $[\boldsymbol{A}_{\langle k\rangle} \backslash \boldsymbol{n}_1] \wedge [\boldsymbol{A}_{\langle k\rangle} \backslash \boldsymbol{n}_1]^* \propto \boldsymbol{I}$, which shows that $\boldsymbol{n}_1 \in \ker([\boldsymbol{A}_{\langle k\rangle} \backslash \boldsymbol{n}_1]^*)$. This is intelligible, because the dual of that space[14] that is orthogonal to a certain vector contains the respective vector again, cf. equation (2.54). As a consequence, it exists a basis for the $n-k+1$-blade $[\boldsymbol{A}_{\langle k\rangle} \backslash \boldsymbol{n}_1]^*$ that includes $\boldsymbol{n}_1$. But this basis, say $\{\boldsymbol{n}_1, \boldsymbol{b}_2, \boldsymbol{b}_3, \ldots, \boldsymbol{b}_{n-k+1}\} \subset \mathbb{R}^{p,q}$, cannot be an

[14] The space of a non-null blade.

orthogonal one; if $\boldsymbol{n}_1 \cdot \boldsymbol{b}_i = 0$, $i \in [2{,}n-k+1]_{\mathbb{Z}}$, including $\boldsymbol{n}_1^2 = 0$, then the expression

$$\boldsymbol{A}^*_{\langle k\rangle} = \boldsymbol{n}_1 \cdot [\boldsymbol{A}_{\langle k\rangle}\backslash\boldsymbol{n}_1]^* \;=\; \sum_{i=1}^{n-k+1} (-1)^{i-1}(\boldsymbol{n}_1 \cdot \boldsymbol{b}_i)\;\Big[[\boldsymbol{A}_{\langle k\rangle}\backslash\boldsymbol{n}_1]^* \backslash \boldsymbol{b}_i\Big]$$

attains zero, which cannot be true as $\boldsymbol{A}^*_{\langle k\rangle} \neq 0$. It must therefore exist at least one vector $\boldsymbol{b}_x \in \mathbb{R}^{p,q}$, $x \in [2{,}n-k+1]_{\mathbb{Z}}$, with $\boldsymbol{n}_1 \cdot \boldsymbol{b}_x \neq 0$. Further, for the corresponding remainder it holds

$$\boldsymbol{n}_1 \in \mathbb{k}\mathrm{er}([[\boldsymbol{A}_{\langle k\rangle}\backslash\boldsymbol{n}_1]^* \backslash \boldsymbol{b}_x]),$$

which proves that $\boldsymbol{n}_1 \in \mathbb{k}\mathrm{er}(\boldsymbol{A}^*_{\langle k\rangle})$ *and* $\boldsymbol{n}_1 \in \mathbb{k}\mathrm{er}(\boldsymbol{A}_{\langle k\rangle})$.

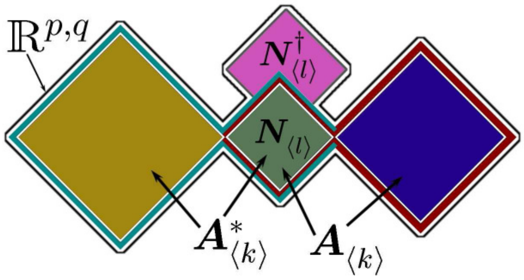

Fig. 2.8: Null blades: if $\boldsymbol{N}_{\langle l\rangle}$ is part of $\boldsymbol{A}_{\langle k\rangle}$ then $\boldsymbol{N}_{\langle l\rangle}$ is part of $\boldsymbol{A}^*_{\langle k\rangle}$ as well. The perpendicularity of the subspaces is indicated by the right angles between the rhombi. $\boldsymbol{N}_{\langle l\rangle}$ and $\boldsymbol{N}^\dagger_{\langle l\rangle}$ are parallel (perpendicular) w.r.t the inner product (Euclidean scalar product), although $\boldsymbol{N}^\dagger_{\langle l\rangle} \wedge \boldsymbol{N}_{\langle l\rangle} \neq 0$.

The next example reinforces the assumption that the conjugate of $\boldsymbol{n}_1$ might be the sought vector $\boldsymbol{b}_x$ for frame of $[\boldsymbol{A}_{\langle k\rangle}\backslash\boldsymbol{n}_1]^*$.

Example 2.14 (Null blade - continuation):
Recall the situation in example 2.13. A possible basis for $[\boldsymbol{A}_{\langle k\rangle}\backslash\boldsymbol{n}]^*$ *arises from the evaluation*

$$\begin{aligned}[\boldsymbol{A}_{\langle k\rangle}\backslash\boldsymbol{n}]^* \;=\; \mathbf{e}_1^* \;=\; -\mathbf{e}_2\mathbf{e}_3\mathbf{e}_4 \;&=\; \tfrac{1}{2}\,\mathbf{e}_2 \wedge (\mathbf{e}_3+\mathbf{e}_4) \wedge (\mathbf{e}_3-\mathbf{e}_4)\\ &=\; \tfrac{1}{2}\,\mathbf{e}_2 \wedge \boldsymbol{n} \wedge \boldsymbol{n}^\dagger.\end{aligned}$$

And even $(\mathbf{e}_1 + \lambda\,\boldsymbol{n})^* = \boldsymbol{n} \wedge \mathbf{e}_2 \wedge (\lambda\mathbf{e}_1 + \boldsymbol{n}^\dagger/2)$, $\lambda \in \mathbb{R}$.

With the help of equation (2.53), and since $[\boldsymbol{A}_{\langle k\rangle}\backslash\boldsymbol{n}_1]$ is not a null blade, it can indeed be substantiated that $\boldsymbol{n}_1^\dagger \in \mathbb{k}\mathrm{er}([\boldsymbol{A}_{\langle k\rangle}\backslash\boldsymbol{n}_1]^*)$

$$\boldsymbol{n}_1^\dagger \wedge [\boldsymbol{A}_{\langle k\rangle}\backslash\boldsymbol{n}_1]^* \;=\; \Big(\boldsymbol{n}_1^\dagger \cdot [\boldsymbol{A}_{\langle k\rangle}\backslash\boldsymbol{n}_1]\Big)^* \;=\; \Big(\boldsymbol{n}_1 \cdot_{\boldsymbol{\varepsilon}} [\boldsymbol{A}_{\langle k\rangle}\backslash\boldsymbol{n}_1]\Big)^* \;=\; 0.$$

Here it is exploited that the basis of $[\boldsymbol{A}_{\langle k\rangle}\backslash\boldsymbol{n}_1]$ is sound regarding $\boldsymbol{n}_1$.

It is now possible to write

$$
\begin{aligned}
\boldsymbol{I} &\propto [\boldsymbol{A}_{\langle k\rangle}\backslash\boldsymbol{n}_1] \wedge [\boldsymbol{A}_{\langle k\rangle}\backslash\boldsymbol{n}_1]^* \\
&\propto [\boldsymbol{A}_{\langle k\rangle}\backslash\boldsymbol{n}_1] \wedge \left[[\boldsymbol{A}_{\langle k\rangle}\backslash\boldsymbol{n}_1]^*\backslash\{\boldsymbol{n}_1, \boldsymbol{n}_1^\dagger\}\right] \wedge \boldsymbol{n}_1 \wedge \boldsymbol{n}_1^\dagger \\
&\propto \boldsymbol{A}_{\langle k\rangle} \wedge \left[[\boldsymbol{A}_{\langle k\rangle}\backslash\boldsymbol{n}_1]^*\backslash\{\boldsymbol{n}_1, \boldsymbol{n}_1^\dagger\}\right] \wedge \boldsymbol{n}_1^\dagger \\
&\propto \boldsymbol{A}_{\langle k\rangle} \wedge (([\boldsymbol{A}_{\langle k\rangle}\backslash\boldsymbol{n}_1]^* \cdot \boldsymbol{n}_1^\dagger) \cdot \boldsymbol{n}_1) \wedge \boldsymbol{n}_1^\dagger \\
&\overset{(2.44),5.}{\propto} \boldsymbol{A}_{\langle k\rangle} \wedge ([\boldsymbol{A}_{\langle k\rangle}\backslash\boldsymbol{n}_1]^* \cdot \boldsymbol{n}_1^\dagger) \\
&\propto \boldsymbol{A}_{\langle k\rangle} \wedge ([\boldsymbol{A}_{\langle k\rangle}\backslash\boldsymbol{n}_1] \wedge \boldsymbol{n}_1^\dagger)^*.
\end{aligned}
$$

Hence the complement of a null blade $\boldsymbol{A}_{\langle k\rangle}$ can be obtained by turning the null vector into its conjugate and building afterwards the dual. This technique may also be extended to the case where more than one null vector is involved, i.e. if $\boldsymbol{A}_{\langle k\rangle} = \boldsymbol{N}_{\langle l\rangle} \wedge \boldsymbol{A'}_{\langle k-l\rangle}$ then

$$
\boldsymbol{I} \propto \left(\boldsymbol{N}_{\langle l\rangle} \wedge \boldsymbol{A'}_{\langle k-l\rangle}\right) \wedge \left(\boldsymbol{N}^\dagger_{\langle l\rangle} \wedge \boldsymbol{A'}_{\langle k-l\rangle}\right)^*.
$$

This result can immediately be verified by means of equation (2.51). Note that a null blade has no *orthogonal* complement w.r.t $\mathbb{R}^{p,q}$ because $\boldsymbol{A}^*_{\langle k\rangle}$ is not a complement of $\boldsymbol{A}_{\langle k\rangle}$ and because $(\boldsymbol{N}^\dagger_{\langle l\rangle} \wedge \boldsymbol{A'}_{\langle k-l\rangle})^*$ is neither orthogonal nor perpendicular to $\boldsymbol{A}_{\langle k\rangle}$.

The following considerations are in particular significant when dealing with the factorization of a blade.

Projecting with Geometric Algebra

Let $\mathbb{B} = \{\boldsymbol{n}_{1\ldots r}\} \cup \{\boldsymbol{z}_{1\ldots s}\}$ be a sound frame for the null blade $\boldsymbol{B}_{\langle l\rangle}$, specifically $\boldsymbol{B}_{\langle l\rangle} = (\bigwedge_{i=1}^r \boldsymbol{n}_i) \wedge (\bigwedge_{i=1}^s \boldsymbol{z}_i)$. An arbitrary vector $\boldsymbol{a} \in \mathbb{R}^{p,q}$ can then be expressed as

$$
\boldsymbol{a} = \overline{\gamma}^i\,\overline{\boldsymbol{z}}_i + \overline{\alpha}^i \boldsymbol{n}_i^\dagger + \alpha^i \boldsymbol{n}_i + \gamma^i \boldsymbol{z}_i,
$$

such that $\overline{\mathbb{B}} = \{\boldsymbol{n}^\dagger{}_{1\ldots r}\} \cup \{\overline{\boldsymbol{z}}_{1\ldots t}\}$ is a sound basis as well. The sets $\{\overline{\boldsymbol{z}}_{1\ldots t}\}$ and $\{\boldsymbol{z}_{1\ldots s}\}$ can be assumed to be orthogonal, too. Consider the inner product

$$
\boldsymbol{a} \cdot \boldsymbol{B}_{\langle l\rangle} = \overline{\alpha}^i (-1)^{i-1} (\boldsymbol{n}_i^\dagger \cdot \boldsymbol{n}_i)\,[\boldsymbol{B}_{\langle l\rangle}\backslash\boldsymbol{n}_i] \;+\; \gamma^j (-1)^{r+j-1}\,\boldsymbol{z}_j^2\,[\boldsymbol{B}_{\langle l\rangle}\backslash\boldsymbol{z}_j].
$$

Hence the $\boldsymbol{n}$-parts of $\boldsymbol{a}$ that lie in $\mathbb{k}\mathrm{er}(\boldsymbol{B}_{\langle l\rangle})$ have no influence, and the $\boldsymbol{n}^\dagger$-parts that do not come from $\mathbb{k}\mathrm{er}(\boldsymbol{B}_{\langle l\rangle})$ produce components in $\boldsymbol{a} \cdot \boldsymbol{B}_{\langle l\rangle}$. This explains why the inner product cannot always be used for projecting in geometric algebra.

This problem cannot be overcome easily. Nevertheless, it is always possible to invoke the 'Euclidean alternative' if $\boldsymbol{A}_{\langle k\rangle} \cdot_{\boldsymbol{\varepsilon}} \boldsymbol{B}_{\langle l\rangle} \neq 0$

$$
\begin{aligned}
\mathbb{k}\mathrm{er}(\boldsymbol{B}_{\langle l\rangle}) \ominus_{\boldsymbol{\varepsilon}} \left(\mathbb{k}\mathrm{er}(\boldsymbol{B}_{\langle l\rangle}) \ominus_{\boldsymbol{\varepsilon}} \mathbb{k}\mathrm{er}(\boldsymbol{A}_{\langle k\rangle})\right) &\overset{k\leq l}{\equiv} \mathbb{k}\mathrm{er}((\boldsymbol{A}_{\langle k\rangle} \cdot_{\boldsymbol{\varepsilon}} \boldsymbol{B}_{\langle l\rangle}) \cdot_{\boldsymbol{\varepsilon}} \boldsymbol{B}_{\langle l\rangle}) \\
&= \mathbb{k}\mathrm{er}((\boldsymbol{A}^\dagger_{\langle k\rangle} \cdot \boldsymbol{B}_{\langle l\rangle})^\dagger \cdot \boldsymbol{B}_{\langle l\rangle}).
\end{aligned}
$$

In this case, $\boldsymbol{A}_{\langle k\rangle}$ is self-evidently perpendicular, but not orthogonal, to the result, that is

$$\boldsymbol{A}_{\langle k\rangle} \cdot \left((\boldsymbol{A}^{\dagger}_{\langle k\rangle} \cdot \boldsymbol{B}_{\langle l\rangle})^{\dagger} \cdot \boldsymbol{B}_{\langle l\rangle} \right) \neq 0.$$

The dedicated projection formula may further be modified as

$$\begin{aligned} (\boldsymbol{A}^{\dagger}_{\langle k\rangle} \cdot \boldsymbol{B}_{\langle l\rangle})^{\dagger} \cdot \boldsymbol{B}_{\langle l\rangle} &= (\boldsymbol{B}^{\dagger}_{\langle l\rangle} \cdot \boldsymbol{A}_{\langle k\rangle}) \cdot \boldsymbol{B}_{\langle l\rangle} && (2.58) \\ &= (-1)^{k(l-1)}\, (\boldsymbol{A}_{\langle k\rangle} \cdot \boldsymbol{B}^{\dagger}_{\langle l\rangle}) \cdot \boldsymbol{B}_{\langle l\rangle}. && (2.59) \end{aligned}$$

Note in this respect that here $(\boldsymbol{A}_{\langle k\rangle} \cdot \boldsymbol{B}^{\dagger}_{\langle l\rangle}) \cdot \boldsymbol{B}_{\langle l\rangle} \neq (\boldsymbol{A}_{\langle k\rangle} \cdot \boldsymbol{B}^{\dagger}_{\langle l\rangle})\boldsymbol{B}_{\langle l\rangle}$ because of the Euclidean derivation. Nevertheless, an even better choice for the projection, which can handle the case $k = l$, is

$$\left\langle (\boldsymbol{A}_{\langle k\rangle} \cdot \boldsymbol{B}^{\dagger}_{\langle l\rangle})\, \boldsymbol{B}_{\langle l\rangle} \right\rangle_k.$$

Any projection must fulfill the condition that the projection of a space onto itself is the space again. Then

$$(-1)^{l(l-1)} \left\langle (\boldsymbol{B}_{\langle l\rangle} \cdot \boldsymbol{B}^{\dagger}_{\langle l\rangle})\boldsymbol{B}_{\langle l\rangle} \right\rangle_l \quad \stackrel{!}{=} \quad \boldsymbol{B}_{\langle l\rangle}$$

implies at first that

$$\boldsymbol{B}^{\dagger}_{\langle l\rangle} \quad \longmapsto \quad \frac{\boldsymbol{B}^{\dagger}_{\langle l\rangle}}{\|\boldsymbol{B}_{\langle l\rangle}\|^2}.$$

Moreover, as the projection has to be an idempotent operation, projecting a projection must not change all prior projections. Let $\mathbf{e}_{\mathbb{v}}$ and $\mathbf{e}_{\mathbb{u}}$ be two basis blades with $\mathbb{v} \subseteq \mathbb{u}$. Hence $\mathbf{e}_{\mathbb{v}}$ can be considered a projection onto $\mathbf{e}_{\mathbb{u}}$. Then

$$(\mathbf{e}_{\mathbb{v}} \cdot \mathbf{e}^{\dagger}_{\mathbb{u}}) \cdot \mathbf{e}_{\mathbb{u}} \;=\; (\mathbf{e}_{\mathbb{v}} \cdot (\mathbf{e}_{\mathbb{u}})^2\, \mathbf{e}_{\mathbb{u}}) \cdot \mathbf{e}_{\mathbb{u}} \;=\; (\mathbf{e}_{\mathbb{u}})^2\, \mathbf{e}_{\mathbb{v}}\mathbf{e}_{\mathbb{u}}\mathbf{e}_{\mathbb{u}} \;=\; \mathbf{e}_{\mathbb{v}}, \tag{2.60}$$

which shows that the sign $(-1)^{k(l-1)}$ must be discarded; recall that equation (2.58) comes from subspace considerations only, i.e. $\mathbb{k}\mathrm{er}((\boldsymbol{A}_{\langle k\rangle} \cdot \boldsymbol{B}^{\dagger}_{\langle l\rangle}) \cdot \boldsymbol{B}_{\langle l\rangle}) = \mathbb{k}\mathrm{er}(-\,(\boldsymbol{A}_{\langle k\rangle} \cdot \boldsymbol{B}^{\dagger}_{\langle l\rangle}) \cdot \boldsymbol{B}_{\langle l\rangle})$.

Definition 2.21 (Euclidean projection operator):
Let $\boldsymbol{A}_{\langle k\rangle}$ and $\boldsymbol{B}_{\langle l\rangle}$ two blades with $k \leq l$. Then the perpendicular projection of $\boldsymbol{A}_{\langle k\rangle}$ onto $\boldsymbol{B}_{\langle l\rangle}$, denoted by $\mathcal{P}_{\boldsymbol{\varepsilon}\boldsymbol{B}_{\langle l\rangle}}(\boldsymbol{A}_{\langle k\rangle})$, is defined as

$$\mathcal{P}_{\boldsymbol{\varepsilon}\boldsymbol{B}_{\langle l\rangle}}(\boldsymbol{A}_{\langle k\rangle}) \;=\; \left\langle \left[\boldsymbol{A}_{\langle k\rangle} \;\cdot\; \frac{\boldsymbol{B}^{\dagger}_{\langle l\rangle}}{\|\boldsymbol{B}_{\langle l\rangle}\|^2} \right] \boldsymbol{B}_{\langle l\rangle} \right\rangle_k.$$

■

Aside: *By the Euclidean projection operator any blade can be factorized into its spanning vectors. An appropriate algorithm is stated in [93]. The obtained frame can then be orthogonalized regarding $\mathbb{R}^{p,q}$.*

If both, $\boldsymbol{A}_{\langle k\rangle}$ and $\boldsymbol{B}_{\langle l\rangle}$, are non-null blades the projection with respect to the inner product can be used.

Definition 2.22 (Orthogonal projection operator):
Let $\boldsymbol{A}_{\langle k\rangle}$ and $\boldsymbol{B}_{\langle l\rangle}$ two non-null blades with $k \leq l$. Then the orthogonal projection of $\boldsymbol{A}_{\langle k\rangle}$ onto $\boldsymbol{B}_{\langle l\rangle}$, denoted by $\mathcal{P}_{\boldsymbol{B}_{\langle l\rangle}}(\boldsymbol{A}_{\langle k\rangle})$, is defined as

$$\mathcal{P}_{\boldsymbol{B}_{\langle l\rangle}}(\boldsymbol{A}_{\langle k\rangle}) \;=\; \left[\boldsymbol{A}_{\langle k\rangle} \cdot \boldsymbol{B}_{\langle l\rangle}^{-1}\right] \boldsymbol{B}_{\langle l\rangle}.$$

■

The respective derivation is very similar to the one of the Euclidean projection operator. Especially, equation (2.60) amounts to the same result in case of definition 2.22. Here the grade projection operator is omitted as

$$\left[\boldsymbol{A}_{\langle k\rangle} \cdot \boldsymbol{B}_{\langle l\rangle}^{-1}\right] \cdot \boldsymbol{B}_{\langle l\rangle} \;\stackrel{k\leq l}{=}\; \left[\boldsymbol{A}_{\langle k\rangle} \cdot \boldsymbol{B}_{\langle l\rangle}^{-1}\right] \boldsymbol{B}_{\langle l\rangle}.$$

The counterpart of the projection is the *rejection*.

Definition 2.23 (Rejection):
Let $\boldsymbol{A}_{\langle k\rangle}$ and $\boldsymbol{B}_{\langle l\rangle}$ two non-null blades with $k \leq l$. Then the rejection of $\boldsymbol{A}_{\langle k\rangle}$ onto $\boldsymbol{B}_{\langle l\rangle}$ is defined as $\boldsymbol{A}_{\langle k\rangle}$ minus the respective projection. The Euclidean rejection, *denoted by $\mathcal{R}_{\boldsymbol{\varepsilon}\boldsymbol{B}_{\langle l\rangle}}(\boldsymbol{A}_{\langle k\rangle})$, is defined as*

$$\mathcal{R}_{\boldsymbol{\varepsilon}\boldsymbol{B}_{\langle l\rangle}}(\boldsymbol{A}_{\langle k\rangle}) \;=\; \boldsymbol{A}_{\langle k\rangle} - \mathcal{P}_{\boldsymbol{\varepsilon}\boldsymbol{B}_{\langle l\rangle}}(\boldsymbol{A}_{\langle k\rangle}).$$

Accordingly, $\mathcal{R}_{\boldsymbol{B}_{\langle l\rangle}}(\boldsymbol{A}_{\langle k\rangle})$ denotes the orthogonal rejection. *It is defined as*

$$\mathcal{R}_{\boldsymbol{B}_{\langle l\rangle}}(\boldsymbol{A}_{\langle k\rangle}) \;=\; \boldsymbol{A}_{\langle k\rangle} - \mathcal{P}_{\boldsymbol{B}_{\langle l\rangle}}(\boldsymbol{A}_{\langle k\rangle}).$$

■

Note that if $\boldsymbol{A}_{\langle k\rangle}$ is a vector $\boldsymbol{a}$, it may be written, similar to equation (2.41) on page 50,

$$\boldsymbol{a}\boldsymbol{B}_{\langle l\rangle}^{-1}\boldsymbol{B}_{\langle l\rangle} \;=\; \underbrace{\left[\boldsymbol{a} \cdot \boldsymbol{B}_{\langle l\rangle}^{-1}\right] \boldsymbol{B}_{\langle l\rangle}}_{\text{projection}} + \underbrace{\left[\boldsymbol{a} \wedge \boldsymbol{B}_{\langle l\rangle}^{-1}\right] \boldsymbol{B}_{\langle l\rangle}}_{\text{rejection}}. \tag{2.61}$$

Now it is being returned to the beginning of the current section, to page 76. Now $\boldsymbol{B}_{\langle l\rangle} = (\bigwedge_{i=1}^{r} \boldsymbol{n}_i) \wedge (\bigwedge_{i=1}^{s} \boldsymbol{z}_i)$ is being represented by $\boldsymbol{B}_{\langle l\rangle} = \boldsymbol{N}_{\langle r\rangle}\boldsymbol{Z}_{\langle s\rangle}$, where $\boldsymbol{N}_{\langle r\rangle} = \boldsymbol{n}_1\boldsymbol{n}_2 \ldots \boldsymbol{n}_r$ and $\boldsymbol{Z}_{\langle s\rangle} = \boldsymbol{z}_1\boldsymbol{z}_2 \ldots \boldsymbol{z}_s$, respectively. Then

$$\left\langle \left[\boldsymbol{A}_{\langle k\rangle} \cdot \frac{\boldsymbol{Z}_{\langle s\rangle}^{-1}\boldsymbol{N}_{\langle r\rangle}^{\dagger}}{\|\boldsymbol{N}_{\langle r\rangle}\|^2}\right] \boldsymbol{B}_{\langle l\rangle} \right\rangle_k \tag{2.62}$$

is an orthogonal projection that is as well defined for null blades. Certainly, the decomposition of $\boldsymbol{B}_{\langle l\rangle}$ is not available beforehand since, to the author's knowledge, it exists no operation $\boldsymbol{N}_{\langle r\rangle}\boldsymbol{Z}_{\langle s\rangle} \longmapsto \widetilde{\boldsymbol{Z}_{\langle s\rangle}}\boldsymbol{N}^\dagger_{\langle r\rangle}$, presuming that $\boldsymbol{Z}^{-1}_{\langle s\rangle} \propto \widetilde{\boldsymbol{Z}_{\langle s\rangle}}$. But if $\widetilde{\boldsymbol{Z}_{\langle s\rangle}}\boldsymbol{N}^\dagger_{\langle r\rangle}$ is at hand, a multiplicity of projections can be carried out.

For simplicity, $\boldsymbol{A}_{\langle k\rangle}$ is being replaced by the vector $\boldsymbol{a} = \alpha\boldsymbol{n}_i + \beta\boldsymbol{z}_j$, represented in the sound basis $\mathbb{B}$ of $\boldsymbol{B}_{\langle l\rangle}$. Components of $\boldsymbol{a}$ that have a representation in terms of $\overline{\mathbb{B}}$ are discarded as they do not contribute. Consider the simplification

$$
\begin{aligned}
\boldsymbol{a}\cdot(\widetilde{\boldsymbol{Z}_{\langle s\rangle}}\boldsymbol{N}^\dagger_{\langle r\rangle}) &= (\alpha\boldsymbol{n}_i+\beta\boldsymbol{z}_j)\cdot(\boldsymbol{z}_s\boldsymbol{z}_{s-1}\dots\boldsymbol{z}_1\boldsymbol{n}^\dagger_r\boldsymbol{n}^\dagger_{r-1}\dots\boldsymbol{n}^\dagger_1)\\
&= (-1)^{k-i}\,\alpha\,(\boldsymbol{n}_i\cdot\boldsymbol{n}^\dagger_i)\;\boldsymbol{z}_s\boldsymbol{z}_{s-1}\dots\boldsymbol{z}_1\boldsymbol{n}^\dagger_r\boldsymbol{n}^\dagger_{r-1}\dots\check{\boldsymbol{n}}^\dagger_i\dots\boldsymbol{n}^\dagger_1\\
&\quad+\;(-1)^{s-j}\,\beta\,(\boldsymbol{z}_j\cdot\boldsymbol{z}_j)\;\boldsymbol{z}_s\boldsymbol{z}_{s-1}\dots\check{\boldsymbol{z}}_j\dots\boldsymbol{z}_1\boldsymbol{n}^\dagger_r\boldsymbol{n}^\dagger_{r-1}\dots\boldsymbol{n}^\dagger_1,
\end{aligned}
$$

where $\boldsymbol{a}_1\boldsymbol{a}_2\dots\check{\boldsymbol{a}}_i\dots\boldsymbol{a}_k$ symbolizes $\boldsymbol{a}_1\boldsymbol{a}_2\dots\boldsymbol{a}_{i-1}\boldsymbol{a}_{i+1}\dots\boldsymbol{a}_k$.

Next consider the first summand $(\alpha\boldsymbol{n}_i\cdot(\widetilde{\boldsymbol{Z}_{\langle s\rangle}}\boldsymbol{N}^\dagger_{\langle r\rangle}))\cdot\boldsymbol{B}_{\langle l\rangle}$ only in the simplified version of equation (2.62)

$$
\begin{aligned}
&(\alpha\boldsymbol{n}_i\cdot(\widetilde{\boldsymbol{Z}_{\langle s\rangle}}\boldsymbol{N}^\dagger_{\langle r\rangle}))\cdot\boldsymbol{B}_{\langle l\rangle}\\
&= \Big[(-1)^{k-i}\,\alpha\,(\boldsymbol{n}_i\cdot\boldsymbol{n}^\dagger_i)\;\boldsymbol{z}_s\boldsymbol{z}_{s-1}\dots\boldsymbol{z}_1\boldsymbol{n}^\dagger_r\boldsymbol{n}^\dagger_{r-1}\dots\check{\boldsymbol{n}}^\dagger_i\dots\boldsymbol{n}^\dagger_1\Big]\cdot\boldsymbol{B}_{\langle l\rangle}\\
&= (-1)^{k-i}\,\alpha\,(\boldsymbol{n}_i\cdot\boldsymbol{n}^\dagger_i)\;\langle\boldsymbol{z}_s...\boldsymbol{z}_1\boldsymbol{n}^\dagger_r...\check{\boldsymbol{n}}^\dagger_i...\boldsymbol{n}^\dagger_1\;\boldsymbol{n}_1...\boldsymbol{n}_r\boldsymbol{z}_1...\boldsymbol{z}_s\rangle_1\\
&= (-1)^{k-i}\,\alpha\,(\boldsymbol{n}_i\cdot\boldsymbol{n}^\dagger_i)\;(-1)^{k-i}\langle\boldsymbol{z}_s...\boldsymbol{z}_1\boldsymbol{n}^\dagger_r...\check{\boldsymbol{n}}^\dagger_i...\boldsymbol{n}^\dagger_1\;\boldsymbol{n}_1...\check{\boldsymbol{n}}_i...\boldsymbol{n}_r\boldsymbol{z}_1...\boldsymbol{z}_s\rangle_0\,\boldsymbol{n}_i\\
&\qquad\qquad\qquad\qquad = \alpha\Big((\widetilde{\boldsymbol{Z}_{\langle s\rangle}}\boldsymbol{N}^\dagger_{\langle r\rangle})\cdot\boldsymbol{B}_{\langle l\rangle}\Big)\boldsymbol{n}_1,
\end{aligned}
$$

where the complete orthogonality of the sound basis is made use of. Hence $\widetilde{\boldsymbol{Z}_{\langle s\rangle}}\boldsymbol{N}^\dagger_{\langle r\rangle}$ has solely to be replaced by $\boldsymbol{Z}^{-1}_{\langle s\rangle}\boldsymbol{N}^\dagger_{\langle r\rangle}/\|\boldsymbol{N}_{\langle r\rangle}\|^2$ in order to obtain $\alpha\boldsymbol{n}_1$. The summand regarding the non-null vector part behaves in the same way.

Chapter 3

The Conformal Geometric Algebra

"The challenge is not necessarily to do new things using geometric algebra (though that is always nice!), but rather to show that a single framework encompasses all previously known results, and does so compactly."

`Leo Dorst in [21]`

3.1 Introduction

Recently it has been shown [104, 106] that the conformal geometry [85] is very attractive for robot vision. Conformal geometric algebra delivers a representation of the Euclidean space with remarkable features: first, the basic geometric entities of conformal geometry are spheres of dimension n. Other geometric entities as points, planes, lines, circles, ... may easily be constructed. These entities are no longer set concepts of a vector space but elements of CGA. Second, the special Euclidean group is a subgroup of the conformal group, which is in CGA an orthogonal group. Therefore, its action on the above mentioned geometric entities is linear. Third, the inversion operation is another subgroup of the conformal group which can be advantageously used in robot vision. Fourth, CGA generalizes the incidence algebra of projective geometry with respect to the above mentioned geometric entities.

As will be seen conformal vectors are embeddings of Euclidean vectors. This tight relationship will make it necessary to introduce a special non-bold notation for the Euclidean vectors, which are at the same time elements of the conformal space. If a vector, with components $\mathbf{e}_1$, $\mathbf{e}_2$ and $\mathbf{e}_3$ only, is supposed to have a specific Euclidean meaning, it may be labeled by an overset arrow[1], e.g.

$$\vec{a} = a_1\mathbf{e}_1 + a_2\mathbf{e}_2 + a_3\mathbf{e}_3.$$

[1]For these elements the vector cross product '$\times$' (from Gibbs's vector algebra) may be utilized.

If the element is known to have unit length, a hat is used rather that the arrow, e.g. $\hat{n}$. The same notation is meant to apply to all elements from $\mathbb{R}_3 \subset \mathbb{R}_{4,1}$, i.e. $\widehat{U}_{\langle 2\rangle} \in \mathbb{R}_3$ may denote a 2-blade with unit magnitude. The usual representation for vectors, e.g. $\boldsymbol{a}$, is kept for general CGA vectors.

In the end it is pointed out that the blade notation, for instance $\boldsymbol{A}_{\langle k\rangle}$, is only made use of if the blade character or the grade of the multivector under consideration is of special importance. Otherwise, for convenience, just capital letters are used, that is $\boldsymbol{C}$ instead of $\boldsymbol{C}_{\langle 2\rangle}$ and likewise $\widehat{U}$ for $\widehat{U}_{\langle 2\rangle}$.

Next an introduction to the *projective conformal space* is given.

3.2 Conformal Space $\mathbb{R}^{4,1}$

Here the *projective conformal space* $\mathbb{R}^{4,1}$ upon which CGA bases is to be constructed. Later on the habit of omitting the word 'projective' will be adopted so that $\mathbb{R}^{4,1}$ is referred to as the 'conformal space' only.

Having its early roots (1816) in the work of Friedrich Ludwig Wachter, a student of Gauss, the *conformal model* has become eminent mainly by the work of Li, Hestenes and Rockwood [76, 77, 78] in 2001. A prerequisite was the introduction of homogeneous coordinates for geometric algebra as done by Hestenes [64, 62]. It also was him in 1966 who initially paved the way for geometric algebra [61, 63]. Not so much impact had the work of the French physicist Angles who derived the conformal model two decades before [3]. He was basically driven by an interest in the transformations of the conformal group, in which respect Penrose's contributions shall be mentioned as well, cf. [90, 91, 92]. For more information on the historical development of the *conformal model* see, for example, [93] and [76].

The subsequent presentation in the main follows [97].

3.2.1 The Construction

As realized in [3], a quadratic space $\mathbb{R}^{a,b}$ must be extended to a space with signature $(p, q) = (a + 1, b + 1)$, i.e.

$$\mathbb{R}^{p,q} \;=\; \mathbb{R}^{a,b} \oplus \mathbb{R}^{1,1}$$

so as to have conformal transformations for $\mathbb{R}^{a,b}$ in the geometric algebra $\mathbb{R}_{p,q}$ of $\mathbb{R}^{p,q}$. In the present case it is self-evidently dealt with the embedding of the Euclidean space $\mathbb{R}^3$ into $\mathbb{R}^{4,1}$, a *Minkowski space*. The additional basis vectors of the *Minkowski plane* $\mathbb{R}^{1,1}$ are denoted by $\mathbf{e}_+$ and $\mathbf{e}_-$, with $\mathbf{e}_+^2 = +1$ and $\mathbf{e}_-^2 = -1$, respectively. The sought embedding of a Euclidean vector $\vec{x} \in \mathbb{R}^3$, denoted by $\mathcal{K}(\vec{x}) \in \mathbb{R}^{4,1}$, can then be determined by requiring that $\mathcal{K}(\vec{x}) - \vec{x} = a\mathbf{e}_+ + b\mathbf{e}_- \in \mathbb{R}^{1,1}$, with unknowns $a, b \in \mathbb{R}$, cf. [3].

Nevertheless, here the approach in concordance with the work of Li, Hestenes and Rockwood is chosen. It well enlightens the notion behind the embedding because in this approach the embedding may be presented in a two-staged bottom-up way.

Note that the three steps of embedding a point into conformal space are illustrated in figure 3.1, which depicts the embedding of a one-dimensional Euclidean space $\mathbb{R}$ into $\mathbb{R}^{2,1} = \mathbb{R} \oplus \mathbb{R}^{1,1}$.

First of all, consider a unit sphere and a plane passing through the center of that sphere. If the plane represents the Euclidean 2D-space, the sphere may be identified with the *Riemann sphere*. It is well known in this respect that it exists a stereographic projection that maps a point on the Riemann sphere to a point on the Euclidean plane and vice versa. Note that although the sphere is two-dimensional it is a manifold contained in a 3D-space. The principle regarding the mapping between sphere and plane may be generalized to higher dimensions, specifically one dimension higher. Hence the Euclidean 3D-space can be thought of as a unit 3-sphere (a three-dimensional unit hypersphere contained in a 4D-space), both connected by a stereographic projection. This is basically the first stage of embedding $\mathbb{R}^3$ into $\mathbb{R}^{4,1}$: introducing the previously mentioned basis vector $\mathbf{e}_+$, the required additional dimension for the hypersphere is obtained, whence the (inverse) stereographic projection reads

$$\mathcal{C}: \qquad \vec{x} \in \mathbb{R}^3 \quad \longmapsto \quad \frac{2}{\vec{x}^2+1}\,\vec{x} \;+\; \frac{\vec{x}^2-1}{\vec{x}^2+1}\,\mathbf{e}_+ \quad \in \mathbb{R}^4,$$

where $\mathcal{C}(\vec{x})$ denotes the corresponding operator. It can easily be verified that $\mathcal{C}(\vec{x})^2 = 1$ holds for all $\vec{x} \in \mathbb{R}^3$. With the help of figure 3.1 it can be seen that

$$\text{zero} \quad \overset{\mathcal{C}}{\longmapsto} \quad -\mathbf{e}_+ \qquad\qquad \text{and} \qquad\qquad \text{infinity} \quad \overset{\mathcal{C}}{\longmapsto} \quad \mathbf{e}_+.$$

Recall that a stereographic projection is a conformal mapping. Thus the points on the unit hypersphere constitute a locally conformal image of the underlying 3D-space $\mathbb{R}^3$ so that $\mathbb{R}^4$ can be regarded as an infinite locally conformal covering of $\mathbb{R}^3$ when also taking into account all non-unit hyperspheres. For this reason, the space $\mathbb{R}^4$ in conjunction with the embedding $\mathcal{C}(\vec{x})$ is referred to as *conformal space*.[2]

In order to arrive at the projective conformal space $\mathbb{R}^{4,1}$, it suffices to add a homogeneous dimension by means of the negatively squaring basis vector $\mathbf{e}_-$ because on defining the embedding

$$\mathcal{H}: \qquad \vec{x} \in \mathbb{R}^3 \quad \longmapsto \quad \mathcal{C}(\vec{x}) \;+\; \mathbf{e}_- \quad \in \mathbb{R}^{4,1}$$

it follows with $\mathcal{C}(\vec{x})^2 = 1$ that

$$\mathcal{H}(\vec{x})^2 \;=\; \Big(\mathcal{C}(\vec{x}) + \mathbf{e}_-\Big)^2 \;=\; 0.$$

The advantages of using null vectors will become apparent soon. Before it should be noted that using the embedding $\mathcal{H}$ the representations for zero and for infinity

[2] Not to be confused with the (projective) conformal space $\mathbb{R}^{4,1}$.

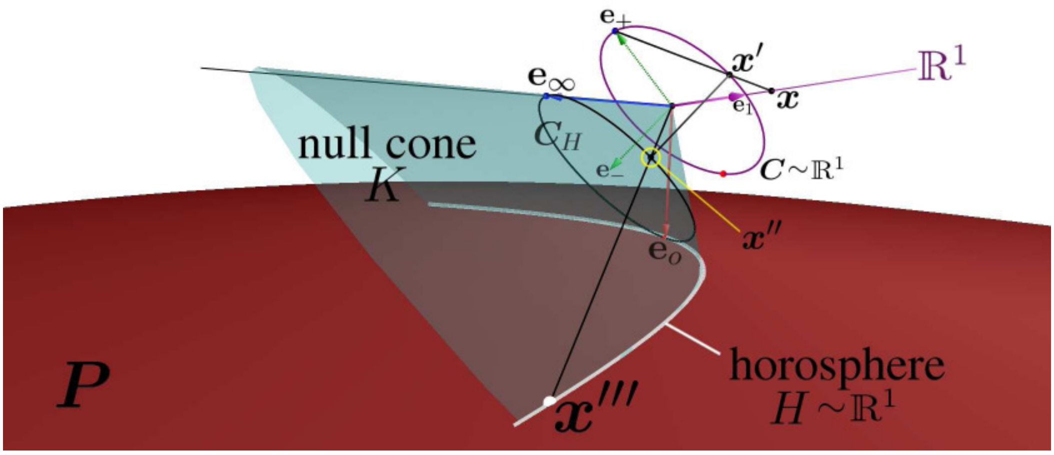

Fig. 3.1: Embedding $\mathbb{R}$ - the conformal space $\mathbb{R}^{2,1}$: $\boldsymbol{x}$ is eventually mapped to $\boldsymbol{x}'''$. Bear in mind that this is a Euclidean view of something non-Euclidean because of $\mathbf{e}_-^2 = -1$.

(which of course is not a proper point), for example, only differ by $2\mathbf{e}_+$, see figure 3.1,

$$\text{zero} \quad \overset{\mathcal{H}}{\longmapsto} \quad \mathbf{e}_- - \mathbf{e}_+ \qquad\qquad \text{and} \qquad\qquad \text{infinity} \quad \overset{\mathcal{H}}{\longmapsto} \quad \mathbf{e}_- + \mathbf{e}_+.$$

This property is certainly not desirable; an amendment to the embedding can be done exploiting that the $\mathbf{e}_-$-component represents a homogeneous coordinate, i.e. $(\alpha\mathcal{H}(\vec{x}))^2 = 0$, $\alpha \in \mathbb{R}$. Consequently, the set of vectors in $\mathbb{R}^{4,1}$ for which a valid preimage in $\mathbb{R}^3$ can be found consists of all null vectors, and it can be figured out that these form the so-called *null cone* in $\mathbb{R}^{4,1}$, see figure 3.1. The question arises whether an individual scale $\alpha(\vec{x}) \in \mathbb{R}$ can be determined such that

- the distribution of the embedded points in $\mathbb{R}^{4,1}$ metrically better resembles the one of the points in $\mathbb{R}^3$ (specifically, when $\vec{x} \to \infty$ then $\alpha(\vec{x}) \to \infty$)
- the origin does not become a distinguished element, e.g. with $\alpha = 0$.

For this purpose consider

$$\begin{aligned}\Big(\alpha_x\mathcal{H}(\vec{x}) - \alpha_y\mathcal{H}(\vec{y})\Big)^2 &= 2\alpha_x\alpha_y\Big(1 - \mathcal{C}(\vec{x})\mathcal{C}(\vec{y})\Big) \\ &= 2\alpha_x\alpha_y\,\frac{2(\vec{x}-\vec{y})^2}{(\vec{x}^2+1)(\vec{y}^2+1)},\end{aligned}$$

which suggests $\alpha(\vec{x}) := \frac{1}{2}(\vec{x}^2 + 1)$.

Hence the *conformal embedding* of a vector $\vec{x} \in \mathbb{R}^3$ into $\mathbb{R}^{4,1}$ can be defined to be $\mathcal{K}(\vec{x}) := \frac{1}{2}(\vec{x}^2+1)\mathcal{H}(\vec{x})$, that is

$$\begin{aligned} \mathcal{K}: \qquad \vec{x} \in \mathbb{R}^3 \quad \longmapsto \quad \boldsymbol{x} \quad &:= \quad \vec{x} \;+\; \tfrac{1}{2}(\vec{x}^2-1)\mathbf{e}_+ \;+\; \tfrac{1}{2}(\vec{x}^2+1)\mathbf{e}_- \quad \in \mathbb{R}^{4,1} \\ &= \quad \vec{x} \;+\; \tfrac{1}{2}\vec{x}^2(\mathbf{e}_+ + \mathbf{e}_-) \;+\; \tfrac{1}{2}(\mathbf{e}_- - \mathbf{e}_+) \\ &= \quad \vec{x} \;+\; \tfrac{1}{2}\vec{x}^2\mathbf{e} \;+\; \mathbf{e}_o \end{aligned} \tag{3.1}$$

where the common *null basis* of $\mathbb{R}^{1,1}$

$$\mathbf{e} \;:=\; \mathbf{e}_+ + \mathbf{e}_- \qquad \text{and} \qquad \mathbf{e}_o \;:=\; \tfrac{1}{2}(\mathbf{e}_- - \mathbf{e}_+)$$

was used. The elements $\boldsymbol{x} = \mathcal{K}(\vec{x} \in \mathbb{R}^3)$ are termed *conformal points*.

This is a great result because given the conformal points $\boldsymbol{x}, \boldsymbol{y} \in \mathbb{R}^{4,1}$, the function $\mathsf{d}_{[\boldsymbol{x},\boldsymbol{y}]} := \sqrt{(\boldsymbol{x}-\boldsymbol{y})^2}$ returns exactly the Euclidean d_2-metric $\sqrt{(\vec{x}-\vec{y})^2}$ for the underlying points $\vec{x} = \mathcal{K}^{-1}(\boldsymbol{x})$ and $\vec{y} = \mathcal{K}^{-1}(\boldsymbol{y})$, respectively.

Hence the derived hypersurface $\mathcal{K}(\mathbb{R}^3)$ of conformal points in $\mathbb{R}^{4,1}$ has a Euclidean intrinsic geometry. It is called *horosphere*, the generalized concept of a *horocycle*[3] in *hyperbolic geometry*. The metric within these objects is Euclidean, cf. [85]. The horosphere can be obtained by intersecting the null cone K with the hyperplane $P := \{\boldsymbol{x} \in \mathbb{R}^{4,1} | \, \mathbf{e} \cdot (\boldsymbol{x} - \mathbf{e}_o) = 0\}$, see figure 3.1. This geometrical view first shows that the origin is indeed an undistinguished element. Second, it nicely reflects a normalization with respect to the $\mathbf{e}_o$-component due to the plane condition $\mathbf{e} \cdot \boldsymbol{x} = \mathbf{e} \cdot \mathbf{e}_o = -1$, [76].

As mentioned in the beginning of this section the embedding into the higher-dimensional space $\mathbb{R}^{4,1}$ as done before has certain implications for the corresponding algebra $\mathbb{R}_{4,1}$: every vector off the null cone, i.e. every non-null vector in $\mathbb{R}_{4,1}$, represents either a reflection or an inversion. These operations belong to the basis transformations of the conformal group, see [79, 22], which justifies why $\mathbb{R}^{4,1}$ is referred to as the conformal space.

Subsequently, it is being discussed if points are the only 'geometric objects' in $\mathbb{R}^{4,1}$.

Subdividing $\mathbb{R}^{4,1}$

Next to their operator being in $\mathbb{R}_{4,1}$ the vectors of $\mathbb{R}^{4,1}$ represent geometric objects regarding the inner product. In particular, $\mathbb{R}^{4,1}$ is a space of spheres.

Varying the $\mathbf{e}$-component of a conformal point $\boldsymbol{x} = \vec{x} + \frac{1}{2}\vec{x}^2\mathbf{e} + \mathbf{e}_o$ corresponds to leaving the horosphere while staying inside the hyperplane P, see figure 3.1. Letting, for example,

$$\boldsymbol{S} \;=\; \vec{s} + \tfrac{1}{2}(\vec{s}^2 - r^2)\mathbf{e} + \mathbf{e}_o, \qquad r \in \mathbb{R},$$

[3] A horocycle is a circle on the *Poincaré disk* (a model of hyperbolic geometry) that touches the border (Greek: 'horos') of the disk, which represents infinity.

it can be seen[4] that

$$\boldsymbol{x} \cdot \boldsymbol{S} \;=\; \tfrac{1}{2}(r^2 - ||\vec{x} - \vec{s}||^2).$$

It is therefore justifiable to identify $\boldsymbol{S}$ with a sphere of radius r. Verify that the same holds for any vector outside the paraboloid, i.e. the horosphere. Hence not all elements in hyperplane P are spheres or points - the vectors inside the paraboloid are referred to as *imaginary spheres* for reasons that will become apparent later on. Due to the homogeneity of the conformal space, the above subdivision must be extended to vectors inside or outside, respectively, the double null cone (includes negative scales as well). Finally, there is the hyperplane of vectors with $\mathbf{e}_o$-component being zero, that is tangent to the null cone. The contained elements represent like points a certain type of sphere: planes - spheres with infinite radius. This remains to be justified, too, but observing that the IPNS of every plane includes $\mathbf{e}$ - the element representing infinity - gives a first hint that this might be correct.

The Elements of the Algebra of the Conformal Space

Previously the conformal space $\mathbb{R}^{4,1}$ has been derived. Now the 32 basis blades emerging from building the conformal geometric algebra $\mathbb{R}_{4,1}$ shall be mentioned:

grade 0	grade 1	grade 2	grade 3	grade 4	grade 5
$\mathbf{e}_0$	$\mathbf{e}_1$	$\mathbf{e}_1\mathbf{e}_2$	$\mathbf{e}_1\mathbf{e}_2\mathbf{e}_3$	$\mathbf{e}_1\mathbf{e}_2\mathbf{e}_3\mathbf{e}_+$	$\mathbf{e}_1\mathbf{e}_2\mathbf{e}_3\mathbf{e}_+\mathbf{e}_-$
	$\mathbf{e}_2$	$\mathbf{e}_2\mathbf{e}_3$	$\mathbf{e}_1\mathbf{e}_2\mathbf{e}_+$	$\mathbf{e}_1\mathbf{e}_2\mathbf{e}_3\mathbf{e}_-$	
	$\mathbf{e}_3$	$\mathbf{e}_3\mathbf{e}_1$	$\mathbf{e}_2\mathbf{e}_3\mathbf{e}_+$	$\mathbf{e}_1\mathbf{e}_2\mathbf{e}_+\mathbf{e}_-$	
	$\mathbf{e}_+$	$\mathbf{e}_1\mathbf{e}_+$	$\mathbf{e}_3\mathbf{e}_1\mathbf{e}_+$	$\mathbf{e}_2\mathbf{e}_3\mathbf{e}_+\mathbf{e}_-$	
	$\mathbf{e}_-$	$\mathbf{e}_2\mathbf{e}_+$	$\mathbf{e}_1\mathbf{e}_2\mathbf{e}_-$	$\mathbf{e}_3\mathbf{e}_1\mathbf{e}_+\mathbf{e}_-$	
		$\mathbf{e}_3\mathbf{e}_+$	$\mathbf{e}_2\mathbf{e}_3\mathbf{e}_-$		
		$\mathbf{e}_1\mathbf{e}_-$	$\mathbf{e}_3\mathbf{e}_1\mathbf{e}_-$		
		$\mathbf{e}_2\mathbf{e}_-$	$\mathbf{e}_1\mathbf{e}_+\mathbf{e}_-$		
		$\mathbf{e}_3\mathbf{e}_-$	$\mathbf{e}_2\mathbf{e}_+\mathbf{e}_-$		
		$\mathbf{e}_+\mathbf{e}_-$	$\mathbf{e}_3\mathbf{e}_+\mathbf{e}_-$		

The map between the $\mathbf{e}_+\mathbf{e}_-$-basis and the null basis is invertible, see equation (3.6) and equation (3.7). The algebra built upon the null basis $\{\mathbf{e}_1, \mathbf{e}_2, \mathbf{e}_3, \mathbf{e}, \mathbf{e}_o\}$ can therefore be obtained by replacing in the above table every occurrence of $\mathbf{e}_+$ with $\mathbf{e}$ and every occurrence of $\mathbf{e}_-$ with $\mathbf{e}_o$, respectively. But it must be taken into account that the orthogonality for basis blades of equal grade is lost, compare

$$\mathbf{e}_1\mathbf{e}_2\mathbf{e}_+ \cdot \mathbf{e}_1\mathbf{e}_2\mathbf{e}_- \;=\; 0 \qquad \text{and} \qquad \mathbf{e}_1\mathbf{e}_2\mathbf{e} \cdot \mathbf{e}_1\mathbf{e}_2\,\mathbf{e}_o \;=\; 1.$$

Note that for traditional, practical and convenience reasons, it is being worked with the null basis, which at that same time admits a better geometric interpretation.

The Euclidean IPNS

The terms ‘eIPNS’ and ‘eOPNS’ will occasionally be used. What is meant simply is the IPNS or OPNS, respectively, constrained to the vectors on the horosphere,

[4] By means of equation (3.14).

that is to the representatives of Euclidean vectors in conformal space. Hence the IPNS, for example, of a blade may include much more vectors than contained in the eIPNS.

3.3 Conformal Analytic Geometry of Euclidean Space

Conformal geometric algebra with its definition of a conformal point provides several geometric entities, for example a circle. These objects are well known from the Euclidean world. Moreover, CGA gives access to this world in such a way as to deal with its objects in an analytic way. The geometric product allows to algebraically combine different elements in a way that the result has a meaningful, sometimes amazing, interpretation. Those calculations upon geometric objects are to be presented subsequently. The section can be considered a toolbox for the work with CGA.

3.3.1 Preliminaries on Subspaces

Recall that the subspace of a blade can be described in terms of the inner (IPNS) or outer product null space (OPNS). The IPNS will here be taken as a standard, that is if $\boldsymbol{L} \in \mathbb{R}_{4,1}$ denotes a blade, representing for example a line, the inner product null space representation for that line is tacitly assumed: some point $\boldsymbol{a} \in \mathbb{R}^{4,1}$ lies on the line iff $\boldsymbol{a} \cdot \boldsymbol{L} = 0$. The OPNS representation is made explicit by the dual. Hence the OPNS line that corresponds to $\boldsymbol{L}$ is simply $\boldsymbol{L}^*$. For the same $\boldsymbol{a}$ one has $\boldsymbol{a} \wedge \boldsymbol{L}^* = 0$ iff the point lies on the line.

For most of the CGA entities to be dealt with here a normalization is being introduced. The reason is clear: multiplying a blade with a scalar factor does not change its subspace. A similar argument holds for versors. Hence if a calculation does not result in a normalized entity, the equivalent sign '≡' is used rather than the equal sign.

It is still to mention that building the inner product of a vector and an IPNS entity corresponds to building the outer product of the vector and the respective OPNS entity, cf. equation (2.52) on page 64. In this regard, the inner product can be though of as a way to expand subspaces.

$$\boldsymbol{a} \cdot \boldsymbol{X} \;=\; \boldsymbol{a} \cdot (\boldsymbol{X}^* \boldsymbol{I}) \;=\; (\underbrace{\boldsymbol{a} \wedge \boldsymbol{X}^*}_{\boldsymbol{Y}^*})\boldsymbol{I} \;=\; \boldsymbol{Y} \tag{3.2}$$

Projection or Rejection

It is worth mentioning that the use of the IPNS changes the roles of projection and rejection. Consider for instance the projection of a point $\boldsymbol{x}$ onto the OPNS blade

$\boldsymbol{A}^*_{\langle k\rangle}$

$$\begin{aligned}
\boldsymbol{x}_p &= (\boldsymbol{x}\cdot\boldsymbol{A}^{*-1}_{\langle k\rangle})\boldsymbol{A}^*_{\langle k\rangle} &(3.3)\\
&= (\boldsymbol{x}\cdot(\boldsymbol{A}_{\langle k\rangle}\boldsymbol{I}^{-1})^{-1})\boldsymbol{A}_{\langle k\rangle}\boldsymbol{I}^{-1}\\
&= \left[\boldsymbol{x}\cdot\frac{(\boldsymbol{A}_{\langle k\rangle}\boldsymbol{I}^{-1})^{\sim}}{(\boldsymbol{A}_{\langle k\rangle}\boldsymbol{I}^{-1})^{\sim}(\boldsymbol{A}_{\langle k\rangle}\boldsymbol{I}^{-1})}\right]\boldsymbol{A}_{\langle k\rangle}\boldsymbol{I}^{-1}\\
&= \left[\boldsymbol{x}\cdot\frac{-\boldsymbol{I}\widetilde{\boldsymbol{A}_{\langle k\rangle}}}{(-\boldsymbol{I}\widetilde{\boldsymbol{A}_{\langle k\rangle}})(-\boldsymbol{A}_{\langle k\rangle}\boldsymbol{I})}\right]\boldsymbol{A}_{\langle k\rangle}\boldsymbol{I}^{-1}\\
&= \left(\boldsymbol{x}\cdot\boldsymbol{A}^{-1}_{\langle k\rangle}\boldsymbol{I}\right)\boldsymbol{A}_{\langle k\rangle}\boldsymbol{I}^{-1}\\
&= \left(\boldsymbol{x}\wedge\boldsymbol{A}^{-1}_{\langle k\rangle}\right)\boldsymbol{I}\boldsymbol{A}_{\langle k\rangle}\boldsymbol{I}^{-1}\\
&= (\boldsymbol{x}\wedge\boldsymbol{A}^{-1}_{\langle k\rangle})\boldsymbol{A}_{\langle k\rangle}, &(3.4)
\end{aligned}$$

where it was used that in $\mathbb{R}_{4,1}$: $\widetilde{\boldsymbol{I}}=\boldsymbol{I}$, $\boldsymbol{I}^{-1}=-\boldsymbol{I}$, $\boldsymbol{I}^2=-1$ and $\boldsymbol{A}_{\langle k\rangle}\boldsymbol{I}=\boldsymbol{I}\boldsymbol{A}_{\langle k\rangle}$. Hence equation (3.4) (which originally represents a rejection, see equation (2.61)) is used instead of equation (3.3).

Where Points Project to Spheres

Next to conformal points, spheres and planes are equally vectors, that is to say elements that can make up a null space[5]. Clearly, projection and rejection split a vector into two orthogonal vector parts. But it will turn out that the manifold of conformal points is not closed under addition; whence it is not surprising that projecting a point may end with a plane or a sphere.

On the Sandwich Product

This important product reappears in this chapter being the subject of several sections. Let $\boldsymbol{A}$ and $\boldsymbol{X}$ be general multivectors. Applying $\boldsymbol{A}$ or its dual to $\boldsymbol{X}$ may at least change the sign of the result, compare

$$\boldsymbol{A}\boldsymbol{X}\boldsymbol{A} = \boldsymbol{A}^*\boldsymbol{I}\boldsymbol{X}\boldsymbol{A}^*\boldsymbol{I} = -\boldsymbol{A}^*\boldsymbol{X}\boldsymbol{A}^*. \tag{3.5}$$

3.3.2 Useful Notes on CGA

It is begun by repeating the most important basis blades.

$$\mathbf{e} = \mathbf{e}_\infty = \mathbf{e}_+ + \mathbf{e}_-$$

[5]When mentioning, for instance, the OPNS of a blade $\boldsymbol{A}_{\langle k\rangle}$, only the underlying set of conformal points is meant rather than all vectors in $\mathbb{k}\mathrm{er}(\boldsymbol{A}_{\langle k\rangle})\subseteq\mathbb{R}^{4,1}$.

and

$$\mathbf{e}_o \;=\; \frac{1}{2}\,(\mathbf{e}_- - \mathbf{e}_+)$$

as well as

$$\boldsymbol{E} \;=\; \mathbf{e}_+ \wedge \mathbf{e}_- = \mathbf{e} \wedge \mathbf{e}_o = \mathbf{e}_{+-}.$$

Conversely it must be

$$\mathbf{e}_+ \;=\; \tfrac{1}{2}\big(\mathbf{e} - 2\,\mathbf{e}_o\big) \tag{3.6}$$

$$\mathbf{e}_- \;=\; \tfrac{1}{2}\big(\mathbf{e} + 2\,\mathbf{e}_o\big). \tag{3.7}$$

The following tables are to be read from the left to the right. They show often occurring products between these 'new' typical elements of CGA.

$*$	$\mathbf{e}$	$\mathbf{e}_o$	$\boldsymbol{E}$	$\mathbf{e}_+$	$\mathbf{e}_-$
$\mathbf{e}$	0	$\boldsymbol{E}-1$	$\mathbf{e}$	$1-\boldsymbol{E}$	$E-1$
$\mathbf{e}_o$	$-(\boldsymbol{E}+1)$	0	$-\,\mathbf{e}_o$	$-\frac{1}{2}(\boldsymbol{E}+1)$	$-\frac{1}{2}(\boldsymbol{E}+1)$
$\boldsymbol{E}$	$-\,\mathbf{e}$	$\mathbf{e}_o$	1	$-\,\mathbf{e}_-$	$-\,\mathbf{e}_+$
$\mathbf{e}_+$	$\boldsymbol{E}+1$	$\frac{1}{2}(\boldsymbol{E}-1)$	$\mathbf{e}_-$	1	$\boldsymbol{E}$
$\mathbf{e}_-$	$-(\boldsymbol{E}+1)$	$\frac{1}{2}(\boldsymbol{E}-1)$	$\mathbf{e}_+$	$-\,\boldsymbol{E}$	-1

(3.8)

The results involving the geometric product with the pseudoscalar $\boldsymbol{I}$ can be inferred from the next table by noting that $\boldsymbol{AI} = \boldsymbol{A}\cdot\boldsymbol{I}$, for every multivector $\boldsymbol{A} \in \mathbb{R}_{4,1}$.

$\cdot$	$\mathbf{e}$	$\mathbf{e}_o$	$\boldsymbol{E}$	$\mathbf{e}_+$	$\mathbf{e}_-$	$\boldsymbol{I}$
$\mathbf{e}$	0	-1	$\mathbf{e}$	1	-1	$-\boldsymbol{I}_E\mathbf{e}$
$\mathbf{e}_o$	-1	0	$-\,\mathbf{e}_o$	$-\,\frac{1}{2}$	$-\,\frac{1}{2}$	$\boldsymbol{I}_E\,\mathbf{e}_o$
$\boldsymbol{E}$	$-\,\mathbf{e}$	$\mathbf{e}_o$	1	$-\,\mathbf{e}_-$	$-\,\mathbf{e}_+$	$\boldsymbol{I}_E$
$\mathbf{e}_+$	1	$-\,\frac{1}{2}$	$\mathbf{e}_-$	1	0	$-\boldsymbol{I}_E\mathbf{e}_-$
$\mathbf{e}_-$	-1	$-\,\frac{1}{2}$	$\mathbf{e}_+$	0	-1	$-\boldsymbol{I}_E\mathbf{e}_+$
$\boldsymbol{I}$	$-\boldsymbol{I}_E\mathbf{e}$	$\boldsymbol{I}_E\,\mathbf{e}_o$	$\boldsymbol{I}_E$	$-\boldsymbol{I}_E\mathbf{e}_-$	$-\boldsymbol{I}_E\mathbf{e}_+$	-1

(3.9)

Notice that $\boldsymbol{I}_E$ symbolizes the Euclidean pseudoscalar $\mathbf{e}_1\mathbf{e}_2\mathbf{e}_3$.

$\wedge$	$\mathbf{e}$	$\mathbf{e}_o$	$\boldsymbol{E}$	$\mathbf{e}_+$	$\mathbf{e}_-$
$\mathbf{e}$	0	$\boldsymbol{E}$	0	$-\,\boldsymbol{E}$	$\boldsymbol{E}$
$\mathbf{e}_o$	$-\,\boldsymbol{E}$	0	0	$-\,\frac{1}{2}\boldsymbol{E}$	$-\,\frac{1}{2}\boldsymbol{E}$
$\boldsymbol{E}$	0	0	0	0	0
$\mathbf{e}_+$	$\boldsymbol{E}$	$\frac{1}{2}\boldsymbol{E}$	0	0	$\boldsymbol{E}$
$\mathbf{e}_-$	$-\,\boldsymbol{E}$	$\frac{1}{2}\boldsymbol{E}$	0	$-\,\boldsymbol{E}$	0

(3.10)

More helpful identities and relations can be found in the appendix A.4.

3.3.3 The Conformal Point and Its Descendants

These descendants mean certain products involving two or more conformal points and giving new geometric entities.

Consider the expression

$$\begin{aligned} \boldsymbol{a} &= \vec{a} + \underbrace{\tfrac{1}{2}(\vec{a}^2 - \rho_a^2)}_{\tau_a}\,\mathbf{e} + \mathbf{e}_o & (3.11) \\ &= (a_1\,\mathbf{e}_1 + a_2\,\mathbf{e}_2 + a_3\,\mathbf{e}_3) \;+\; a_4\,\mathbf{e} \;+\; a_5\,\mathbf{e}_o, & (3.12) \end{aligned}$$

and recall that the vector $\boldsymbol{a} \in \mathbb{R}_{4,1}$ represents a (possibly imaginary[6]) sphere with radius ρ_a unless ρ_a is zero. In this case $\boldsymbol{a}$ denotes the conformal point $\boldsymbol{a} = \mathcal{K}(\vec{a})$. But depending on the coefficients a_4 and a_5 there are more interpretations for the vector. These are summarized by the following table.

	$a_5 = 0$	$a_5 \neq 0$
$a_4 = 0$	plane including the origin	sphere/point located at the origin
$a_4 \neq 0$	plane not including the origin	sphere/point not located at the origin

Aside: *Note that spheres, points and planes may as well be denoted by capital letters, e.g.* $\boldsymbol{S}$, $\boldsymbol{X}$ *or* $\boldsymbol{P}$. *Particularly, a sphere may be expressed by means of*

$$\boldsymbol{S} \;=\; \boldsymbol{s} - \tfrac{1}{2}r_s^2\mathbf{e},$$

where $\boldsymbol{s}$ *represents the conformal point at the center of the sphere and* r_s *the radius.*

Let the conformal points/spheres $\boldsymbol{a}$, $\boldsymbol{b}$, $\boldsymbol{c}$ and $\boldsymbol{d}$ be defined in accordance with equation (3.11). In particular, it is henceforth assumed that conformal points are normalized w.r.t. their $\mathbf{e}_o$-component. Then the following geometric relationships and objects arise.

The inner product of two conformal points is negative definite:

$$\begin{aligned} \boldsymbol{a}\cdot\boldsymbol{b} &= \vec{a}\cdot\vec{b} \;-\; \tfrac{1}{2}\left[(\vec{a}^2 - \rho_a^2) + (\vec{b}^2 - \rho_b^2)\right] & (3.13) \\ &= \tfrac{1}{2}\big(\,\rho_a^2 + \rho_b^2 \;-\; \|\vec{a} - \vec{b}\|^2\,\big) & (3.14) \\ &= \rho_a\,\rho_b\,\cos\gamma & (3.15) \end{aligned}$$

$$\Longleftrightarrow$$

$$(\rho_a + \rho_b) \;\geq\; \|\vec{a} - \vec{b}\| \;\geq\; |\rho_a - \rho_b| \qquad (3.16)$$

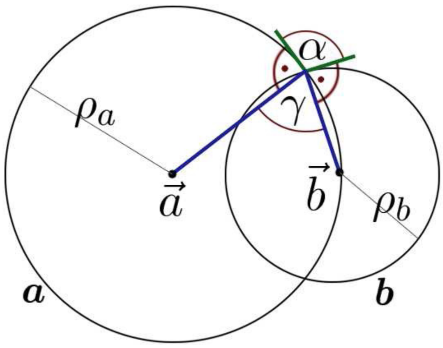

Fig. 3.2: Intersection of spheres: the two spheres $\boldsymbol{a}$ and $\boldsymbol{b}$ do almost intersect at right angles, i.e. $\alpha \approx \pi/2$. The related supplementary angle $\gamma = \pi - \alpha$ can be computed by means of equation (3.15).

Hence if $\boldsymbol{a}$ and $\boldsymbol{b}$ denote two intersecting spheres, their inner product can be used to determine the local angle $\alpha = \pi - \gamma$ between the (tangent planes of the) surfaces of the two spheres (law of cosines), see figure 3.2.

$$\begin{aligned} \boldsymbol{a} \wedge \boldsymbol{b} \;&=\; \vec{a} \wedge \vec{b} \;+\; (\vec{a} - \vec{b}) \wedge \mathbf{e}_o \\ &+\; \tfrac{1}{2}\left[(\vec{b}^2 - \rho_b^2)\vec{a} - (\vec{a}^2 - \rho_a^2)\vec{b}\right] \wedge \mathbf{e} \\ &+\; \tfrac{1}{2}\left[(\vec{a}^2 - \rho_a^2) - (\vec{b}^2 - \rho_b^2)\right] \boldsymbol{E} \end{aligned} \tag{3.17}$$

(OPNS point pair)

$$\mathbf{e} \wedge \boldsymbol{a} \wedge \boldsymbol{b} \;=\; \mathbf{e} \wedge \vec{a} \wedge \vec{b} \;+\; (\vec{b} - \vec{a})\, \boldsymbol{E} \tag{3.18}$$

(OPNS line)

$$\begin{aligned} \boldsymbol{a} \wedge \boldsymbol{b} \wedge \boldsymbol{c} \;&=\; \vec{a} \wedge \vec{b} \wedge \vec{c} \;+\; \overbrace{\left[\vec{a} \wedge \vec{b} \,-\, \vec{a} \wedge \vec{c} + \vec{b} \wedge \vec{c}\right]}^{[(\vec{b}-\vec{a}) \wedge (\vec{c}-\vec{a})]} \wedge \mathbf{e}_o \\ &+\; \left[\tau_a(\vec{b} \wedge \vec{c}) - \tau_b(\vec{a} \wedge \vec{c}) + \tau_c(\vec{a} \wedge \vec{b})\right] \wedge \mathbf{e} \\ &+\; \left[(\tau_b \,-\, \tau_c)\, \vec{a} + (\tau_c \,-\, \tau_a)\vec{b} + (\tau_a \,-\, \tau_b)\vec{c}\right] \boldsymbol{E} \end{aligned} \tag{3.19}$$

(OPNS circle)

$$\begin{aligned} \mathbf{e} \wedge \boldsymbol{a} \wedge \boldsymbol{b} \wedge \boldsymbol{c} \;&=\; \mathbf{e} \wedge \vec{a} \wedge \vec{b} \wedge \vec{c} \;+\; \left[\vec{a} \wedge \vec{b} \,-\, \vec{a} \wedge \vec{c} + \vec{b} \wedge \vec{c}\right] \boldsymbol{E} \\ &=\; \mathbf{e} \wedge \vec{a} \wedge \vec{b} \wedge \vec{c} \;+\; \left[(\vec{b} - \vec{a}) \,\wedge\, (\vec{c} - \vec{a})\right] \boldsymbol{E} \end{aligned} \tag{3.20}$$

[6] An imaginary sphere is meant to denote a sphere whose radius may be regarded as imaginary, more specifically if $a_4 = \tau_a = \frac{1}{2}(\vec{a}^2 + \rho_a^2)$, cf. equation (3.11) or section 3.3.6.

(OPNS plane)

$$
\begin{aligned}
\boldsymbol{Q}^* \;&=\; \boldsymbol{a} \wedge \boldsymbol{b} \wedge \boldsymbol{c} \wedge \boldsymbol{d} \qquad (3.21)\\
&=\; \overbrace{\left[\vec{a} \wedge \vec{b} \wedge \vec{c} \,-\, \vec{a} \wedge \vec{b} \wedge \vec{d} \,+\, \vec{a} \wedge \vec{c} \wedge \vec{d} \,-\, \vec{b} \wedge \vec{c} \wedge \vec{d}\right]}^{\left[(\vec{b}-\vec{a}) \wedge (\vec{d}-\vec{a}) \wedge (\vec{c}-\vec{a})\right]} \wedge \mathbf{e}_o\\
&+\; \left[\tau_d(\vec{a} \wedge \vec{b} \wedge \vec{c}) - \tau_a(\vec{b} \wedge \vec{c} \wedge \vec{d}) + \tau_b(\vec{a} \wedge \vec{c} \wedge \vec{d}) - \tau_c(\vec{a} \wedge \vec{b} \wedge \vec{d})\right] \wedge \mathbf{e}\\
&+\; \Big[\; (\tau_a - \tau_d)(\vec{b} \wedge \vec{c}) \,+\, (\tau_d - \tau_b)(\vec{a} \wedge \vec{c}) \,+\, (\tau_c - \tau_d)(\vec{a} \wedge \vec{b})\\
&+\; \quad (\tau_b - \tau_c)(\vec{a} \wedge \vec{d}) \,+\, (\tau_c - \tau_a)(\vec{b} \wedge \vec{d}) \,+\, (\tau_a - \tau_b)(\vec{c} \wedge \vec{d}) \;\Big] \boldsymbol{E}
\end{aligned}
$$

(OPNS sphere)

Note that the respective IPNS entities can be build by multiplying with the pseudoscalar $\boldsymbol{I}$, for example

$$\boldsymbol{Q} \;=\; \boldsymbol{Q}^* \, \boldsymbol{I}.$$

Specifically, the IPNS representation of a sphere or a plane is given by a vector of the form (3.11) or (3.12).

Next an interlude dealing with intersections in conformal geometric algebra is given because it simplifies matters in the rest of this chapter.

3.3.4 Intersecting in CGA

For several pairs of entities intersections may be computed simply by building the outer product of the IPNS entities, which is one reason for choosing the IPNS representation as a standard in this chapter. The result is again an IPNS entity. Intersecting two planes, defined, for example, by the points $\boldsymbol{a}_1, \boldsymbol{a}_2, \boldsymbol{a}_3$ and $\boldsymbol{b}_1, \boldsymbol{b}_2, \boldsymbol{b}_3$, respectively, can be done by means of

$$\boldsymbol{L} \;=\; [(\mathbf{e} \wedge \boldsymbol{a}_1 \wedge \boldsymbol{a}_2 \wedge \boldsymbol{a}_3)\boldsymbol{I}] \wedge [(\mathbf{e} \wedge \boldsymbol{b}_1 \wedge \boldsymbol{b}_2 \wedge \boldsymbol{b}_3)\boldsymbol{I}].$$

If the OPNS representation of the line $\boldsymbol{L}$ is preferred, the dual of $\boldsymbol{L}$ has to be built.

This kind of intersection works in all cases in which the join of the respective OPNS entities is $\boldsymbol{I}$. Let $\boldsymbol{A}^*_{\langle k \rangle}$ and $\boldsymbol{B}^*_{\langle l \rangle}$ be two OPNS entities to be intersected. It must not exist a subspace of $\mathbb{R}_{4,1}$ that is orthogonal to $\boldsymbol{A}^*_{\langle k \rangle}$ and to $\boldsymbol{B}^*_{\langle l \rangle}$ at the same time. To see this, suppose that such a subspace exists, given by the blade $\boldsymbol{D}_{\langle s \rangle}$. Let $\boldsymbol{d}$ denote a vector in $\boldsymbol{D}_{\langle s \rangle}$. Pursuant to the elucidations on page 71 it is

$$
\begin{aligned}
\boldsymbol{d} \cdot \boldsymbol{A}^*_{\langle k \rangle} \;=\; 0 \quad &\Longleftrightarrow \quad \boldsymbol{d} \in \mathbb{k}\mathrm{er}^{\boldsymbol{*}}(\boldsymbol{A}^*_{\langle k \rangle})\\
&\Longleftrightarrow \quad \boldsymbol{d} \in \mathbb{k}\mathrm{er}(\boldsymbol{A}_{\langle k \rangle})\\
&\Longleftrightarrow \quad \boldsymbol{d} \wedge \boldsymbol{A}_{\langle k \rangle} \;=\; 0.
\end{aligned}
$$

Hence $\boldsymbol{D}_{\langle s\rangle}$ is part of $\boldsymbol{A}_{\langle k\rangle}$ and $\boldsymbol{B}_{\langle l\rangle}$: the dual of $\boldsymbol{A}^*_{\langle k\rangle}$ and $\boldsymbol{B}^*_{\langle l\rangle}$ may be expressed as $\boldsymbol{A}_{\langle k\rangle} = \boldsymbol{D}_{\langle s\rangle} \wedge \boldsymbol{X}_{\langle n-(k+s)\rangle}$ and $\boldsymbol{B}_{\langle l\rangle} = \boldsymbol{D}_{\langle s\rangle} \wedge \boldsymbol{Y}_{\langle n-(l+s)\rangle}$, for some suitable blades $\boldsymbol{X}_{\langle n-(k+s)\rangle}$ and $\boldsymbol{Y}_{\langle n-(l+s)\rangle}$. Consequently, the outer product of the IPNS representations attains zero

$$\boldsymbol{A}_{\langle k\rangle} \wedge \boldsymbol{B}_{\langle l\rangle} \;=\; \boldsymbol{D}_{\langle s\rangle} \wedge \boldsymbol{X}_{\langle n-(k+s)\rangle} \;\wedge\; \boldsymbol{D}_{\langle s\rangle} \wedge \boldsymbol{Y}_{\langle n-(l+s)\rangle} \;=\; 0.$$

In conformal geometric algebra $\mathbb{R}_{4,1}$ it is mostly the case that the subspace $\boldsymbol{D}_{\langle s\rangle}$ does not exist. The table below shows which kind of objects certain intersections produce, provided that they do intersect.

$\wedge$	Sphere	Plane	Line	Circle
Sphere	Circle	Circle	Point pair*	Point pair*
Plane		Line	Projective point*	Point pair*
Line			$--$	Point*
Circle				Point*

Note that all entries with a superset asterisk are OPNS elements.

Exceptions

But it must be taken care when using the table. If, for example, a circle and a line (being in the circle plane) shall be intersected, the outer product method cannot be used. In such coplanarity situations it exists a direction orthogonal to the common plane, with the result that the join of the entities is not the entire space $\boldsymbol{I}$. Thus a subspace $\boldsymbol{D}_{\langle s\rangle}$ exists. Likewise the outer product intersection of two circles does only exist if the circles intersect in just one point. Otherwise, if they have two points in common, they share a common sphere. It is therefore helpful to imagine entities in terms of the primitives sphere and plane. If the IPNS entities that are to be intersected, can be split in such a way that they share a plane or a sphere, the outer product must be zero.

In the following example, the circle $\boldsymbol{C}$ and the coplanar line $\boldsymbol{L}$ can be expressed by means of a sphere $\boldsymbol{S}$, a plane $\boldsymbol{P}'$ and the common plane $\boldsymbol{P}$. Thus

$$\boldsymbol{C} \wedge \boldsymbol{L} \;=\; \underbrace{\boldsymbol{S} \wedge \boldsymbol{P}}_{\boldsymbol{C}} \;\wedge\; \underbrace{\boldsymbol{P} \wedge \boldsymbol{P}'}_{\boldsymbol{L}} \;=\; 0.$$

Another important operation in CGA is the reflection. It is discussed in section 3.3.8.

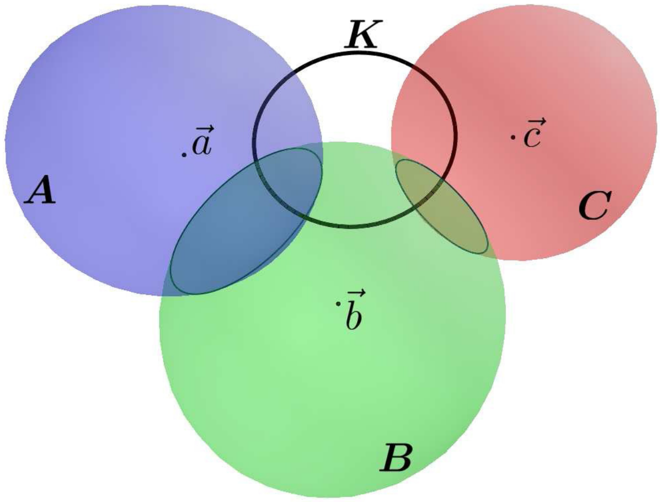

Fig. 3.3: Circle from spheres: the circle $\boldsymbol{K}^* = \boldsymbol{A} \wedge \boldsymbol{B} \wedge \boldsymbol{C}$ hits all the spheres at right angles (it does not pass through the centers).

Orthogonality and Perpendicularity

It is worthwhile to take a closer look at the inner product of IPNS entities. As can be deduced from equation (3.14), the inner product of two intersecting spheres is zero iff their surfaces intersect at right angles. Similarly, the same applies for two perpendicular planes or a plane and a sphere, compare equation (3.34) and equation (3.33), respectively. Higher order entities, which can be represented by an intersection (see above), inherit this property, for example, by the relationship

$$\boldsymbol{a} \cdot (\boldsymbol{b} \wedge \boldsymbol{c}) \;=\; (\boldsymbol{a} \cdot \boldsymbol{b})\boldsymbol{c} - (\boldsymbol{a} \cdot \boldsymbol{c})\boldsymbol{b}.$$

Thus a new meaningful kind of (locally Euclidean) perpendicularity is provided by geometric algebra which is more than a pure orthogonality of null spaces – especially if this orthogonality is inherently non-Euclidean.

Consider in this respect the outer product of three spheres $\boldsymbol{A}$, $\boldsymbol{B}$ and $\boldsymbol{C}$ as depicted in figure 3.3. It is

$$\boldsymbol{K} \;=\; (\boldsymbol{A} \wedge \boldsymbol{B} \wedge \boldsymbol{C})\boldsymbol{I} \qquad \text{and e.g.} \qquad \boldsymbol{A} \cdot \boldsymbol{K} \;=\; 0.$$

All contributing spheres must therefore be orthogonal to the circle $\boldsymbol{K}$. The effect is that the outer product of three spheres yields a circle that does not pass through the centers of the spheres any more – instead the circle intersects each of the spheres at right angles. It seems that such a circle is unique. The setup is illustrated in figure 3.3.
The line $\boldsymbol{L}^* = \mathbf{e} \wedge \boldsymbol{A} \wedge \boldsymbol{B}$, on the other hand, would include the centers because the thought elongation of the segment between the centers of $\boldsymbol{A}$ and $\boldsymbol{B}$ to infinity ($\mathbf{e}$) always intersects the spheres at right angles.

Note that the outer product of any four non-coplanar spheres that intersect in a single conformal point $\boldsymbol{x} \in \mathbb{R}^{4,1}$ gives $\alpha \boldsymbol{x}^*$, $\alpha \in \mathbb{R}$. Hence in the same way that a circle has (infinitely) many representations in terms of the intersection of two spheres, a simple point has comparably more representations. This multiplicity of possible representations is one of the strengths of GA.

Subsequently, all geometric objects that can be represented by a vector only, i.e. points, spheres and planes, will be detailed.

3.3.5 Conformal Points

Many equations in this chapter refer to conformal points which are not necessarily normalized regarding their $\mathbf{e}_o$-coordinate. Such a normalization can easily be achieved by

$$\boldsymbol{a} \;\mapsto\; \frac{\boldsymbol{a}}{-\mathbf{e}\cdot\boldsymbol{a}}.$$

A Particularity

The fact that conformal points square to zero implies, given a blade $\boldsymbol{A}_{\langle k\rangle}$ and a point $\boldsymbol{x}$, that

$$(\boldsymbol{x}\cdot\boldsymbol{A}_{\langle k\rangle})^2 \;=\; (\boldsymbol{x}\wedge\boldsymbol{A}_{\langle k\rangle})^2 \;=\; \tfrac{1}{2}\,\boldsymbol{x}\cdot(\boldsymbol{A}_{\langle k\rangle}\boldsymbol{x}\boldsymbol{A}_{\langle k\rangle}). \tag{3.22}$$

For a proof it is referred to page 31, where it is stated that inner and outer product between a vector and a blade/κ-vector can be expressed by the commutator and anti-commutator, respectively. Now the $\pm$-symbol is being used to represent commutator and anti-commutator at the same time (disregarding the factor 0.5). The result is independent of the sign

$$\begin{aligned}(\boldsymbol{x}\boldsymbol{A}_{\langle k\rangle} \pm \boldsymbol{A}_{\langle k\rangle}\boldsymbol{x})^2 \;&=\; +\boldsymbol{x}\boldsymbol{A}_{\langle k\rangle}\boldsymbol{x}\boldsymbol{A}_{\langle k\rangle} \\ &\quad\; \pm\boldsymbol{x}\underbrace{\boldsymbol{A}_{\langle k\rangle}\boldsymbol{A}_{\langle k\rangle}}_{\in\mathbb{R}}\boldsymbol{x} \;\pm\; \boldsymbol{A}_{\langle k\rangle}\underbrace{\boldsymbol{x}\boldsymbol{x}}_{0}\boldsymbol{A}_{\langle k\rangle} \\ &\quad\; +\boldsymbol{A}_{\langle k\rangle}\boldsymbol{x}\boldsymbol{A}_{\langle k\rangle}\boldsymbol{x} \\ &=\; \boldsymbol{x}\boldsymbol{A}_{\langle k\rangle}\boldsymbol{x}\boldsymbol{A}_{\langle k\rangle} \;+\; \boldsymbol{A}_{\langle k\rangle}\boldsymbol{x}\boldsymbol{A}_{\langle k\rangle}\boldsymbol{x},\end{aligned}$$

and therefore independent of whether inner or outer product is chosen.

Distance

The distance between two conformal points $\boldsymbol{a}$ and $\boldsymbol{b}$ (the distance between the underlying Euclidean points $\vec{a}$ and $\vec{b}$, respectively) can be determined with the help of the inner product, cf. equation (3.14). It is henceforth being denoted by $\mathtt{d}_{[\boldsymbol{a},\boldsymbol{b}]}$.

$$\mathtt{d}_{[\boldsymbol{a},\boldsymbol{b}]} \;=\; \sqrt{-2(\boldsymbol{a}\cdot\boldsymbol{b})} \tag{3.23}$$

Observing that $-2(\boldsymbol{a}\cdot\boldsymbol{b}) = \boldsymbol{a}^2 - 2(\boldsymbol{a}\cdot\boldsymbol{b}) + \boldsymbol{b}^2 = (\boldsymbol{a}-\boldsymbol{b})^2$ it can be inferred that

$$\mathtt{d}_{[\boldsymbol{a},\boldsymbol{b}]} \;=\; \sqrt{(\boldsymbol{a}-\boldsymbol{b})^2}. \tag{3.24}$$

Self-evidently, the square root and the square may not neutralize each other.

Summation

Here the arithmetic mean of k points $\boldsymbol{x}_1, \boldsymbol{x}_2, \ldots, \boldsymbol{x}_k$ is to be analyzed by identifying it with the equation of a sphere $\boldsymbol{S}$. An unexpected relationship regarding the variance of the points will be obtained.

$$\begin{aligned}
\boldsymbol{S} = \frac{1}{k}\sum_{i=1}^{k}\boldsymbol{x}_i \quad &= \quad \overbrace{\frac{1}{k}\sum_{i=1}^{k}\vec{x}_i}^{\vec{s}} + \overbrace{\tfrac{1}{2}\left(\frac{1}{k}\sum_{i=1}^{k}\vec{x}_i^{\,2}\right)}^{\frac{1}{2}(\vec{s}^2-\rho^2)}\mathbf{e} + \mathbf{e}_o \\
&= \quad \vec{s} + \tfrac{1}{2}\left(\vec{s}^{\,2} - \rho^2\right)\mathbf{e} + \mathbf{e}_o .
\end{aligned}$$

Using the above definitions of $\vec{s}$ and ρ it follows[7]

$$\begin{aligned}
& \left(\frac{1}{k}\sum_{i=1}^{k}\vec{x}_i\right)^2 - \rho^2 = \left(\frac{1}{k}\sum_{i=1}^{k}\vec{x}_i^{\,2}\right) \\
\iff \quad & \\
& \rho^2 = \underbrace{\left(\frac{1}{k}\sum_{i=1}^{k}\vec{x}_i\right)^2}_{\mathrm{E}(\underset{\sim}{\vec{x}})^2} - \underbrace{\left(\frac{1}{k}\sum_{i=1}^{k}\vec{x}_i^{\,2}\right)}_{\mathrm{E}(\underset{\sim}{\vec{x}}^2)} \\
\implies \quad & \\
& \rho = \sqrt{-\operatorname{Var}(\underset{\sim}{\vec{x}})}.
\end{aligned} \tag{3.25}$$

Hence the sphere is imaginary. As a matter of fact, its center $\vec{s}$ corresponds to the barycenter of the points and the radius is related to the variance of the points by

$$\operatorname{Var}(\underset{\sim}{\vec{x}}) = -\rho^2 = -\boldsymbol{S}^2,$$

where equation (3.14) was used.

3.3.6 Spheres

Spheres can be considered the most general geometric objects in CGA.

The center $\vec{s}$ of a sphere $\boldsymbol{S} = \vec{s} + \frac{1}{2}(\vec{s}^{\,2} - r_s^2)\mathbf{e} + \mathbf{e}_o$ with radius r_s may be determined by directly looking at the Euclidean parts, i.e.

$$\vec{s} = \sum_{i=1}^{3}(\mathbf{e}_i \cdot \boldsymbol{S})\mathbf{e}_i$$

or alternatively algebraically, see equation (A.33), with

$$\vec{s} = \boldsymbol{E} \cdot (\boldsymbol{E} \wedge \boldsymbol{S}).$$

[7] The underset tilde serves to indicate a random variable, see page 146.

It can further be verified, irrespective of whether the sphere is imaginary or not, that

$$\boldsymbol{S}\,\mathbf{e}\boldsymbol{S} \;=\; -2\boldsymbol{s} \qquad \Longleftrightarrow \qquad \boldsymbol{s} \;=\; \frac{\boldsymbol{S}\,\mathbf{e}\boldsymbol{S}}{-2}, \tag{3.26}$$

where $\boldsymbol{s} = \mathcal{K}(\vec{s})$. This is an important result which is to be discussed in section 3.3.9, starting on page 104.

Radius

As already mentioned, the radius r_s of a sphere can be calculated using

$$r_s^2 \;=\; \boldsymbol{S}^2.$$

However, in certain cases a sphere squares to a negative value so that the radius r_s can be viewed as an imaginary number. Correspondingly, the sphere is said to be imaginary. Assuming a real radius r_s, the equation for such spheres can be stated as

$$\boldsymbol{S}_s \;=\; \vec{s} + \tfrac{1}{2}(\vec{s}^{\,2} \;+\; r_s^2)\mathbf{e} + \mathbf{e}_o.$$

Calculating the inner product of $\boldsymbol{S}_s$ and another sphere $\boldsymbol{K} = \vec{k} + \frac{1}{2}(\vec{k}^2 - r_K^2)\mathbf{e} + \mathbf{e}_o$

$$\begin{aligned} \boldsymbol{S}_s \cdot \boldsymbol{K} \;&=\; \vec{s} \cdot \vec{k} - \tfrac{1}{2}(\vec{s}^{\,2} + r_s^2 + \vec{k}^2 - r_K^2) \\ &=\; \tfrac{1}{2}\left[\, r_K^2 - (r_s^2 + ||\vec{k} - \vec{s}||^2) \,\right], \end{aligned}$$

shows that spheres $\boldsymbol{K}$ with radius $r_K = \sqrt{r_s^2 + ||\vec{k} - \vec{s}||^2}$, but not conformal points, cause the inner product to attain zero. As a consequence, imaginary spheres do not have a Euclidean inner product null space – these spheres cannot be created using equation (3.21).

Conversion of Imaginary Spheres

It is not difficult to realize that, given an imaginary sphere $\boldsymbol{K}$, the real counterpart $\boldsymbol{S}$, with radius $r = \sqrt{-\boldsymbol{K}^2}$, can be computed by means of the simple relation

$$\boldsymbol{S} \;=\; \boldsymbol{K} + \boldsymbol{K}^2\mathbf{e}. \tag{3.27}$$

It is crucial to observe that making a sphere real changes the inner product. That means an imaginary sphere that is initially orthogonal to another sphere cannot be orthogonal after the conversion, and vice versa. The orthogonality with respect to a plane, however, is always preserved, see equation (3.33).

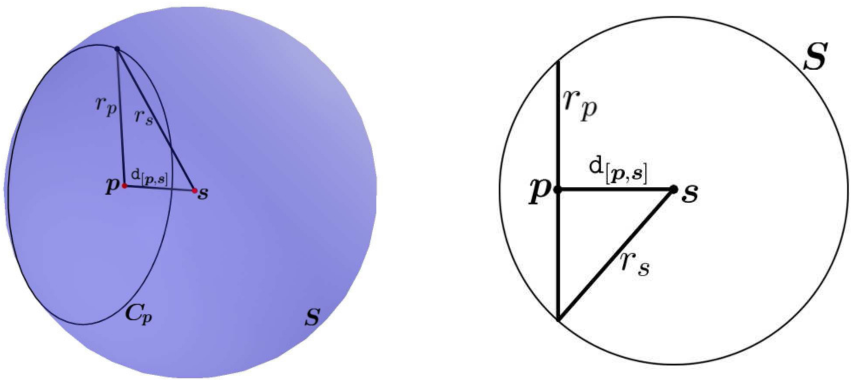

Fig. 3.4: Inner product between a sphere and a point inside of it. The right side depicts a cross-section only.

Point - Sphere

Consider a point $\boldsymbol{p}$ and a sphere $\boldsymbol{S} = \vec{s} + \frac{1}{2}(\vec{s}^2 - r_s^2)\mathbf{e} + \mathbf{e}_o$. Assume that $\boldsymbol{p}$ lies outside $\boldsymbol{S}$. Then the inner product $\boldsymbol{p} \cdot \boldsymbol{S} =: \alpha\, r_p^2$, with $\alpha = -0.5$, gives the radius r_p of a sphere $\boldsymbol{S}_p$ centered at $\boldsymbol{p}$ in such a way that $\boldsymbol{S}_p$ is orthogonal[8] to $\boldsymbol{S}$, i.e. $\boldsymbol{S}_p \cdot \boldsymbol{S} = 0$. The sphere $\boldsymbol{S}_p$ can be built by

$$\boldsymbol{S}_p = \boldsymbol{p} + (\boldsymbol{p} \cdot \boldsymbol{S})\mathbf{e}. \tag{3.28}$$

To see this, compare

$$\boldsymbol{S}_p \cdot \boldsymbol{S} \;=\; (\boldsymbol{p} + (\boldsymbol{p} \cdot \boldsymbol{S})\mathbf{e}) \cdot \boldsymbol{S} \;=\; \boldsymbol{p} \cdot \boldsymbol{S} - \boldsymbol{p} \cdot \boldsymbol{S} \;=\; 0.$$

Note that r_p^2 is the *power of point* $\boldsymbol{p}$ with respect to the sphere $\boldsymbol{S}$ if $\boldsymbol{p}$ lies outside $\boldsymbol{S}$, cf. [111, 19, 107]. Thus given a chord passing through the points $\boldsymbol{a}$, $\boldsymbol{b}$ and $\boldsymbol{p}$, where $\boldsymbol{a}$ and $\boldsymbol{b}$ are assumed to lie on $\boldsymbol{S}$, it holds that

$$\mathsf{d}_{[\boldsymbol{p},\boldsymbol{a}]}\ \mathsf{d}_{[\boldsymbol{p},\boldsymbol{b}]} \overset{\text{const}}{=} r_p^2.$$

If $\boldsymbol{p}$ lies inside $\boldsymbol{S}$ (see below), the inner product becomes positive such that it must be considered that $r_p^2 < 0$. This implies that the sphere $\boldsymbol{S}_p$ becomes imaginary.

Thus by looking at the sign of the inner product it can be determined whether a point is inside or outside a sphere

$$\boldsymbol{p} \cdot \boldsymbol{S} \;<\; 0 \qquad \overset{\boldsymbol{S}^2 > 0}{\Longleftrightarrow} \qquad \text{point } \boldsymbol{p} \text{ lies outside } \boldsymbol{S}.$$

This relationship is exploited by Banarer [9] who utilizes CGA spheres in a neural architecture to define so-called *hypersphere neurones* so as to achieve a non-linear, that is a hyperspherical, separation in classification problems.

Now let $\boldsymbol{p}$ be a point in the inside of the sphere $\boldsymbol{S} := \boldsymbol{s} - \frac{1}{2}r_s^2\mathbf{e}$. The scenario is illustrated in figure 3.4. According to equation (3.14) the inner product is

$$\boldsymbol{p} \cdot \boldsymbol{S} \;=\; \tfrac{1}{2}(r_s^2 - \mathsf{d}_{[\boldsymbol{p},\boldsymbol{s}]}^2) \;=:\; \tfrac{1}{2}r_p^2,$$

where in this case r_p denotes the radius of circle $\boldsymbol{C}_p$, which is depicted on the left side of the figure.

[8] Recall that this means that the respective surfaces are perpendicular.

3.3.7 Planes

Planes are the last vector valued elements that are mentioned. Recall that a plane can be considered a special sphere with infinite radius. This notion has a solid base; replacing the fourth point $\boldsymbol{d}$ in equation (3.21), the OPNS representation of a sphere, with 'the point' $\mathbf{e}$, should consistently yield a sphere passing through infinity. The resulting OPNS expression does in effect match the plane equation (3.20).

The IPNS of planes representation is succinct

$$\boldsymbol{P} \;=\; \hat{n} + d\mathbf{e}, \qquad d \geq 0 \tag{3.29}$$

where $\hat{n}$, $||\hat{n}|| = 1$, denotes the normal vector of the plane and d stands for the distance to the origin $\mathbf{e}_o$. If the plane is not normalized right from the beginning, for example $\boldsymbol{P} = \vec{n} + t\mathbf{e}$ and $||\vec{n}|| \neq 1$, it can be divided by $\boldsymbol{P}^2 = \vec{n}^2 + t(\vec{n}\mathbf{e} + \mathbf{e}\vec{n}) = \vec{n}^2$. A plane, as defined above, has to fulfill two conditions

$$\boldsymbol{P}^2 \;=\; 1 \qquad \text{and} \qquad \mathbf{e}_o \cdot \boldsymbol{P} \leq 0.$$

Notice that planes with $d < 0$ are simply oppositely oriented and occur equally frequently.

Distance d and normal vector $\hat{n}$ can easily be extracted

$$\begin{aligned} d &= \boldsymbol{P} \cdot \mathbf{e}_+ \\ \hat{n} &= \boldsymbol{E} \cdot (\boldsymbol{E} \wedge \boldsymbol{P}). \end{aligned}$$

The two parameters $\hat{n}$ and d appear as well in the OPNS formula (3.20): building the IPNS representation of the first component $\mathbf{e} \wedge \vec{a} \wedge \vec{b} \wedge \vec{c}$, only, in equation (3.20) yields

$$\begin{aligned} (\mathbf{e} \wedge \vec{a} \wedge \vec{b} \wedge \vec{c})\, \boldsymbol{I} &= -\left(\vec{a} \cdot (\vec{b} \times \vec{c})\right) \mathbf{e} \\ &= \alpha\, (d\, \mathbf{e}) \qquad \alpha \in \mathbb{R}. \end{aligned}$$

For the second component it is

$$\begin{aligned} ((\vec{b} - \vec{a}) \wedge (\vec{c} - \vec{a}))\, \boldsymbol{E}\, \boldsymbol{I} &= (\vec{c} - \vec{a}) \;\times\; (\vec{b} - \vec{a}) \\ &= \alpha\, \hat{n}, \end{aligned} \tag{3.30}$$

for the same $\alpha \in \mathbb{R}$ as above. Its value is the magnitude of $(\vec{b} - \vec{a}) \wedge (\vec{c} - \vec{a})$ and can be computed by means of equation (2.16).

Hence if a plane is created by means of the OPNS representation, its orientation $\hat{n}$ can be determined with a hand rule[9]: the fingers of the left hand are curled to match the direction given by the point sequence ***a*-*b*-*c***; then the thumb indicates the direction of the plane.

[9] Right hand sequence: ***a*-*c*-*b***.

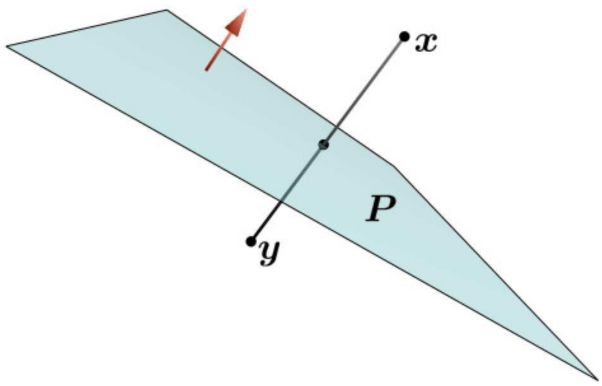

Fig. 3.5: Creating planes: the expression $\boldsymbol{x}-\boldsymbol{y}$ represents the bisecting plane $\boldsymbol{P}$ indicated by the cyan area.

Creating Planes

An easy way to create a plane is to subtract two conformal points so that the $\mathbf{e}_o$-component vanishes, for example $\boldsymbol{P} \equiv \boldsymbol{x}-\boldsymbol{y}$. In order to normalize $\boldsymbol{P}$ it must be divided by $\sqrt{\boldsymbol{P}^2}$

$$\boldsymbol{P} \;=\; \frac{\boldsymbol{x}-\boldsymbol{y}}{\sqrt{(\boldsymbol{x}-\boldsymbol{y})^2}} \;=\; \frac{\boldsymbol{x}-\boldsymbol{y}}{\sqrt{-2(\boldsymbol{x}\cdot\boldsymbol{y})}} \;=\; \frac{\boldsymbol{x}-\boldsymbol{y}}{\mathtt{d}_{[\boldsymbol{x},\boldsymbol{y}]}}.$$

Moreover, in order to comply with equation (3.29), which defines a plane, the $\mathbf{e}$-component must be positive. That means $\boldsymbol{x}$ must be further away from the origin than $\boldsymbol{y}$. The exact expression is therefore

$$\mathtt{d}_{[\,\mathbf{e}_o,\boldsymbol{x}]} \geq \mathtt{d}_{[\,\mathbf{e}_o,\boldsymbol{y}]} \qquad \Longrightarrow \qquad \boldsymbol{P} \;=\; \frac{\boldsymbol{x}-\boldsymbol{y}}{\mathtt{d}_{[\boldsymbol{x},\boldsymbol{y}]}}. \tag{3.31}$$

The inner product of $\boldsymbol{P}$ with a vector $\boldsymbol{a}$ results in

$$\boldsymbol{a}\cdot\boldsymbol{P} \;=\; \frac{\boldsymbol{a}\cdot\boldsymbol{x}-\boldsymbol{a}\cdot\boldsymbol{y}}{\mathtt{d}_{[\boldsymbol{x},\boldsymbol{y}]}} \;=\; \frac{\mathtt{d}^2_{[\boldsymbol{a},\boldsymbol{y}]}-\mathtt{d}^2_{[\boldsymbol{a},\boldsymbol{x}]}}{2\,\mathtt{d}_{[\boldsymbol{x},\boldsymbol{y}]}}.$$

This shows that the eIPNS of $\boldsymbol{P}$ consists of all points $\boldsymbol{a}$ fulfilling $\mathtt{d}_{[\boldsymbol{a},\boldsymbol{x}]} = \mathtt{d}_{[\boldsymbol{a},\boldsymbol{y}]}$ or equivalently of all points lying on the perpendicular bisecting plane of the line that connects $\boldsymbol{x}$ and $\boldsymbol{y}$.

Distance Point - Plane

To evaluate the distance between a point $\boldsymbol{x}$ and a normalized plane $\boldsymbol{P}$ a virtual point $\boldsymbol{y}$ can temporarily be introduced that serves as the reflected version of $\boldsymbol{x}$ in the plane $\boldsymbol{P}$. Note that $\boldsymbol{x}$ and $\boldsymbol{y}$ lie on different sides of $\boldsymbol{P}$. Assume at first and in accordance to the condition imposed by equation (3.31) that $\mathtt{d}_{[\,\mathbf{e}_o,\boldsymbol{x}]} \geq \mathtt{d}_{[\,\mathbf{e}_o,\boldsymbol{y}]}$. Then $\boldsymbol{P}$ can be expressed in terms of the two points by

$$\boldsymbol{P} \;=\; \frac{\boldsymbol{x}-\boldsymbol{y}}{\mathtt{d}_{[\boldsymbol{x},\boldsymbol{y}]}}.$$

The inner product $\boldsymbol{x}\cdot\boldsymbol{P}$ gives

$$\boldsymbol{x}\cdot\boldsymbol{P} \;=\; \frac{-\,\boldsymbol{x}\cdot\boldsymbol{y}}{\mathtt{d}_{[\boldsymbol{x},\boldsymbol{y}]}} \;=\; \frac{\mathtt{d}^2_{[\boldsymbol{x},\boldsymbol{y}]}}{2\,\mathtt{d}_{[\boldsymbol{x},\boldsymbol{y}]}} \;=\; \frac{\mathtt{d}_{[\boldsymbol{x},\boldsymbol{y}]}}{2}.$$

If the condition $\mathtt{d}_{[\mathbf{e}_o,\boldsymbol{x}]} \geq \mathtt{d}_{[\mathbf{e}_o,\boldsymbol{y}]}$ is not fulfilled, $\boldsymbol{P} = (\boldsymbol{y}-\boldsymbol{x})/\,\mathtt{d}_{[\boldsymbol{x},\boldsymbol{y}]}$ must be considered, which introduces a minus sign $\boldsymbol{x}\cdot\boldsymbol{P} = -\,\mathtt{d}_{[\boldsymbol{x},\boldsymbol{y}]}/2$. Hence depending on which side of $\boldsymbol{P}$ $\boldsymbol{x}$ lies, the inner product may be positive or negative.

Since the distance $\mathtt{d}_{[\boldsymbol{x},\boldsymbol{y}]}$ is twice the sought distance $\mathtt{d}_{[\boldsymbol{x},\boldsymbol{P}]}$, it can be figured out that

$$\mathtt{d}_{[\boldsymbol{x},\boldsymbol{P}]} \;=\; |\boldsymbol{x}\cdot\boldsymbol{P}|. \tag{3.32}$$

A plane $\boldsymbol{P} = \hat{n} + d\mathbf{e}$ has, just like the closely related sphere, two distinct sides; a point on the same side as the origin yields a negative inner product

$$\boldsymbol{x}\cdot\boldsymbol{P} \leq 0 \qquad \overset{d>0}{\Longleftrightarrow} \qquad \boldsymbol{x} \text{ lies on the same side as } \mathbf{e}_o.$$

The gradient of $\mathcal{K}(\vec{x})\cdot\boldsymbol{P}$ w.r.t. $\vec{x}$ is the normal vector $\hat{n}$. Consequently, the value of the inner product increases if $\boldsymbol{x}$ is moved in the direction of $\hat{n}$. The inner product $\boldsymbol{x}\cdot\boldsymbol{P}$ with a plane passing through the origin ($d=0$) is positive iff $\boldsymbol{x}\neq\mathbf{e}_o$ lies on the same side as $\hat{n}$ points to.

Sphere - Plane

These two entities do essentially differ in that a plane has no $\mathbf{e}_o$-component. As a result, the $\mathbf{e}$-component of a sphere, which holds its radius, has no impact if the inner product between a sphere $\boldsymbol{S}$ and a plane $\boldsymbol{P}$ is built. Hence a sphere $\boldsymbol{S} = \boldsymbol{s} - \frac{1}{2}r_s^2\mathbf{e}$, $\boldsymbol{s}^2 = 0$, behaves as the point $\boldsymbol{s}$ in its center

$$\boldsymbol{S}\cdot\boldsymbol{P} \;=\; (\boldsymbol{s} - \tfrac{1}{2}r_s^2\mathbf{e})\cdot\boldsymbol{P} \;=\; \boldsymbol{s}\cdot\boldsymbol{P} \;=\; \pm\,\mathtt{d}_{[\boldsymbol{s},\boldsymbol{P}]}. \tag{3.33}$$

Consequently, the inner product of a sphere and a plane is zero iff the center of the sphere lies on the plane or equivalently iff the sphere (surface) is perpendicular to the plane.

Anti-Commuting Planes

As the inner product of two planes $\boldsymbol{P}_1 = \hat{n}_1 + d_1\mathbf{e}$ and $\boldsymbol{P}_2 = \hat{n}_2 + d_2\mathbf{e}$ amounts to

$$\begin{aligned} \boldsymbol{P}_1\cdot\boldsymbol{P}_2 \;&=\; (\hat{n}_1 + d_1\,\mathbf{e})\cdot(\hat{n}_2 + d_2\,\mathbf{e}) \\ &=\; \hat{n}_1\cdot\hat{n}_2 \\ &=\; \cos(\theta), \end{aligned} \tag{3.34}$$

where θ denotes the angle between the planes, two planes anti-commute iff they are orthogonal

$$\big(\boldsymbol{P}_1\,\boldsymbol{P}_2 \;=\; -\,\boldsymbol{P}_2\,\boldsymbol{P}_1\big) \quad\Longleftrightarrow\quad \boldsymbol{P}_1 \perp \boldsymbol{P}_2. \tag{3.35}$$

Projection

The projection of a point $\boldsymbol{x}$ onto a plane $\boldsymbol{P} = \hat{n} + d\mathbf{e} = \boldsymbol{P}^{-1}$ results in an imaginary sphere $\boldsymbol{S}_p = \boldsymbol{s}_p - \frac{1}{2}r_p^2\mathbf{e}$. Let $\kappa := \operatorname{sgn}(\boldsymbol{x}\cdot\boldsymbol{P})$ then

$$\begin{aligned}\boldsymbol{S}_p = (\boldsymbol{x}\wedge\boldsymbol{P}^{-1})\boldsymbol{P} &\overset{(2.44,1.)}{=} \boldsymbol{x} - \overbrace{(\boldsymbol{x}\cdot\boldsymbol{P})\boldsymbol{P}}^{\text{rejection}} = \boldsymbol{x} - \kappa\,\mathtt{d}_{[\boldsymbol{x},\boldsymbol{P}]}\boldsymbol{P}\\ &= \boldsymbol{x} - \kappa\,\mathtt{d}_{[\boldsymbol{x},\boldsymbol{P}]}\hat{n} - \kappa\,\mathtt{d}_{[\boldsymbol{x},\boldsymbol{P}]}\,\mathtt{d}_{[\mathbf{e}_o,\boldsymbol{P}]}\mathbf{e}\end{aligned}$$

with an imaginary radius r_p:

$$\begin{aligned} r_p^2 &= \boldsymbol{S}_p^2 = (\boldsymbol{x} - \kappa\,\mathtt{d}_{[\boldsymbol{x},\boldsymbol{P}]}\boldsymbol{P})^2 = \boldsymbol{x}^2 - \kappa\,\mathtt{d}_{[\boldsymbol{x},\boldsymbol{P}]}\underbrace{(\boldsymbol{x}\boldsymbol{P} + \boldsymbol{P}\boldsymbol{x})}_{2\boldsymbol{x}\cdot\boldsymbol{P}} + \mathtt{d}^2_{[\boldsymbol{x},\boldsymbol{P}]}\boldsymbol{P}^2\\ &= -2\,\mathtt{d}^2_{[\boldsymbol{x},\boldsymbol{P}]} + \mathtt{d}^2_{[\boldsymbol{x},\boldsymbol{P}]}\\ &= -\,\mathtt{d}^2_{[\boldsymbol{x},\boldsymbol{P}]}\end{aligned}$$

Since $\boldsymbol{s}_p = \mathcal{K}(\vec{x} - \kappa\,\mathtt{d}_{[\boldsymbol{x},\boldsymbol{P}]}\hat{n})$, it follows $\mathtt{d}_{[\boldsymbol{x},\boldsymbol{s}_p]} = \mathtt{d}_{[\boldsymbol{x},\boldsymbol{P}]} = |r_p|$. The point $\boldsymbol{s}_p$ lies on $\boldsymbol{P}$ because of $\boldsymbol{S}_p\cdot\boldsymbol{P} = 0$ and

$$\boldsymbol{s}_p\cdot\boldsymbol{P} = (\boldsymbol{S}_p - \tfrac{1}{2}\,\mathtt{d}^2_{[\boldsymbol{x},\boldsymbol{P}]}\mathbf{e})\cdot\boldsymbol{P} = \boldsymbol{S}_p\cdot\boldsymbol{P} - \tfrac{1}{2}\,\mathtt{d}^2_{[\boldsymbol{x},\boldsymbol{P}]}\mathbf{e}\cdot\boldsymbol{P} = 0.$$

Hence $\boldsymbol{s}_p$ represents the Euclidean projection of $\boldsymbol{x}$ onto $\boldsymbol{P}$. There are several ways to determine $\boldsymbol{s}_p$. Using equation (3.26), for example, it can be figured out that

$$\boldsymbol{s}_p = \frac{(\boldsymbol{x}\wedge\boldsymbol{P})\mathbf{e}(\boldsymbol{x}\wedge\boldsymbol{P})}{-2}.$$

Summation of Planes

Consider two normalized planes $\boldsymbol{P}_1$, $\boldsymbol{P}_2$ in the notation of equation (3.29). The average $\boldsymbol{P}_3 := \frac{1}{2}(\boldsymbol{P}_1 + \boldsymbol{P}_2)$ is now being analyzed. Clearly, $\boldsymbol{P}_3$ is still a vector with $\mathbf{e}$ and without $\mathbf{e}_o$-component identifying itself as a plane.

Two settings are distinguished. First let the planes be parallel. Building the average $\boldsymbol{P}_3$ results in a plane with identical normal vector and a correct distance such that $\boldsymbol{P}_3$ lies centered between $\boldsymbol{P}_1$ and $\boldsymbol{P}_2$, as expected. Otherwise, what if the planes intersect? Let $\boldsymbol{L} = \boldsymbol{P}_1\wedge\boldsymbol{P}_2$ be the line of intersection. It can be seen that $\boldsymbol{P}_1\wedge\boldsymbol{P}_3$ equals $\boldsymbol{P}_2\wedge\boldsymbol{P}_3$, that is $\pm\frac{1}{2}\boldsymbol{L}$, which represents the same line as $\boldsymbol{L}$. Thus $\boldsymbol{L}$ lies on all planes, $\boldsymbol{P}_1$, $\boldsymbol{P}_2$ and $\boldsymbol{P}_3$, at the same time. Furthermore the average of two normalized direction vectors gives a new direction vector representing the angle bisector. This shows that $\boldsymbol{P}_3$ is correctly orientated, whence it can be concluded that $\boldsymbol{P}_3$ has as well the correct distance. In conclusion, the algebraic mean plane $\boldsymbol{P}_3$ is also the (geometrically) bisecting plane. Note that an afterwards normalization of $\boldsymbol{P}_3$ can easily be achieved by $\boldsymbol{P}_3 \mapsto \boldsymbol{P}_3/\boldsymbol{P}_3^2$.

3.3.8 Reflecting with CGA

A vital aspect of CGA is the reflection. It is, in general, explained in chapter 2. Here the reflection in a plane and in a sphere (inversion) are being discussed.

Let $\boldsymbol{P}$ denote a plane that is created according to equation (3.31), i.e. by subtracting two conformal points $\boldsymbol{x}$ and $\boldsymbol{y}$

$$\boldsymbol{P} \;=\; \frac{\boldsymbol{x}-\boldsymbol{y}}{\sqrt{-2(\boldsymbol{x}\cdot\boldsymbol{y})}}, \qquad \text{with} \quad \boldsymbol{P}^2 = 1.$$

Recall that in GA reflections are carried out by means of a sandwich product. By the result of equation (2.40), that is $\boldsymbol{A}_{\langle k\rangle}\boldsymbol{b}\boldsymbol{A}_{\langle k\rangle} \in \mathbb{R}^{p,q}$, is the reflection $\boldsymbol{PaP}$ of $\boldsymbol{a}$ in $\boldsymbol{P}$ again a vector. Moreover, a conformal point

$$(\boldsymbol{PaP})^2 \;=\; \boldsymbol{P}\underbrace{\boldsymbol{a}\overbrace{\boldsymbol{PP}}^{1}\boldsymbol{a}}_{0}\boldsymbol{P} \;=\; 0.$$

In addition, it can be seen that the reflection of the reflection in the same plane is again the initial point

$$\boldsymbol{P}(\boldsymbol{PaP})\boldsymbol{P} \;=\; \boldsymbol{a}. \tag{3.36}$$

However, observing that

$$\boldsymbol{PxP} \;=\; \frac{(\boldsymbol{x}-\boldsymbol{y})\boldsymbol{x}(\boldsymbol{x}-\boldsymbol{y})}{-2(\boldsymbol{x}\cdot\boldsymbol{y})} \;=\; \frac{\boldsymbol{yxy}}{-2(\boldsymbol{x}\cdot\boldsymbol{y})} \;\overset{(A.27)}{=}\; \frac{2(\boldsymbol{x}\cdot\boldsymbol{y})\boldsymbol{y}}{-2(\boldsymbol{x}\cdot\boldsymbol{y})} \;=\; -\boldsymbol{y},$$

unveils that the reflection, irrespective on which side of $\boldsymbol{P}$ point $\boldsymbol{x}$ lies, introduces a scalar factor -1, which disappears if $\boldsymbol{P}$ is applied twice, see equation (3.36).

Now it is being shown that the sandwich product $\boldsymbol{PaP}$ in fact represents a reflection. Taking into account the minus sign, the difference between an arbitrary point $\boldsymbol{a}$ (not on $\boldsymbol{P}$) and its reflected version $-\boldsymbol{PaP}$ must be the plane again, hence

$$\begin{aligned}\frac{\boldsymbol{a}+\boldsymbol{PaP}}{\sqrt{(\boldsymbol{a}+\boldsymbol{PaP})^2}} \;&\overset{(A.24)}{=}\; \frac{\boldsymbol{a}+2(\boldsymbol{P}\cdot\boldsymbol{a})\boldsymbol{P}-\boldsymbol{a}}{\sqrt{(\boldsymbol{a}+\boldsymbol{PaP})^2}} \;=\; \frac{2(\boldsymbol{P}\cdot\boldsymbol{a})\boldsymbol{P}}{\sqrt{\boldsymbol{aPaP}+\boldsymbol{PaPa}}}\\ &=\; \frac{2(\boldsymbol{P}\cdot\boldsymbol{a})\boldsymbol{P}}{\sqrt{2\boldsymbol{a}\cdot(\boldsymbol{PaP})}} \;=\; \frac{2(\boldsymbol{P}\cdot\boldsymbol{a})\boldsymbol{P}}{\sqrt{4(\boldsymbol{P}\cdot\boldsymbol{a})^2}} \;=\; \boldsymbol{P},\end{aligned}$$

where the denominator serves as a normalization.

Eventually, consider the distance $\mathtt{d}_{[\boldsymbol{a},\boldsymbol{a}']}$ between a point $\boldsymbol{a}$ and its reflection $\boldsymbol{a}' = -\boldsymbol{PaP}$

$$\begin{aligned}&-\tfrac{1}{2}\,\mathtt{d}^2_{[\boldsymbol{a},\boldsymbol{a}']} \;=\; \boldsymbol{a}\cdot\boldsymbol{a}' \;=\; -2(\boldsymbol{a}\cdot\boldsymbol{P})^2 \;=\; -2\,\mathtt{d}^2_{[\boldsymbol{a},\boldsymbol{P}]}\\ \Longleftrightarrow\quad &\\ &\mathtt{d}_{[\boldsymbol{a},\boldsymbol{a}']} \;=\; 2\,\mathtt{d}_{[\boldsymbol{a},\boldsymbol{P}]}.\end{aligned}$$

This further substantiates that

$$\boldsymbol{a}' \;=\; -\boldsymbol{PaP} \tag{3.37}$$

does indeed represent the reflection $\boldsymbol{a}'$ of $\boldsymbol{a}$ in $\boldsymbol{P}$.

To summarize, there should be sufficient evidence confirming that $-\boldsymbol{PaP}$ represents a reflection, although it is not outright proven.

Example: Point Pairs

The entity point pair is not being discussed explicitly. These 2-blades often arise from intersections, for instance between a plane and a circle.

Consider the point pair $\boldsymbol{a} \wedge \boldsymbol{b}$ and let $\boldsymbol{P}$ denote the (normalized) plane halfway between $\boldsymbol{a}$ and $\boldsymbol{b}$, e.g. $\boldsymbol{P} \equiv \boldsymbol{b} - \boldsymbol{a}$. Point $\boldsymbol{b}$ may then be replaced by the reflected version of $\boldsymbol{a}$

$$\begin{aligned} \boldsymbol{a} \wedge \boldsymbol{b} &= \boldsymbol{a} \wedge (-\boldsymbol{PaP}) \\ &= \boldsymbol{PaP} \wedge \boldsymbol{a} \\ &\overset{(A.24)}{=} (2(\boldsymbol{a} \cdot \boldsymbol{P})\boldsymbol{P} - \boldsymbol{a}) \wedge \boldsymbol{a} \\ &= 2(\boldsymbol{a} \cdot \boldsymbol{P})\boldsymbol{P} \wedge \boldsymbol{a} \\ &= \mathtt{d}_{[\boldsymbol{a},\boldsymbol{b}]}\, \boldsymbol{P} \wedge \boldsymbol{a}. \end{aligned} \tag{3.38}$$

If $\boldsymbol{P}$ was oppositely oriented, i.e. $\boldsymbol{P}' = -\boldsymbol{P}$, it would likewise be $\boldsymbol{a} \wedge \boldsymbol{b} = -\,\mathtt{d}_{[\boldsymbol{a},\boldsymbol{b}]}\, \boldsymbol{P}' \wedge \boldsymbol{a} = \mathtt{d}_{[\boldsymbol{a},\boldsymbol{b}]}\, \boldsymbol{P} \wedge \boldsymbol{a}$ such that $\boldsymbol{P}$ can be assumed to be oriented towards $\boldsymbol{a}$.

Hence a point pair can equally be represented as the outer product between a point and a plane[10].

3.3.9 Inversion

The existence of a spherical reflection, the inversion, has – phenomenologically – already been deduced in section 1.1.3. Now it is to be proven that the expression $\boldsymbol{x}' = \boldsymbol{SxS}$ indeed describes the inversion of a conformal point $\boldsymbol{x}$ in the sphere $\boldsymbol{S} = \boldsymbol{s} - \frac{1}{2}r_s^2\mathbf{e}$. For this purpose, first $\boldsymbol{x}'$ is analyzed. Then the product $\boldsymbol{x}'' = \boldsymbol{Sx}'\boldsymbol{S}$ is built which is supposed to be $\boldsymbol{x}$ again.

Let $\boldsymbol{x}$ be a point outside $\boldsymbol{S}$, i.e. $\boldsymbol{x} \cdot \boldsymbol{S} < 0$. Pursuant to section 3.3.6, it is

$$\begin{aligned} \boldsymbol{x}' \equiv \boldsymbol{SxS} &\overset{(A.24)}{=} 2(\boldsymbol{x} \cdot \boldsymbol{S})\boldsymbol{S} - \boldsymbol{S}^2\,\boldsymbol{x} \\ &= -(r_x^2\boldsymbol{S} + r_s^2\boldsymbol{x}), \end{aligned}$$

where $\boldsymbol{x}' \equiv \ldots$ indicates that $\boldsymbol{x}'$ is not normalized w.r.t. $\mathbf{e}_o$.

Recall that, according to equation (3.28), r_x is the radius of the sphere $\boldsymbol{S}_x := \boldsymbol{x} + (\boldsymbol{x} \cdot \boldsymbol{S})\mathbf{e}$ at $\boldsymbol{x}$ that is orthogonal to $\boldsymbol{S}$. This corresponds to an angle of $\gamma = \pi/2$ in figure 3.2 so that

$$\mathtt{d}^2_{[\boldsymbol{x},\boldsymbol{s}]} = r_x^2 + r_s^2.$$

The $\mathbf{e}_o$-component of $\boldsymbol{x}'$ therefore takes the value $-\,\mathtt{d}^2_{[\boldsymbol{x},\boldsymbol{s}]}$. Thus

$$\boldsymbol{x}' = \frac{\boldsymbol{SxS}}{-\,\mathtt{d}^2_{[\boldsymbol{x},\boldsymbol{s}]}}.$$

[10] Clearly, it is $\boldsymbol{a} \wedge \boldsymbol{P} \equiv \boldsymbol{a} \wedge (\boldsymbol{b} - \boldsymbol{a}) = \boldsymbol{a} \wedge \boldsymbol{b}$.

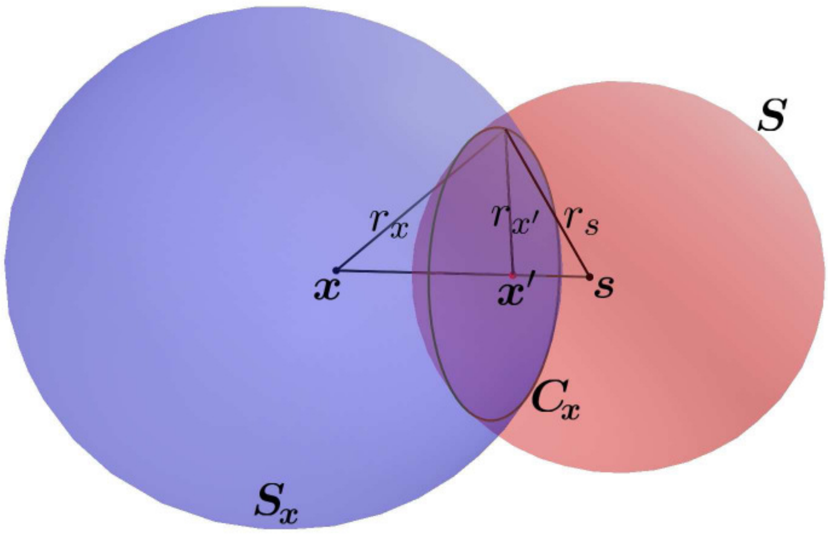

Fig. 3.6: Inversion: the inversion $\boldsymbol{x}'$ of point $\boldsymbol{x}$ ($\boldsymbol{s}$) in the sphere $\boldsymbol{S}$ ($\boldsymbol{S}_x$) represents the center of the circle $\boldsymbol{C}_x = \boldsymbol{S} \wedge \boldsymbol{S}_x$, where $\boldsymbol{S}_x := \boldsymbol{x} + (\boldsymbol{x} \cdot \boldsymbol{S})\mathbf{e}$.

The new point lies inside $\boldsymbol{S}$ due to

$$\boldsymbol{x}' \cdot \boldsymbol{S} \;=\; \frac{2(\boldsymbol{x}\cdot\boldsymbol{S})\boldsymbol{S}^2 - \boldsymbol{S}^2(\boldsymbol{x}\cdot\boldsymbol{S})}{-\,\mathsf{d}^2_{[\boldsymbol{x},\boldsymbol{s}]}} \;=\; \frac{(\boldsymbol{x}\cdot\boldsymbol{S})\boldsymbol{S}^2}{-\,\mathsf{d}^2_{[\boldsymbol{x},\boldsymbol{s}]}} > 0.$$

Now the term $\boldsymbol{x}'' = \boldsymbol{S}\boldsymbol{x}'\boldsymbol{S} = \boldsymbol{S}^4\boldsymbol{x} = r_s^4\,\boldsymbol{x}$ is being focused on. Since $\boldsymbol{x}'$ is in the inside of $\boldsymbol{S}$, the inner product $\boldsymbol{x}'\cdot\boldsymbol{S} = \frac{1}{2}r_{x'}^2$ yields a positive value with a different interpretation as before, cf. figure 3.6,

$$\begin{aligned}\boldsymbol{x}'' \equiv \boldsymbol{S}\boldsymbol{x}'\boldsymbol{S} \;&=\; 2(\boldsymbol{x}'\cdot\boldsymbol{S})\boldsymbol{S} - \boldsymbol{S}^2\,\boldsymbol{x}' \\ &=\; r_{x'}^2\boldsymbol{S} - r_s^2\boldsymbol{x}' \;=\; (r_s^2 - \mathsf{d}^2_{[\boldsymbol{x}',\boldsymbol{s}]})\boldsymbol{S} - r_s^2\boldsymbol{x}'.\end{aligned}$$

By solely looking at the $\mathbf{e}_o$-component of $\boldsymbol{x}''$, it follows the normalized point $\boldsymbol{x}'' = \boldsymbol{x}$ and thus the identity

$$\boldsymbol{x}'' \;=\; \frac{\boldsymbol{S}\boldsymbol{x}'\boldsymbol{S}}{-\,\mathsf{d}^2_{[\boldsymbol{x}',\boldsymbol{s}]}} \;=\; \frac{\boldsymbol{S}\boldsymbol{S}\boldsymbol{x}\boldsymbol{S}\boldsymbol{S}}{(-\,\mathsf{d}^2_{[\boldsymbol{x}',\boldsymbol{s}]})(-\,\mathsf{d}^2_{[\boldsymbol{x},\boldsymbol{s}]})} \;=\; \frac{r_s^4\,\boldsymbol{x}}{(-\,\mathsf{d}^2_{[\boldsymbol{x}',\boldsymbol{s}]})(-\,\mathsf{d}^2_{[\boldsymbol{x},\boldsymbol{s}]})} \;=\; \boldsymbol{x}.$$

This finally implies the relationship

$$\frac{r_s^4}{\mathsf{d}^2_{[\boldsymbol{x}',\boldsymbol{s}]}\,\mathsf{d}^2_{[\boldsymbol{x},\boldsymbol{s}]}} \;=\; 1 \qquad\Longleftrightarrow\qquad \frac{r_s}{\mathsf{d}_{[\boldsymbol{x}',\boldsymbol{s}]}} \;=\; \frac{\mathsf{d}_{[\boldsymbol{x},\boldsymbol{s}]}}{r_s} \tag{3.39}$$

that defines the inversion in a sphere with radius r_s, as expected.

As a general result[11] it may be formulated that the inversion of a point $\boldsymbol{x}$ in a sphere $\boldsymbol{S} = \boldsymbol{s} - \frac{1}{2}r_s^2\mathbf{e}$ gives a scaled inversion point $\boldsymbol{x}'$ according to

$$\boldsymbol{S}\boldsymbol{x}\boldsymbol{S} \;=\; -\,\mathsf{d}^2_{[\boldsymbol{x},\boldsymbol{s}]}\;\boldsymbol{x}'. \tag{3.40}$$

[11] The only exception represents equation (3.26), i.e. $\boldsymbol{S}\mathbf{e}\boldsymbol{S} = -2\boldsymbol{s}$, in that $\sqrt{2}$ is not the distance between $\boldsymbol{s}$ and infinity ($\mathbf{e}$). However, that the inversion of infinity yields the center $\boldsymbol{s}$ of the inversion sphere $\boldsymbol{S}$ is phenomenologically sound.

Symmetries

Previously, it was shown that $\boldsymbol{x}'$ is the inversion of $\boldsymbol{x}$ in $\boldsymbol{S}$. Now it is to be examined whether $\boldsymbol{x}'$ could likewise be the inversion of $\boldsymbol{s}$, the center of $\boldsymbol{S}$, in the sphere $\boldsymbol{S}_x$. For this purpose consider

$$\begin{aligned} r_x^2 + r_s^2 \;=\; \mathtt{d}^2_{[\boldsymbol{x},\boldsymbol{s}]} \quad &= \quad \left(\mathtt{d}_{[\boldsymbol{x},\boldsymbol{x}']} + \mathtt{d}_{[\boldsymbol{x}',\boldsymbol{s}]}\right)\mathtt{d}_{[\boldsymbol{x},\boldsymbol{s}]} \\ &\overset{(3.39)}{=} \quad \mathtt{d}_{[\boldsymbol{x},\boldsymbol{x}']}\,\mathtt{d}_{[\boldsymbol{x},\boldsymbol{s}]} + r_s^2 . \end{aligned}$$

Hence a relation equivalent to relation (3.39) holds so that the proposition $\boldsymbol{x}' \equiv \boldsymbol{S}_x \boldsymbol{s} \boldsymbol{S}_x$ must be true as well.

Comparing

$$\begin{aligned} r_x^2 + r_s^2 \;=\; \mathtt{d}^2_{[\boldsymbol{x},\boldsymbol{s}]} \quad &= \quad \left(\mathtt{d}_{[\boldsymbol{x},\boldsymbol{x}']} + \mathtt{d}_{[\boldsymbol{x}',\boldsymbol{s}]}\right)^2 \\ &= \quad \mathtt{d}^2_{[\boldsymbol{x},\boldsymbol{x}']} + 2\,\mathtt{d}_{[\boldsymbol{x},\boldsymbol{x}']}\,\mathtt{d}_{[\boldsymbol{x}',\boldsymbol{s}]} + \mathtt{d}^2_{[\boldsymbol{x}',\boldsymbol{s}]} \end{aligned}$$

and

$$\begin{aligned} r_x^2 + r_s^2 \quad &= \quad \left(\mathtt{d}^2_{[\boldsymbol{x},\boldsymbol{x}']} + r_{x'}^2\right) + \left(\mathtt{d}^2_{[\boldsymbol{x}',\boldsymbol{s}]} + r_{x'}^2\right) \\ &= \quad \mathtt{d}^2_{[\boldsymbol{x},\boldsymbol{x}']} + 2\,r_{x'}^2 + \mathtt{d}^2_{[\boldsymbol{x}',\boldsymbol{s}]} \end{aligned}$$

gives the altitude theorem – one of the Pythagorean theorems

$$\mathtt{d}_{[\boldsymbol{x},\boldsymbol{x}']}\,\mathtt{d}_{[\boldsymbol{x}',\boldsymbol{s}]} \;=\; r_{x'}^2, \tag{3.41}$$

which ultimately shows that $\boldsymbol{x}'$ coincides with the foot of the altitude. Consequently, $\boldsymbol{x}'$ is the center of circle $\boldsymbol{C}_x$, see figure 3.6.

Invariant Objects

It is as well a question of symmetry that orthogonal spheres are invariant, up to a scalar factor, under inversion. Let $\boldsymbol{S}$ and $\boldsymbol{K}$ denote two orthogonal spheres. The proposition can then be figured out as follows

$$\begin{aligned} \boldsymbol{SK} = \boldsymbol{SK} \quad &\Longleftrightarrow \quad \boldsymbol{SK} = -\boldsymbol{KS} \\ &\Longleftrightarrow \quad \boldsymbol{S}^2\boldsymbol{K} = -\boldsymbol{SKS} \quad \Longleftrightarrow \quad \boldsymbol{K} = -\frac{\boldsymbol{SKS}}{\boldsymbol{S}^2} \\ &\Longleftrightarrow \quad \boldsymbol{K} \equiv \boldsymbol{SKS}. \end{aligned}$$

A Connection to the Conjugate

A special versor is the basis vector $\mathbf{e}_-$ – the imaginary unit sphere $\mathbf{e}_- = \frac{1}{2}\mathbf{e} + \mathbf{e}_o$ centered at the origin. It can be used to algebraically perform a conjugation of blades. Recall that the conjugate negates those basis vectors of a vector that would square to minus one. Hence for some basis vector $\mathbf{e}_i \in \mathbb{R}^{4,1}$ it holds that

$$\mathbf{e}_i \neq \mathbf{e}_- \qquad \Longrightarrow \qquad \mathbf{e}_-\mathbf{e}_i\mathbf{e}_- \;=\; -\mathbf{e}_-^2\mathbf{e}_i \;=\; \mathbf{e}_i$$

If, however, $\mathbf{e}_i = \mathbf{e}_-$

$$\mathbf{e}_-\mathbf{e}_-\mathbf{e}_- \;=\; -\mathbf{e}_-,$$

so that, given a vector $\boldsymbol{a} \in \mathbb{R}^{4,1}$,

$$\boldsymbol{a}^\dagger \;=\; \mathbf{e}_-\boldsymbol{a}\mathbf{e}_-.$$

By the versor outermorphism, see section 2.3.4, it is

$$\boldsymbol{A}^\dagger_{\langle k\rangle} \;=\; \begin{cases} \mathbf{e}_-\widetilde{\boldsymbol{A}_{\langle k\rangle}}\mathbf{e}_-, & k \text{ odd} \\ -\,\mathbf{e}_-\widetilde{\boldsymbol{A}_{\langle k\rangle}}\mathbf{e}_-, & k \text{ even} \end{cases}$$

or simply

$$\boldsymbol{A}^\dagger_{\langle k\rangle} \;=\; (-1)^{\frac{(k-1)(k+2)}{2}}\; \mathbf{e}_-\,\boldsymbol{A}_{\langle k\rangle}\,\mathbf{e}_-.$$

3.3.10 Projective Points

A special point pair is the *projective conformal point*, cf. [76, 61, 64]. It is defined by

$$\boldsymbol{P}^* \;=\; \mathbf{e}\wedge\boldsymbol{p} \;=\; \mathbf{e}\wedge\vec{p} \;+\; \boldsymbol{E}. \tag{3.42}$$

In this case component $\boldsymbol{E}$ takes over the role of a homogeneous coordinate. This becomes apparent by noting that

$$\boldsymbol{P}^* \;=\; \mathbf{e}\wedge\vec{p} \;+\; \boldsymbol{E} \;=\; \mathbf{e}\wedge\,\underbrace{(\vec{p}+\mathbf{e}_-)}_{\text{projective point}}.$$

The projective point can be reobtained by using

$$\boldsymbol{P}^* \;\mapsto\; \mathbf{e}_+\cdot\boldsymbol{P}^* \;=\; \vec{p}+\mathbf{e}_-.$$

Note that more on this kind of switching between different spaces can be found in [104, 106]. There the authors extend Faugeras' *stratification hierarchy* [28], inspired by vector space calculus, to the algebras of the Euclidean, projective and conformal space. Especially the formalization of the pose estimation problem is shown in [104] to have roots throughout all *strata*, that means levels of representation.

Dehomogenization

If $\boldsymbol{P}^*$ is normalized w.r.t. the $\boldsymbol{E}$-component, its Euclidean representative $\vec{p}$ can be calculated via

$$\vec{p} \;=\; \boldsymbol{E}\cdot(\mathbf{e}_+\wedge\boldsymbol{P}^*).$$

In practical issues it is often of interest to determine the underlying conformal point $\boldsymbol{p}$ from $\boldsymbol{P}^*$. For this purpose a special operator can be created. Let

$$\boldsymbol{Q} \;:=\; \tfrac{1}{2}(1\,+\,\boldsymbol{P}^*), \qquad \text{with} \qquad \boldsymbol{Q}\,\widetilde{\boldsymbol{Q}} \;=\; 0,$$

then

$$\boldsymbol{p} \;=\; \boldsymbol{Q}\;\mathbf{e}_o\,\widetilde{\boldsymbol{Q}}.$$

Point Reflection in Projective Points

A projective point $\boldsymbol{X} = (\mathrm{e} \wedge \boldsymbol{x})\boldsymbol{I}$ can be used to describe a reflection in itself via

$$\boldsymbol{b} \;=\; \boldsymbol{X}\boldsymbol{a}\boldsymbol{X}.$$

Using relationship (3.5) and exploiting that $\mathbf{e} \wedge \boldsymbol{x} = \mathbf{e}\boldsymbol{x} + 1$, it is

$$\begin{aligned}
\boldsymbol{b} &= \boldsymbol{X}\boldsymbol{a}\boldsymbol{X} \;=\; (\mathbf{e}\boldsymbol{x} + 1)\boldsymbol{a}(\boldsymbol{x}\mathbf{e} + 1) \\
&\overset{(A.27,A.29)}{=} -4(\boldsymbol{a} \cdot \boldsymbol{x})\mathrm{e} + \mathbf{e}\boldsymbol{x}\boldsymbol{a} + \boldsymbol{a}\boldsymbol{x}\mathbf{e} + \boldsymbol{a} \\
&\overset{(A.24)}{=} -4(\boldsymbol{a} \cdot \boldsymbol{x})\mathrm{e} + 2(\boldsymbol{x} - \boldsymbol{a} + (\boldsymbol{a} \cdot \boldsymbol{x})\mathrm{e}) + \boldsymbol{a} \\
&= \boldsymbol{x} + (\boldsymbol{x} - \boldsymbol{a}) + \mathsf{d}^2_{[\boldsymbol{a},\boldsymbol{x}]}\mathbf{e}.
\end{aligned}$$

It can easily be seen that $\vec{b} = \vec{x} + (\vec{x} - \vec{a})$ and further

$$\boldsymbol{b}^2 \;=\; \boldsymbol{X}\,\underbrace{\boldsymbol{a}\overbrace{\boldsymbol{X}\boldsymbol{X}}^{-1}\boldsymbol{a}}_{0}\,\boldsymbol{X} \;=\; 0,$$

showing that $\boldsymbol{b}$ embodies a (point reflected) conformal point.

3.3.11 Circles

Circles are one of the most inspiring objects in conformal geometric algebra. A reason might be that six parameters are needed to uniquely define a circle in $\mathbb{R}^3$, which makes circles the most complex geometric objects in CGA.

Circles may most easily be constructed according to equation (3.19), that is in terms of the outer product of three points $\boldsymbol{a}$, $\boldsymbol{b}$ and $\boldsymbol{c}$ which are supposed to be on the locus of the circle

$$\boldsymbol{C} \;=\; (\boldsymbol{a} \wedge \boldsymbol{b} \wedge \boldsymbol{c})\boldsymbol{I}.$$

Even more comfortable is the possibility to create a circle by intersecting a sphere $\boldsymbol{S}$ and a plane $\boldsymbol{P}$ or two spheres $\boldsymbol{S}_1$, $\wedge\boldsymbol{S}_2$, respectively

$$\boldsymbol{C} \;=\; \boldsymbol{S}_1 \wedge \boldsymbol{S}_2 \qquad \text{or} \qquad \boldsymbol{C} \;=\; \boldsymbol{P} \wedge \boldsymbol{S}. \tag{3.43}$$

Self-evidently, for every sphere or plane incident[12] with a circle, there exist infinitely many suitable spheres, such that an intersection yields the circle again. Among them it exists a unique sphere being orthogonal to its counterpart; see section 1.1.3 in this respect.

[12] Here incidence means a 'lies on' (containment) relation. Different elements can only be incident if they are of different dimension (regarding their hypersurface), e.g. a 1d-circle and a 2d-sphere.

The Parametric Form

The aim is now to derive a sensible algebraic expression for an IPNS circle $\boldsymbol{C}$ in terms of the parameters: center $\vec{m}$, radius r and normal vector $\hat{n}$ indicating the orientation of the circle. Hence a circle has six degrees of freedom.

For this issue the orthogonal intersection of a sphere $\boldsymbol{S}_C$ and a plane $\boldsymbol{P}_C$ is considered, that is w.l.o.g. $\boldsymbol{P}_C \cdot \boldsymbol{S}_C = 0$ and consequently

$$\boldsymbol{C} \;=\; \boldsymbol{P}_C \wedge \boldsymbol{S}_C \;=\; \boldsymbol{P}_C \boldsymbol{S}_C.$$

The circle equation can, for instance, be obtained by expanding the outer product expression $\boldsymbol{P}_C \wedge \boldsymbol{S}_C$, with $\boldsymbol{P} = \hat{n} + d\,\mathbf{e}$ and $\boldsymbol{S}_C = \vec{m} + \frac{1}{2}\,(\vec{m}^2 - r^2)\,\mathbf{e} + \mathbf{e}_o$, i.e.

$$\begin{aligned}
\boldsymbol{C} &= \boldsymbol{P}_C \wedge \boldsymbol{S}_C \\
&= (\hat{n} + d\,\mathbf{e}) \wedge \big(\vec{m} + \tfrac{1}{2}\,(\vec{m}^2 - r^2)\,\mathbf{e} + \mathbf{e}_o\big) \qquad \text{where} \qquad d = \vec{m} \cdot \hat{n} \\
&= \hat{n} \wedge \vec{m} \,+\, \hat{n}\,\mathbf{e}_o \,+\, \tfrac{1}{2}\Big[(\vec{m}^2 - r^2)\hat{n} - 2\,(\vec{m} \cdot \hat{n})\vec{m}\Big]\mathbf{e} \,+\, (\vec{m} \cdot \hat{n})\boldsymbol{E}.
\end{aligned}$$

Observing that $\vec{m}^2\hat{n} - 2(\vec{m} \cdot \hat{n})\vec{m} = -\vec{m}\,\hat{n}\,\vec{m}$ it may likewise be written

$$\boldsymbol{C} \;=\; \hat{n} \wedge (\vec{m} - \tfrac{1}{2}r^2\mathbf{e} + \mathbf{e}_o) \;-\; \tfrac{1}{2}(\vec{m}\,\hat{n}\;\vec{m})\mathbf{e} \;+\; (\vec{m} \cdot \hat{n})\boldsymbol{E}.$$

Just like the previously introduced entities it is favorable to have a normalization. Evaluating the square of a circle, a 2-blade, gives

$$\begin{aligned}
\boldsymbol{C}^2 &= (\boldsymbol{P}_C\,\boldsymbol{S}_C)(\boldsymbol{P}_C\,\boldsymbol{S}_C) \;=\; -\,(\boldsymbol{S}_C\,\boldsymbol{P}_C)(\boldsymbol{P}_C\,\boldsymbol{S}_C) \\
&= -\,\boldsymbol{S}_C\,\boldsymbol{S}_C \;=\; -\,r^2.
\end{aligned}$$

It is therefore suggesting to require $\boldsymbol{C}^2 = -1$. Hence with $d = \vec{m} \cdot \hat{n} \geq 0$

$$\boldsymbol{C} \;=\; \frac{\boldsymbol{P}_C \boldsymbol{S}_C}{r} \;=\; \frac{\hat{n}\wedge\vec{m} \,+\, \hat{n}\,\mathbf{e}_o \,+\, \frac{1}{2}\Big[(\vec{m}^2 - r^2)\hat{n} - 2d\vec{m}\Big]\mathbf{e} \,+\, d\boldsymbol{E}}{r} \tag{3.44}$$

In analogy to the equation of a plane it remains to fix the sign of $\boldsymbol{C}$. Since the parameters r and d are supposed to be positive, it is reasonable to demand that the sign of the $\boldsymbol{E}$-component is positive as well. The component may algebraically be accessed by means of equation (A.34), i.e.

$$\mathbf{e}_+ \cdot (\mathbf{e} \cdot \boldsymbol{C}) \geq 0 \tag{3.45}$$

or in this case where $\boldsymbol{C}$ is a pure 2-blade

$$\boldsymbol{E} \cdot \boldsymbol{C} \geq 0$$

Evaluation of Circle Parameters

First the circle must be normalized w.r.t. condition (3.45) and such that $\boldsymbol{C}^2 = -1$. As a next step the circle plane $\boldsymbol{P}_C$ and the radius r can be determined

$$\boldsymbol{P}'_C \;=\; (\mathbf{e} \wedge \boldsymbol{C}^*)\boldsymbol{I} \;=\; \mathbf{e} \cdot \boldsymbol{C} \;=\; \mathbf{e} \cdot \frac{\boldsymbol{P}_C \wedge \boldsymbol{S}_C}{r} \;=\; \frac{\boldsymbol{P}_C}{r}, \qquad r^2 = \frac{1}{{\boldsymbol{P}'_C}^2}. \tag{3.46}$$

Having $\boldsymbol{P}_C$ at hand, the normal vector $\hat{n}$ and the distance $d = \vec{m} \cdot \hat{n}$ can be computed. Observing that

$$\boldsymbol{C}\mathbf{e}\widetilde{\boldsymbol{C}} \;=\; \frac{\boldsymbol{P}_C \boldsymbol{S}_C \mathbf{e} \boldsymbol{S}_C \boldsymbol{P}_C}{r^2} \overset{(3.26)}{=} \frac{-2\boldsymbol{P}_C \boldsymbol{m} \boldsymbol{P}_C}{r^2} \overset{(3.37)}{=} \frac{2}{r^2}\,\boldsymbol{m}, \tag{3.47}$$

shows a neat possibility to get the center $\boldsymbol{m} = \mathcal{K}(\vec{m})$ of the circle.

A new term shall be now coined: let the $\boldsymbol{C}$*-sphere* denote the unique *inscribed sphere (insphere)*, hence with minimal radius, contained within the circle $\boldsymbol{C}$.

Evaluating the $\boldsymbol{C}$-sphere

Recall that $\mathbf{e} \cdot \boldsymbol{C} = \boldsymbol{P}_C / r$. It seems that the $\boldsymbol{C}$-sphere is basically the rejection of $\mathbf{e}$ as

$$-\mathcal{R}_{\boldsymbol{C}}(\mathbf{e}) \;=\; (\mathbf{e} \cdot \boldsymbol{C})\boldsymbol{C} \;=\; \frac{\boldsymbol{P}_C(\boldsymbol{P}_C \boldsymbol{S}_C)}{r^2} \;=\; \frac{\boldsymbol{S}_C}{r^2} \;=:\; \boldsymbol{S}'_C,$$

where $-\boldsymbol{C} = \boldsymbol{C}^{-1}$ was used. With normalization it eventually follows

$$\boldsymbol{S}_C \;=\; \frac{\boldsymbol{S}'_C}{-\mathbf{e} \cdot \boldsymbol{S}'_C}.$$

Degenerate Circles - Tangency

A circle reflects the intersection between a sphere and a plane or another sphere. But many situations are thinkable in which there is no intersection at all. In addition, what does an intersection look like if one or both entities are imaginary. The answer is simple – an imaginary circle. It is not being derived here, but these entities do not square to negative values.

Interesting is also the case in which a point is used instead of a sphere, see figure 3.7. Since a point is algebraically a sphere with radius zero, an intersection between a point and a plane or rather a sphere may be declared. Particularly, a point pair can be regarded as a circle. Consequently, the entity point could have been included in the table on page 93 that summarizes all possible intersections.

If the point lies on the surface of the sphere/plane, a circle with radius zero - a null blade - is obtained:

$$(\boldsymbol{x} \wedge \boldsymbol{S})^2 \overset{(3.22)}{=} (\boldsymbol{x} \cdot \boldsymbol{S})^2 \;=\; 0$$

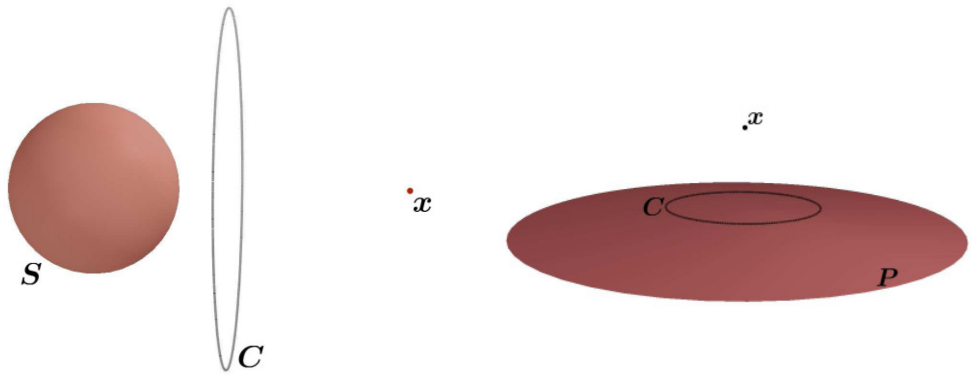

Fig. 3.7: Degenerate circles: points, here $\boldsymbol{x}$, are treated as spheres with radius zero. The outer product $\boldsymbol{C} = \boldsymbol{x} \wedge \boldsymbol{S}$, where $\boldsymbol{S}$ might be imaginary, gives the imaginary circle $\boldsymbol{C}$. The same holds if a plane $\boldsymbol{P}$ is used.

Both null spaces, eIPNS and eOPNS, coincide and consist solely of the point. This can be seen using the orthogonality[13] $\boldsymbol{x} \cdot \boldsymbol{S} = 0$

$$\boldsymbol{x}(\boldsymbol{x} \wedge \boldsymbol{S}) \;=\; \boldsymbol{x}(\boldsymbol{x}\boldsymbol{S}) \;=\; 0 \qquad \Longrightarrow \qquad \begin{cases} \boldsymbol{x} \cdot (\boldsymbol{x} \wedge \boldsymbol{S}) & = \; 0 \\ \boldsymbol{x} \wedge (\boldsymbol{x} \wedge \boldsymbol{S}) & = \; 0. \end{cases}$$

These objects can be though of as *oriented points* because in contrast to a conformal point or a projective point an additional orientation information is contained[14]. And just like conformal points they are null blades. Recalling that the intersection formally still represents a circle, the plane $\boldsymbol{P}_t$ tangent to a point $\boldsymbol{x}$ on a sphere $\boldsymbol{S}$ can be determined with the help of equation (3.46)

$$\boldsymbol{x} \cdot \boldsymbol{S} = 0 \qquad \Longrightarrow \qquad \boldsymbol{P}_t \;\equiv\; \mathbf{e} \cdot (\boldsymbol{x} \wedge \boldsymbol{S}). \tag{3.48}$$

However, in general it is not advisable to work with null blades.

Inner Product with a Point

Let $\boldsymbol{C} = (\boldsymbol{a}_1 \wedge \boldsymbol{a}_2 \wedge \boldsymbol{a}_3)\boldsymbol{I}$ be the circle passing through the points $\boldsymbol{a}_1$, $\boldsymbol{a}_2$ and $\boldsymbol{a}_3$. Then the inner product of $\boldsymbol{C}$ and a point $\boldsymbol{x}$, not on the circle, yields a plane if all four points are coplanar. Otherwise, a sphere $\boldsymbol{S}$ including the four points is obtained

$$\begin{aligned} \boldsymbol{S} \;&=\; \boldsymbol{x} \cdot \boldsymbol{C} \\ &=\; \boldsymbol{x} \cdot (\boldsymbol{C}^* \boldsymbol{I}) \\ &=\; (\boldsymbol{x} \wedge \boldsymbol{C}^*)\, \boldsymbol{I} \\ &=\; (\boldsymbol{x} \wedge \boldsymbol{a}_1 \wedge \boldsymbol{a}_2 \wedge \boldsymbol{a}_3)\, \boldsymbol{I}. \end{aligned}$$

[13] Or generally by equation (2.44, 5.), i.e. $(\boldsymbol{A}_{\langle k \rangle} \wedge \boldsymbol{b}) \cdot \boldsymbol{c} = \boldsymbol{A}_{\langle k \rangle}(\boldsymbol{b} \cdot \boldsymbol{c}) - (\boldsymbol{A}_{\langle k \rangle} \cdot \boldsymbol{c}) \wedge \boldsymbol{b}$.

[14] According to equation (3.17), the orientation information is held by the $\mathbf{e}_o$-component.

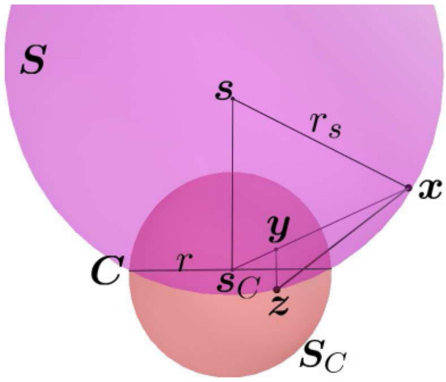

Fig. 3.8: The product $\boldsymbol{S} = \boldsymbol{x} \cdot \boldsymbol{C}$: point $\boldsymbol{x}$ lies with circle $\boldsymbol{C}$ on the common sphere $\boldsymbol{S}$. Note that $\boldsymbol{z} \equiv \boldsymbol{CxC}$ does also lie on $\boldsymbol{S}$.

Employing representation (3.44), i.e. $\boldsymbol{C} = \boldsymbol{P}_C \boldsymbol{S}_C / r$, the $\mathbf{e}_o$-component of $\boldsymbol{S}$ can be computed via

$$\begin{aligned} -\mathbf{e} \cdot (\boldsymbol{x} \cdot \boldsymbol{C}) &= -(\mathbf{e} \wedge \boldsymbol{x}) \cdot \boldsymbol{C} \;=\; \boldsymbol{x} \cdot (\mathbf{e} \cdot \boldsymbol{C}) \\ &= \boldsymbol{x} \cdot (\mathbf{e} \cdot (\boldsymbol{P}_C \wedge \boldsymbol{S}_C))/r \;=\; \boldsymbol{x} \cdot ((-\mathbf{e} \cdot \boldsymbol{S}_C)\boldsymbol{P}_C)/r \\ &= \boldsymbol{x} \cdot \boldsymbol{P}_C / r \;=\; \pm\, \mathtt{d}_{[\boldsymbol{x},\boldsymbol{P}_C]}/r \end{aligned}$$

On defining $\boldsymbol{S}_C = \boldsymbol{s}_C - \frac{1}{2}r^2\mathbf{e}$, $\boldsymbol{y} = \boldsymbol{S}_C \boldsymbol{x} \boldsymbol{S}_C / -\, \mathtt{d}^2_{[\boldsymbol{x},\boldsymbol{s}_C]}$ and $\boldsymbol{z} = -\boldsymbol{P}_C \boldsymbol{y} \boldsymbol{P}_C$, it can be seen that

$$\begin{aligned} \boldsymbol{S}^2 = (\boldsymbol{x} \cdot \boldsymbol{C})^2 \;\overset{(3.22)}{=}\; & \boldsymbol{x} \cdot \frac{\boldsymbol{CxC}}{2} \;=\; -\boldsymbol{x} \cdot \frac{\boldsymbol{P}_C \boldsymbol{S}_C \boldsymbol{x} \boldsymbol{S}_C \boldsymbol{P}_C}{2\,r^2} \\ =\; & -\boldsymbol{x} \cdot \frac{\boldsymbol{P}_C(-\,\mathtt{d}^2_{[\boldsymbol{x},\boldsymbol{s}_C]}\boldsymbol{y})\boldsymbol{P}_C}{2\,r^2} \;=\; -\frac{\mathtt{d}^2_{[\boldsymbol{x},\boldsymbol{s}_C]}}{2\,r^2}\,\boldsymbol{x} \cdot \boldsymbol{z} \\ =\; & \left(\frac{\mathtt{d}_{[\boldsymbol{x},\boldsymbol{s}_C]}\,\mathtt{d}_{[\boldsymbol{x},\boldsymbol{z}]}}{2\,r}\right)^2 \end{aligned}$$

Regarding the radius r_s of the normalized sphere $\frac{r\boldsymbol{S}}{\pm\,\mathtt{d}_{[\boldsymbol{x},\boldsymbol{P}_C]}}$ it follows

$$r_s \;=\; \sqrt{\left(\frac{r\,\boldsymbol{S}}{\mathtt{d}_{[\boldsymbol{x},\boldsymbol{P}_C]}}\right)^2} \;=\; \frac{\mathtt{d}_{[\boldsymbol{x},\boldsymbol{s}_C]}\,\mathtt{d}_{[\boldsymbol{x},\boldsymbol{z}]}}{2\,\mathtt{d}_{[\boldsymbol{x},\boldsymbol{P}_C]}}$$

The normal

There are infinitely many pairs of spheres, $\boldsymbol{S}_1$ and $\boldsymbol{S}_2$, the intersection of which results in an identical circle $\boldsymbol{C}$. Pursuant to equation (3.18), the outer product $\mathbf{e} \wedge \boldsymbol{S}_1 \wedge \boldsymbol{S}_2 = \mathbf{e} \wedge \boldsymbol{C}$ represents an OPNS line. The respective IPNS line $\boldsymbol{L}$, passing

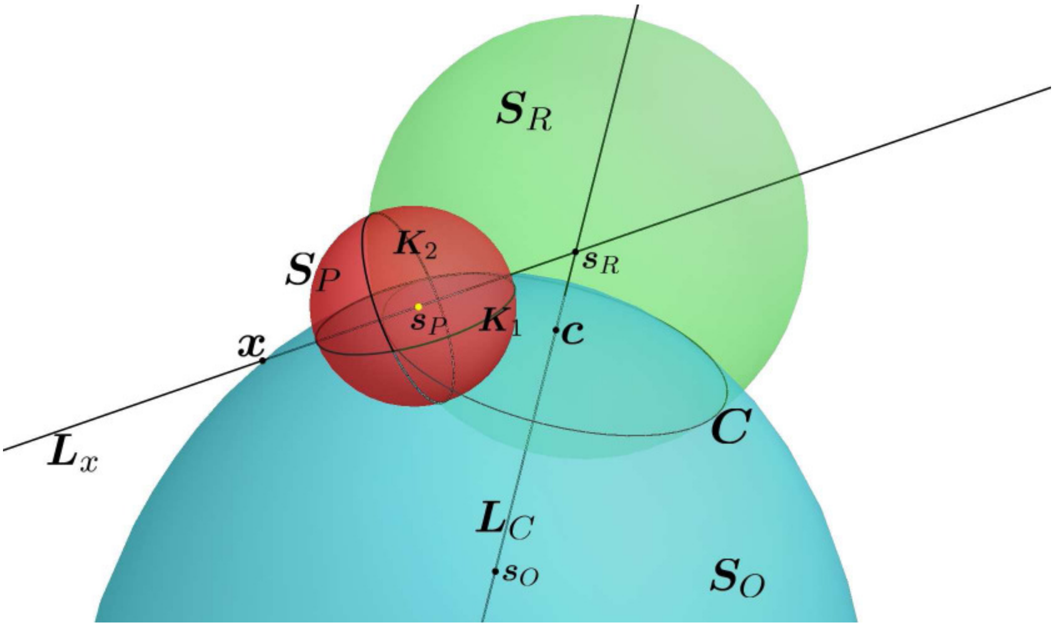

Fig. 3.9: Circles: projection S_P and rejection S_R of a point x

$$\begin{array}{lll} S_O \equiv x \cdot C & L_C \equiv \mathrm{e} \cdot C^* & L_x \equiv (\mathrm{e} \wedge x \wedge S_R) I \\ S_R \equiv (x \cdot C^{-1}) C & S_P \equiv (x \wedge C^{-1}) C & (S_P \ \text{imaginary}) \end{array}$$

through the center C, can thus be determined using

$$\begin{aligned} & L' = (\mathrm{e} \wedge C)\, I = \mathrm{e} \cdot (C\, I) = -\mathrm{e} \cdot C^* \\ \Longleftrightarrow \quad & \\ & L'^2 = -(\mathrm{e} \wedge C)^2 \overset{(3.22)}{=} -(\mathrm{e} \cdot C)^2 \overset{(3.46)}{=} -\frac{P_C^2}{r^2} = -\frac{1}{r^2} \\ \Longleftrightarrow \quad & \\ & L = \pm r(\mathrm{e} \cdot C^*) \quad \Longleftrightarrow \quad L^2 = -1. \end{aligned} \tag{3.49}$$

Regarding the choice of the sign it is referred to section 3.3.12, which deals with lines.

In this way an infinite number of circles, which may vary in their position along the line or in the radius, correspond to the same line. These degrees of freedom make the formula attractive for being used to replace lines with circles.

Figure 3.9 may serve as an example. There the perpendiculars L_C, w.r.t circle C, and L_x, respectively are depicted. The latter line belongs to circle K_2.

Projection

Figure 3.9 summarizes several products, among others, the projection S_P and the rejection S_R of a point x with respect to a circle C. The center s_P of the imaginary sphere S_P lies on the plane of the circle, i.e. P_C. Note that line L_x does, in general, not intersect with $\boldsymbol{C}$. Clearly, since projection and rejection are orthogonal, one has $\boldsymbol{S}_P \cdot \boldsymbol{S}_R = 0$. Moreover, it holds that $\boldsymbol{C} = \boldsymbol{S}_O \boldsymbol{S}_R$ because of the orthogonality of the spheres:

$$\boldsymbol{S}_O \cdot \boldsymbol{S}_R \;=\; -\boldsymbol{S}_O \cdot (\boldsymbol{S}_O \boldsymbol{C}) \;=\; -\boldsymbol{S}_O \cdot (\boldsymbol{S}_O \cdot \boldsymbol{C}) \;=\; -(\boldsymbol{S}_O \wedge \boldsymbol{S}_O) \cdot \boldsymbol{C} \;=\; 0$$

It must also be mentioned that the depicted intersection circles $\boldsymbol{K}_1$ and $\boldsymbol{K}_2$ were built using the real version of $\boldsymbol{S}_P$, cf. equation (3.27), that means

$$\boldsymbol{K}_1 \;\equiv\; \boldsymbol{S}_O \wedge (\boldsymbol{S}_P + \boldsymbol{S}_P^2 \mathbf{e}) \qquad \text{and} \qquad \boldsymbol{K}_2 \;\equiv\; \boldsymbol{S}_R \wedge (\boldsymbol{S}_P + \boldsymbol{S}_P^2 \mathbf{e}).$$

3.3.12 Lines

In the OPNS equation (3.18) can be used to describe a line

$$\begin{aligned} \boldsymbol{L}^* \;&=\; \mathbf{e} \wedge \boldsymbol{a} \wedge \boldsymbol{b} \;=\; \mathbf{e} \wedge \underbrace{\vec{a} \wedge \vec{b}}_{\vec{p} \wedge \vec{r}} \;+\; \underbrace{(\vec{b} - \vec{a})}_{\vec{r} = l\,\hat{r}}\, \boldsymbol{E} & l \in \mathbb{R} \\ &=\; l(\mathbf{e} \wedge \vec{p} \wedge \hat{r} \;+\; \hat{r}\, \boldsymbol{E}), & \vec{p} \perp_{\boldsymbol{\varepsilon}} \vec{r} \end{aligned}$$

where $\vec{p}$ and $\hat{r}$ denote the foot (of the perpendicular passing through the origin $\mathbf{e}_o$) and the unit direction vector, respectively, of $\boldsymbol{L}$. Figure 3.10 gives a visualization. The equality of $\vec{a} \wedge \vec{b} = \vec{p} \wedge (\vec{p} + \vec{r}) = \vec{p} \wedge \vec{r}$ was already shown in equation (2.15) on page 24.

On defining

$$\widehat{U} \;=\; \hat{r}\, \boldsymbol{I}_E, \tag{3.50}$$

a 2-blade in $\langle \mathbb{R}_3 \rangle_2 \subset \mathbb{R}_{4,1}$ that contains $\vec{p}$, the IPNS representation becomes

$$\begin{aligned} (\underbrace{\mathbf{e} \wedge \vec{p} \wedge \hat{r}}_{\vec{p}\,\hat{r}\,\mathbf{e}})\boldsymbol{I} + \hat{r}\, \boldsymbol{E}\boldsymbol{I} \quad &\overset{(A.19, A.20)}{=} \quad (\mathbf{e} \wedge \vec{p} \wedge \hat{r} + \hat{r})\boldsymbol{I}_E \\ &= \quad \mathbf{e}\,(\vec{p} \cdot \widehat{U}) + \widehat{U} \end{aligned}$$

so that

$$\boldsymbol{L}^2 \;=\; \underbrace{(\mathbf{e}(\vec{p} \cdot \widehat{U})) \cdot \widehat{U}}_{0} + \underbrace{\widehat{U}^2}_{(\hat{r}\boldsymbol{I}_E)^2 = -\hat{r}^2} + \underbrace{\widehat{U} \cdot (\mathbf{e}(\vec{p} \cdot \widehat{U}))}_{0} + \underbrace{(\mathbf{e}(\vec{p} \cdot \widehat{U}))^2}_{0} \;=\; -1.$$

With the help of equation (A.32), the *unit binormal vector* $\hat{b}$ can be introduced in terms of the vector cross product

$$\hat{b} \;=\; \frac{1}{d}\,\vec{p} \cdot \widehat{U} \;=\; \frac{1}{d}\,\hat{r} \times \vec{p}, \qquad \text{where} \;\; d \;:=\; \|\vec{p}\|.$$

The final representation of a line regarding the IPNS is thus

$$\boldsymbol{L} \quad = \quad \widehat{U} \;-\; (\vec{p} \cdot \widehat{U})\,\mathbf{e} \quad = \quad \widehat{U} \;-\; d\,\hat{b}\,\mathbf{e} \tag{3.51}$$

with $\widehat{U} = \hat{r}\boldsymbol{I}_E$ and where $d = \|\vec{p}\| \in \mathbb{R}$ denotes $\boldsymbol{L}$'s distance from the origin $\mathbf{e}_o$.

Aside: *Note that the signs of lines, planes passing through the origin and circles centered at the origin, respectively, cannot be fixed because the origin* $\mathbf{e}_o$*, as the only reference point, is not sufficient for uniquely attributing an orientation, i.e. sign, in a coordinate-free manner to the entities.*

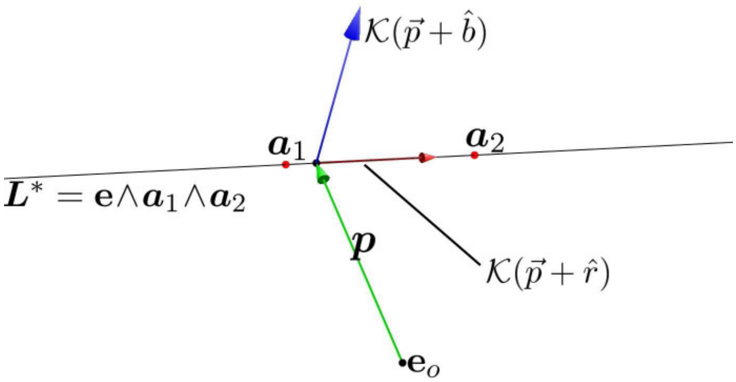

Fig. 3.10: Line $\boldsymbol{L}$ passing through the points $\boldsymbol{a}_1$ and $\boldsymbol{a}_2$: the mutually orthogonal vectors $\hat{r}$, $\vec{p}$ and $\hat{b}$ form a right-handed system, $\hat{b} = \hat{r} \times \vec{p}/d$.

Construction by Intersection

The intersection of two planes gives a line. Let $\boldsymbol{P}_1 = \hat{n}_1 + d_1\,\mathbf{e}$ and $\boldsymbol{P}_2 = \hat{n}_2 + d_2\,\mathbf{e}$ denote two non-parallel planes.

$$\begin{aligned}\boldsymbol{L} &\equiv (\hat{n}_1 + d_1\,\mathbf{e}) \wedge (\hat{n}_2 + d_2\,\mathbf{e}) \\ &= \hat{n}_1 \wedge \hat{n}_2 + \underbrace{(d_2\,\hat{n}_1 - d_1\,\hat{n}_2)\,\mathbf{e}}_{-(\boldsymbol{p}\cdot(\hat{n}_1\wedge\hat{n}_2))\,\mathbf{e}}, \qquad \vec{U} := \hat{n}_1 \wedge \hat{n}_2, \\ &= \vec{U} - \left(\vec{p}\cdot\vec{U}\right)\mathbf{e}.\end{aligned}$$

Since $\boldsymbol{p}$ lies on each of the planes at the same time, it has a positive inner product with both normal vectors, that is $\boldsymbol{p}\cdot\hat{n}_i \geq 0$, $i \in \{1,2\}$. Correspondingly, it is $\mathtt{d}_{[\boldsymbol{P}_i,\,\mathbf{e}_o]} = d_i = \boldsymbol{p}\cdot\hat{n}_i$.

The normalized line can be computed by[15]

$$\boldsymbol{L} = \widehat{U} - \left(\vec{p}\cdot\widehat{U}\right)\mathbf{e} = \frac{\boldsymbol{P}_1 \wedge \boldsymbol{P}_2}{\sqrt{-(\boldsymbol{P}_1 \wedge \boldsymbol{P}_2)^2}} \qquad \text{with} \qquad \widehat{U} = \frac{\hat{n}_1 \wedge \hat{n}_2}{\|\hat{n}_1 \wedge \hat{n}_2\|}.$$

Especially if the planes are orthogonal, it may effortlessly be verified that $\boldsymbol{L}^2 = -1$

$$\boldsymbol{P}_1 \cdot \boldsymbol{P}_2 = 0 \quad \Longleftrightarrow \quad \boldsymbol{L} = \boldsymbol{P}_1\boldsymbol{P}_2 \quad \Longleftrightarrow \quad \boldsymbol{L}^2 = \boldsymbol{P}_1\,\underbrace{\boldsymbol{P}_2\boldsymbol{P}_1}_{-\boldsymbol{P}_1\boldsymbol{P}_2}\,\boldsymbol{P}_2 = -1.$$

An alternative way to create a line is proposed in equation (3.49); circles are utilized as representatives of lines because the line perpendicularly passing through the center of a circle $\boldsymbol{C}$ is unique. It can be obtained by evaluating $\boldsymbol{L} \equiv \mathbf{e}\cdot\boldsymbol{C}^*$.

[15] Recall that $\sqrt{-(\boldsymbol{P}_1 \wedge \boldsymbol{P}_2)^2} \neq \|\boldsymbol{P}_1 \wedge \boldsymbol{P}_2\| = \sqrt{(\boldsymbol{P}_1 \wedge \boldsymbol{P}_2)^\dagger \cdot (\boldsymbol{P}_1 \wedge \boldsymbol{P}_2)}$ (magnitude, see page 61).

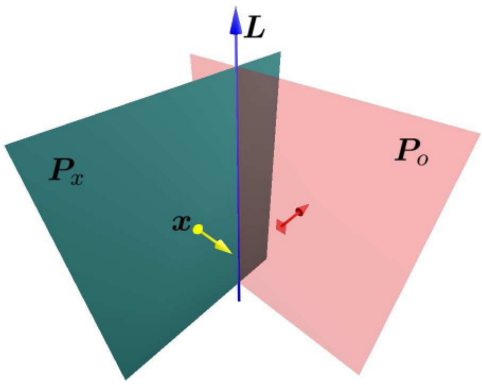

Fig. 3.11: Representation of a line w.r.t. a point $\boldsymbol{x}$: the geometric product of the orthogonal planes gives the line $\boldsymbol{L} = \boldsymbol{P}_x\boldsymbol{P}_o$ (arrows indicate orientations). The orientations of the planes may also by flipped, i.e. $\boldsymbol{L} = (-\boldsymbol{P}_x)(-\boldsymbol{P}_o)$.

Point Dependent Representation

Let $\boldsymbol{x}$ be a point not on the line given by $\boldsymbol{L}$. Then exists a plane, denoted by $\boldsymbol{P}_x$, that is incident with both, line $\boldsymbol{L}$ and point $\boldsymbol{x}$. It further exists a plane, say $\boldsymbol{P}_o$, orthogonal to that 'parallel' plane being incident with $\boldsymbol{L}$ as well. Thus the line can be written as $\boldsymbol{L} = \boldsymbol{P}_x \wedge \boldsymbol{P}_o = \boldsymbol{P}_x\boldsymbol{P}_o$. One scenario is pictured in figure 3.11. Note that the orientations of $\boldsymbol{P}_x$, $\boldsymbol{P}_o$ and $\boldsymbol{L}$ must form a right-handed system.

By the principle expressed in equation (3.2) the inner product of a point $\boldsymbol{x}$ with a line $\boldsymbol{L} \equiv (\mathbf{e}\wedge\boldsymbol{a}\wedge\boldsymbol{b})\boldsymbol{I}$ yields the plane spanned by the points $\boldsymbol{x}$, $\boldsymbol{a}$ and $\boldsymbol{b}$. Specifically, it is

$$\boldsymbol{x} \cdot ((\mathbf{e} \wedge \boldsymbol{a} \wedge \boldsymbol{b})\boldsymbol{I}) \;=\; (\boldsymbol{x} \wedge \mathbf{e} \wedge \boldsymbol{a} \wedge \boldsymbol{b})\boldsymbol{I} \;=\; (\mathbf{e} \wedge \boldsymbol{a} \wedge \boldsymbol{x} \wedge \boldsymbol{b})\boldsymbol{I} \;\overset{(3.20)}{\equiv}\; \boldsymbol{P}_x$$

According to equation (3.30), the orientation of $\boldsymbol{P}_x$ is given by $(\vec{b} - \vec{a}) \times (\vec{x} - \vec{a})$, where $\vec{r} = \vec{b} - \vec{a}$ denotes the direction vector of $\boldsymbol{L}$. For an example see figure 3.11.

Evaluation of Line Parameters

If a line was created by means of the OPNS formula, hence $\boldsymbol{L}^* = \mathbf{e} \wedge \boldsymbol{a} \wedge \boldsymbol{b}$, the distance $l \in \mathbb{R}$ between the points $\boldsymbol{a}$ and $\boldsymbol{b}$ can be computed via

$$l \;=\; \sqrt{\boldsymbol{L}^{*2}} \qquad \text{or equally} \qquad l \;=\; \sqrt{-\boldsymbol{L}^2}. \tag{3.52}$$

The unit normal vector $\hat{r}$ simply arises from

$$\hat{r} \;=\; -\boldsymbol{L} \cdot \boldsymbol{I}_E.$$

Since $\boldsymbol{P}_r := \hat{r}$ defines a plane, the foot $\boldsymbol{p}$ of $\boldsymbol{L}$ with respect to $\mathbf{e}_o$ can be determined by the intersection $\boldsymbol{X}_p \equiv \boldsymbol{P}_r \wedge \boldsymbol{L}$. As $\boldsymbol{X}_p$ represents a projective point, the methods described in section 3.3.10 can be used to retrieve the corresponding conformal

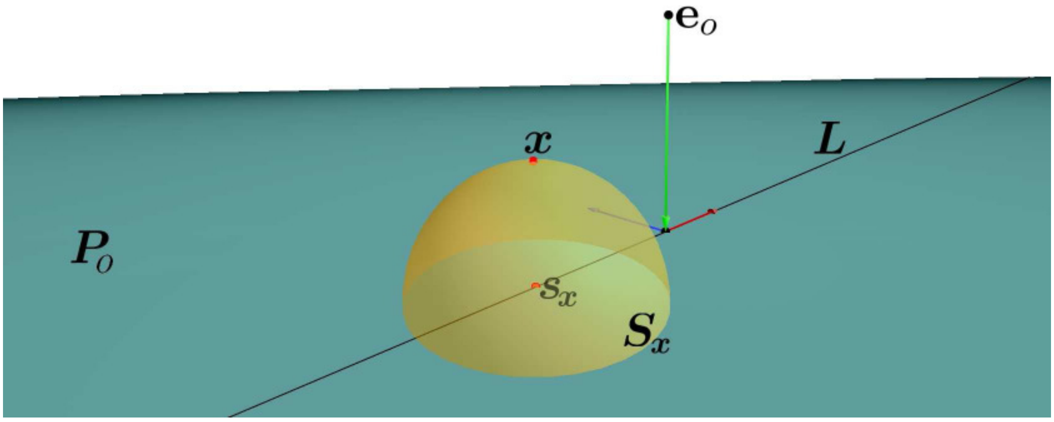

Fig. 3.12: Projection onto a line: the result is the imaginary sphere $\boldsymbol{S}_x$ with center $\boldsymbol{s}_x$ on the line $\boldsymbol{L}$. Rejection $\boldsymbol{P}_o$ is solely coincidentally aligned with the plane spanned by the direction vector and the binormal vector of $\boldsymbol{L}$.

point $\boldsymbol{p}$ from $\boldsymbol{X}_p^* = \mathbf{e} \wedge \boldsymbol{p}$.
However, $\boldsymbol{p}$ may most easily be obtained by the projection of $\mathbf{e}_o$ onto $\boldsymbol{L}$, see below.

The distance $d = \|\vec{p}\|$ from the origin can be computed according to equation (3.55), i.e.

$$d \;=\; \sqrt{(\mathbf{e}_o \cdot \boldsymbol{L})^2} \qquad \text{or} \qquad d \;=\; \sqrt{(\mathbf{e}_o \wedge \boldsymbol{L})^2}$$

Is the distance available, the binormal vector $\hat{b}$ is

$$\hat{b} \;=\; -\,\mathbf{e}_o \cdot \boldsymbol{L}/d.$$

Projection

It is begun with calculating the rejection, where w.l.o.g. the representation of $\boldsymbol{L}$ as depicted in figure 3.11 is used, i.e. $\boldsymbol{L} = \boldsymbol{P}_x\boldsymbol{P}_o$. Note that the direction vector of $\boldsymbol{P}_o$ points away from $\boldsymbol{x}$ such that $\boldsymbol{x} \cdot \boldsymbol{P}_o = -\,\mathtt{d}_{[\boldsymbol{x},\boldsymbol{P}_o]}$. Building the inner product reveals that

$$\boldsymbol{x} \cdot \boldsymbol{L} \;=\; \boldsymbol{x} \cdot (\boldsymbol{P}_x \wedge \boldsymbol{P}_o) \;=\; (\boldsymbol{x} \cdot \boldsymbol{P}_x)\boldsymbol{P}_o - (\boldsymbol{x} \cdot \boldsymbol{P}_o)\boldsymbol{P}_x \;\stackrel{(3.32)}{=}\; \mathtt{d}_{[\boldsymbol{x},\boldsymbol{P}_o]}\boldsymbol{P}_x \tag{3.53}$$

By the chosen configuration of the planes it must be inferred that $\mathtt{d}_{[\boldsymbol{x},\boldsymbol{P}_o]} = \mathtt{d}_{[\boldsymbol{x},\boldsymbol{L}]}$. Due to $\boldsymbol{L}^{-1} = -\boldsymbol{L}$, the rejection is

$$\begin{aligned}\mathcal{R}_{\boldsymbol{L}}(\boldsymbol{x}) \;=\; (\boldsymbol{x} \cdot \boldsymbol{L}^{-1})\boldsymbol{L} \;&\stackrel{\text{cor. 2.14}}{=}\; -\,\mathtt{d}_{[\boldsymbol{x},\boldsymbol{L}]}\boldsymbol{P}_x \cdot \boldsymbol{L} \;=\; -\,\mathtt{d}_{[\boldsymbol{x},\boldsymbol{L}]}\boldsymbol{P}_x \cdot (\boldsymbol{P}_x \wedge \boldsymbol{P}_o)\\ &=\; -\,\mathtt{d}_{[\boldsymbol{x},\boldsymbol{L}]}\boldsymbol{P}_o\end{aligned} \tag{3.54}$$

Now the projection $\mathcal{P}_{\boldsymbol{L}}(\boldsymbol{x}) = \boldsymbol{x} - \mathcal{R}_{\boldsymbol{L}}(\boldsymbol{x}) = \boldsymbol{x} + \mathtt{d}_{[\boldsymbol{x},\boldsymbol{L}]}\boldsymbol{P}_o$ is being tackled. First of all, adding/subtracting a plane from a point gives a sphere as the $\mathbf{e}_o$-component is left unchanged (one). Let $\boldsymbol{S}_x = \mathcal{P}_{\boldsymbol{L}}(\boldsymbol{x}) = \boldsymbol{s}_x - \frac{1}{2}r_s^2\mathbf{e}$. The center $\boldsymbol{s}_x$ of the sphere is determined by the displacement of the scaled unit normal vector of $\boldsymbol{P}_o$. It may be figured out that value of the factor $\mathtt{d}_{[\boldsymbol{x},\boldsymbol{L}]}$ in $\mathcal{R}_{\boldsymbol{L}}(\boldsymbol{x})$ guarantees that $\boldsymbol{s}_x$ comes to lie on $\boldsymbol{L}$. Hence the first result is that the projection embodies a sphere orthogonal to $\boldsymbol{L}$, $\boldsymbol{P}_x$ and $\boldsymbol{P}_o$. The analytical derivation of the radius by means of geometric considerations is quite thorny. Instead the radius is being evaluated by squaring the projection, which is known to be a sphere.

$$\begin{aligned}
(\mathcal{P}_{\boldsymbol{L}}(\boldsymbol{x}))^2 &= (-(\boldsymbol{x}\wedge\boldsymbol{L})\boldsymbol{L})^2 \;=\; (\boldsymbol{x}\wedge\boldsymbol{L})\boldsymbol{L}(\boldsymbol{x}\wedge\boldsymbol{L})\boldsymbol{L} \\
&\overset{\text{cor. 2.5}}{=} (-1)^{2\cdot 3-2}\,(\boldsymbol{x}\wedge\boldsymbol{L})\boldsymbol{L}^2(\boldsymbol{x}\wedge\boldsymbol{L}) \\
&= -(\boldsymbol{x}\wedge\boldsymbol{L})^2 \\
&\overset{(3.22)}{=} -(\boldsymbol{x}\cdot\boldsymbol{L})^2 \\
&\overset{\text{above}}{=} -(\,\mathtt{d}_{[\boldsymbol{x},\boldsymbol{L}]}\boldsymbol{P}_x)^2 \\
&= -\,\mathtt{d}^2_{[\boldsymbol{x},\boldsymbol{L}]},
\end{aligned}$$

where corollary 2.14 was additionally used. Thus the projection of a point onto a line is an imaginary sphere with radius equal to the distance between point and line. The center $\boldsymbol{s}_x$ of the sphere coincides with that point which corresponds to the Euclidean projection of $\boldsymbol{x}$ onto $\boldsymbol{L}$, see figure 3.12.

Distance Point - Line

Along the above lines the distance between a point and a line can be computed as

$$\mathtt{d}_{[\boldsymbol{x},\boldsymbol{L}]} \;=\; \sqrt{(\boldsymbol{x}\cdot\boldsymbol{L})^2} \;=\; \sqrt{(\boldsymbol{x}\wedge\boldsymbol{L})^2} \tag{3.55}$$

Outer Product with a Point

Clearly, a line has the representation in terms of two planes, i.e. $\boldsymbol{L} = \boldsymbol{P}_1\wedge\boldsymbol{P}_2$. The OPNS product $\boldsymbol{x}\wedge\boldsymbol{L}$ must therefore be a curve orthogonally passing through $\boldsymbol{x}$ and the planes. The red circle $\boldsymbol{C}_x = (\boldsymbol{x}\wedge\boldsymbol{L})\boldsymbol{I}$, see the figure to the right, meets these requirements. Similarly to equation (3.49) it is

$$\boldsymbol{C}_x \;=\; (\boldsymbol{x}\wedge\boldsymbol{L})\boldsymbol{I} \;=\; -\boldsymbol{x}\cdot\boldsymbol{L}^*.$$

Note that $\boldsymbol{S}_x$ represents the projection of $\boldsymbol{x}$ onto $\boldsymbol{L}$, compare figure 3.12.

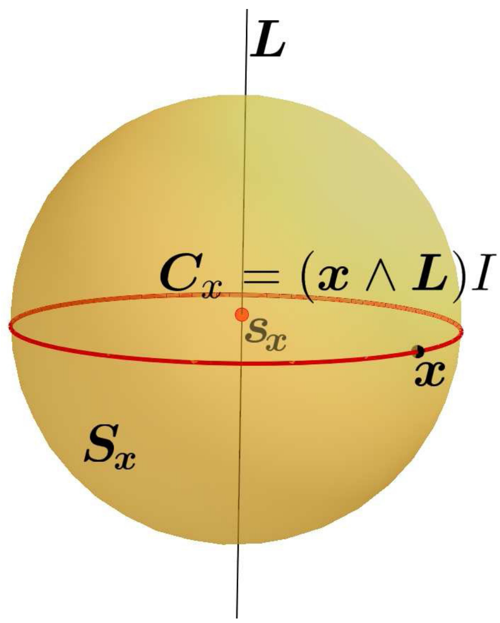

Fig. 3.13: The product $(\boldsymbol{x}\wedge\boldsymbol{L})\boldsymbol{I}$.

Example: Intersection with a Sphere

In the scope of omnidirectional vision it is often a necessity to project a point onto a sphere. Intersecting the corresponding projection ray with the sphere yields a point pair. Now it is being deduced how the correct point – the closer point – can be determined algebraically, cf. [80].

For this purpose, let $\boldsymbol{S} = \boldsymbol{s} - \frac{1}{2}r^2\mathbf{e}$ denote the sphere onto which the point $\boldsymbol{x}$ is to be projected. The respective projection ray is given by the line $\boldsymbol{L} = (\mathbf{e} \wedge \boldsymbol{S} \wedge \boldsymbol{x})\boldsymbol{I}$, with $\boldsymbol{L}^2 = -l^2 = -\,\mathtt{d}^2_{[\boldsymbol{s},\boldsymbol{x}]}$, see equation (3.52). The point pair, a 3-blade in the IPNS, is then

$$\boldsymbol{C} \;=\; \boldsymbol{S} \wedge \boldsymbol{L}.$$

Now it is used that a point pair can similarly be expressed as a degenerate circle, i.e. by the outer product of a plane $\boldsymbol{P}$ and a point $\boldsymbol{q}$. According to equation (3.38) it is

$$\boldsymbol{C}^* \;\equiv\; \boldsymbol{P} \wedge \boldsymbol{q},$$

where $\boldsymbol{q}$ is meant to be the sought projection of $\boldsymbol{x}$ on $\boldsymbol{S}$. Besides, $\boldsymbol{P}$, with $\boldsymbol{P}^2 = 1$, has to be a plane passing through the center $\boldsymbol{s}$ of $\boldsymbol{S}$. Comparing

$$(\boldsymbol{C}^*)^2 \;=\; -\boldsymbol{C}^2 \;\overset{\boldsymbol{S}\cdot\boldsymbol{L}=0}{=}\; -(\boldsymbol{S}\boldsymbol{L})^2 \;\overset{\boldsymbol{S}\times\boldsymbol{L}=0}{=}\; -\boldsymbol{S}^2\boldsymbol{L}^2 \;=\; r^2\,\mathtt{d}^2_{[\boldsymbol{s},\boldsymbol{x}]}$$

and

$$(\boldsymbol{P} \wedge \boldsymbol{q})^2 \;\overset{(3.22)}{=}\; (\boldsymbol{P}\cdot\boldsymbol{q})^2 \;=\; r^2$$

it can be inferred that[16]

$$\boldsymbol{C}^* \;=\; \mathtt{d}_{[\boldsymbol{s},\boldsymbol{x}]}\,\boldsymbol{P} \wedge \boldsymbol{q}.$$

Now $\boldsymbol{q}$ can be retrieved from $\boldsymbol{C}^*$ using the invertibility of the geometric product

$$\begin{aligned} \mathtt{d}_{[\boldsymbol{s},\boldsymbol{x}]}\,\boldsymbol{P}\boldsymbol{q} \;&=\; \boldsymbol{C}^* + \mathtt{d}_{[\boldsymbol{s},\boldsymbol{x}]}\,\boldsymbol{P}\cdot\boldsymbol{q} \\ &=\; \boldsymbol{C}^* + r\,\mathtt{d}_{[\boldsymbol{s},\boldsymbol{x}]} \;=\; \boldsymbol{C}^* + \sqrt{(\boldsymbol{C}^*)^2}. \end{aligned}$$

Observing that $\mathbf{e}\cdot\boldsymbol{P} = 0$ and thus $\mathbf{e}\cdot\boldsymbol{C}^* = \mathtt{d}_{[\boldsymbol{s},\boldsymbol{x}]}\boldsymbol{P}$, it follows

$$\boldsymbol{q} \;=\; (\mathbf{e}\cdot\boldsymbol{C}^*)^{-1}\Big(\boldsymbol{C}^* + \sqrt{(\boldsymbol{C}^*)^2}\Big).$$

Correspondingly, the oppositely located point $\boldsymbol{q}'$ on $\boldsymbol{S}$ is given by

$$\boldsymbol{q}' \;=\; (\mathbf{e}\cdot\boldsymbol{C}^*)^{-1}\Big(\boldsymbol{C}^* - \sqrt{(\boldsymbol{C}^*)^2}\Big)$$

such that

$$\boldsymbol{C}^* \;\equiv\; \boldsymbol{q} \wedge \boldsymbol{q}'.$$

[16] A closer look substantiates that no minus sign must be introduced.

Fig. 3.14: Translator $\boldsymbol{T} = \boldsymbol{P}_2\boldsymbol{P}_1$.

3.4 The Operators of CGA

First and foremost it is to be mentioned that the main operation of CGA, which is the reflection in a vector (a sphere or a plane), is the subject of section 3.3.8 and section 3.3.9. The operators to be dealt with here are compositions of reflections and are correspondingly represented by higher versors, see page 67. Bear in mind that a versor is not necessarily a blade. It is begun with the *translator*, a versor that expresses a translation in space. Self-evidently, a translation does not add a five-dimensional offset to a conformal point; instead all operators do only act on the represented (underlying) Euclidean points, which is inherited from the reflection.

While the reflection is the basic transformation of the *Euclidean group*, the basic transformation of the *conformal group* is the inversion. As the reflection can be considered an inversion in a sphere with infinite radius, the Euclidean group, consisting of *isometries*[17], is a subgroup of the conformal group, which additionally comprises the locally angle preserving transformations.

3.4.1 Translator

Consider two parallel and identically orientated planes $\boldsymbol{P}_1 = \hat{n} + d_1\mathbf{e}$ and $\boldsymbol{P}_2 = \hat{n} + d_2\mathbf{e}$, where $d_2 > d_1$. Let, at first, $\boldsymbol{x}$ be a point such that the reflection $\boldsymbol{x}' = -\boldsymbol{P}_1\boldsymbol{x}\boldsymbol{P}_1$ lies between the planes $\boldsymbol{P}_1$ and $\boldsymbol{P}_2$, respectively. Reflecting $\boldsymbol{x}'$ in $\boldsymbol{P}_2$ gives point $\boldsymbol{x}'' = -\boldsymbol{P}_2\boldsymbol{x}'\boldsymbol{P}_2$ with the result, shown in figure 3.14, that the planes lie between the points $\boldsymbol{x}$ and $\boldsymbol{x}''$.

Since the distance between $\boldsymbol{x}$ and $\boldsymbol{x}''$ is $2(\,\mathtt{d}_{[\boldsymbol{x},\boldsymbol{P}_1]} + \,\mathtt{d}_{[\boldsymbol{x}',\boldsymbol{P}_2]})$ and noting that the distance between the planes is $d_2 - d_1 = \mathtt{d}_{[\boldsymbol{x},\boldsymbol{P}_1]} + \mathtt{d}_{[\boldsymbol{x}',\boldsymbol{P}_2]}$, it is intuitively clear that the (unitary) versor $\boldsymbol{T} = \boldsymbol{P}_2\boldsymbol{P}_1$ describes a translation of length two times the distance between the planes along $\hat{n}$. On defining $\vec{t} = 2(d_2 - d_1)\hat{n}$ the representation of a translator becomes

$$\begin{aligned}\boldsymbol{T} \;=\; \boldsymbol{P}_2\boldsymbol{P}_1 &= (\hat{n} + d_1\mathbf{e})(\hat{n} + d_2\mathbf{e}) \\ &= 1 + (d_2 - d_1)\mathbf{e}\hat{n} \\ &= 1 - \tfrac{1}{2}\,\vec{t}\,\mathbf{e}.\end{aligned}$$

Hence $\boldsymbol{T}$ displaces objects by the offset $\vec{t}$.

To shown that this is also true for cases deviating from the above scenario the impact of $\boldsymbol{T}$ upon an arbitrarily located point/sphere $\boldsymbol{x} = \vec{x} + \frac{1}{2}(\vec{x}^2 - r_x^2)\mathbf{e} + \mathbf{e}_o$ is

[17] Rigid body motions (RBM) that preserve angles and distances

analyzed

$$\begin{aligned}\boldsymbol{y} \;=\; \boldsymbol{T}\,\boldsymbol{x}\,\widetilde{\boldsymbol{T}} \quad &= \quad \boldsymbol{x} + (\vec{t}\cdot\vec{x})\mathbf{e} + \tfrac{1}{2}\vec{t}^{\,2}\,\mathbf{e} + \vec{t} \\ &= \quad (\vec{x}+\vec{t}) + \tfrac{1}{2}\,\left((\vec{x}+\vec{t})^2 - r_x^2\right)\mathbf{e} + \mathbf{e}_o \\ &\overset{\vec{y}:=\vec{x}+\vec{t}}{=} \quad \vec{y} + \tfrac{1}{2}\,(\vec{y}^{\,2} - r_x^2)\,\mathbf{e} + \mathbf{e}_o.\end{aligned}$$

It can be seen that $\vec{x}$ is offset by $\vec{t}$ and that the $\mathbf{e}$-component is maintained as well.

Commutation of Translators

Given two translators their order of execution should, logically, be arbitrary. This may be proven algebraically. Let $\boldsymbol{T}_u = 1 - \frac{1}{2}\vec{u}\,\mathbf{e}$ and $\boldsymbol{T}_v = 1 - \frac{1}{2}\vec{v}\,\mathbf{e}$, respectively, be the translators. Hence

$$\boldsymbol{T}_u\boldsymbol{T}_v \;=\; 1 - \tfrac{1}{2}\vec{u}\,\mathbf{e} - \tfrac{1}{2}\vec{v}\,\mathbf{e} + \frac{1}{4}\,\underbrace{\vec{u}\,\mathbf{e}\,\vec{v}\,\mathbf{e}}_{-\vec{u}\vec{v}\,\mathbf{e}^2=0} \;=\; 1 - \tfrac{1}{2}\vec{v}\,\mathbf{e} - \tfrac{1}{2}\vec{u}\,\mathbf{e} + \frac{1}{4}\,\underbrace{\vec{v}\,\mathbf{e}\,\vec{u}\,\mathbf{e}}_{0} \;=\; \boldsymbol{T}_v\boldsymbol{T}_u.$$

Exponential Representation

Using the Taylor series expansion of the exponential function it can be seen that

$$\exp(-\tfrac{1}{2}\vec{t}\,\mathbf{e}) \;=\; \sum_{k=0}^{\infty}\frac{(-\frac{1}{2}\vec{t}\,\mathbf{e})^k}{k!} \;=\; 1 - \tfrac{1}{2}\vec{t}\,\mathbf{e}$$

because all terms with $k > 1$ take the value zero

$$(-\tfrac{1}{2}\vec{t}\,\mathbf{e})^2 \;=\; \frac{1}{4}\,\vec{t}\,\mathbf{e}\vec{t}\,\mathbf{e} \;=\; -\frac{1}{4}\,\vec{t}^{\,2}\,\mathbf{e}^2 \;=\; 0.$$

3.4.2 Dilator

A very related and often useful operator is the dilator. Due to its rather little significance for this thesis, it is not being treated in full detail.

A dilator can be described by two concentric spheres, for example

$$\boldsymbol{D} \equiv \boldsymbol{S}_2\boldsymbol{S}_1,$$

which shows the similarity to a translator. In this respect, a dilator performs two consecutive reflections in the spheres, which results in an isotropic ‘translation’ with respect to the center $\boldsymbol{m}$ of the spheres. Specifically, dilating a point means scaling that point by a constant factor $D \in \mathbb{R}$ with respect to $\boldsymbol{m}$.

Assume at first that the spheres are centered at the origin, i.e. $\boldsymbol{m} = \mathbf{e}_o$. Let the radii of the spheres $\boldsymbol{S}_1$ and $\boldsymbol{S}_2$ be denoted by r_{S_1} and r_{S_2}, respectively. From equation (3.39) it can be seen that

$$\mathtt{d}_{[\boldsymbol{x}',\,\mathbf{e}_o]} \;=\; \frac{r_{S_1}^2}{\mathtt{d}_{[\boldsymbol{x},\,\mathbf{e}_o]}} \quad\text{and}\quad \mathtt{d}_{[\boldsymbol{x}'',\,\mathbf{e}_o]} \;=\; \frac{r_{S_2}^2}{\mathtt{d}_{[\boldsymbol{x}',\,\mathbf{e}_o]}} \quad\Longrightarrow\quad \mathtt{d}_{[\boldsymbol{x}'',\,\mathbf{e}_o]} \;=\; \frac{r_{S_2}^2}{r_{S_2}^2}\,\mathtt{d}_{[\boldsymbol{x},\,\mathbf{e}_o]},$$

where $\boldsymbol{x}' \equiv \boldsymbol{S}_1\boldsymbol{x}\boldsymbol{S}_1$ and $\boldsymbol{x}'' \equiv \boldsymbol{D}\boldsymbol{x}\widetilde{\boldsymbol{D}} \equiv \boldsymbol{S}_2\boldsymbol{x}'\boldsymbol{S}_2$ was assumed. Hence the amount of dilation is given by the ratio $D := (r_{S_2}/r_{S_1})^2$.

By means of equation (3.40) it can be deduced that

$$\boldsymbol{D}\boldsymbol{x}\widetilde{\boldsymbol{D}} \;\equiv\; \boldsymbol{S}_2\boldsymbol{S}_1\boldsymbol{x}\boldsymbol{S}_1\boldsymbol{S}_2 \;=\; \mathsf{d}^2_{[\boldsymbol{x},\,\mathbf{e}_o]}\;\mathsf{d}^2_{[\boldsymbol{x}',\,\mathbf{e}_o]}\;\boldsymbol{x}'' \;=\; r^4_{S_1}\boldsymbol{x}''$$

suggesting that

$$\boldsymbol{D} \;:=\; \frac{\boldsymbol{S}_2\boldsymbol{S}_1}{r^2_{S_1}} \tag{3.56}$$

such that, finally, $\boldsymbol{D}\widetilde{\boldsymbol{D}} = D$.

As already mentioned, a dilation may be carried out with respect to any point $\boldsymbol{m}$. To see this, a translator $\boldsymbol{T}$, with $\boldsymbol{T}\,\mathbf{e}_o\widetilde{\boldsymbol{T}} = \boldsymbol{m}$, can be applied to the above derived dilator $\boldsymbol{D}$, i.e. consider $\boldsymbol{D}' = \boldsymbol{T}\boldsymbol{D}\widetilde{\boldsymbol{T}}$.

To summarize, there is one degree of freedom: the choice of the sphere $\boldsymbol{S}_1$. Sphere $\boldsymbol{S}_2$ must be concentric with $\boldsymbol{S}_1$ and its radius r_{S_2} must satisfy $r_{S_2} = \sqrt{D}\,r_{S_1}$ so as to have the dilation D. Hence $\boldsymbol{S}_2$ is fully determined after $\boldsymbol{S}_1$ has been chosen.

Componentwise Representation

Here it is focused on the multivector components of a dilator $\boldsymbol{D}$ as defined by equation (3.56). Again, let $\boldsymbol{m} = \mathbf{e}_o$. Hence let $\boldsymbol{S}_1 = -\frac{1}{2}r^2\mathbf{e} + \mathbf{e}_o$ and $\boldsymbol{S}_2 = -\frac{1}{2}D\,r^2\mathbf{e} + \mathbf{e}_o$. Pursuant to equation (3.14) and equation (3.17) it follows

$$\frac{\boldsymbol{S}_2\cdot\boldsymbol{S}_1}{r^2} \;=\; \tfrac{1}{2}(1+D) \qquad\text{and}\qquad \frac{\boldsymbol{S}_2\wedge\boldsymbol{S}_1}{r^2} \;=\; \tfrac{1}{2}(1-D)\boldsymbol{E}$$

so that

$$\boldsymbol{D} \;=\; \tfrac{1}{2}(1+D) \;+\; \tfrac{1}{2}(1-D)\boldsymbol{E}.$$

Ultimately applying the translator $\boldsymbol{T} := 1 - \frac{1}{2}\vec{m}\mathbf{e}$, with $\boldsymbol{T}\,\mathbf{e}_o\widetilde{\boldsymbol{T}} = \boldsymbol{m}$, to the components of $\boldsymbol{D}$ yields

$$\boldsymbol{T}\,1\,\widetilde{\boldsymbol{T}} \;=\; 1 \qquad\text{and}\qquad \boldsymbol{T}\boldsymbol{E}\widetilde{\boldsymbol{T}} \;=\; \boldsymbol{E} - \vec{m}\mathbf{e}.$$

The general formula for a dilator $\boldsymbol{D}$ at $\boldsymbol{m}$ with delation D is therefore

$$\boldsymbol{D} \;=\; \tfrac{1}{2}(1+D) \;+\; \tfrac{1}{2}(1-D)(\boldsymbol{E} - \vec{m}\mathbf{e}). \tag{3.57}$$

3.4.3 Rotor

A rotor describes a pure rotation, that means a rotation about an axis passing through the origin only. It therefore has an equivalent representation in terms of a 3×3-rotation matrix. Alike the translator, a rotor may be expressed by means of two consecutive reflections in planes passing through the origin. Figure 3.15 may serve as an example: the first reflection $\boldsymbol{x}' = -\boldsymbol{P}_1\boldsymbol{x}\boldsymbol{P}_1$ of point $\boldsymbol{x}$ is further reflected in the plane $\boldsymbol{P}_2$ and gives the rotation $\boldsymbol{x}'' = \boldsymbol{R}\boldsymbol{x}\widetilde{\boldsymbol{R}}$.

Let $\boldsymbol{P}_1 = \hat{n}$ and $\boldsymbol{P}_2 = \hat{m}$ be the planes of the rotor

$$\boldsymbol{R} \;=\; \boldsymbol{P}_2\boldsymbol{P}_1 \;=\; \hat{m}\cdot\hat{n} \;+\; \hat{m}\wedge\hat{n}.$$

Next it is being demonstrated that such a multivector in fact represents a rotation.

Recalling that $\mathtt{d}_{[\mathbf{e}_o,\boldsymbol{x}]} = \sqrt{-2\,\mathbf{e}_o\cdot\boldsymbol{x}}$, it is immediately clear that a rotor retains the distance from the origin because

$$\mathbf{e}_o\cdot(\boldsymbol{R}\boldsymbol{x}\widetilde{\boldsymbol{R}}) \;\stackrel{(A.26)}{=}\; \mathbf{e}_o\cdot\boldsymbol{x}.$$

The line of intersection $\boldsymbol{L} = \boldsymbol{P}_1\wedge\boldsymbol{P}_2$ is supposed to be invariant under $\boldsymbol{R}$ and indeed

$$\begin{aligned}
\boldsymbol{R}\boldsymbol{L}\widetilde{\boldsymbol{R}} &= \boldsymbol{P}_2\boldsymbol{P}_1\Big(\tfrac{1}{2}(\boldsymbol{P}_1\boldsymbol{P}_2 - \boldsymbol{P}_2\boldsymbol{P}_1)\Big)\boldsymbol{P}_1\boldsymbol{P}_2\\
&= \tfrac{1}{2}\Big(\boldsymbol{P}_2\boldsymbol{P}_1\boldsymbol{P}_1\boldsymbol{P}_2\boldsymbol{P}_1\boldsymbol{P}_2 - \boldsymbol{P}_2\boldsymbol{P}_1\boldsymbol{P}_2\boldsymbol{P}_1\boldsymbol{P}_1\boldsymbol{P}_2\Big)\\
&= \tfrac{1}{2}(\boldsymbol{P}_1\boldsymbol{P}_2 - \boldsymbol{P}_2\boldsymbol{P}_1)\\
&= \boldsymbol{L}.
\end{aligned}$$

Let $\hat{n}'$ and $\hat{m}'$ denote rotations of $\hat{n}$ and $\hat{m}$, respectively, about line $\boldsymbol{L}$ (all vectors are coplanar). By equation (2.39) or the early elucidations on page 23 it is known that $\hat{m}'\wedge\hat{n}' = \hat{m}\wedge\hat{n}$ and likewise $\hat{m}'\cdot\hat{n}' = \hat{m}\cdot\hat{n}$. Thus given a point $\boldsymbol{x}$, two planes $\boldsymbol{P}_1' = \hat{n}'$ and $\boldsymbol{P}_2' = \hat{m}'$ can be chosen such that $\boldsymbol{x}$ lies on $\boldsymbol{P}_1'$, i.e. $\boldsymbol{x}\cdot\boldsymbol{P}_1' = 0$, and additionally $\boldsymbol{R} = \boldsymbol{P}_2\boldsymbol{P}_1 = \boldsymbol{P}_2'\boldsymbol{P}_1'$. Now if θ denotes the angle between the planes, i.e. $\boldsymbol{P}_1\cdot\boldsymbol{P}_2 = \cos\theta$, the angle between $\boldsymbol{x}$ and its 'reflection' $\boldsymbol{R}\boldsymbol{x}\widetilde{\boldsymbol{R}} = -\boldsymbol{P}_2'\boldsymbol{x}\boldsymbol{P}_2'$ amounts to 2θ. This shows that, irrespective of which pair of planes is chosen, it is rotated by twice the angle between the planes.

Definition

Let $\frac{1}{2}\theta$ be the angle between the planes $\boldsymbol{P}_1 = \hat{n}$ and $\boldsymbol{P}_2 = \hat{m}$. Upon defining the normalized line $\widehat{L} \in \langle\mathbb{R}_3\rangle_2 \subset \mathbb{R}_{4,1}$

$$\widehat{L} \;=\; -\frac{\hat{m}\wedge\hat{n}}{\|\hat{m}\wedge\hat{n}\|} \qquad \text{where} \qquad \|\hat{m}\wedge\hat{n}\| \stackrel{(A.31)}{=} \left|\sin\left(\frac{\theta}{2}\right)\right|, \tag{3.58}$$

the rotor for a rotation by an angle θ may be defined as

$$\boldsymbol{R} \;=\; \boldsymbol{m}\boldsymbol{n} \;=\; \cos\left(\frac{\theta}{2}\right) \;-\; \sin\left(\frac{\theta}{2}\right)\widehat{L}. \tag{3.59}$$

Note that a minus sign is introduced so as to have a right-handed rotation in respect to the line $\widehat{L}$; regarding the oppositely oriented line $\hat{m}\wedge\hat{n}$ the rotor $\boldsymbol{R} = \hat{m}\hat{n}$ would rotate in a negative sense, as illustrated in figure 3.15.

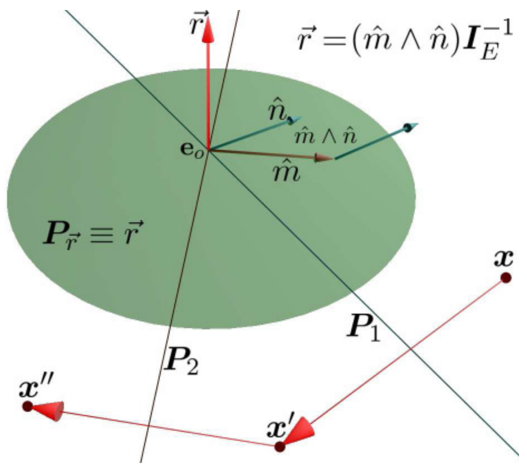

Fig. 3.15: Rotation of $\boldsymbol{x}$ by $\boldsymbol{R} = \boldsymbol{P}_2\boldsymbol{P}_1$, where $\boldsymbol{P}_1 = \hat{n}$ and $\boldsymbol{P}_2 = \hat{m}$ (planes indicated by lines only). The vector $\vec{r}$ denotes the orientation (see page 25) of the rotation plane $\boldsymbol{P}_{\vec{r}} \equiv \vec{r} = (\hat{m} \wedge \hat{n})\boldsymbol{I}_E^{-1} = \hat{m} \times \hat{n}$. Note that $\boldsymbol{x}$ is negatively rotated, i.e. in a non-right-handed sense, regarding $\vec{r}$.

Exponential Representation

Since equation (3.59) strongly resembles *Euler's formula* – only $\widehat{L}$ has to be replaced with the imaginary unit $i \in \mathbb{C}$ – and since $\widehat{L}^2 = i^2 = -1$, it may directly be deduced that

$$\boldsymbol{R} \;=\; \exp\left(-\frac{\theta}{2}\,\widehat{L}\right). \tag{3.60}$$

Example

Let the rotation axis be given by the vector $\vec{n} = 3\mathbf{e}_1 + 4\mathbf{e}_2 + 5\mathbf{e}_3$. Assume that it is to be rotated by an angle $\theta = \frac{70}{180}\pi$. Normalizing $\vec{n}$ results in the vector

$$\hat{n} \;=\; 0.4243\mathbf{e}_1 + 0.5657\mathbf{e}_2 + 0.7071\mathbf{e}_3.$$

With equation (3.50), the line $\widehat{L} = \hat{n}\boldsymbol{I}_E$ can be calculated

$$\widehat{L} \;=\; 0.7071\,\mathbf{e}_{12} - 0.5657\,\mathbf{e}_{13} + 0.4243\,\mathbf{e}_{23}.$$

Multiplying with $-\sin(\theta/2)$ and adding the scalar part $\cos(\theta/2) = 0.8192$ finally yields the rotor

$$\boldsymbol{R} \;=\; 0.8192 \;-\; 0.4056\,\mathbf{e}_{12} \;+\; 0.3245\,\mathbf{e}_{13} \;-\; 0.2433\,\mathbf{e}_{23}.$$

The parameters can be retrieved very easily from the rotor. This is detailed for a *motor*, the most general transformation to be discussed here, in section 3.4.5.

As a comparison consider the representation of a rotation matrix $\mathsf{R} \in \mathbb{R}^{3\times3}$ below. Similarly, it describes a rotation around a unit normal vector $\hat{n} = n_x\mathbf{e}_1 + n_y\mathbf{e}_2 + n_z\mathbf{e}_3$

by an angle θ. Notice that it is refrained from expressing the rotation in terms of *Euler angles*.

$$\mathsf{R} \;=\; \begin{bmatrix} n_x^2(1-\cos\theta)+\cos\theta & n_x n_y(1-\cos\theta)-n_z\sin\theta & n_x n_z(1-\cos\theta)+n_y\sin\theta \\ n_x n_y(1-\cos\theta)+n_z\sin\theta & n_y^2(1-\cos\theta)+\cos\theta & n_y n_z(1-\cos\theta)-n_x\sin\theta \\ n_x n_z(1-\cos\theta)-n_y\sin\theta & n_y n_z(1-\cos\theta)+n_x\sin\theta & n_z^2(1-\cos\theta)+\cos\theta \end{bmatrix}$$

Both approaches have certain advantages. The matrix representation is probably more efficient, i.e. less multiplications and additions are required to carry out a rotation, but using a rotor is much more intuitive and handy. Besides, the representation by means of a rotor is condensed in that four components hold the three necessary parameters. Last but not least, the parameters are not so strongly mixed up.

3.4.4 General Rotor

A so-called *general rotor* allows for rotations about arbitrary axes in space. It shall be discussed shortly because it differs only slightly from a rotor or a motor.

As one might expect, a general rotor differs from a rotor only in that the intersecting planes are not bound anymore to pass through the origin. Like before, the general rotor rotates by twice the included angle. Similarly, the rotation axis is given by the line $\boldsymbol{L} \equiv -\boldsymbol{P}_2 \wedge \boldsymbol{P}_1$ if the rotor (for brevity, the term 'general' may be omitted from now on) was defined by $\boldsymbol{R} = \boldsymbol{P}_2\boldsymbol{P}_1$.

Example

Say a general rotor is given by $\boldsymbol{R}_\phi = \boldsymbol{P}_b\boldsymbol{P}_a$, where the opening angle between the planes amounts to $\frac{1}{2}\phi$. It shall, however, be rotated by the different angle θ. The rotation axis $\boldsymbol{L}$ can be retrieved by

$$\boldsymbol{L}' \;=\; \langle \boldsymbol{R}_\phi \rangle_2,$$

and for a normalization and a correct orientation

$$\boldsymbol{L} = \frac{-\boldsymbol{L}'}{\sqrt{-\boldsymbol{L}'^2}} \qquad \text{or equally} \qquad \boldsymbol{L} = \frac{-\boldsymbol{P}_b \wedge \boldsymbol{P}_a}{\sqrt{-(\boldsymbol{P}_b \wedge \boldsymbol{P}_a)^2}}.$$

The new rotor is then obtained with

$$\boldsymbol{R}_\theta \;=\; \exp\left(-\frac{\theta}{2}\boldsymbol{L}\right). \tag{3.61}$$

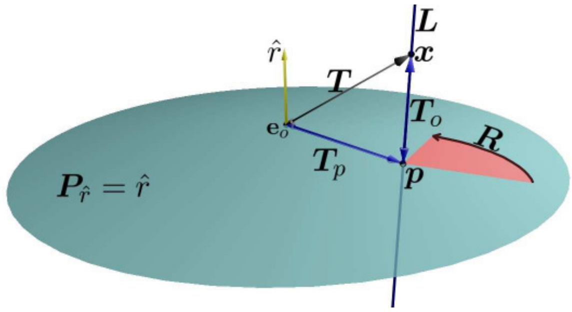

Fig. 3.16: Rotation about an arbitrary line in space.

Displacing a Pure Rotation

A general rotor can also be viewed as an offset pure rotation. This can be accomplished by means of a translator $\boldsymbol{T}$. Hence if $\boldsymbol{R}_p$ denotes a pure rotor, the shifted (general) rotor $\boldsymbol{R}$ can be expressed via

$$\boldsymbol{R} \;=\; \boldsymbol{T}\boldsymbol{R}_p\widetilde{\boldsymbol{T}}. \tag{3.62}$$

Clearly, if $\boldsymbol{R}_p = \boldsymbol{P}_2'\boldsymbol{P}_1'$ then $\boldsymbol{R} = (\boldsymbol{T}\boldsymbol{P}_2'\widetilde{\boldsymbol{T}})(\boldsymbol{T}\boldsymbol{P}_1'\widetilde{\boldsymbol{T}}) = \boldsymbol{P}_2\boldsymbol{P}_1$.

But transformation (3.62) can also be interpreted stepwise: the leftmost and therefore first subtransformation $\widetilde{\boldsymbol{T}}$ of $\boldsymbol{R}$ rigidly moves the coordinate frame centered at $\boldsymbol{x} = \boldsymbol{T}\,\mathbf{e}_o\widetilde{\boldsymbol{T}}$, see figure 3.16, to the origin where the pure rotation of $\boldsymbol{R}_p$ is carried out. Finally, $\boldsymbol{T}$ undoes the change of the coordinate frame.

Using the pure rotor $\boldsymbol{R}_p = \hat{m}\,\hat{n}$ and the translator $\boldsymbol{T} = 1 - \frac{1}{2}\vec{t}\,\mathbf{e}$, the general rotor $\boldsymbol{R}$ becomes

$$\begin{aligned}
\boldsymbol{R} \;&=\; \left(1 - \tfrac{1}{2}\vec{t}\,\mathbf{e}\right)\,\hat{m}\,\hat{n}\,\left(1 + \tfrac{1}{2}\vec{t}\,\mathbf{e}\right)\\
&=\; \hat{m}\,\hat{n} \;-\; (\,\vec{t}\,\mathbf{e}) \times (\,\hat{m}\,\hat{n}\,)\\
&=\; \boldsymbol{R}_p \;-\; \left(\vec{t}\cdot(\hat{m}\wedge\hat{n})\right)\mathbf{e}\\
&\overset{(3.58)}{=}\; \cos\left(\frac{\theta}{2}\right) \;-\; \sin\left(\frac{\theta}{2}\right)\widehat{L} \;+\; \sin\left(\frac{\theta}{2}\right)\left(\vec{t}\cdot\widehat{L}\right)\mathbf{e}\\
&=\; \cos\left(\frac{\theta}{2}\right) \;-\; \sin\left(\frac{\theta}{2}\right)\left[\widehat{L} \;-\; \left(\vec{t}\cdot\widehat{L}\right)\mathbf{e}\right]\\
&\overset{(3.51)}{=}\; \cos\left(\frac{\theta}{2}\right) \;-\; \sin\left(\frac{\theta}{2}\right)\boldsymbol{L},
\end{aligned} \tag{3.63}$$

in analogy with equation (3.61).

Exponential Representation

The exponential representation is now being derived by means of the exponential representation of $\boldsymbol{R}_p$ as stated in equation (3.60). Let $\boldsymbol{L}_p$ denote the rotation axis of $\boldsymbol{R}_p$. Thus

$$\begin{aligned}
\boldsymbol{R} &= \boldsymbol{T}\boldsymbol{R}_p\widetilde{\boldsymbol{T}} \;=\; \boldsymbol{T}\left(\sum_{k=0}^{\infty}\frac{(-\frac{\theta}{2}\boldsymbol{L}_p)^k}{k!}\right)\widetilde{\boldsymbol{T}} \\
&= \left(\sum_{k=0}^{\infty}\frac{(-\frac{\theta}{2})^k\,\boldsymbol{T}\boldsymbol{L}_p^k\widetilde{\boldsymbol{T}}}{k!}\right) \;=\; \left(\sum_{k=0}^{\infty}\frac{(-\frac{\theta}{2})^k\,(\boldsymbol{T}\boldsymbol{L}_p\widetilde{\boldsymbol{T}})^k}{k!}\right) \\
&= \exp\left(-\frac{\theta}{2}\boldsymbol{T}\boldsymbol{L}_p\widetilde{\boldsymbol{T}}\right) \;=\; \exp\left(-\frac{\theta}{2}\boldsymbol{L}\right),
\end{aligned}$$

where $\boldsymbol{L} := \boldsymbol{T}\boldsymbol{L}_p\widetilde{\boldsymbol{T}}$.

Note that the versor outermorphism for $\boldsymbol{T}$, with $\boldsymbol{T}\widetilde{\boldsymbol{T}} = 1$, was used; it is, for instance, $\boldsymbol{T}\boldsymbol{L}^2\widetilde{\boldsymbol{T}} = \boldsymbol{T}\boldsymbol{L}\widetilde{\boldsymbol{T}}\boldsymbol{T}\boldsymbol{L}\widetilde{\boldsymbol{T}} = (\boldsymbol{T}\boldsymbol{L}\widetilde{\boldsymbol{T}})^2$.

Rotation in Detail

Let $\boldsymbol{R}$ be a general rotor. The expressions $\cos(\frac{\theta}{2})$ and $\sin(\frac{\theta}{2})$ are being abbreviated to c and s, respectively. Expanding $\boldsymbol{y} = \boldsymbol{R}\boldsymbol{x}\widetilde{\boldsymbol{R}}$ then gives

$$\begin{aligned}
\boldsymbol{y} &= (c - s\boldsymbol{L})\,\boldsymbol{x}\,(c + s\boldsymbol{L}) \\
&= c^2\boldsymbol{x} + 2cs(\boldsymbol{x}\cdot\boldsymbol{L}) - s^2\boldsymbol{L}\,\boldsymbol{x}\,\boldsymbol{L} \\
&= x + 2\,cs(\boldsymbol{x}\cdot\boldsymbol{L}) + 2\,s^2(\boldsymbol{x}\cdot\boldsymbol{L})\boldsymbol{L},
\end{aligned}$$

where is was used that

$$\begin{aligned}
(\boldsymbol{x}\cdot\boldsymbol{L})\cdot\boldsymbol{L} &= (\boldsymbol{x}\underline{\times}\boldsymbol{L})\underline{\times}\boldsymbol{L} \\
&= (\boldsymbol{x}\boldsymbol{L}\boldsymbol{L} - \boldsymbol{L}\boldsymbol{x}\boldsymbol{L} - \boldsymbol{L}\boldsymbol{x}\boldsymbol{L} + \boldsymbol{L}\boldsymbol{L}\boldsymbol{x})/4 \\
&= -\tfrac{\boldsymbol{x}}{2} - \tfrac{\boldsymbol{L}\boldsymbol{x}\boldsymbol{L}}{2} \\
\Longleftrightarrow \qquad -\boldsymbol{L}\boldsymbol{x}\boldsymbol{L} &= \boldsymbol{x} + 2(\boldsymbol{x}\cdot\boldsymbol{L})\boldsymbol{L},
\end{aligned}$$

which describes the reflection $\boldsymbol{L}\boldsymbol{x}\widetilde{\boldsymbol{L}}$ of $\boldsymbol{x}$ in $\boldsymbol{L}$ (rotation about $\boldsymbol{L}$ by 180°). Applying the results (3.53) and (3.54) gives

$$\begin{aligned}
\boldsymbol{R}\,\boldsymbol{x}\,\widetilde{\boldsymbol{R}} &= \boldsymbol{x} + \mathsf{d}_{[\boldsymbol{x},\boldsymbol{L}]}\left(2\,cs\,\boldsymbol{P}_x - 2\,s^2\,\boldsymbol{P}_o\right) \\
&= \boldsymbol{x} + \mathsf{d}_{[\boldsymbol{x},\boldsymbol{L}]}\Big(\sin\theta\,\boldsymbol{P}_x + (\cos\theta - 1)\,\boldsymbol{P}_o\Big),
\end{aligned} \tag{3.64}$$

where the point dependent representation $\boldsymbol{L} = \boldsymbol{P}_x\boldsymbol{P}_o$ was used.
For an interpretation the (pure) rotation of a vector[18] $\mathsf{u} \in \mathbb{R}^3$ is now being analyzed.

On defining the skew symmetric matrix $\mathsf{A} \in \mathbb{R}^{3\times 3}$

$$\mathsf{A} = \begin{bmatrix} 0 & -r_3 & r_2 \\ r_3 & 0 & -r_1 \\ -r_2 & r_1 & 0 \end{bmatrix} \quad \overset{\mathsf{r}:=[r_1,r_2,r_3]^\mathsf{T}}{\Longrightarrow} \quad \mathsf{A}\mathsf{u} = \mathsf{r}\times\mathsf{u}, \quad \mathsf{u}\in\mathbb{R}^3$$

[18] Temporary use of the matrix notation!

and setting $\theta = \|\mathsf{r}\|$, *Rodrigues's formula* (1840), cf. [56, 37], states that

$$e^{\mathsf{A}} = \mathsf{I}_3 + \frac{\sin\theta}{\theta}\mathsf{A} + \frac{(1-\cos\theta)}{\theta^2}\mathsf{A}^2 =: \mathsf{R}, \tag{3.65}$$

where R denotes a rotation matrix for rotating about the vector $\mathsf{r} \in \mathbb{R}^3$ by an angle $\theta = \|\mathsf{r}\|$. Thus with $\hat{\mathsf{r}} := \mathsf{r}/\theta$ it holds that

$$\mathsf{Ru} = \mathsf{u} + \sin\theta\,\hat{\mathsf{r}} \times \mathsf{u} + (1-\cos\theta)\,\hat{\mathsf{r}} \times (\hat{\mathsf{r}} \times \mathsf{u}). \tag{3.66}$$

Identifying $\hat{r} := \hat{\mathsf{r}}$ with the direction vector of a line $\widehat{L} \in \langle\mathbb{R}_3\rangle_2 \subset \mathbb{R}_{4,1}$ passing through the origin, the line may be expressed in respect of point $\boldsymbol{u} := \mathcal{K}(\vec{u} := \mathsf{u})$, that is $\widehat{L} = (\hat{n}_u \wedge \hat{n}_o)\boldsymbol{I}_E^{-1}$ (see page 116), such that

$$\begin{aligned} \hat{r} \times \vec{u} &= ((\hat{n}_u \wedge \hat{n}_o)\boldsymbol{I}_E^{-1} \wedge \vec{u})\boldsymbol{I}_E^{-1} = -(\vec{u} \wedge (\hat{n}_u \wedge \hat{n}_o)\boldsymbol{I}_E^{-1})\boldsymbol{I}_E^{-1} \\ &= \vec{u} \cdot ((\hat{n}_u \wedge \hat{n}_o)\boldsymbol{I}_E^{-1}\boldsymbol{I}_E) = \vec{u} \cdot \widehat{L} = \mathsf{d}_{[\boldsymbol{u},\widehat{L}]}\boldsymbol{P}_u. \end{aligned}$$

This shows the connection or equality, respectively, between equation (3.64) and equation (3.66); only $\boldsymbol{u}$ has to be replaced with $\boldsymbol{x}$.

The Orthogonal Part

Like in figure 3.16, the translation of $\boldsymbol{T}$ may be separated into a translation $\boldsymbol{T}_p$ parallel or inside, respectively, the rotation plane $\boldsymbol{P}_{\hat{r}}$ and an orthogonal translation $\boldsymbol{T}_o$ along the rotation axis $\boldsymbol{L}$. Hence let $\boldsymbol{T} = \boldsymbol{T}_p\boldsymbol{T}_o = \boldsymbol{T}_o\boldsymbol{T}_p$, with $\boldsymbol{T}_o = \boldsymbol{P}_v\boldsymbol{P}_u$ where $\{\boldsymbol{P}_v, \boldsymbol{P}_u\} \parallel \boldsymbol{P}_{\hat{r}}$. Again let $\boldsymbol{R}_p = \boldsymbol{P}_2'\boldsymbol{P}_1'$. Due to $\{\boldsymbol{P}_2', \boldsymbol{P}_1'\} \perp \boldsymbol{P}_{\hat{r}}$, the planes of $\boldsymbol{T}_o$ and $\boldsymbol{R}_p$, respectively, anti-commute such that

$$\boldsymbol{R} = (\boldsymbol{T}_p\boldsymbol{T}_o)\boldsymbol{R}_p(\widetilde{\boldsymbol{T}_o}\widetilde{\boldsymbol{T}_p}) = \boldsymbol{T}_p\boldsymbol{P}_v\boldsymbol{P}_u\boldsymbol{P}_2'\overbrace{\boldsymbol{P}_1'\boldsymbol{P}_u}^{-\boldsymbol{P}_u\boldsymbol{P}_1'}\boldsymbol{P}_v\widetilde{\boldsymbol{T}_p} \stackrel{...}{=} \boldsymbol{T}_p\boldsymbol{P}_2'\boldsymbol{P}_1'\widetilde{\boldsymbol{T}_p} = \boldsymbol{T}_p\boldsymbol{R}_p\widetilde{\boldsymbol{T}_p}.$$

Consequently, a general rotor $\boldsymbol{R}$ commutes with an orthogonal translator $\boldsymbol{T}_o$

$$\boldsymbol{R}\boldsymbol{T}_o = \boldsymbol{T}_o\boldsymbol{R}.$$

This suggests a new operator, namely the *motor*, which can be viewed as a *screw motion*[19].

3.4.5 Motor

For an introduction consider at first two congruent objects, or simply two point clouds, $\boldsymbol{X}_1$ and $\boldsymbol{X}_2$ in 3D-space $\mathbb{R}^3$; both have a distinct position and orientation.

[19]The alternating execution of arbitrary small portions of general rotor and orthogonal translator can be thought of as a screw motion.

Now let $\widetilde{\boldsymbol{T}_1}$ and $\widetilde{\boldsymbol{T}_2}$ be translators that move the barycenters of $\boldsymbol{X}_1$ and $\boldsymbol{X}_2$, respectively, to the origin $\mathbf{e}_o$. It then exists a (pure) rotation $\boldsymbol{R}_p$ that aligns the copy of $\boldsymbol{X}_2$ with the copy of $\boldsymbol{X}_1$, cf. [5, 25]. It may be inferred that

$$\begin{aligned} & \widetilde{\boldsymbol{T}_1}\boldsymbol{X}_1\boldsymbol{T}_1 \;=\; \boldsymbol{R}_p(\widetilde{\boldsymbol{T}_2}\boldsymbol{X}_2\boldsymbol{T}_2)\widetilde{\boldsymbol{R}_p} \\ \iff \quad & \boldsymbol{X}_1 \;=\; \underbrace{\boldsymbol{T}_1\boldsymbol{R}_p\widetilde{\boldsymbol{T}_2}}_{=:\,\boldsymbol{M}}\,\boldsymbol{X}_2\,\boldsymbol{T}_2\widetilde{\boldsymbol{R}_p}\widetilde{\boldsymbol{T}_1}. \end{aligned}$$

The transformation of $\boldsymbol{M}$ is taken as the most general case for a rigid body motion, whence $\boldsymbol{M}$ is called a motor. It is now being shown that there is always a decomposition of $\boldsymbol{M}$ into a translation and a pure rotation, i.e. $\boldsymbol{M} = \boldsymbol{T}_m\boldsymbol{R}_p$. In addition, a motor may always be represented by means of a general rotation $\boldsymbol{R}$ and an orthogonal translation $\boldsymbol{T}_o$ as suggested at the end of the previous section.

Clearly, each of the translators may be split into a parallel and an orthogonal part, denoted by a superset '$\perp$', regarding the rotation plane of $\boldsymbol{R}_p$. Let $\boldsymbol{T}_1 = \boldsymbol{T}_1'\boldsymbol{T}_1^{\perp}$ and $\boldsymbol{T}_2 = \boldsymbol{T}_2'\boldsymbol{T}_2^{\perp}$ such that

$$\boldsymbol{M} \;=\; \boldsymbol{T}_1'\boldsymbol{T}_1^{\perp}\boldsymbol{R}_p\widetilde{\boldsymbol{T}_2}^{\perp}\widetilde{\boldsymbol{T}_2'} \;=\; \underbrace{\boldsymbol{T}_1^{\perp}\widetilde{\boldsymbol{T}_2}^{\perp}}_{=:\,\boldsymbol{T}_o}\boldsymbol{T}_1'\boldsymbol{R}_p\widetilde{\boldsymbol{T}_2'} \;=\; \boldsymbol{T}_o\,\boldsymbol{T}_1'\boldsymbol{R}_p\widetilde{\boldsymbol{T}_2'}.$$

Since a rotated translator still is a translator it follows

$$\boldsymbol{M} \;=\; \boldsymbol{T}_o\,\overbrace{\boldsymbol{T}_1'\,\boldsymbol{R}_p\widetilde{\boldsymbol{T}_2'}\widetilde{\boldsymbol{R}_p}}^{\boldsymbol{T}_L:=\boldsymbol{T}_1'(\boldsymbol{R}_p\boldsymbol{T}_2'\widetilde{\boldsymbol{R}_p})^{\sim}}\;\boldsymbol{R}_p \;=\; \overbrace{\boldsymbol{T}_o\boldsymbol{T}_L}^{\boldsymbol{T}_m:=}\boldsymbol{R}_p \;=\; \boldsymbol{T}_m\boldsymbol{R}_p,$$

which is the preferred and also an intuitive representation for a motor[20].

As the orthogonal part $\boldsymbol{T}_o$ commutes with the rest of $\boldsymbol{M}$ it is disregarded for a while. In order to show that $\boldsymbol{T}_L\boldsymbol{R}_p$ is a general rotation $\boldsymbol{T}_p\boldsymbol{R}_p\widetilde{\boldsymbol{T}_p}$ let $\boldsymbol{R}_p = c - s\widehat{L}$ and $\boldsymbol{T}_L = 1 - \frac{1}{2}\vec{t}\,\mathbf{e}$. Exploiting that $\vec{t}$ lies on the plane defined by $\widehat{L} \in \langle\mathbb{R}_3\rangle_2$, i.e. $\vec{t} = -\vec{t}\,\widehat{L}^2 = -(\vec{t}\cdot\widehat{L})\cdot\widehat{L}$, one has

$$\begin{aligned} \boldsymbol{T}_L\boldsymbol{R}_p \;=\; (1 - \tfrac{1}{2}\vec{t}\,\mathbf{e})(c - s\widehat{L}) \quad &= \quad c - s\widehat{L} \,+\, \tfrac{1}{2}(\,s\,\vec{t}\,\widehat{L} \,-\, c\,\vec{t}\,)\,\mathbf{e} \\ &= \quad c - s\widehat{L} \,+\, \Big(\tfrac{1}{2}(s\,\vec{t} + c\,\vec{t}\cdot\widehat{L}\,)\cdot\widehat{L}\Big)\,\mathbf{e} \end{aligned}$$

Ultimately setting $\vec{p} = \frac{c}{2s}\,\vec{t}\cdot\widehat{L} + \frac{\vec{t}}{2}$ it can be seen that

$$\boldsymbol{T}_L\boldsymbol{R}_p \;=\; c - s\Big(\widehat{L} - (\vec{p}\cdot\widehat{L})\,\mathbf{e}\Big) \;\overset{(3.51)}{=}\; c - s\boldsymbol{L} \;=\; \boldsymbol{R}$$

is in effect a general rotation $\boldsymbol{R} = \boldsymbol{T}_p\boldsymbol{R}_p\widetilde{\boldsymbol{T}_p}$ about line $\boldsymbol{L}$ with foot $\mathcal{K}(\vec{p})$. Finally two major representations can be subsumed

$$\boldsymbol{M} \;=\; \boldsymbol{T}_m\boldsymbol{R}_p \;=\; \boldsymbol{T}_o(\boldsymbol{T}_p\boldsymbol{R}_p\widetilde{\boldsymbol{T}_p}). \tag{3.67}$$

[20] Likewise, defining $\boldsymbol{T}_R = \widetilde{\boldsymbol{R}_p}\boldsymbol{T}_1'\boldsymbol{R}_p\widetilde{\boldsymbol{T}_2'}$ shows that $\boldsymbol{R}_p\boldsymbol{T}_R = \boldsymbol{T}_L\boldsymbol{R}_p$.

Exponential Representation

Let the motor $\boldsymbol{M}$ be given in terms of the general rotor $\boldsymbol{R} = c - s\boldsymbol{L}$ and the orthogonal translator $\boldsymbol{T}_o = 1 - \frac{1}{2}\vec{t}_o\mathbf{e}$. Hence let $\boldsymbol{M} = \boldsymbol{T}_o\boldsymbol{R}$. In this case the commutation of $\boldsymbol{R}$ and $\boldsymbol{T}_o$ implies that the respective arguments of their exponential representation commute as well, that means

$$(-\tfrac{1}{2}\vec{t}_o\mathbf{e}) \veebar (-\frac{\theta}{2}\boldsymbol{L}) \;=\; 0.$$

Hence a general result from *Lie theory*, see [12] for an introduction, can be used

$$A \veebar B = 0 \qquad \Longleftrightarrow \qquad \exp(A)\exp(B) = \exp(A+B).$$

This may be proven directly, as in [37], or by means of the BCH (*Baker Campbell Hausdorff*) formula [24], which exploits the commutator formalism.

Thus

$$\begin{aligned} \boldsymbol{M} \;=\; \boldsymbol{T}_o\boldsymbol{R} \;&=\; \exp(-\tfrac{1}{2}\vec{t}_o\mathbf{e})\exp(-\frac{\theta}{2}\boldsymbol{L}) \\ &=\; \exp\left(-\tfrac{1}{2}\vec{t}_o\mathbf{e} - \frac{\theta}{2}\boldsymbol{L}\right). \end{aligned}$$

Note that the bivector in the argument of the exponential function is not a blade any more.

Componentwise Representation

Employing $\boldsymbol{L} = \widehat{L} - (\vec{p}\cdot\widehat{L})\mathbf{e}$, with $\widehat{L} = \hat{r}\boldsymbol{I}_E$, the expanded form of a motor reads

$$\boldsymbol{M} \;=\; \underbrace{c - s\widehat{L}}_{\boldsymbol{R}_p} + \Big(s(\vec{p}\cdot\widehat{L}) - \tfrac{1}{2}c\,\vec{t}_o\Big)\mathbf{e} + \tfrac{1}{2}\,s\,t\,\boldsymbol{I}_E\,\mathbf{e}, \qquad \text{with} \qquad t := \vec{t}_o\cdot\hat{r}.$$

Hence a motor differs from a general rotor in that it has the additional 4-vector component $\frac{1}{2}\,t\sin(\theta/2)\,\boldsymbol{I}_E\,\mathbf{e}$, where $t\in\mathbb{R}$ denotes the (signed) amount of translation along the direction $\hat{r} = \widehat{L}\boldsymbol{I}_E^{-1}$ of $\boldsymbol{L}$.

Factorizing a Motor

Here it is focused on the determination of the components $\boldsymbol{R}_p$, $\boldsymbol{T}_p$, $\boldsymbol{T}_o$ and $\boldsymbol{T}_m$. First of all, given a motor $\boldsymbol{M}$, the pure rotor $\boldsymbol{R}_p$ can be extracted via

$$\boldsymbol{R}_p \overset{(A.33)}{=} \boldsymbol{E}\cdot(\boldsymbol{E}\wedge\boldsymbol{M}) \tag{3.68}$$

Now $\boldsymbol{T}_m$ can easily be computed, see equation (3.67), via

$$\boldsymbol{T}_m \;=\; \boldsymbol{M}\widetilde{\boldsymbol{R}_p}. \tag{3.69}$$

The orthogonal translator $\boldsymbol{T}_o$ can be obtained by evaluating

$$\boldsymbol{T}_o \;=\; \frac{\boldsymbol{R}_p \cdot \boldsymbol{M}}{\boldsymbol{R}_p \cdot \boldsymbol{R}_p}. \tag{3.70}$$

To see this let $\boldsymbol{M} = \boldsymbol{T}_o\boldsymbol{R}$, where $\boldsymbol{R} = \boldsymbol{T}_p\boldsymbol{R}_p\widetilde{\boldsymbol{T}_p}$ denotes a general rotation. Assume further the special configuration of planes

$$\begin{aligned} \boldsymbol{R}_p &= c + s\boldsymbol{P}_1' \wedge \boldsymbol{P}_2' & \qquad \boldsymbol{P}_1' \cdot \boldsymbol{P}_2' &= 0 \\ \boldsymbol{T}_o &= 1 + \boldsymbol{P}_a \wedge \boldsymbol{P}_b & \boldsymbol{P}_a \cdot \boldsymbol{P}_b &= 1 \\ \boldsymbol{R} &= c + s\boldsymbol{P}_1 \wedge \boldsymbol{P}_2 & \boldsymbol{P}_1 \cdot \boldsymbol{P}_2 &= 0, \end{aligned}$$

where, as usual, c and s stand for $\cos(\theta/2)$ and $\sin(\theta/2)$, respectively. Note that $\boldsymbol{P}_1$ and $\boldsymbol{P}_2$ are translated versions of $\boldsymbol{P}_1'$ and $\boldsymbol{P}_2'$. It follows

$$\begin{aligned} \boldsymbol{R}_p \cdot \boldsymbol{M} &= (c + s\boldsymbol{P}_1' \wedge \boldsymbol{P}_2') \cdot ((1 + \boldsymbol{P}_a \wedge \boldsymbol{P}_b)(c + s\boldsymbol{P}_1 \wedge \boldsymbol{P}_2)) \\ &= (c + s\boldsymbol{P}_1' \wedge \boldsymbol{P}_2') \cdot (c + s\boldsymbol{P}_1 \wedge \boldsymbol{P}_2 + c\boldsymbol{P}_a \wedge \boldsymbol{P}_b + s(\boldsymbol{P}_a \wedge \boldsymbol{P}_b)(\boldsymbol{P}_1 \wedge \boldsymbol{P}_2)) \end{aligned}$$

All products involving a scalar can be disregarded as they take the value zero. Also the inner product with the term $c\boldsymbol{P}_a \wedge \boldsymbol{P}_b$ is zero due to the mutual orthogonality of the planes. It remains

$$(s\boldsymbol{P}_1' \wedge \boldsymbol{P}_2') \cdot (s\boldsymbol{P}_1 \wedge \boldsymbol{P}_2) \;\overset{(2.45)}{=}\; -s^2(\boldsymbol{P}_1' \cdot \boldsymbol{P}_1)(\boldsymbol{P}_2' \cdot \boldsymbol{P}_2) \;=\; -s^2. \tag{3.71}$$

The orthogonality allows for $(\boldsymbol{P}_a \wedge \boldsymbol{P}_b)(\boldsymbol{P}_1 \wedge \boldsymbol{P}_2) = \boldsymbol{P}_a\boldsymbol{P}_b\boldsymbol{P}_1\boldsymbol{P}_2 = \boldsymbol{P}_a \wedge \boldsymbol{P}_b \wedge \boldsymbol{P}_1 \wedge \boldsymbol{P}_2$. By means of corollary 2.15 (and particularly by example 2.9) the last inner product gives

$$\begin{aligned} (s\boldsymbol{P}_1' \wedge \boldsymbol{P}_2') \cdot (s\boldsymbol{P}_a \wedge \boldsymbol{P}_b \wedge \boldsymbol{P}_1 \wedge \boldsymbol{P}_2) &= s^2\Big((\boldsymbol{P}_1' \cdot \boldsymbol{P}_1) \cdot (\boldsymbol{P}_1 \wedge \boldsymbol{P}_2)\Big)(\boldsymbol{P}_a \wedge \boldsymbol{P}_b) \\ &= -s^2\, \boldsymbol{P}_a \wedge \boldsymbol{P}_b. \end{aligned} \tag{3.72}$$

Combining equation (3.71) and equation (3.72) yields

$$\boldsymbol{R}_p \cdot \boldsymbol{M} \;=\; -s^2\,(1 + \boldsymbol{P}_a \wedge \boldsymbol{P}_b) \;=\; -s^2\, \boldsymbol{T}_o.$$

Proposition (3.70) follows observing that

$$\boldsymbol{R}_p \cdot \boldsymbol{R}_p \;=\; (c - s\widehat{L}) \cdot (c - s\widehat{L}) \;=\; s^2\,\widehat{L}^2 \;=\; -s^2. \tag{3.73}$$

In order to calculate translator $\boldsymbol{T}_p = 1 - \frac{1}{2}\vec{t}\mathbf{e}$, the second row of equation (3.63) is taken into account. Using that $\vec{t}\mathbf{e} = 2(1 - \boldsymbol{T}_p)$, the equation can be converted to

$$\begin{aligned} \boldsymbol{R} &= \boldsymbol{R}_p - [2(1 - \boldsymbol{T}_p)] \,\underline{\times}\, \boldsymbol{R}_p \\ &= \boldsymbol{R}_p - (\boldsymbol{R}_p - \boldsymbol{T}_p\boldsymbol{R}_p - \boldsymbol{R}_p + \boldsymbol{R}_p\boldsymbol{T}_p) \\ &= \boldsymbol{R}_p + \boldsymbol{T}_p\boldsymbol{R}_p - \boldsymbol{R}_p\boldsymbol{T}_p \end{aligned}$$

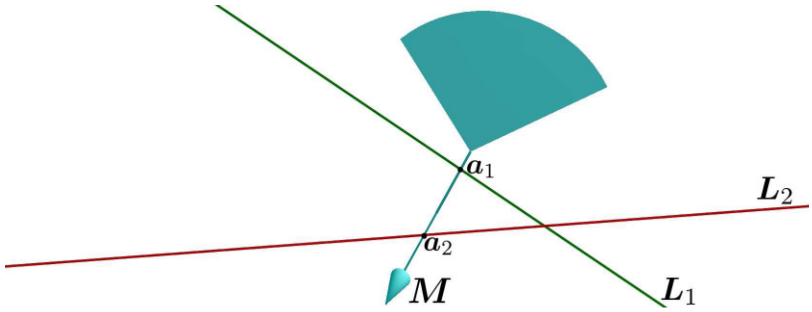

Fig. 3.17: Reflecting in line $\boldsymbol{L}_1$ and then in line $\boldsymbol{L}_2$ gives the motor $\boldsymbol{M} = \boldsymbol{L}_2\boldsymbol{L}_1$.

Now consider the expression

$$\begin{aligned} \boldsymbol{R} \veebar \widetilde{\boldsymbol{R}_p} &= \tfrac{1}{2}\Big((\boldsymbol{R}_p + \boldsymbol{T}_p\boldsymbol{R}_p - \boldsymbol{R}_p\boldsymbol{T}_p)\widetilde{\boldsymbol{R}_p} - \widetilde{\boldsymbol{R}_p}(\boldsymbol{R}_p + \boldsymbol{T}_p\boldsymbol{R}_p - \boldsymbol{R}_p\boldsymbol{T}_p)\Big) \\ &= \boldsymbol{T}_p - \tfrac{1}{2}(\boldsymbol{R}_p\boldsymbol{T}_p\widetilde{\boldsymbol{R}_p} + \widetilde{\boldsymbol{R}_p}\boldsymbol{T}_p\boldsymbol{R}_p). \end{aligned} \tag{3.74}$$

The latter term reminds of the complex numbers; identifying the complex plane with the rotation plane of $\boldsymbol{R}_p$ and $\boldsymbol{T}_p$ with $\exp(i\,0) = 1$, the last term reflects building the average of a complex number $\exp(i\,\theta)$ and its conjugate $\exp(-i\,\theta)$, which gives the real part (parallel to $\boldsymbol{T}_p$). Hence the last term represents a dilated version of $\boldsymbol{T}_p$. The result in the complex plane would be $\cos(\theta)$ and likewise

$$\boldsymbol{T}_p' := \tfrac{1}{2}(\boldsymbol{R}_p\boldsymbol{T}_p\widetilde{\boldsymbol{R}_p} + \widetilde{\boldsymbol{R}_p}\boldsymbol{T}_p\boldsymbol{R}_p) = 1 - \tfrac{1}{2}\cos(\theta)\vec{t}\,\mathbf{e}.$$

Substituting $\boldsymbol{T}_p'$ back into equation (3.74) gives

$$\boldsymbol{R} \veebar \widetilde{\boldsymbol{R}_p} = \boldsymbol{T}_p - \boldsymbol{T}_p' = \tfrac{1}{2}\Big(\cos(\theta) - 1\Big)\vec{t}\,\mathbf{e} = \boldsymbol{R}_p \veebar \boldsymbol{R},$$

where the last equality comes from

$$\begin{aligned} \boldsymbol{R} \veebar \widetilde{\boldsymbol{R}_p} &= (c - s\boldsymbol{L}) \veebar (c + s\widehat{L}) = -s^2\boldsymbol{L} \veebar \widehat{L} = s^2\widehat{L} \veebar \boldsymbol{L} = s^2(-\widehat{L}) \veebar (-\boldsymbol{L}) \\ &= (c - s\widehat{L}) \veebar (c - s\boldsymbol{L}) = \boldsymbol{R}_p \veebar \boldsymbol{R}. \end{aligned}$$

Finally noting that $\cos(2\,\tfrac{1}{2}\theta) - 1 = -2\sin^2(\theta/2)$, equation (3.73) can be used such that

$$\boldsymbol{T}_p = 1 - \tfrac{1}{2}\frac{\boldsymbol{R}_p \veebar \boldsymbol{M}}{\boldsymbol{R}_p \cdot \boldsymbol{R}_p}. \tag{3.75}$$

where $\boldsymbol{R}_p \veebar \boldsymbol{M} = (\boldsymbol{R}_p \veebar \boldsymbol{R})\boldsymbol{T}_o = \boldsymbol{R}_p \veebar \boldsymbol{R}$ was additionally used.

Example

Here one possibility to calculate the distance between two lines is proposed. A single line can be seen as a general rotor with angle $\theta = 180°$. Reflecting twice, however, results in a motor as depicted in figure 3.17.

Given two lines $\boldsymbol{L}_1$ and $\boldsymbol{L}_2$, a pair of parallel planes can be found such that each line lies on a plane, say $\boldsymbol{L}_i$ lies on plane $\boldsymbol{P}_i$, $i \in \{1, 2\}$. The distance between these planes corresponds to the distance between the lines. For each line $\boldsymbol{L}_i$, on its plane $\boldsymbol{P}_i$, a unique orthogonal plane $\boldsymbol{Q}_i$ can be found such that $\boldsymbol{L}_i = \boldsymbol{P}_i\boldsymbol{Q}_i$. It may be deduced that $\boldsymbol{Q}_i \cdot \boldsymbol{P}_j = 0$, $i, j \in \{1, 2\}$. Hence

$$\boldsymbol{M} \;:=\; \boldsymbol{L}_2\boldsymbol{L}_1 \;=\; \boldsymbol{P}_2\boldsymbol{Q}_2\boldsymbol{P}_1\boldsymbol{Q}_1 \;=\; -\overbrace{\boldsymbol{P}_2\boldsymbol{P}_1}^{\boldsymbol{T}_o}\overbrace{\boldsymbol{Q}_2\boldsymbol{Q}_1}^{\boldsymbol{R}} \;\equiv\; \boldsymbol{T}_o\boldsymbol{R}.$$

Therefore, equation (3.70) can be used to extract $\boldsymbol{T}_o$. Given a point $\boldsymbol{a}$, the distance between the lines may then be computed by means of

$$\mathtt{d}_{[\boldsymbol{L}_1,\boldsymbol{L}_2]} \;=\; \mathtt{d}_{[\boldsymbol{a},\boldsymbol{T}_o\boldsymbol{a}\widetilde{\boldsymbol{T}_o}]} \;=\; \sqrt{-2\boldsymbol{a}\cdot(\boldsymbol{T}_o\boldsymbol{a}\widetilde{\boldsymbol{T}_o})},$$

where, for instance, $\boldsymbol{a} = \mathbf{e}_o$ can be selected.

Chapter 4

A Primer on Pose Estimation with CGA

In this chapter it is delved into the subject of perspective pose estimation, specifically from a CGA standpoint. A method for estimating the pose of a camera from one image of a known object is to be presented. The method emerges from a purely geometric approach and does entirely reside in conformal geometric algebra.

In pose estimation the orientation and position of one internally calibrated camera is recovered from its images. For example, when a criminal investigator tries to infer the perspective from which a photo was initially taken, he basically does pose estimation. If the same task is to be automated, as here, all information must be made available in a digitized form: the 3D-point model of at least one pictured object is assumed to be known together with a set of correspondences, which correctly interrelate model points and image points. This kind of pose estimation is often referred to as the 'perspective N-point problem' (PNP).

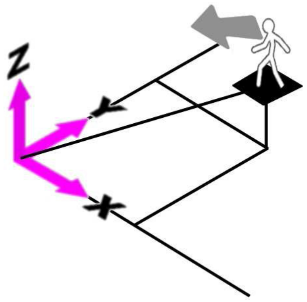

Fig. 4.1: Pose in general: position and orientation

One step prior to pose estimation is usually to assure to have an internally calibrated camera. This involves the determination of all those camera parameters that do not depend on position and orientation of the camera in space. These so-called *intrinsic parameters* are the principal point offset (the coordinates of the pixel where the optical axis hits the image plane), the focal length and, if needed, the distortion coefficients.

If the pictured 3D-object is described in camera coordinates, with origin at the optical center of the camera, it is possible to specify the equation of every *projection ray* given the respective image point of an internally calibrated camera. However, having the 3D-point model in terms of the camera coordinate system is very unlikely, except the model has been transformed, as the camera may move around.

If the projection rays, and thus the whole imaging system, are to be expressed with respect to an external world coordinate system, six additional *extrinsic parameters* have to be introduced. They reflect a *rigid body motion* (RBM), consisting of a rotation and a translation, so as to allow for an arbitrary position and orientation of the camera in respect to the external coordinate system. So in short, determining the RBM is pose estimation.

4.1 The overall Principle

The general approach to the pose estimation problem in the text bases on the following key assumptions:

1. a 3D-point model of the pictured object, given in respect to an external world coordinate system, is available
2. for each point in the object model the corresponding image point (object pixel) can be determined if it exists (view dependent)[1]
3. for each object pixel a projection ray, expressed in terms of the camera coordinate system, can be computed

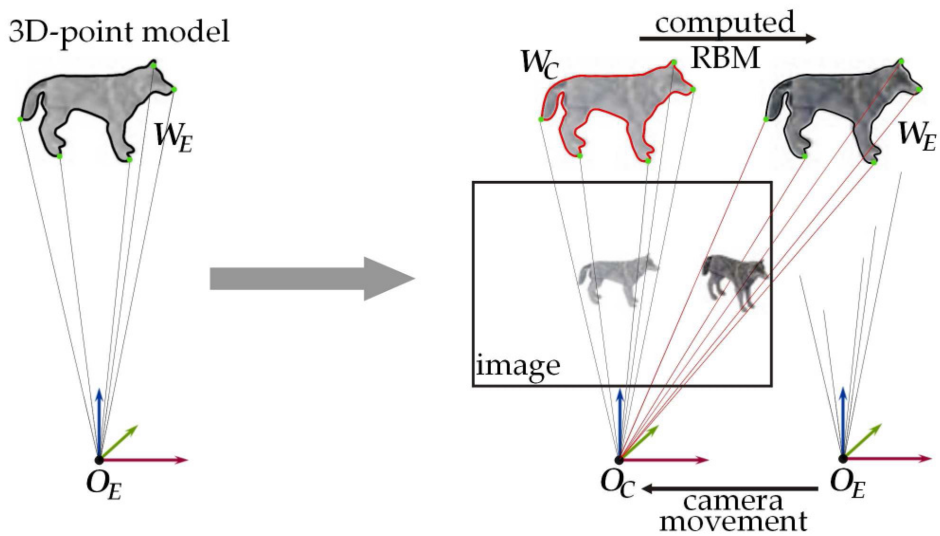

Fig. 4.2: Pose estimation: fitting the red wolf $\boldsymbol{W}_C$ to the computed red projection rays, the black wolf $\boldsymbol{W}_E$ is obtained being the connection to the external coordinate system $\boldsymbol{O}_E$. The inverse RBM (a translation only) then reflects the camera pose.

The principle shall be demonstrated with the help of figure 4.2. There the 'object model' is given by the wolf $\boldsymbol{W}_E$. It is defined with respect to the external coordinate system at $\boldsymbol{O}_E$. The camera with its optical center $\boldsymbol{O}_C$ is assumed to move off the coordinate system at $\boldsymbol{O}_E$ in a fronto-parallel manner, i.e. sideways on, with respect to the flank of the wolf.

[1]The correspondence problem is referred to as 'matching'.

Since the wolf $\boldsymbol{W}_E$ is rigidly connected to its coordinate system by means of the coordinates themselves, any transformation of the wolf can likewise be considered a transformation of its coordinate system. Now if the wolf $\boldsymbol{W}_E$, in its $\boldsymbol{O}_E$-representation, is placed in the camera coordinate system, the wolf $\boldsymbol{W}_C$ is obtained; it would project to the left palish drawn wolf on the image plane. The idea for solving the pose estimation problem is to rigidly transform $\boldsymbol{W}_C$ such that its projection comes into agreement with the 2D-sensory data of the camera, i.e. if the pale and dark wolf coincide. Note that, technically, the agreement is established in 3D rather than on the image plane; the 3D-point model is transformed such that each model point comes to lie on its respective projection ray[2] (expressed as a conformal line), see the figures 4.2 and 4.3. This technique is referred to as *2D-3D pose estimation*, cf. [57, 105]. Of central importance for PNP, also regarding later chapters, is the corresponding CGA condition equation

$$(\boldsymbol{M}\boldsymbol{a}_{\underline{\mathrm{i}}}\widetilde{\boldsymbol{M}}) \cdot \boldsymbol{L}_{\underline{\mathrm{i}}} \stackrel{!}{=} \mathbf{0}, \tag{4.1}$$

which has to be fulfilled by the RBM $\boldsymbol{M}$ for every pair of model point and projection ray $(\boldsymbol{a}_{\underline{\mathrm{i}}}, \boldsymbol{L}_{\underline{\mathrm{i}}})$, $1 \leq \underline{\mathrm{i}} \leq N$. Provided this condition holds, both wolves, $\boldsymbol{W}_E$ and the transformation of $\boldsymbol{W}_C$, coincide. Especially, if the computed RBM is applied to the basis vectors at $\boldsymbol{O}_C$, the coordinate frame at $\boldsymbol{O}_E$ is obtained, and the pose of the camera is given by the inverse RBM.

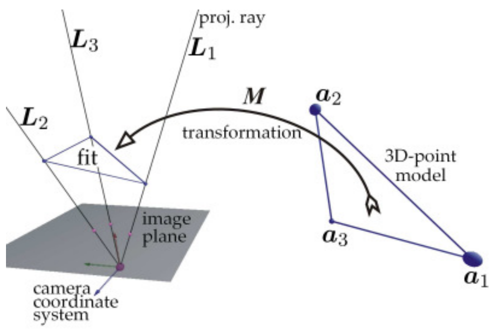

Fig. 4.3: 3-point pose estimation in 3D

Hence the technique for solving the pose estimation problem consists in finding the best position and orientation of the 3D-point model inside the projection rays, which is called *fitting*. This best *fit* is equivalent to the camera pose in that both can be calculated from each other.

4.2 Overview

The method to be presented here [42] can be subdivided as follows: initially problems covering only subsets of three feature points are solved and globally assessed. For this purpose the object model is pruned and rigidly fitted to the three corresponding projection rays by evaluating a succinct CGA expression which will be

[2]This method is unique if four or more model points are involved unless they form a critical configuration, see [4]. Clearly, in case of symmetries in the model multiple solutions arise.

derived from geometric considerations. It results a set of 3-point poses each given by a motor. These spinor elements of CGA embody rigid body motions from the manifold $SE(3)$, see section 3.4.5. The poses are then to be averaged according to their quality. This is the second key aspect of this chapter as the respective motors do not come from a linear space and averaging must be carried out appropriately [55]. Accordingly, a technique called weighted intrinsic mean is used.

The geometric formulation of P3P by means of CGA simultaneously motivates a sound subset selection strategy for *point triplets* (a group of three points), i.e. not all possible 3-combinations in the correspondences must be considered. It will become apparent that the respective P3P-solution is fully determined by a certain angle θ^* only. The geometric approach further leads to an algebraic function $h(\theta) \in \mathbb{R}$, with θ^* being a root of which. For each root the corresponding RBM is globally assessed regarding its effect on the entire N-point scenario. The set of 3-point candidate solutions can then be reduced by solutions from obviously false correspondences. This relaxes the requirement of knowing all correspondences beforehand. The remaining RBMs, at most one for every triplet considered, are finally averaged by means of the weighted intrinsic mean, which is tailored to elements of $SE(3)$.

4.3 Related Work PNP

The classic but challenging task of pose estimation is from the field of computer vision. Most approaches to that subject are iterative, highly non-linear or require an initialization. Closed form solutions to the 3-point problem (P3P), where the number of correspondences is three, exist [58, 86] but may result in up to four distinct solutions because P3P is not necessarily unique. As extension to P3P it is also possible to consider four points. Fischler and Bolles [31], for example, take subsets and perform consistency checks to eliminate the P3P ambiguity for most point configurations. In [101] Quan and Lan present an algorithm capable of finding the unique solution to PNP. They first generate a global system of linear equations based on all correspondences. Next, the exact 3D-vectors to the object points w.r.t. the camera coordinate system are estimated. Finally, camera orientation and position are evaluated one after another. But this class of techniques is shown in [66] to improperly model the physical imaging, i.e. a perspective projection must be considered. Rosenhahn and Sommer [104] formulate algebraic constraints with CGA. They obtain a hybrid system of linear equations based on correspondences between points, lines and between point and line. Starting from an initialization the pose is iteratively estimated in 3D. It is to mention that such global PNP approaches are not able to spot and disregard false or noisy correspondences.

4.4 Thales' Theorem Revisited

In this section it is demonstrate how a simple geometric theorem motivates a solution to P3P.

The generalization of Thales' theorem states that, given a circle $\boldsymbol{K}$, the centric angle $\angle(\boldsymbol{x}_1',\boldsymbol{m},\boldsymbol{x}_1)$ at $\boldsymbol{m}$ is twice the peripheral angle $\angle(\boldsymbol{x}_1',\boldsymbol{O},\boldsymbol{x}_1)$ at $\boldsymbol{O}$, cf. figure 4.4. This fact can be used to define two successive rotations: the first rotates $\boldsymbol{x}_1$ to $\boldsymbol{x}_1'$ and the second rotates $\boldsymbol{x}_1'$ back onto the straight line connecting $\boldsymbol{O}$ and $\boldsymbol{x}_1$; the point $\boldsymbol{x}_1''$ is obtained. It is crucial that any second point $\boldsymbol{x}_2$ on $\boldsymbol{K}$ also moves directly towards $\boldsymbol{O}$ when applying the same rotations. Moreover, the distance from $\boldsymbol{x}_1$ to $\boldsymbol{x}_2$ stays constant since rotations are distance preserving.

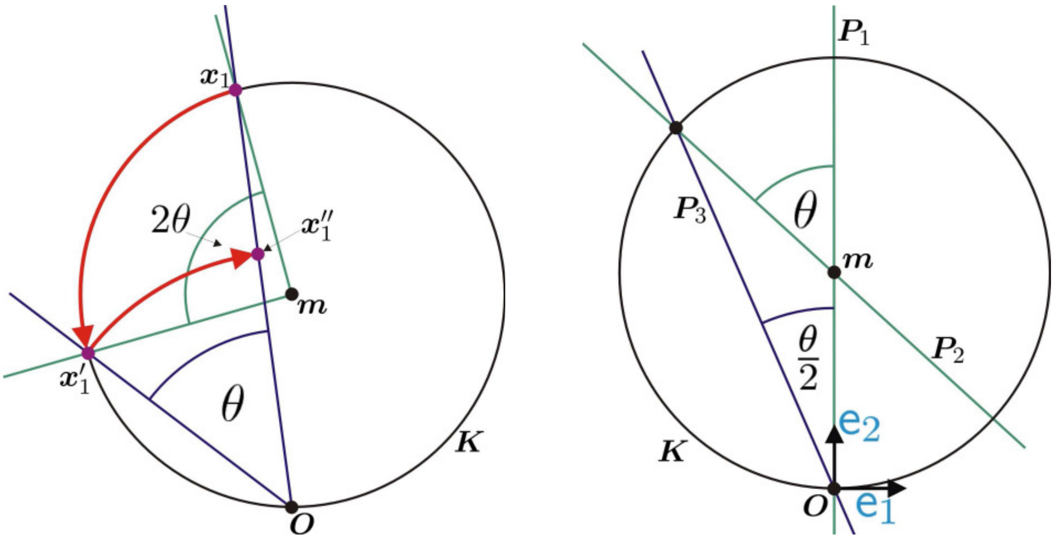

Fig. 4.4: Left: the generalization of Thales' theorem explains why two successive rotations form a translation. Right: the transformation can be realized by a sequence of four reflections in three well-chosen planes $\boldsymbol{P}_1$, $\boldsymbol{P}_2$ and $\boldsymbol{P}_3$. The overall transformation is then $\boldsymbol{R}_\theta = \boldsymbol{P}_1\boldsymbol{P}_3\boldsymbol{P}_2\boldsymbol{P}_1$.

Before the value of this observation is enlightened, the coupled transformation, denoted by $\boldsymbol{R}_\theta$, is being worked out in terms of a CGA expression. Therefore each of the two rotations is replaced by two reflections in suitable planes as indicated on the right side of figure 4.4. Two rules have to be obeyed: the dihedral angle between two planes that are supposed to represent a rotation must be half the rotation angle. Further, the line of intersection between the planes must coincide with the rotation axis. The two rotations can ultimately be realized by four reflections in the three planes $\boldsymbol{P}_1$, $\boldsymbol{P}_2$ and $\boldsymbol{P}_3$ because plane $\boldsymbol{P}_1$ can be used twice. The order of application must be $\boldsymbol{P}_1$, $\boldsymbol{P}_2$, $\boldsymbol{P}_3$ and $\boldsymbol{P}_1$ again. From this the motor $\boldsymbol{R}_\theta = \boldsymbol{P}_1\boldsymbol{P}_3\boldsymbol{P}_2\boldsymbol{P}_1$ can be obtained, cf. section 3.4.3. For the derivation a canonical coordinate system can be taken as a basis, cf. section 2.3.4, page 68. Let

$$\begin{aligned}
\boldsymbol{P}_1 &= \mathbf{e}_1, \\
\boldsymbol{P}_2 &= \cos(\theta)\,\mathbf{e}_1 + \sin(\theta)\,(\mathbf{e}_2 + r\,\mathbf{e}) \qquad \text{and} \\
\boldsymbol{P}_3 &= \cos(\theta/2)\,\mathbf{e}_1 + \sin(\theta/2)\,\mathbf{e}_2,
\end{aligned}$$

where r denotes the radius of circle $\boldsymbol{K}$. After some algebra it follows

$$\begin{aligned}\boldsymbol{R}_\theta &= \cos(\theta/2) + \sin(\theta/2)\Big[\underbrace{\mathbf{e}_1\mathbf{e}_2 + r\Big((\cos(\theta)+1)\mathbf{e}_1\mathbf{e} + \sin(\theta)\mathbf{e}_2\mathbf{e}\Big)}_{\boldsymbol{L}_\theta}\Big] \\ &= \exp\Big(\theta/2\ \boldsymbol{L}_\theta\Big)\,. \end{aligned} \tag{4.2}$$

The element $\boldsymbol{L}_\theta$ is a line representing the rotation axis of $\boldsymbol{R}_\theta$ and plays the role of the imaginary unit i of complex numbers, for $\boldsymbol{L}_\theta^2 = -1$[3]. On writing

$$\boldsymbol{R}_\theta = \boldsymbol{P}_1(\boldsymbol{P}_3\boldsymbol{P}_2)\boldsymbol{P}_1$$

it can be recognized that $\boldsymbol{R}_\theta$ is the reflection of $\boldsymbol{R}'_\theta := \boldsymbol{P}_3\boldsymbol{P}_2$ in plane $\boldsymbol{P}_1$. Hence $\boldsymbol{R}_\theta$ rotates by an angle θ being twice the dihedral angle between $\boldsymbol{P}_3$ and $\boldsymbol{P}_2$. The position of $\boldsymbol{R}_\theta$ is depicted on the left of figure 4.5.

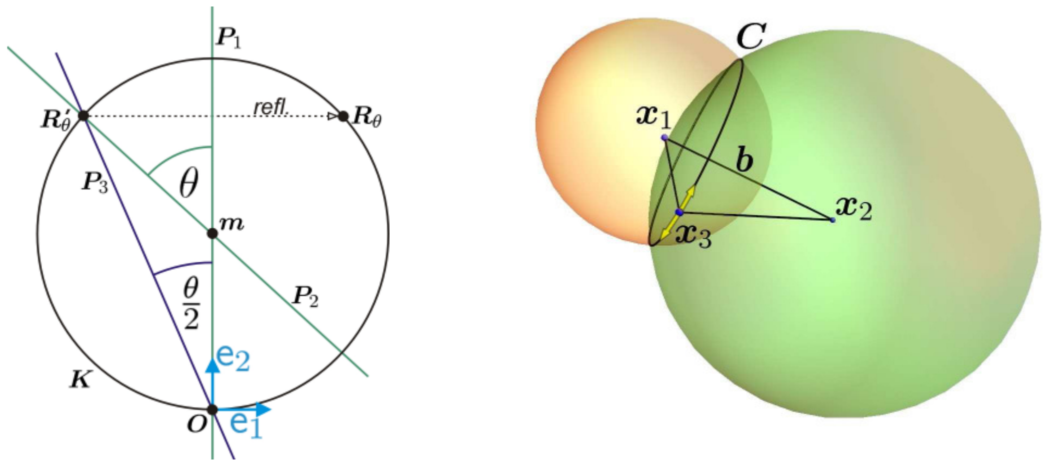

Fig. 4.5: Left: depending on the angle θ, the motor $\boldsymbol{R}_\theta$ 'orbits' around circle $\boldsymbol{K}$. Right: each point $\boldsymbol{x}_3$ on the circle $\boldsymbol{C}$ guarantees a congruent triangle.

Recall that initially 3-point problems are to be tackled. Thus 3-point models (triangles) have to be fitted to three corresponding projection rays. Clearly, a two-point model can easily be fitted: simply follow the angle bisector of two projection rays until the model forms an isosceles triangle with the projection rays, where $\boldsymbol{O}$ is considered the optical center of the camera. Then one possible 2-point fit is accomplished. Now let $\boldsymbol{K}$ be the unique circumcircle of that triangle, whence the canonical coordinate system[4] and the motor $\boldsymbol{R}_\theta$ can be defined. Thus a two-point model can rigidly be moved such that the constituent model points $\{\boldsymbol{x}_1, \boldsymbol{x}_2\}$ remain on their respective projection rays, i.e. the 2-point fit may be varied w.r.t. θ. Note that certain fits must necessarily be extendable to 3-point fits if these exist.

[3]Not to be confused with one of the projection rays.
[4]Notice that the canonical coordinate system is actually made use of.

For this purpose it has to be figured out where a third model point $\boldsymbol{x}_3$ can be if $\boldsymbol{x}_1$ and $\boldsymbol{x}_2$ are already fix. As illustrated on the right side of figure 4.5, the locus of possible points is given by a circle $\boldsymbol{C}$. In which way this result may contribute to a solution of the 3-point problem is discussed in the next section.

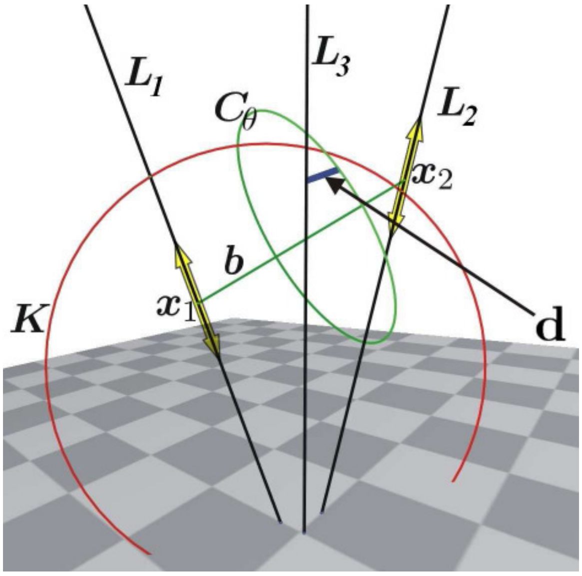

Fig. 4.6: Distance **d** between circle $\boldsymbol{C}_\theta$ and the third projection ray $\boldsymbol{L}_3$.

4.5 The Perspective 3-Point Problem

To recap, three 3D-model points $\{\boldsymbol{x}_1, \boldsymbol{x}_2, \boldsymbol{x}_3\}$ in conjunction with their corresponding image points are considered. From these the respective projection rays $\{\boldsymbol{L}_1, \boldsymbol{L}_2, \boldsymbol{L}_3\}$ are computed so as to fit the model.

Assume that the circle $\boldsymbol{C}$, the locus of the third point $\boldsymbol{x}_3$, would likewise be subjected to $\boldsymbol{R}_\theta$ while the same transformation is used to move $\boldsymbol{x}_1$ and $\boldsymbol{x}_2$ along their respective projection rays[5], see figure 4.6. Let $\boldsymbol{C}_\theta$, $\theta \in (-\pi, \pi]$, denote this rotated version of the circle $\boldsymbol{C} = \boldsymbol{C}_0$, i.e.

$$\boldsymbol{C}_\theta \;:=\; \boldsymbol{R}_\theta \boldsymbol{C} \widetilde{\boldsymbol{R}_\theta}.$$

Note that $\boldsymbol{C}$ denotes the initial circle where $\boldsymbol{x}_1, \boldsymbol{x}_2$ and $\boldsymbol{O}$ form the isosceles triangle ($\boldsymbol{x}_1, \boldsymbol{x}_2$ lie on $\boldsymbol{K}$). Then a possible 3-point fit is obtained if $\boldsymbol{C}_\theta$ intersects the third projection ray $\boldsymbol{L}_3$; the point of intersection is the sought position of $\boldsymbol{x}_3$. Subsequently, a way for determining θ is presented.

As shown in the table on page 93, the intersection of a line (projection ray) and a circle gives a point, unless line and circle do not intersect. Generally, the corresponding CGA expression $\boldsymbol{C}_\theta \wedge \boldsymbol{L}_3$ represents a sphere. Since only degenerate

[5]The assumed $\mathbf{e}_1\mathbf{e}_2$-coordinate system is accordingly extended to three dimensions.

spheres, these are conformal points, square to zero, a suitable function for retrieving θ is

$$h(\theta) \;=\; (\boldsymbol{C}_\theta \wedge \boldsymbol{L}_3)^2 \;\in \mathbb{R}. \tag{4.3}$$

It is a relatively simple, univariate and scalar valued algebraic distance function with compact support. In order to evaluate the, at most four, roots $\Theta = \{\theta_1, \theta_2, \ldots, \theta_k\}$, $k \leq 4$ of $h(\theta)$, the iterative *Newton-Raphson* method is employed because all derivatives are analytically available.

The derivative of $h(\theta) = (\boldsymbol{R}_\theta \boldsymbol{C} \widetilde{\boldsymbol{R}_\theta} \wedge \boldsymbol{L})^2$ w.r.t. angle θ can be calculated by taking advantage of the chain rule. Differentiation of the inner term yields

$$\frac{d}{d\theta}\Big(\boldsymbol{R}_\theta \boldsymbol{C} \widetilde{\boldsymbol{R}_\theta} \wedge \boldsymbol{L}_3\Big) \;=\; \left[\left(\frac{d\boldsymbol{R}_\theta}{d\theta}\right) \boldsymbol{C} \widetilde{\boldsymbol{R}_\theta} + \boldsymbol{R}_\theta \boldsymbol{C} \left(\frac{d\widetilde{\boldsymbol{R}_\theta}}{d\theta}\right)\right] \wedge \boldsymbol{L}_3.$$

According to the previous result in equation (4.2), it can be seen that

$$\frac{d\boldsymbol{R}_\theta}{d\theta} \;=\; \frac{\boldsymbol{R}_\theta}{2}\Big[\boldsymbol{L}_\theta + \theta\,\frac{d\boldsymbol{L}_\theta}{d\theta}\Big].$$

It remains to build the derivative of the orbiting line $\boldsymbol{L}_\theta$, which turns out to be

$$\frac{d\boldsymbol{L}_\theta}{d\theta} \;=\; r\,(\cos(\theta)\mathbf{e}_2\mathbf{e} - \sin(\theta)\mathbf{e}_1\mathbf{e}).$$

At this point the derivative of equation (4.3) follows after substituting, in reverse order, the partial solutions into each other.

Let θ_i^k, $k \in \mathbb{N}_0$, be the value of iteration k that belongs to the i^{th} root of $h(\theta)$. Then a typical Newton-Raphson update step is

$$\theta_i^{k+1} \;=\; \theta_i^k \;-\; \left[h(\theta) / \frac{d}{d\theta}h(\theta)\right]_{\theta\,=\,\theta_i^k}$$

Being in the possession of the roots $\Theta = \{\theta_1, \theta_2, \ldots, \theta_k\}$ P3P is not yet solved: at first, the respective motors $\boldsymbol{R}_{\theta\in\Theta}$ and 3-point fits are calculated. In a second step each fit is carried over from the canonical coordinate system back to the camera coordinate system. There the interrelating motor[6] $\boldsymbol{M}_\theta$, being the connection between camera and world coordinate system, is estimated by means of standard methods, see [5, 72]. In case of perfect measurements, i.e. if all data was free from errors, one of the motors $\boldsymbol{M}_{\theta\in\Theta}$ would already be the solution to the entire N-point problem so that identity (4.1) would be fulfilled. Since this is unrealistic, the aim must be to pick the best pose candidate available. Consequently, each motor is applied to the N-point model. Next the Euclidean distances between transformed model points and corresponding projection rays are calculated, which eventually yields a set of root mean square distances; the motor with the smallest distance is selected as the solution to P3P.

[6] In this case a transformation between two congruent point triplets (not collinear).

4.5.1 Crucial triplets

It remains to specify the subset selection strategy for triplets in order to put a limit on the computational complexity $\binom{N}{3}$. The solution arises from the observation that the impact of noise on two nearby projection rays is much stronger than the impact on two distant ones when subjected to pose estimation algorithms. Hence those triplets are selected the image points of which form maximum area triangles on the image plane. Then the effects caused by the noise of the image point coordinates are minimized as the possible uncertainty of the model in the projection rays cannot carry much weight in a relative sense. As a byproduct, cases in which all three projections rays are (nearly) coplanar are avoided.

The selection procedure is as follows: point by point, a suitable supplementary point pair is selected such that the resultant triplet fulfils the maximum area condition. In case a triangle is already assigned, the next biggest triangle is considered. Thus each point is at least once contained in a 'big' triangle. Eventually, N triplets are obtained, which are all to be input to the three point algorithm. The respective results, i.e. the motors $\{\boldsymbol{M}_1, \boldsymbol{M}_2, \ldots, \boldsymbol{M}_N\}$, have to be merged if one decides against a 'the winner takes it all'-strategy. This process in particular has to be done correctly.

4.6 The Perspective N-Point Problem

As already announced, the issue regarding the fusion of the P3P motors $\{\boldsymbol{M}_1, \boldsymbol{M}_2, \ldots, \boldsymbol{M}_N\}$ is the second key aspect. Since any motor is from the Lie group $SE(3)$, being a manifold, the customary arithmetic mean must not be used:

$$A, B \in SE(3) \quad \not\Rightarrow \quad A + B \in SE(3).$$

The Lie group $SE(3)$ is connected to its Lie algebra $se(3)$ (tangent space to the identity element of $SE(3)$) by the `exp`/`log` map. Note that in $se(3)$ any customary mean can be built as the algebra elements form a vector space. This is exploited by the 'weighted intrinsic mean', in which the `log` map [22] is used to compute first-order mean approximations via the tangent space, see [33, 14]. The N motors are input to the outlined algorithm below, where the weights w_i, $1 \leq i \leq N$, reflect the motor assessments. Starting from the motor $\boldsymbol{M} = \texttt{identity}$ the subsequent three steps are repeated until $||\texttt{log}(\Delta\boldsymbol{M})||$ falls below a certain threshold ϵ.

$$\begin{array}{llcll} 1. & \Delta\boldsymbol{A}_i & = & \log\big(\boldsymbol{M}^{-1}\boldsymbol{M}_i\big) & 1 \leq i \leq N \\ 2. & \Delta\boldsymbol{M} & = & \exp\Big(\frac{1}{W}\sum_{i=1}^{N} w_i\,\Delta\boldsymbol{A}_i\Big) & W = \sum_{i=1}^{N} w_i \\ 3. & \boldsymbol{M} & = & \boldsymbol{M}\,\Delta\boldsymbol{M} & \end{array} \tag{4.4}$$

Notice that the motor $\boldsymbol{M}$ is repeatedly updated by the residuals $\Delta\boldsymbol{M}$, which originate from the weighted averaging of algebra elements $\Delta\boldsymbol{A}_i$, $1 \leq i \leq N$. The term

$\boldsymbol{M}^{-1}\boldsymbol{M}_i$ in step 1 moves the input closer to the identity element of $SE(3)$ in order to minimize the averaging error in step 2. A derivation of the algorithm and a uniqueness proof is given in [16].

Experimental results can be found in section 7.3.1, where the presented method serves to provide initial estimates.

Chapter 5

Parameter Estimation

The combination of a stochastic parameter estimation with geometric algebra is one of the fundamental aspects of this work. What makes these two concepts go well together is the bilinearity of the main algebra product - the geometric product.

The throughout employed estimation method, hereafter called the *Gauss-Helmert* method (GH-method), amounts to the most general from of least squares adjustment, cf. [74]. It is founded on the homonymous linear model, which has basically been introduced by Helmert in 1872 [60].

In this chapter, all relevant aspects concerning the parameter estimation as used in the scope of this thesis are detailed, but an introduction to the underlying probability theory cannot be provided. At first, a brief overview and a theoretical categorization of the most common estimation methods, together with the respective terminology, is given. All then following explanations and derivations are intended to be from a practical point of view.

5.1 Introduction

In general, the object of estimation theory is the inference about a population of entities by appropriately analyzing observations, that is samples, drawn from the respective population. This can include testing a hypothesis, making a prediction and of course estimating parameters. These are more or less explicitly the parameters of a probability density function (pdf); the parameters used in a functional model that describes the observation-generating process possess a distribution, too. If a distribution is to be estimated in terms of the pdf itself, it must be differentiated between two philosophies:

Parametric estimation: The outcome are parameters, or confidence intervals of which, that characterize a certain aspect, e.g. the pdf, of the problem at hand. Several assumptions can flow into the estimation: the type of the distribution might be known a priori or knowledge about the functional model, say a linear dependence between the samples and the parameters, may be incorporated.

Non-parametric estimation: If a distribution cannot be parameterized in a sensible way, like by the first two moments in case of the normal (Gaussian) distribution, it is advisable to employ the non-parametric estimation. No assumption about the distribution of the population is made. As a benefit, no wrong assumptions can be made. The outcome is, comparable to interpolation, an approximation of the pdf. The simplest example would be a histogram. Further to mention is the kernel density estimation.

Subsequently, the key ideas concerning parametric estimation are to be conveyed. Besides, the five quality criteria *unbiasedness, minimal variance, consistency, efficiency, sufficiency and robustness* for estimators are briefly explained. After that a small example on parameter estimation is given.

Note that *random variables* are labeled with an underset tilde, e.g. $\utilde{\mathsf{y}}$. However, most of the time it is dealt with *realizations* y of random variables $\utilde{\mathsf{y}}$.

5.1.1 Point Estimation: a Motivation

A case in point is the estimation of the mean. Let $\utilde{X}_1, \ldots, \utilde{X}_k$ be independent and identically distributed (i.i.d.) random variables. Assume a normal distribution with mean μ and variance σ^2, denoted by $\utilde{X}_i \sim N(\mu; \sigma^2)$. Let $x_1 \ldots x_k$ be a *sample* from the random variables $\utilde{X}_1 \ldots \utilde{X}_k$. Then the *sample mean*

$$\overline{x} \; := \; \frac{1}{n} \sum_{i=1}^{k} x_i$$

is an estimator for the *population mean* μ.

So generally, the result of estimating a parameter from one realization of the random variables $\utilde{X}_1, \ldots, \utilde{X}_k$, $k \geq 1$, is referred to as *point estimation.* If, in contrast, the intervals are to be determined in which a parameter (or a function of which) lies with a certain given probability, an *interval estimation* must be used. A point estimator can be considered a zero-length interval estimator because this corresponds to finding the (infinitesimal) interval of maximal probability. In the following, however, it is only dealt with point estimation.

Calculating the expectation $\mathrm{E}(\overline{\utilde{X}})$ of the respective $\overline{\utilde{X}}$

$$\mathrm{E}(\overline{\utilde{X}}) \; = \; \mathrm{E}(\frac{1}{k} \sum_{i=1}^{k} \utilde{X}_i) \; = \; \frac{1}{k} \sum_{i=1}^{k} \mathrm{E}(\utilde{X}_i) \; = \; \frac{1}{k} \sum_{i=1}^{k} \mu \; = \; \mu \; = \; \mathrm{E}(\utilde{X}_i),$$

where $i \in [1,k]_{\mathbb{Z}}$, shows that the estimator is *unbiased*, which means that no systematic error is introduced. This is not natural: in order to estimate σ^2, the *corrected* sample variance s_x^2 must be used, that is it must be divided by $k-1$ rather than by k

$$s_x^2 \; := \; \frac{1}{k-1} \sum_{i=1}^{k} (x_i - \overline{x})^2,$$

otherwise an (asymptotically vanishing) bias would occur.

As an estimator depends on the samples it computes the estimate from, the estimator itself is a random variable as well. An estimate[1], denoted by $\hat{\theta}(x_1, \ldots, x_k)$, of the true parameter $\check{\theta}$ is a realization of its estimator, denoted by $\underset{\smile}{\hat{\theta}}(\underset{\smile}{X}_1, \ldots, \underset{\smile}{X}_k)$.

Aside: *In estimation theory, the estimation is usually extended to real valued functions $\gamma(\check{\theta})$ of the parameter(s), for example $\gamma(\check{\theta}) = 1/\check{\theta}^2$ or $\gamma(\check{\theta}) = \alpha_1\check{\theta}_1 + \alpha_2\check{\theta}_2$, such that $\gamma(\check{\theta})$ is to be estimated. An estimator is defined as a real valued measurable function defined on the sample space.*

Next to an expectation, as determined above, the estimator must possess a variance, too. A further criterion, next to unbiasedness, for a good estimator $\underset{\smile}{\hat{\theta}}$ is therefore the *minimal variance property*

$$\forall \theta \in \Theta : \qquad \underset{\smile}{\hat{\theta}}(\underset{\smile}{X}_1, \ldots, \underset{\smile}{X}_k) \;=\; \underset{\underset{\smile}{\hat{\theta}}^* \text{ unbiased}}{\operatorname{argmin}} \; \operatorname{Var}(\underset{\smile}{\hat{\theta}}^*(\underset{\smile}{X}_1, \ldots, \underset{\smile}{X}_k)),$$

where Θ is the *parameter space*. The unbiased minimum-variance estimator (MVUE) is uniquely defined. However, the general error of an estimator is measured by its mean square error (MSE)

$$\operatorname{MSE}(\underset{\smile}{\hat{\theta}}) \;=\; \big[\underbrace{\gamma(\check{\theta}) \;-\; \operatorname{E}(\underset{\smile}{\hat{\theta}})}_{\text{bias}}\big]^2 \;+\; \operatorname{Var}(\underset{\smile}{\hat{\theta}}).$$

Consequently, it must be taken into account that there may be a biased estimator with a lower error than the unbiased minimum-variance estimator.

For an (infinitely) increasing number of samples the estimate $\hat{\theta}$ should get arbitrarily close to the true parameter $\gamma(\check{\theta})$ (*consistency* criterion); the estimator is required to converge in probability to the estimate

$$\forall \epsilon > 0 : \qquad \lim_{k \to \infty} P(|\, \underset{\smile}{\hat{\theta}}(\underset{\smile}{X}_1, \ldots, \underset{\smile}{X}_k) \;-\; \gamma(\check{\theta})\,| < \epsilon\,) \;=\; 1,$$

where $P(A)$ denotes the probability of some event A.

The next three criteria are somewhat involved and do not have enough relevance for this work to give a comprehensive discussion.

An estimator is said to be *efficient* if its variance attains the theoretically minimal possible variance. Hence only unbiased minimum-variance estimators can fulfill the efficiency requirement.

An estimator is called *sufficient* if all the relevant information about $\check{\theta}$ contained in $\underset{\smile}{X}_1, \ldots, \underset{\smile}{X}_k$ is as well available to $\underset{\smile}{\hat{\theta}}(\underset{\smile}{X}_1, \ldots, \underset{\smile}{X}_k)$. For example, let the i.i.d. random variables $\underset{\smile}{X}_1, \ldots, \underset{\smile}{X}_k$ be normally distributed $\underset{\smile}{X}_i \sim N(\mu; \sigma^2)$ with probability density function

$$\begin{aligned} f(x_1, \ldots, x_k) \;&=\; (\sqrt{2\pi}\,\sigma)^{-k}\, e^{-\frac{1}{2\sigma^2} \sum\limits_{i=1}^{k} (\mu - x_i)^2} \\ &=\; (\sqrt{2\pi}\,\sigma)^{-k}\, e^{-\frac{k\mu^2}{2\sigma^2}}\, e^{-\frac{1}{2\sigma^2} \sum\limits_{i=1}^{k} x_i^2}\, e^{\frac{\mu}{\sigma^2} \sum\limits_{i=1}^{k} x_i}. \end{aligned}$$

[1] A hat on top of a variable usually indicates estimates and estimators, whereas a check ($\check{\theta}$) always denotes the true parameter(s).

Hence the pdf can be expressed in terms of $G_1(x_1,\dots,x_k) := \sum_{i=1}^k x_i$ and similarly $G_2(x_1,\dots,x_k) := \sum_{i=1}^k x_i^2$ such that the reduced information $(x_1,\dots,x_k) \mapsto (G_1,G_2) \in \mathbb{R}^2$ is still sufficient to estimate the parameters of the distribution. The corrected sample variance can be estimated via

$$\begin{aligned} s_x^2 &= \frac{1}{k-1}\sum_{i=1}^{k}(x_i-\overline{x})^2 = \frac{1}{k-1}\Big(\sum_{i=1}^{k} x_i^2 - \frac{1}{k}\big(\textstyle\sum_{i=1}^k x_i\big)^2\Big) \\ &= \frac{G_2(x) - k\,G_1(x)^2}{k-1}. \end{aligned}$$

Likewise, it is $\overline{x} = G_1(x)/k$.

It is often possible to state an optimal estimator with respect to the above criteria and to the assumed model. But what if this model is not fully appropriate? Wrong decisions would be the consequence. Moreover, as samples ultimately represent (noisy) measurements, there might be outliers - caused either manually by a human observer or even automatically, for example, by an algorithm. Estimators that are less sensitive to a poorly chosen model and that are tolerant of outliers are termed *robust* estimators. The median, for instance, can be considered a robust estimator of the mean.

5.1.2 Parameter Estimation Methods

Here a short overview of various estimation methods is given. The method of least squares adjustment is detailed in section 5.2 so as to emphasize its special importance. After that the Gauss-Helmert method is explained in detail in section 5.3.

Method of Moments

The principle of the method of moments is simply to compute the parameters of a pdf from the sample moments. The already stated estimator $\overline{x}$ for the sample mean, for example, is obtained by this method. Estimating the sample variance gives the biased version $\frac{k-1}{k}\,s_x^2$. Consider the uniform distribution with pdf

$$f(x,k_1,k_2) = \frac{\mathbf{1}_{[k_1,k_2]}(x)}{k_2-k_1},$$

where the indicator function is employed. The population mean and variance are

$$\mu = \frac{k_1+k_2}{2} \qquad \text{and} \qquad \sigma^2 = \frac{(k_2-k_1)^2}{12}, \text{ respectively.}$$

By identifying $\mu \approx \overline{x}$, it follows $k_1 \approx 2\overline{x} - k_2$ and consequently $s_x^2 \approx 4(k_2-\overline{x})/12 = (k_2-\overline{x})/3$. Thus

$$\hat{k}_{1/2} = \overline{x} \mp \sqrt{3\,s_x^2}.$$

Generalized Method of Moments

In case of the generalized method of moments (GMM), a technique widely used in econometrics, a parameter vector is estimated by minimizing the sum of squares of the differences between the population moments and the sample moments. The key to the GMM are the orthogonality or moment conditions

$$\mathrm{E}(\mathsf{m}(\check{\boldsymbol{\theta}}, \utilde{\mathsf{y}}_t)) \;=\; \mathsf{0}, \qquad t \in \{1, 2, \ldots, k\}$$

where $\mathsf{m} : \mathbb{R}^{M\times T} \to \mathbb{R}^Q$ can be an arbitrary non-linear function of the true parameters $\check{\boldsymbol{\theta}} \in \mathbb{R}^M$ and k i.i.d. observations[2] $\mathsf{y}_t \in \mathbb{R}^T$. By the law of large numbers it can be assumed that the population quantity

$$\overline{\mathsf{m}}(\check{\boldsymbol{\theta}}) \;:=\; \frac{1}{k}\sum_{i=1}^{k} \mathsf{m}(\check{\boldsymbol{\theta}}, \mathsf{y}_i)$$

converges in probability to $\mathrm{E}(\mathsf{m}(\check{\boldsymbol{\theta}}, \utilde{\mathsf{y}}_t))$. Hence the respective sample counterpart

$$\overline{\mathsf{m}}(\hat{\boldsymbol{\theta}}_{gm}) \;:=\; \frac{1}{k}\sum_{i=1}^{k} \mathsf{m}(\hat{\boldsymbol{\theta}}_{gm}, \mathsf{y}_i)$$

is supposed to be as close as possible to zero. The least squares solution is therefore $\hat{\boldsymbol{\theta}}_{gm} = \mathrm{argmin}_{\boldsymbol{\theta}\in\boldsymbol{\Theta}}\, \overline{\mathsf{m}}^{\mathsf{T}}\mathsf{W}\overline{\mathsf{m}}$, where $\mathsf{W}(\boldsymbol{\theta})$ denotes a weighting matrix that counteracts scalings of the moments. It exists an optimal weighting matrix $\mathsf{W}^{\mathrm{opt}}(\boldsymbol{\theta})$ which minimizes the asymptotic variance of the estimator. Unfortunately, $\mathsf{W}^{\mathrm{opt}}(\boldsymbol{\theta})$ depends on $\boldsymbol{\theta}$, such that an iterative scheme must be applied. Starting with the identity matrix $\mathsf{W}^{[0]} = \mathsf{I}_Q$, the estimation process is iterated until convergence

$$\hat{\boldsymbol{\theta}}_{gm}^{[j+1]} \;=\; \underset{\boldsymbol{\theta}}{\mathrm{argmin}}\; \overline{\mathsf{m}}^{\mathsf{T}}\mathsf{W}^{[j]}\,\overline{\mathsf{m}}, \qquad j = \{0, 1, \ldots\},$$

where $\mathsf{W}^{[j]} = \mathsf{W}^{[j]}(\hat{\boldsymbol{\theta}}_{gm}^{[j]})$.

Consider, for example, the classical linear regression model $\mathsf{y} = \mathsf{X}\check{\boldsymbol{\beta}} + \boldsymbol{\epsilon}$, where $\mathsf{y} \in \mathbb{R}^k$ is a vector of observations, $\mathsf{X} \in \mathbb{R}^{k\times M}$, $\check{\boldsymbol{\beta}} \in \mathbb{R}^M$, $\boldsymbol{\epsilon} \in \mathbb{R}^k$ and $\mathrm{E}(\utilde{\boldsymbol{\epsilon}}) = \mathsf{0}$. The (componentwise) moment conditions are $\mathrm{Var}(\utilde{\boldsymbol{\epsilon}}_t) = \sigma^2$, $\mathrm{E}(\utilde{\boldsymbol{\epsilon}}_t\utilde{\boldsymbol{\epsilon}}_{s\neq t}) = 0$ and, with $\mathsf{x}^{\mathsf{T}} := \mathsf{X}|_t$, $\mathrm{E}(\utilde{\boldsymbol{\epsilon}}_t\mathsf{x}) = \mathrm{E}((\utilde{\mathsf{y}}_t - \mathsf{x}^{\mathsf{T}}\check{\boldsymbol{\beta}})\mathsf{x}) = 0$. Note that with $\mathsf{x}_1 = 1$, $\mathrm{E}(\utilde{\boldsymbol{\epsilon}}_t) = 0$ is obtained. By the latter assumption, the condition $\mathrm{E}(\utilde{\boldsymbol{\epsilon}}_t\mathsf{x}_{i\neq 1}) = 0$ states[3] that there is no correlation between the variables in X (if regarded as random variables) and the errors $\boldsymbol{\epsilon}$. Notice that this is assumed by default in standard regression problems: the ordinary least squares estimate for the one-dimensional linear model $y_i = \check{\beta}x_i + \epsilon_i$ is

$$\hat{\beta}_{ls} \;=\; \textstyle\sum_i x_i y_i \Big/ \sum_i x_i^2 \;=\; \sum_i x_i(\check{\beta}x_i + \epsilon_i)\Big/\sum_i x_i^2 \;=\; \check{\beta} \;+\; \sum_i x_i\epsilon_i \Big/ \sum_i x_i^2.$$

[2]If the y_t are realizations of a stochastic process, stationarity is required.

[3]$\mathrm{Cov}(\utilde{\boldsymbol{\epsilon}}_t, \utilde{\mathsf{x}}_{i\neq 1}) = \mathrm{E}(\utilde{\boldsymbol{\epsilon}}_t\utilde{\mathsf{x}}_{i\neq 1}) + \mathrm{E}(\utilde{\boldsymbol{\epsilon}}_t)\mathrm{E}(\utilde{\mathsf{x}}_{i\neq 1}) = \mathrm{E}(\utilde{\boldsymbol{\epsilon}}_t\utilde{\mathsf{x}}_{i\neq 1})$

Hence the estimate $\hat{\beta}_{ls}$ only converges to $\check{\beta}$ if x_i and the error ϵ_i are uncorrelated. Otherwise the criteria unbiasedness and consistency are violated.

The sample counterpart of the moment condition $\mathrm{E}((\mathsf{y}_t - \mathsf{x}^\mathsf{T}\check{\boldsymbol{\beta}})\mathsf{x}) = 0$ is

$$\overline{\mathsf{m}}(\hat{\boldsymbol{\beta}}_{gm}) \;=\; \frac{1}{k}\sum_{i=1}^{k}(\mathsf{y}_i - \mathsf{x}^\mathsf{T}\hat{\boldsymbol{\beta}}_{gm})\mathsf{x} \;=\; \frac{1}{k}\mathsf{X}^\mathsf{T}(\mathsf{y} - \mathsf{X}\hat{\boldsymbol{\beta}}_{gm}) \;\overset{!}{\approx}\; 0,$$

which leads, for the chosen model, to the ordinary least squares estimate

$$\hat{\boldsymbol{\beta}}_{gm} \;=\; \hat{\boldsymbol{\beta}}_{ls} \;=\; (\mathsf{X}^\mathsf{T}\mathsf{X})^{-1}\mathsf{X}^\mathsf{T}\mathsf{y}.$$

Bayesian Estimation

The Bayesian framework mainly bases on Bayes' famous theorem

$$P(A_i|E) \;=\; \frac{P(E|A_i)\,P(A_i)}{\sum_j P(E|A_j)P(A_j)},$$

where E and A_i denote events. The denominator represents the *total probability* $P(E) = \sum_j P(E|A_j)P(A_j)$, where it must be assumed that the event space can be partitioned into disjoint events $\{A_1, A_2, \ldots\}$. Bayes' formula can thus be interpreted as an inversion of conditional probabilities.

In Bayesian estimation theory the random character of the parameters comes to the fore. The uncertainty of the parameters $\boldsymbol{\theta} = [\theta_1, \ldots, \theta_m]^\mathsf{T}$ is modeled by a probability distribution $\pi(\boldsymbol{\theta})$ (pdf), called prior. The name reflects the fact that the prior has to be manually chosen according to some *a priori* knowledge, which might not always be available. Let $\underset{\smile}{X}_1, \ldots, \underset{\smile}{X}_k$ be the observations generating random variables under consideration. The conditional probability density function of the $\underset{\smile}{X}_1, \ldots, \underset{\smile}{X}_k$, given the parameters, denoted by $f(\mathsf{x}|\boldsymbol{\theta})$, has to be modeled, that is an appropriate distribution type for the $\underset{\smile}{X}_1, \ldots, \underset{\smile}{X}_k$ has to be chosen. Note that $f(\mathsf{x}|\boldsymbol{\theta})$ is referred to as *likelihood* (function). According to Bayes' theorem inference can now be drawn from

$$f(\boldsymbol{\theta}|\mathsf{x}) \;=\; \frac{f(\mathsf{x}|\boldsymbol{\theta})\,\pi(\boldsymbol{\theta})}{\int_{\boldsymbol{\Theta}} f(\mathsf{x}|\boldsymbol{\theta}')\,\pi(\boldsymbol{\theta}')\,d\boldsymbol{\theta}'} \;=\; \frac{f(\mathsf{x}|\boldsymbol{\theta})\,\pi(\boldsymbol{\theta})}{f(\mathsf{x})},$$

where $f(\mathsf{x})$ is the *marginal density* of $\underset{\smile}{\mathsf{x}}$. The function $f(\boldsymbol{\theta}|\mathsf{x})$ is the pdf belonging to the *posterior distribution* of $\boldsymbol{\theta}$. This can be interpreted as updating or sharpening the prior after taking into account the data. The *Bayes estimate* $\hat{\boldsymbol{\theta}}_B(\mathsf{x})$ of $\check{\boldsymbol{\theta}}$ can be obtained by calculating the expectation $\mathrm{E}(\underset{\smile}{\boldsymbol{\theta}}|\underset{\smile}{\mathsf{x}})$

$$\hat{\boldsymbol{\theta}}_B(\mathsf{x}) \;=\; \int_{\boldsymbol{\Theta}} \boldsymbol{\theta}\, f(\boldsymbol{\theta}|\mathsf{x})\,d\boldsymbol{\theta}. \tag{5.1}$$

From the property $\operatorname{argmin}_{a\in\mathbb{R}} \mathrm{E}((\underset{\smile}{X} - a)^2) \;=\; \mathrm{E}(\underset{\smile}{X})$ for every square-integrable random variable $\underset{\smile}{X}$, it can be inferred that

$$\underset{\boldsymbol{\theta}'\in\boldsymbol{\Theta}}{\operatorname{argmin}}\, \mathrm{E}(\|\underset{\smile}{\boldsymbol{\theta}} - \boldsymbol{\theta}'\|^2|\underset{\smile}{\mathsf{x}}) \;=\; \underset{\boldsymbol{\theta}'\in\boldsymbol{\Theta}}{\operatorname{argmin}} \int_{\boldsymbol{\Theta}} \|\boldsymbol{\theta} - \boldsymbol{\theta}'\|^2 f(\boldsymbol{\theta}|\mathsf{x})\,d\boldsymbol{\theta} \;=\; \mathrm{E}(\underset{\smile}{\boldsymbol{\theta}}|\underset{\smile}{\mathsf{x}}) = \hat{\boldsymbol{\theta}}_B(\mathsf{x}).$$

As the integral in the middle term represents the mean square error of the estimate $\boldsymbol{\theta}'(\mathsf{x})$, $\hat{\boldsymbol{\theta}}_B(\mathsf{x})$ must be optimal in this sense. Due to $\inf_{a\in\mathbb{R}} \mathrm{E}((\underset{\smile}{X} - a)^2) = \mathrm{Var}(\underset{\smile}{X})$ the MSE of $\hat{\boldsymbol{\theta}}_B(\mathsf{x})$ is equal to the variance of the posterior.

Note that besides the expectation (mean), it is likewise possible to take the median or the mode of the posterior into account, cf. the next section. It can be mentioned in this respect that for skew distributions, sample mean, median and mode do not coincide. The median lies in between the mode and the sample mean[4].

Maximum a Posteriori Estimation

The *maximum a posteriori* (MAP) estimation is a Bayesian estimation method: instead of computing the expectation of equation (5.1), the mode of the posterior distribution $f(\boldsymbol{\theta}|\mathsf{x})$ is built

$$\hat{\boldsymbol{\theta}}_{map}(\mathsf{x}) \;=\; \underset{\boldsymbol{\theta}\in\boldsymbol{\Theta}}{\operatorname{argmax}} \; \frac{f(\mathsf{x}|\boldsymbol{\theta})\,\pi(\boldsymbol{\theta})}{\int_{\boldsymbol{\Theta}} f(\mathsf{x}|\boldsymbol{\theta}')\,\pi(\boldsymbol{\theta}')\,d\boldsymbol{\theta}'} \;=\; \underset{\boldsymbol{\theta}\in\boldsymbol{\Theta}}{\operatorname{argmax}} \; f(\mathsf{x}|\boldsymbol{\theta})\,\pi(\boldsymbol{\theta}).$$

Note that, for computational convenience, the estimate can equally be obtained by maximizing the expression $\ln f(\boldsymbol{\theta}|\mathsf{x})$

$$\hat{\boldsymbol{\theta}}_{map}(\mathsf{x}) \;=\; \underset{\boldsymbol{\theta}\in\boldsymbol{\Theta}}{\operatorname{argmax}} \; \ln(f(\mathsf{x}|\boldsymbol{\theta})\,\pi(\boldsymbol{\theta})) \;=\; \underset{\boldsymbol{\theta}\in\boldsymbol{\Theta}}{\operatorname{argmax}} \; \Big[\ln f(\mathsf{x}|\boldsymbol{\theta}) + \ln \pi(\boldsymbol{\theta})\Big].$$

Maximum Likelihood Estimator

Another, very popular, Bayesian estimation method is the *maximum likelihood* (ML) method. This technique differs from the MAP strategy in that it is additionally assumed that the a priori probabilities, i.e. $\pi(\boldsymbol{\theta})$, are constant. Hence they are disregarded. Just like the MAP estimator, the ML method is generically applicable to cases in which the functional model, which describes the observation generating process, is not known[5]. On the other hand, if it was a linear model, one would certainly decide on a pure least squares approach. However, in any case, the functional form of the density of the observations, i.e. $f(\mathsf{x}|\boldsymbol{\theta})$, has to be specified. Especially in regard to the ML method, the function $\boldsymbol{\theta} \mapsto f(\mathsf{x}|\boldsymbol{\theta})$ with x fixed, is called the *likelihood* (function). It is usually denoted by $L(\boldsymbol{\theta}) = f(\mathsf{x}|\boldsymbol{\theta})$. The ML estimate is

$$\hat{\boldsymbol{\theta}}_{ml}(\mathsf{x}) \;=\; \underset{\boldsymbol{\theta}\in\boldsymbol{\Theta}}{\operatorname{argmax}} \; f(\mathsf{x}|\boldsymbol{\theta}) \;=\; \underset{\boldsymbol{\theta}\in\boldsymbol{\Theta}}{\operatorname{argmax}} \; \ln f(\mathsf{x}|\boldsymbol{\theta}).$$

This corresponds to determining the mode of the joint density function $f(\mathsf{x}|\boldsymbol{\theta}) = f(\mathsf{x}_1,\ldots,\mathsf{x}_k\,|\boldsymbol{\theta})$. Hence the parameters are determined in such a way that the observed data are precisely the most likely samples to expect.

[4] An empirical rule of thumb for a unimodal skew distribution is: mean-mode $\approx$ 3(mean-median).

[5] Say the observations y_i are normally distributed with expectation μ but underly some unknown model $g(\mathsf{x}_i, \check{\boldsymbol{\theta}})$ such that $\mathrm{E}(\underset{\smile}{y}_i) = g(\mathsf{x}_i, \check{\boldsymbol{\theta}}) = \mu$. Then μ rather than $\check{\boldsymbol{\theta}}$ can be estimated.

It is usually assumed that the observations are i.i.d., which considerably simplifies the problem as the joint density function can be written as

$$f(\mathsf{x}_1, \ldots, \mathsf{x}_k \,|\boldsymbol{\theta}) \overset{\text{i.i.d.}}{=} \prod_{i=1}^{k} f(\mathsf{x}_i \,|\boldsymbol{\theta}) \qquad \Longrightarrow \qquad \ln f(\mathsf{x}|\boldsymbol{\theta}) \overset{\text{i.i.d.}}{=} \sum_{i=1}^{k} \ln\, f(\mathsf{x}_i \,|\boldsymbol{\theta}).$$

As a ML example, reconsider the classical linear model $\mathsf{y} = \mathsf{X}\check{\boldsymbol{\beta}} + \boldsymbol{\epsilon}$, with $\mathrm{E}(\underset{\smile}{\epsilon}_i) = 0$. Let Σ_{yy} be the (non-singular) covariance matrix of the observations $\mathsf{y} \in \mathbb{R}^k$. Then the joint pdf takes on the (multivariate) form

$$f(\mathsf{y}|\boldsymbol{\beta}) \;=\; \frac{1}{(2\pi)^{k/2}\sqrt{\det(\Sigma_{\mathsf{yy}})}}\; \exp\Big[-\frac{1}{2}(\mathsf{y}-\mathsf{X}\boldsymbol{\beta})^{\mathsf{T}}\Sigma_{\mathsf{yy}}^{-1}(\mathsf{y}-\mathsf{X}\boldsymbol{\beta})\Big],$$

and the problem condenses into

$$\hat{\boldsymbol{\beta}}_{ml}(\mathsf{y}) \;=\; \underset{\boldsymbol{\beta}\in\boldsymbol{\Theta}}{\operatorname{argmax}}\; \ln f(\mathsf{y}|\boldsymbol{\beta}) \;=\; \underset{\boldsymbol{\beta}\in\boldsymbol{\Theta}}{\operatorname{argmin}}\; \frac{1}{2}(\mathsf{y}-\mathsf{X}\boldsymbol{\beta})^{\mathsf{T}}\,\Sigma_{\mathsf{yy}}^{-1}\,(\mathsf{y}-\mathsf{X}\boldsymbol{\beta}),$$

which is the ordinary least squares approach to the problem. Note that the derivation is not restricted to linear models. Moreover, in case of normally distributed observations, the maximum likelihood method and the method of least squares are obviously identical. Under these circumstances, the method of least squares can be considered a Bayesian estimation method as well.

It remains to say that the ML estimator is only asymptotically unbiased. Under the assumption that $\Sigma_{\mathsf{yy}} = \sigma^2\mathsf{I}_k$ (i.i.d. case) and $\mathsf{X}\check{\boldsymbol{\beta}} = \boldsymbol{\mu}$, for instance, the ML estimate of the variance in the above example is uncorrected, i.e. $\hat{\sigma}^2_{ml}(\mathsf{y}) = \frac{1}{k}\,(\mathsf{y} - \hat{\boldsymbol{\mu}}_{ml})^{\mathsf{T}}(\mathsf{y} - \hat{\boldsymbol{\mu}}_{ml})$ rather that $s^2_{\mathsf{y}} = \frac{1}{k-1}\,(\mathsf{y} - \hat{\boldsymbol{\mu}}_{ml})^{\mathsf{T}}(\mathsf{y} - \hat{\boldsymbol{\mu}}_{ml})$.

5.2 Least Squares Adjustment

Here an primer on the method of least squares (LS) is given. Applying a LS estimation is often referred to as *fitting*.

In order to overcome the inherent noisiness of measurements one typically introduces a redundancy by drawing much more samples than necessary to uniquely describe the process under consideration. So, in general, each time the number of observations exceeds the number of unknowns an additional criterion has to be introduced. Such criterions, usually a functional model of the process, can be incorporated by the method of least squares. This provides a way to derive a unique solution (in a least squares sense). The term ‘*adjustment*’ emphasizes that the estimation has to handle redundancy appropriately, that is in an compensatory way. Besides, it hints at the fact that the LS method yields the *adjusted observations*, those ‘observations’ which fully comply with the imposed functional model.

The LS method is founded on the assumption that the *true value* $\check{y} \in \mathbb{R}$ of an observable quantity $\underset{\smile}{y} \in \mathbb{R}$, the true value $\check{\boldsymbol{\theta}} \in \mathbb{R}^M$ of the unknown parameters (*parameter vector*) and the vector $\mathsf{a} \in \mathbb{R}^V$ of known constants[6] fulfill a functional model[7], which may be implicit, i.e. $g(\check{y}_i, \mathsf{a}_{\underline{i}}, \check{\boldsymbol{\theta}}) = 0$ or explicit, i.e. $\check{y}_i = g(\mathsf{a}_{\underline{i}}, \check{\boldsymbol{\theta}})$. Hence the model imposes conditions that interrelate all involved quantities. It may henceforth be referred to g as *condition function*. Note that the impact of the model is necessarily essential for the estimation. A case in point is the classical linear model $\check{y}_i = \mathsf{x}_{\underline{i}}^{\mathsf{T}} \check{\boldsymbol{\beta}}$, where $\mathsf{x}_{\underline{i}}$ is a function of $\mathsf{a}_{\underline{i}}$. The parameters are to be estimated from measurements of $\check{y}$; hence by drawing samples y from the respective random variable $\underset{\frown}{y}$. Clearly, a sample y_i will never exactly fulfill the model in terms of the true parameters $\check{\boldsymbol{\theta}}$ because of the associated measurement error ϵ_i. By including the error the model can be made consistent again

$$y_i + \epsilon_i \;=\; g(\mathsf{a}_{\underline{i}}, \check{\boldsymbol{\theta}}) \;=\; \check{y}_i, \tag{5.2}$$

where ϵ_i may be interpreted as the true correction of y_i. Equations of the form (5.2) are known as *error equations* or *observation equations*. As it is more likely to have a small error than a big one, and since negative and positive errors of equal magnitude should occur with equal frequency, it can be inferred that $\mathrm{E}(g(\mathsf{a}_{\underline{i}}, \check{\boldsymbol{\theta}}) - \underset{\frown}{y}_i) = \mathrm{E}(\underset{\frown}{\epsilon}_i) = 0$ or equally $\mathrm{E}(\underset{\frown}{y}_i) \;=\; g(\mathsf{a}_{\underline{i}}, \check{\boldsymbol{\theta}})$.

Self-evidently, the aim of the least squares estimation is to obtain an estimate $\hat{\boldsymbol{\theta}}$ such that all deviations $\Delta y_i = g(\mathsf{a}_{\underline{i}}, \hat{\boldsymbol{\theta}}) - y_i$, $i \in [1,k]_{\mathbb{Z}}$, in total, attain a minimum. This *best fit*, in a least squares sense, is defined as the estimate $\hat{\boldsymbol{\theta}}$ which minimizes the sum of (weighted) squares of the deviations, that is

$$\hat{\boldsymbol{\theta}} \;:=\; \underset{\boldsymbol{\theta}\in\boldsymbol{\Theta}}{\operatorname{argmin}} \; (\mathsf{y} - \mathsf{g}(\mathsf{a}, \boldsymbol{\theta}))^{\mathsf{T}} \; \mathsf{W} \; (\mathsf{y} - \mathsf{g}(\mathsf{a}, \boldsymbol{\theta})), \tag{5.3}$$

where $\mathsf{y} = [y_1, \ldots, y_k]^{\mathsf{T}}$ and $\mathsf{g}(\mathsf{a}, \boldsymbol{\theta}) \in \mathbb{R}^k$, correspondingly. The matrix $\mathsf{W} \in \mathbb{R}^{k\times k}$ is called the weight matrix. Generally, the weights reflect to which extent an observation should influence the estimation; bigger weights should be attributed to more accurate or constraining observations. In this respect, the weight matrix can be chosen to be the inverse of the covariance matrix if regular, i.e. $\mathsf{W} = \Sigma_{\mathsf{yy}}^{-1}$. In particular, in case of i.i.d. observations with variance σ^2, it is $\mathsf{W} = \frac{1}{\sigma^2}\mathsf{I}_k$. The weight matrix can be interpreted as an error metric as all deviations $\Delta\mathsf{y}$, with $||\Delta\mathsf{y}|| =$ const, on the hypersurface implicitly given by the ellipsoid $d_M^{\,2} = \Delta\mathsf{y}^{\mathsf{T}}\mathsf{W}\Delta\mathsf{y}$ represent equally good choices - each deviation has the same so-called *Mahalanobis distance* d_M.

Note that varying $\mathsf{y} - \mathsf{g}(\mathsf{a}, \boldsymbol{\theta})$ in $\boldsymbol{\theta}$, see equation (5.3), corresponds to varying the deviation $\Delta\mathsf{y}$, which is why not the (unobservable) error $\epsilon_i = \check{y}_i - y_i$ is subjected to the minimization but the so-called residuals[8], i.e. deviations Δy_i. Keeping changes

[6] The constant $\mathsf{a}_{\underline{i}j} \in \mathbb{R}$ can, for instance, denote the j^{th} coordinate in the i^{th} sample y_i from a hypersurface $z : \mathbb{R}^{V\times M} \to \mathbb{R}$ such that $\check{y}_i = z(\mathsf{a}_{\underline{i}}, \check{\boldsymbol{\theta}}) = z(\mathsf{a}_{\underline{i}1}, \ldots, \mathsf{a}_{\underline{i}V}, \check{\boldsymbol{\theta}}) \in \mathbb{R}$.

[7] The arguments of $g(\mathsf{a}_{\underline{i}}, \check{\boldsymbol{\theta}})$ are chosen to be vector valued because g might represent one component of a vector valued model of $\check{\boldsymbol{y}}_{\underline{i}} \in \mathbb{R}^T$.

[8] *Corrections, updates and residuals* are meant to mean the same. However, in non-linear problems corrections or updates are increments w.r.t. the actual iteration, whereas a residual can be seen as the correction w.r.t the original observation, see figure 5.4. The former three terms are not to be confused with the (statistical) *error* which is the deviation of the realization of a random variable from its expectation (population mean).

minimal makes sense as observations are the best that is available. Given $\hat{\boldsymbol{\theta}}$, the estimate $\hat{\mathsf{y}} = \mathsf{g}(\mathsf{a}, \hat{\boldsymbol{\theta}})$ is referred to as the adjusted observations. They would most likely be observed if all measurements were totally free from errors. In this sense, $\hat{y}_i$ represents the most plausible value for $\check{y}_i$ regarding the given model. It may be written

$$\hat{\mathsf{y}} = \mathsf{y} + \hat{\boldsymbol{\epsilon}}, \qquad \text{with} \qquad \hat{\mathsf{y}} = \mathsf{g}(\mathsf{a}, \hat{\boldsymbol{\theta}}), \tag{5.4}$$

so that $\hat{e}_i$ is an estimate for the true error ϵ_i. This kind of equation may be referred to as *adjustment equations*.

5.2.1 Linearization

The principle of the least squares method can be stated without distinction between having a linear or a non-linear model. In practice, it is inevitable to linearize the equations since there is no closed form solution for the non-linear LS problem. However, in few cases it can be circumvented to work with partial derivatives; if, for example, the model obeys $\check{y}_i = \check{\theta}_1 e^{\check{\theta}_2 a_i}$, where a_i is a known constant, then $\ln(\check{y}_i) = \ln(\check{\theta}_1) + \check{\theta}_2 a_i$ is a linear model for the new observations[9] $z_i := \ln(y_i)$. Similarly, given a model $g(\check{y}_i, \mathsf{a}_{\underline{i}}, \check{\boldsymbol{\theta}})$, there are several possibilities for functions $q : \mathbb{R} \to \mathbb{R}$ such that $q(g)$ represents a model as well, and vice versa.

In all other cases, a linearization of the functional model in terms of a first-order Taylor series expansion must be done. Consequently, an initial parameter estimate $\hat{\boldsymbol{\theta}}^{[0]}$ must be provided, which should already be a fairly good approximation to the sought true $\check{\boldsymbol{\theta}}$. The issue of finding an initial estimate is of special importance as, depending on the character of the condition function g, an estimation can get stuck in local minima, the convergence can be extremely slow or it diverges at all. Note in this respect that the estimation procedure set forth hereunder is the *Gauss-Newton algorithm* such that the respective convergence properties hold[10]. It may also be mentioned that here the objective function g is first approximated and then subjected to a norm (the square of the linearized deviation (5.5) is minimized), while *Newton-Raphson* related methods, cf. [54], usually minimize an approximation of g^2 through solving $\nabla(g^2) = 0$, see [51].

Estimation turns into an iterative process in which the locally best LS corrections $\Delta\hat{\boldsymbol{\theta}}^{[t]}$ for a current $\hat{\boldsymbol{\theta}}^{[t]}$ are to be estimated. The designated estimate is successively updated by the rule $\hat{\boldsymbol{\theta}}^{[t+1]} = \hat{\boldsymbol{\theta}}^{[t]} + \Delta\hat{\boldsymbol{\theta}}^{[t]}$. Starting from $g(\mathsf{a}_{\underline{i}}, \hat{\boldsymbol{\theta}}^{[t]})$ the linearization reads

$$g^{[t]}(\mathsf{a}_{\underline{i}}, \boldsymbol{\theta}) \approx g(\mathsf{a}_{\underline{i}}, \hat{\boldsymbol{\theta}}^{[t]}) + \frac{\partial g(\mathsf{a}_{\underline{i}}, \boldsymbol{\theta})}{\partial \boldsymbol{\theta}} \left(\hat{\boldsymbol{\theta}}^{[t]}\right) \Delta\boldsymbol{\theta}^{[t]},$$

where $\Delta\boldsymbol{\theta}^{[t]} = \boldsymbol{\theta} - \hat{\boldsymbol{\theta}}^{[t]}$. By setting the *Jacobian matrix* $\mathsf{j}^{[t]}_{g_i, \hat{\boldsymbol{\theta}}} := \frac{\partial g(\mathsf{a}_{\underline{i}}, \boldsymbol{\theta}')}{\partial \boldsymbol{\theta}'}(\hat{\boldsymbol{\theta}}^{[t]}) \in \mathbb{R}^{1\times M}$

[9] The covariance Σ_{yy} of y has to be propagated according to $\Sigma_{\mathsf{zz}} = \mathsf{J}\Sigma_{\mathsf{yy}}\mathsf{J}^\mathsf{T}$, with the Jacobian matrix $\mathsf{J} = \frac{\partial \mathsf{z}}{\partial \mathsf{y}}(\mathsf{y})$, i.e. $\mathsf{J}_{ij} = \delta_{ij}/y_i$. Thus $[\Sigma_{\mathsf{zz}}]_{ij} = [\Sigma_{\mathsf{yy}}]_{ij}/(y_i y_j)$.

[10] Teunissen[115] showed that, in order to have convergence, the vector of observations y has to lie within a certain hypersphere S centered at (the unknown point) $\mathsf{g}(\mathsf{a}, \check{\boldsymbol{\theta}})$. The radius of S is given by the smallest radius of curvature at $\mathsf{g}(\mathsf{a}, \check{\boldsymbol{\theta}})$.

(a row vector) and further $g_i^{[t]} := g(\mathsf{a}_{\underline{i}}, \hat{\boldsymbol{\theta}}^{[t]})$, the updates can be approximated via

$$\Delta y_i(\boldsymbol{\theta}) \;=\; y_i - g(\mathsf{a}_{\underline{i}}, \boldsymbol{\theta}) \;\approx\; \underbrace{y_i \;-\; g_i^{[t]}}_{c_i^{[t]}} - \mathsf{j}^{[t]}_{g_i,\hat{\boldsymbol{\theta}}}\, \Delta\boldsymbol{\theta}^{[t]}. \tag{5.5}$$

Bear in mind that the Jacobians always have to be evaluated at the current $\hat{\boldsymbol{\theta}}^{[t]}$, see [100].

Let $\underset{\smile}{C}_i^{[t]}$ denote the random variable belonging to new shifted observations $c_i^{[t]} = y_i - g_i^{[t]}$. It is $\mathrm{E}(\underset{\smile}{C}_i^{[t]}) = \mathrm{E}(\underset{\smile}{y}_i) - g_i^{[t]}$ and $\Sigma_{\mathsf{cc}} = \Sigma_{\mathsf{yy}}$, which shows that weight matrices W do not have to be altered while iterating. The resulting linear model is

$$\underset{\smile}{C}_i^{[t]} \;=\; \mathsf{j}^{[t]}_{g_i,\hat{\boldsymbol{\theta}}}\, \breve{\Delta\boldsymbol{\theta}}^{[t]}, \tag{5.6}$$

where $\breve{\Delta\boldsymbol{\theta}}^{[t]} = \breve{\boldsymbol{\theta}} - \hat{\boldsymbol{\theta}}^{[t]}$. Let $\mathsf{J}^{[t]}_{g,\hat{\boldsymbol{\theta}}} \in \mathbb{R}^{k\times M}$ be the Jacobian matrix such that $\mathsf{j}^{[t]}_{g_i,\hat{\boldsymbol{\theta}}}$ is its i^{th} row. The estimate of the update can then be evaluated by

$$\Delta\hat{\boldsymbol{\theta}}^{[t+1]} \;=\; \underset{\boldsymbol{\theta}\in\boldsymbol{\Theta}}{\operatorname{argmin}}\; (\mathsf{c}^{[t]} - \mathsf{J}^{[t]}_{g,\hat{\boldsymbol{\theta}}}\, \boldsymbol{\theta})^{\mathsf{T}}\, \mathsf{W}\, (\mathsf{c}^{[t]} - \mathsf{J}^{[t]}_{g,\hat{\boldsymbol{\theta}}}\, \boldsymbol{\theta}). \tag{5.7}$$

The solution to this linear problem is detailed in the following section. For a graphical illustration of the non-linear least squares principle see figure 5.2, which shows the iteration step from $t \to t+1$.

The model (5.6) does usually not lead to an unbiased minimum-variance estimate of $\breve{\boldsymbol{\theta}}$ because the estimation is restricted to the tangent hyperplane of $\mathsf{g}(\mathsf{a}, \boldsymbol{\theta})$, and the meaningfulness of which is strongly dependent on the proximity of $\hat{\boldsymbol{\theta}}^{[t]}$ to $\breve{\boldsymbol{\theta}}$. Generally, the LS estimate $\hat{\boldsymbol{\theta}}$ for a non-linear model (for existence and uniqueness see [88, 108]) is well known to be biased; Box derives in [13] an approximate value for the bias of $\hat{\boldsymbol{\theta}}$. Nonetheless, applying the Gauss-Newton algorithm in non-linear LS is a standard technique. Besides, *outliers* in the observations account for really serious problems as they can induce a considerable bias.

5.2.2 The Linear Model

Here the case is considered that $g(\mathsf{a}_{\underline{i}}, \boldsymbol{\theta})$ is a linear function. It is common to use $\boldsymbol{\beta} \in \boldsymbol{\Theta} \subseteq \mathbb{R}^M$, instead of $\boldsymbol{\theta}$, as the vector of parameters. Each observation is assumed to be a linear combination of the parameters, i.e. $y_i + \epsilon_i = \mathsf{x}_{\underline{i}}^{\mathsf{T}}\breve{\boldsymbol{\beta}}$ with $\mathrm{E}(\underset{\smile}{\epsilon}_i) = 0$. The linear model for k observations $\mathsf{y} \in \mathbb{R}^k$ is given by

$$\mathrm{E}(\underset{\smile}{\mathsf{y}}) \;=\; \mathsf{X}\breve{\boldsymbol{\beta}} \qquad \overset{\mathrm{E}(\underset{\smile}{\boldsymbol{\epsilon}})=0}{\text{or equally}} \qquad \mathsf{y} + \boldsymbol{\epsilon} \;=\; \mathsf{X}\breve{\boldsymbol{\beta}}, \tag{5.8}$$

in conjunction with a positive definite covariance matrix

$$\Sigma_{\mathsf{yy}} \;=\; \sigma^2\, \mathsf{W}^{-1}, \qquad (\sigma^2 \text{ unknown})$$

where $\mathsf{X} \in \mathbb{R}^{k \times M}$ is a matrix of constants such that $\mathsf{X}|_i = \mathsf{x}_{\underset{\smile}{i}}^{\mathsf{T}}$. It is sometimes referred to X as *design matrix*. Let X have full column rank, i.e. $\operatorname{rank}(\mathsf{X}) = M$, requiring that the number of observations is at least as high as the number of parameters (*overdetermined problem*, $k \geq M$).

Note that no assumptions are made about the distribution of the errors and on their independence. Instead, a covariance matrix is assumed to be given up to an unknown variance factor σ^2. The model can be simplified a bit.
Say a the linear model is given by $\mathsf{y}' + \boldsymbol{\epsilon}' = \mathsf{X}'\check{\boldsymbol{\beta}}$. Let $\Sigma_{\mathsf{y}'\mathsf{y}'} = \Sigma_{\boldsymbol{\epsilon}'\boldsymbol{\epsilon}'}$ be the respective (positive definite) covariance matrix of the observations (and the errors). By factoring out a (for the moment basically arbitrary) variance σ^2 of $\Sigma_{\mathsf{y}'\mathsf{y}'}$, one defines the *cofactor matrix* $\mathsf{Q}_{\mathsf{y}'\mathsf{y}'}$, such that $\Sigma_{\mathsf{y}'\mathsf{y}'} = \sigma^2 \mathsf{Q}_{\mathsf{y}'\mathsf{y}'}$. The primed model can then be transferred into a so-called *homoscedastic* model $\mathsf{y} + \boldsymbol{\epsilon} = \mathsf{X}\check{\boldsymbol{\beta}}$ in which the observations are uncorrelated and have equal variance σ^2. The transformation[11] is called *homogenization* and can be expressed as follows

$$\mathsf{T}_C(\mathsf{X}'\check{\boldsymbol{\beta}} - \mathsf{y}' - \boldsymbol{\epsilon}') \;=\; \mathsf{T}_C\mathsf{X}'\check{\boldsymbol{\beta}} - \mathsf{T}_C\mathsf{y}' - \mathsf{T}_C\boldsymbol{\epsilon}' \;=\; \mathsf{X}\check{\boldsymbol{\beta}} - \mathsf{y} - \boldsymbol{\epsilon}. \tag{5.9}$$

The matrix $\mathsf{T}_C \in \mathbb{R}^{k \times k}$ is a regular upper triangular matrix that uniquely arises from the *Cholesky decomposition* of $\mathsf{Q}_{\mathsf{y}'\mathsf{y}'}^{-1}$, i.e. $\mathsf{T}_C^{\mathsf{T}}\mathsf{T}_C = \mathsf{Q}_{\mathsf{y}'\mathsf{y}'}^{-1}$. Consequently, it is $\mathrm{E}(\underset{\smile}{\boldsymbol{\epsilon}}) = \mathrm{E}(\mathsf{T}_C\underset{\smile}{\boldsymbol{\epsilon}}') = \mathsf{T}_C\mathrm{E}(\underset{\smile}{\boldsymbol{\epsilon}}) = 0$ and

$$\Sigma_{\mathsf{yy}} \;=\; \mathrm{Cov}(\mathsf{T}_C\underset{\smile}{\mathsf{y}}', \mathsf{T}_C\underset{\smile}{\mathsf{y}}') \;=\; \mathsf{T}_C\Sigma_{\mathsf{y}'\mathsf{y}'}\mathsf{T}_C^{\mathsf{T}} \;=\; \sigma^2\mathsf{T}_C(\overbrace{\mathsf{T}_C^{\mathsf{T}}\mathsf{T}_C}^{\mathsf{Q}_{\mathsf{y}'\mathsf{y}'}^{-1}})^{-1}\mathsf{T}_C^{\mathsf{T}} \;=\; \sigma^2\mathsf{I}_k,$$

where it is used that

$$\mathrm{Cov}(\mathsf{A}\underset{\smile}{\mathsf{a}}, \mathsf{B}\underset{\smile}{\mathsf{b}}) = \mathsf{A}\mathrm{Cov}(\underset{\smile}{\mathsf{a}}, \underset{\smile}{\mathsf{b}})\mathsf{B}^{\mathsf{T}} \tag{5.10}$$

for suitable matrices A, B and random vectors $\underset{\smile}{\mathsf{a}}$ and $\underset{\smile}{\mathsf{b}}$, confer e.g. [82]. Such a model can equivalently be treated, and afterwards it can be reverted to the original problem by substituting, for example, $\mathsf{T}_C\mathsf{y}'$ for y. It is therefore proceeded on the assumption that a homoscedastic problem is already at hand.

5.2.3 The Solution for the Linear Case

Here the least squares solution for the homoscedastic case, i.e. $\Sigma_{\mathsf{yy}} = \sigma^2\mathsf{I}_k$, is being derived. In concordance with equation (5.7) the problem

$$\hat{\boldsymbol{\beta}} \;=\; \underset{\boldsymbol{\beta}\in\boldsymbol{\Theta}}{\mathrm{argmin}}\; \frac{1}{\sigma^2}\,(\mathsf{y} - \mathsf{X}\,\boldsymbol{\beta})^{\mathsf{T}}(\mathsf{y} - \mathsf{X}\,\boldsymbol{\beta}). \tag{5.11}$$

has to be solved. Setting the derivative to zero, that is

$$\frac{1}{\sigma^2}\,\frac{\partial(\mathsf{y} - \mathsf{X}\,\boldsymbol{\beta})^{\mathsf{T}}(\mathsf{y} - \mathsf{X}\,\boldsymbol{\beta})}{\partial\boldsymbol{\beta}} \;=\; \frac{1}{\sigma^2}\,2\mathsf{X}^{\mathsf{T}}\mathsf{X}\boldsymbol{\beta} - 2\mathsf{X}^{\mathsf{T}}\mathsf{y} \;=\; 0,$$

[11] In this context the *principal component analysis* (PCA) shall be mentioned. By means of a PCA, a vector $\mathsf{y}' \in \mathbb{R}^k$ is subjected to $\mathsf{y} = \mathsf{U}^{\mathsf{T}}\mathsf{y}'$, where $\mathsf{U} \in \mathbb{R}^{k \times k}$ is the eigenvector matrix of $\Sigma_{\mathsf{y}'\mathsf{y}'}$ with $\mathsf{U}\mathsf{U}^{\mathsf{T}} = \mathsf{I}_k$. This amounts to a decorrelation of y' as $\forall\, i \in [1,k]_{\mathbb{Z}} : \Sigma_{\mathsf{yy}} = \mathsf{U}^{\mathsf{T}}\Sigma_{\mathsf{y}'\mathsf{y}'}\mathsf{U} = \mathsf{I}_k\boldsymbol{\lambda}$, with $\Sigma_{\mathsf{y}'\mathsf{y}'}\mathsf{u}_{\underset{\smile}{i}} = \boldsymbol{\lambda}_i\mathsf{u}_{\underset{\smile}{i}}$ and the i^{th} eigenvector $\mathsf{u}_{\underset{\smile}{i}} = \mathsf{U}|^i$ of $\Sigma_{\mathsf{y}'\mathsf{y}'}$.

implies the *normal equation*

$$\mathsf{X}^\mathsf{T}\mathsf{y} = \mathsf{X}^\mathsf{T}\mathsf{X}\hat{\boldsymbol{\beta}} \tag{5.12}$$

and hence the familiar result follows

$$\hat{\boldsymbol{\beta}} \;=\; (\mathsf{X}^\mathsf{T}\mathsf{X})^{-1}\mathsf{X}^\mathsf{T}\mathsf{y}, \tag{5.13}$$

or rather, in concordance with equation (5.9), i.e. by $\mathsf{X} \mapsto \mathsf{T}_C\mathsf{X}$, $\mathsf{y} \mapsto \mathsf{T}_C\mathsf{y}$ and $\mathsf{T}_C^\mathsf{T}\mathsf{T}_C = \mathsf{Q}_{\mathsf{yy}}^{-1}$

$$\begin{aligned}
\hat{\boldsymbol{\beta}} &= (\mathsf{X}^\mathsf{T}\mathsf{T}_C^\mathsf{T}\mathsf{T}_C\mathsf{X})^{-1}\mathsf{X}^\mathsf{T}\mathsf{T}_C^\mathsf{T}\mathsf{T}_C\mathsf{y} \\
&= (\mathsf{X}^\mathsf{T}\mathsf{Q}_{\mathsf{yy}}^{-1}\mathsf{X})^{-1}\mathsf{X}^\mathsf{T}\mathsf{Q}_{\mathsf{yy}}^{-1}\mathsf{y} \qquad\qquad \mathsf{Q}_{\mathsf{yy}} = \Sigma_{\mathsf{yy}}/\sigma^2 \\
&= (\mathsf{X}^\mathsf{T}\sigma^2\Sigma_{\mathsf{yy}}^{-1}\mathsf{X})^{-1}\mathsf{X}^\mathsf{T}\sigma^2\Sigma_{\mathsf{yy}}^{-1}\mathsf{y} \\
&= (\mathsf{X}^\mathsf{T}\Sigma_{\mathsf{yy}}^{-1}\mathsf{X})^{-1}\mathsf{X}^\mathsf{T}\Sigma_{\mathsf{yy}}^{-1}\mathsf{y}.
\end{aligned} \tag{5.14}$$

The inverse of $\mathsf{X}^\mathsf{T}\mathsf{X}$ exists as X is assumed to have full column rank. By the rule (5.10), the covariance of $\hat{\boldsymbol{\beta}}$, as stated in equation (5.13), can be determined to be

$$\Sigma_{\hat{\boldsymbol{\beta}}\hat{\boldsymbol{\beta}}} \;=\; (\mathsf{X}^\mathsf{T}\mathsf{X})^{-1}\mathsf{X}^\mathsf{T}\,\Sigma_{\mathsf{yy}}\,\mathsf{X}(\mathsf{X}^\mathsf{T}\mathsf{X})^{-1} \;=\; \frac{1}{\sigma^2}(\mathsf{X}^\mathsf{T}\mathsf{X})^{-1}. \tag{5.15}$$

Note that according to the condition imposed by the normal equation (5.12), the residuals have to be orthogonal to the adjusted observations $\hat{\mathsf{y}}$ because

$$\mathsf{X}^\mathsf{T}(\mathsf{X}\hat{\boldsymbol{\beta}} - \mathsf{y}) \overset{(5.4)}{=} \mathsf{X}^\mathsf{T}\hat{\boldsymbol{\epsilon}} \;=\; 0 \qquad \Longrightarrow \qquad \hat{\mathsf{y}}^\mathsf{T}\hat{\boldsymbol{\epsilon}} \;=\; (\mathsf{X}\hat{\boldsymbol{\beta}})^\mathsf{T}\hat{\boldsymbol{\epsilon}} \;=\; \hat{\boldsymbol{\beta}}^\mathsf{T}\mathsf{X}^\mathsf{T}\hat{\boldsymbol{\epsilon}} \;=\; 0.$$

This is evident since minimizing the residuals in equation (5.11) means finding a point $\mathsf{X}\boldsymbol{\beta}$, $\boldsymbol{\beta} \in \boldsymbol{\Theta}$, in the *column space* $\mathrm{col}(\mathsf{X})$ of X such that the distance to the observed y becomes a minimum. The solution, where $\hat{\mathsf{y}}^\mathsf{T}\hat{\boldsymbol{\epsilon}} = 0$, must be the orthogonal projection of y onto $\mathrm{col}(\mathsf{X})$, see figure 5.1. The projection $\hat{\mathsf{y}} = \mathsf{X}\hat{\boldsymbol{\beta}}$ of y is therefore given by $\mathcal{P}_\mathsf{X}(\mathsf{y}) := \mathsf{X}(\mathsf{X}^\mathsf{T}\mathsf{X})^{-1}\mathsf{X}^\mathsf{T}\mathsf{y}$. It is readily checked that $\mathcal{P}_\mathsf{X}(\mathsf{y})$ is indeed a projection by observing that $\mathcal{P}_\mathsf{X}(\mathsf{y})$ is idempotent

$$\mathcal{P}_\mathsf{X}\Big(\mathcal{P}_\mathsf{X}(\mathsf{y})\Big) \;=\; \mathsf{X}(\mathsf{X}^\mathsf{T}\mathsf{X})^{-1}\mathsf{X}^\mathsf{T}\Big(\mathsf{X}(\mathsf{X}^\mathsf{T}\mathsf{X})^{-1}\mathsf{X}^\mathsf{T}\mathsf{y}\Big) \;=\; \mathsf{X}(\mathsf{X}^\mathsf{T}\mathsf{X})^{-1}\mathsf{X}^\mathsf{T}\mathsf{y} \;=\; \mathcal{P}_\mathsf{X}(\mathsf{y}).$$

Moreover, the column space of X is invariant under the projection; for every vector $\mathsf{a} \in \mathbb{R}^M$ it holds $\mathcal{P}_\mathsf{X}(\mathsf{Xa}) = \mathsf{X}(\mathsf{X}^\mathsf{T}\mathsf{X})^{-1}\mathsf{X}^\mathsf{T}\mathsf{Xa} = \mathsf{Xa}$. The orthogonality of $\hat{\mathsf{y}}$ and $\hat{\boldsymbol{\epsilon}} = \hat{\mathsf{y}} - \mathsf{y} = (\mathcal{P}_\mathsf{X}(\mathsf{I}_k) - \mathsf{I}_k)\mathsf{y}$ implies the *zero-correlation* (no linear dependence)

$$\Sigma_{\hat{\mathsf{y}}\hat{\boldsymbol{\epsilon}}} \;=\; \mathrm{Cov}\Big(\mathsf{X}(\mathsf{X}^\mathsf{T}\mathsf{X})^{-1}\mathsf{X}^\mathsf{T}\underset{\sim}{\mathsf{y}},\; \Big(\mathsf{X}(\mathsf{X}^\mathsf{T}\mathsf{X})^{-1}\mathsf{X}^\mathsf{T} \;-\; \mathsf{I}_k\Big)\underset{\sim}{\mathsf{y}}\Big) \;=\; 0.$$

Note that the estimate $\hat{\boldsymbol{\beta}} = (\mathsf{X}^\mathsf{T}\mathsf{X})^{-1}\mathsf{X}^\mathsf{T}\mathsf{y}$ does not explicitly depend on the unknown variance σ^2, which shows that the scale of a covariance or a weight matrix is not decisive. By observing that the rank of a projection matrix is determined by the dimension of the subspace it projects onto, it is $\mathrm{rank}(\mathcal{P}_\mathsf{X}(\mathsf{I}_k)) = \mathrm{rank}(\mathrm{col}(\mathsf{X})) = M$ and hence $\mathrm{rank}(\mathcal{P}_\mathsf{X}(\mathsf{I}_k) - \mathsf{I}_k) = k - M$. By exploiting that $\hat{\boldsymbol{\epsilon}}^\mathsf{T}\hat{\boldsymbol{\epsilon}} = \mathsf{y}^\mathsf{T}\mathsf{y} - \hat{\mathsf{y}}^\mathsf{T}\hat{\mathsf{y}}$, it

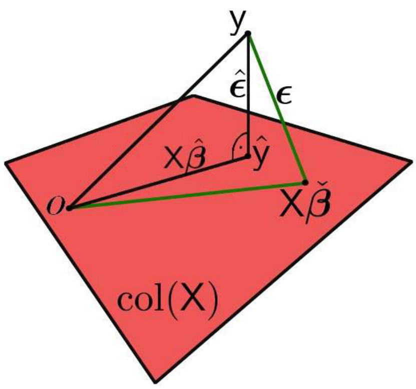

Fig. 5.1: LS principle for the linear model: orthogonal projection of y onto the *expectation surface* $\mathrm{col}(\mathsf{X})(\boldsymbol{\beta}) = \mathsf{X}\boldsymbol{\beta}$ for the homoscedastic case; $\hat{\mathsf{y}} = \mathsf{X}\hat{\boldsymbol{\beta}}$ is most plausible if y was observed.

may then be shown that $\mathrm{E}(\undertilde{\hat{\boldsymbol{\epsilon}}}^{\mathsf{T}}\undertilde{\hat{\boldsymbol{\epsilon}}}) = \sigma^2\,(k-m)$. The unknown variance σ^2 can be estimated via

$$\hat{\sigma}^2 \;=\; \hat{\boldsymbol{\epsilon}}^{\mathsf{T}}\hat{\boldsymbol{\epsilon}}\Big/(k-M).$$

Consequently, $\hat{\sigma}^2$ is unbiased. It also possesses the minimal variance property. For details see [70, 74].

It is now being shown that the least squares estimate for the linear model, as stated in equation (5.13), is unbiased. For this purpose, it is harked back to the comment on page 147, that is a function $\gamma(\check{\boldsymbol{\theta}}) \in \mathbb{R}$ of the parameters is to be estimated. Let, for a given $\boldsymbol{\lambda} \in \mathbb{R}^M$, the linear function $\gamma(\check{\boldsymbol{\beta}}) := \boldsymbol{\lambda}^{\mathsf{T}}\check{\boldsymbol{\beta}}$ be defined. Note that $\gamma(\hat{\boldsymbol{\beta}})$ can equally be considered an estimate for $\hat{\boldsymbol{\beta}}$ by the relation $\hat{\boldsymbol{\beta}}_i = \mathsf{e}_{\underline{\mathsf{i}}}^{\mathsf{T}}\hat{\boldsymbol{\beta}}$, i.e. by substituting the i^{th} canonical basis vector $\mathsf{e}_{\underline{\mathsf{i}}}$, $i \in [1,M]_{\mathbb{Z}}$, for $\boldsymbol{\lambda}$. Building the expectation verifies the unbiasedness

$$\begin{aligned}
\mathrm{E}(\boldsymbol{\lambda}^{\mathsf{T}}\undertilde{\hat{\boldsymbol{\beta}}}) &= \boldsymbol{\lambda}^{\mathsf{T}}\mathrm{E}(\undertilde{\hat{\boldsymbol{\beta}}}) \\
&= \boldsymbol{\lambda}^{\mathsf{T}}\mathrm{E}((\mathsf{X}^{\mathsf{T}}\mathsf{X})^{-1}\mathsf{X}^{\mathsf{T}}\undertilde{\mathsf{y}}) \\
&= \boldsymbol{\lambda}^{\mathsf{T}}(\mathsf{X}^{\mathsf{T}}\mathsf{X})^{-1}\mathsf{X}^{\mathsf{T}}\mathrm{E}(\undertilde{\mathsf{y}}) \\
&= \boldsymbol{\lambda}^{\mathsf{T}}(\mathsf{X}^{\mathsf{T}}\mathsf{X})^{-1}\mathsf{X}^{\mathsf{T}}\mathsf{X}\check{\boldsymbol{\beta}} \\
&= \boldsymbol{\lambda}^{\mathsf{T}}\check{\boldsymbol{\beta}}.
\end{aligned}$$

Next it is demonstrated that $\hat{\boldsymbol{\beta}}$ fulfills the minimum-variance property, too.

Direct Derivation of the Best Linear Unbiased Estimator

In the above case the estimator of $\gamma(\check{\boldsymbol{\beta}})$ is already known to be $\boldsymbol{\lambda}^{\mathsf{T}}\undertilde{\hat{\boldsymbol{\beta}}}(\undertilde{\mathsf{y}})$. Let $\undertilde{\hat{\omega}}(\undertilde{\mathsf{y}})$ be a general estimator of $\gamma(\check{\boldsymbol{\beta}})$. The condition for unbiasedness is then $\mathrm{E}(\undertilde{\hat{\omega}}(\undertilde{\mathsf{y}})) = \gamma(\check{\boldsymbol{\beta}})$. Having a linear combination $\gamma(\check{\boldsymbol{\beta}}) = \boldsymbol{\lambda}^{\mathsf{T}}\check{\boldsymbol{\beta}}$ of parameters $\check{\beta}_i$, $i \in [1,M]_{\mathbb{Z}}$, the corresponding estimator in the linear model is a linear combination of the observations y_j, $j \in [1,k]_{\mathbb{Z}}$; for a given $\boldsymbol{\lambda} \in \mathbb{R}^M$ let $\underset{\smile}{\hat{\omega}}(\underset{\smile}{\mathsf{y}}) = \boldsymbol{\zeta}^\mathsf{T}\underset{\smile}{\mathsf{y}}$ be an applicable estimator, where $\boldsymbol{\zeta} \in \mathbb{R}^k$ is to be determined. Requiring unbiasedness supposes

$$\mathrm{E}(\underset{\smile}{\hat{\omega}}(\underset{\smile}{\mathsf{y}})) \;=\; \mathrm{E}(\boldsymbol{\zeta}^\mathsf{T}\underset{\smile}{\mathsf{y}}) \;=\; \boldsymbol{\zeta}^\mathsf{T}\mathrm{E}(\underset{\smile}{\mathsf{y}}) \;=\; \boldsymbol{\zeta}^\mathsf{T}\mathsf{X}\check{\boldsymbol{\beta}} \;\overset{!}{=}\; \boldsymbol{\lambda}^\mathsf{T}\check{\boldsymbol{\beta}},$$

which gives the constraint

$$\boldsymbol{\zeta}^\mathsf{T}\mathsf{X} = \boldsymbol{\lambda}^\mathsf{T}. \tag{5.16}$$

Demanding a minimal variance, i.e. $\operatorname{argmin}_{\boldsymbol{\zeta}\in\mathbb{R}^k} \mathrm{Var}(\boldsymbol{\zeta}^\mathsf{T}\underset{\smile}{\mathsf{y}})$, subject to the constraint (5.16), can be solved by the *method of Lagrange multipliers* (LS with constraints). At first, the variance term may be expanded as follows $\mathrm{Var}(\boldsymbol{\zeta}^\mathsf{T}\underset{\smile}{\mathsf{y}}) = \boldsymbol{\zeta}^\mathsf{T}\mathrm{Var}(\underset{\smile}{\mathsf{y}})\boldsymbol{\zeta} = \sigma^2\boldsymbol{\zeta}^\mathsf{T}\boldsymbol{\zeta}$. Setting the partial derivatives of the respective Lagrange function $\Psi(\boldsymbol{\zeta},\mathsf{k}) := \frac{1}{2}\sigma^2\boldsymbol{\zeta}^\mathsf{T}\boldsymbol{\zeta} - \mathsf{k}^\mathsf{T}(\mathsf{X}^\mathsf{T}\boldsymbol{\zeta} - \boldsymbol{\lambda})$ to zero, e.g. $\partial\Psi(\boldsymbol{\zeta},\mathsf{k})/\partial\boldsymbol{\zeta} = \mathsf{0}$, yields

$$\sigma^2\boldsymbol{\zeta} - \mathsf{X}\mathsf{k} \;=\; \mathsf{0} \qquad \text{and} \qquad \mathsf{X}^\mathsf{T}\boldsymbol{\zeta} - \boldsymbol{\lambda} \;=\; \mathsf{0},$$

whence $\boldsymbol{\zeta} \;=\; \mathsf{X}(\mathsf{X}^\mathsf{T}\mathsf{X})^{-1}\boldsymbol{\lambda}$ with final and unique solution [74]

$$\hat{\omega}(\mathsf{y}) \;=\; \boldsymbol{\lambda}^\mathsf{T}\underbrace{(\mathsf{X}^\mathsf{T}\mathsf{X})^{-1}\mathsf{X}^\mathsf{T}\mathsf{y}}_{\hat{\boldsymbol{\beta}}} \;=\; \boldsymbol{\lambda}^\mathsf{T}\hat{\boldsymbol{\beta}}.$$

Thus by choosing $\boldsymbol{\lambda} = \mathsf{e}_\mathrm{i}$, $i \in [1,M]_{\mathbb{Z}}$, the component $\hat{\boldsymbol{\beta}}_i$ is obtained, with the result that the best linear unbiased estimator coincides with the least squares result given by equation (5.13).

5.2.4 Non-Linear Least Squares Illustrated

Having a notion of what happens in the linear model the whole LS estimation process can be elucidated. It is built on section 5.2.1.

Consider the case where the functional model $\mathsf{g}(\mathsf{a},\boldsymbol{\theta})$ in non-linear. A set of k observations, gathered in the vector y, is to be fitted to the model. Assume a non-diagonal covariance matrix Σ_{yy} (observations are not stochastically independent). Such a situation is depicted in figure 5.2. It shows the iteration step $t \to t+1$ in a non-linear LS estimation, where t might be zero as well. The solution to the problem is indicated by the point $\mathsf{g}(\mathsf{a},\check{\boldsymbol{\theta}})$. It lies on the curved hypersurface $\mathsf{g}(\mathsf{a},\boldsymbol{\theta}) \subset \mathbb{R}^k$ which is a parameterization with respect to the variable $\boldsymbol{\theta}$ (a is fix). By the relation $\mathrm{E}(\underset{\smile}{\mathsf{y}}) = \mathsf{g}(\mathsf{a},\check{\boldsymbol{\theta}})$, the surface is referred to as *expectation surface.* Assume an initial estimate $\hat{\boldsymbol{\theta}}^{[t]}$ is available. The linearization of $\mathsf{g}(\mathsf{a},\boldsymbol{\theta})$ at $\hat{\boldsymbol{\theta}}^{[t]}$ yields the linear expectation surface $\mathsf{g}_L(\mathsf{a},\boldsymbol{\theta})$ and the linear model of equation (5.6). This time a homogenization is disregarded so that the solution to the linearized problem is not an orthogonal projection of y. Instead, a point $\hat{\mathsf{y}} \in \mathbb{R}^k$ on $\mathsf{g}_L(\mathsf{a},\boldsymbol{\theta})$ is sought which minimizes the Mahalanobis distance $d_M = \sqrt{(\hat{\mathsf{y}}-\mathsf{y})^\mathsf{T}\Sigma_{\mathsf{yy}}^{-1}(\hat{\mathsf{y}}-\mathsf{y})}$ between y and $\mathsf{g}_L(\mathsf{a},\boldsymbol{\theta})$. This point possesses the smallest deviation d_M from y which, at the same time, satisfies the condition $\mathsf{g}_L(\mathsf{a},\boldsymbol{\theta})$. The point can be determined (graphically) by varying the size of the ellipsoid, given by $\Sigma_{\mathsf{yy}}^{-1}$ and centered at y, such that it touches $\mathsf{g}_L(\mathsf{a},\boldsymbol{\theta})$. However, the solution (5.13) for the linear model yields the update $\Delta\hat{\boldsymbol{\theta}}^{[t+1]}$, which hopefully directs towards $\check{\boldsymbol{\theta}}$. Refining $\hat{\boldsymbol{\theta}}$ is stopped when the magnitude of the vector of residuals falls below a certain threshold or when no further improvement can be achieved by iterating.

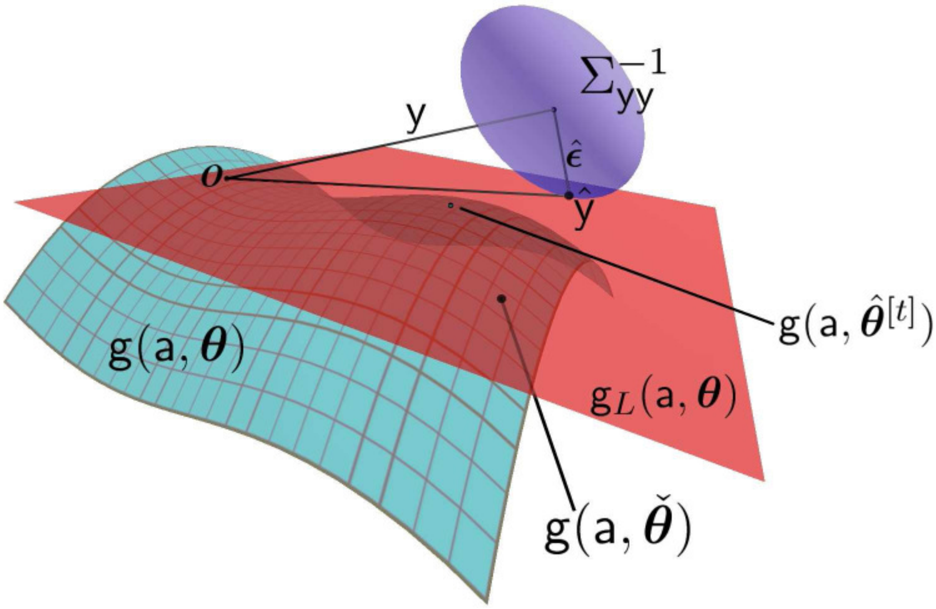

Fig. 5.2: Non-linear LS iteration: The linearization of $\mathsf{g}(\mathsf{a}, \boldsymbol{\theta})$ at $\hat{\boldsymbol{\theta}}^{[t]}$ gives $\mathsf{g}_L(\mathsf{a}, \boldsymbol{\theta})$ onto which y is (non-orthogonally) projected: the projection $\hat{\mathsf{y}}$, from which the update $\Delta\hat{\boldsymbol{\theta}}^{[t+1]}$ is to be determined, is the point where the ellipsoid $\mathbb{S}_d = \{\mathsf{s} | (\mathsf{s} - \mathsf{y})^\mathsf{T} \Sigma_{\mathsf{yy}}^{-1} (\mathsf{s} - \mathsf{y}) = d\}$ touches $\mathsf{g}_L(\mathsf{a}, \boldsymbol{\theta})$ ($\Rightarrow d = \hat{\boldsymbol{\epsilon}}^\mathsf{T} \Sigma_{\mathsf{yy}}^{-1} \hat{\boldsymbol{\epsilon}}$).

5.2.5 Simple Least Squares Adjustment Example I

Here an example of least squares adjustment is given.

Task: Estimate the shape of a triangle (uniquely defined by two angles).

Given: Three measured angles $\{y_1, y_2, y_3\}$ ($\rightarrow$ redundancy of one) with covariance matrix Σ_{yy}.

Hence a pure adjustment problem in the absence of parameters is to be solved. This is called an *adjustment of (conditioned) observations only*. Let $\mathsf{y} = [y_1, y_2, y_3]^\mathsf{T}$. The aim is to estimate the most plausible $\hat{\mathsf{y}}$, which can be written as $\hat{\mathsf{y}} = \mathsf{y} + \Delta\mathsf{y}$, where $\Delta\mathsf{y}$ are the most plausible corrections to the data y. Then the minimization of the corrections $\Delta\mathsf{y} = \hat{\mathsf{y}} - \mathsf{y}$ by $\frac{1}{2}\Delta\mathsf{y}^\mathsf{T}\Sigma_{yy}^{-1}\Delta\mathsf{y} \rightarrow \min$ in conjunction with the condition $\hat{y}_1 + \hat{y}_2 + \hat{y}_3 = 180$ is sufficient to solve the problem. With the help of the method of Lagrange multipliers the function

$$\Psi(\Delta\mathsf{y}, \lambda) \;=\; \tfrac{1}{2}\Delta\mathsf{y}^\mathsf{T}\Sigma_{yy}^{-1}\Delta\mathsf{y} \;+\; \lambda\Big(\mathsf{o}^\mathsf{T}(\mathsf{y} + \Delta\mathsf{y}) - 180\Big), \qquad \mathsf{o} := [1, 1, 1]^\mathsf{T},$$

has to be minimized. Building the partial derivatives, which have to be zero, yields

$$\frac{\partial\Psi}{\partial\Delta\mathsf{y}} \;=\; \Sigma_{yy}^{-1}\Delta\mathsf{y} \;+\; \lambda\mathsf{o}$$

$$\frac{\partial\Psi}{\partial\lambda} \;=\; \mathsf{o}^\mathsf{T}\mathsf{y} + \mathsf{o}^\mathsf{T}\Delta\mathsf{y} - 180.$$

Thus inserting $\Delta \mathsf{y} = -\lambda \Sigma_{yy} \mathsf{o}$ from the first equation into the second gives

$$\lambda = -\frac{180 - \mathsf{o}^\mathsf{T} \mathsf{y}}{\mathsf{o}^\mathsf{T} \Sigma_{yy} \mathsf{o}},$$

and finally

$$\Delta \mathsf{y} = \frac{180 - \mathsf{o}^\mathsf{T} \mathsf{y}}{\mathsf{o}^\mathsf{T} \Sigma_{yy} \mathsf{o}} \Sigma_{yy} \mathsf{o}.$$

If, for example, $\Sigma_{yy} = \mathrm{diag}([\sigma_1^2, \sigma_2^2, \sigma_3^2])$, then the correction Δy_i, $i \in [1{,}3]_\mathbb{Z}$, is proportional to the uncertainty σ_i^2.

5.2.6 Simple Least Squares Adjustment Example II

In this second example, the estimation of a 2D-circle, parameterized by radius r and center (m_x, m_y), from a set of k points is presented. The condition that the i^{th} sampled point $\mathsf{y}_{\underline{\mathsf{i}}} := [x_i; y_i]$, $i \in [1{,}k]_\mathbb{Z}$, lies on the circle is simply given by the implicit function

$$\begin{aligned} g(\check{\boldsymbol{y}}_{\underline{\mathsf{i}}}, \check{\boldsymbol{\theta}}) &:= r^2 - (\check{x}_i - \check{m}_x)^2 - (\check{y}_i - \check{m}_y)^2 \\ &= r^2 - (x_i + \boldsymbol{\epsilon}_{\underline{\mathsf{i}}1} - \check{m}_x)^2 - (y_i + \boldsymbol{\epsilon}_{\underline{\mathsf{i}}2} - \check{m}_y)^2, \end{aligned}$$

where $\boldsymbol{\theta} := [r; m_x; m_y]$ and $\check{\boldsymbol{y}}_{\underline{\mathsf{i}}} = \mathsf{y}_{\underline{\mathsf{i}}} + \boldsymbol{\epsilon}_{\underline{\mathsf{i}}} \in \mathbb{R}^2$.

The subsequently described estimation is employed for calibration purposes in omnidirectional vision, see chapter 8. It is of peculiar interest as it - in a single step - exactly yields the iteratively computed result of the least squares solution (5.13), pursuant to the derivations on pages 154-157.

A necessary condition for a minimum is that the partial derivatives of $\sum_i g(\mathsf{y}_{\underline{\mathsf{i}}}, \boldsymbol{\theta})^2$ w.r.t. the parameters are zero, that is

$$\begin{aligned} \partial/\partial r \quad & \sum_{i=1}^{k} \left(r^2 - (x_i - m_x)^2 - (y_i - m_y)^2\right)^2 &= 0 \\ \partial/\partial m_x \quad & \sum_{i=1}^{k} \left(r^2 - (x_i - m_x)^2 - (y_i - m_y)^2\right)^2 &= 0 \\ \partial/\partial m_y \quad & \sum_{i=1}^{k} \left(r^2 - (x_i - m_x)^2 - (y_i - m_y)^2\right)^2 &= 0 \end{aligned}$$

The first condition immediately gives

$$r^2 = \frac{1}{k} \sum_{i=1}^{k} (x_i - m_x)^2 + (y_i - m_y)^2.$$

On substituting this result into the remaining two conditions, it follows after some algebra

$$2 \begin{bmatrix} \sum_i x_i(x_i - \overline{x}) & \sum_i x_i(y_i - \overline{y}) \\ \sum_i y_i(x_i - \overline{x}) & \sum_i y_i(y_i - \overline{y}) \end{bmatrix} \begin{bmatrix} m_x \\ m_y \end{bmatrix} = \begin{bmatrix} \sum_i x_i(x_i^2 - \overline{\overline{x}} + y_i^2 - \overline{\overline{y}}) \\ \sum_i y_i(x_i^2 - \overline{\overline{x}} + y_i^2 - \overline{\overline{y}}) \end{bmatrix},$$

where $\overline{x} = \sum_i x_i/k$ and $\overline{\overline{x}} = \sum_i x_i^2/k$ was defined ($\overline{y}$, $\overline{\overline{y}}$ analogously). The solution can easily be evaluated, for example, by means of *Cramer's rule*.

5.3 Gauss-Helmert Model Based Estimation

In this section, the technique of least squares adjustment applied to the Gauss-Helmert (GH) model is to be detailed. For brevity, this approach is also called the *Gauss-Helmert method.* It is begun by introducing three basic types of adjustment problems, each characterized by a certain type of observation or rather by the way the observations are integrated into the respective functional model (equations).

5.3.1 Types of Adjustment Problems

At first the issue of *adjustment of observations only* is dealt with. Then the general case including parameters is introduced.

Direct Observations

This is the most straightforward case of adjustment; it occurs if each observation y_i yields a single model equation of the form

$$y_i + \epsilon_i \;=\; \breve{y}_i.$$

Hence the functional model $\breve{y}_i = g(\mathsf{a}_{\underset{\sim}{i}}, \breve{\boldsymbol{\theta}})$ is reduced to $\breve{y}_i = g(i)$, i.e. parameters $\boldsymbol{\theta}$ or constants $\mathsf{a}_{\underset{\sim}{i}}$ do not appear. Such error equations arise if the same quantity, for instance a time difference or a length, is repeatedly measured in order to increase accuracy. Self-evidently, the adjusted observations are given by the arithmetic mean $\hat{y} = \overline{y} = \frac{y_1+\ldots+y_k}{k}$.

On the other hand, by setting $\breve{y}_i = g(\mathsf{a}_{\underset{\sim}{i}}, \breve{\boldsymbol{\theta}}) \stackrel{!}{=} \breve{\beta}$, a most simple linear model - *with* parameter - is obtained. Given k observations, as usual by $\mathsf{y} \in \mathbb{R}^k$, the functional model is

$$\mathrm{E}(\underset{\sim}{\mathsf{y}}) = \mathsf{X}\breve{\boldsymbol{\beta}}, \qquad \text{with} \quad \breve{\boldsymbol{\beta}} = \breve{\beta} \in \mathbb{R} \quad \text{and} \quad \mathsf{X} = \begin{bmatrix} 1 \\ 1 \\ \vdots \\ 1 \end{bmatrix} \in \mathbb{R}^{k\times 1}. \tag{5.17}$$

If the observations have different uncertainties σ_i^2 (say the accuracy of the respective measuring device depends on the ambient temperature), collected in the diagonal covariance matrix, i.e. $\sigma_i^2 = [\Sigma_{\mathsf{yy}}]_{ii}$, equation (5.14) can be used to evaluate the result

$$\hat{\beta} \;=\; \hat{y} \;=\; (\mathsf{X}^\mathsf{T}\Sigma_{\mathsf{yy}}^{-1}\mathsf{X})^{-1}\mathsf{X}^\mathsf{T}\Sigma_{\mathsf{yy}}^{-1}\mathsf{y} \;=\; \frac{\sum_{i=1}^k w_i\,\mathsf{y}_i}{\sum_{i=1}^k w_i}, \qquad w_i := 1/\sigma_i^2,$$

which is a weighted average. Certainly, in case of $\Sigma_{\mathsf{yy}} = \sigma^2\mathsf{I}_k$, the above arithmetic mean $\overline{y}$ is obtained again. This exemplifies that there is often more than one possibility to approach an estimation problem.

Conditioned Observations

It often happens that observations are interrelated by known mathematical conditions, see, for instance, section 5.2.5. There are a multiplicity of further examples, such as that the sum of measured voltages in a series circuit must be equal to the voltage across the source. Both, the true values of the observations and the adjusted observations have to satisfy the same conditions. Note that these are assumed to be parameter-free (adjustment of observations only), otherwise refer section 5.3.2. Consider at first the linear case with m conditions: for given coefficients[12] $\{o_i,\, z_{i1}, \ldots, z_{ik}\}$, $i \in [1,m]_{\mathbb{Z}}$, and k observations $\mathsf{y} := [y_1, \ldots, y_k]^{\mathsf{T}}$, the i^{th} condition on the true values $\breve{y}_i = y_i + \epsilon_i$ may be expressed as

$$0 \;=\; o_i + z_{i1}(y_1\,+\,\epsilon_1) + z_{i2}(y_2\,+\,\epsilon_2) + \ldots + z_{ik}(y_k\,+\,\epsilon_k).$$

or equally with $\mathsf{z}_{\underline{\mathsf{i}}} := [z_{i1}, \ldots, z_{ik}]^{\mathsf{T}}$

$$0 \;=\; \underbrace{o_i + \mathsf{z}_{\underline{\mathsf{i}}}^{\mathsf{T}}\mathsf{y}}_{=:\,-z_i} + \mathsf{z}_{\underline{\mathsf{i}}}^{\mathsf{T}}\boldsymbol{\epsilon} \qquad\Longleftrightarrow\qquad \mathsf{z}_{\underline{\mathsf{i}}}^{\mathsf{T}}\boldsymbol{\epsilon} \;=\; z_i.$$

As the estimate $\hat{\boldsymbol{\epsilon}}$ has to fulfill the conditions as well these are rephrased in terms of the residuals (which are to be minimized)

$$\mathsf{z}_{\underline{\mathsf{i}}}^{\mathsf{T}}\Delta\mathsf{y} \;=\; z_i. \tag{5.18}$$

For the non-linear case, consider the implicit functional model $g_{\underline{\mathsf{i}}}(\breve{\mathsf{y}}) := g_{\underline{\mathsf{i}}}(\mathsf{a}_{\underline{\mathsf{i}}}, \breve{\mathsf{y}}) = 0 \in \mathbb{R}$ representing the i^{th} condition. A linearization at y yields

$$g_{\underline{\mathsf{i}}}(\mathsf{y} + \Delta\mathsf{y}) \;\approx\; \underbrace{g_{\underline{\mathsf{i}}}(\mathsf{y})}_{=:\,-z_i} \;+\; \underbrace{\sum_{j=1}^{k} \frac{\partial\, g_{\underline{\mathsf{i}}}}{\partial y_j}(\mathsf{y})\;\Delta y_j}_{\mathsf{z}_{\underline{\mathsf{i}}}^{\mathsf{T}}\Delta\mathsf{y}}$$

such that equation (5.18) is reobtained.

On defining $\mathsf{Z} := [\![\mathsf{z}_{\underline{\mathsf{i}}j}]\!] \in \mathbb{R}^{m\times k}$ and $\mathsf{z} := [z_1, \ldots, z_m]^{\mathsf{T}} \in \mathbb{R}^m$ all $m \leq k$ condition equations can be subsumed to

$$\mathsf{Z}\Delta\mathsf{y} \;=\; \mathsf{z}. \tag{5.19}$$

Let W be a symmetric positive definite weight matrix for y. The minimization of the residuals $\Delta\mathsf{y}$ subject to the conditions on the observations can be expressed by means of the method of Lagrange multipliers

$$\Psi(\Delta\mathsf{y}, \boldsymbol{\lambda}) \;=\; \tfrac{1}{2}\Delta\mathsf{y}^{\mathsf{T}}\mathsf{W}\Delta\mathsf{y} \;+\; \boldsymbol{\lambda}^{\mathsf{T}}(\mathsf{Z}\Delta\mathsf{y} - \mathsf{z}) \quad\rightarrow\quad \min.$$

The minimal residuals are thus given by

$$\hat{\boldsymbol{\epsilon}} \;=\; \mathsf{W}^{-1}\mathsf{Z}^{\mathsf{T}}(\mathsf{Z}\mathsf{W}^{-1}\mathsf{Z}^{\mathsf{T}})^{-1}\,\mathsf{z}. \tag{5.20}$$

[12]Recall that coefficients, such as $\{o_i,\, z_{i1}, \ldots, z_{ik}\}$, are captured by $\mathsf{a}_{\underline{\mathsf{i}}}$ (page 153).

Indirect Observations

Indirect observations are exactly those which are described by the error equation (5.2): $y_i + \epsilon_i = g(\mathsf{a}_{\underline{i}}, \check{\boldsymbol{\theta}})$. Thus there is exactly one condition function (of the parameters) for each observation. According to the linear model (section 5.2.2) $\mathrm{E}(\mathsf{y}) = \mathsf{X}\check{\boldsymbol{\beta}}$, $\mathsf{y} \in \mathbb{R}^k$, indirect observations are supposed to satisfy

$$y_i + e_i \;=\; \mathsf{x}_{\underline{i}1}\check{\boldsymbol{\beta}}_1 + \mathsf{x}_{\underline{i}2}\check{\boldsymbol{\beta}}_2 + \ldots + \mathsf{x}_{\underline{i}M}\check{\boldsymbol{\beta}}_M, \qquad i \in [1,k]_{\mathbb{Z}},$$

where the coefficient matrix $\mathsf{X} := [\![\mathsf{x}_{\underline{i}j}]\!] \in \mathbb{R}^{k\times M}$ is assumed to consist of known constants. As indirect observations are already covered by section 5.2, it is refrained from giving a comprehensive illustration here, too.

It is to mention that the previously given considerations on this class of problems, where one variable y_i (random) depends on one or more independent variables $\mathsf{x}_{\underline{i}1}, \ldots, \mathsf{x}_{\underline{i}M}$ (non-random) in a linear manner, belong to the *linear regression analysis*. Note that this may also include functional models like the linear polynomial model [74], for instance $y_i + \epsilon_i = \check{\boldsymbol{\beta}}_0 + x_i\check{\boldsymbol{\beta}}_1 + x_i^2\check{\boldsymbol{\beta}}_2 + \ldots + x_i^{M-1}\check{\boldsymbol{\beta}}_{M-1}$.

Derived Observations

'As a specific problem, let a number of measurements be made upon the diameter of a circle, with the object of determining its area. That is, the quantity really sought is the area, but the direct measurements are made upon the diameter, a function of the area. Supposing the observations to be all made in the same manner, the question arises, what is the most probable value of the area? Is it the arithmetical mean of the areas computed from the separate measurements on the diameter, or is it the area determined by taking, as the diameter, the mean of the measurements upon it?'

L. D. Weld in [119]

According to the principle of least squares adjustment an optimal solution consists in minimizing the residuals belonging to the observed quantities. Hence the answer to the above question is to calculate the area from the arithmetic mean of the measurements of the diameters. It is however mostly possible to work with derived observations, these are function values of the original observations. Note that the number of derived observations may not exceed the number of original observations, and in particular error propagation must be used to propagate the covariances for the new observations (which can then be correlated). An example is to compute an angle from two measured directions. Is the function linear, it does not matter whether the observations or the derived observations are used. In case of non-linearity, the solution can be found iteratively after a linearization. In the absence of a condition function, as in the area-diameter example, iterating is difficult since the LS solution is found in one step. As a consequence, the right solution is not found even with correctly propagated covariances. Assume, for instance, that two diameters were measured, $\mathsf{d} := [d_1, d_2]^\mathsf{T}$. The respective areas are $\mathsf{f} := [d_1^2, d_2^2]^\mathsf{T}\,\pi/4$.

Let $\mathsf{X} = [1,1]^\mathsf{T}$ according to the model (5.17) for direct observations. The special solution then reads

$$\begin{aligned} \pi/4\,\overline{d}^{\,2} &= \pi/4\left(\frac{d_1+d_2}{2}\right)^2 = \pi/4\left[(\mathsf{X}^\mathsf{T}\mathsf{X})^{-1}\mathsf{X}^\mathsf{T}\,\mathsf{d}\right]^2 \\ &= (\mathsf{X}^\mathsf{T}\mathsf{Q}_{\mathsf{ff}}^{-1}\mathsf{X})^{-1}\mathsf{X}^\mathsf{T}\mathsf{Q}_{\mathsf{ff}}^{-1}\,\mathsf{f}, \end{aligned}$$

where $\mathsf{Q}_{\mathsf{ff}} = \mathrm{diag}([\,3d_1 + d_2,\, 3d_2 + d_1\,])$ was manually determined; note that Q_{ff} is not obtained by error propagation on the function $f(d) = d^2\,\pi/4$.

5.3.2 General Case of Least Squares Adjustment

Here the so-called *mixed model* is being introduced [74]. It was first established by Helmert [60], but it is based on the work of Gauss who invented the method of least squares [39, 40]. For this reason, the model bears the name *Gauss-Helmert model* (GH-model) [120].

As might be expected from a 'general case' the observations allowed in the GH-model resemble a fusion of conditioned and indirect observations, that is to say the i^{th} of m conditions may be written as

$$0 \;=\; o_i + z_{i1}(y_1 \,+\, \epsilon_1) + \ldots + z_{ik}(y_k \,+\, \epsilon_k) \;+\; x_{i1}\check{\beta}_1 + \ldots + x_{iM}\check{\beta}_M$$

or equally

$$0 \;=\; \overbrace{o_i + \mathsf{z}_{\underline{\mathsf{i}}}^\mathsf{T}\mathsf{y}}^{=:\,-z_i} + \mathsf{z}_{\underline{\mathsf{i}}}^\mathsf{T}\boldsymbol{\epsilon} + \mathsf{x}_{\underline{\mathsf{i}}}^\mathsf{T}\check{\boldsymbol{\beta}},$$

$\Longleftrightarrow$

$$\mathsf{x}_{\underline{\mathsf{i}}}^\mathsf{T}\check{\boldsymbol{\beta}} \;+\; \mathsf{z}_{\underline{\mathsf{i}}}^\mathsf{T}\boldsymbol{\epsilon} \;=\; z_i,$$

where $\check{\boldsymbol{\beta}} \in \mathbb{R}^M$ is the vector of unknown (true) parameters, $o_i \in \mathbb{R}$, $\mathsf{x}_{\underline{\mathsf{i}}} \in \mathbb{R}^M$ and $\mathsf{z}_{\underline{\mathsf{i}}} \in \mathbb{R}^k$ are known constants (gathered in the model parameter $\mathsf{a}_{\underline{\mathsf{i}}}$) and $\mathsf{y} + \boldsymbol{\epsilon} = \check{\mathsf{y}} \in \mathbb{R}^k$ as usual. Subsuming all condition equations yields the linear Gauss-Helmert model

$$\mathsf{X}\check{\boldsymbol{\beta}} + \mathsf{Z}\boldsymbol{\epsilon} \;=\; \mathsf{z} \quad \text{with} \quad \mathrm{E}(\underset{\smile}{\boldsymbol{\epsilon}}) = 0, \tag{5.21}$$

where z can be interpreted as a vector of 'new' observations. Thus if Σ_{yy} (being equal to $\Sigma_{\boldsymbol{\epsilon\epsilon}}$) denotes a covariance matrix of the measured observations then $\Sigma_{\mathsf{zz}} = \mathsf{Z}\Sigma_{\mathsf{yy}}\mathsf{Z}^\mathsf{T}$ is the (propagated) covariance matrix for the new observations held in z.

Note that this model extends the linear model (5.8) in that the errors $\boldsymbol{\epsilon}$ are treated as random parameters with zero-mean. Certainly, by setting $\boldsymbol{\epsilon}_z = -\mathsf{Z}\boldsymbol{\epsilon}$ a linear model $\mathsf{z} + \boldsymbol{\epsilon}_z = \mathsf{X}\check{\boldsymbol{\beta}}$ is reobtained with $\mathrm{E}(\underset{\smile}{\boldsymbol{\epsilon}_z}) = \mathsf{0}$ and therefore

$$\hat{\boldsymbol{\beta}} \;=\; (\mathsf{X}^\mathsf{T}(\mathsf{Z}\Sigma_{\mathsf{yy}}\mathsf{Z}^\mathsf{T})^{-1}\mathsf{X})^{-1}\mathsf{X}^\mathsf{T}(\mathsf{Z}\Sigma_{\mathsf{yy}}\mathsf{Z}^\mathsf{T})^{-1}\,\mathsf{z} \tag{5.22}$$

or to put it more concisely

$$\hat{\boldsymbol{\beta}} \;=\; (\mathsf{X}^\mathsf{T}\Sigma_{\mathsf{zz}}^{-1}\mathsf{X})^{-1}\mathsf{X}^\mathsf{T}\Sigma_{\mathsf{zz}}^{-1}\,\mathsf{z}. \tag{5.23}$$

Substituting the result back into the GH-model (5.21) gives a condition function involving conditioned observations, i.e.

$$\mathsf{Z}\boldsymbol{\epsilon} \;=\; (\mathsf{z} - \mathsf{X}\hat{\boldsymbol{\beta}}).$$

Using the respective solution given in equation (5.20) it can be figured out that

$$\hat{\boldsymbol{\epsilon}} \;=\; \Sigma_{\mathsf{yy}}\mathsf{Z}^{\mathsf{T}}\left(\mathsf{Z}\Sigma_{\mathsf{yy}}\mathsf{Z}^{\mathsf{T}}\right)^{-1}(\mathsf{z} - \mathsf{X}\hat{\boldsymbol{\beta}}) \;=\; \Sigma_{\mathsf{yz}}\Sigma_{\mathsf{zz}}^{-1}(\mathsf{z} - \mathsf{X}\hat{\boldsymbol{\beta}}), \tag{5.24}$$

whence the estimate $\hat{\mathsf{y}}$ may be determined. Another but more detailed derivation can be found in [74].

Further Extensions

One extension to the GH-model is obtained by treating all occurring variables in the functional model in a unified manner. Specifically, all variables are considered as observations. The vague distinction between observations and parameters has already been touched in the context of direct observations, page 162. But yet the notion of parameters does not have to be abolished, it simply gets more 'fuzzy'. The optimal tool to realize fuzziness is a covariance matrix or rather a cofactor matrix for the (former) parameters: by utilizing an a priori variance for each parameter it can be controlled whether a parameter update is allowed to vary freely (variance tends to big values) or whether it should be treated almost as a constant (variance tends to zero). As a result, an adjustment of observations only is obtained. This variant form of LS adjustment is referred to as the *unified approach*. It is discussed in [82].

5.3.3 Example

Here the simple example of fitting observed points to a line in 2D is considered. On the assumption that solely the ordinates are affected by a random error, the linear model (5.8), i.e. $\mathrm{E}(\underset{\sim}{\mathsf{y}}) = \mathsf{X}\check{\boldsymbol{\beta}}$, could be used. This would correspond to a linear regression, see the remark on page 164. But if the so-called independent variables in X are not error-free or at least show a not insignificant error, it is advisable to use the method of *total least squares* (TLS), cf. [54]. There the sum of squared residuals in y and in X are to be minimized simultaneously. Geometrically, this kind of 'best fit' corresponds to minimizing the sum of squared distances from the observed points to the sought line, which seems more intuitive. The difference is illustrated by figure 5.3; the green linear regression line in the left plot looks unfair (although it is correct) as it seems that the upper point of the lower point pair and the lower point of the upper point pair are preferred. The blue line indicates the TLS solution assuming equal uncertainties in x and y. A very detailed study of the TLS problem can be found in [67].

[14] The depicted line is not a computed solution; it is drawn on the off chance.

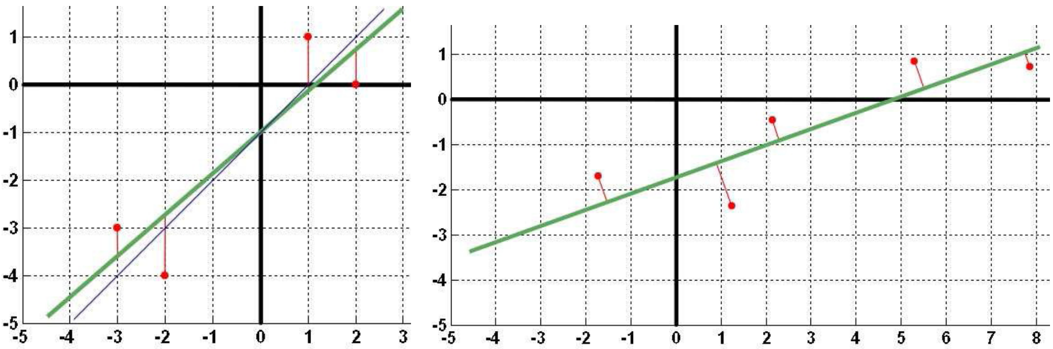

Fig. 5.3: *Left*: linear regression (abscissa values are assumed to be known constants). The blue line shows the expected TLS fit. *Right*: TLS fit[14] (uncertainty is attributed to both coordinates).

Let $\mathsf{y}_{\underline{i}} = [y_{i1}, y_{i2}]^\mathsf{T}$ denote the i^{th} observed point. Using the *Hesse normal form*, the sought line can be parameterized by the angle φ and the distance d to the origin, i.e. the i^{th} observation has to obey the functional model $g(\check{\mathsf{y}}_{\underline{i}}, \check{\boldsymbol{\theta}})$, where $\check{\boldsymbol{\theta}} := [\check{\varphi}, \check{d}]^\mathsf{T}$,

$$\check{y}_{i1} \cos\check{\varphi} + \check{y}_{i2} \sin\check{\varphi} - \check{d} \;=\; 0.$$

For all k observed points the block matrix condition equation may be set up

$$\underbrace{\begin{bmatrix} \cos\check{\varphi} & \sin\check{\varphi} & & & & \mathsf{0} \\ & & \cos\check{\varphi} & \sin\check{\varphi} & & \\ & & & \ddots & & \\ \mathsf{0} & & & & \cos\check{\varphi} & \sin\check{\varphi} \end{bmatrix}}_{\mathsf{Z}_{\check{\varphi}} \in \mathbb{R}^{k \times 2k}} \underbrace{\begin{bmatrix} \check{\mathsf{y}}_{\underline{1}} \\ \check{\mathsf{y}}_{\underline{2}} \\ \vdots \\ \check{\mathsf{y}}_{\underline{k}} \end{bmatrix}}_{\check{\mathsf{y}} \in \mathbb{R}^{2k}} - \underbrace{\begin{bmatrix} \check{d} \\ \check{d} \\ \vdots \\ \check{d} \end{bmatrix}}_{\check{\mathsf{d}} \in \mathbb{R}^{2k}} \;=\; \mathsf{0},$$

and thus

$$\mathsf{g}(\check{\mathsf{y}}, \check{\boldsymbol{\theta}}) \;=\; \mathsf{Z}_{\check{\varphi}} \check{\mathsf{y}} - \check{\mathsf{d}} \;=\; \mathsf{0}.$$

Hence the problem is linear in the observations $\mathsf{y} \in \mathbb{R}^{2k}$ and non-linear in the parameters. Given an initial estimate $\hat{\boldsymbol{\theta}}^{[0]} = [\hat{\varphi}^{[0]}, \hat{d}^{\,[0]}]^\mathsf{T}$ for the true parameters $\check{\boldsymbol{\theta}}$, the adjustment task is to iteratively solve for the updates $\Delta\boldsymbol{\theta} = \hat{\boldsymbol{\theta}}^{[t+1]} - \hat{\boldsymbol{\theta}}^{[t]}$, $t \in \mathbb{N}_0$. Likewise, the approximate value $\hat{\mathsf{y}}^{[0]}$ needed for the update $\Delta\mathsf{y} = \hat{\mathsf{y}}^{[t+1]} - \hat{\mathsf{y}}^{[t]}$ can be set to $\hat{\mathsf{y}}^{[0]} = \mathsf{y}$. The functional model $\mathsf{g}(\check{\mathsf{y}}, \check{\boldsymbol{\theta}}) = \mathsf{0}$ for the updated variables $\hat{\mathsf{y}}^{[t]} + \Delta\mathsf{y}$ and $\hat{\boldsymbol{\theta}}^{[t]} + \Delta\boldsymbol{\theta}$, i.e. in terms of the corrections, can be approximated as

$$\begin{aligned} \mathsf{g}(\hat{\mathsf{y}}^{[t+1]},\, \hat{\boldsymbol{\theta}}^{[t+1]}) \;&=\; \mathsf{g}(\hat{\mathsf{y}}^{[t]} + \Delta\mathsf{y},\, \hat{\boldsymbol{\theta}}^{[t]} + \Delta\boldsymbol{\theta}) \\ &\approx\; \mathsf{g}(\hat{\mathsf{y}}^{[t]}, \hat{\boldsymbol{\theta}}^{[t]}) \;+\; \frac{\partial \mathsf{g}}{\partial \mathsf{y}}(\hat{\mathsf{y}}^{[t]}, \hat{\boldsymbol{\theta}}^{[t]})\, \Delta\mathsf{y} \;+\; \frac{\partial \mathsf{g}}{\partial \boldsymbol{\theta}}(\hat{\mathsf{y}}^{[t]}, \hat{\boldsymbol{\theta}}^{[t]})\, \Delta\boldsymbol{\theta} \\ &=\; \mathsf{Z}_{\hat{\varphi}} \hat{\mathsf{y}}^{[t]} - \hat{\mathsf{d}}^{\,[t]} \;+\; \mathsf{Z}_{\hat{\varphi}} \Delta\mathsf{y} \;+\; \mathsf{X}_{\hat{\mathsf{y}},\hat{\varphi}} \Delta\boldsymbol{\theta}, \end{aligned} \tag{5.25}$$

where $\hat{\mathsf{d}}^{\,[t]} = [\hat{d}^{\,[t]}, \hat{d}^{\,[t]}, \ldots, \hat{d}^{\,[t]}]^\mathsf{T} \in \mathbb{R}^{2k}$. It is important that the defined Jacobians

$$\mathsf{Z}_{\hat\varphi} \;:=\; \left.\frac{\partial \mathsf{g}(\mathsf{y},\boldsymbol{\theta})}{\partial \mathsf{y}}\right|_{\substack{\mathsf{y}=\hat{\mathsf{y}}^{[t]}\\ \boldsymbol{\theta}=\hat{\boldsymbol{\theta}}^{[t]}}} \;=\; \left.\frac{\partial \mathsf{g}(\mathsf{y},\boldsymbol{\theta})}{\partial \mathsf{y}}\right|_{\varphi=\hat\varphi^{[t]}} \qquad \text{and} \qquad \mathsf{X}_{\hat{\mathsf{y}},\hat\varphi} \;:=\; \left.\frac{\partial \mathsf{g}(\mathsf{y},\boldsymbol{\theta})}{\partial \boldsymbol{\theta}}\right|_{\substack{\mathsf{y}=\hat{\mathsf{y}}^{[t]}\\ \varphi=\hat\varphi^{[t]}}}$$

always have to be evaluated for the estimated quantities $\hat{\mathsf{y}}^{[t]}$ and $\hat{\boldsymbol{\theta}}^{[t]}$ of the t^{th} iteration. $\mathsf{X}_{\hat{\mathsf{y}},\hat\varphi} \in \mathbb{R}^{k,2}$ may be declared in terms of $\mathsf{A}_{\hat\varphi} = \partial_\varphi \mathsf{Z}_{\hat\varphi}$, i.e.

$$\mathsf{A}_{\hat\varphi} \;:=\; \begin{bmatrix} -\sin\hat\varphi^{[t]} & \cos\hat\varphi^{[t]} & & & & & \\ & & -\sin\hat\varphi^{[t]} & \cos\hat\varphi^{[t]} & & & \\ & & & & \ddots & & \\ & & & & & -\sin\hat\varphi^{[t]} & \cos\hat\varphi^{[t]} \end{bmatrix} \;\in\; \mathbb{R}^{k\times 2k}$$

such that

$$\mathsf{X}_{\hat{\mathsf{y}},\hat\varphi} \;:=\; \left[\mathsf{A}_{\hat\varphi}\hat{\mathsf{y}}^{[t]},\; \begin{bmatrix} -1 \\ \vdots \\ -1 \end{bmatrix}\right] \qquad \Longleftrightarrow \qquad \mathsf{X}_{\hat{\mathsf{y}},\hat\varphi}\Delta\boldsymbol{\theta} \;=\; \Delta\varphi\,\mathsf{A}_{\hat\varphi}\hat{\mathsf{y}}^{[t]} \;-\; \Delta d \begin{bmatrix} -1 \\ \vdots \\ -1 \end{bmatrix}.$$

According to figure 5.4 on page 171, relation (5.27) can now be used such that linearization (5.25) finally becomes

$$\begin{aligned} \mathsf{Z}_{\hat\varphi}\mathsf{y}^{[t]} - \hat{\mathsf{d}}^{\,[t]} + \mathsf{Z}_{\hat\varphi}\Delta\mathsf{y} + \mathsf{X}_{\hat{\mathsf{y}},\hat\varphi}\Delta\boldsymbol{\theta} \;&=\; \mathsf{Z}_{\hat\varphi}\mathsf{y}^{[t]} - \hat{\mathsf{d}}^{\,[t]} + \mathsf{Z}_{\hat\varphi}(\boldsymbol{\epsilon} - (\hat{\mathsf{y}}^{[t]} - \mathsf{y})) + \mathsf{X}_{\hat{\mathsf{y}},\hat\varphi}\Delta\boldsymbol{\theta} \\ &=\; \underbrace{\mathsf{Z}_{\hat\varphi}\mathsf{y} - \hat{\mathsf{d}}^{\,[t]}}_{=:\,-\mathsf{z}} + \mathsf{Z}_{\hat\varphi}\boldsymbol{\epsilon} \;+\; \mathsf{X}_{\hat{\mathsf{y}},\hat\varphi}\Delta\boldsymbol{\theta}. \end{aligned}$$

Thus the linearization perfectly matches the GH-model (5.21)

$$\mathsf{X}_{\hat{\mathsf{y}},\hat\varphi}\Delta\boldsymbol{\theta} \;+\; \mathsf{Z}_{\hat\varphi}\boldsymbol{\epsilon} \;=\; \mathsf{z}.$$

Iterating the solutions (5.23) and (5.24) several times converges to the TLS solution, including $\hat{\boldsymbol{\theta}} = [\hat\varphi, \hat d\,]^{\mathsf{T}}$.

It is worth mentioning that in this case the TLS solution can be computed directly by means of a PCA; the sample covariance matrix $\Sigma_{YY} \in \mathbb{R}^{2\times 2}$

$$\underset{u,v\in\{1,2\}}{[\Sigma_{YY}]_{uv}} \;:=\; \frac{1}{k-1}\sum_{i=1}^{k}(y_{iu}-\overline{y}_u)(y_{iv}-\overline{y}_v) \qquad \underset{j\in\{1,2\}}{\overline{y}_j} \;=\; \sum_{i=1}^{k} y_{ij}\Big/ k$$

can be subjected to an Eigenvalue decomposition $\Sigma_{YY} = \mathsf{U}\mathsf{D}\mathsf{U}^{\mathsf{T}}$, where $\mathsf{U}\mathsf{U}^{\mathsf{T}} = \mathsf{I}_2$. Let $\mathsf{U} = [\mathsf{u}_{\underline{1}}, \mathsf{u}_{\underline{2}}]$ such that $\mathsf{u}_{\underline{1}}$ is the eigenvector belonging to the smaller eigenvalue. Then the following relationships are satisfied $\mathsf{u}_{\underline{1}} = [\cos\hat\varphi,\, \sin\hat\varphi]^{\mathsf{T}}$ and $\hat d = [\overline{y}_1,\, \overline{y}_2]\mathsf{u}_{\underline{1}}$ since the line estimated by the TLS method is supposed to pass through the barycenter (centroid) of the point cloud. For further explanations see [89] (1901).

5.3.4 The Gauss-Helmert Method for Block Observations

Now the GH-method as used in this thesis is to be derived. *Block observations* were already used in the previous example - each observed point can be considered as one block observation consisting of the y_1- and y_2-coordinate. There was one condition function for each block observation and all blocks shared the same parameters. It may already be speculated that there is a variety of possible adjustment scenarios [121, 74]. Fortunately, the example is solely extended to having more than one condition function for each block. In particular [36, 122] focus on the GH-model in the context of this kind of block adjustment.

From now on it will be necessary to differentiate between conditions and *constraints*: equations in which observations occur are termed condition equations, whereas equations that only relate parameters to each other are called constraints (on the parameters). These are necessary if there are functional dependencies between the parameters. Consider, for example, the parameterization of a Euclidean normal vector $\mathsf{n} \in \mathbb{R}^3$ by means of the three variables n_1, n_2 and n_3 such that $\mathsf{n} = [n_1, n_2, n_3]^\mathsf{T}$. This is an overparameterization and the constraint $\mathsf{n}^\mathsf{T}\mathsf{n} = 1$ has to be introduced. Similar to the example in section 5.3.3, a constraint can be avoided by using spherical coordinates α and φ, i.e. $\mathsf{n} = [\cos\alpha\cos\varphi, \cos\alpha\sin\varphi, \sin\alpha]^\mathsf{T}$.

As before, the condition equation $\mathsf{g}(\check{\mathsf{y}}_{\underline{\mathsf{i}}}, \mathsf{a}_{\underline{\mathsf{i}}}, \check{\boldsymbol{\theta}}) = \mathsf{0}$ reflects the functional model. Constraints are represented by the function $\mathsf{h}(\check{\boldsymbol{\theta}}) = \mathsf{0}$. In the following sections, it is referred to the functions g and h as G-condition and H-constraint, respectively. Subsequently it is proceeded on the assumption that both are non-linear.

Estimation Synopsis

A short synopsis of the estimation problem is given beforehand

$$
\begin{array}{rccl}
\text{Parameters} & \boldsymbol{\theta} & \in & \mathbb{R}^M \\
\text{Number of block observations} & k & & \\
i^{th}\text{ block observation} & \mathsf{y}_{\underline{\mathsf{i}}} & \in & \mathbb{R}^{\kappa_i} \\
\text{Condition equation for the } i^{th}\text{ block} & \mathsf{g}_{\underline{\mathsf{i}}} & \in & \mathbb{R}^{\eta_i} \\
\\
\text{Overall number of observations} & K & := & \sum_{i=1}^k \kappa_i \\
\text{Overall number of conditions} & N_g & := & \sum_{i=1}^k \eta_i \\
\text{Number of constraints} & N_h & & \\
\\
\text{Vector of observations} & \mathsf{y} & \in & \mathbb{R}^K \\
\text{Vector of conditions} & \mathsf{g} & \in & \mathbb{R}^{N_g} \\
\text{Vector of constraints} & \mathsf{h} & \in & \mathbb{R}^{N_h}
\end{array}
$$

where $\mathsf{y} := [\mathsf{y}_{\underline{1}}; \ldots; \mathsf{y}_{\underline{\mathsf{k}}}]$ and $\mathsf{g} := [\mathsf{g}_{\underline{1}}; \ldots; \mathsf{g}_{\underline{\mathsf{k}}}]$.

For each observation vector $\mathsf{y}_{\underline{i}} \in \mathbb{R}^{\kappa_i}$ it is assumed that a covariance matrix[15] $\Sigma_{\mathsf{y}_{\underline{i}}\mathsf{y}_{\underline{i}}}$ is given. The covariance matrix for the total observation vector $\mathsf{y} \in \mathbb{R}^K$ is therefore

$$\Sigma_{\mathsf{yy}} := \begin{bmatrix} \Sigma_{\mathsf{y}_{\underline{1}}\mathsf{y}_{\underline{1}}} & & 0 \\ & \ddots & \\ 0 & & \Sigma_{\mathsf{y}_{\underline{k}}\mathsf{y}_{\underline{k}}} \end{bmatrix}.$$

The Condition Equations

Note that the observation vectors for different observations $\mathsf{y}_{\underline{i}}$ can be of different dimensions κ_i. For each observation a condition of the form

$$\mathsf{g}_{\underline{i}}(\check{\mathsf{y}}_{\underline{i}}, \check{\boldsymbol{\theta}}) := \mathsf{g}(\check{\mathsf{y}}_{\underline{i}}, \mathsf{a}_{\underline{i}}, \check{\boldsymbol{\theta}}) \in \mathbb{R}^{\eta_i}, \qquad i \in [1,k]_{\mathbb{Z}}$$

is given, that is the dimension of $\mathsf{g}_{\underline{i}}$ can also differ for different observations.

Now a linearization as described in section 5.2.1 shall be done with respect to the variables y and $\boldsymbol{\theta}$. Thus let $\hat{\boldsymbol{\theta}}^{[0]}$ be an adequate initial estimate for the parameters. In case of the observations, it is chosen $\hat{\mathsf{y}}_{\underline{i}}^{[0]} := \mathsf{y}_{\underline{i}}$. The sought corrections regarding the t^{th} iteration may then be written as

$$\Delta\boldsymbol{\theta} = \hat{\boldsymbol{\theta}}^{[t+1]} - \hat{\boldsymbol{\theta}}^{[t]} \qquad \text{and} \qquad \Delta\mathsf{y}_{\underline{i}} = \hat{\mathsf{y}}_{\underline{i}}^{[t+1]} - \hat{\mathsf{y}}_{\underline{i}}^{[t]}, \qquad i \in [1,k]_{\mathbb{Z}}.$$

The i^{th} condition can then be approximated by

$$\begin{aligned} \mathsf{g}_{\underline{i}}(\hat{\mathsf{y}}_{\underline{i}}^{[t+1]}, \hat{\boldsymbol{\theta}}^{[t+1]}) &= \mathsf{g}_{\underline{i}}(\hat{\mathsf{y}}_{\underline{i}}^{[t]} + \Delta\mathsf{y}_{\underline{i}}, \hat{\boldsymbol{\theta}}^{[t]} + \Delta\boldsymbol{\theta}) \\ &\approx \mathsf{g}_{\underline{i}}(\hat{\mathsf{y}}_{\underline{i}}^{[t]}, \hat{\boldsymbol{\theta}}^{[t]}) + \frac{\partial \mathsf{g}_{\underline{i}}}{\partial \mathsf{y}_{\underline{i}}}(\hat{\mathsf{y}}_{\underline{i}}^{[t]}, \hat{\boldsymbol{\theta}}^{[t]})\, \Delta\mathsf{y}_{\underline{i}} + \frac{\partial \mathsf{g}_{\underline{i}}}{\partial \boldsymbol{\theta}}(\hat{\mathsf{y}}_{\underline{i}}^{[t]}, \hat{\boldsymbol{\theta}}^{[t]})\, \Delta\boldsymbol{\theta} \\ &= -\mathsf{z}'_{\underline{i}} + \mathsf{Z}_{\underline{i}}\Delta\mathsf{y}_{\underline{i}} + \mathsf{X}_{\underline{i}}\Delta\boldsymbol{\theta}, \end{aligned}$$

where is was defined

$$\begin{aligned} \mathsf{Z}_{\underline{i}} &:= \partial_{\mathsf{y}_{\underline{i}}}\, \mathsf{g}_{\underline{i}}(\mathsf{y}_{\underline{i}}, \boldsymbol{\theta})\Big|_{\substack{\mathsf{y}_{\underline{i}} = \hat{\mathsf{y}}_{\underline{i}}^{[t]} \\ \boldsymbol{\theta} = \hat{\boldsymbol{\theta}}^{[t]}}} &&\in \mathbb{R}^{\eta_i \times \kappa_i} \\ \mathsf{X}_{\underline{i}} &:= \partial_{\boldsymbol{\theta}}\, \mathsf{g}_{\underline{i}}(\mathsf{y}_{\underline{i}}, \boldsymbol{\theta})\Big|_{\substack{\mathsf{y}_{\underline{i}} = \hat{\mathsf{y}}_{\underline{i}}^{[t]} \\ \boldsymbol{\theta} = \hat{\boldsymbol{\theta}}^{[t]}}} &&\in \mathbb{R}^{\eta_i \times M} \qquad (5.26) \\ \text{and} \qquad \mathsf{z}'_{\underline{i}} &:= -\mathsf{g}_{\underline{i}}(\hat{\mathsf{y}}_{\underline{i}}^{[t]}, \hat{\boldsymbol{\theta}}^{[t]}) &&\in \mathbb{R}^{\eta_i}. \end{aligned}$$

Note that the Jacobians always have to be evaluated at the positions of the fitted observations $\hat{\mathsf{y}}_{\underline{i}}^{[t]}$ and parameters $\hat{\boldsymbol{\theta}}^{[t]}$, respectively. It is focussed on this kind of popular pitfalls in [100].

[15] Employing $\Sigma_{\mathsf{y}_{\underline{i}}\mathsf{y}_{\underline{i}}} = \sigma^2\, \mathsf{Q}_{\mathsf{y}_{\underline{i}}\mathsf{y}_{\underline{i}}}$, the derivation can equally be expressed in terms of the respective cofactor matrices $\mathsf{Q}_{\mathsf{y}_{\underline{i}}\mathsf{y}_{\underline{i}}}$.

Combining all conditions into a single block matrix equation then gives

$$\underbrace{\begin{bmatrix} \mathsf{X}_{\underline{1}} \\ \vdots \\ \mathsf{X}_{\underline{k}} \end{bmatrix}}_{=:\ \mathsf{X}} \Delta\boldsymbol{\theta} + \underbrace{\begin{bmatrix} \mathsf{Z}_{\underline{1}} & & 0 \\ & \ddots & \\ 0 & & \mathsf{Z}_{\underline{k}} \end{bmatrix}}_{=:\ \mathsf{Z}} \underbrace{\begin{bmatrix} \Delta\mathsf{y}_{\underline{1}} \\ \vdots \\ \Delta\mathsf{y}_{\underline{1}} \end{bmatrix}}_{=:\ \Delta\mathsf{y}} = \underbrace{\begin{bmatrix} \mathsf{z}'_{\underline{1}} \\ \vdots \\ \mathsf{z}'_{\underline{k}} \end{bmatrix}}_{=:\ \mathsf{z}'_g},$$

where $\mathsf{X} \in \mathbb{R}^{N_g \times M}$, $\mathsf{Z} \in \mathbb{R}^{N_g \times K}$, $\Delta\mathsf{y} \in \mathbb{R}^K$ and correspondingly $\mathsf{z}'_g \in \mathbb{R}^{N_g}$.

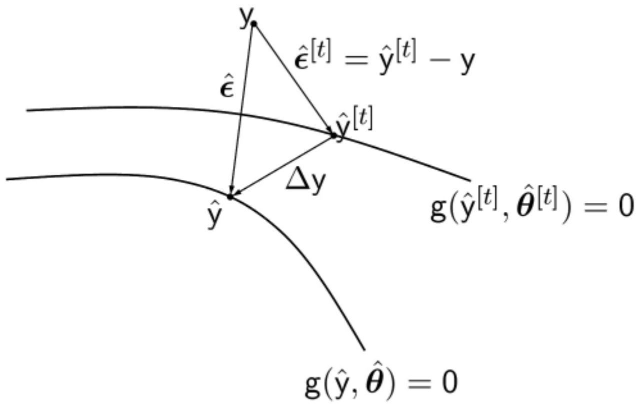

Fig. 5.4: Situation after the t^{th} iteration: estimated values should in each iteration fulfill the G-condition. After linearization, the relation $\Delta\mathsf{y} = \boldsymbol{\epsilon} - (\hat{\mathsf{y}}^{[t]} - \mathsf{y})$ has to be obeyed, cf. [34].

Taking into account the situation depicted in figure 5.4 the important relation

$$\Delta\mathsf{y} \;=\; \boldsymbol{\epsilon} - (\hat{\mathsf{y}}^{[t]} - \mathsf{y}) \tag{5.27}$$

can be inferred. This is, for example, shown by Förstner in [34]. It follows that

$$\begin{aligned} -\mathsf{z}'_g + \mathsf{Z}\Delta\mathsf{y} + \mathsf{X}\Delta\boldsymbol{\theta} \;&=\; \mathsf{g}(\hat{\mathsf{y}}^{[t]}, \hat{\boldsymbol{\theta}}^{[t]}) + \mathsf{Z}(\mathsf{y} - \hat{\mathsf{y}}^{[t]}) + \mathsf{Z}\boldsymbol{\epsilon} + \mathsf{X}\Delta\boldsymbol{\theta} \\ &=\; \underbrace{\mathsf{g}(\mathsf{y}, \hat{\boldsymbol{\theta}}^{[t]})}_{=:\,-\mathsf{z}_g} + \mathsf{Z}\boldsymbol{\epsilon} + \mathsf{X}\Delta\boldsymbol{\theta}, \end{aligned}$$

where the unprimed z_g denotes the contradictions. Hence by means of the block Jacobians X and Z, the pendant of the GH-model (5.21) in terms of the residuals is

$$\mathsf{X}\Delta\boldsymbol{\theta} + \mathsf{Z}\boldsymbol{\epsilon} = \mathsf{z}_g. \tag{5.28}$$

The Constraint Equations

The respective Taylor series expansion of first order for the H-constraint reads

$$\begin{aligned} \mathsf{h}(\hat{\boldsymbol{\theta}}^{[t]} + \Delta\boldsymbol{\theta}) \;&\approx\; \mathsf{h}(\hat{\boldsymbol{\theta}}^{[t]}) + \frac{\partial\mathsf{h}}{\partial\boldsymbol{\theta}}(\hat{\boldsymbol{\theta}}^{[t]})\, \Delta\boldsymbol{\theta} \\ &=\; -\mathsf{z}_h + \mathsf{H}\Delta\boldsymbol{\theta}. \end{aligned}$$

On these implicit definitions the H-constraint becomes

$$\mathsf{H}\Delta\boldsymbol{\theta} \;=\; \mathsf{z}_h,$$

with $\mathsf{H} \in \mathbb{R}^{N_h \times M}$ and $\mathsf{z}_h \in \mathbb{R}^{N_h}$.

Further Proceeding

The whole of conditions and constraints can be rendered by the matrix formalism as

$$\begin{bmatrix} \mathsf{X} & \mathsf{Z} \\ \mathsf{H} & 0 \end{bmatrix} \begin{bmatrix} \Delta\boldsymbol{\theta} \\ \Delta\mathsf{y} \end{bmatrix} \;=\; \begin{bmatrix} \mathsf{z}_g \\ \mathsf{z}_h \end{bmatrix}.$$

Recall the GH-model as stated in (5.21): $\mathsf{X}\check{\boldsymbol{\beta}} + \mathsf{Z}\boldsymbol{\epsilon} = \mathsf{z}$ with $\mathrm{E}(\underset{\sim}{\boldsymbol{\epsilon}}) = \mathsf{0}$. It is now proceeded in same way as on page 165, i.e. the vector z_g is considered a vector of new 'pseudo' observations. Setting again $\boldsymbol{\epsilon}_z = -\mathsf{Z}\boldsymbol{\epsilon}$, for the present case the linear model

$$\mathsf{z}_g + \boldsymbol{\epsilon}_z \;=\; \mathsf{X}\check{\Delta\boldsymbol{\theta}}$$

is obtained with $\mathrm{E}(\underset{\sim}{\boldsymbol{\epsilon}_z}) = \mathsf{0}$.

Next, this reduced estimation problem is solved, subject to the H-constraint. The solution is then used to evaluate the update $\Delta\mathsf{y}$.

Least Squares Minimization

According to the previous elucidations only the system

$$\begin{bmatrix} \mathsf{X} \\ \mathsf{H} \end{bmatrix} \Delta\boldsymbol{\theta} \;=\; \begin{bmatrix} \mathsf{z}_g \\ \mathsf{z}_h \end{bmatrix}. \tag{5.29}$$

must be taken into account.

Note that a transition to pseudo observations z_g is made. Setting $\Delta\mathsf{z}_g := \boldsymbol{\epsilon}_z$ the expression $\Delta\mathsf{z}_g^{\mathsf{T}}\Sigma_{\mathsf{z}_g\mathsf{z}_g}^{-1}\Delta\mathsf{z}_g$, with

$$\Delta\mathsf{z}_g \;:=\; -\mathsf{Z}\boldsymbol{\epsilon} \;\stackrel{(5.28)}{=}\; \mathsf{X}\Delta\boldsymbol{\theta} \;-\; \mathsf{z}_g, \tag{5.30}$$

has to be minimized, which is why the corresponding covariance matrix $\Sigma_{\Delta\mathsf{z}_g\Delta\mathsf{z}_g}$ is required. Due to

$$\mathrm{Cov}(\underset{\sim}{\mathsf{z}_g}, \underset{\sim}{\mathsf{z}_g}) \;=\; \mathrm{Cov}(\underset{\sim}{\boldsymbol{\epsilon}_z}, \underset{\sim}{\boldsymbol{\epsilon}_z}) \stackrel{\boldsymbol{\epsilon}_z = -\mathsf{Z}\boldsymbol{\epsilon}}{=} \mathsf{Z}\mathrm{Cov}(\underset{\sim}{\boldsymbol{\epsilon}}, \underset{\sim}{\boldsymbol{\epsilon}})\mathsf{Z}^{\mathsf{T}} \;=\; \mathsf{Z}\mathrm{Cov}(\underset{\sim}{\mathsf{y}}, \underset{\sim}{\mathsf{y}})\mathsf{Z}^{\mathsf{T}},$$

it follows[16], as on page 165,

$$\Sigma_{\mathsf{z}_g\mathsf{z}_g} \;=\; \mathsf{Z}\Sigma_{\mathsf{yy}}\mathsf{Z}^{\mathsf{T}} \tag{5.31}$$

[16] For readability, $\Sigma_{\mathsf{z}_g\mathsf{z}_g} \;=\; \Sigma_{\Delta\mathsf{z}_g\Delta\mathsf{z}_g}$ is being used in the following.

or rather, for some $i \in [1,k]_{\mathbb{Z}}$

$$\Sigma_{\mathsf{z}_{\underline{i}}\mathsf{z}_{\underline{i}}} \;=\; \mathsf{Z}_{\underline{i}}\Sigma_{\mathsf{y}_{\underline{i}}\mathsf{y}_{\underline{i}}}\mathsf{Z}_{\underline{i}}^{\mathsf{T}}. \tag{5.32}$$

Hence $\Sigma_{\mathsf{z}_g\mathsf{z}_g}$ has the same block diagonal structure as Σ_{yy}.

The minimization of $\Delta\mathsf{z}_g^{\mathsf{T}}\Sigma_{\mathsf{z}_g\mathsf{z}_g}^{-1}\Delta\mathsf{z}_g$ subject to (5.29) is now being formulated by using the method of Lagrange multipliers. For this purpose a new function Ψ is being defined, whose minimum is to be determined

$$\begin{aligned}\Psi(\Delta\boldsymbol{\theta},\boldsymbol{\lambda}) \;&:=\; \tfrac{1}{2}(\mathsf{X}\Delta\boldsymbol{\theta} \;-\; \mathsf{z}_g)^{\mathsf{T}}\,\Sigma_{\mathsf{z}_g\mathsf{z}_g}^{-1}\,(\mathsf{X}\Delta\boldsymbol{\theta} \;-\; \mathsf{z}_g)\\ &\quad+\;\; \boldsymbol{\lambda}^{\mathsf{T}}(\mathsf{H}\Delta\boldsymbol{\theta} \;-\; \mathsf{z}_h),\end{aligned} \tag{5.33}$$

where $\boldsymbol{\lambda} \in \mathbb{R}^{N_h}$ symbolizes the Lagrange multiplier. The derivative with respect to $\Delta\boldsymbol{\theta}$ is built so as to find the normal equations

$$\frac{\partial\Psi}{\partial\Delta\boldsymbol{\theta}}(\Delta\boldsymbol{\theta},\boldsymbol{\lambda}) \;=\; \mathsf{X}^{\mathsf{T}}\Sigma_{\mathsf{z}_g\mathsf{z}_g}^{-1}\mathsf{X}\Delta\boldsymbol{\theta} \;-\; \mathsf{X}^{\mathsf{T}}\Sigma_{\mathsf{z}_g\mathsf{z}_g}^{-1}\mathsf{z}_g \;+\; \mathsf{H}^{\mathsf{T}}\boldsymbol{\lambda}.$$

On defining

$$\mathsf{N} \;:=\; \mathsf{X}^{\mathsf{T}}\Sigma_{\mathsf{z}_g\mathsf{z}_g}^{-1}\mathsf{X} \qquad \text{and} \qquad \mathsf{z}_N \;:=\; \mathsf{X}^{\mathsf{T}}\Sigma_{\mathsf{z}_g\mathsf{z}_g}^{-1}\mathsf{z}_g \tag{5.34}$$

the derivative becomes

$$\frac{\partial\Psi}{\partial\Delta\boldsymbol{\theta}}(\Delta\boldsymbol{\theta},\boldsymbol{\lambda}) \;=\; \mathsf{N}\Delta\boldsymbol{\theta} \;+\; \mathsf{H}^{\mathsf{T}}\boldsymbol{\lambda} \;-\; \mathsf{z}_N.$$

This result in conjunction with the original H-constraint yields the normal equations

$$\begin{array}{l}\texttt{I.}\\ \texttt{II.}\end{array} \qquad \begin{bmatrix}\mathsf{N} & \mathsf{H}^{\mathsf{T}}\\ \mathsf{H} & 0\end{bmatrix}\begin{bmatrix}\Delta\boldsymbol{\theta}\\ \boldsymbol{\lambda}\end{bmatrix} = \begin{bmatrix}\mathsf{z}_N\\ \mathsf{z}_h\end{bmatrix}. \tag{5.35}$$

Note that this system of equations may already be directly solved by building the inverse of the first matrix. Nonetheless, solving for $\Delta\boldsymbol{\theta}$ by means of the normal equations can be approached as follows: using (`I.`) an expression for $\Delta\boldsymbol{\theta}(\boldsymbol{\lambda})$ can be determined. Second, substituting the result into (`II.`) , it can be solved for $\boldsymbol{\lambda}$. Third, (`I.`) can be consulted again, that is

$$\overset{\texttt{I.}}{\Longrightarrow} \quad \Delta\boldsymbol{\theta}(\boldsymbol{\lambda}) \quad \overset{\texttt{II.}}{\Longrightarrow} \quad \boldsymbol{\lambda} \quad \overset{\texttt{I.}}{\Longrightarrow} \quad \Delta\boldsymbol{\theta}.$$

Consequently, with (`I.`)

$$\texttt{III.} \qquad \Delta\boldsymbol{\theta}(\boldsymbol{\lambda}) \;=\; \mathsf{N}^{-1}(\mathsf{z}_N \;-\; \mathsf{H}^{\mathsf{T}}\boldsymbol{\lambda})$$

and (`II.`)

$$\begin{aligned}&\mathsf{H}\mathsf{N}^{-1}(\mathsf{z}_N \;-\; \mathsf{H}^{\mathsf{T}}\boldsymbol{\lambda}) \;=\; \mathsf{z}_h\\ \Longleftrightarrow\quad &\boldsymbol{\lambda} \;=\; (\mathsf{H}\mathsf{N}^{-1}\mathsf{H}^{\mathsf{T}})^{-1}\left(\mathsf{H}\mathsf{N}^{-1}\mathsf{z}_N \;-\; \mathsf{z}_h\right)\end{aligned}$$

and (`I.`) , or rather (`III.`) , again it follows

$$\begin{aligned}\widehat{\Delta\boldsymbol{\theta}} &= \mathsf{N}^{-1}\left(\mathsf{z}_N - \mathsf{H}^\mathsf{T}(\mathsf{HN}^{-1}\mathsf{H}^\mathsf{T})^{-1}\left(\mathsf{HN}^{-1}\mathsf{z}_N - \mathsf{z}_h\right)\right)\\ &= \left(\mathsf{N}^{-1} - \mathsf{N}^{-1}\mathsf{H}^\mathsf{T}(\mathsf{HN}^{-1}\mathsf{H}^\mathsf{T})^{-1}\mathsf{HN}^{-1}\right)\mathsf{z}_N\\ &\quad + \mathsf{N}^{-1}\mathsf{H}^\mathsf{T}(\mathsf{HN}^{-1}\mathsf{H}^\mathsf{T})^{-1}\,\mathsf{z}_h.\end{aligned} \tag{5.36}$$

The estimate $\widehat{\Delta\boldsymbol{\theta}}$ will later on be used to derive an expression for the uncertainty of $\widehat{\Delta\boldsymbol{\theta}}$.

It remains to compute the corrections $\Delta\mathsf{y}$. In concordance to page 165, the estimate $\widehat{\Delta\boldsymbol{\theta}}$ can be substituted back into the GH-model. As a result, the simple functional model for conditioned observations of the form

$$\mathsf{Z}\boldsymbol{\epsilon} = \mathsf{z}_g - \mathsf{X}\widehat{\Delta\boldsymbol{\theta}}$$

is obtained, compare equation (5.30). Following figure 5.4, $\boldsymbol{\epsilon}^\mathsf{T}\Sigma_{\mathsf{yy}}^{-1}\boldsymbol{\epsilon}$ has to be minimized subject to the condition $\mathsf{Z}\boldsymbol{\epsilon} = \mathsf{z}_g - \mathsf{X}\widehat{\Delta\boldsymbol{\theta}}$. The solution is given by equation (5.20)

$$\begin{aligned}\hat{\boldsymbol{\epsilon}} &= \Sigma_{\mathsf{yy}}\mathsf{Z}^\mathsf{T}(\mathsf{Z}\Sigma_{\mathsf{yy}}\mathsf{Z}^\mathsf{T})^{-1}(\mathsf{z}_g - \mathsf{X}\widehat{\Delta\boldsymbol{\theta}})\\ &= \Sigma_{\mathsf{yy}}\mathsf{Z}^\mathsf{T}\Sigma_{\mathsf{z}_g\mathsf{z}_g}^{-1}(\mathsf{z}_g - \mathsf{X}\widehat{\Delta\boldsymbol{\theta}}).\end{aligned}$$

Leaving the block matrix concept, i.e. recalling that $\mathsf{Z}_{\underline{\mathsf{i}}}\boldsymbol{\epsilon}_{\underline{\mathsf{i}}} = \mathsf{z}_{\underline{\mathsf{i}}} - \mathsf{X}_{\underline{\mathsf{i}}}\widehat{\Delta\boldsymbol{\theta}}$, it can be inferred that the individual residuals can be independently estimated via

$$\hat{\boldsymbol{\epsilon}}_{\underline{\mathsf{i}}} = \Sigma_{\mathsf{y}_{\underline{\mathsf{i}}}\mathsf{y}_{\underline{\mathsf{i}}}}\mathsf{Z}_{\underline{\mathsf{i}}}^\mathsf{T}\Sigma_{\mathsf{z}_{\underline{\mathsf{i}}}\mathsf{z}_{\underline{\mathsf{i}}}}^{-1}(\mathsf{z}_{\underline{\mathsf{i}}} - \mathsf{X}_{\underline{\mathsf{i}}}\widehat{\Delta\boldsymbol{\theta}}), \tag{5.37}$$

whence the update $\widehat{\Delta\mathsf{y}}_{\underline{\mathsf{i}}}$ could be computed according to (5.27)

$$\widehat{\Delta\mathsf{y}_{\underline{\mathsf{i}}}} = \hat{\boldsymbol{\epsilon}}_{\underline{\mathsf{i}}} - (\hat{\mathsf{y}}_{\underline{\mathsf{i}}}^{[t]} - \mathsf{y}_{\underline{\mathsf{i}}})$$

such that finally

$$\hat{\mathsf{y}}_{\underline{\mathsf{i}}}^{[t+1]} = \hat{\mathsf{y}}_{\underline{\mathsf{i}}}^{[t]} + \widehat{\Delta\mathsf{y}_{\underline{\mathsf{i}}}} = \mathsf{y}_{\underline{\mathsf{i}}} + \hat{\boldsymbol{\epsilon}}_{\underline{\mathsf{i}}}. \tag{5.38}$$

In the following subsection a discussion on the uncertainty of the estimated (corrections of the) parameters $\widehat{\Delta\boldsymbol{\theta}}$ is given.

Derivation of the Covariance Matrix $\Sigma_{\Delta\boldsymbol{\theta}\Delta\boldsymbol{\theta}}$

Recall that an estimator must be considered a random variable. As the estimate ultimately is a function of the observations, the covariance of the estimator can be computed by means of error propagation, see for instance equation (5.15) on page 157. In the present case, the derived solution for $\widehat{\Delta\boldsymbol{\theta}}$ depends on z_N and z_h, respectively

$$\widehat{\Delta\boldsymbol{\theta}} \overset{(5.36)}{=} \underbrace{\left(\mathsf{N}^{-1} - \mathsf{N}^{-1}\mathsf{H}^\mathsf{T}(\mathsf{H}\mathsf{N}^{-1}\mathsf{H}^\mathsf{T})^{-1}\mathsf{H}\mathsf{N}^{-1}\right)}_{\mathsf{A}} \mathsf{z}_N \;+\; \underbrace{\mathsf{N}^{-1}\mathsf{H}^\mathsf{T}(\mathsf{H}\mathsf{N}^{-1}\mathsf{H}^\mathsf{T})^{-1}}_{\mathsf{B}^\mathsf{T}} \mathsf{z}_h,$$

or more succinctly

$$\widehat{\Delta\boldsymbol{\theta}} \;=\; \mathsf{A}\mathsf{z}_N \;+\; \mathsf{B}^\mathsf{T}\mathsf{z}_h. \tag{5.39}$$

As z_h stems from the constraints (on the parameters only), it can be disregarded in the error propagation. The vector z_N, on the contrary, must have an uncertainty because of its dependence on $\mathsf{z}_g \sim \Sigma_{\mathsf{z}_g\mathsf{z}_g}$; from the definition (5.34)

$$\mathsf{z}_N \;=\; \underbrace{\mathsf{X}^\mathsf{T}\Sigma^{-1}_{\mathsf{z}_g\mathsf{z}_g}}_{\mathsf{C}} \mathsf{z}_g$$

and the often used rule (5.10), the covariance matrix associated with z_N can be derived to be

$$\Sigma_{\mathsf{z}_N\mathsf{z}_N} \;=\; \mathsf{C}\Sigma_{\mathsf{z}_g\mathsf{z}_g}\mathsf{C}^\mathsf{T} \;=\; \mathsf{X}^\mathsf{T}\Sigma^{-1}_{\mathsf{z}_g\mathsf{z}_g}\Sigma_{\mathsf{z}_g\mathsf{z}_g}\Sigma^{-1}_{\mathsf{z}_g\mathsf{z}_g}\mathsf{X} \;=\; \mathsf{X}^\mathsf{T}\Sigma^{-1}_{\mathsf{z}_g\mathsf{z}_g}\mathsf{X} \;\overset{!}{=}\; \mathsf{N}.$$

In order to derive the covariance matrix $\Sigma_{\Delta\boldsymbol{\theta}\Delta\boldsymbol{\theta}}$, error propagation must be carried on, that is

$$\begin{aligned}
\Sigma_{\Delta\boldsymbol{\theta}\Delta\boldsymbol{\theta}} \;&=\; \mathsf{A}\Sigma_{\mathsf{z}_N\mathsf{z}_N}\mathsf{A}^\mathsf{T} \;=\; \mathsf{A}\mathsf{N}\mathsf{A}^\mathsf{T} \\
&=\; \left(\mathsf{N}^{-1} - \mathsf{N}^{-1}\,\mathsf{H}^\mathsf{T}\,(\mathsf{H}\,\mathsf{N}^{-1}\,\mathsf{H}^\mathsf{T})^{-1}\,\mathsf{H}\,\mathsf{N}^{-1}\right)\mathsf{N} \\
&\qquad\qquad \left(\mathsf{N}^{-1} - \mathsf{N}^{-1}\,\mathsf{H}^\mathsf{T}\,(\mathsf{H}\,\mathsf{N}^{-1}\,\mathsf{H}^\mathsf{T})^{-1}\,\mathsf{H}\,\mathsf{N}^{-1}\right) \\
&=\; \mathsf{N}^{-1} + \mathsf{N}^{-1}\,\mathsf{H}^\mathsf{T}\,(\mathsf{H}\,\mathsf{N}^{-1}\,\mathsf{H}^\mathsf{T})^{-1}\,\mathsf{H}\,\mathsf{N}^{-1}\,\mathsf{H}^\mathsf{T}\,(\mathsf{H}\,\mathsf{N}^{-1}\,\mathsf{H}^\mathsf{T})^{-1}\,\mathsf{H}\,\mathsf{N}^{-1} \\
&\qquad -2\,\mathsf{N}^{-1}\,\mathsf{H}^\mathsf{T}\,(\mathsf{H}\,\mathsf{N}^{-1}\,\mathsf{H}^\mathsf{T})^{-1}\,\mathsf{H}\mathsf{N}^{-1} \\
&=\; \mathsf{N}^{-1} - \mathsf{N}^{-1}\,\mathsf{H}^\mathsf{T}\,(\mathsf{H}\,\mathsf{N}^{-1}\,\mathsf{H}^\mathsf{T})^{-1}\,\mathsf{H}\,\mathsf{N}^{-1} \quad \overset{!}{=} \quad \mathsf{A}.
\end{aligned}$$

Block Matrix Considerations

As already mentioned, it is likewise possible to solve the system of normal equations (5.35) directly. This alternative is now being examined. Opposing the inverse of the normal equations (5.35) with the succinct representation (5.39) for $\widehat{\Delta\boldsymbol{\theta}}$ yields[17]

$$\begin{bmatrix} \widehat{\Delta\boldsymbol{\theta}} \\ \boldsymbol{\lambda} \end{bmatrix} = \begin{bmatrix} \mathsf{N} & \mathsf{H}^\mathsf{T} \\ \mathsf{H} & 0 \end{bmatrix}^{-1} \begin{bmatrix} \mathsf{z}_N \\ \mathsf{z}_h \end{bmatrix} = \begin{bmatrix} \mathsf{A} & \mathsf{B}^\mathsf{T} \\ \mathsf{B} & \cdot \end{bmatrix} \begin{bmatrix} \mathsf{z}_N \\ \mathsf{z}_h \end{bmatrix},$$

[17] In fact, it can easily be shown that the question mark in the rightmost 2×2-matrix equates to $(\mathsf{H}\mathsf{N}^{-1}\mathsf{H}^\mathsf{T})^{-1}$, cf. [74].

where is was exploited that the inverse of a symmetric regular matrix is symmetric again. It may hence be figured out that

$$\begin{bmatrix} \mathsf{N} & \mathsf{H}^\mathsf{T} \\ \mathsf{H} & 0 \end{bmatrix}^{-1} \sim \begin{bmatrix} \Sigma_{\Delta\boldsymbol{\theta}\Delta\boldsymbol{\theta}} & \cdot \\ \cdot & \cdot \end{bmatrix}.$$

The inverse comprises the covariance matrix for $\widehat{\Delta\boldsymbol{\theta}}$. Solving the normal equations directly may therefore be advisable. Especially the aspect that $\mathsf{N} \in \mathbb{R}^{M\times M}$ is a relatively small square symmetric matrix encourages this idea. The matrix N is now being analyzed for that purpose.

Note at fist that the inverse of a block diagonal matrix (a matrix with square matrices on its diagonal) is again block diagonal. Especially, if $\{\mathsf{A}_1, \ldots, \mathsf{A}_k\}$ are regular square matrices it holds that

$$\begin{bmatrix} \mathsf{A}_1 & & & 0 \\ & \mathsf{A}_2 & & \\ & & \ddots & \\ 0 & & & \mathsf{A}_k \end{bmatrix}^{-1} = \begin{bmatrix} \mathsf{A}_1^{-1} & & & 0 \\ & \mathsf{A}_2^{-1} & & \\ & & \ddots & \\ 0 & & & \mathsf{A}_k^{-1} \end{bmatrix}.$$

or more concisely $\mathrm{diag}([\mathsf{A}_1, \ldots, \mathsf{A}_k])^{-1} = \mathrm{diag}([\mathsf{A}_1^{-1}, \ldots, \mathsf{A}_k^{-1}])$. Because of $\mathsf{N} = \mathsf{X}^\mathsf{T}\Sigma_{\mathsf{z}_g\mathsf{z}_g}^{-1}\mathsf{X}$, the inverse of the block diagonal matrix $\Sigma_{\mathsf{z}_g\mathsf{z}_g}$ has to be evaluated in the present case. It follows with equation (5.32) that

$$\Sigma_{\mathsf{z}_g\mathsf{z}_g}^{-1} = \mathrm{diag}([\Sigma_{\mathsf{z}_{\underline{1}}\mathsf{z}_{\underline{1}}}^{-1}, \ldots, \Sigma_{\mathsf{z}_{\underline{k}}\mathsf{z}_{\underline{k}}}^{-1}]).$$

Recall that $\mathsf{X} = [\mathsf{X}_{\underline{1}}; \ldots; \mathsf{X}_{\underline{k}}]$. Hence

$$\mathsf{N} = \mathsf{X}^\mathsf{T}\Sigma_{\mathsf{z}_g\mathsf{z}_g}^{-1}\mathsf{X} = \left[\mathsf{X}_{\underline{1}}^\mathsf{T}, \ldots, \mathsf{X}_{\underline{k}}^\mathsf{T}\right] \begin{bmatrix} \Sigma_{\mathsf{z}_{\underline{1}}\mathsf{z}_{\underline{1}}}^{-1} & & & 0 \\ & \Sigma_{\mathsf{z}_{\underline{2}}\mathsf{z}_{\underline{2}}}^{-1} & & \\ & & \ddots & \\ 0 & & & \Sigma_{\mathsf{z}_{\underline{k}}\mathsf{z}_{\underline{k}}}^{-1} \end{bmatrix} \begin{bmatrix} \mathsf{X}_{\underline{1}} \\ \vdots \\ \mathsf{X}_{\underline{k}} \end{bmatrix}.$$

By noting that the dimensions match, i.e. $\mathsf{X}_{\underline{i}} \in \mathbb{R}^{\eta_i\times M}$, $\mathsf{X}_{\underline{i}}^\mathsf{T} \in \mathbb{R}^{M\times\eta_i}$ and $\Sigma_{\mathsf{z}_{\underline{i}}\mathsf{z}_{\underline{i}}}^{-1} \in \mathbb{R}^{\eta_i\times\eta_i}$, it is easy to see that with $\mathsf{N}_{\underline{i}} := \mathsf{X}_{\underline{i}}^\mathsf{T}\Sigma_{\mathsf{z}_{\underline{i}}\mathsf{z}_{\underline{i}}}^{-1}\mathsf{X}_{\underline{i}}$

$$\mathsf{N} = \sum_{i=1}^{k} \mathsf{N}_{\underline{i}} = \sum_{i=1}^{k} \mathsf{X}_{\underline{i}}^\mathsf{T}\Sigma_{\mathsf{z}_{\underline{i}}\mathsf{z}_{\underline{i}}}^{-1}\mathsf{X}_{\underline{i}} = \sum_{i=1}^{k} \mathsf{X}_{\underline{i}}^\mathsf{T}(\mathsf{Z}_{\underline{i}}\Sigma_{\mathsf{y}_{\underline{i}}\mathsf{y}_{\underline{i}}}\mathsf{Z}_{\underline{i}}^\mathsf{T})^{-1}\mathsf{X}_{\underline{i}}. \tag{5.40}$$

Similarly it can be deduced that

$$\mathsf{z}_N = \mathsf{X}^\mathsf{T}\Sigma_{\mathsf{z}_g\mathsf{z}_g}^{-1}\mathsf{z}_g = \sum_{i=1}^{k} \mathsf{X}_{\underline{i}}^\mathsf{T}\Sigma_{\mathsf{z}_{\underline{i}}\mathsf{z}_{\underline{i}}}^{-1}\mathsf{z}_{\underline{i}} = \sum_{i=1}^{k} \mathsf{X}_{\underline{i}}^\mathsf{T}(\mathsf{Z}_{\underline{i}}\Sigma_{\mathsf{y}_{\underline{i}}\mathsf{y}_{\underline{i}}}\mathsf{Z}_{\underline{i}}^\mathsf{T})^{-1}\mathsf{z}_{\underline{i}}. \tag{5.41}$$

Hence, the construction of huge block matrices can be avoided by using the above two sums.

Brief Summary of the GH-Method

Having all necessary linearizations at hand the system of normal equations (5.35) is set up by using the sums (5.40) and (5.41) for N and z_N, respectively. In combination with the H-constraint the inverse of the normal equations is built, which gives the corrections $\widehat{\Delta\boldsymbol{\theta}}$ and the associated covariance matrix $\Sigma_{\Delta\boldsymbol{\theta}\Delta\boldsymbol{\theta}}$. Consequently, the individual updates $\widehat{\Delta\mathsf{y}}_{\mathrm{i}}$, $i \in [1,k]_{\mathbb{Z}}$, for the fitted observations can be evaluated by means of equation (5.38).

Chapter 6

Practical Aspects of Geometric Algebra

On the one side there is the framework of geometric algebra and on the other side there is a parameter estimation method that bases on matrices and vectors. It is therefore natural to ask how these two concepts can be combined in a reasonable way.

Every Clifford algebra has a certain matrix representation [6], where the geometric product can be evaluated simply by using the normal matrix multiplication. A case in point are the *Pauli matrices* σ_x, σ_y and σ_z which can be considered a basis of $\mathbb{R}_3$ [61]. An orthogonal matrix basis of the conformal geometric algebra, for example, can be derived from the set of 8×8-matrices:

$$\mathbf{e}_1 = \begin{bmatrix} 0 & 0 & 0 & 0 & 0 & 0 & 1 & 0 \\ 0 & 0 & 0 & 0 & 0 & 0 & 0 & 1 \\ 0 & 0 & 0 & 0 & 1 & 0 & 0 & 0 \\ 0 & 0 & 0 & 0 & 0 & 1 & 0 & 0 \\ 0 & 0 & 1 & 0 & 0 & 0 & 0 & 0 \\ 0 & 0 & 0 & 1 & 0 & 0 & 0 & 0 \\ 1 & 0 & 0 & 0 & 0 & 0 & 0 & 0 \\ 0 & 1 & 0 & 0 & 0 & 0 & 0 & 0 \end{bmatrix}$$

$$\mathbf{e}_2 = \begin{bmatrix} 0 & 0 & 0 & 0 & 0 & 0 & 0 & 1 \\ 0 & 0 & 0 & 0 & 0 & 0 & -1 & 0 \\ 0 & 0 & 0 & 0 & 0 & -1 & 0 & 0 \\ 0 & 0 & 0 & 0 & 1 & 0 & 0 & 0 \\ 0 & 0 & 0 & 1 & 0 & 0 & 0 & 0 \\ 0 & 0 & -1 & 0 & 0 & 0 & 0 & 0 \\ 0 & -1 & 0 & 0 & 0 & 0 & 0 & 0 \\ 1 & 0 & 0 & 0 & 0 & 0 & 0 & 0 \end{bmatrix} \qquad \mathbf{e}_3 = \begin{bmatrix} 0 & 0 & 0 & 0 & 1 & 0 & 0 & 0 \\ 0 & 0 & 0 & 0 & 0 & 1 & 0 & 0 \\ 0 & 0 & 0 & 0 & 0 & 0 & -1 & 0 \\ 0 & 0 & 0 & 0 & 0 & 0 & 0 & -1 \\ 1 & 0 & 0 & 0 & 0 & 0 & 0 & 0 \\ 0 & 1 & 0 & 0 & 0 & 0 & 0 & 0 \\ 0 & 0 & -1 & 0 & 0 & 0 & 0 & 0 \\ 0 & 0 & 0 & -1 & 0 & 0 & 0 & 0 \end{bmatrix}$$

$$\mathbf{e} = \begin{bmatrix} 1 & 0 & 0 & 0 & -1 & 0 & 0 & 0 \\ 0 & 1 & 0 & 0 & 0 & -1 & 0 & 0 \\ 0 & 0 & 1 & 0 & 0 & 0 & -1 & 0 \\ 0 & 0 & 0 & 1 & 0 & 0 & 0 & -1 \\ 1 & 0 & 0 & 0 & -1 & 0 & 0 & 0 \\ 0 & 1 & 0 & 0 & 0 & -1 & 0 & 0 \\ 0 & 0 & 1 & 0 & 0 & 0 & -1 & 0 \\ 0 & 0 & 0 & 1 & 0 & 0 & 0 & -1 \end{bmatrix} \qquad \mathbf{e}_o = \begin{bmatrix} -\frac{1}{2} & 0 & 0 & 0 & -\frac{1}{2} & 0 & 0 & 0 \\ 0 & -\frac{1}{2} & 0 & 0 & 0 & -\frac{1}{2} & 0 & 0 \\ 0 & 0 & -\frac{1}{2} & 0 & 0 & 0 & -\frac{1}{2} & 0 \\ 0 & 0 & 0 & -\frac{1}{2} & 0 & 0 & 0 & -\frac{1}{2} \\ \frac{1}{2} & 0 & 0 & 0 & \frac{1}{2} & 0 & 0 & 0 \\ 0 & \frac{1}{2} & 0 & 0 & 0 & \frac{1}{2} & 0 & 0 \\ 0 & 0 & \frac{1}{2} & 0 & 0 & 0 & \frac{1}{2} & 0 \\ 0 & 0 & 0 & \frac{1}{2} & 0 & 0 & 0 & \frac{1}{2} \end{bmatrix}$$

It may easily be verified that, for instance, $\mathbf{e}_o^2 = \mathsf{0}$ (a matrix with zeros only) or $\mathbf{e}_1^2 = \mathsf{I}_8$. The fourth and fifth basis vector, $\mathbf{e}_+$ and $\mathbf{e}_-$, can then be calculated from $\mathbf{e}$ and $\mathbf{e}_o$ according to equation (3.6) and equation (3.7), respectively.
Note that basis blade $\mathbf{e}_{12}$, for example, corresponds to the product of the matrices for $\mathbf{e}_1$ and $\mathbf{e}_2$.

Nevertheless, the chosen numerical CGA representation is much more trivial; the coefficients of the 32 components of a multivector are merely put into a vector. Hence using the matrix notation every element of $\mathbb{R}_{4,1}$ can be expressed as a vector in $\mathbb{R}^{32}$. This is detailed in the following.

6.1 Geometric Algebra and its Tensor Notation

Now a closer look beyond the symbolic level of geometric algebra is taken. It is questioned how the structure of GA can be realized numerically. The solution which is being presented makes direct use of the tensor representation inherent in GA.

Let $\{\boldsymbol{E}_1, \boldsymbol{E}_2, \ldots, \boldsymbol{E}_{2^n}\}$ denote the numbered basis of the 2^n-dimensional geometric algebra $\mathbb{R}_n$, see page 19. A multivector, say $\boldsymbol{A} \in \mathbb{R}_n$, can thus be written as the linear combination $\boldsymbol{A} = \mathsf{a}^i\, \boldsymbol{E}_i$, where a^i denotes the i^{th} component of a vector $\mathsf{a} \in \mathbb{R}^{2^n}$ and a sum over the repeated index i is implied (Einstein summation convention, see page 256). Clearly, a holds the coefficients of $\boldsymbol{A}$. Operations as the geometric product may be included in the same manner.

If $\boldsymbol{B} = \mathsf{b}^i\, \boldsymbol{E}_i$ and $\boldsymbol{C} = \mathsf{c}^i\, \boldsymbol{E}_i$, then the components of $\boldsymbol{C}$, given by the algebra equation $\boldsymbol{C} = \boldsymbol{A} \circ \boldsymbol{B}$ ('$\circ$' is a placeholder for some algebra product), can be evaluated via $\mathsf{c}^k = \mathsf{a}^i\, \mathsf{b}^j\, \mathsf{G}^k{}_{ij}$, that is

$$\begin{array}{ccccc} \boldsymbol{C} & = & \boldsymbol{A} & \circ & \boldsymbol{B} \\ \downarrow & & \downarrow & \downarrow & \downarrow \\ \mathsf{c}^k & = & \mathsf{a}^i & \mathsf{G}^k{}_{ij} & \mathsf{b}^j, \end{array} \tag{6.1}$$

where $\mathsf{G}_{kij} \in \mathbb{R}^{2^n \times 2^n \times 2^n}$ is a 3-valence tensor encoding the product '$\circ$'. The index that directly succeeds the tensor, in this case 'k', is typically associated with the result dimension. It is noteworthy that each component of the vector $\mathsf{c} \in \mathbb{R}^{2^n}$ can be written as a quadratic form as the tensor $\mathsf{G} = [\![\mathsf{G}_{kij}]\!]$ gets two-dimensional for any fixed index k, i.e. $\mathsf{G}_k = (\mathsf{G}_{kij})_{i \times j} \in \mathbb{R}^{2^n \times 2^n}$. Consider, for example, the scalar part $\langle \boldsymbol{C} \rangle$, where $k = 0$

$$\langle \boldsymbol{C} \rangle \;=\; \mathsf{c}_0 \;=\; \mathsf{a}^{\mathsf{T}} \mathsf{G}_0\, \mathsf{b}.$$

Aside: *The bilinearity in the algebra products manifests itself on defining the matrices* $\mathsf{U}, \mathsf{V} \in \mathbb{R}^{2^n \times 2^n}$ *as* $\mathsf{U}(\mathsf{a}) := [\![\mathsf{a}^i\, \mathsf{G}^k{}_{ij}]\!]$ *and* $\mathsf{V}(\mathsf{b}) := [\![\mathsf{b}^j\, \mathsf{G}^k{}_{ij}]\!]$, *respectively, because* $\mathsf{c} = \mathsf{U}(\mathsf{a})\, \mathsf{b} = \mathsf{V}(\mathsf{b})\, \mathsf{a}$ *is obviously linear in* b *and linear in* a *at the same time.*

For more explicitness a map Φ_f can be introduced

$$\begin{array}{rccc} \Phi_f : & \mathbb{R}_{p,q} & \longrightarrow & \mathbb{R}^n \\ & \boldsymbol{X} & \longmapsto & \mathsf{x} \end{array}$$

By means of Φ_f it becomes possible to assign vectors to algebra elements. Hence regarding the preceding text it is $\Phi_f(\boldsymbol{A}) = \mathsf{a}$, $\Phi_f(\boldsymbol{B}) = \mathsf{b}$ and $\Phi_f(\boldsymbol{C}) = \mathsf{c}$.

It is quite scaring that every CGA tensor that corresponds to a binary operation (a unary operation, by contrast, is e.g. the reverse) consists of $2^{5^3} = 32768$ coefficients. This would cause some CGA expressions to be inoperable. So, in practice, the complexity of calculations can be reduced considerably by using masked multivectors. A line $\boldsymbol{L}$, for example, can internally be stored by six coefficients with associated mask

$$\begin{array}{c} \boldsymbol{L} \;=\; 0.45\,\mathbf{e}_{12} + 0.89\,\mathbf{e}_{23} + 0.47\,\mathbf{e}_2\mathbf{e} \\ \downarrow \\ \Big(\texttt{line mask},\ [0.45 \quad 0.89 \quad 0 \quad 0 \quad 0.47 \quad 0]\Big), \end{array}$$

where

$$\texttt{line mask} = \left[\begin{array}{cccccccccc} 0 & & & & & & & & & \\ 0 & 0 & 0 & 0 & 0 & & & & & \\ 1 & 2 & 3 & 4 & 5 & 6 & 4 & 5 & 6 & 0 \\ 0 & 0 & 0 & 0 & 0 & 0 & 0 & 0 & 0 & 0 \\ 0 & 0 & 0 & 0 & 0 & & & & & \\ 0 & & & & & & & & & \end{array}\right]$$

Aside: *The line mask contains double indices because basis blades like* $0.47\,\mathbf{e}_2\mathbf{e}$ *correspond to the two components* $0.47\,\mathbf{e}_2\mathbf{e}_+$ *and* $0.47\,\mathbf{e}_2\mathbf{e}_-$*, respectively, due to* $\mathbf{e} = \mathbf{e}_+ + \mathbf{e}_-$ *(internally the* $\mathbf{e}_+\mathbf{e}_-$*-basis is used), see page 85.*

Accordingly, a map Φ can be defined that replaces Φ_f - the full mapping. The new Φ only maps the minimum number of coefficients necessary presuming the corresponding mask is known

$$\begin{array}{rcll} \Phi: \quad \mathbb{R}_{p,q} & \longrightarrow & \mathbb{R}^k, & \qquad k \leq n \\ \boldsymbol{X} & \longmapsto & \mathsf{x} & \end{array}$$

To understand this consider an OPNS circle $\boldsymbol{C}^*$ from which a line $\boldsymbol{L}_C = -\mathbf{e} \cdot \boldsymbol{C}^*$ is to be calculated according to equation (3.49). As it is known beforehand that $\boldsymbol{C}^*$ is a 3-blade, it follows

$$\begin{array}{rcl} \Phi(\boldsymbol{C}^*) & \longmapsto & \mathsf{c} \in \mathbb{R}^{10} \\ \Phi(\mathbf{e}) & \longmapsto & \mathsf{e} \in \mathbb{R}^{1} \\ \Phi(\boldsymbol{L}) & \longmapsto & \mathsf{l} \in \mathbb{R}^{6}. \end{array}$$

Note that generally the outer product of two vectors, for instance, will not produce 3-vector components such that these can be disregarded. Analogously, with the help of Φ the dimensions of the product tensor for the inner product $-\mathbf{e} \cdot \boldsymbol{C}^*$, in the following denoted by Q, can be restricted to only those components of the multivectors that are actually needed. Then Q can be determined such that

$$\mathsf{l}^k \;=\; -\mathsf{e}^i \mathsf{Q}^k{}_{ij}\, \mathsf{c}^j \qquad \text{with} \qquad \mathsf{Q} \;\in\; \mathbb{R}^{6\times 1\times 10}.$$

So exploiting the internal structure of CGA elements, the operation can effectively be carried out by means of a 6-by-10 matrix rather than by a 3-valence tensor with 32768 elements.

6.2 Error Propagation with CGA

Besides the necessity to provide covariance matrices as required by the Gauss-Helmert method introduced in chapter 5, it would also be senseless to not be able to go on calculating with the obtained uncertain multivectors. Consequently, an error propagation approach must be chosen that may cope with typically occurring geometric algebra functions.

The error propagation to be presented here is *standard error propagation*, which means that moments of grade higher than two are disregarded. Hence error propagation as used for this thesis bases on the concepts expectation and covariance. The alternative would be to either consider higher moments or to work with analytically derived pdfs. In both cases it must be taken into account that multivector valued functions are usually highly multivariate, especially if more than one multivector is involved. As a result, the complexity of maintaining and numerically representing the uncertainty information explodes. Despite that one must be aware that standard error propagation is mostly an approximation as it can be derived from a second order Taylor expansion of the function under consideration [82, 74]. This may only be alleviated by two things: first, the employed GH-method is likewise not capable of taking advantage of uncertainty information other than covariance matrices, nor can it provide such kind of information. Second, in the field of computer vision, and above all in geometric algebra, most of the time bilinear problems of the form (6.1) are encountered. This type of expression comes as close as possible to linear equations, for which error propagation is in effect exact.

Error propagation starts with the initial uncertain observations, which are typically assumed to be normally distributed. Since propagation relies on a Taylor approximation at the mean of a random variable two circumstances should be present: the function at hand is supposed to be locally well approximated by its tangent at the mean, and likewise the related pdf should quickly taper off within a certain validity region around that mean. Note that this does not automatically require a Gaussian distribution, as provided by the initial observations. Consequently, if an error propagation result is given in terms of a mean and a variance, it does not say that the solution corresponds to the mean itself, although this is often tacitely assumed. As an example, consider the case where the resultant density distribution is symmetric bimodal (M-shaped).

Non-Gaussian distributions can easily come up as shown in figure 6.1 and figure 6.2. The first figure geometrically explains why the product distribution of two Gaussians cannot be Gaussian. This is then substantiated by the second figure.

Subsequently, it is dealt with the question of how the first two moments of a random variable are propagated when a function is applied. In the univariate case, i.e. for one random variable $\underset{\smile}{X}$ and a function $h : \mathbb{R} \rightarrow \mathbb{R}$, it is well known that

$$\mathrm{E}(h(\underset{\smile}{X})) \approx h(\mathrm{E}(\underset{\smile}{X})) + \tfrac{1}{2} h''(\mathrm{E}(\underset{\smile}{X}))\,\mathrm{Var}(\underset{\smile}{X})$$

and

$$\mathrm{Var}(h(\underset{\smile}{X})) \approx h'(\mathrm{E}(\underset{\smile}{X}))^2\,\mathrm{Var}(\underset{\smile}{X}).$$

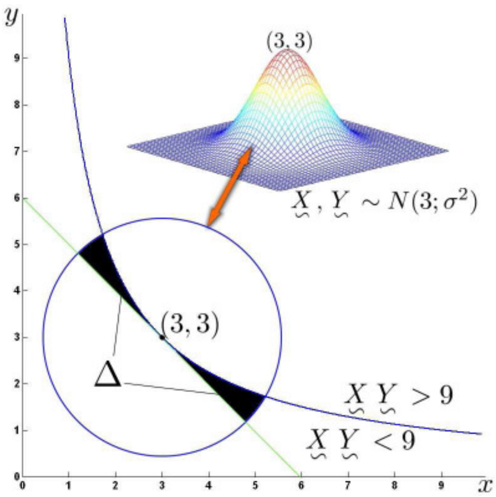

Fig. 6.1: Product of Gaussians: the random variable $\underset{\sim}{Z} = \underset{\sim}{X}\underset{\sim}{Y}$, $\sigma = 3/5$, cannot be Gaussian as there are more values smaller than nine (the mean of $\underset{\sim}{Z}$) than values greater than nine, cf. figure 6.2; the difference can be though of as twice the area denoted with Δ.

If a function $h(\underset{\sim}{\mathsf{x}}) \in \mathbb{R}$ is to be examined, where $\underset{\sim}{\mathsf{x}} \in \mathbb{R}^s$ denotes a random vector, the multivariate Taylor expansion at the mean, here denoted by $\bar{\mathsf{x}} := \mathrm{E}(\underset{\sim}{\mathsf{x}})$, must be used

$$h(\underset{\sim}{\mathsf{x}}) \;=\; \sum_{k=0}^{\infty} \frac{1}{k!} \sum_{m_1+\ldots+m_s=k} \frac{k!}{m_1!\ldots m_s!} \left(\prod_{i=1}^{s} \Delta \mathsf{x}_i^{m_i} \right) \left(\prod_{i=1}^{s} \frac{\partial^{m_i}}{\partial \mathsf{x}_i^{m_i}} \right) h(\underset{\sim}{\mathsf{x}}) \Big|_{\underset{\sim}{\mathsf{x}} = \bar{\mathsf{x}}},$$

where $\Delta \mathsf{x}_i := \mathsf{x}_i - \bar{\mathsf{x}}_i$. Along the above lines it suffices to set $k := 2$. Let $h_{\mathsf{x}_i}(\mathsf{x}) := \frac{\partial}{\partial \mathsf{x}_i} h(\mathsf{x})$ and correspondingly $h_{\mathsf{x}_i \mathsf{x}_j}(\mathsf{x}) := \frac{\partial}{\partial \mathsf{x}_i} \frac{\partial}{\partial \mathsf{x}_j} h(\mathsf{x})$. The second order approximation then reads

$$h(\underset{\sim}{\mathsf{x}} = \mathsf{x}) \;\approx\; h(\bar{\mathsf{x}}) + \sum_{i=1}^{s} \Delta \mathsf{x}_i \, h_{\mathsf{x}_i}(\bar{\mathsf{x}}) + \tfrac{1}{2} \sum_{i,j=1}^{s} \Delta \mathsf{x}_i \Delta \mathsf{x}_j \, h_{\mathsf{x}_i \mathsf{x}_j}(\bar{\mathsf{x}}).$$

Building the expectation with the help of the marginal distributions $f(\mathsf{x}_i, \mathsf{x}_j)$, obtained from the joint density distribution $f(\mathsf{x}) = f(\mathsf{x}_1, \mathsf{x}_2, \ldots, \mathsf{x}_s)$, it follows

$$\mathrm{E}(h(\underset{\sim}{\mathsf{x}})) \;\approx\; h(\bar{\mathsf{x}}) + \tfrac{1}{2} \sum_{i,j=1}^{s} [\Sigma_{\mathsf{xx}}]_{ij} \, h_{\mathsf{x}_i \mathsf{x}_j}(\bar{\mathsf{x}}), \tag{6.2}$$

where Σ_{xx} symbolizes the covariance matrix of $\underset{\sim}{\mathsf{x}}$.

This can be extended to a function of two vectors by splitting x into two parts, i.e. $\mathsf{x} \rightsquigarrow [\mathsf{x}; \mathsf{y}]$ with $\mathsf{x} \in \mathbb{R}^s$ and $\mathsf{y} \in \mathbb{R}^t$, see also [74] page 102. The original covariance matrix must be partitioned as well

$$\Sigma_{\mathsf{xx}} \;\rightsquigarrow\; \begin{bmatrix} \Sigma_{\mathsf{xx}} & \Sigma_{\mathsf{xy}} \\ \Sigma_{\mathsf{yx}} & \Sigma_{\mathsf{yy}} \end{bmatrix}. \tag{6.3}$$

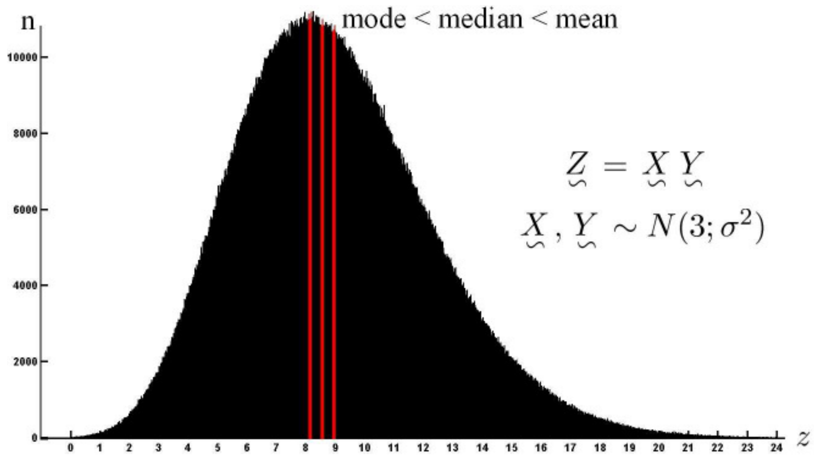

Fig. 6.2: Histogram over 3000000 samples from $\utilde{Z}$. The skewness of the distribution is obvious as mean (9), median (8.7) and mode (≈ 8.2) do not coincide. 53.5% of the samples lie below $\mathrm{E}(\utilde{Z}) = 9$.

Thus exploiting that $h_{\mathsf{x}_i\mathsf{y}_j} = h_{\mathsf{y}_j\mathsf{x}_i}$

$$\begin{aligned}\mathrm{E}(h(\utilde{\mathsf{x}},\utilde{\mathsf{y}})) \;\approx\; h(\bar{\mathsf{x}},\bar{\mathsf{y}}) \;&+\; \tfrac{1}{2}\sum_{i,j=1}^{s}[\Sigma_{\mathsf{xx}}]_{ij}\; h_{\mathsf{x}_i\mathsf{x}_j}(\bar{\mathsf{x}},\bar{\mathsf{y}}) \\ &+\; \tfrac{1}{2}\sum_{i,j=1}^{t}[\Sigma_{\mathsf{yy}}]_{ij}\; h_{\mathsf{y}_i\mathsf{y}_j}(\bar{\mathsf{x}},\bar{\mathsf{y}}) \\ &+\; \sum_{i=1}^{s}\sum_{j=1}^{t}[\Sigma_{\mathsf{xy}}]_{ij}\; h_{\mathsf{x}_i\mathsf{y}_j}(\bar{\mathsf{x}},\bar{\mathsf{y}}),\end{aligned} \tag{6.4}$$

Now consider a typical bilinear algebra product as given by equation (6.1): let $\utilde{\boldsymbol{H}} = \utilde{\boldsymbol{X}} \circ \utilde{\boldsymbol{Y}}$ such that the usage of Φ yields

$$\utilde{\mathsf{h}}^k \;=\; \utilde{\mathsf{x}}^i\, \mathsf{G}^k{}_{ij}\; \utilde{\mathsf{y}}^j. \tag{6.5}$$

Note that by the bilinearity of $\utilde{\mathsf{h}}^k$ it cannot be differentiated twice with respect to the same variable, for instance $\utilde{\mathsf{x}}$. It is thus clear from the preceding elucidations that applying equation (6.4) gives

$$\begin{aligned}\mathrm{E}(\utilde{\mathsf{h}}^k) \;&=\; \mathsf{h}^k(\bar{\mathsf{x}},\bar{\mathsf{y}}) \;+\; \sum_{i,j}[\Sigma_{\mathsf{xy}}]_{ij}\; \mathsf{h}^k_{\mathsf{x}_i\mathsf{y}_j}(\bar{\mathsf{x}},\bar{\mathsf{y}}) \\ &=\; \mathsf{h}^k(\bar{\mathsf{x}},\bar{\mathsf{y}}) \;+\; [\Sigma_{\mathsf{xy}}]^{ij}\; \mathsf{G}^k{}_{ij}\end{aligned}$$

It is crucial to note that this result is not an approximation since even a complete Taylor series expansion will not provide terms higher than the first order derivatives: error propagation for the mean of a bilinear function is exact irrespective of the underlying distribution.

Now that the expectation $\mathrm{E}(\utilde{\mathsf{h}})$ of a random vector with functional dependence $\mathsf{h}(\mathsf{x}, \mathsf{y})$ can be evaluated it remains to look for an appropriate expression for the covariance matrix of $\utilde{\mathsf{h}}$. Starting again from $h(\utilde{\mathsf{x}} \in \mathbb{R}^s) \in \mathbb{R}$ equation (6.2) can be utilized in

$$\mathrm{Cov}(\utilde{X}, \utilde{Y}) \;=\; \mathrm{E}(\utilde{X}\utilde{Y}) - \mathrm{E}(\utilde{X})\mathrm{E}(\utilde{Y}) \tag{6.6}$$

to derive the familiar expression

$$\Sigma_{\mathsf{zz}} \;\approx\; \mathsf{J}_{\mathsf{h},\mathsf{x}}(\bar{\mathsf{x}}) \;\Sigma_{\mathsf{xx}}\; \mathsf{J}_{\mathsf{h},\mathsf{x}}(\bar{\mathsf{x}})^{\mathsf{T}}, \tag{6.7}$$

where $\utilde{\mathsf{z}} := \mathsf{h}(\utilde{\mathsf{x}})$ was used. The Jacobian $\mathsf{J}_{\mathsf{h},\mathsf{x}}(\mathsf{x})$ is defined as

$$\Big[\mathsf{J}_{\mathsf{h},\mathsf{x}}(\mathsf{x})\Big]_{ij} \;:=\; \frac{\partial}{\partial \mathsf{x}_j}\mathsf{h}_i(\mathsf{x}).$$

At this point the splitting (6.3) can be reused, i.e. substituting $\mathsf{x} \rightsquigarrow [\mathsf{x};\mathsf{y}]$ yields the covariance matrix for $\utilde{\mathsf{z}} := \mathsf{h}(\utilde{\mathsf{x}}, \utilde{\mathsf{y}})$

$$\Sigma_{\mathsf{zz}} \;\approx\; \Big[\mathsf{J}_{\mathsf{h},\mathsf{x}}(\bar{\mathsf{x}},\bar{\mathsf{y}}) \quad \mathsf{J}_{\mathsf{h},\mathsf{y}}(\bar{\mathsf{x}},\bar{\mathsf{y}})\Big] \begin{bmatrix} \Sigma_{\mathsf{xx}} & \Sigma_{\mathsf{xy}} \\ \Sigma_{\mathsf{yx}} & \Sigma_{\mathsf{yy}} \end{bmatrix} \begin{bmatrix} \mathsf{J}_{\mathsf{h},\mathsf{x}}(\bar{\mathsf{x}},\bar{\mathsf{y}})^{\mathsf{T}} \\ \mathsf{J}_{\mathsf{h},\mathsf{y}}(\bar{\mathsf{x}},\bar{\mathsf{y}})^{\mathsf{T}} \end{bmatrix} \tag{6.8}$$

On multiplying out this result it can be seen that each term is a variant of the linear equivalent (5.10).

For the concerns of this thesis the accuracy of equation (6.8) regarding bilinear functions must still be investigated. As it was resorted to a second order Taylor expansion one could expect that error propagation of covariances is exact in the bilinear case. But it has to be taken into account that because of equation (6.6) terms like $\mathrm{E}(\utilde{\mathsf{h}}^a\utilde{\mathsf{h}}^b)$ may occur, that is in the notation (6.5)

$$\mathrm{E}(\utilde{\mathsf{h}}^a\utilde{\mathsf{h}}^b) \;\approx\; \mathrm{E}\Big(\utilde{\mathsf{x}}^{i_1}\; \utilde{\mathsf{x}}^{i_2}\; \utilde{\mathsf{y}}^{j_1}\; \utilde{\mathsf{y}}^{j_2}\; \mathsf{G}^a{}_{i_1 j_1}\; \mathsf{G}^b{}_{i_2 j_2}\Big).$$

Correspondingly, second derivatives might no longer be adequate - instead a Taylor approximation of order four would be necessary. This is gone through in [93, 96] with the result that an additional bias term is to be added to equation (6.8) so as to reach exactness[1]. Here a different method is chosen to provide the bias term: it is proven in [74], page 134, that the covariance of two symmetric quadratic forms $\utilde{\mathsf{v}}^{\mathsf{T}}\mathsf{A}\utilde{\mathsf{v}}$ and $\utilde{\mathsf{v}}^{\mathsf{T}}\mathsf{B}\utilde{\mathsf{v}}$, respectively, is given by

$$\mathrm{Cov}(\utilde{\mathsf{v}}^{\mathsf{T}}\mathsf{A}\utilde{\mathsf{v}}, \utilde{\mathsf{v}}^{\mathsf{T}}\mathsf{B}\utilde{\mathsf{v}}) \;=\; 4\,\bar{\mathsf{v}}^{\mathsf{T}}\mathsf{A}\Sigma_{\mathsf{vv}}\mathsf{B}\,\bar{\mathsf{v}} \;+\; 2\,\mathrm{tr}(\mathsf{A}\Sigma_{\mathsf{vv}}\mathsf{B}\Sigma_{\mathsf{vv}}) \tag{6.9}$$

where $\utilde{\mathsf{v}} \in \mathbb{R}^v$ denotes a normally distributed random vector with expectation $\bar{\mathsf{v}} := \mathrm{E}(\utilde{\mathsf{v}})$ and covariance matrix $\Sigma_{\mathsf{vv}} = \mathrm{Cov}(\utilde{\mathsf{v}}, \utilde{\mathsf{v}})$, as usual. Now let w.l.o.g.

$$\utilde{\mathsf{v}} = [\utilde{\mathsf{x}};\, \utilde{\mathsf{y}}], \qquad \mathsf{A} \;:=\; \tfrac{1}{2}\begin{bmatrix} 0 & \mathsf{G}^a \\ \mathsf{G}^{a\mathsf{T}} & 0 \end{bmatrix} \qquad \text{and} \qquad \mathsf{B} \;:=\; \tfrac{1}{2}\begin{bmatrix} 0 & \mathsf{G}^b \\ \mathsf{G}^{b\mathsf{T}} & 0 \end{bmatrix}$$

[1] Assuming normality for $\utilde{\mathsf{x}}$ and $\utilde{\mathsf{y}}$.

where $\utilde{\mathsf{x}} \in \mathbb{R}^x$, $\utilde{\mathsf{y}} \in \mathbb{R}^y$ and $\mathsf{G}^a, \mathsf{G}^b \in \mathbb{R}^{x \times y}$ such that

$$v = x + y, \qquad \utilde{\mathsf{v}}^\mathsf{T}\mathsf{A}\utilde{\mathsf{v}} \;=\; \utilde{\mathsf{x}}^\mathsf{T}\mathsf{G}^a\utilde{\mathsf{y}} \qquad \text{and} \qquad \utilde{\mathsf{v}}^\mathsf{T}\mathsf{B}\utilde{\mathsf{v}} \;=\; \utilde{\mathsf{x}}^\mathsf{T}\mathsf{G}^b\utilde{\mathsf{y}}.$$

The subexpression $\mathsf{A}\Sigma_{\mathsf{vv}}\mathsf{B}$ in equation (6.9) yields

$$\tfrac{1}{4}\begin{bmatrix} 0 & \mathsf{G}^a \\ \mathsf{G}^{a\mathsf{T}} & 0 \end{bmatrix}\begin{bmatrix} \Sigma_{\mathsf{xx}} & \Sigma_{\mathsf{xy}} \\ \Sigma_{\mathsf{yx}} & \Sigma_{\mathsf{yy}} \end{bmatrix}\begin{bmatrix} 0 & \mathsf{G}^b \\ \mathsf{G}^{b\mathsf{T}} & 0 \end{bmatrix} = \tfrac{1}{4}\begin{bmatrix} \mathsf{G}^a\Sigma_{\mathsf{yy}}\mathsf{G}^{b\mathsf{T}} & \mathsf{G}^a\Sigma_{\mathsf{yx}}\mathsf{G}^b \\ \mathsf{G}^{a\mathsf{T}}\Sigma_{\mathsf{xy}}\mathsf{G}^{b\mathsf{T}} & \mathsf{G}^{a\mathsf{T}}\Sigma_{\mathsf{xx}}\mathsf{G}^b \end{bmatrix}, \tag{6.10}$$

where it was used that

$$\Sigma_{\mathsf{vv}} \;=\; \begin{bmatrix} \Sigma_{\mathsf{xx}} & \Sigma_{\mathsf{xy}} \\ \Sigma_{\mathsf{yx}} & \Sigma_{\mathsf{yy}} \end{bmatrix}.$$

Setting again $\utilde{\mathsf{z}} = \mathsf{h}(\utilde{\mathsf{x}}, \utilde{\mathsf{y}}) := [\utilde{\mathsf{x}}^\mathsf{T}\mathsf{G}^a\utilde{\mathsf{y}}; \utilde{\mathsf{x}}^\mathsf{T}\mathsf{G}^b\utilde{\mathsf{y}}] \in \mathbb{R}^2$ it follows with

$$\mathsf{J}_{\mathsf{h},\mathsf{x}}(\bar{\mathsf{x}}, \bar{\mathsf{y}}) \;=\; \begin{bmatrix} \bar{\mathsf{y}}^\mathsf{T}\mathsf{G}^{a\mathsf{T}} \\ \bar{\mathsf{y}}^\mathsf{T}\mathsf{G}^{b\mathsf{T}} \end{bmatrix} \qquad \text{and} \qquad \mathsf{J}_{\mathsf{h},\mathsf{y}}(\bar{\mathsf{x}}, \bar{\mathsf{y}}) \;=\; \begin{bmatrix} \bar{\mathsf{x}}^\mathsf{T}\mathsf{G}^a \\ \bar{\mathsf{x}}^\mathsf{T}\mathsf{G}^b \end{bmatrix}$$

that according to approximation (6.8)

$$\Sigma_{\mathsf{zz}} \;\approx\; \begin{bmatrix} \bar{\mathsf{y}}^\mathsf{T}\mathsf{G}^{a\mathsf{T}} & \bar{\mathsf{x}}^\mathsf{T}\mathsf{G}^a \\ \bar{\mathsf{y}}^\mathsf{T}\mathsf{G}^{b\mathsf{T}} & \bar{\mathsf{x}}^\mathsf{T}\mathsf{G}^b \end{bmatrix}\begin{bmatrix} \Sigma_{\mathsf{xx}} & \Sigma_{\mathsf{xy}} \\ \Sigma_{\mathsf{yx}} & \Sigma_{\mathsf{yy}} \end{bmatrix}\begin{bmatrix} \mathsf{G}^a\bar{\mathsf{y}} & \mathsf{G}^b\bar{\mathsf{y}} \\ \mathsf{G}^{a\mathsf{T}}\bar{\mathsf{x}} & \mathsf{G}^{b\mathsf{T}}\bar{\mathsf{x}} \end{bmatrix}.$$

Particularly interesting is of course the covariance

$$\begin{aligned} \mathrm{Cov}(\utilde{\mathsf{v}}^\mathsf{T}\mathsf{A}\utilde{\mathsf{v}}, \utilde{\mathsf{v}}^\mathsf{T}\mathsf{B}\utilde{\mathsf{v}}) \;=\; [\Sigma_{\mathsf{zz}}]_{12} \;\;&\approx\;\; \bar{\mathsf{y}}^\mathsf{T}\mathsf{G}^{a\mathsf{T}}\Sigma_{\mathsf{xx}}\mathsf{G}^b\bar{\mathsf{y}} \;+\; \bar{\mathsf{x}}^\mathsf{T}\mathsf{G}^a\Sigma_{\mathsf{yx}}\mathsf{G}^b\bar{\mathsf{y}} \\ &\quad+\; \bar{\mathsf{y}}^\mathsf{T}\mathsf{G}^{a\mathsf{T}}\Sigma_{\mathsf{xy}}\mathsf{G}^{b\mathsf{T}}\bar{\mathsf{x}} \;+\; \bar{\mathsf{x}}^\mathsf{T}\mathsf{G}^a\Sigma_{\mathsf{yy}}\mathsf{G}^{b\mathsf{T}}\bar{\mathsf{x}} \\ &\overset{!}{=}\;\; 4\,\bar{\mathsf{v}}^\mathsf{T}\mathsf{A}\Sigma_{\mathsf{vv}}\mathsf{B}\,\bar{\mathsf{v}}. \end{aligned} \tag{6.11}$$

The last equality can be inferred from equation (6.10). It is crucial to notice that this is the first term of the non-approximative equation (6.9). Hence the rectification must consist in the second term $2\,\mathrm{tr}(\mathsf{A}\Sigma_{\mathsf{vv}}\mathsf{B}\Sigma_{\mathsf{vv}})$. For a deeper analysis of this term, it is now being used that, given two matrices A and B, it holds that $\mathrm{tr}(\mathsf{A}^\mathsf{T}\mathsf{B}) = \mathrm{vec}(\mathsf{A})^\mathsf{T}\,\mathrm{vec}(\mathsf{B}) = \mathsf{A}^{ij}\mathsf{B}_{ij}$. Exploiting the symmetric block structure of all involved matrices it is

$$\begin{aligned} 2\,\mathrm{tr}(\mathsf{A}\Sigma_{\mathsf{vv}}\mathsf{B}\Sigma_{\mathsf{vv}}) \;&=\; 2\,\mathrm{vec}(\Sigma_{\mathsf{vv}}\mathsf{A})^\mathsf{T}\,\mathrm{vec}(\mathsf{B}\Sigma_{\mathsf{vv}}) \\ &=\; \frac{2}{4}\begin{bmatrix} \Sigma_{\mathsf{xy}}\mathsf{G}^{a\mathsf{T}} & \Sigma_{\mathsf{xx}}\mathsf{G}^a \\ \Sigma_{\mathsf{yy}}\mathsf{G}^{a\mathsf{T}} & \Sigma_{\mathsf{yx}}\mathsf{G}^a \end{bmatrix}^{ij}\begin{bmatrix} \mathsf{G}^b\Sigma_{\mathsf{yx}} & \mathsf{G}^b\Sigma_{\mathsf{yy}} \\ \mathsf{G}^{b\mathsf{T}}\Sigma_{\mathsf{xx}} & \mathsf{G}^{b\mathsf{T}}\Sigma_{\mathsf{xy}} \end{bmatrix}_{ij} \\ &=\; \tfrac{1}{2}\Big([\Sigma_{\mathsf{xy}}\mathsf{G}^{a\mathsf{T}}]^{ij}\,[\mathsf{G}^b\Sigma_{\mathsf{yx}}]_{ij} + [\Sigma_{\mathsf{yx}}\mathsf{G}^a]^{ij}\,[\mathsf{G}^{b\mathsf{T}}\Sigma_{\mathsf{xy}}]_{ij} \\ &\qquad + [\Sigma_{\mathsf{xx}}\mathsf{G}^a]^{ij}\,[\mathsf{G}^b\Sigma_{\mathsf{yy}}]_{ij} + [\Sigma_{\mathsf{yy}}\mathsf{G}^{a\mathsf{T}}]^{ij}\,[\mathsf{G}^{b\mathsf{T}}\Sigma_{\mathsf{xx}}]_{ij}\Big). \end{aligned} \tag{6.12}$$

For a simplification it can further be used that $\mathrm{tr}(\mathsf{AB}) = \mathrm{tr}(\mathsf{BA})$. Thus

$$\begin{aligned}\mathrm{vec}(\mathsf{AB})^{\mathsf{T}}\,\mathrm{vec}(\mathsf{CD}) &= \mathrm{tr}((\mathsf{AB})^{\mathsf{T}}\mathsf{CD}) \;=\; \mathrm{tr}(\mathsf{B}^{\mathsf{T}}\mathsf{A}^{\mathsf{T}}\mathsf{CD}) \\ &= \mathrm{tr}(\mathsf{DB}^{\mathsf{T}}\mathsf{A}^{\mathsf{T}}\mathsf{C}) \;=\; \mathrm{tr}((\mathsf{BD}^{\mathsf{T}})^{\mathsf{T}}\mathsf{A}^{\mathsf{T}}\mathsf{C}) \;=\; \mathrm{vec}(\mathsf{BD}^{\mathsf{T}})^{\mathsf{T}}\,\mathrm{vec}(\mathsf{A}^{\mathsf{T}}\mathsf{C}). \qquad (6.13)\end{aligned}$$

The repeated application of this shifting scheme eventually gives

$$[\mathsf{AB}]^{ij}\,[\mathsf{CD}]_{ij} \;=\; [\mathsf{BD}^{\mathsf{T}}]^{ij}\,[\mathsf{A}^{\mathsf{T}}\mathsf{C}]_{ij} \;=\; [\mathsf{D}^{\mathsf{T}}\mathsf{C}^{\mathsf{T}}]^{ij}\,[\mathsf{B}^{\mathsf{T}}\mathsf{A}^{\mathsf{T}}]_{ij} \;=\; [\mathsf{C}^{\mathsf{T}}\mathsf{A}]^{ij}\,[\mathsf{DB}^{\mathsf{T}}]_{ij}.$$

This shows that there are the identities

$$\begin{aligned}[\Sigma_{\mathsf{xx}}\mathsf{G}^{a}]^{ij}\,[\mathsf{G}^{b}\Sigma_{\mathsf{yy}}]_{ij} &= [\Sigma_{\mathsf{yy}}\mathsf{G}^{a\mathsf{T}}]^{ij}\,[\mathsf{G}^{b\mathsf{T}}\Sigma_{\mathsf{xx}}]_{ij} \\ [\Sigma_{\mathsf{xy}}\mathsf{G}^{a\mathsf{T}}]^{ij}\,[\mathsf{G}^{b}\Sigma_{\mathsf{yx}}]_{ij} &= [\Sigma_{\mathsf{yx}}\mathsf{G}^{a}]^{ij}\,[\mathsf{G}^{b\mathsf{T}}\Sigma_{\mathsf{xy}}]_{ij}\end{aligned}$$

in equation (6.12) such that finally

$$2\,\mathrm{tr}(\mathsf{A}\Sigma_{\mathsf{vv}}\mathsf{B}\Sigma_{\mathsf{vv}}) \;=\; [\Sigma_{\mathsf{xx}}\mathsf{G}^{a}]^{ij}\,[\mathsf{G}^{b}\Sigma_{\mathsf{yy}}]_{ij} \;+\; [\Sigma_{\mathsf{xy}}\mathsf{G}^{a\mathsf{T}}]^{ij}\,[\mathsf{G}^{b}\Sigma_{\mathsf{yx}}]_{ij}. \qquad (6.14)$$

To conclude, the covariance matrix regarding a general multivariate bilinear expression $\utilde{\mathsf{z}} = \mathsf{h}(\utilde{\mathsf{x}}, \utilde{\mathsf{y}}) \in \mathbb{R}^{K}$, as given by equation (6.5), can be derived from equation (6.9): the elements of the respective $\Sigma_{\mathsf{zz}} \in \mathbb{R}^{K\times K}$ can thus be computed by combining equations (6.11) and (6.14), that is

$$\begin{aligned}[\Sigma_{\mathsf{zz}}]_{ab} \;=\; & \bar{\mathsf{y}}^{\mathsf{T}}\mathsf{G}^{a\mathsf{T}}\Sigma_{\mathsf{xx}}\mathsf{G}^{b}\bar{\mathsf{y}} + \bar{\mathsf{x}}^{\mathsf{T}}\mathsf{G}^{a}\Sigma_{\mathsf{yx}}\mathsf{G}^{b}\bar{\mathsf{y}} + \bar{\mathsf{y}}^{\mathsf{T}}\mathsf{G}^{a\mathsf{T}}\Sigma_{\mathsf{xy}}\mathsf{G}^{b\mathsf{T}}\bar{\mathsf{x}} + \bar{\mathsf{x}}^{\mathsf{T}}\mathsf{G}^{a}\Sigma_{\mathsf{yy}}\mathsf{G}^{b\mathsf{T}}\bar{\mathsf{x}} \\ & + \mathrm{vec}(\Sigma_{\mathsf{xx}}\mathsf{G}^{a})^{\mathsf{T}}\mathrm{vec}(\mathsf{G}^{b}\Sigma_{\mathsf{yy}}) + \mathrm{vec}(\Sigma_{\mathsf{xy}}\mathsf{G}^{a\mathsf{T}})^{\mathsf{T}}\mathrm{vec}(\mathsf{G}^{b}\Sigma_{\mathsf{yx}}). \qquad (6.15)\end{aligned}$$

The resultant distribution of $\utilde{\mathsf{z}}$ does however not follow a normal distribution: let again $\utilde{Z} = \utilde{X}\utilde{Y}$, where this time $\utilde{X} \sim N(0, \sigma_x^2)$ and $\utilde{Y} \sim N(0, \sigma_y^2)$ with $\mathrm{Cov}(\utilde{X}, \utilde{Y}) = 0$. By means of equation (6.15) it is

$$\mathrm{Var}(\utilde{Z}) \;=\; \sigma_x^2\sigma_y^2.$$

A histogram sampled from the distribution is shown on the right.

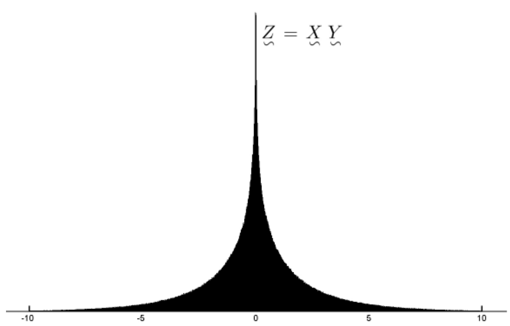

Fig. 6.3: Non-Gaussian distribution

Despite the exactness of equation (6.15), it is equation (6.8) that is being favored as its simple matrix form allows for an efficient processing where thousands of covariances have to be propagated.

6.2.1 Conformal Embedding - the Stochastic Supplement

The rules of error propagation have to be obeyed as well when embedding points into the conformal space by means of the function $\mathcal{K}$ as defined by equation (3.1). A Euclidean point $\vec{x} = x_1\mathbf{e}_1 + x_2\mathbf{e}_2 + x_3\mathbf{e}_3 \in \mathbb{R}^3$ (given in the notation of chapter 3) can clearly be identified with a Gaussian distributed random vector $\underset{\smile}{\mathsf{x}} = [\underset{\smile}{x}_1;\, \underset{\smile}{x}_2;\, \underset{\smile}{x}_3] \in \mathbb{R}^3$. Let, at variance with the former representation $\bar{\mathsf{x}} = \mathrm{E}(\underset{\smile}{\mathsf{x}})$, the expectation of $\underset{\smile}{\mathsf{x}}$ be denoted by the point itself, that is[2] $\mathrm{E}(\underset{\smile}{\mathsf{x}}) = \vec{x}$. Let, as before, the respective covariance matrix be given by $\Sigma_{\mathsf{xx}} \in \mathbb{R}^{3\times 3}$.

For the purpose of propagating the expectation $\mathrm{E}(\mathcal{K}(\underset{\smile}{\mathsf{x}}))$ equation (6.2) can be used with $\mathsf{h}(\underset{\smile}{\mathsf{x}}) := \Phi(\mathcal{K}(\underset{\smile}{\mathsf{x}})) \in \mathbb{R}^5$. According to equation (3.1) it follows at first

$$\mathsf{h}(\underset{\smile}{\mathsf{x}} = \Phi(\vec{x})) \;=\; \Phi(\vec{x} \;+\; \tfrac{1}{2}\vec{x}^2\mathbf{e} \;+\; \mathbf{e}_o) \;\overset{\Phi(\vec{x})\,=\,\bar{\mathsf{x}}}{=}\; [\,\bar{x}_1;\; \bar{x}_2;\; \bar{x}_3;\; \tfrac{1}{2}\bar{\mathsf{x}}^{\mathsf{T}}\bar{\mathsf{x}};\; 1\,]. \tag{6.16}$$

It can be seen that only the fourth component h^4 will produce second order derivatives different from zero, specifically

$$\mathsf{h}^4_{\mathsf{x}_i\mathsf{x}_j}(\bar{\mathsf{x}}) \;=\; \delta_{ij}$$

such that the expectation for the $\mathbf{e}$-component becomes

$$\mathrm{E}(\mathsf{h}^4(\underset{\smile}{\mathsf{x}})) \;=\; \mathrm{E}(\tfrac{1}{2}\underset{\smile}{\mathsf{x}}^{\mathsf{T}}\underset{\smile}{\mathsf{x}}) \;\overset{(6.2)}{\approx}\; \mathsf{h}^4(\bar{\mathsf{x}}) \;+\; \tfrac{1}{2}[\Sigma_{\mathsf{xx}}]^{ij}\, \mathsf{h}^4_{\mathsf{x}_i\mathsf{x}_j}(\bar{\mathsf{x}}) \;=\; \tfrac{1}{2}\bar{\mathsf{x}}^{\mathsf{T}}\bar{\mathsf{x}} \;+\; \tfrac{1}{2}\,\mathrm{tr}(\Sigma_{\mathsf{xx}}).$$

The uncertain representative in conformal space, i.e. the stochastic supplement for $\boldsymbol{x} := \mathcal{K}(\vec{x})$, is thus determined by a sphere with imaginary radius

$$\mathrm{E}(\mathcal{K}(\underset{\smile}{\mathsf{x}})) \;\approx\; \boldsymbol{x} + \tfrac{1}{2}\,\mathrm{tr}(\Sigma_{\mathsf{xx}})\,\mathbf{e}, \tag{6.17}$$

see equation (3.11), rather than by the pure conformal point $\boldsymbol{x}$. However it is refrained from using the exact term (6.17) since the advantages of conformal points over spheres with imaginary radius empirically outbalance the numerical error by far.

The 5×5 covariance matrix $\Sigma_{\boldsymbol{xx}}$ belonging to $\boldsymbol{x} \in \mathbb{R}^{4,1}$ can easily be computed by means of equation (6.7), which is in this case more adequate than equation (6.8)

$$\Sigma_{\boldsymbol{xx}} \;\approx\; \mathsf{J}_{\mathsf{h},\mathsf{x}}(\bar{\mathsf{x}})\,\Sigma_{\mathsf{xx}}\,\mathsf{J}_{\mathsf{h},\mathsf{x}}(\bar{\mathsf{x}})^{\mathsf{T}}.$$

The respective Jacobians can directly be deduced from the vector representation on the right in equation (6.16)

$$\mathsf{J}_{\mathsf{h},\mathsf{x}}(\bar{\mathsf{x}}) \;=\; \left.\frac{\partial \mathsf{h}(\mathsf{x})}{\partial \mathsf{x}}\right|_{\mathsf{x}=\bar{\mathsf{x}}} \;=\; \begin{bmatrix} 1 & 0 & 0 \\ 0 & 1 & 0 \\ 0 & 0 & 1 \\ \bar{x}_1 & \bar{x}_2 & \bar{x}_3 \\ 0 & 0 & 0 \end{bmatrix}.$$

[2] Hence $\vec{x}$ can be regarded as a maximum likelihood estimate built from a set of samples of size one. It may likewise be stated $\vec{x} = \Phi^{-1}(\bar{\mathsf{x}})$.

Chapter 7

Applications in Computer Vision

This is the first time that all concepts of this thesis are being brought together. Three different parameter estimation examples shall demonstrate the goodness of the previously derived GH-method, see preferably section 5.3.4, when applied to problems expressed in the language of conformal geometric algebra. It is begun with a simple example of fitting a circle to a set of uncertain points in 3D, which was also one of the first experiments with the GH-method. The elucidations culminate in the presentation of a solution to the perspective pose estimation problem as introduced in chapter 4. The subsequent descriptions clearly builds on CGA, but subjects such as error propagation are prerequisites as well; refer to chapter 6 in this respect. In the end, experimental results including comparisons to standard approaches are presented.

Recall that, in general, the aim is to find multivectors that satisfy a particular condition that depends on a set of uncertain measurements. The specific problem and the type of multivector, representing a geometric entity or a geometric operator, determine this condition. Here point measurements from Euclidean 3D-space are considered, where the respective uncertainties are assumed to be given by covariance matrices.

Related Work

A discussion regarding the linear estimation of rotation operators in geometric algebra can be found in [98], albeit without taking account of uncertainty. In the scope of perspective pose estimation Rosenhahn and Sommer [104] derived a method for estimating rotation/translation operators by means of conformal geometric algebra. Their approach is mainly based on the stratification hierarchy of Euclidean, projective and affine spaces. Based on previous works by Förstner et al. [35] and Heuel [65], where uncertain points, lines and planes were treated in a unified manner, the estimation of uncertain CGA operators was introduced in [95], which can be viewed as a foundation for this text.

Notation for Succeeding Sections

In the field of computer vision the variables x and y are typically designated for representing image coordinates. Hence it is necessary to (partly) give up the classically stochastic notation given in the synopsis on page 169 so as to avoid confusing the meanings. Especially the Jacobians of definition (5.26) have to be adapted. The following changes arise:

$$\begin{array}{rcccl}
\text{Parameters} & \boldsymbol{\theta} & \longrightarrow & \mathsf{p} & \in & \mathbb{R}^M \\
\text{Number of block observations} & k & \longrightarrow & N & & \\
i^{th}\text{ block observation} & \mathsf{y}_{\underline{\mathsf{i}}} & \longrightarrow & \mathsf{b}_{\underline{\mathsf{i}}} & \in & \mathbb{R}^{K_i} \\
\text{Vector of observations} & \mathsf{y} & \longrightarrow & \mathsf{b} & \in & \mathbb{R}^K \\
\text{Jacobian w.r.t. parameters} & \mathsf{X}(\mathsf{y}) & \longrightarrow & \mathsf{U}(\mathsf{b}) & \in & \mathbb{R}^{N_g \times M} \\
\text{Jacobian w.r.t. observations} & \mathsf{Z}(\boldsymbol{\theta}) & \longrightarrow & \mathsf{V}(\mathsf{p}) & \in & \mathbb{R}^{N_g \times K}
\end{array}$$

7.1 Fitting a Circle in 3D

The first example is a classical parameter estimation problem: fitting a circle to a set of points.

Given a set of N observations, that is Euclidean 3D-points with associated covariance matrices, their stochastic embedding into the conformal space, as described in section 6.2.1, yields a set of conformal points $\{\boldsymbol{b}_{\underline{1}\ldots\underline{N}}\}$, together with the propagated 5×5 covariance matrices, denoted by $\{\Sigma_{\mathsf{b}_{\underline{1}}\mathsf{b}_{\underline{1}}}, \Sigma_{\mathsf{b}_{\underline{2}}\mathsf{b}_{\underline{2}}}, \ldots, \Sigma_{\mathsf{b}_{\underline{N}}\mathsf{b}_{\underline{N}}}\}$.

Note that henceforth a stochastic embedding as above is implicitly assumed throughout all remaining sections dealing with estimation.

7.1.1 The Functional Model

For the purpose of fitting a circle to the data a functional model must be present. Remarkably, it arises right from the definition of a circle in CGA (page 108): the inner product null space. Hence a point $\boldsymbol{x}$ lies on the circle $\boldsymbol{C}$ iff it fulfills the simple condition

$$\boldsymbol{x} \cdot \boldsymbol{C} \;=\; 0,$$

where the 2-blade $\boldsymbol{C} = \boldsymbol{C}_{\langle 2 \rangle}$ can be thought of as an intersection of two spheres, say $\boldsymbol{S}_1$ and $\boldsymbol{S}2$, see equation (3.43). In fact, it is

$$\boldsymbol{x} \cdot \boldsymbol{C} \;=\; \boldsymbol{x} \cdot (\boldsymbol{S}_1 \wedge \boldsymbol{S}_2) \;=\; \underbrace{(\boldsymbol{x} \cdot \boldsymbol{S}_1)}_{\in \mathbb{R}} \boldsymbol{S}_2 \;-\; \underbrace{(\boldsymbol{x} \cdot \boldsymbol{S}_2)}_{\in \mathbb{R}} \boldsymbol{S}_1$$

an expression being different from zero[1] unless $\boldsymbol{x}$ lies on both of the spheres at the same time, which is equivalent to $\boldsymbol{x}$ being a point on the circle. Now isomorphism

[1]The expression may also be zero if the spheres are not linearly independent. However, this would imply that $\boldsymbol{S}_1$ and $\boldsymbol{S}_2$ represent the same sphere.

Φ can be used to transfer the inner product expression to an equivalent matrix representation, which may then already be used as the necessary G-condition for the GH-method. The parameter vector p that describes the sought circle $\boldsymbol{C}$ is ten-dimensional as there are ten basis blades of grade two in $\mathbb{R}_{4,1}$. Accordingly

$$\begin{array}{rcll} \Phi(\boldsymbol{b}_{\underline{i}}) & \longmapsto & \mathsf{b}_{\underline{i}} \in \mathbb{R}^5, & i \in [1,N]_{\mathbb{Z}} \\ \Phi(\boldsymbol{C}_{\langle 2\rangle}) & \longmapsto & \mathsf{p} \in \mathbb{R}^{10}. & \end{array}$$

Note that the inner product of a vector with a bivector results in a vector. Since a vector has five components, the condition equation $\mathsf{g}_{\underline{i}}$ for the i^{th} (block) observation is five-dimensional

$$\mathsf{g}_{\underline{i}}(\mathsf{b}_{\underline{i}}, \mathsf{p}) \;:=\; \Phi(\boldsymbol{b}_{\underline{i}} \cdot \boldsymbol{C}) \;=\; 0 \quad \in \quad \mathbb{R}^5.$$

The respective Jacobians $\mathsf{U}_{\underline{i}}(\mathsf{b}_{\underline{i}})$ and $\mathsf{V}_{\underline{i}}(\mathsf{p})$ can be obtained from the tensor representation of the G-condition; the t^{th} component of $\mathsf{g}_{\underline{i}} = [\![\mathsf{b}_{\underline{i}}^r \mathsf{G}^t{}_{rs} \mathsf{p}^s]\!] \in \mathbb{R}^5$ reads

$$[\mathsf{g}_{\underline{i}}(\mathsf{b}_{\underline{i}}, \mathsf{p})]_t \;=\; \mathsf{b}_{\underline{i}}^r \mathsf{G}^t{}_{rs} \mathsf{p}^s, \qquad 1 \le t \le 5,$$

where the product tensor $\mathsf{G} \in \mathbb{R}^{5\times5\times10}$ is assumed to realize the inner product. Differentiating thus gives the matrices

$$\begin{aligned} \mathsf{U}_{\underline{i}}(\mathsf{b}_{\underline{i}}) &= [\![\mathsf{b}_{\underline{i}}^r \mathsf{G}^t{}_{rs}]\!] \in \mathbb{R}^{5\times10} \\ \mathsf{V}_{\underline{i}}(\mathsf{p}) &= [\![\mathsf{G}^t{}_{rs} \mathsf{p}^s]\!] \in \mathbb{R}^{5\times5}, \end{aligned}$$

where[2] $\mathsf{V} := \mathsf{V}_{\underline{i}}$ is constant over $1 \le \underline{i} \le N$. These matrices are nearly sparse due to the particularly simple structure of the G-tensor for the inner product. For example,

$$\mathsf{U}_{\underline{i}}(\mathsf{b}_{\underline{i}}) \;=\; \begin{bmatrix} -\mathsf{b}_{\underline{i}2} & 0 & \mathsf{b}_{\underline{i}3} & -\mathsf{b}_{\underline{i}4} & 0 & 0 & \mathsf{b}_{\underline{i}5} & 0 & 0 & 0 \\ \mathsf{b}_{\underline{i}1} & -\mathsf{b}_{\underline{i}3} & 0 & 0 & -\mathsf{b}_{\underline{i}4} & 0 & 0 & \mathsf{b}_{\underline{i}5} & 0 & 0 \\ 0 & \mathsf{b}_{\underline{i}2} & -\mathsf{b}_{\underline{i}1} & 0 & 0 & -\mathsf{b}_{\underline{i}4} & 0 & 0 & \mathsf{b}_{\underline{i}5} & 0 \\ 0 & 0 & 0 & \mathsf{b}_{\underline{i}1} & \mathsf{b}_{\underline{i}2} & \mathsf{b}_{\underline{i}3} & 0 & 0 & 0 & \mathsf{b}_{\underline{i}5} \\ 0 & 0 & 0 & 0 & 0 & 0 & \mathsf{b}_{\underline{i}1} & \mathsf{b}_{\underline{i}2} & \mathsf{b}_{\underline{i}3} & \mathsf{b}_{\underline{i}4} \end{bmatrix}.$$

It is important to notice that algebraically fitting a circle is obviously a linear problem as it may be written

$$\mathsf{g}_{\underline{i}}(\mathsf{b}_{\underline{i}}, \mathsf{p}) \;=\; \mathsf{U}_{\underline{i}}(\mathsf{b}_{\underline{i}})\,\mathsf{p}. \tag{7.1}$$

Later on, the linear relationship is used to determine an initial estimate for the circle, which is possible because the parameter vector p does apparently lie in a common nullspace of the matrices $\mathsf{U}_{\underline{i}}(\mathsf{b}_{\underline{i}})$, $\underline{i} \in [1,N]_{\mathbb{Z}}$.

It can easily be demonstrated that the imposed conditions are indeed algebraic but not geometric. Picture 7.1 shows a circle and lines of equal inner product (norm of the inner product). These isolines were chosen to be equidistant in the circle plane, and it can be seen that their respective curves deviate from concentric circles as they would occur if the inner product returned the Euclidean distance to the circle. So in case of imperfect data the algebraic fit can slightly differ from a geometric fit.

[2] It is $[\![\mathsf{G}^t{}_{rs}\mathsf{p}^s]\!] = (\mathsf{G}^t{}_{rs}\mathsf{p}^s)_{t\times r}$ or equally $[\![\mathsf{G}^t{}_{rs}\mathsf{p}^s]\!]_{ij} = \mathsf{G}^i{}_{js}\mathsf{p}^s$, consult appendix C.

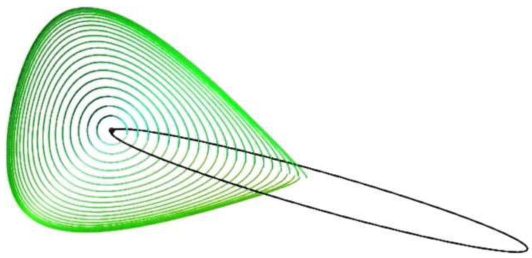

Fig. 7.1: Inner product isolines: the inner product of a point and a circle tends to be isotropic with decreasing proximity to the circle.

7.1.2 Constraints

It must not be overlooked that additional constraints are necessary. The reason is an overparameterization of the circle. A circle in 3D needs six parameters to be uniquely defined (three for the center, two for the circle plane and one for the radius) - the parameter vector p does however have ten components so that a functional dependency of $4 = 10 - 6$ is present. In order to fix the overparameterization, an H-constraint on the parameters, forcing $\boldsymbol{C} \wedge \boldsymbol{C}$ to zero, is introduced, which constrains $\boldsymbol{C} = \Phi^{-1}(\mathsf{p})$ to be a 2-blade (proved in section A.3.1). Let $\mathsf{O} \in \mathbb{R}^{5\times10\times10}$ denote the tensor for the outer product. The result dimension is again five-dimensional because $\boldsymbol{C} \wedge \boldsymbol{C}$ yields a quadvector, see page 86. The vector of constraints $\mathsf{h} \in \mathbb{R}^5$ is thus

$$\mathsf{h}(\mathsf{p}) \;=\; \Phi(\boldsymbol{C} \wedge \boldsymbol{C}) \;=\; [\![\mathsf{p}^r \mathsf{O}^t{}_{rs} \mathsf{p}^s]\!],$$

whence the matrix H is obtained

$$\mathsf{H}(\mathsf{p}) \;=\; \partial_{\mathsf{p}'} \mathsf{h}(\mathsf{p}')\Big|_{\mathsf{p}'=\mathsf{p}} \;=\; 2[\![\mathsf{p}^r \mathsf{O}^t{}_{rs}]\!] \quad \in \mathbb{R}^{5\times10}.$$

The matrix is at most of rank five but it turns out that $\operatorname{rank}(\mathsf{H}) = 3$, which is why a further constraint has to be added so as to completely remedy the functional dependency. Recall that CGA entities may vary in scale because a change in scale does not change the inner or outer product null space. The last constraint is therefore a kind of standard constraint inherent in CGA. W.l.o.g. it can be demanded

$$\mathsf{h}'(\mathsf{p}) \;:=\; \mathsf{p}^\mathsf{T}\mathsf{p} - 1 \;=\; 0 \quad \in \mathbb{R} \qquad \Longleftrightarrow \qquad \mathsf{H}'(\mathsf{p}) \;=\; 2[\![\mathsf{p}_r]\!]^\mathsf{T} \;=\; 2\mathsf{p}^\mathsf{T} \quad \in \mathbb{R}^{1\times10}.$$

Combining the matrices H and H' as $\mathsf{H} \rightsquigarrow [\mathsf{H};\mathsf{H}']$ gives

$$\mathsf{H} \;=\; 2\;\begin{array}{c}
\begin{array}{cccccccccc}
1 & 2 & 3 & 4 & 5 & 6 & 7 & 8 & 9 & 10 \\
\mathbf{e}_1\mathbf{e}_2 & \mathbf{e}_2\mathbf{e}_3 & \mathbf{e}_3\mathbf{e}_1 & \mathbf{e}_1\mathbf{e}_+ & \mathbf{e}_2\mathbf{e}_+ & \mathbf{e}_3\mathbf{e}_+ & \mathbf{e}_1\mathbf{e}_- & \mathbf{e}_2\mathbf{e}_- & \mathbf{e}_3\mathbf{e}_- & \mathbf{e}_+\mathbf{e}_-
\end{array} \\
\begin{bmatrix}
\mathsf{p}_6 & \mathsf{p}_4 & \mathsf{p}_5 & \mathsf{p}_2 & \mathsf{p}_3 & \mathsf{p}_1 & 0 & 0 & 0 & 0 \\
\mathsf{p}_9 & \mathsf{p}_7 & \mathsf{p}_8 & 0 & 0 & 0 & \mathsf{p}_2 & \mathsf{p}_3 & \mathsf{p}_1 & 0 \\
\mathsf{p}_{10} & 0 & 0 & -\mathsf{p}_8 & \mathsf{p}_7 & 0 & \mathsf{p}_5 & -\mathsf{p}_4 & 0 & \mathsf{p}_1 \\
0 & \mathsf{p}_{10} & 0 & 0 & -\mathsf{p}_9 & \mathsf{p}_8 & 0 & \mathsf{p}_6 & -\mathsf{p}_5 & \mathsf{p}_2 \\
0 & 0 & \mathsf{p}_{10} & \mathsf{p}_9 & 0 & -\mathsf{p}_7 & -\mathsf{p}_6 & 0 & \mathsf{p}_4 & \mathsf{p}_3 \\
\mathsf{p}_1 & \mathsf{p}_2 & \mathsf{p}_3 & \mathsf{p}_4 & \mathsf{p}_5 & \mathsf{p}_6 & \mathsf{p}_7 & \mathsf{p}_8 & \mathsf{p}_9 & \mathsf{p}_{10}
\end{bmatrix}
\end{array}
.\;
\begin{array}{l}
\\ \\
\mathbf{e}_1\mathbf{e}_2\mathbf{e}_3\mathbf{e}_+ \\
\mathbf{e}_1\mathbf{e}_2\mathbf{e}_3\mathbf{e}_- \\
\mathbf{e}_1\mathbf{e}_2\mathbf{e}_+\mathbf{e}_- \\
\mathbf{e}_2\mathbf{e}_3\mathbf{e}_+\mathbf{e}_- \\
\mathbf{e}_3\mathbf{e}_1\mathbf{e}_+\mathbf{e}_- \\
\\
\end{array}$$

The elements on the right indicate the basis blade that a constraint-row aims at. The elements above H indicate to which basis blade the columns belong to.

7.1.3 Proceeding

Since it is iterative in nature, it was previously assumed that it exists an initial starting point for the GH-method; clearly, regarding the data the observations themselves can be taken, but an initial estimate for the parameter vector has to be provided as well. By means of equation (7.1) it follows that the parameter vector p must satisfy

$$\mathsf{g} = \underbrace{\begin{bmatrix} \mathsf{U}_{\underline{1}}(\mathsf{b}_{\underline{1}}) \\ \mathsf{U}_{\underline{2}}(\mathsf{b}_{\underline{2}}) \\ \vdots \\ \mathsf{U}_{\underline{\mathsf{N}}}(\mathsf{b}_{\underline{\mathsf{N}}}) \end{bmatrix}}_{\mathsf{U}(\mathsf{b})} \mathsf{p} = 0.$$

Thus p lies in the common nullspace of the $\mathsf{U}_{\underline{\mathsf{i}}}$, $\underline{\mathsf{i}} \in [1, N]_{\mathbb{Z}}$, whence a simple singular value decomposition (SVD) of $\mathsf{U}(\mathsf{b})$ can be used to compute the initial estimate.

Having all the necessary matrices at hand the GH-method can be applied, i.e. it can be solved for the corrections $\Delta\mathsf{p}$ and $\{\Delta\mathsf{b}_{1\ldots N}\}$. Experimental results and comparisons that show the quality of the GH-method applied to the illustrative example of a circle-fit problem, can be found in the introductory paper of Perwass, Gebken and Sommer [95]. It likewise comprises experimental results for the problem stated in section 7.2.

7.1.4 Visualizing Uncertainty

As derived on page 174, the method as well provides the covariance matrix Σ_{pp} of p. It tells how reliable the model fits the observations and how advantageously these are distributed. It does not reflect to which extend the estimate deviates from a potentially perfect fit regarding ground truth (because this cannot be known), i.e. it is no quality measure for the method. Figure 7.2 illustrates the uncertainty of an estimated circle. The surrounding tubes, indicated by slices, show the standard deviation of the estimates.

Because a line has one degree of freedom fewer than a circle (it has no $\boldsymbol{E}$-component), adding a further constraint is sufficient to enforce the estimation to yield lines. It is likewise possible to simply omit the entry in p that represents the $\boldsymbol{E}$-component so that one is left with a nine- rather than ten-dimensional vector p; the constraints will then still make sure that the estimate is a blade. The uncertainty of an estimated line is depicted by figure 7.3.

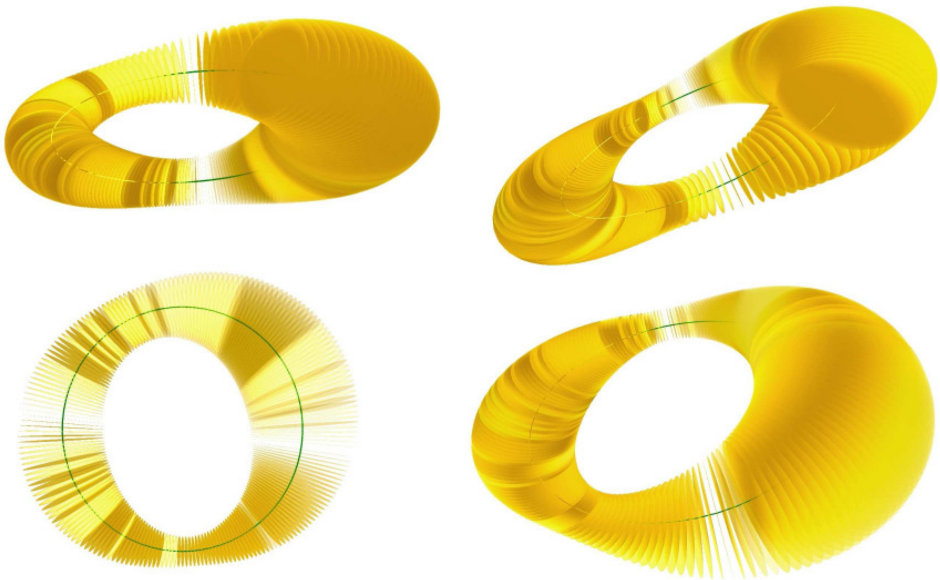

Fig. 7.2: Fitting a circle: the uncertainty, i.e. standard deviation, of an estimated circle in four different views. The image in the lower left depicts a top view of the circle.

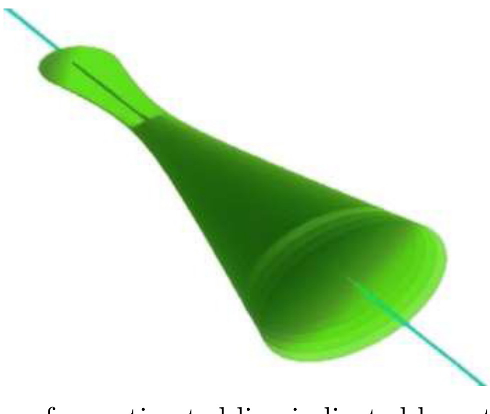

Fig. 7.3: Uncertainty of an estimated line indicated by a twisted elliptic tube.

7.2 Estimating a Rigid Body Motion

This section is preparatory for the coming sections dealing with pose estimation in that not a geometric object but a geometric operator, namely a motor, is estimated. Such an element is also the objective of the estimation presented in chapter 4, where an approach completely different from the GH-method is chosen. A comprehensive discussion of motors can be found in section 3.4.5.

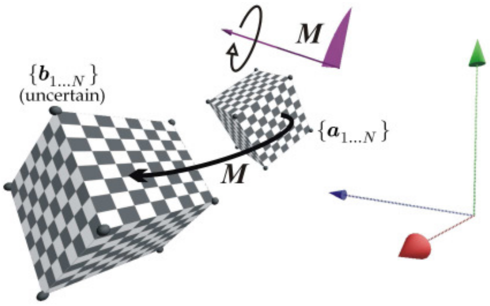

Fig. 7.4: The estimation of an RBM with points forming a cube.

Now it is being focused on the transformation interrelating two (almost) congruent sets of 3D-points. Let $\{\boldsymbol{a}_{1\ldots N}\}$ and $\{\boldsymbol{b}_{1\ldots N}\}$ be the two sets, where it is assumed that each point $\boldsymbol{a}_{\underline{i}} \in \mathbb{R}^{4,1}$ is a constant, whereas the corresponding point $\boldsymbol{b}_{\underline{i}} \in \mathbb{R}^{4,1}$ represents an observation with associated uncertainty $\Sigma_{\mathsf{b}_{\underline{i}}\mathsf{b}_{\underline{i}}} \in \mathbb{R}^{5\times 5}$, $\underline{i} \in [1, N]_{\mathbb{Z}}$. An example scenario is depicted in figure 7.4. Recall that in CGA, transformations are expressed in the form of

$$\boldsymbol{M}\boldsymbol{a}\widetilde{\boldsymbol{M}} = \boldsymbol{b}. \tag{7.2}$$

Unfortunately, it is no particular algebraic operation known by means of which the motor $\boldsymbol{M}$ that best transforms the points $\{\boldsymbol{a}_{1\ldots N}\}$ into $\{\boldsymbol{b}_{1\ldots N}\}$ could be computed at once. However, switching to the tensor representation of CGA the above equation can be reformulated [98]. The first step consists in exploiting that a motor is a unitary versor, i.e. $\boldsymbol{M}\widetilde{\boldsymbol{M}} = \mathbf{1}$. On multiplying with $\boldsymbol{M}$ from the right, equation (7.2) can be rewritten as

$$\boldsymbol{M}\boldsymbol{a}\widetilde{\boldsymbol{M}} = \boldsymbol{b} \quad \Longleftrightarrow \quad \boldsymbol{M}\boldsymbol{a} - \boldsymbol{b}\boldsymbol{M} = \mathbf{0},$$

whence the tensor representation follows as

$$\Phi : \begin{array}{ccccccccc} \boldsymbol{M} & & \boldsymbol{a}_{\underline{i}} & - & \boldsymbol{b}_{\underline{i}} & & \boldsymbol{M} & = & \mathbf{0} \\ \downarrow & & \downarrow & & \downarrow & & \downarrow & & \downarrow \\ \mathsf{p}^k & \mathsf{G}^t{}_{kl} & \mathsf{a}_{\underline{i}}{}^l & - & \mathsf{b}_{\underline{i}}{}^l & \mathsf{G}^t{}_{lk} & \mathsf{p}^k & = & \mathsf{0}^t \end{array}, \qquad \begin{array}{rcl} 1 \leq & t & \leq 5 \\ 1 \leq & \underline{i} & \leq N. \end{array} \tag{7.3}$$

It is $\Phi(\boldsymbol{a}) = \mathsf{a} \in \mathbb{R}^5$, $\Phi(\boldsymbol{b}) = \mathsf{b} \in \mathbb{R}^5$ and $\Phi(\boldsymbol{M}) = \mathsf{p} \in \mathbb{R}^8$, which includes the scalar component of a motor, see below. Accordingly, the tensor for the geometric product is $[\![\mathsf{G}^t{}_{kl}]\!] \in \mathbb{R}^{5\times 8\times 5}$ and $[\![\mathsf{G}^t{}_{lk}]\!] \in \mathbb{R}^{5\times 5\times 8}$, respectively. The Φ-mask associated with the motor, see page 181, is

$$
\begin{array}{ll}
\texttt{RBM mask} = [& 1 \\
& 0\ 0\ 0\ 0\ 0 \\
& 2\ 3\ 4\ 5\ 6\ 7\ 5\ 6\ 7\ 0 \\
& 0\ 0\ 0\ 0\ 0\ 0\ 0\ 0\ 0\ 0 \\
& 8\ 8\ 0\ 0\ 0 \\
& 0 \qquad\qquad\qquad\qquad].
\end{array}
\tag{7.4}
$$

As expected, equation (7.3) lends itself to being used as the functional model. A differentiation w.r.t. p and $\mathsf{b}_{\underline{\mathsf{i}}}$, respectively, yields the familiar matrices

$$
\Longrightarrow \quad
\begin{array}{rcll}
\mathsf{g}_{\underline{\mathsf{i}}}(\mathsf{b}_{\underline{\mathsf{i}}}, \mathsf{p}) & := & [\![\mathsf{p}^k \mathsf{G}^t{}_{kl} \mathsf{a}_{\underline{\mathsf{i}}}{}^l - \mathsf{b}_{\underline{\mathsf{i}}}{}^l \mathsf{G}^t{}_{lk} \mathsf{p}^k]\!] = 0 & \in \mathbb{R}^5 \\
\mathsf{U}(\mathsf{b}_{\underline{\mathsf{i}}}) & = & [\![\mathsf{G}^t{}_{kl} \mathsf{a}_{\underline{\mathsf{i}}}{}^l - \mathsf{b}_{\underline{\mathsf{i}}}{}^l \mathsf{G}^t{}_{lk}]\!] & \in \mathbb{R}^{5\times 8} \\
\mathsf{V}(\mathsf{p}) & = & [\![-\mathsf{p}^k \mathsf{G}^t{}_{lk}]\!] & \in \mathbb{R}^{5\times 5}.
\end{array}
\tag{7.5}
$$

Since a rigid body motion is defined by six rather than by eight parameters, constraints become necessary. It may be chosen

$$
\mathsf{h}(\mathsf{p}) := \Phi_f(\boldsymbol{M}\widetilde{\boldsymbol{M}} - \mathbf{1}) = [\![\mathsf{p}^k\, \mathsf{G}^t{}_{km}\, \mathsf{R}^m{}_l\, \mathsf{p}^l - \delta^{t1}]\!] \in \mathbb{R}^{32},
$$

where G and R denote the tensors for the geometric product and the reverse operation, respectively. Symbolically evaluating $\mathsf{h}(\mathsf{p})$ for multivectors with a structure imposed by the RBM mask reveals that $\mathsf{h}(\mathsf{p})$ is sparse - only the entries h_1, h_{27} and h_{28} are non-zero:

$$
\begin{array}{rcll}
\mathsf{h}_1 & = & \mathsf{p}_1^2 + \mathsf{p}_2^2 + \mathsf{p}_3^2 + \mathsf{p}_4^2 - 1 & = 0 \\
\mathsf{h}_{27} & = & 2(\mathsf{p}_8\mathsf{p}_1 - \mathsf{p}_5\mathsf{p}_2 - \mathsf{p}_6\mathsf{p}_3 - \mathsf{p}_7\mathsf{p}_4) & = 0 \\
\mathsf{h}_{28} & = & \mathsf{h}_{27} &
\end{array}
\tag{7.6}
$$

Thus the condition $\boldsymbol{M}\widetilde{\boldsymbol{M}} = \mathbf{1}$ provides exactly the two required constraints. Differentiating gives

$$
\mathsf{H}(\mathsf{p}) = 2 \begin{bmatrix} \mathsf{p}_1 & \mathsf{p}_2 & \mathsf{p}_3 & \mathsf{p}_4 & 0 & 0 & 0 & 0 \\ \mathsf{p}_8 & -\mathsf{p}_5 & -\mathsf{p}_6 & -\mathsf{p}_7 & -\mathsf{p}_2 & -\mathsf{p}_3 & -\mathsf{p}_4 & \mathsf{p}_1 \end{bmatrix}.
\tag{7.7}
$$

These two constraints in conjunction with the implicit structural constraint imposed by the RBM mask are sufficient to describe a motor, an element from the Lie group $SE(3)$, cf. chapter 4. The encoding, which is also free from trigonometric functions, is therefore remarkably dense, for example, in comparison to a rotation matrix, which needs six constraints for nine parameters (three degrees of freedom).

By simply substituting the derived matrices U, V and H into the respective equations given in the theoretical part, the estimate for $\boldsymbol{M}$ can be computed in an iterative way. An initial estimate may easily be obtained by using the SVD-method described in section 7.1.3, applied to the U-matrices given by equation (7.5), or by using the rotation matrix based standard approach in [5].

7.2.1 Experiments

To show the quality of the GH-estimation method, synthetic experiments were conducted, see [95].

In the experiment, the points $\{\boldsymbol{a}_{1\ldots N}\}$, from now on referred to as the 'true' points, are Gaussian distributed about the origin with a standard deviation 0.8. These are subsequently transformed by the ground truth motor $\boldsymbol{M}_0$, which gives $\{\boldsymbol{a'}_{1\ldots N}\}$, the transformed true points. Afterwards, noise is added to build the data points $\{\boldsymbol{b}_{1\ldots N}\}$. Notice that the noise is exactly generated in compliance with the respective, randomly chosen, covariance matrices $\{\Sigma_{\mathsf{b}_{\underline{1}}\mathsf{b}_{\underline{1}}}, \Sigma_{\mathsf{b}_{\underline{2}}\mathsf{b}_{\underline{2}}}, \ldots, \Sigma_{\mathsf{b}_{\underline{N}}\mathsf{b}_{\underline{N}}}\}$.

The above procedure is repeated: for each of 40 sets of true points, 40 data point sets are generated such that a total of 1600 motors is estimated. Finally, the true points are rotated by means of the corresponding estimates $\{\{\widehat{\boldsymbol{M}}_{1\ldots 40}\}_{1\ldots 40}\}$ to give $\{\{\{\hat{\boldsymbol{a}}_{1\ldots N}\}_{1\ldots 40}\}_{1\ldots 40}\}$. For each of the 1600 runs, Euclidean distance vectors $\{\mathsf{d}_{1\ldots N}\}$, defined as

$$\mathsf{d}_{\underline{i}} \;=\; \mathcal{K}^{-1}(\boldsymbol{a}'_{\underline{i}}) \;-\; \mathcal{K}^{-1}(\hat{\boldsymbol{a}}_{\underline{i}}) \quad \in \mathbb{R}^3, \qquad 1 \le \underline{i} \le N,$$

are computed. From these values two different quality measures are calculated: the Euclidean RMS[3]-distance

$$\delta_E \;:=\; \sqrt{\frac{1}{N}\sum\nolimits_{\underline{i}} \mathsf{d}_{\underline{i}}^{\mathsf{T}}\, \mathsf{d}_{\underline{i}}}$$

and the Mahalanobis RMS-distance, which already occurred on page 153,

$$\delta_\Sigma \;:=\; \sqrt{\frac{1}{N}\sum\nolimits_{\underline{i}} \mathsf{d}_{\underline{i}}^{\mathsf{T}}\, \Sigma_{\mathsf{b}_{\underline{i}}\mathsf{b}_{\underline{i}}}^{-1}\, \mathsf{d}_{\underline{i}}}.$$

For each true point set, the mean and standard deviation of the δ_E and δ_Σ over all 40 data point sets is denoted by Δ_E, σ_E and Δ_Σ, σ_Σ, respectively. It then remains to average over the true point sets, i.e. over Δ_E, σ_E and Δ_Σ, σ_Σ. The ultimately obtained values are denoted by $\bar{\Delta}_E$, $\bar{\sigma}_E$ and $\bar{\Delta}_\Sigma$, $\bar{\sigma}_\Sigma$, respectively. Furthermore, the experiments were conducted for different rotation angles.

	$\bar{\Delta}_\Sigma$ ($\bar{\sigma}_\Sigma$)			$\bar{\Delta}_E$ ($\bar{\sigma}_E$)		
σ_r	Std	SVD	GH	Std	SVD	GH
0.09	1.44 (0.59)	1.47 (0.63)	0.68 (0.22)	0.037 (0.011)	0.037 (0.012)	0.024 (0.009)
0.18	1.47 (0.62)	1.53 (0.67)	0.72 (0.25)	0.078 (0.024)	0.079 (0.026)	0.052 (0.019)

Table 7.1: Result of general rotation estimation for standard method (Std), SVD method (SVD) and Gauss-Helmert method (GH).

Table 7.1 compares the results of the GH-method (GH) with those from the initial SVD estimate and with those given by the standard approach (Std) described in [5].

[3] RMS stands for 'root mean square'.

Since the quality measures did not give significantly different results for rotation angles between 3 and 160 degrees, the means of the respective values over all rotation angles are shown in the table. The rotation axis always points along the z-axis and is moved one unit away from the origin along the x-axis. In all experiments $N = 10$ points are used.

It can be seen that for different levels of ground noise σ_r (according to which the covariance matrices $\Sigma_{\mathsf{b_i b_i}}$ are created) the Gauss-Helmert method always performs significantly better in the mean quality and the mean standard deviation than the other two. The Euclidean measure $\bar{\Delta}_E$ is approximately doubled when σ_r is doubled, whereas the stochastic measure $\bar{\Delta}_\Sigma$ increases only slightly. Note that $\bar{\Delta}_\Sigma < 1$ implies that the points $\{\{\{\hat{\boldsymbol{a}}_{1\ldots N}\}_{1\ldots 40}\}_{1\ldots 40}\}$ do mostly lie inside the standard deviation ellipsoids of the corresponding $\{\{\boldsymbol{a}'_{1\ldots N}\}_{1\ldots 40}\}$.

7.3 Perspective Pose Estimation

Although the problem (PNP, cf. the introduction in chapter 4) seems very similar to what is presented in the previous section, it is completely different: before the problem was linear in the parameters, here it will turn out to be quadratic. The reason is that points are no longer mapped to points but to lines - the projection rays, see the illustration in figure 7.5.

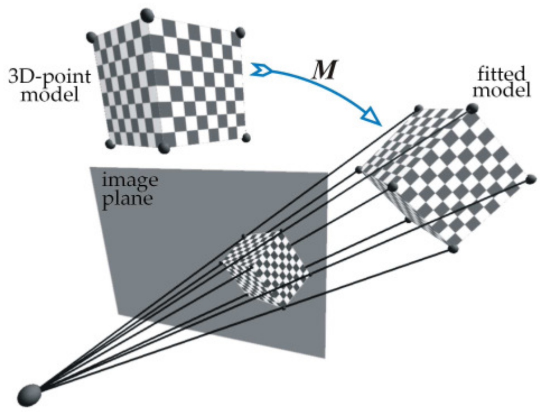

Fig. 7.5: Perspective pose estimation using 7 of 8 model points.

The present situation is typically associated with the pinhole camera model, so here too. Hence the same assumptions are in effect as in section 4.1. Let the object model be given by the (visible) points $\{\boldsymbol{a}_{1\ldots N}\}$. The uncertain observations $\{\boldsymbol{b}_{1\ldots N}\}$ are the corresponding image points from which the respective projections rays are to be computed. This issue shall be clarified first. If $\mathbf{e}_o$ is identified with the optical center, the line representing the projection ray through an image point $\boldsymbol{b} = \mathcal{K}(\vec{b})$ is simply given by

$$\begin{aligned}
\boldsymbol{B} &\overset{(3.18)}{=} (\mathbf{e} \wedge \mathbf{e}_o \wedge \boldsymbol{b})\boldsymbol{I} = (\boldsymbol{E} \wedge \boldsymbol{b})\boldsymbol{I} = \boldsymbol{E}\vec{b}\boldsymbol{I} = \vec{b}\boldsymbol{E}\boldsymbol{I} \overset{(3.9)}{=} \vec{b}\boldsymbol{I}_E = \vec{b} \cdot \boldsymbol{I}_E \\
&= b_3\mathbf{e}_{12} + b_1\mathbf{e}_{23} + b_2\mathbf{e}_{31} \iff \vec{b} = b_1\mathbf{e}_1 + b_2\mathbf{e}_2 + b_3\mathbf{e}_3,
\end{aligned}$$

where $\{b_1, b_2, b_3\} \subset \mathbb{R}$. This linear relationship shows that the projection rays may likewise be taken as the observations. In this case, error propagation, as presented in section 6.2, is not only linear (and thus exact), the 3×3-covariance matrix of $\boldsymbol{B}$ is even a cyclically shifted version of the one belonging to $\vec{b}$.
Nonetheless, it is a standard procedure to use barycentric coordinates in computer vision, which is why the optical center might deviate from $\mathbf{e}_o$. Although lines not passing through the origin may have up to six parameters, cf. the line mask given on page 181, the computation of the projection rays still does not involve any approximation. Hence let $\Phi(\boldsymbol{B}(\boldsymbol{b})) = \mathsf{b} \in \mathbb{R}^6$.

It is now being focused on the functional model and the constraints. Note that the subsequent identities are crucial not only for the current section.

Let $\boldsymbol{B}_{\underline{\mathrm{i}}}$ be the i^{th} projection ray belonging to the i^{th} image point $\boldsymbol{b}_{\underline{\mathrm{i}}}$, $1 \leq \underline{\mathrm{i}} \leq N$. In concordance with the elucidations on page 137, equation (4.1) is used for the G-condition, i.e.

$$(\boldsymbol{M}\boldsymbol{a}_{\underline{\mathrm{i}}}\widetilde{\boldsymbol{M}}) \;\cdot\; \boldsymbol{B}_{\underline{\mathrm{i}}} \;=\; 0.$$

On setting $\Phi(\boldsymbol{a}_{\underline{\mathrm{i}}}) := \mathsf{a}_{\underline{\mathrm{i}}} \in \mathbb{R}^5$ and $\Phi(\boldsymbol{M}) := \mathsf{p} \in \mathbb{R}^8$, it may be written[4]

$$\mathsf{g}_{\underline{\mathrm{i}}}(\mathsf{b}_{\underline{\mathrm{i}}}, \mathsf{p}) \;:=\; [\![\mathsf{p}^k\, \mathsf{p}^l\, \mathsf{a}_{\underline{\mathrm{i}}}{}^r\, \mathsf{b}_{\underline{\mathrm{i}}}{}^s\, \Pi^t{}_{klrs}]\!] \;=\; \mathsf{0} \in \mathbb{R}^5, \tag{7.8}$$

where the product tensor Π arises from contracting all constituent product tensors

$$\Pi \;:=\; (\mathsf{G}^a{}_{kr}\, \mathsf{G}^c{}_{ab}\, \mathsf{R}^b{}_l\, \mathsf{N}^t{}_{cs})_{t\times k\times l\times r\times s} \quad \in \mathbb{R}^{5\times 8\times 8\times 5\times 6}. \tag{7.9}$$

Here G, R and N denote the tensors encoding the geometric product, the reverse operation and the inner product, respectively. It can be seen that the G-condition (7.8) is indeed quadratic in p such that the difficulty of iterating to a solution is brought to a higher level. The derivatives are

$$\begin{aligned} \mathsf{U}(\mathsf{b}_{\underline{\mathrm{i}}}) \;&=\; [\![\mathsf{p}^l\, (\Pi^t{}_{lkrs} + \Pi^t{}_{klrs})\, \mathsf{a}_{\underline{\mathrm{i}}}{}^r\, \mathsf{b}_{\underline{\mathrm{i}}}{}^s]\!] \quad &\in \mathbb{R}^{5\times 8} \\ \mathsf{V}(\mathsf{p}) \;&=\; [\![\mathsf{p}^k\, \mathsf{p}^l\, \mathsf{a}_{\underline{\mathrm{i}}}{}^r\, \Pi^t{}_{klrs}]\!] \quad &\in \mathbb{R}^{5\times 6}. \end{aligned} \tag{7.10}$$

The H-constraint is self-evidently the one given by equation (7.7) from the preceding section, i.e. $\boldsymbol{M}\widetilde{\boldsymbol{M}} = \mathbf{1}$. The Gauss-Helmert method may thus be applied as soon as an initial estimate is available. Very good results in this respect produces the geometric method introduced in chapter 4, see the experiments.

7.3.1 Experiments

The subsequently presented results are in the main taken from [41].

The assumed pinhole camera imaging geometry basically resembles a normalized one [27]: the optical axis is aligned to the x-axis, the focal point is at the origin $(0, 0, 0)$ and the image plane is centered at the point $(1, 0, 0)$, i.e. it has unit distance to the focal point.

[4] The whole expression reads $\mathsf{g}_{\underline{\mathrm{i}}}(\mathsf{b}_{\underline{\mathrm{i}}}, \mathsf{p}) \;=\; [\![\mathsf{p}^k\, \mathsf{G}^a{}_{kr}\, \mathsf{a}_{\underline{\mathrm{i}}}{}^r\, \mathsf{G}^c{}_{ab}\, \mathsf{R}^b{}_l\, \mathsf{p}^l\, \mathsf{N}^t{}_{cs}\, \mathsf{b}_{\underline{\mathrm{i}}}{}^s]\!]$.

Multiple synthetic experiments are conducted: in the beginning, a cloud of N Gaussian distributed points $\{\vec{x}'_{1\ldots N}\}$ with a standard deviation of $\sqrt{2}$ and a bias of $(7,0,0)$ is generated directly in front of the camera. Given the ground truth motor, denoted by $\boldsymbol{M}_0$, these points are displaced yielding the points $\{\boldsymbol{a}_{1\ldots N}\} := \boldsymbol{M}\mathcal{K}(\{\vec{x}'_{1\ldots N}\})\widetilde{\boldsymbol{M}}$, which are intended to represent the object model. A set of N 3×3-covariance matrices $\{\Sigma_{\mathsf{r}_{\underline{1}}\mathsf{r}_{\underline{1}}}, \Sigma_{\mathsf{r}_{\underline{2}}\mathsf{r}_{\underline{2}}}, \ldots, \Sigma_{\mathsf{r}_{\underline{N}}\mathsf{r}_{\underline{N}}}\}$ is generated at random so as to account for image noise. None of those introduces an uncertainty parallel to the optical axis (the uncertainty that is to be attributed to the image points is always bounded to the image plane).

For each experimental run the following procedure applied: for each $\vec{x}'_{\underline{i}}$, $1 \leq \underline{i} \leq N$, the corresponding $\Sigma_{\mathsf{r}_{\underline{i}}\mathsf{r}_{\underline{i}}}$ is used to generate a Gaussian distributed error vector $\vec{r}_{\underline{i}} \in \mathbb{R}^3$, which is in turn used to translate $\vec{x}'_{\underline{i}}$ so as to obtain the (noisy) point $\boldsymbol{x}_{\underline{i}} = \mathcal{K}(\vec{x}'_{\underline{i}} + \vec{r}_{\underline{i}})$. The associated covariance matrix $\Sigma_{\mathsf{x}_{\underline{i}}\mathsf{x}_{\underline{i}}}$ is evaluated by means of the elucidations in section 6.2.1. Next the projection rays $\{\boldsymbol{B}_{1\ldots N}\}$ passing through the 3D-point cloud $\{\boldsymbol{x}_{1\ldots N}\}$ are calculated[5] via $\boldsymbol{B}_{\underline{i}} = (\mathbf{e} \wedge \mathbf{e}_o \wedge \boldsymbol{x}_{\underline{i}})\boldsymbol{I}$, where error propagation must again be obeyed when evaluating the covariance matrices $\{\Sigma_{\mathsf{b}_{\underline{1}}\mathsf{b}_{\underline{1}}}, \Sigma_{\mathsf{b}_{\underline{2}}\mathsf{b}_{\underline{2}}}, \ldots, \Sigma_{\mathsf{b}_{\underline{N}}\mathsf{b}_{\underline{N}}}\} \subset \mathbb{R}^{6\times 6}$. Hence the best motor $\widehat{\boldsymbol{M}}$ is estimated, which fits the $\{\boldsymbol{a}_{1\ldots N}\}$ to the corresponding uncertain $\{\boldsymbol{B}_{1\ldots N}\}$. Notice that the ground truth motor $\boldsymbol{M}_0$ is not necessarily the optimal solution for a single run.

Each experiment - involving 100 runs with $N = 15$ points - is characterized by three values: the rotation angle of $\boldsymbol{M}_0$, denoted ω, the angle between the rotation axis and the optical axis, denoted ϕ, and the noise level μ_r, being the arithmetic mean of the set $\{\|\vec{r}\|_{1\ldots N}\}$.

Three motors are compared: the motor $\boldsymbol{M}_0$ (TRUE) and the motor estimated by the GH-method (GH). This time no SVD-motor is available to serve as an initial estimate. Hence the geometric method (GEM) as introduced in chapter 4 represents the third motor, which at the same time plays the role of the initial estimate for the GH-method. The quality of an estimated motor, here denoted by $\boldsymbol{M}$, is assessed by applying it to the actual problem setup, i.e. by transforming the model $\{\boldsymbol{a}_{1\ldots N}\}$ into the point set $\{\hat{\boldsymbol{b}}_{1\ldots N}\} := \boldsymbol{M}\{\boldsymbol{a}_{1\ldots N}\}\widetilde{\boldsymbol{M}}$. Next the distances between the $\{\hat{\boldsymbol{b}}_{1\ldots N}\}$ and their respective projection rays $\{\boldsymbol{B}_{1\ldots N}\}$ is calculated, for example with the help of equation (3.55). The N distances of every single run are averaged, whence the RMS distance over all 100 runs, denoted by μ, is computed. The standard deviation is given by σ.

	Angle ω	$10°$	$40°$	$70°$	$100°$
Method	TRUE	0.223	0.230	0.229	0.226
	GEM	0.229	0.237	0.235	0.230
	GH	0.215	0.219	0.215	0.213

Table 7.2: Pose estimation: means μ for varying rotation angles ($\mu_r = 0.2$).

[5] Image plane and image points are thus only fictive entities in this experiment.

	TRUE		GEM		GH	
μ_r	μ	σ	μ	σ	μ	σ
0.200	0.227	0.037	0.233	0.045	0.215	0.040
0.283	0.320	0.051	0.330	0.066	0.304	0.055
0.416	0.470	0.074	0.476	0.095	0.441	0.081

Table 7.3: Pose estimation accuracy for the GH-method (GH), the geometric method (GEM) and the ground truth (TRUE) for varying noise levels μ_r.

The results of the pose estimation experiments are presented in table 7.2 and table 7.3, respectively. As there was no recognizable difference in the results when varying angle ϕ between $20°$ and $50°$, it is refrained from breaking down the results in this regard.

It can be seen that the overall fit quality of the GH-method consistently improves the results provided by the geometric approach. The results are even better than those of the true motor, which are supposed to be superior if the number of observations tends to infinity ($\boldsymbol{M}_0$ will then, on average, optimally fit the model). Besides, table 7.3 shows that the standard deviation is smaller compared to the input obtained from the geometric method.

In the next chapter, the parameter estimation by means of the GH-method is adapted to the more complex case of a perspective pose estimation using a catadioptric omnidirectional vision system that provides 360°-panoramic images.

Chapter 8

Applications in Omnidirectional Vision

Here a sophisticated application of the parameter estimation from uncertain data is presented. It shows even stronger geometric streaks than the problems presented in previous sections.

It is first sketched what is meant when talking about omnidirectional vision: single-viewpoint catadioptric[1] vision sensors combine a conventional camera with one or two mirrors and provide a horizontally panoramic view of 360° (→ 'omnidirectional'). The vertical direction of the view does typically subtend an angle notably fewer than the theoretical maximum of 180°.
The imaging system used in this thesis is a so-called folded system as the objective consists of two parabolic mirrors and one lens to provide a scaled ideally orthographic projection from the main mirror, see figure 8.1. The objective represents the actual catadioptric system because it is mounted directly in front of the CCD chip of the camera (no additional lens). In the present case, the model `Remote Reality Netvision 360` is employed. Its vertical view comprises ca. 57.5°. Generally, a configuration involving parabolic mirrors may be termed a paracatadioptric ('parabolic catadioptric') system.

Folded vision systems may, according to the work of Nayar et al [84], equivalently be treated as a single-mirror device. This simplifies matters substantially since solely a parabolic mirror needs to be modeled. Note that, henceforth, a single-viewpoint zero-lens catadioptric vision system with one parabolic mirror is considered.

Pose estimation certainly is a well-studied subject [4, 101, 105, 103, 58] but not in case of an omnidirectional vision sensor. The objective in the first parts of the current chapter is thus to develop an accurate pose estimation for omnidirectional vision, given imprecise image features, i.e. 2D-sensory data. Two approaches are presented: the first one again uses point-line correspondences, like in the previous

[1] The term 'catadioptric' is a compound made up of 'catoptrics' and 'dioptrics'. The words denote the sciences dealing with image formation by means of mirrors (reflecting elements) and lenses (refracting elements), respectively.

sections, while the second one associates object lines with the corresponding projection planes. Hence the object model consists of lines connecting points, rather than the points themselves.

Fig. 8.1: Paracatadioptric imaging system[2]

Comparable to triangulation, the accuracy of an estimated pose likewise improves if the known landmarks are perceived at angles being as different as possible. But the most significant advantage of omnidirectional vision in view of pose estimation is related to navigation: the objects remain on the image plane under most camera movements. This alleviates issues like tracking or 3D-reconstruction.

In the last part of this chapter it is dealt with the epipolar geometry between two omnidirectional images, a prerequisite for 3D-reconstruction. Initially, a geometric modeling with CGA provides certain conditions that express pose relationships between two omnidirectional images of (approximately) the same scene. As a result, the familiar and approved combination of geometric algebra and the Gauss-Helmert method can be applied to estimate the RBM describing the related camera movement. Observing that this is equivalent to a description of the epipolar geometry by means of the essential/fundamental matrix, finally gives access to methods for solving the correspondence problem and for reconstructing the whole 3D-scene. Especially the connection between the essential/fundamental matrix and the motor interrelating the two respective 3D-scenes is of importance in this last part.

The following preliminaries on omnidirectional imaging at the same time demonstrate the advantages of representing geometric problems within the framework of conformal geometric algebra.

[2]For the purpose of the red dot on top of the device see section 8.4.5.

8.1 Omnidirectional Imaging

Omnidirectional imaging subsumes a large variety of imaging techniques; a rotating camera, for instance, may as well be called an omnidirectional imaging system. A detailed survey can be found in [123]. The subsequent explanations solely refer to a parabolic catadioptric vision system. Moreover, a single-viewpoint system, where all incident rays of light intersect at one point (the effective pinhole [114]), is considered. The advantage over a multiple viewpoint system is that geometrically correct perspective images may be calculated ('unwarping') from the acquired images [7], whence a multiplicity of customary and ready-to-use algorithms, designed for the pinhole camera model, become applicable. Discussions on multiple viewpoint systems can be found in [114, 110, 20, 113, 29].

Sample images can be seen in figure 8.15 or 8.19. Unwarped images are depicted in figure 8.13. Next the actual imaging process is being described.

Consider a camera K, focused at infinity, which looks upward at a coaxial parabolic mirror/reflector M. A cross-section of this setup, including the incident ray of light $\boldsymbol{R}$, is shown on the left of figure 8.2.

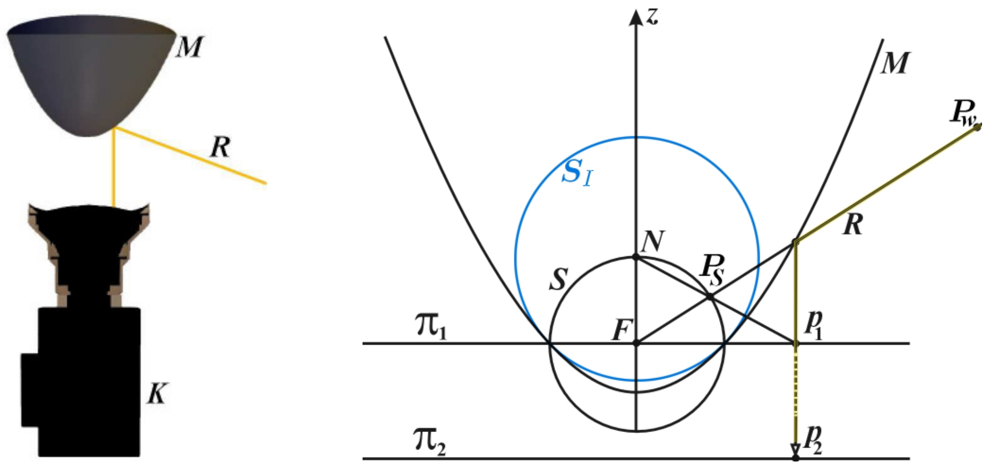

Fig. 8.2: Left: catadioptric vision sensor (camera K + parabolic mirror M). Right: mapping of the world point $\boldsymbol{P}_w \rightarrow$ the image planes $\boldsymbol{\pi}_1$ and $\boldsymbol{\pi}_2$ are identical.

For illustrative purposes, all rays of light except those emitted from the world point $\boldsymbol{P}_w$, see figure 8.2, are disregarded. Besides the rays causing image blur, only one ray of light is involved in the image formation: it suffices to look at the ray of light that would pass through the focal point[3] $\boldsymbol{F}$ of the parabolic mirror M. These rays are the projection rays. The one from $\boldsymbol{P}_w$, i.e. $\boldsymbol{R}$, is reflected in M to a ray of light parallel to the central/optical axis of M and gives point $\boldsymbol{p}_2$ on image plane $\boldsymbol{\pi}_2$. A camera placed beneath the mirror, focused at infinity, thus generates a sharp image on $\boldsymbol{\pi}_2$. For catadioptric image formation, including a discussion on the defocus blur, refer to [7, 8, 10].

[3]The effective pinhole

Introducing the sphere $\boldsymbol{S}$, centered at $\boldsymbol{F}$ with radius twice the focal length f, an elementary alternative to the above imaging scheme arises, cf. [48, 47]. On intersecting all projection rays with $\boldsymbol{S}$ an omnidirectional perspective image is formed on the sphere. Note that a stereographic projection regarding the North pole $\boldsymbol{N}$ on $\boldsymbol{S}$ yields a plane version of the image on $\boldsymbol{S}$ on $\boldsymbol{\pi}_1$, see figure 8.2. Hence, $\boldsymbol{P}_w$ maps to $\boldsymbol{P}_S$ and further to $\boldsymbol{p}_1$. The point is that the image obtained on $\boldsymbol{\pi}_1$ is identical to that on $\boldsymbol{\pi}_2$. The equivalence between the orthogonal projection from a parabola and the stereographic projection is geometrically established in [91], page 13. The paraboloid is thus of no use any more and can be discarded.

To internalize the new imaging scheme solely in terms of the projection sphere $\boldsymbol{S}$ and the image plane $\boldsymbol{\pi}_1$ it is useful to look at figure 8.3. It shows two 3D-views of the same scene: a line $\boldsymbol{L}$ (and a point on it) is mapped to the image plane $\boldsymbol{\pi}$. By means of figure 8.2 it is intuitively clear that infinitely extended lines form great circles on $\boldsymbol{S}$. Moreover, a subsequent stereographic projection to $\boldsymbol{\pi}$, being a conformal mapping, must result in circles. A special case is a (vertical) line parallel to the optical axis, which is mapped to line on the image as well. The reason is that the respective circle on $\boldsymbol{S}$ contains the North pole $\boldsymbol{N}$, which represents (the point at) infinity. The stereographic projection to $\boldsymbol{\pi}$ is therefore a circle with infinite radius passing through $\boldsymbol{F}$. This example makes clear that the resultant circles on $\boldsymbol{\pi}$ are not concentric in general.

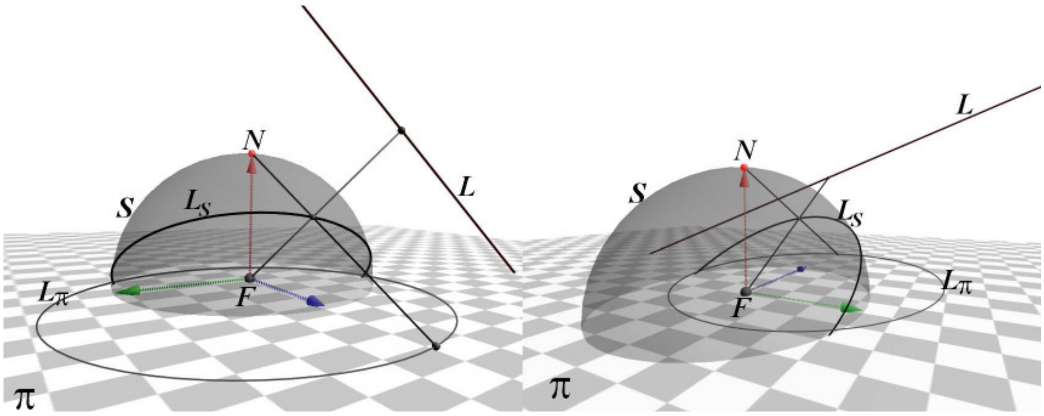

Fig. 8.3: Two views of the mapping of line $\boldsymbol{L}$ to $\boldsymbol{L}_\pi$ via great circle $\boldsymbol{L_S}$ on $\boldsymbol{S}$. The mapping of a sample point on $\boldsymbol{L}$ to the corresponding point on $\boldsymbol{L}_\pi$ is shown as well.

The relevance of the new mapping scheme in context of conformal geometric algebra is immediately disclosed when noting that the stereographic projection can also be done in terms of an inversion. The necessary inversion sphere, denoted by $\boldsymbol{S}_I \in \mathbb{R}^{4,1}$, is centered at the North Pole $\boldsymbol{N}$ of $\boldsymbol{S}$. For the scenario of figure 8.2, it can easily be verify that the radius r_I of $\boldsymbol{S}_I$ must be

$$r_I \;=\; \sqrt{2}\, r_S, \tag{8.1}$$

where r_S denotes the radius of the projection sphere $\boldsymbol{S}$. Using CGA the mapping between the points $\boldsymbol{p}_1, \boldsymbol{P}_S \in \mathbb{R}^{4,1}$ may simply be expressed as

$$\boldsymbol{P}_S \;=\; \boldsymbol{S}_I \boldsymbol{p}_1 \boldsymbol{S}_I \quad \in \mathbb{R}^{4,1}. \tag{8.2}$$

Note that, given an image point, the corresponding projection ray may effortlessly be calculated by $\boldsymbol{R} = (\boldsymbol{e} \wedge \boldsymbol{F} \wedge (\boldsymbol{S}_I \boldsymbol{p}_1 \boldsymbol{S}_I))\boldsymbol{I}$.

Other approaches connecting CGA with omnidirectional vision are rare, but see for example [96, 99, 116, 80, 11].

8.2 Pose Estimation

Due to its large field of view, omnidirectional vision is highly beneficial for robot navigation and thus for pose estimation.

The advantages emerging from omnidirectional vision are recognized; the amount of research on the subjects in this field is increasing. Approaches based on (single camera) stereo matching or motion estimation can be found in [81, 117, 52, 71]. Methods dealing with pose estimation or localization, mostly related to robot navigation, are presented in [15, 30, 87]. Navigation involving a generation of a topology map is investigated in [53, 38]. The latter analyzes eigenimages obtained from a multi-viewpoint spherical mirror system. A multi-camera localization technique based on the estimation of configurations between robot soccer players, each equipped with one sensor, is proposed in [83]. In this context the popular 'RoboCup' competition must be mentioned.

Now two different approaches are being presented concurrently. Both of which exploit the approved combination of the Gauss-Helmert method and the conformal geometric algebra. Both approaches rely on the concise principle of 2D-3D pose estimation 'to rigidly move the object model in 3D such that it comes into agreement with the 2D-sensory data of the camera'. However, while the first technique tries to fit a point model to projection rays [44], the second one tries to fit a line model to projection planes [45, 109]. It is referred to them as the point-line and the line-plane method/version, respectively.

8.2.1 The General Omnidirectional Approach

First of all, note that once the projection rays are computed, the further proceeding is identical to that in ordinary pose estimation assuming the pinhole camera model. To illustrate the whole pose estimation process consider figure 8.4. It is suitable to describe both versions: three image points constitute the triangle-like[4] imaged object $T_{\boldsymbol{\pi}}$, which is stereographically back-projected to T_S on $\boldsymbol{S}$. In conjunction with the focal point $\boldsymbol{F}$, the projection rays or planes, respectively, can be calculated. The correct RBM then moves the model triangle T' so that either the model points come to lie on the corresponding projection rays or the model lines come to lie on the corresponding projection planes.

[4] In the figure, $T_{\boldsymbol{\pi}}$ and T_S are drawn as triangles, although their sides are supposed to be arcs rather than lines.

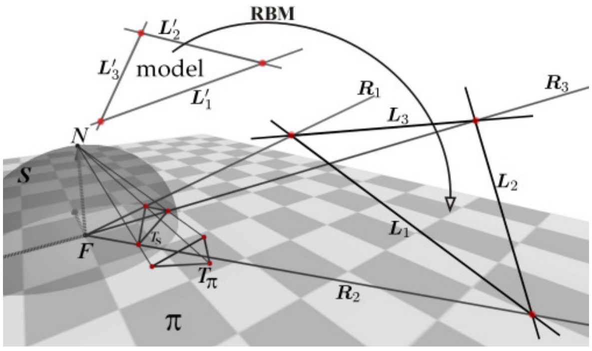

Fig. 8.4: P3P: the omnidirectional analogue of figure 4.3.

Parameters

Typical quantities to consider are radial distortion, skew and aspect ratio of the sensor, focal length f and the image center $\vec{m}$, where the optical axis intersects the image plane. This equally holds for a parabolic catadioptric vision system, as in the present case. Skew and aspect ratio may be remedied beforehand as shown in [47]; it is, for example, possible to constrain the outer boundary of the mirror as it appears in the image, see the left side of figure 8.6, to be circular. Radial distortion [18, 32] is not taken into account at all. The related effects can, however, be corrected by the methods introduced in [99, 75]. Of specific interest are therefore the three values

- the focal length[5] f, measured in pixel
- the coordinates of the image center $\vec{m} \in \mathbb{R}^2$.

It is crucial to note that on using the inversion based imaging (not as in illustration 8.5), the image center and the focal point do necessarily coincide, i.e. $\vec{m} \equiv \boldsymbol{F} := \mathbf{e}_o$. Recall that the focal length f is connected to the radius r_S of the projection sphere $\boldsymbol{S}$ by the relationship, cf. [48],

$$r_S = 2f. \tag{8.3}$$

In order to determine the image center $\vec{m}$, the center of the inner or outer boundary of the iris-like omnidirectional image, see figure 8.6, can be estimated. If, as in the experimental part of the current pose estimation section, the focal length is only known in terms of a metric unit, e.g. `mm`, it must be converted to `pixel`. For this purpose, the radius r_M of the mirror, if known, can be related to the outer radius r_d of the iris, see figure 8.5. Hence,

$$f = f_{\texttt{mm}} \frac{r_d}{r_M}. \tag{8.4}$$

Both values, $\vec{m}$ and r_d, are estimated by fitting circles to the iris by means of the direct technique described in section 5.2.6. A good survey of other circle estimation

[5]The combined focal length of the mirror and the lens

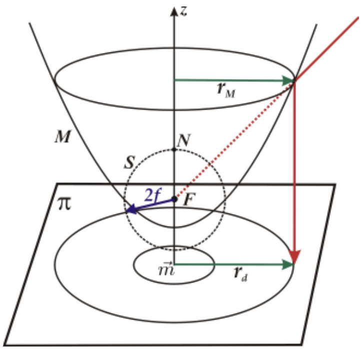

Fig. 8.5: The parameters used to describe the omnidirectional sensor.

methods can be found in [1]. Note that the contours[6] of monochrome iris images, as shown on the left side of figure 8.6, are used for the circle estimation. A similar methodology is used in [26] for calibration. The monochrome images are obtained after using a rank filter [59], thresholding and applying a morphologic operator (closing). If a sequence of images is available the pixel-wise maximum is built beforehand.

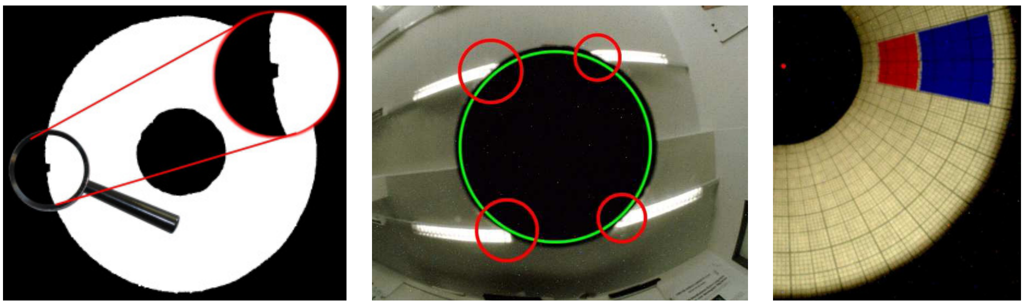

Fig. 8.6: Left/middle: the severe problems on determining parameters as the outer radius r_d or the image center $\vec{m} \in \mathbb{R}^2$, see figure 8.5. Right: non-uniform imaging resolution (the objective is wrapped up in graph paper). The blue and the red area do both cover a grid of size 4×4 on the graph paper.

The above three parameters can self-evidently be determined through calibrating. This is detailed in section 8.3.

Point-Line

Let the object model be given by the points $\{\boldsymbol{a}_{1\ldots N}\}$. The uncertain observations $\{\boldsymbol{b}_{1\ldots N}\}$ are the embedded image points from which the projections rays are to be computed. Hence $\boldsymbol{b}_{\underline{i}} = \mathcal{K}(\vec{b}_{\underline{i}} \in \mathbb{R}^2)$, $\underline{i} \in [1,N]_{\mathbb{Z}}$, where the $\{\vec{b}_{1\ldots N}\}$ denote the underlying pixel coordinates given with respect to the coordinate system centered at $\vec{m}$. The respective pixel uncertainties are assumed to be be independent and

[6] In practice, the contours are highly influenced by the incident light as demonstrated on the right of figure 8.6.

identically distributed (i.i.d.). Moreover, each associated covariance matrix reads

$$\Sigma_{\text{pixel}} := \begin{bmatrix} 1 & 0 \\ 0 & 1 \end{bmatrix}. \tag{8.5}$$

This is possible, as stated on page 157, since the overall scale of the covariance matrices has no impact on the estimation. Note that these i.i.d. uncertainties are transformed by means of error propagation which eventually gives distinct uncertainties that appropriately account for the imaging geometry. The mapping of a far image point to a point close to the North Pole on $\boldsymbol{S}$, for example, is less affected by noise and will thus inhere with a higher confidence, i.e. smaller variance.

Error propagation is employed three times:

1. The image points are embedded into conformal space, see section 6.2.1
   $\vec{b}_{\underline{i}} \longmapsto \boldsymbol{b}_{\underline{i}}$

2. An inversion in $\boldsymbol{S}_I$ is carried out
   $\boldsymbol{b}_{\underline{i}} \longmapsto \boldsymbol{b}'_{\underline{i}} := \boldsymbol{S}_I \boldsymbol{b}_{\underline{i}} \boldsymbol{S}_I$

3. The projection rays are built
   $\boldsymbol{b}'_{\underline{i}} \longmapsto \boldsymbol{B}_{\underline{i}} := (\mathbf{e} \wedge \boldsymbol{F} \wedge \boldsymbol{b}'_{\underline{i}})\boldsymbol{I}$

Consequently, a new situation is present in which the model points $\{\boldsymbol{a}_{1\ldots N}\}$ are to be fitted to the newly computed projection rays $\{\boldsymbol{B}_{1\ldots N}\}$. Their uncertainty is captured by the covariance matrices $\{\Sigma_{\mathsf{b}_{\underline{1}}\mathsf{b}_{\underline{1}}}, \Sigma_{\mathsf{b}_{\underline{2}}\mathsf{b}_{\underline{2}}}, \ldots, \Sigma_{\mathsf{b}_{\underline{N}}\mathsf{b}_{\underline{N}}}\} \subset \mathbb{R}^{6\times 6}$. Hence a scenario identical to the one derived in section 7.3 is obtained. It is proceeded with the estimation in concordance to the elucidations on page 199.

Line-Plane

Let the object model be given by the lines[7] $\{\boldsymbol{A}_{1\ldots N}\}$, and let the uncertain observations be sets of image points, denoted by $\{\{\vec{b}_{1\ldots N_{\underline{i}}}\}_{1\ldots N}\} \subset \mathbb{R}^2$, $1 \leq \underline{i} \leq N$, with uncertainties (8.5), as before. Each set $\{\vec{b}_{1\ldots N_{\underline{i}}}\}$ contains $N_{\underline{i}}$ points from the circular arc on the image plane that represents the projection of the i^{th} world line. After an embedding the points $\{\{\boldsymbol{b}_{1\ldots N_{\underline{i}}}\}_{1\ldots N}\} \subset \mathbb{R}^{4,1}$, including propagated uncertainties, are obtained.

In order to perform the line-plane fitting, artificial plane observations have to be derived from the point observations. Given a set of image points $\{\boldsymbol{b}_{1\ldots N_{\underline{i}}}\}$, there are basically two possibilities: the circle passing through the image points is estimated and then brought[8] to the projection sphere $\boldsymbol{S}$ or the great circle passing through the points on $\boldsymbol{S}$ is estimated after the points were brought to $\boldsymbol{S}$. In each case, the sought projection plane is the plane containing the great circle. Here it is opted for

[7] IPNS lines (bivectors)

[8] All entities on the image plane may be back-projected in the same way, i.e. by an inversion in $\boldsymbol{S}_I$.

the second alternative since estimating a great circle (passes through the center $\boldsymbol{F}$ of the sphere) involves solely two unknowns describing the orientation of the great circle. In [118], for example, the authors tackle the former problem of localizing projected lines on the image plane from uncalibrated paracatadioptric views. In [10] a model for the general central catadioptric line imaging is presented.

The estimation of the projection planes, denoted by $\{\boldsymbol{B}_{1\ldots N}\}$, is now being outlined. It can be done in very much the same way as the circle estimation described in section 7.1. The planes could, in theory, be extracted from estimated circles via relationship (3.46). Nevertheless, a separate GH-estimation for planes is more sensible: each plane is parameterized by three values giving the orientation, $\mathsf{b}_{\underline{i}} := \Phi(\boldsymbol{B}_{\underline{i}}) \in \mathbb{R}^3$. The redundancy of one can be remedied by means of the H-constraint $\mathsf{b}_{\underline{i}}^{\mathsf{T}}\mathsf{b}_{\underline{i}} = 1$. Let the stereographically back-projected points $\{\boldsymbol{b}_{1\ldots N_{\underline{i}}}\}$ on $\boldsymbol{S}$ be denoted by $\{\boldsymbol{b'}_{1\ldots N_{\underline{i}}}\}$. Hence every point $\boldsymbol{b}'_{\underline{j}}$, $1 \leq \underline{j} \leq N_{\underline{i}}$, gives one G-condition $\boldsymbol{b}'_{\underline{j}} \cdot \boldsymbol{B}_{\underline{i}} = \mathbf{0}$. As before, the GH-method can be started from an initial SVD estimate. Note that every run yields a covariance matrix $\Sigma_{\mathsf{b}_{\underline{i}}\mathsf{b}_{\underline{i}}} \in \mathbb{R}^{3\times 3}$, too, which in turn serves as input for the final pose estimation.

The actual estimation scenario is given by the model lines $\{\boldsymbol{A}_{1\ldots N}\}$ and the projection planes $\{\boldsymbol{B}_{1\ldots N}\}$ with associated uncertainties $\{\Sigma_{\mathsf{b}_{\underline{1}}\mathsf{b}_{\underline{1}}}, \Sigma_{\mathsf{b}_{\underline{2}}\mathsf{b}_{\underline{2}}}, \ldots, \Sigma_{\mathsf{b}_{\underline{N}}\mathsf{b}_{\underline{N}}}\} \subset \mathbb{R}^{3\times 3}$. A G-condition expressing the incidence of line and plane must set up. Clearly, if an IPNS line $\boldsymbol{L}$ lies on an IPNS plane $\boldsymbol{P}$, a suitable plane $\boldsymbol{P}'$ can be determined such that the line may be expressed as $\boldsymbol{L} = \boldsymbol{P} \wedge \boldsymbol{P}'$. Hence the outer product of line and plane, in this case $(\boldsymbol{P} \wedge \boldsymbol{P}') \wedge \boldsymbol{P}$, vanishes unless the line protrudes from the plane. By means of the dual operation, particularly by equation (2.52), an equivalent inner product expression can be figured out. The resultant condition for the line-plane pose estimation looks familiar

$$\boldsymbol{M}\,\boldsymbol{A}_{\underline{i}}^{*}\,\widetilde{\boldsymbol{M}} \;\cdot\; \boldsymbol{B}_{\underline{i}} \;=\; \mathbf{0}, \qquad \underline{i} \in [1,N]_{\mathbb{Z}}. \tag{8.6}$$

This is, in principle, again the same condition equation as the one given in section 7.3. The tensor for building the dual of the $\{\boldsymbol{A}_{1\ldots N}\}$ does not necessarily need to be used; it may equally be assumed that $\{\boldsymbol{A}^{*}{}_{1\ldots N}\}$ (3-blades) is given from the outset. Hence choosing $\Phi(\boldsymbol{A}_{\underline{i}}^{*}) := \mathsf{a}_{\underline{i}} \in \mathbb{R}^6$, $\Phi(\boldsymbol{B}_{\underline{i}}) := \mathsf{b}_{\underline{i}} \in \mathbb{R}^3$ and $\Phi(\boldsymbol{M}) := \mathsf{p} \in \mathbb{R}^8$, the expressions of section 7.3 can be reused. Typically, the inner product of an OPNS line with a plane gives a bivector with seven non-zero components, with solely four of them being distinct from one another. However, a random multivector, created only in accordance with the structural RBM mask (7.4), can, if used in equation (8.6), produce all ten basis blades of grade two. Although it would not do any harm to utilize all ten conditions, i.e. $\mathsf{g}_{\underline{i}}(\mathsf{b}_{\underline{i}}, \mathsf{p}) \in \mathbb{R}^{10}$, it is refrained from doing so because the H-constraint (7.7) is already in use. Thus unlike condition (7.8) on page 199, it is

$$\mathsf{g}_{\underline{i}}(\mathsf{b}_{\underline{i}}, \mathsf{p}) \in \mathbb{R}^4 \qquad \text{and} \qquad \Pi \in \mathbb{R}^{4\times 8\times 8\times 6\times 3}.$$

Note that four conditions are used since three of the seven conditions are structure-related linearly dependent. Differentiating with respect to p and $\mathsf{b}_{\underline{i}}$ implies

$$\mathsf{U}(\mathsf{b}_{\underline{i}}) \in \mathbb{R}^{4\times 8} \qquad \text{and} \qquad \mathsf{V}(\mathsf{p}) \in \mathbb{R}^{4\times 3},$$

respectively.

8.2.2 Initial Estimates

In case of the point-line method simply the approved geometric technique introduced in chapter 4, which is also used in section 7.3 to provide the initial estimate, is employed.

The initial estimate for the line-plane estimation can be provided at very low costs. Moreover, it shortens the overall computation time. The aim is to rotate the model such that the unit direction vectors, denoted by $\{\hat{\mathsf{d}}_{1\ldots N}\}$, of the lines come to lie on the respective projection planes. Let the normal vectors of the planes be given by $\{\hat{\mathsf{n}}_{1\ldots N}\}$. Hence pre-aligning the model means finding a rotation matrix $\mathsf{R} \in \mathbb{R}^{3\times 3}$ such that

$$(\forall i): \quad \hat{\mathsf{n}}_{\underline{i}}^{\mathsf{T}} \, \mathsf{R} \, \hat{\mathsf{d}}_{\underline{i}} \; = \; 0.$$

By Rodrigues's formula (3.65), it is known that the matrix R describing a rotation through angle θ about a fixed axis, given by a unit normal vector $\hat{\mathsf{a}} = [a_1; a_2; a_3]$, can be calculated by

$$\begin{aligned} \mathsf{R} \;&=\; \exp(\theta \mathsf{A}) \\ &=\; \mathsf{I}_3 + \sin\theta \, \mathsf{A} + (1-\cos\theta)\mathsf{A}^2, \end{aligned} \qquad \mathsf{A} \;:=\; \begin{bmatrix} 0 & -a_3 & a_2 \\ a_3 & 0 & -a_1 \\ -a_2 & a_1 & 0 \end{bmatrix}.$$

For small angles,

$$\mathsf{R} \;\approx\; \mathsf{I}_3 + \theta \mathsf{A}$$

can be used as a good approximation. With this relationship and due to the skew symmetric structure of $\mathsf{A}' := \theta\mathsf{A}$, it is possible to solve for $\mathsf{a}' = [\theta a_1; \theta a_2; \theta a_3]$: each correspondence pair $(\hat{\mathsf{n}}_{\underline{i}}, \hat{\mathsf{d}}_{\underline{i}})$ gives one row

$$\begin{aligned} & \hat{\mathsf{n}}_{\underline{i}}^{\mathsf{T}} \, \mathsf{A}' \, \hat{\mathsf{d}}_{\underline{i}} \;=\; -\hat{\mathsf{n}}_{\underline{i}}^{\mathsf{T}} \, \hat{\mathsf{d}}_{\underline{i}} \\ \Longleftrightarrow \quad & \mathrm{vec}(\hat{\mathsf{d}}_{\underline{i}} \hat{\mathsf{n}}_{\underline{i}}^{\mathsf{T}})^{\mathsf{T}} \, \mathrm{vec}(\mathsf{A}') \;=\; -\hat{\mathsf{n}}_{\underline{i}}^{\mathsf{T}} \, \hat{\mathsf{d}}_{\underline{i}} \\ \Longleftrightarrow \quad & (\hat{\mathsf{d}}_{\underline{i}3} \hat{\mathsf{n}}_{\underline{i}2} - \hat{\mathsf{d}}_{\underline{i}2} \hat{\mathsf{n}}_{\underline{i}3}) \, \mathsf{a}'_1 + (\hat{\mathsf{d}}_{\underline{i}1} \hat{\mathsf{n}}_{\underline{i}3} - \hat{\mathsf{d}}_{\underline{i}3} \hat{\mathsf{n}}_{\underline{i}1}) \, \mathsf{a}'_2 + (\hat{\mathsf{d}}_{\underline{i}2} \hat{\mathsf{n}}_{\underline{i}1} - \hat{\mathsf{d}}_{\underline{i}1} \hat{\mathsf{n}}_{\underline{i}2}) \, \mathsf{a}'_3 \;=\; -\hat{\mathsf{n}}_{\underline{i}}^{\mathsf{T}} \, \hat{\mathsf{d}}_{\underline{i}} \end{aligned}$$

of an overdetermined system of linear equations. Using the solution a' a first approximation $\mathsf{R}^{[1]}$ of R can be computed. After transforming the lines by means of $\mathsf{R}^{[1]}$, the method can be reapplied. Any such succeeding iteration yields a new rotation until the procedure is stopped because the lines were close enough to the planes. It can be inferred that after t iterations

$$\mathsf{R} \;\approx\; \mathsf{R}^{[t]} \ldots \mathsf{R}^{[2]} \, \mathsf{R}^{[1]}.$$

The convergence of this method is analyzed in [102] with the result that very few (below five) iterations are necessary to maintain a high accuracy, even if the amount of rotation is nearly 180° (and despite assuming small angles). What makes this technique so effective is the detour via the Lie algebra $so(3)$ instead of directly searching the Lie group $SO(3)$, which comprises R, see section 4.6.

8.2.3 Experiments

The experiments presented here are throughout real world experiments. For both methods no rigorous calibration was carried out. The only thing that was done was to determine the focal length and the image center from the outline of the iris-like image as described on page 208. For equation (8.4) the mirror radius $r_M = 40\,\mathrm{mm}$ and the focal length $f_{\mathtt{mm}} = 16.7\,\mathrm{mm}$ were used as intrinsic parameters. Note that these values come directly from the manufacturer.

Throughout all experiments, observations were taken from the sensory data by hand. The reason is a lack of sufficiently robust and accurate automatic methods coping with sensitivity regarding lighting conditions, 'curvy' mappings of straight lines, especially for loosely calibrated systems, and the related non-uniform imaging resolution, which decreases towards the image center as demonstrated on the right side of figure 8.6. Another issue is the correspondence problem, see item 2 of the general pose estimation assumptions on page 136, which is likely the biggest challenge in pose estimation. A human observer can, under these circumstances and with some effort, ensure that the underlying assumptions are not violated. Thus assessing the method as such, i.e. its consistency, is possible.

Point-Line

Two experiments were conducted using a `Sony DxC-151AP` camera with a resolution of 768×576 pixels.

In the first set of experiments, a pose estimation with respect to a model house was done. Tags were attached to the house at certain positions so as to allow for a smooth feature point retrieval from the omnidirectional pictures; each tag reflects one vertex in the known house model. The image coordinates corresponding to these points of interest were extracted manually. One illustrative view of the model house and all visible feature points, as extracted, is depicted on the left side of figure 8.8 (showing only the relevant part of the sensed image). The house dimensions in cm are approximately $21 \times 15 \times 21$.

Fig. 8.7: Camera, but with pinhole objective

Two sequences were conducted, one with 35.1 cm (A) and one with 52.4 cm (B) orthogonal distance between the house and the optical axis of the sensor. In order to simplify the acquisition of ground truths the rotation plane was perpendicular to the optical axis. The house was rotated in 10° steps from 60° down to 0°. The respective errors relative to the 60°-rotation were measured.

The results are listed in table 8.1. Note that the house appears flat in the 0°-image, i.e. the usable 3D-model points are nearly coplanar such that the estimation result is affected. The mean error in the rotation was 1.65° and the mean error in the planar distance was 0.43 cm. The estimated height of the sensor relative to the house was $27.5 \pm 0.4\,\mathrm{cm}$, which is within the measurement error of ground truth $27.55 \pm 0.4\,\mathrm{cm}$.

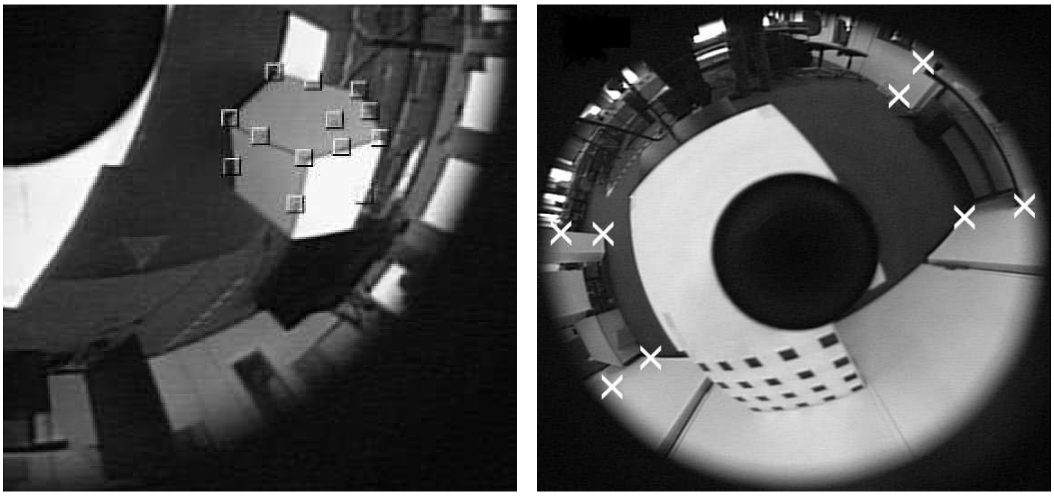

Fig. 8.8: Examples: the model house (left) and the room navigation (right) experiment. Model points and markers are graphically highlighted.

Rotation	Abs. error angle		Abs. error distance	
[°]	A [°]	B [°]	A [cm]	B [cm]
50 to 60	2.8	0.4	0.65	0.10
40 to 60	2.6	0.2	0.40	0.30
30 to 60	1.3	0.5	0.54	0.33
20 to 60	0.3	0.8	0.70	0.04
10 to 60	0.7	6.4	0.90	1.12
0 to 60	3.0	6.3	3.90	1.20

Table 8.1: Results of the pose estimation w.r.t. the model house.

In the second set of experiments, the sensor was moved to six positions inside a $5.3 \times 2.2\,\mathrm{m}^2$ room. The room model, as indicated by white crosses on the right side of figure 8.8, was defined by four pairs of markers, each vertically aligned. In each of the six positions, the sensor was rotated by 0°, 30° and 70°. The results are illustrated in figure 8.9.

The error regarding the planar distances to the ground truth positions was 2.45 ± 1.74 cm. The estimated height of the sensor has an error of 3.22 ± 1.0 cm. These are comparable results to those given by Aliaga [2]; there the authors obtained an average planar error of 2.8 cm within a room of comparable dimension. Nevertheless, Aliaga made a thorough calibration and used a high-precision 3-CCD chip camera with a superior resolution of 1360×1024 pixels, which is almost twice the resolution of the Sony camera. Cauchois et el [17] obtained as good results as here taking the room size into account, which was noticeably smaller. Further sensible comparisons are difficult due to varying circumstances or missing data in the publications.

In addition to the large movements, the accuracy of estimating smaller displace-

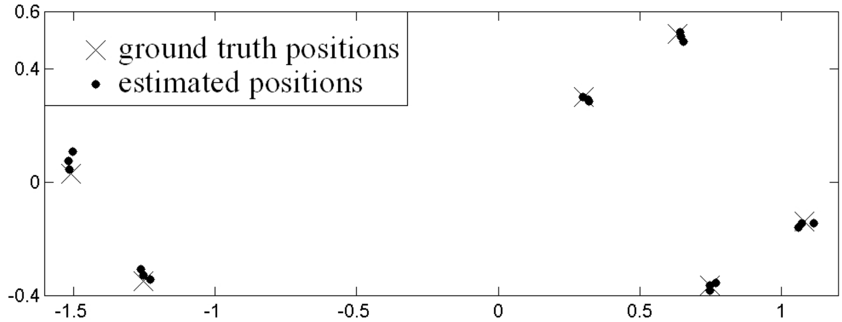

Fig. 8.9: Pose estimation for room navigation. Units in meters.

ments and rotations was studied separately, with the sensor being in the center of the room. The sensor was moved along a line in steps of 1, 5 and 10 cm. This gave a mean error of 0.5 cm. The error did not depend on the length of the translation. In addition, the camera was rotated in steps of 5°, from a starting position 0° to 90°. The mean error in the rotation estimation was 0.4°.

Line-plane

Just like for the point-line method, the aim is to show the goodness of the line-plane variant by conducting navigation and pose estimation experiments. In this case a `Kamerawerk Dresden Loglux i5` camera was used. The whole sensor is depicted in figure 8.1. Omnidirectional images were acquired with a resolution of 1280×1024 pixels. Here the focus is on line observations, i.e. imaged 3D-lines; these were extracted by selecting seven points per line. After that the artificial plane observations were built.

	Abs. error [mm]	Rel. error [%]	Angle error [°]
mean	10.4	3.5	0.9
std	4.8	1.7	0.4
min	0.9	0.4	0.12
max	21.3	11.5	2.4

Table 8.2: The errors of the house pose estimation.

In the first experiment, a model house was moved with a robot arm to 21 different positions. The robot arm gives ground truth of the positions, and thus of the translations between different positions, with millimeter accuracy. The magnitude of these motions was between 7.7 cm and 62.4 cm, and the distance between the model house and the optical center of the catadioptric sensor ranged between 31.4 cm and 82.8 cm. For each of the 21 acquired images, a line-plane pose estimation w.r.t. the model house was done. Note that this time the house model is given by means of lines connecting the tags (see the point-line part). The estimates are then used to compute intermediate RBMs between pairs of fits so as to mimic the robot motions. The results are given in table 8.2.

Fig. 8.10: The 3D-line model (right) of the entrance hall was built from point measurements (red dots, left) using a laser device. The blue dots in the right image indicate the 25 sensor positions.

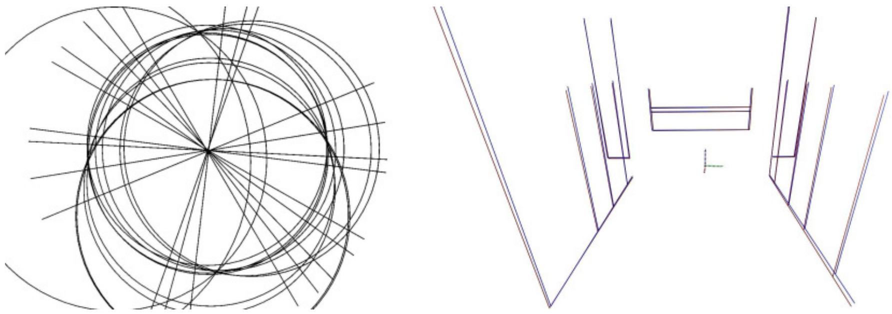

Fig. 8.11: Left: the picture shows a set of imaged world lines as they occurred in the hall experiment. Note that the radial lines (circles with infinite radius) belong to vertical world lines, for instance, the edges of pillars. Right: A fit of average quality.

In the second experiment, the sensor (attached on top of a tripod) was moved to 25 different positions in a hallway, see figure 8.10. The model was defined by lines clearly visible in most of the images. The walls in the hallway were assumed to be perpendicular to the floor and all corners were assumed to be right angled. With these assumptions, an accuracy of roughly 2 cm for the positions of the model lines was obtained. The model consisted of in total 51 lines, from which on average 20 lines were visible in an image. The maximal orthogonal distance between these lines was 18.1 m, the minimal distance 3.8 m, and the sensor movements were made within an area of size $8 \times 2\,\mathrm{m}^2$. Two methods compete against each other: the Gauss-Helmert (G-H) method and an ordinary least squares approach, based on the Gauss-Markov model[9] (G-M). Navigation results were computed not only for 3D but also for 2D, where the height component of the sensor was disregarded. Note that a ground truth for the rotation information could not be determined such that no qualitative analysis of the entire pose information can be given. Instead it is confined to the position information. Empirically, however, the rotational error is supposed to be less than one degree as can be guessed from the right side of figure 8.11.

[9]The classical homoscedastic linear model

The results for the navigational error are given in table 8.3. Moreover, the left side of figure 8.12 visualizes the individual estimation results, where 'Truth' denotes the measured ground truth positions of the sensor.

	Mean error [cm]	RMS error [cm]	min [cm]	max [cm]
G-M 3D	7.6	9.4	3.6	32.2
G-M 2D	5.1	7.7	0.4	32.0
G-H 3D	6.4	6.5	2.7	8.3
G-H 2D	3.5	3.9	0.5	5.7

Table 8.3: The errors of the navigation.

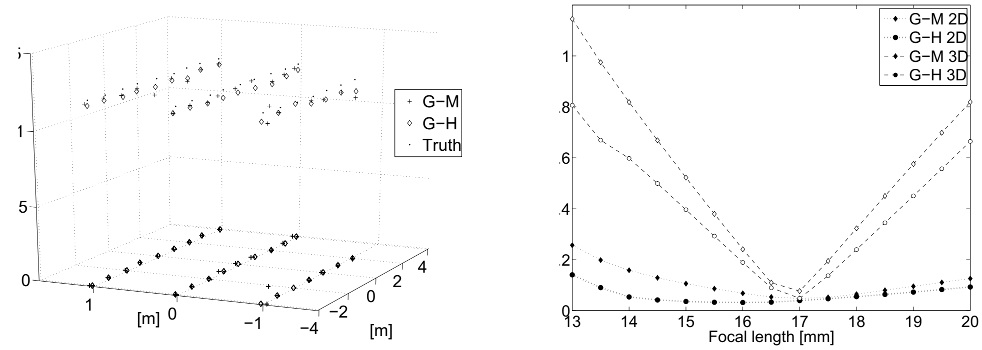

Fig. 8.12: Left: navigation results. The 3D positions are also projected to plane for clarity. Right: focal length vs. mean error.

In addition to the pose estimation, the robustness of the two methods with respect to changes of the focal length was tested. The results are given on the right side of figure 8.12. It can be seen that the GH-method always outperforms the standard least squares approach G-M. The 2D-estimation is much less affected when the focal length is varied than the 3D-variant. A reason might be that the images of vertical world lines are invariant to changes in focal length while these, at the same time, strongly contribute to the horizontal estimation accuracy. The best encountered 3D-result was an RMS error of 4.2 cm using $f_{\mathtt{mm}} = 16.9$ mm for the GH-method and 5.8 cm using $f_{\mathtt{mm}} = 16.8$ mm for the opponent G-M, respectively.

For the 3D-case it is still difficult to relate the results to those from other approaches due to the limited number of really comparable publications. The presented 2D-results are comparable to those given by Aliaga [2]; after calibration, the authors obtained an average horizontal error of 2.8 cm within a room of 5 meters diameter. Cauchois et el [17] reached about 1 cm accuracy (2D) using an image database method with a conical mirror and a room of size $2 \times 3\,\mathrm{m}^2$.

8.3 Calibration

For the presentation of the epipole estimation in the next section a calibration is inevitable. Very good papers regarding the calibration of catadioptric image sensors are [26, 46], where the last one is probably the most known. In [10] a calibration from only three projected lines is suggested by determining the parameters that describe the absolute conic.

Here a method for evaluating the focal length f and the image center $\vec{m} := x_0\mathbf{e}_1 + y_0\mathbf{e}_2$ in the paracatadioptric case is described. Let R_i, $\vec{c}_i := c_i^x\mathbf{e}_1 + c_i^y\mathbf{e}_2$ and $r_S = 2f$ denote the radius of the i^{th} image circle, its center and the radius of the projection sphere, respectively. Three approaches may be distinguished

- Reconsider figure 8.3 showing the projection of a world line $\boldsymbol{L}$. It also demonstrates that the inversion of the great circle $\boldsymbol{L_S}$ is the circle $\boldsymbol{L_\pi}$. On the other hand, the inversion of the plane $\boldsymbol{\pi}$, containing $\boldsymbol{L_\pi}$, gives the sphere $\boldsymbol{S}$. It is natural to ask for the inversion of the plane containing the circle $\boldsymbol{L_S}$. It is clearly a sphere incident with $\boldsymbol{L_\pi}$. Moreover, the North Pole $\boldsymbol{N}$ must lie on this sphere because $\boldsymbol{N}$ symbolizes the inversion of infinity being part of every plane. Finally, the South Pole must lie on the sphere since it is the inversion of $\boldsymbol{F}$. Thus by symmetry the radius of the sphere under consideration must be equal to the radius of $\boldsymbol{L_\pi}$. Because $\boldsymbol{N}$, with coordinates $[x_0, y_0, r_S]$, is a common point of all circle-spheres, it can be seen that calibrating amounts to the minimization of
$$\sum_i \left((\vec{m} - \vec{c}_i)^2 + r_S^2 - R_i^2\right)^2.$$
- The radii of the circles obtained after the inversion of the image circles must be equal to the radius of the projection sphere because they are supposed to be great circles.
- By the same argument, the distance between the center of a great circle and the origin (x_0, y_0) must be zero.

Using the CGA expression (3.44) for a circle, it can easily be shown that the last two approaches both lead to the identical formula. The same formula is given by Geyer and Daniilidis in [48], however, with another derivation. Note that a minimum of three lines must be known to do the calibration.

8.4 Estimating Epipoles

Here the epipolar geometry between two omnidirectional images, acquired by a moving single-viewpoint paracatadioptric vision sensor, is studied [43].

Approaches to epipolar geometry, but regarding general catadioptric vision systems, are presented in [112, 49]. Issues related to stereo matching and motion estimation can be found in [81, 117, 52]. The authors of [15, 71] try to accomplish a 3D-reconstruction from two omnidirectional views. Naturally, there is a strong overlap between the mentioned papers as, for instance, reconstruction mostly includes the aspect of stereo matching.

This work in particular deals with the stochastic estimation of epipoles by means of the Gauss-Helmert method. Specifically, conformal geometric algebra is used to show the existence of a 3×3 essential matrix, which describes the underlying epipolar geometry. Since it can be estimated from less data, the essential matrix is preferable to the 4×4 fundamental matrix, which additionally comprises the fixed intrinsic parameters. Actually, the essential matrix is used to obtain an initial estimate for the stochastic epipole computation, which is a key aspect of this work. Next to the stochastically optimal positions of the epipoles the method computes the rigid body motion (RBM) between two camera positions.

8.4.1 Epipolar Geometry

Epipolar geometry is one way to model stereo vision systems. In general, epipolar geometry considers the projection of projection rays from different cameras. The resulting image curve is called epipolar line. The projection of a focal point of another camera is called epipole. Certainly, all epipolar lines must pass through the epipoles. The advantage of epipolar geometry is the search space reduction when doing stereo correspondence analysis: given a pixel in one image the corresponding pixel (if not occluded) must be located on the respective epipolar line. This relation is also expressed by the singular fundamental matrix F, the quadratic form of which attains zero in case a left-image pixel lies on the epipolar line belonging to the right-image pixel, and vice versa. The fundamental matrix contains all geometric information necessary, that is intrinsic and extrinsic parameters, for establishing correspondences between two images. If the intrinsic parameters as focal length or the optical image center are known, the so-called essential matrix E describes the imaging in terms of normalized image coordinates, cf. [27].

The Moving Sensor Illustrated

Roughly speaking, on horizontal movement $A \rightarrow B$, the epipole is a place in the image taken at A where the sensor would appear after moving to B (if this was possible). Camera movement and the position of the epipole is depicted in figure 8.13. Note that all the red-rimmed regions correspond to each other. The figure shows the original image on the right. An unwarped 360° panoramic view is shown on the bottom left. Finally, on the top left, the unwarped right lateral 180° view from the sensor is show. Its right side represents the epipole.
To understand this recall that projecting a line results in a circle in the image, see figure 8.3. It will be detailed later on, but epipolar 'lines' are therefore circles passing through the epipole. Since all respective great circles on the projection sphere $\boldsymbol{S}$ have to intersect in two points, the same must be true for the epipolar circles on the image plane. Hence an epipole always has a diametrically opposite counterpart;

when the sensor approaches an object it becomes taller - the diametrically opposite object becomes smaller. When the senor moves, the image points move along the epipolar circles, see figure 8.16.
Each line in the top left image of figure 8.13 is sampled from the lower half of an epipolar circle between the epipole and its diametrically opposite counterpart. Such rectifications are usually employed in stereo vision because any customary scan line based stereo matching algorithm can then compute the corresponding disparities which ultimately provide the 3D-reconstruction of a scene. Nevertheless, it must be taken into account that only the green-rimmed area in the figure can effectively be used.

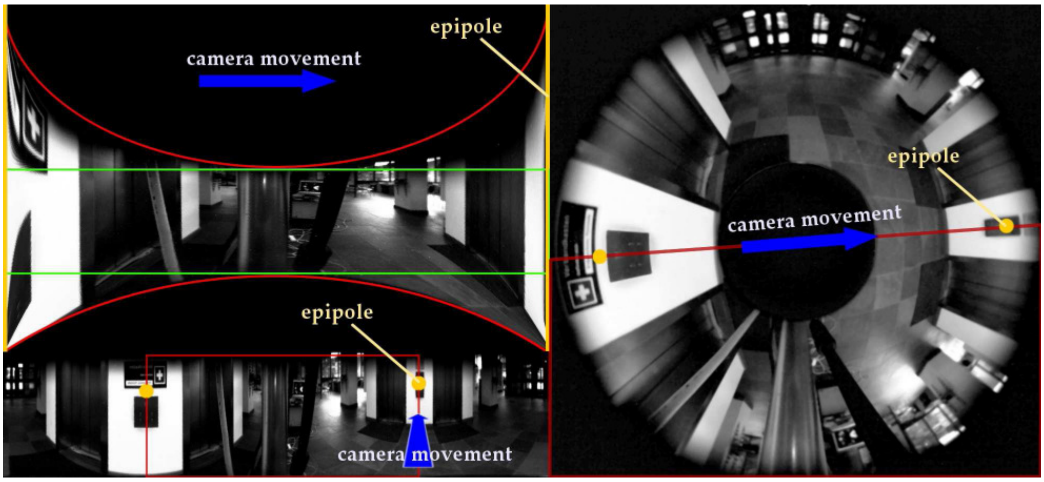

Fig. 8.13: On the role of the epipoles.

8.4.2 Discovering Catadioptric Stereo Vision with CGA

Now a condition for the matching of image points is formulated. This enables the derivation of the fundamental matrix F and the essential matrix E for the parabolic catadioptric case.

Consider the stereo setup of figure 8.14 in which the imaging of world point $\boldsymbol{P}_w$ is depicted. Each of the projection spheres $\boldsymbol{S}$ and $\boldsymbol{S}'$ represents the catadioptric imaging device, but at different positions. The interrelating RBM indicates the sensor movement - from the original to the primed coordinate system. The centers of the coordinate systems are assumed to coincide with the respective focal points, i.e. $\boldsymbol{F}$ and $\boldsymbol{F}'$. Note that the (left) primed coordinate system is also rotated about the vertical axis.

The two projections of $\boldsymbol{P}_w$ are $\boldsymbol{X}$ and $\boldsymbol{Y}'$. Let $\boldsymbol{x}$ and $\boldsymbol{y}$ be their corresponding image points, given as conformal embeddings $\{\boldsymbol{x}, \boldsymbol{y}\} = \mathcal{K}(\{\vec{x}, \vec{y}\} \subset \mathbb{R}^3)$ of the pixel coordinates w.r.t. the image center $\boldsymbol{F}$. The inverse stereographic projection (from the plane to the sphere) of $\boldsymbol{x}$ and $\boldsymbol{y}$ yields the points $\boldsymbol{X}$ and $\boldsymbol{Y}$, represented in the unprimed coordinate system. In order to do stereo, considerations must involve the RBM, which is denoted by $\boldsymbol{M}$. Hence one can write

$$\boldsymbol{Y}' = \boldsymbol{M}\boldsymbol{Y}\widetilde{\boldsymbol{M}},$$

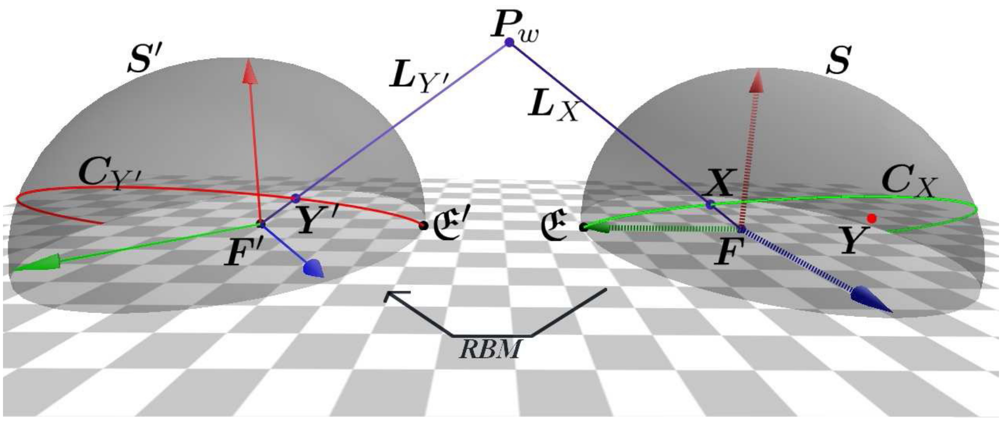

Fig. 8.14: Omnidirectional stereo vision: the projection of ray $\boldsymbol{L}_X$ ($\boldsymbol{L}_{Y'}$) is the great circle $\boldsymbol{C}_{Y'}$ ($\boldsymbol{C}_X$). The 3D-epipole $\mathfrak{E}$ ($\mathfrak{E}'$) is the projection of the focal point $\boldsymbol{F}'$ ($\boldsymbol{F}$) onto the sphere $\boldsymbol{S}$ ($\boldsymbol{S}'$).

$\boldsymbol{S}' = \boldsymbol{M}\boldsymbol{S}\widetilde{\boldsymbol{M}}$ and $\boldsymbol{F}' = \boldsymbol{M}\boldsymbol{F}\widetilde{\boldsymbol{M}}$, etc.

World point $\boldsymbol{P}_w$ has two projection rays, $\boldsymbol{L}_X$ and $\boldsymbol{L}_{Y'}$. Each ray may be projected to the opposite projection sphere. The projection of $\boldsymbol{L}_X$ on $\boldsymbol{S}'$, for example, gives the circle $\boldsymbol{C}_{Y'}$ including $\boldsymbol{Y}'$. This motivates the underlying epipolar geometry since all these great circles must pass through the point $\mathfrak{E}'$ being the projection of $\boldsymbol{F}$. This must be the case because independent of $\boldsymbol{P}_w$ all triangles $\overline{\boldsymbol{F}\boldsymbol{P}_w\boldsymbol{F}'}$ have the line connecting $\boldsymbol{F}$ and $\boldsymbol{F}'$, called baseline, in common. Subsequently it is referred to the 3D-points $\mathfrak{E}$ and $\mathfrak{E}'$ as *3D-epipoles*. Note that a 3D-epipole does not need to lie on the image plane; a tilted sensor lets the 3D-epipoles wander off the image plane.

Intelligibly, the two projection rays $\boldsymbol{L}_X$ and $\boldsymbol{L}_{Y'}$ intersect if the four points $\boldsymbol{F}', \boldsymbol{Y}', \boldsymbol{X}$ and $\boldsymbol{F}$ are coplanar. This condition is now being expressed in terms of CGA. The outer product of four conformal points, say $\boldsymbol{a}_1, \boldsymbol{a}_2, \boldsymbol{a}_3$ and $\boldsymbol{a}_4$, results in the sphere $\boldsymbol{K}_A = \boldsymbol{a}_1 \wedge \boldsymbol{a}_2 \wedge \boldsymbol{a}_3 \wedge \boldsymbol{a}_4$ comprising the points. If these are coplanar the sphere degenerates to the special sphere with infinite radius - which is a plane. Recall from section 3.3 that a plane lacks the $\mathbf{e}_o$-component in contrast to a sphere. The explanation is that the $\mathbf{e}_o$-component carries the value $(\vec{a}_2 - \vec{a}_1) \wedge (\vec{a}_3 - \vec{a}_1) \wedge (\vec{a}_4 - \vec{a}_1)$ which amounts to the triple product (utilizing the vector cross product)

$$(\vec{a}_2 - \vec{a}_1) \cdot ((\vec{a}_3 - \vec{a}_1) \times (\vec{a}_4 - \vec{a}_1)),$$

where $\boldsymbol{a}_i = \mathcal{K}(\vec{a}_i \in \mathbb{R}^3)$, $1 \le i \le 4$. The condition must therefore ensure the $\mathbf{e}_o^*$-component[10] to be zero, i.e.

$$\boldsymbol{G} \;=\; \boldsymbol{F} \wedge \boldsymbol{X} \wedge \boldsymbol{F}' \wedge \boldsymbol{Y}' \;=\; (\boldsymbol{F} \wedge \boldsymbol{X}) \;\wedge\; \boldsymbol{M}\big(\boldsymbol{F} \wedge \boldsymbol{Y}\big)\widetilde{\boldsymbol{M}} \;\; \overset{\mathbf{e}_o^*}{=} \;\; 0\,. \tag{8.7}$$

Using the abbreviations $\underline{\boldsymbol{X}} = \boldsymbol{F} \wedge \boldsymbol{X}$ and $\underline{\boldsymbol{Y}} = \boldsymbol{F} \wedge \boldsymbol{Y}$ the upper formula reads $\boldsymbol{G} = \underline{\boldsymbol{X}} \wedge \boldsymbol{M}\underline{\boldsymbol{Y}}\widetilde{\boldsymbol{M}} \overset{\mathbf{e}_o^*}{=} 0$. Now the tensor representation as introduced in section

[10]The component dual to $\mathbf{e}_o$-component (denoted $\mathbf{e}_o^*$) must be zero as the outer product representation is dual to the sphere representation given in section 3.3.

6.1 can be exploited such that every pair of correspondence points $(\underline{\mathsf{x}}, \underline{\mathsf{y}})$ yields the G-condition

$$\mathsf{g}^t(\mathsf{p}, \underline{\mathsf{x}}, \underline{\mathsf{y}}) \;=\; \underline{\mathsf{x}}^k\, \mathsf{O}^t{}_{kc}\, (\mathsf{p}^r\, \mathsf{G}^a{}_{rl}\, \underline{\mathsf{y}}^l\, \mathsf{G}^c{}_{ab}\, \mathsf{R}^b{}_s\, \mathsf{p}^s), \tag{8.8}$$

where $\Phi(\boldsymbol{G}) = \mathsf{g}$, $\Phi(\underline{\boldsymbol{X}}) = \underline{\mathsf{x}}$, $\Phi(\underline{\boldsymbol{Y}}) = \underline{\mathsf{y}}$ and $\Phi(\boldsymbol{M}) = \mathsf{p}$. As usual, the product tensors O, G and R denote the outer product, the geometric product and the reverse, respectively. Likewise, for the motor $\boldsymbol{M}$ the familiar parameterization $\mathsf{p} \in \mathbb{R}^8$ is chosen.
Note that only a particular index $t = t^{\diamond}$, that is the one indexing to the $\mathbf{e}_o^*$-component of the result, has to be taken into account. After setting $\boldsymbol{F} = \mathbf{e}_o$ it can be shown that $\underline{\mathsf{x}}$ and $\underline{\mathsf{y}}$ in fact denote the Euclidean 3D-coordinates on the projection spheres, i.e. $\underline{\mathsf{x}}, \underline{\mathsf{y}} \in \mathbb{R}^3$. Considering the motor p as constant, the bilinear form

$$g(\underline{\mathsf{x}}, \underline{\mathsf{y}}) \;=\; \underline{\mathsf{x}}^k\, \mathsf{E}_{kl}\, \underline{\mathsf{y}}^l \;\in\; \mathbb{R}$$

with

$$\mathsf{E}_{kl} \;=\; \mathsf{O}^{t^{\diamond}}{}_{kc}\, \mathsf{p}^r\, \mathsf{G}^a{}_{rl}\, \mathsf{G}^c{}_{ab}\, \mathsf{R}^b{}_s\, \mathsf{p}^s$$

is obtained. The condition is linear in $\underline{\boldsymbol{X}}$ and linear in $\underline{\boldsymbol{Y}}$ as expected by the bilinearity of the geometric product. Its succinct matrix notation is

$$\underline{\mathsf{x}}^{\mathsf{T}}\mathsf{E}\,\underline{\mathsf{y}} \;=\; 0\,, \tag{8.9}$$

where $\mathsf{E} \in \mathbb{R}^{3\times 3}$ denotes the essential matrix of the epipolar geometry. No proof is given, but it is mentioned that equation (8.9), which ultimately reflects a triple product, is zero if and only if there is coplanarity between the four points $\boldsymbol{F}', \boldsymbol{Y}', \boldsymbol{X}$ and $\boldsymbol{F}$. Next, if setting $\boldsymbol{Y}' = \mathfrak{E}'$ or $\boldsymbol{X} = \mathfrak{E}$ one gets $\mathsf{E}\,\underline{\mathsf{y}} = \mathsf{0}$ and $\underline{\mathsf{x}}^{\mathsf{T}}\mathsf{E} = \mathsf{0}$, respectively. Otherwise, say $\mathsf{E}\,\underline{\mathsf{y}} = \mathsf{n} \in \mathbb{R}^3$, an $\boldsymbol{X}$ can be chosen such that the corresponding $\underline{\mathsf{x}}$ is not orthogonal to n, whence $\underline{\mathsf{x}}^{\mathsf{T}}\mathsf{E}\,\underline{\mathsf{y}} \neq 0$. This would imply that the points $\boldsymbol{F}', \mathfrak{E}', \boldsymbol{F}$ and the chosen $\boldsymbol{X}$ are not coplanar, which must be a contradiction since $\boldsymbol{F}', \mathfrak{E}'$ and $\boldsymbol{F}$ are already collinear. Hence the 3D-epipoles reflect the left and right null space of E, and it can be inferred that the rank of E can be at most two.

Because E does solely depend on the motor $\boldsymbol{M}$, which embodies the extrinsic parameters, it can not be a fundamental matrix, which must include the intrinsic parameters as well. Fortunately, the previous derivations can easily be extended to obtain the fundamental matrix F. Recall the image points $\boldsymbol{x}$ and $\boldsymbol{y}$. They are related to $\boldsymbol{X}$ and $\boldsymbol{Y}$ in terms of a stereographic projection. As already stated in section 8.1, a stereographic projection is equal to an inversion in a certain sphere, but inversion is the most fundamental operation in CGA. In accordance with figure 8.2 it can be used $\boldsymbol{X} = \boldsymbol{S}_I \boldsymbol{x} \boldsymbol{S}_I$. Note that the inversion sphere $\boldsymbol{S}_I$ depends on the focal length of the parabolic mirror. In this way equation (8.7) becomes

$$\boldsymbol{G} \;=\; \boldsymbol{F} \wedge (\boldsymbol{S}_I \boldsymbol{x} \boldsymbol{S}_I) \wedge \boldsymbol{F}' \wedge (\boldsymbol{S}_I \boldsymbol{y}' \boldsymbol{S}_I) \;\overset{\mathbf{e}_o^*}{=}\; 0.$$

In addition, the image center (specifically, the coordinates of the pixel where the optical axis hits the image plane) can be included by introducing a suitable translator $\boldsymbol{T}_C$. Hence $\boldsymbol{S}_I$ would have to be replaced by the compound operator $\boldsymbol{Z} := \boldsymbol{S}_I \boldsymbol{T}_C$

$$\boldsymbol{G} \;=\; \boldsymbol{F} \wedge (\boldsymbol{Z}\boldsymbol{x}\widetilde{\boldsymbol{Z}}) \wedge \boldsymbol{F}' \wedge (\boldsymbol{Z}\boldsymbol{y}'\widetilde{\boldsymbol{Z}}) \quad \overset{\mathbf{e}_o^*}{=} \quad 0. \tag{8.10}$$

However, equation (8.10) is still linear in the points $\boldsymbol{x}$ and $\boldsymbol{y}$. It is refrained from specifying the corresponding tensor representation or the fundamental matrix, respectively. Instead a connection to the work of Geyer and Daniilidis [50] is shown. They have derived a catadioptric fundamental matrix of dimension 4×4 for what they call lifted image points. These entities live in the 4D-Minkowski space (the fourth basis vector squares to -1). The lifting raises an image point, say $\mathsf{w} := [u, v]^\mathsf{T}$, onto a unit sphere, centered at the origin, such that the lifted point $\tilde{\mathsf{w}} \in \mathbb{R}^{3,1}$ is collinear with w and the North Pole $\boldsymbol{N}$ of the sphere. Thus the lifting corresponds to a stereographic projection. The lifting of w is defined as

$$\tilde{\mathsf{w}} \;=\; [2u, 2v, u^2 + v^2 - 1, u^2 + v^2 + 1]^\mathsf{T}. \tag{8.11}$$

Compare the conformal embedding $\boldsymbol{w} = \mathcal{K}(\mathsf{w}) = u\,\mathbf{e}_1 + v\,\mathbf{e}_2 + \frac{1}{2}(u^2 + v^2)\,\mathbf{e} + 1\;\mathbf{e}_o$ in the $\mathbf{e}\,\mathbf{e}_o$-coordinate system (Φ discards the $\mathbf{e}_3$-coordinate as it is zero)

$$\Phi(\boldsymbol{w}) = [u, v, \tfrac{1}{2}(u^2 + v^2), 1]^\mathsf{T}\,.$$

It can be switched back to the $\mathbf{e}_+\mathbf{e}_-$-coordinate system of the conformal space by means of the linear (basis) transformation $\mathfrak{L} \in \mathbb{R}^{5\times 5}$

$$\mathfrak{L} \;:=\; \begin{bmatrix} 1 & 0 & 0 & 0 \\ 0 & 1 & 0 & 0 \\ 0 & 0 & 1 & -\frac{1}{2} \\ 0 & 0 & 1 & +\frac{1}{2} \end{bmatrix}.$$

$$\mathfrak{L}\;\Phi(\boldsymbol{w}) \;=\; \begin{bmatrix} 1 & 0 & 0 & 0 \\ 0 & 1 & 0 & 0 \\ 0 & 0 & 1 & -\frac{1}{2} \\ 0 & 0 & 1 & +\frac{1}{2} \end{bmatrix} \begin{bmatrix} u \\ v \\ \frac{1}{2}(u^2 + v^2) \\ 1 \end{bmatrix} = \begin{bmatrix} u \\ v \\ \frac{1}{2}(u^2 + v^2 - 1) \\ \frac{1}{2}(u^2 + v^2 + 1) \end{bmatrix}.$$

The lifting in equation (8.11) is therefore identical to the conformal embedding up to the scalar factor 2. At first, this implies that $\tilde{\mathsf{w}} = 2\mathfrak{L}\;\Phi(\boldsymbol{w}) = 2\mathfrak{L}\;\Phi(\mathcal{K}(\mathsf{w}))$. Second, if $\tilde{\mathsf{F}} \in \mathbb{R}^{4\times 4}$ denotes a fundamental matrix for lifted points then, by analogy, $\mathsf{F} = 4\,\mathfrak{L}^\mathsf{T}\tilde{\mathsf{F}}\mathfrak{L}$ is the fundamental matrix that would be obtained from equation (8.10).

8.4.3 Pre-Estimating Epipoles

The results of the previous section are now applied to the epipole estimation. The essential matrix E is used to estimate the epipoles for two reasons. First, the intrinsic parameters do not change while the imaging device moves; one initial calibration is enough. Second, the rank-2 essential matrix is only of dimension 3×3 such that at least eight points are needed for the estimation.

Here nine pairs of corresponding image points are chosen. Then considering the respective points on the projection sphere, the expression

$$\underline{\mathsf{x}} \;=\; \Phi(\,\mathbf{e}_o \wedge \boldsymbol{X}) \quad \in \mathbb{R}^3 \tag{8.12}$$

is evaluated. This gives $\mathbb{X} = \{\underline{\mathsf{x}}_{1\ldots9}\}$ and $\mathbb{Y} = \{\underline{\mathsf{y}}_{1\ldots9}\}$, respectively. Every $\underline{\mathsf{x}}$-$\underline{\mathsf{y}}$-pair must satisfy equation (8.9) which can be rephrased as

$$\mathrm{vec}(\underline{\mathsf{x}}\,\underline{\mathsf{y}}^{\mathsf{T}})^{\mathsf{T}}\,\mathrm{vec}(\mathsf{E}) \;=\; 0.$$

Recall that vec(·) reshapes a matrix into a column vector. Hence the best least-squares approximation of vec(E) is the right-singular vector to the smallest singular value of the matrix consisting of the row vectors $\mathrm{vec}(\underline{\mathsf{x}}_{\underline{\mathsf{i}}}\underline{\mathsf{y}}_{\underline{\mathsf{i}}}^{\mathsf{T}})^{\mathsf{T}}$, $1 \le \underline{\mathsf{i}} \le 9$. Let $\mathsf{E}^{\diamond}$ be the so estimated essential matrix. The left- and right-singular vectors to the smallest singular value of $\mathsf{E}^{\diamond}$ are then the sought approximations to the 3D-epipoles, as described above. The epipoles then serve as a first guess for the stochastic epipole estimation explained in the following section.

8.4.4 Stochastic Epipole Estimation

Now it is being detailed how the GH-method can be invoked. The role of the previously derived initial estimates in the actual stochastic estimation will thereby become evident, too.
Estimating the epipoles is simply done by estimating the motor $\boldsymbol{M}$, parameterized by $\mathsf{p} \in \mathbb{R}^8$: knowing $\boldsymbol{M}$ the directions to the 3D-epipoles can be extracted from the points $\boldsymbol{M}\boldsymbol{F}\widetilde{\boldsymbol{M}}$ and $\widetilde{\boldsymbol{M}}\boldsymbol{F}\boldsymbol{M}$, respectively, as can be inferred from figure 8.14. The former point, for instance, equals $\boldsymbol{F}'$.

As input data all N pairs of corresponding points are used, i.e. $\mathbb{X} := \{\underline{\mathsf{x}}_{1\ldots N}\}$ and $\mathbb{Y} := \{\underline{\mathsf{y}}_{1\ldots N}\}$. The sets are computed by means of equation (8.12). An observation is a pair $(\underline{\mathsf{x}}_{\underline{\mathsf{i}}},\, \underline{\mathsf{y}}_{\underline{\mathsf{i}}})$, $1 \le \underline{\mathsf{i}} \le N$. Note that internally the compound observation vector $\underline{\mathsf{b}}_{\underline{\mathsf{i}}} := [\underline{\mathsf{x}}_{\underline{\mathsf{i}}};\underline{\mathsf{y}}_{\underline{\mathsf{i}}}] \in \mathbb{R}^6$ is used. The related uncertainties[11] can be computed either by equation (8.12) or more directly by equation (8.11), where independence of $\underline{\mathsf{x}}_{\underline{\mathsf{i}}}$ and $\underline{\mathsf{y}}_{\underline{\mathsf{i}}}$ is assumed, i.e.

$$\Sigma_{\underline{\mathsf{b}}_{\underline{\mathsf{i}}},\underline{\mathsf{b}}_{\underline{\mathsf{i}}}} \;=\; \begin{bmatrix} \Sigma_{\underline{\mathsf{x}}_{\underline{\mathsf{i}}}\underline{\mathsf{x}}_{\underline{\mathsf{i}}}} & \mathsf{0} \\ \mathsf{0} & \Sigma_{\underline{\mathsf{y}}_{\underline{\mathsf{i}}}\underline{\mathsf{y}}_{\underline{\mathsf{i}}}} \end{bmatrix} \in \mathbb{R}^{6\times6}, \qquad 1 \le \underline{\mathsf{i}} \le N.$$

The functional model, derived from geometric considerations, is self-evidently given by equation (8.8) for $t = t^{\diamond}$. Hence the G-constraint is

$$g^t_{\underline{\mathsf{i}}}(\mathsf{p}, \underline{\mathsf{x}}_{\underline{\mathsf{i}}}, \underline{\mathsf{y}}_{\underline{\mathsf{i}}}) \;=\; \mathsf{p}^r\,\mathsf{p}^s\;\; \underline{\mathsf{x}}^k_{\underline{\mathsf{i}}}\,\underline{\mathsf{y}}^l_{\underline{\mathsf{i}}}\;\; \mathsf{O}^t{}_{kc}\,\mathsf{G}^a{}_{rl}\,\mathsf{G}^c{}_{ab}\,\mathsf{R}^b{}_s, \qquad 1 \le \underline{\mathsf{i}} \le N, \tag{8.13}$$

Differentiating with respect to $\underline{\mathsf{b}}_{\underline{\mathsf{i}}}$ and p yields the required matrices V and U, respectively. Again, the standard H-constraint (7.7) can be used. But additionally it has to be constrained that $\boldsymbol{M}$ does not converge to the identity element $\boldsymbol{M} = \mathbf{1}$. Otherwise, the condition equation (8.7) would become $\boldsymbol{G} = \boldsymbol{F} \wedge \boldsymbol{X} \wedge \boldsymbol{F} \wedge \boldsymbol{Y}$ being zero at all times. This is achieved by constraining the $\mathbf{e}$-component of $\boldsymbol{F}' = \boldsymbol{M}\boldsymbol{F}\widetilde{\boldsymbol{M}}$,

[11]The distribution of the acquired pixel coordinates is assumed to be i.i.d., as usual.

$\boldsymbol{F} = \mathbf{e}_o$, to be 0.5. Thus the distance d between $\boldsymbol{F}$ and $\boldsymbol{F}'$ is set to one[12]. The needed conformal geometric algebra expression is simply

$$d^2 = \left\langle -2\,\mathbf{e}_o \cdot (\boldsymbol{M}\,\mathbf{e}_o\widetilde{\boldsymbol{M}}) \right\rangle$$

if $\boldsymbol{M}$ was an outright motor. In the iterative estimation process $\boldsymbol{M}$ must effectively be considered a general multivector with structural restrictions imposed by the RBM mask (7.4). Using the matrix representation of CGA, as outlined in chapter 6, a motor $\mathsf{p} = \Phi(\boldsymbol{M})$ has the structure

$$\boldsymbol{M} \equiv \begin{bmatrix} \mathsf{p}_1+\mathsf{p}_7 & -\mathsf{p}_4-\mathsf{p}_8 & \mathsf{p}_3+\mathsf{p}_5 & -\mathsf{p}_2+\mathsf{p}_6 & -\mathsf{p}_7 & \mathsf{p}_8 & -\mathsf{p}_5 & -\mathsf{p}_6 \\ \mathsf{p}_4+\mathsf{p}_8 & \mathsf{p}_1+\mathsf{p}_7 & \mathsf{p}_2-\mathsf{p}_6 & \mathsf{p}_3+\mathsf{p}_5 & -\mathsf{p}_8 & -\mathsf{p}_7 & \mathsf{p}_6 & -\mathsf{p}_5 \\ -\mathsf{p}_3+\mathsf{p}_5 & -\mathsf{p}_2-\mathsf{p}_6 & \mathsf{p}_1-\mathsf{p}_7 & \mathsf{p}_4-\mathsf{p}_8 & -\mathsf{p}_5 & \mathsf{p}_6 & \mathsf{p}_7 & \mathsf{p}_8 \\ \mathsf{p}_2+\mathsf{p}_6 & -\mathsf{p}_3+\mathsf{p}_5 & -\mathsf{p}_4+\mathsf{p}_8 & \mathsf{p}_1-\mathsf{p}_7 & -\mathsf{p}_6 & -\mathsf{p}_5 & -\mathsf{p}_8 & \mathsf{p}_7 \\ \mathsf{p}_7 & -\mathsf{p}_8 & \mathsf{p}_5 & \mathsf{p}_6 & \mathsf{p}_1-\mathsf{p}_7 & -\mathsf{p}_4+\mathsf{p}_8 & \mathsf{p}_3-\mathsf{p}_5 & -\mathsf{p}_2-\mathsf{p}_6 \\ \mathsf{p}_8 & \mathsf{p}_7 & -\mathsf{p}_6 & \mathsf{p}_5 & \mathsf{p}_4-\mathsf{p}_8 & \mathsf{p}_1-\mathsf{p}_7 & \mathsf{p}_2+\mathsf{p}_6 & \mathsf{p}_3-\mathsf{p}_5 \\ \mathsf{p}_5 & -\mathsf{p}_6 & -\mathsf{p}_7 & -\mathsf{p}_8 & -\mathsf{p}_3-\mathsf{p}_5 & -\mathsf{p}_2+\mathsf{p}_6 & \mathsf{p}_1+\mathsf{p}_7 & \mathsf{p}_4+\mathsf{p}_8 \\ \mathsf{p}_6 & \mathsf{p}_5 & \mathsf{p}_8 & -\mathsf{p}_7 & \mathsf{p}_2-\mathsf{p}_6 & -\mathsf{p}_3-\mathsf{p}_5 & -\mathsf{p}_4-\mathsf{p}_8 & \mathsf{p}_1+\mathsf{p}_7 \end{bmatrix}.$$

This makes it possible to derive the constraint via simple matrix calculations. Since, in the present case, $\boldsymbol{M}\,\mathbf{e}_o\widetilde{\boldsymbol{M}}$ can only give vector and 5-vector components, the anti-commutator can be used to expand the inner product as

$$\boldsymbol{Q} := -2\,\mathbf{e}_o \cdot (\boldsymbol{M}\,\mathbf{e}_o\widetilde{\boldsymbol{M}}) = -(\,\mathbf{e}_o\boldsymbol{M}\,\mathbf{e}_o\widetilde{\boldsymbol{M}} + \boldsymbol{M}\,\mathbf{e}_o\widetilde{\boldsymbol{M}}\,\mathbf{e}_o). \tag{8.14}$$

In CGA the reverse operation always amounts to negating the 20 bivector and trivector components of a multivector. Hence $\widetilde{\boldsymbol{M}}$ can be obtained by applying a sign change to the components $\{\mathsf{p}_{2\ldots7}\}$ in the above $\boldsymbol{M}$-matrix. Evaluating equation (8.14) gives a multivector $\boldsymbol{Q}$ with only three non-zero components in $\mathsf{q} = \Phi_f(\boldsymbol{Q})$:

$$\begin{array}{lll} \mathsf{q}_1: & 4(\mathsf{p}_5^2+\mathsf{p}_6^2+\mathsf{p}_7^2+\mathsf{p}_8^2) & \stackrel{!}{=} 1 \\ \mathsf{q}_{27}: & 2(\mathsf{p}_1\mathsf{p}_8-\mathsf{p}_2\mathsf{p}_5-\mathsf{p}_3\mathsf{p}_6-\mathsf{p}_4\mathsf{p}_7) & \stackrel{!}{=} 0 \\ \mathsf{q}_{28}: & -\mathsf{q}_{27} & \stackrel{!}{=} 0. \end{array}$$

The rightmost column shows the value the component should take. Note that the last two constraints are already part of the $\boldsymbol{M}\widetilde{\boldsymbol{M}} = \mathbf{1}$ constraint (7.6), cf. page 196. Adding the constraint $\mathsf{p}_5^2+\mathsf{p}_6^2+\mathsf{p}_7^2+\mathsf{p}_8^2 = 1/4$ and differentiating ultimately gives

$$\mathsf{H}(\mathsf{p}) = 2\begin{bmatrix} \mathsf{p}_1 & \mathsf{p}_2 & \mathsf{p}_3 & \mathsf{p}_4 & 0 & 0 & 0 & 0 \\ 0 & 0 & 0 & 0 & \mathsf{p}_5 & \mathsf{p}_6 & \mathsf{p}_7 & \mathsf{p}_8 \\ \mathsf{p}_8 & -\mathsf{p}_5 & -\mathsf{p}_6 & -\mathsf{p}_7 & -\mathsf{p}_2 & -\mathsf{p}_3 & -\mathsf{p}_4 & \mathsf{p}_1 \end{bmatrix}.$$

It remains to enlighten the usage of the pre-estimated 3D-epipoles. But this issue coincides with the requirement to provide an initial estimate for the GH-method: the initial estimate for p is the unit length translator $\boldsymbol{T}_E$ - being a special motor - along the direction of the initial estimate for the 3D-epipole $\mathfrak{E}$ from section 8.4.3, i.e. $\mathsf{p}^{[0]} := \Phi(\boldsymbol{T}_E)$.

[12]This can be done as the true distance between $\boldsymbol{F}$ and $\boldsymbol{F}'$ cannot be recovered from the image data.

Scenario	1x2	2x3	3x4	4x5	5x6	6x7	7x8	8x9
Displacement	37cm	58cm	64cm	16cm	46cm	89cm	18cm	20cm

Table 8.4: Camera displacements between successive positions.

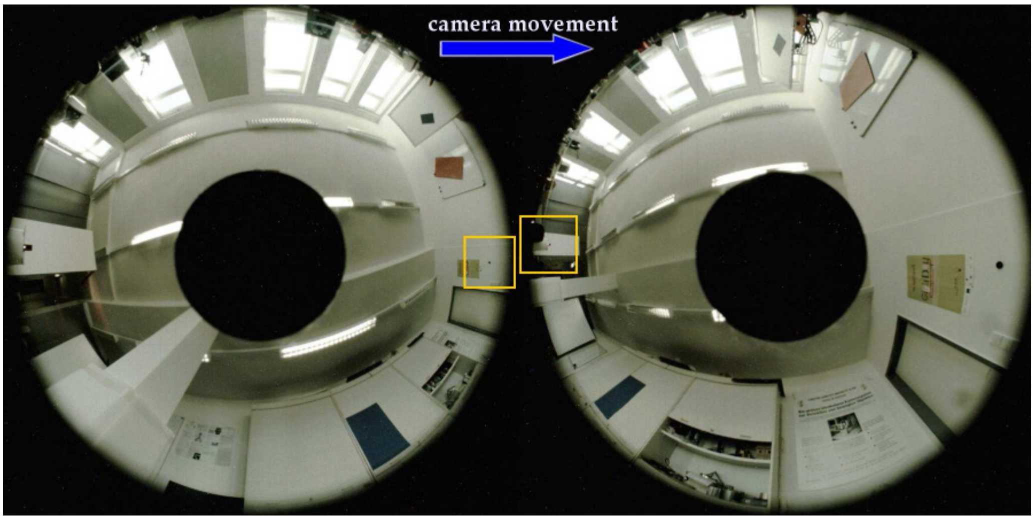

Fig. 8.15: Stereo setup. The epipoles are highlighted by the orange rectangles. The right image was taken after moving the sensor 3.5 m towards the black marker point on the wall in the center of the left orange rectangle. Note the immense difference in the perceived environment.

8.4.5 Experimental Results

For the experimental verification of the derived epipole estimation procedure the vision system shown in figure 8.1 was used again. It was, upright as in the figure, mounted on top of a tripod. The sensor was then translated (on a planar surface, avoiding rotations) by hand along a laser beam. The red dot in figure 8.1 shows the place where the laser beam hit the device. Nine images were taken at distances 1.82 m, 2.19 m, 2.77 m, 3.41 m, 3.57 m, 4.03 m, 4.92 m, 5.1 m and 5.3 m. Thus the overall movement was about 3.5 m. Table 8.4 summarizes the displacements between consecutive sensor positions. Each of the 36 2-combinations of images reflects one experimental scenario, i.e. $\{(1,2),(1,3),\ldots,(8,9)\}$. Scenario $(1,9)$, for example, is shown in figure 8.15. On average, 112 feature points were manually selected in each image. Further, for each scenario on average 94 feature point correspondences were manually established. The entire image series was subjected to the calibration as described in section 8.3. In the last but one step, 3D-epipoles were pre-estimated according to the method, referred to as SVD-method, presented in section 8.4.3. Note that all rather than nine correspondence points were used to determine the initial guess. The subsequently presented results indicate the gain in accuracy on applying the Gauss-Helmert method to the initial estimates.

For each scenario there are two initial estimates of the 3D-epipoles - one for each

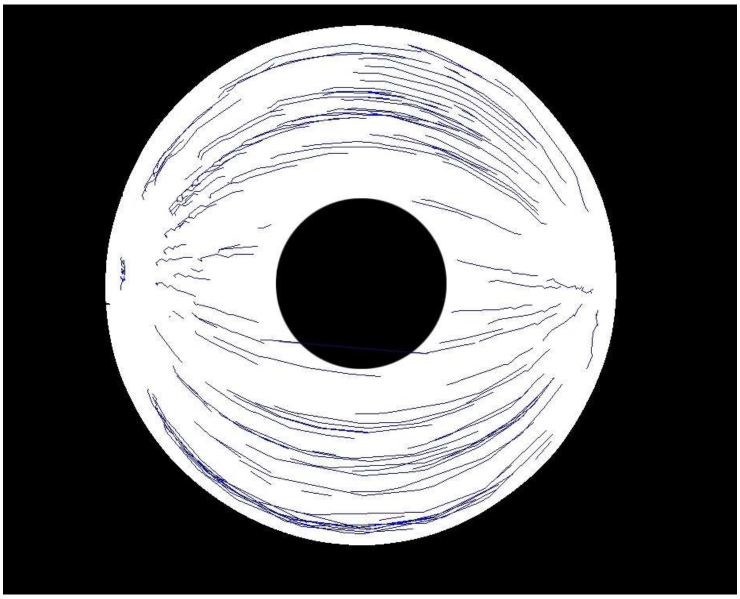

Fig. 8.16: Movement of correspondence points across (at most) nine images. Each trajectory represents the connected positions of one feature point. Some trajectories show jaggies; these are caused by unwillingly done rotations of the camera.

image/sensor position. In order to compare the GH-method and the SVD-method, an SVD-motor $\boldsymbol{M}_{\mathrm{SVD}}$ is computed from these 3D-epipoles. It consists of a horizontal rotation to align both 3D-epipoles. This is necessary so as to account for accidental rotations of the sensor. As a consequence, the sensor coordinate axis are no longer aligned. The other part is the unit length translator $\boldsymbol{T}_E$. Hence a situation similar to that of figure 8.14 is created.
The goodness of the GH-results is demonstrated in two different ways. Let the GH-motor be denoted by $\boldsymbol{M}_{\mathrm{GH}}$. For each scenario and each of the motors $\boldsymbol{M}_{\mathrm{SVD}}$ and $\boldsymbol{M}_{\mathrm{GH}}$ the following evaluations were carried out.

1. Using the motor all projection rays of the scenario can be reconstructed. Ideally, corresponding projection rays intersect. Hence the respective distances in 3D are calculated, cf. page 132. The mean of the distances serves as a quality measure.

2. The adjustments in the directions of the 3D-epipoles in degree are calculated.

The results regarding the 3D-reconstruction (item 1) are depicted in figure 8.17. It can be seen that the average improvement of 42.44%$\pm$ 20% is considerably. Moreover, it is always positive. This justifies the second quality measure, the improvements regarding the angular directions as presented in figure 8.18. The stated mean correction of almost one degree, which corresponds to seven pixels in the image, can be vital in practical applications. Convincing evidence for the goodness of the proposed epipole estimation give figure 8.18 and figure 8.20, respectively. It is somewhat empirical, but throughout all scenarios the GH-method (green cross) offset the SVD-result (red cross) for the epipole towards the black dot, which was targeted at by the laser while the experiment was conducted. Hence the dot represents the ground truth regarding the epipoles.

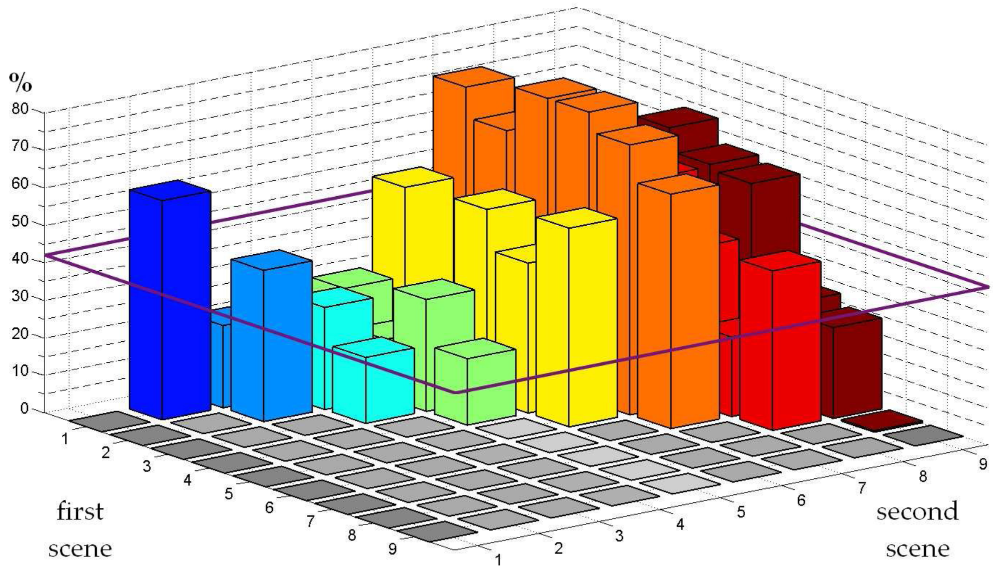

Fig. 8.17: GH-improvements in percent w.r.t. the quality of the 3D-reconstruction from the correspondence points. The min/average/max improvement is 0.43%, 42.44%± 20% (violet line) and 77%, respectively.

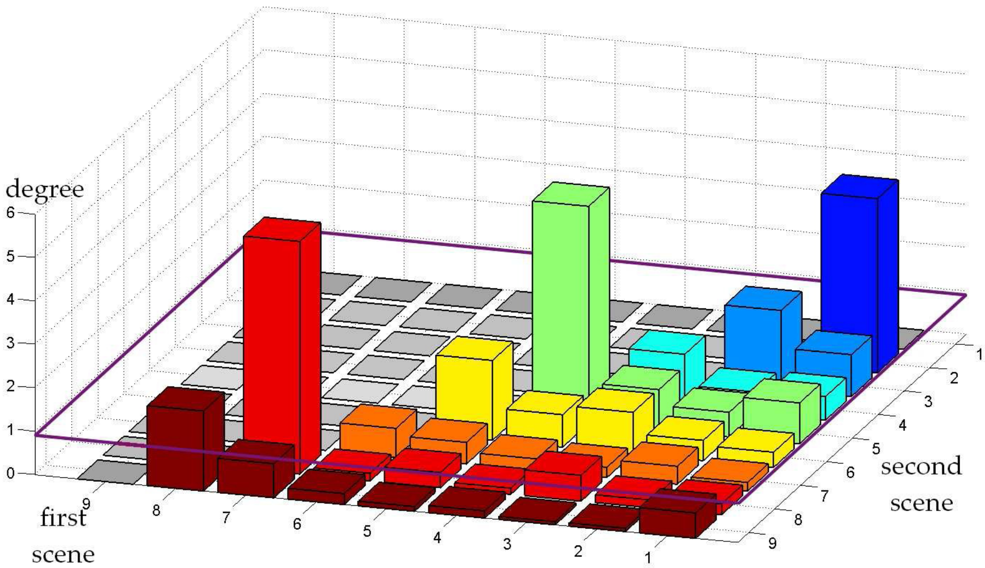

Fig. 8.18: Adjustments in the directions of the 3D-epipoles. The mean correction is $0.95° \pm 1.25°$ (violet line) corresponding to $7px \pm 9px$ (pixel) on the image plane.

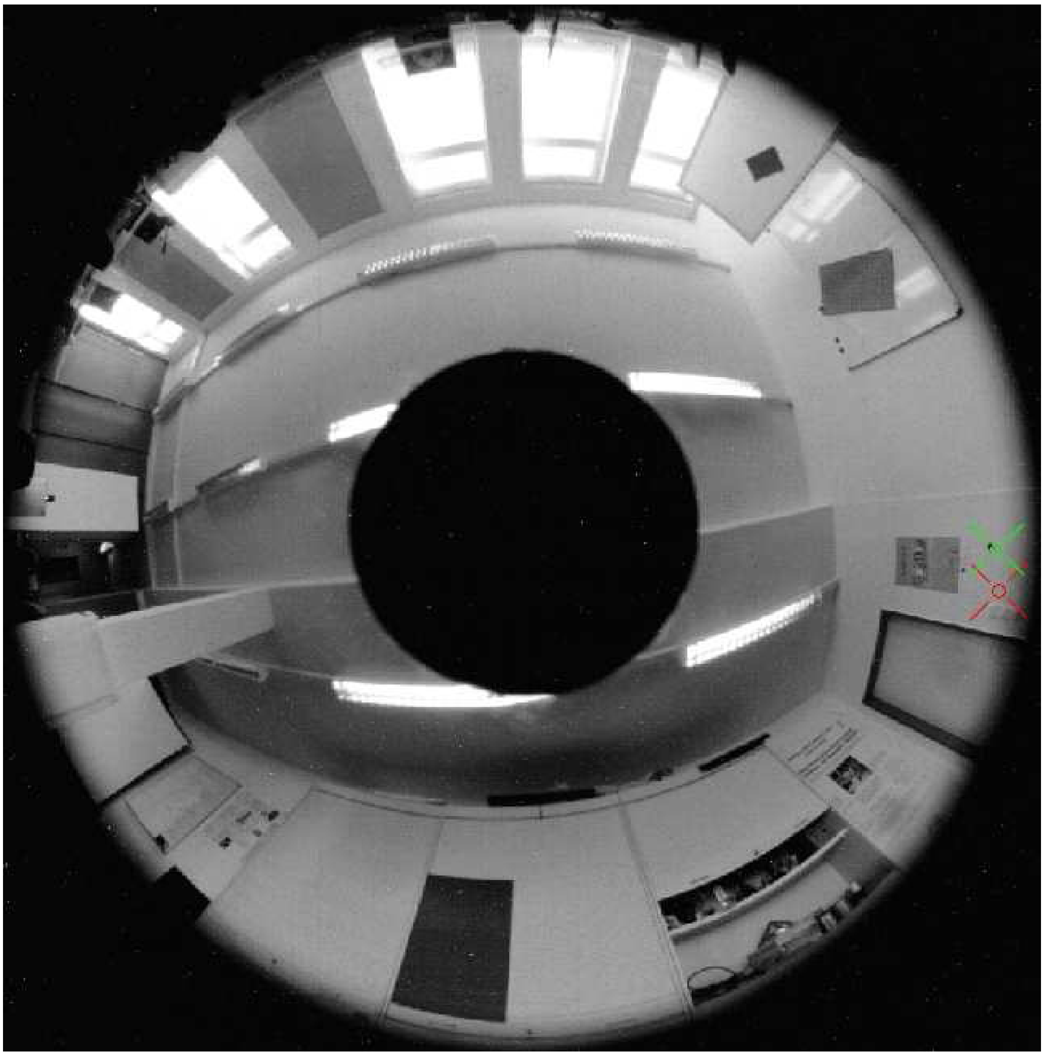

Fig. 8.19: Estimated epipoles: setup 4x5 (see figure 8.20). The guess of the SVD-method (lower red cross) and the refinement by the GH-method (upper green cross).

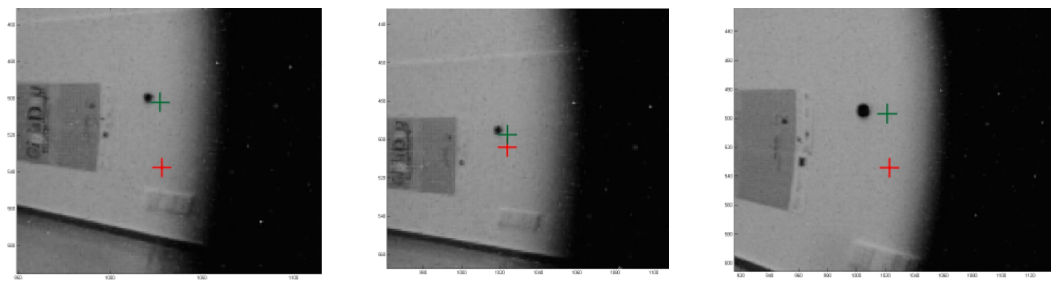

Fig. 8.20: Estimated epipoles: magnification for the scenarios 4x5 (l), 3x5 (c) and 7x8 (r). The differences in pixel are 34, 7 and 37, respectively. Scenario 3x5 represents an average situation.

Chapter 9

Conclusion

It was intended to demonstrate that combining conformal geometric algebra with the method of least squares adjustment is best suited for a wide range of applications, especially those from the field of computer vision. The main topic dealt with from this subject is pose estimation. But the individual contributions of the chapters shall be subsumed first.

- A thorough and formal introduction to GA with vivid examples and several connections to the standard vector algebra is given. The outer product and its momentous consequence - the blade - is derived in every detail. Sophisticated algebra expressions are analyzed and broken down into intelligible representations. Operations as the reverse, the magnitude, the conjugate, the inverse, the projection or the rejection are explained. Vital concepts as duality and outermorphism are elucidated. The relevance of versors and null blades is discussed.

- The conformal space and its underlying embedding is illustratively derived. Conformal geometric algebra, its rich subspace concept and the transformations from the conformal group, which can act on the geometric objects that live in the subspaces, are enlightened. The multivectors inhering with these properties are analyzed in detail with respect to their structure and their mutual relationships. An entirely algebraic factorization of motors (rigid body motions) into specific translational and rotational parts is proposed.

- The principle of pose estimation is succinctly rephrased using CGA. Starting from a clear geometric concept, a new geometric view on the 3-point pose estimation is obtained. The solution so inspired amounts to finding a root of a well-behaved scalar valued function of an angle. An n-point problem is shown to be solvable by taking the algebraic group nature of motors into account; a technique called intrinsic mean builds a weighted average of several 3-point solutions exploiting the tight relationship to the Lie algebra of the motors. The resultant method is robust, sound and provides accurate estimates.

- The method of least squares adjustment and the whole frame of parameter estimation is illustrated. This includes a survey of the different types of observations and their corresponding adjustment problems. The focus is on the linear Gauss-Helmert model, which can account for all types of observations simultaneously. The estimation method, i.e. the GH-method, that arises from the model is hence the most general case of least squares adjustment. In the end, the GH-method for block observations as used throughout this work is derived.

- The matrix representation and the crucial tensor representation of GA is explained. On this basis, standard error propagation is adapted to CGA, that is given a product of two uncertain multivectors the mean and covariance of the resultant multivector is derived. Error propagation is also applied to the conformal embedding as it ultimately represents a function of uncertain arguments.

- Three standard problems are chosen to demonstrate the effectiveness of combining CGA with the GH-method: first, the estimation of the best circle passing through a set of uncertain points in 3D. Second, fitting an RBM to two 3D-point sets, one of which consists of observations. Third, the perspective pose estimation problem based on point features. Each of these issues clarifies several important aspects: first, the ease with which such problems can be modeled if CGA is used. Second, the way the tensor representation of GA makes algebraic condition and constraint equations available to the GH-method. Third, how smoothly and with which accuracy error propagation may be integrated into the framework of geometric algebra. Fourth, the availability of a covariance matrix for the determined parameters that reflects how well the estimate approximates the observations.
  For each problem, the goodness of the respective GH-solution is experimentally substantiated.

- Omnidirectional imaging using a single-viewpoint paracatadioptric vision system, with its strengths and weaknesses, is introduced. A simple method for calibrating such a system is proposed. Due to its structure, conformal geometric algebra offers the ideally matching framework to model omnidirectional imaging in a straightforward manner. This and especially the importance of the related inversion operation is brought to the fore. To keep track of uncertainties under omnidirectional image formation, error propagation for CGA expressions is employed. The GH-method is applied to three problems: a pose estimation based on point features (a 3D-point model is fitted to projection rays), a pose estimation based on line features (a 3D-line model is fitted to projection planes) and an epipole estimation.
  For the latter concern, epipolar geometry is entirely modeled within CGA. As a result, a representation for the essential matrix and the fundamental matrix, respectively, in terms of CGA elements arises. Epipole estimation is lastly established on the basis of the essential matrix. This provides, as a byproduct, the motion estimation between the two considered omnidirectional images. It is further proven that the renowned authors of [50] make

implicit use of a conformal embedding of image points in their standard vector algebra derivation of the fundamental matrix. This impressively shows the appropriateness of CGA.
The conducted experiments show that the proposed approaches to the three problems produce considerably exact results.

It has been demonstrated many times that CGA is not without reason *the* language for geometric computing; it not only gives intuitive access to many geometric problems but also provides a powerful analytical tool to derive the respective solutions. The universal character of CGA compared to the standard vector algebra has been encountered and revealed several times indicating that CGA should be the preferable starting point to model problems.

By means of the tensor representation of GA, the approved GH-method has successfully been incorporated into the framework of geometric algebra. In the same way, error propagation has been made available for all GA operations such that working with uncertain multivectors became feasible. The established combination of the GH-method with CGA represents a sound new estimation technique. Its competitiveness with respect to the reached accuracy has been corroborated experimentally.

Another conclusion that can certainly be drawn is that the approached problems effortlessly and with elegance integrate into the framework of geometric algebra. The wide range of addressable geometric problems likewise demonstrates the variability of the method.

Appendix A

Selected Aspects Underlying this Work

This chapter serves as a repository for text parts which are too extensive or too basic to be given in the main text. It is also tailored to convey the minimal knowledge necessary to follow the elucidations in this thesis.

A.1 Linear Algebra

Linear algebra is the theory of vector spaces over fields. A natural way is therefore to begin with a characterization of a field. The remaining step, that is to introduce the vector space, is then explained easily.

Definition A.1 (Field):
A field is a triple $(\mathbb{K}, +, \cdot)$ *consisting of a set* $\mathbb{K}$ *and two functions*

$$\begin{array}{rcll} + : \mathbb{K}\times\mathbb{K} & \longrightarrow & \mathbb{K} & \\ (\lambda,\mu) & \longmapsto & \lambda+\mu & \quad \textit{(addition)} \end{array}$$

and

$$\begin{array}{rcll} \cdot : \mathbb{K}\times\mathbb{K} & \longrightarrow & \mathbb{K} & \\ (\lambda,\mu) & \longmapsto & \lambda\,\mu & \quad \textit{(multiplication)} \end{array}$$

such that the following axioms are fulfilled:

1. **Associativity of addition**
   For all $\lambda,\mu,\nu\in\mathbb{K}$ *one has* $(\lambda+\mu)+\nu \,=\, \lambda+(\mu+\nu)$.
2. **Commutativity of addition**
   For all $\lambda,\mu\in\mathbb{K}$ *one has* $\lambda+\mu \,=\, \mu+\lambda$.

3. **Identity element of addition (zero element)**
   It exists an element $0 \in \mathbb{K}$ *such that* $\lambda + 0 = \lambda$ *for all* $\lambda \in \mathbb{K}$.

4. **Inverse element of addition**
   For each $\lambda \in \mathbb{K}$ *it exists an element* $-\lambda \in \mathbb{K}$ *such that* $\lambda + (-\lambda) = 0$.

5. **Associativity of multiplication**
   For all $\lambda, \mu, \nu \in \mathbb{K}$ *one has* $(\lambda\,\mu)\,\nu = \lambda\,(\mu\,\nu)$.

6. **Commutativity of multiplication**
   For all $\lambda, \mu \in \mathbb{K}$ *one has* $\lambda\,\mu = \mu\,\lambda$.

7. **Identity element of multiplication**
   It exists an element $1 \in \mathbb{K}$, $1 \neq 0$, *such that* $1\lambda = \lambda$ *for all* $\lambda \in \mathbb{K}$.

8. **Inverse element of multiplication**
   For each $\lambda \in \mathbb{K}$ *and* $\lambda \neq 0$ *it exists an* $\lambda^{-1} \in \mathbb{K}$ *such that* $\lambda^{-1}\,\lambda = 1$.

9. **Distributivity**
   For all $\lambda, \mu, \nu \in \mathbb{K}$ *one has* $\lambda\,(\mu + \nu) = \lambda\,\mu + \lambda\,\nu$.

■

The uniqueness of the elements mentioned at point 3 and 7 can easily be deduced from the axioms given above. Also, the elements $-\lambda$ and λ^{-1} are uniquely defined. There is a vast number of examples but the two most common representatives of a field are the reals $\mathbb{R}$ and the complex numbers $\mathbb{C}$ together with the standard addition $(+)$ and multiplication $(\cdot)$. A field is the scalar domain required for vector spaces.

Definition A.2 (Vector space):
A triple $(V, +, \cdot)$ *consisting of a set* V, *a function (called addition)*

$$\begin{aligned} + : V \times V &\longrightarrow V \\ (x, y) &\longmapsto x + y \end{aligned}$$

and a function (called scalar multiplication)

$$\begin{aligned} \cdot : \mathbb{K} \times V &\longrightarrow V \\ (\lambda, x) &\longmapsto \lambda\, x \end{aligned}$$

is called a vector space (over the field $\mathbb{K}$*), if the subsequent axioms hold for the addition (+) and multiplication (·):*

1. **Associativity of addition**
   $(x + y) + z = x + (y + z)$ *for all* $x, y, z \in V$.

2. **Commutativity of addition**
   $x + y = y + x$ *for all* $x, y \in V$.

3. **Identity element of addition (zero element)**
   It exists an element $0 \in V$ such that $x + 0 = x$ for all $x \in V$.

4. **Inverse element of addition**
   For each $x \in V$ it exists an element $-x \in V$ such that $x + (-x) = 0$.

5. **Associativity of scalar multiplication**
   $\lambda(\mu x) = (\lambda\,\mu)\,x$ *for all* $\lambda, \mu \in \mathbb{K}$, $x \in V$.

6. **Identity element of scalar multiplication**
   $1\,x = x$ *for all* $x \in V$ *and* $1 \in \mathbb{K}$ *is the identity element of multiplication of* $\mathbb{K}$, *too.*

7. **Distributivity**
   a) $\lambda(x + y) = \lambda\,x + \lambda\,y$ *for all* $x, y \in V$, $\lambda \in \mathbb{K}$.
   b) $(\lambda + \mu)\,x = \lambda\,x + \mu\,x$ *for all* $\lambda, \mu \in \mathbb{K}$, $x \in V$.

■

Naturally, the elements of a vector space V are termed 'vectors'. The most famous vector spaces are $\mathbb{R}^2$ and $\mathbb{R}^3$ - known from vector analysis in school. A basic but important concept is the linear combination of vectors.

Definition A.3 (Linear combination):
Let V be a vector space over the field $\mathbb{K}$ with vectors $v_1, v_2, \ldots, v_r \in V$ and scalars $\lambda_1, \lambda_2, \ldots, \lambda_r \in \mathbb{K}$. Then $\lambda_1 v_1 + \lambda_2 v_2 + \ldots + \lambda_r v_r \in V$ is called a linear combination of the vectors $v_1, v_2, \ldots, v_r$. ■

Definition A.4 (Linear span):
Let V be a $\mathbb{K}$-vector space with vectors $v_1, v_2, \ldots, v_r \in V$. The set of all linear combinations

$$\mathrm{span}\{v_1, v_2, \ldots, v_r\} = \{\lambda_1 v_1 + \lambda_2 v_2 + \ldots + \lambda_r v_r \mid \lambda_t \in \mathbb{K}, 1 \leq t \leq r\}$$

is called the linear span of $v_1, v_2, \ldots, v_r$. ■

Definition A.5 (Linear independence):
Let V be a $\mathbb{K}$-vector space with vectors $v_1, v_2, \ldots, v_r \in V$. The vectors are called linearly independent if

$$\lambda_1 v_1 + \lambda_2 v_2 + \ldots + \lambda_r v_r = 0 \quad \Longrightarrow \quad \lambda_1 = \lambda_2 = \ldots = \lambda_r = 0$$

holds for every set of scalars $\lambda_1, \lambda_2, \ldots, \lambda_r \in \mathbb{K}$. ■

It may easily be verified that the span of a set of linearly independent vectors in V generates a linear subspace of V, where the subspace inherits the vector space operations defined on V. Moreover, with the help of Zorn's lemma it can be proven that every vector space owns a minimal set of linearly independent vectors spanning that vector space:

Definition A.6 (Basis):
Let V be a vector space over the field $\mathbb{K}$. A set of linearly independent vectors $v_1, v_2, \ldots, v_r \in V$ is called basis of V if $\operatorname{span}\{v_1, v_2, \ldots, v_r\} = V$. ∎

A basis can equally be termed a **frame**.

Note that the term **canonical basis** refers to the standard basis of an n-dimensional vector space, i.e. the simplest basis possible is meant. For instance, the canonical basis $\{e_1, e_2, e_3\}$ of a 3D-vector space may be written

$$e_1 = [1,0,0]^\mathsf{T} \qquad e_2 = [0,1,0]^\mathsf{T} \qquad e_3 = [0,0,1]^\mathsf{T} \,.$$

Definition A.7 (Scalar product):
Let V be a $\mathbb{K}$-vector space. A scalar product is a function

$$\begin{aligned} \langle,\rangle \,:\, V \times V &\longrightarrow \mathbb{K} \\ (x,y) &\longmapsto \langle x,y\rangle \end{aligned}$$

satisfying the following conditions

1. **Bilinearity**
   The mapping $\langle x,y\rangle$ is linear in both $x \in V$ and $y \in V$, respectively.

2. **Symmetry**
   $\langle x,y\rangle = \langle y,x\rangle$ *for all* $x, y \in V$.

An equivalent notation for the scalar product is indicated by '$*$', hence $x*y = \langle x,y\rangle$. The product $\langle x,x\rangle$ may be abbreviated to x^2 as well. ∎

Remark (scalar product)

Unlike the common definition, the scalar product, as it is understood in this thesis, is allowed to be **indefinite**. This means the scalar product does not have to be positive definite, that is $\langle x,x\rangle > 0$ for all $x \in V$. Even the semi-definite case $\langle x,x\rangle \geq 0$ for all $x \in V$ is not required. This kind of scalar product does not necessarily induce a norm $||\cdot||$ or a metric on a vector space because important relations like $||x|| = 0 \iff x = 0$ or the triangle inequality do not hold unless the scalar product is positive definite.

Definition A.8 (Euclidean vector space):
A $\mathbb{K}$-vector space V equipped with a scalar product such that $\langle x,x\rangle > 0$ for all

$x \in V$ is termed Euclidean vector space. ∎

The positive definite **Euclidean scalar product** is denote by '$*_{\varepsilon}$'.

A scalar product may be associated with a (possibly indefinite) **quadratic form** Q via $Q(x) := \langle x, x\rangle$. Conversely, one has $\langle x, y\rangle = \frac{1}{2}\big(Q(x+y) - Q(x) - Q(y)\big)$. The scalar product is referred to as the associated bilinear form of Q. An important term in the context of this thesis is **quadratic space**, which is a pair (V, Q) where V is a $\mathbb{K}$-vector space and $Q : V \to \mathbb{K}$ is a quadratic form on V. The axiomatic derivation of geometric algebra starting at page 17, for instance, bases upon the quadratic space $\mathbb{R}^{p,q}$. A quadratic form can be defined in terms of its associated bilinear form as follows.

Definition A.9 (Quadratic form):
Let V be a $\mathbb{K}$-vector space. A map

$$\begin{aligned} Q : V &\longrightarrow \mathbb{K} \\ x &\longmapsto \lambda \end{aligned}$$

is called a quadratic form on V if

1. *$Q(\lambda x) = \lambda^2 Q(x)$ for all $x \in V$ and $\lambda \in \mathbb{K}$.*
2. *$B(x, y) = Q(x+y) - Q(x) - Q(y)$ defines a bilinear form on V.*

∎

Definition A.10 (Null vector):
Let V be a $\mathbb{K}$-vector space equipped with a scalar product $\langle , \rangle$. A vector $x \in V$ is a null vector or just null if $x^2 = 0$. ∎

As an example, let $e_+, e_- \in V$ denote two canonical basis vectors with an appropriate scalar product such that $e_+^2 = +1$ and $e_-^2 = -1$. Then $e_+ + e_-$ and $e_- - e_+$ are null vectors.

Definition A.11 (Orthogonality):
Let V be a $\mathbb{K}$-vector space equipped with a scalar product $\langle , \rangle$. Any two different non-zero vectors $x, y \in V$ are called (indicated by $x \perp y$) orthogonal to each other if $\langle x, y\rangle = 0$. ∎

Two vectors are called **perpendicular** to each other if they are orthogonal and if they stem from a Euclidean vector space. A set of two or more vectors is termed (mutually) orthogonal if the vectors in it are pairwise orthogonal to each other.

Lemma A.1 (Orthogonality):
A set of orthogonal non-null vectors is always linearly independent.

Proof: *Let the vectors $v_1, v_2, \ldots, v_r \in V$ be orthogonal and non-null. Let $\lambda_1 v_1 + \lambda_2 v_2 + \ldots + \lambda_r v_r = 0$. Then the scalar product $\langle \lambda_1 v_1 + \lambda_2 v_2 + \ldots + \lambda_r v_r,\, v_t \rangle$, $1 \leq t \leq r$, must be $\lambda_t \langle v_t, v_t \rangle = 0$. Hence zero can only be combined with the trivial solution and so the vectors are linearly independent.*

■

Definition A.12 (Associative algebra):

A vector space V over the field $\mathbb{K}$ together with a bilinear multiplication (termed algebra product)

$$\begin{array}{ccc} V \times V & \longrightarrow & V \\ (x, y) & \longrightarrow & x\, y \end{array}$$

is called associative algebra $\mathcal{A}$ over $\mathbb{K}$ if the associative law holds for any three elements $x, y, z \in V$

$$x\,(y\,z) \;=\; (x\,y)\,z\,.$$

An algebra is called **degenerate** *if there exist at least two non-zero elements $x \neq 0$ and $y \neq 0$ such that $xy \;=\; 0$.*

■

The distributivity of the algebra $\mathcal{A}$ is equivalent to the required bilinearity of the algebra product. Hence for any three elements $x, y, z \in \mathcal{A}$ $(\in V)$

$$x\,(y + z) \;=\; xy + xz$$

holds. The bilinearity also allows for $\lambda(\,xy) = (\lambda x)\,y = x(\lambda y)$ given that $x, y \in \mathcal{A}$ and $\lambda \in \mathbb{K}$. Surely, no axiom for the closure of $\mathcal{A}$ must be stated since it is already implicit in the definition of the algebra product. The dimension of the algebra is its dimension as a $\mathbb{K}$-vector space.

Notice, as a counterexample, that $\mathbb{R}^3$ in conjunction with the non-associative vector cross product '$\times$' can not be an associative algebra - instead a *Lie algebra* is formed.

A.2 Commutator and Anti-Commutator

In linear algebra commutator and anti-commutator are important tools when dealing with analytic calculations. Any linear associative multiplication of two elements A and B, in the following indicated by the juxtaposition AB, can be expressed as the sum of commutator $A \underline{\times} B$ and anti-commutator $A \overline{\times} B$. The minimal algebraic structure necessary is thus a **ring**. A ring differs from a field (page 235) in that axiom 6 (commutativity of multiplication) or axiom 8 (inverse element of multiplication) does not need to be fulfilled. The next definition, however, makes clear why at least axiom 6 must not be fulfilled in order to have a reasonable decomposition of AB.

Definition A.13 (Commutator and anti-commutator[1]):
Let A and B two elements of a non-commutative ring or an associative algebra. The commutator product of A and B is defined as

$$A \veebar B \;=\; \tfrac{1}{2}\Big(AB \,-\, BA\Big)\,.$$

The anti-commutator product of A and B is defined as

$$A \barwedge B \;=\; \tfrac{1}{2}\Big(AB \,+\, BA\Big)\,.$$

It is therefore

$$AB \;=\; A \veebar B \;+\; A \barwedge B\,.$$

■

It immediately follows from the definition that the commutator and anti-commutator product are **distributive** but **not associative** operations. Moreover

$$\begin{array}{lllllll} A \veebar B & = & -\,B \veebar A & \qquad & A \barwedge B & = & B \barwedge A \\ A \veebar A & = & 0 & \qquad & A \barwedge A & = & A \end{array}\,.$$

If there exists an element B^{-1} such that $BB^{-1} = 1$ then a split of identity can easily be accomplished as

$$BB^{-1} = 1 \quad \Longleftrightarrow \quad A \;=\; ABB^{-1} \;=\; (A \veebar B)B^{-1} + (A \barwedge B)B^{-1}\,.$$

Notice that commutator and anti-commutator are assumed to bind stronger than the multiplication, e.g. $A \veebar BC = (A \veebar B)C$. Here a redundant bracketing is intended to increase readability.

A simple but powerful expansion can be obtained with the **Leibniz rule**

$$(AB) \veebar C \;=\; A(B \veebar C) \;+\; (A \veebar C)B\,.$$

The Leibniz rule can be generalized. Using four variables it becomes

$$(ABC) \veebar D \;=\; AB(C \veebar D) \;+\; A(B \veebar D)C \;+\; (A \veebar D)BC\,.$$

After multiplying the latter equation with 2 and expanding the terms it is

$$ABCD - DABC \;=\; ABCD \underbrace{- ABDC \;+\; ABDC - ADBC \;+\; ADBC}_{0} - DABC\,.$$

Hence all intermediate terms neutralize each other. The generalization of the Leibniz rule then reads

$$(A_1A_2 \ldots A_k) \veebar B \;=\; \sum_{i=0}^{k-1} A_1A_2 \ldots A_{(k-i)-1}(A_{k-i} \veebar B)A_{(k-i)+1} \ldots A_k\,,$$

[1] In the literature commutator and anti-commutator are commonly denoted by brackets $[A, B] = A \veebar B$ and curly brackets $\{A, B\} = A \barwedge B$, respectively. Apart from that, the notation $[A, B]_- = A \veebar B$ and $[A, B]_+ = A \barwedge B$ is typical.

where the summands are ordered such that $A_1 A_2 \dots A_{k-1}(A_k \underline{\times} B)$ and $(A_1 \underline{\times} B) A_2 \dots A_k$ are the first and last summand, respectively. An even more general formula includes anti-commutators as well. It can then be inferred that

$$\begin{aligned}
(AB)\underline{\times}C &= A(B\underline{\times}C) \;+\; (A\underline{\times}C)B \\
(AB)\overline{\times}C &= A(B\underline{\times}C) \;+\; (A\overline{\times}C)B \\
(AB)\overline{\times}C &= A(B\overline{\times}C) \;-\; (A\underline{\times}C)B \\
(AB)\underline{\times}C &= A(B\overline{\times}C) \;-\; (A\overline{\times}C)B .
\end{aligned}$$

Very similar expansion rules that rely on the same, above mentioned, neutralization principle are

$$\begin{aligned}
(AB)\underline{\times}C &= A\underline{\times}(BC) + B\underline{\times}(CA) \\
(AB)\overline{\times}C &= A\underline{\times}(BC) + B\overline{\times}(CA) \\
(AB)\overline{\times}C &= A\overline{\times}(BC) - B\underline{\times}(CA) \\
(AB)\underline{\times}C &= A\overline{\times}(BC) - B\overline{\times}(CA).
\end{aligned}$$

The most popular equation is the **Jacobi identity**

$$A\underline{\times}(B\underline{\times}C) \;+\; B\underline{\times}(C\underline{\times}A) \;+\; C\underline{\times}(A\underline{\times}B) \;=\; 0\,.$$

For a possible generalization see [68, 69].

<u>Proof</u>: *Consider the full expansion of all terms. This yields*

$$\begin{aligned}
&4\Big(A\underline{\times}(B\underline{\times}C) \;+\; B\underline{\times}(C\underline{\times}A) \;+\; C\underline{\times}(A\underline{\times}B) \Big) \\
&= \quad ABC - ACB - BCA + CBA \\
&\qquad + BCA - BAC - CAB + ACB \\
&\qquad + CAB - CBA - ABC + BAC \\
&= \quad A\,(BC - CB + CB - BC) \\
&\qquad + B\,(CA - AC + AC - CA) \\
&\qquad + C\,(BA - BA + AB - AB) \\
&= \quad 0\,.
\end{aligned}$$

■

Similar, likewise important, expansions are

$$
\begin{aligned}
(A\underline{\times}B)\underline{\times}C &= A\underline{\times}(B\underline{\times}C) + (A\underline{\times}C)\underline{\times}B && \text{(A.1)}\\
(A\underline{\times}B)\underline{\times}C &= A\overline{\times}(B\overline{\times}C) - (A\overline{\times}C)\overline{\times}B && \text{(A.2)}\\[1ex]
(A\underline{\times}B)\overline{\times}C &= A\overline{\times}(B\underline{\times}C) + (A\overline{\times}C)\underline{\times}B && \text{(A.3)}\\
(A\underline{\times}B)\overline{\times}C &= A\underline{\times}(B\overline{\times}C) - (A\underline{\times}C)\overline{\times}B && \text{(A.4)}\\[1ex]
(A\overline{\times}B)\underline{\times}C &= A\underline{\times}(B\overline{\times}C) - (A\overline{\times}C)\underline{\times}B && \text{(A.5)}\\
(A\overline{\times}B)\underline{\times}C &= A\overline{\times}(B\underline{\times}C) + (A\underline{\times}C)\overline{\times}B && \text{(A.6)}\\[1ex]
(A\overline{\times}B)\overline{\times}C &= A\overline{\times}(B\overline{\times}C) - (A\underline{\times}C)\underline{\times}B && \text{(A.7)}\\
(A\overline{\times}B)\overline{\times}C &= A\underline{\times}(B\underline{\times}C) + (A\overline{\times}C)\overline{\times}B\,. && \text{(A.8)}
\end{aligned}
$$

Note that equation (A.1) is again the Jacobi identity.

It might sometime be necessary to expand a nested (anti-) commutator expression, for instance

$$A\underline{\times}(B\underline{\times}(C\underline{\times}(D\underline{\times}(E\underline{\times}(F\underline{\times}G)))))\,.$$

A solution to the problem with k operands $A_1, A_2, \ldots, A_k$ is given by equation (A.9). In principle, the sum extends over all 2^{k-1} possible disjoint partitions of an index set $I := \{1, 2, \ldots, k-1\}$ into two sets. This is formalized in terms of the sum over (u, v)-shuffles (page 54). Notice that every summand itself is a product that can be considered two-part with respect to the element A_k. The left-hand (right-hand) elements w.r.t. A_k have to be in an ascending (descending) order, where the respective indices come from the first (second) partition of I. The sorting is indicated, for example, by $\sigma_1 < \sigma_2 < \ldots < \sigma_{k-i}$. The way the products are built is illustrated in figure A.1.

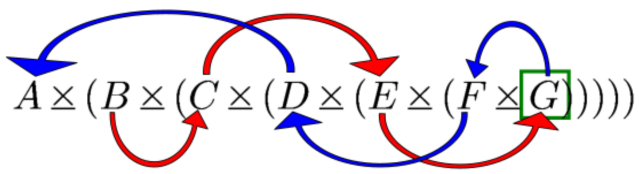

Fig. A.1: Expansion of a nested commutator expression: the term $-BCEGFDA$ is one of the summands that would appear in equation (A.9).

It is refrained from giving the proof of the formula because it would claim too much place measured against its relevance. The expansion formula reads

$$
\begin{gathered}
A_1\underline{\times}(A_2\underline{\times}(A_3\underline{\times}\ldots(A_{k-2}\underline{\times}(A_{k-1}\underline{\times}A_k))\ldots))\\
=\\
\frac{1}{2^{k-1}}\sum_{i=1}^{k}(-1)^{i-1}\sum_{\substack{\sigma\,\in\\ \mathcal{S}(k-i,i-1)}}\underbrace{A_{\sigma_1}A_{\sigma_2}\ldots A_{\sigma_{k-i}}}_{\sigma_1<\sigma_2<\ldots<\sigma_{k-i}}\;A_k\;\underbrace{A_{\sigma_{k-1}}A_{\sigma_{k-2}}\ldots A_{\sigma_{k-i+1}}}_{\sigma_{k-1}>\sigma_{k-2}>\ldots>\sigma_{k-i+1}},
\end{gathered}
\qquad \text{(A.9)}
$$

where $\sigma_i := \sigma(i)$, $1 \leq \sigma_i \leq k-1$. In case of a pure anti-commutator expression, the prefactor $(-1)^{i-1}$ vanishes. Mixed expressions may also be taken into account, but this, in general, makes it necessary to introduce an additional formalism that captures the configuration of commutators and anti-commutators. Nevertheless, two outstanding special cases will be treated now.

Let $\sigma \in \mathcal{S}(k-i, i-1)$ be a (u, v)-shuffle with $\sigma_i := \sigma(i)$, $1 \leq \sigma_i \leq k-1$, as before. Then

$$\omega(\sigma) \; := \; (\sigma_1, \sigma_2, \ldots, \sigma_{k-i},\, k,\, \sigma_{k-1}, \sigma_{k-2}, \ldots, \sigma_{k-i+1}) \tag{A.10}$$

can be regarded as a permutation $\omega \in \mathcal{S}(k)$. With this definition, it is

$$\begin{gathered} \ldots \quad (A_{k-4} \overline{\times} (A_{k-3} \underline{\times} (A_{k-2} \overline{\times} (A_{k-1} \underline{\times} A_k))))... \\ = \\ \frac{1}{2^{k-1}} \sum_{i=1}^{k} \sum_{\substack{\sigma \in \\ \mathcal{S}(k-i,i-1)}} \operatorname{sgn}\big(\omega(\sigma)\big) \; \underbrace{A_{\sigma_1} A_{\sigma_2} \ldots A_{\sigma_{k-i}}}_{\sigma_1 < \sigma_2 < \ldots < \sigma_{k-i}} \; A_k \; \underbrace{A_{\sigma_{k-1}} A_{\sigma_{k-2}} \ldots A_{\sigma_{k-i+1}}}_{\sigma_{k-1} > \sigma_{k-2} > \ldots > \sigma_{k-i+1}} . \end{gathered} \tag{A.11}$$

Note that this formula can be used to expand equation (2.34) - the commutator representation of the **outer product** - which is crucial in geometric algebra.

If the innermost operation is an anti-commutator rather than a commutator like in equation (A.11), a slightly modified formula is obtained:

$$\begin{gathered} \ldots \quad (A_{k-4} \underline{\times} (A_{k-3} \overline{\times} (A_{k-2} \underline{\times} (A_{k-1} \overline{\times} A_k))))... \\ = \\ \frac{1}{2^{k-1}} \sum_{i=1}^{k} (-1)^{i-1} \sum_{\substack{\sigma \in \\ \mathcal{S}(k-i,i-1)}} \operatorname{sgn}\big(\omega(\sigma)\big) \; A_{\sigma_1} A_{\sigma_2} \ldots A_{\sigma_{k-i}} \; A_k \; A_{\sigma_{k-1}} A_{\sigma_{k-2}} \ldots A_{\sigma_{k-i+1}} , \end{gathered} \tag{A.12}$$

with $\omega(\sigma)$ as before (according to equation (A.10)). Note that both equation (A.11) and equation (A.12) can be used to evaluate the **inner product**, see corollary 2.9 on page 45.

A.3 Proofs and Derivations

Extensive proofs which otherwise would interfere with an undiminished understanding of the content are shifted to this place.

A.3.1 Proof of Proposition 2.3

Here it is to be proven, as quoted on page 43, that the outer product of a bivector $\boldsymbol{C} = \boldsymbol{C}_{[2]} \in \mathbb{R}_{p,q}$ with itself is zero iff the bivector represents a 2-blade. This is done by means of an induction on the algebra dimension $n = p + q$. The obvious direction $\boldsymbol{C} = \boldsymbol{C}_{\langle 2 \rangle} \implies \boldsymbol{C} \wedge \boldsymbol{C} = 0$, however, is omitted.

Let $\boldsymbol{C} = \langle \boldsymbol{C} \rangle_2$ be the bivector under consideration. It remains to prove that $\boldsymbol{C} \wedge \boldsymbol{C} = 0$ implies that $\boldsymbol{C}$ is a 2-blade.

Proof:
Induction basis: *let $n = 2$ such that $\boldsymbol{C}$ is definitely a 2-blade.*

Induction hypothesis: *proposition 2.3 is true for algebra dimension n.*

Inductive step: *let $\boldsymbol{C}$ be a bivector from $\mathbb{R}_{n+1}$ with $\boldsymbol{C} \wedge \boldsymbol{C} = 0$. Then $\boldsymbol{C}$ can be subdivided into two summands like*

$$\boldsymbol{C} \;=\; \boldsymbol{C}_n \;+\; \boldsymbol{C}_{n+1},$$

such that $\boldsymbol{C}_{n+1}$ contains all basis blades of $\boldsymbol{C}$ that include the additional basis vector $\mathbf{e}_{n+1}$, i.e. $\boldsymbol{C}_{n+1}$ is the 2-blade

$$\boldsymbol{C}_{n+1} \;=\; \mathbf{e}_{n+1} \wedge \boldsymbol{c}, \qquad \textit{with suitable} \quad \boldsymbol{c} = \sum_{i=1}^{n} c_i \mathbf{e}_i \in \mathbb{R}^n.$$

Accordingly, the remaining basis 2-blades of $\boldsymbol{C}$ compose $\boldsymbol{C}_n$. On evaluating the outer product $\boldsymbol{C} \wedge \boldsymbol{C}$ it is

$$\boldsymbol{C} \wedge \boldsymbol{C} \;=\; \underbrace{\boldsymbol{C}_{n+1} \wedge \boldsymbol{C}_{n+1}}_{0} \;+\; \underbrace{2\,\boldsymbol{C}_{n+1} \wedge \boldsymbol{C}_n \;+\; \boldsymbol{C}_n \wedge \boldsymbol{C}_n}_{0} \;=\; 0.$$

Note that every term of $\boldsymbol{C}_{n+1} \wedge \boldsymbol{C}_n$ does necessarily contain element $\mathbf{e}_{n+1}$, whereas it cannot occur in $\boldsymbol{C}_n \wedge \boldsymbol{C}_n$. Hence both outer products cannot zero themselves and consequently

$$\boldsymbol{C}_{n+1} \wedge \boldsymbol{C}_n \;=\; 0 \qquad \textit{and} \qquad \boldsymbol{C}_n \wedge \boldsymbol{C}_n \;=\; 0.$$

Now the induction hypothesis can be applied to the right expression showing that $\boldsymbol{C}_n$ represents a 2-blade as well. Moreover the first identity

$$\boldsymbol{C}_{n+1} \wedge \boldsymbol{C}_n \;=\; 0 \qquad \Longleftrightarrow \qquad \mathbf{e}_{n+1} \wedge \boldsymbol{c} \wedge \boldsymbol{C}_n \;=\; 0$$

implies that $\boldsymbol{c} \in \mathbb{k}\mathrm{er}(\boldsymbol{C}_n)$ because $\mathbf{e}_{n+1}$ is per definition not part of the OPNS of $\boldsymbol{C}_n$. It therefore exists a supplementary vector $\boldsymbol{c}'$ (pp. 42 sqq.) such that

$$\boldsymbol{C}_n \;=\; \boldsymbol{c}' \wedge \boldsymbol{c},$$

and ultimately, by the distributivity of the outer product,

$$\boldsymbol{C} \;=\; \mathbf{e}_{n+1} \wedge \boldsymbol{c} + \boldsymbol{c}' \wedge \boldsymbol{c} \;=\; (\mathbf{e}_{n+1} + \boldsymbol{c}') \wedge \boldsymbol{c} \;\overset{!}{=}\; \boldsymbol{C}_{\langle 2 \rangle}.$$

■

A.3.2 The Coefficients of Equation (2.27)

At page 33 it has been inferred that equation (2.27)

$$\boldsymbol{f}(\boldsymbol{a}_1, \boldsymbol{a}_2, \ldots, \boldsymbol{a}_k) \;=\; \sum_{\sigma \in \mathcal{S}(k)} \theta_\sigma\, \boldsymbol{a}_{\sigma(1)} \boldsymbol{a}_{\sigma(2)} \ldots \boldsymbol{a}_{\sigma(k)}\,, \qquad \theta_\sigma \in \mathbb{R}\,.$$

is the most general form the outer product of k vectors $\boldsymbol{a}_1$, $\boldsymbol{a}_2$, …, $\boldsymbol{a}_k$ may take on. A condition, or rather the definition for this general case is that each summand of equation (2.27) has to occur. It is therefore assumed that $\theta_\sigma \neq 0$ for all $\sigma \in \mathcal{S}(k)$. Here it is shown that the coefficients θ_σ must then all be equal in their absolute value, that is $|\theta_\sigma| = \text{const}$.

Consider two arbitrary terms of the sum in equation (2.27)

$$\boldsymbol{f}_\sigma \;=\; \theta_\sigma\, \boldsymbol{a}_{\sigma(1)}\boldsymbol{a}_{\sigma(2)}\cdots\boldsymbol{a}_{\sigma(k)} \quad \text{and} \quad \boldsymbol{f}_{\tilde\sigma} \;=\; \theta_{\tilde\sigma}\, \boldsymbol{a}_{\tilde\sigma(1)}\boldsymbol{a}_{\tilde\sigma(2)}\cdots\boldsymbol{a}_{\tilde\sigma(k)}.$$

It exists a permutation $\pi \in \mathcal{S}(k)$ so that $\pi \circ \sigma = \tilde\sigma$ or $\tilde\sigma^{-1} = \sigma^{-1} \circ \pi^{-1}$, equivalently. Note that with the concatenation $\omega := \tilde\sigma^{-1} \circ \sigma$, $\omega \in \mathcal{S}(k)$, and so with $\omega = \sigma^{-1} \circ \pi^{-1} \circ \sigma$, it is $\tilde\sigma \circ \omega = \sigma$. Hence permuting the vectors $\boldsymbol{a}_1, \boldsymbol{a}_2, \ldots, \boldsymbol{a}_k$ with ω beforehand yields

$$\begin{aligned} \boldsymbol{f}_{\tilde\sigma}(\boldsymbol{a}_{\omega(1)}, \boldsymbol{a}_{\omega(2)}, \ldots, \boldsymbol{a}_{\omega(k)}) &= \theta_{\tilde\sigma}\, \boldsymbol{a}_{\sigma(1)}\boldsymbol{a}_{\sigma(2)}\cdots\boldsymbol{a}_{\sigma(k)} \\ &= \theta_{\tilde\sigma}\, \boldsymbol{f}_\sigma(\boldsymbol{a}_1, \boldsymbol{a}_2, \ldots, \boldsymbol{a}_k)/\theta_\sigma\,. \end{aligned}$$

But $\boldsymbol{f}$ is supposed to be alternating which, on the other hand, implies

$$\boldsymbol{f}(\boldsymbol{a}_{\omega(1)}, \boldsymbol{a}_{\omega(2)}, \ldots, \boldsymbol{a}_{\omega(k)}) \;=\; \operatorname{sgn}(\omega)\, \boldsymbol{f}(\boldsymbol{a}_1, \boldsymbol{a}_2, \ldots, \boldsymbol{a}_k)\,.$$

Thus given two arbitrary permutations σ and $\tilde\sigma$, a permutation ω of the argument vectors of $\boldsymbol{f}$ can be found in such a way that the summand $\boldsymbol{f}_\sigma$ plays the role of $\boldsymbol{f}_{\tilde\sigma}$, and vice versa. Consequently, for the quotient $\theta_{\tilde\sigma}/\theta_\sigma$ it is required that[2]

$$\frac{\theta_{\tilde\sigma}}{\theta_\sigma} \;=\; \operatorname{sgn}(\omega) = \operatorname{sgn}(\sigma^{-1})\operatorname{sgn}(\pi^{-1})\operatorname{sgn}(\sigma) = \operatorname{sgn}(\pi) \tag{A.13}$$

since $\operatorname{sgn}(\sigma^{-1})\operatorname{sgn}(\sigma) = 1$ and $\operatorname{sgn}(\pi^{-1}) = \operatorname{sgn}(\pi)$. This already shows that the absolute values $|\theta_\sigma|$ of the summands in equation (2.27) must be identical. Moreover, from $\pi \circ \sigma = \tilde\sigma$ it can be deduced that

$$\operatorname{sgn}(\pi \circ \sigma) = \operatorname{sgn}(\tilde\sigma) \qquad \Longleftrightarrow \qquad \operatorname{sgn}(\pi) \;=\; \frac{\operatorname{sgn}(\tilde\sigma)}{\operatorname{sgn}(\sigma)}\,.$$

In conjunction with equation (A.13) it may eventually be defined

$$\theta_\sigma := c\operatorname{sgn}(\sigma)\,, \qquad c > 0\,, \tag{A.14}$$

where $c = \text{const}$ denotes a positive scalar from the reals $\mathbb{R}$.

[2]The sgn function is a group homomorphism. It therefore holds that

$$\operatorname{sgn}(\sigma_1 \circ \sigma_2) = \operatorname{sgn}(\sigma_1)\operatorname{sgn}(\sigma_2) \qquad \sigma_1, \sigma_2 \in \mathcal{S}\,.$$

A.3.3 Proof of Proposition 2.8

The pending proof of proposition 2.8 set forth hereunder bases on proposition 2.7. The respective equations are restated for a better accessibility:

$$\boldsymbol{A}_{\langle k\rangle} \cdot \boldsymbol{B}_{\langle l\rangle} = \sum_{\sigma\,\in\,\mathcal{S}(k,l-k)} \operatorname{sgn}(\sigma) \Big(\boldsymbol{A}_{\langle k\rangle} \cdot (\boldsymbol{b}_{\sigma_1} \wedge \boldsymbol{b}_{\sigma_2} \wedge ... \wedge \boldsymbol{b}_{\sigma_k})\Big) \Big[\boldsymbol{B}_{\langle l\rangle} \setminus \bigcup_{r=1}^{k} \boldsymbol{b}_{\sigma_r}\Big], \quad \text{(A.15)}$$

with the abbreviation $\sigma_i := \sigma(i)$, $1 \le i \le l$.

$$\boldsymbol{a} \cdot \boldsymbol{B}_{\langle l\rangle} = \sum_{i=1}^{l} (-1)^{i-1} (\boldsymbol{a} \cdot \boldsymbol{b}_i)\ [\boldsymbol{B}_{\langle l\rangle} \setminus \boldsymbol{b}_i] \quad \text{(A.16)}$$

Proof: *According to equation (2.38) it may be written*

$$\boldsymbol{A}_{\langle k\rangle} \cdot \boldsymbol{B}_{\langle l\rangle} = \boldsymbol{a}_1 \cdot (\boldsymbol{a}_2 \cdot\ \dots\ (\boldsymbol{a}_{k-1} \cdot (\boldsymbol{a}_k \cdot \boldsymbol{B}_{\langle l\rangle}))...),\ k \le l$$

As a motivation, consider at first the triple application of proposition 2.7

$$\boldsymbol{a}_3 \cdot (\boldsymbol{a}_2 \cdot (\boldsymbol{a}_1 \cdot \boldsymbol{B}_{\langle l\rangle})) = \sum_{i_3=1}^{l-2} \sum_{i_2=1}^{l-1} \sum_{i_1=1}^{l} (-1)^{i_3-1} (-1)^{i_2-1} (-1)^{i_1-1} \dots$$
$$\dots (\boldsymbol{a}_3 \cdot \boldsymbol{b}''_{i_3})(\boldsymbol{a}_2 \cdot \boldsymbol{b}'_{i_2})(\boldsymbol{a}_1 \cdot \boldsymbol{b}_{i_1})\ \underbrace{[[[\boldsymbol{B}_{\langle l\rangle} \setminus \boldsymbol{b}_{i_1}] \setminus \boldsymbol{b}'_{i_2}] \setminus \boldsymbol{b}''_{i_3}]}_{\textit{remainder}},$$

where $\boldsymbol{b}'_{i_2}$ *denotes the* i_2^{th} *vector in* $[\boldsymbol{B}_{\langle l\rangle} \setminus \boldsymbol{b}_{i_1}]$. *Note that* $\boldsymbol{b}'_{i_2}$ *differs from* $\boldsymbol{b}_{i_2}$, *the* i_2^{th} *vector in* $\boldsymbol{B}_{\langle l\rangle}$, *whenever* $\boldsymbol{b}_{i_1}$ *precedes* $\boldsymbol{b}_{i_2}$ *in* $\boldsymbol{B}_{\langle l\rangle}$, *so if* $i_1 < i_2$. $\boldsymbol{b}''_{i_3}$ *is defined analogously. The index combination* $(i_1, i_2, i_3) = (1, 1, 1)$, *for example, would correspond to* $\boldsymbol{b}_1$ *(* i_1*),* $\boldsymbol{b}_2$ *(* i_2*) and* $\boldsymbol{b}_3$ *(* i_3*). Moreover, an index combination* $(i_1, i_2, i_3) = (3, 2, 1)$ *results in an identical remainder* $[[[\boldsymbol{B}_{\langle l\rangle} \setminus \boldsymbol{b}_{i_1}] \setminus \boldsymbol{b}'_{i_2}] \setminus \boldsymbol{b}''_{i_3}]$.

The aim is now to identify parts of the k-fold application of proposition 2.7 with the corresponding parts of the formula given in proposition 2.8. But it seems that the index combinations $(i_1, i_2, \dots)$, *which define the order in which the vectors* $\boldsymbol{b}$ *are taken out of* $\boldsymbol{B}_{\langle l\rangle}$ *, cause a problem. Hence it is being focused on this now.*

Let $\mathsf{v} \in \mathbb{N}^k$, $k \le l$, *denote a k-tuple that encodes in which order which vectors are to be taken out of* $\boldsymbol{B}_{\langle l\rangle}$ *, e.g. the (vector-) sequence* $\mathsf{v} := (v_1, v_2, \dots, v_k)$. *The first element* v_1 *of* v *specifies that* $\boldsymbol{b}_{\mathsf{v}_1}$ *must be taken out first.*

For every valid sequence v *it exists a unique corresponding index combination* $\mathsf{w} := (i_1, i_2, \dots, i_k) \in \mathbb{N}^k$, $k \le l$. *These tuples are important as they eventually define the sign of the summands. Regarding the above example,* $k = 3$, *it is*

$$\mathsf{v} = (1, 2, 3) \qquad \longleftrightarrow \qquad \mathsf{w} = (1, 1, 1).$$

Next it is analyzed how w *changes under an elementary transposition of an element from* v *with a neighboring element not in* v. *It is ultimately intended to learn how* w *changes under a couple of elementary transpositions so that those summands with identical remainder can be grouped together. In this*

$$\begin{array}{ccc} \overset{(A)}{\boldsymbol{b}_1 \wedge \boldsymbol{b}_2 \wedge \boldsymbol{b}_3 \wedge \boldsymbol{b}_4 \wedge \boldsymbol{b}_5 \wedge \boldsymbol{b}_6} & \longrightarrow & \overset{(B)}{(\ \boldsymbol{b}_2 \wedge \boldsymbol{b}_4 \wedge \boldsymbol{b}_6\ ) \wedge \boldsymbol{b}_1 \wedge \boldsymbol{b}_3 \wedge \boldsymbol{b}_5} \\ \uparrow \quad \uparrow \quad \uparrow & & \uparrow \quad \uparrow \quad \uparrow \\ \mathsf{v}_1 \quad \mathsf{v}_2 \quad \mathsf{v}_3 & \longrightarrow & \mathsf{v}'_1 \quad \mathsf{v}'_2 \quad \mathsf{v}'_3 \end{array} \tag{A.17}$$

example, several elementary transpositions lead to $\mathsf{v} = \mathsf{v}' = (2, 4, 6)$ *but* $\mathsf{w} = (2, 3, 4) \longrightarrow \mathsf{w}' = (1, 1, 1)$. *It is easy to see that moving a vector from* v *by one position to the left, e.g.* $\boldsymbol{b}_3 \wedge \boldsymbol{b}_4 \curvearrowright \boldsymbol{b}_4 \wedge \boldsymbol{b}_3$ *(the right, e.g.* $\boldsymbol{b}_4 \wedge \boldsymbol{b}_5 \curvearrowright \boldsymbol{b}_5 \wedge \boldsymbol{b}_4$*) causes the respective index in* w *to decrease (increase) by one. In the* $\mathsf{v} = (2, 4, 6)$ *example one obtains* $\Delta\mathsf{w} = (-1, -2, -3)$.

Another thing to reflect about is what happens to w *if two neighboring elements in* v *are exchanged, so if for example* $\mathsf{v} = (2, 4, 6) \longrightarrow \mathsf{v}' = (4, 2, 6)$. *First of all, since the elements are neighboring, their composite action regarding the effects on* w *is atomic, i.e. the uninvolved indices of* w *stay unchanged. The situation may be subsumed as follows*

$$\begin{array}{ccccc} \mathsf{v}_i, & \mathsf{v}_{i+1} & \longrightarrow & \mathsf{v}'_i := \mathsf{v}_{i+1}, & \mathsf{v}'_{i+1} := \mathsf{v}_i \\ \mathsf{w}_i, & \mathsf{w}_{i+1} & \longrightarrow & \mathsf{w}'_i = ?, & \mathsf{w}'_{i+1} = ? \end{array} \qquad 1 \le i \le k-1.$$

Two cases must be taken into account when exchanging v_i *and* v_{i+1}*: first, assume that* $\mathsf{v}_i < \mathsf{v}_{i+1}$. *Then,* $\boldsymbol{b}_{\mathsf{v}_i}$ *precedes* $\boldsymbol{b}_{\mathsf{v}_{i+1}}$ *in* $\boldsymbol{B}_{\langle l\rangle}$ *so that the effect of taking out* $\boldsymbol{b}_{\mathsf{v}_i}$ *from* $\boldsymbol{B}_{\langle l\rangle}$ *prior to* $\boldsymbol{b}_{\mathsf{v}_{i+1}}$ *must be that the index* w_{i+1} *is already decreased by one. Note that, as a consequence,* $\mathsf{w}_i = \mathsf{v}_i - (i-1)$ *if the elements in* v *are in ascending order. Conversely, if* $\mathsf{v}_i > \mathsf{v}_{i+1}$ *then the removal of* $\boldsymbol{b}_{\mathsf{v}_i}$ *does not affect the index* w_{i+1}. *After exchanging* v_i *and* v_{i+1} *the update for* w *is*

$$\begin{array}{ccccc} \mathsf{v}_i < \mathsf{v}_{i+1} & \Longrightarrow & \mathsf{w}'_i = \mathsf{w}_{i+1} + 1 & \textit{and} & \mathsf{w}'_{i+1} = \mathsf{w}_i \\ \mathsf{v}_i > \mathsf{v}_{i+1} & \Longrightarrow & \mathsf{w}'_i = \mathsf{w}_{i+1} & \textit{and} & \mathsf{w}'_{i+1} = \mathsf{w}_i - 1. \end{array} \tag{A.18}$$

For example, $\mathsf{v} = (1, 2, \ldots, \mathbf{6}, \mathbf{9}, 7, 8) \longleftrightarrow \mathsf{v}' = (1, 2, \ldots, \mathbf{9}, \mathbf{6}, 7, 8)$ *corresponds to* $\mathsf{w} = (1, 1, \ldots, \mathbf{1}, \mathbf{3}, 1, 1) \longleftrightarrow \mathsf{w}' = (1, 1, \ldots, \mathbf{4}, \mathbf{1}, 1, 1)$.

The sum in equation (A.15) consists of $\binom{l}{k} = \frac{l\,(l-1)\,\ldots\,(l-k+1)}{k!}$ *terms whereas the sum in the* k*-fold application of equation (A.16) is to be taken over* $l\,(l-1)\ \ldots\ (l-k+1)$ *summands, where* $k!$ *of them can each be grouped together as they belong to the same remainder. This becomes clear by observing that there are* $k!$ *permutations of a sequence* $\mathsf{v} = (v_1, v_2, \ldots, v_k)$. *It is thus planned to rearrange the* k*-fold application of equation (A.16) such that it resembles equation (A.15) in proposition 2.8.*

The next equation shows a first generalization towards the k*-fold application of proposition 2.7. The sum* $\sum_{\mathsf{w}}$ *in the formula is intended to be taken over all valid* *index combinations* $\mathsf{w} = (i_1, i_2, \dots, i_k) \in \mathbb{N}^k$*. Besides,* v *is well-defined*[3] *in terms of* w*, and vice versa. This property is indicated by writing* $\mathsf{v}(\mathsf{w})$ *or* $\mathsf{w}(\mathsf{v})$*, respectively.*

$$\boldsymbol{A}_{\langle k\rangle} \cdot \boldsymbol{B}_{\langle l\rangle} \;=\; \sum_{\mathsf{w}} (-1)^{\sum_{i=1}^k \mathsf{w}_i \pm k} \prod_{j=1}^{k} \left(\boldsymbol{a}_{k-(j-1)} \cdot \boldsymbol{b}_{\mathsf{v}(\mathsf{w})_j}\right) \left[\boldsymbol{B}_{\langle l\rangle} \setminus \bigcup_{r=1}^{k} \boldsymbol{b}_{\mathsf{v}(\mathsf{w})_r}\right]$$

This formula may be rewritten in terms of a sum extending over all valid sequences $\mathsf{v} \in \mathbb{N}^k$*. More precisely, the sum is split into two sums such that the outer one captures all* $\binom{l}{k}$ *k-combinations for which a common remainder exists. The inner sum captures all* $k!$ *permutations of the indices* $v_1 < v_2 < \dots < v_k$ *in* v *that belong to the actual remainder.*

$$\boldsymbol{A}_{\langle k\rangle} \cdot \boldsymbol{B}_{\langle l\rangle} \;=\; \sum_{\substack{1 \le v_1 < v_2 < \dots < v_k \le l \\ \mathsf{v}=(v_1, v_2, \dots, v_k)}} \; \sum_{\pi \in \mathcal{S}(k)} \dots$$

$$\dots\; (-1)^{\sum_{i=1}^k \mathsf{w}(\mathsf{v}_\pi)_i \pm k} \prod_{j=1}^{k} \left(\boldsymbol{a}_{k-(j-1)} \cdot \boldsymbol{b}_{\mathsf{v}_{\pi(j)}}\right) \left[\boldsymbol{B}_{\langle l\rangle} \setminus \bigcup_{r=1}^{k} \boldsymbol{b}_{\mathsf{v}_r}\right],$$

where $\mathsf{v}_\pi := (v_{\pi(1)}, v_{\pi(2)}, \dots, v_{\pi(k)})$*. According to equation (A.18), every elementary transposition of elements in* v *alters the sign of* $(-1)^{\sum_{i=1}^k \mathsf{w}_i}$*. The overall number of transpositions to rearrange* v_π *into* v *is determined by the permutation* $\pi \in \mathcal{S}(k)$*. Thus*

$$(-1)^{\sum_{i=1}^k \mathsf{w}(\mathsf{v}_\pi)_i} \;=\; sgn(\pi)\, (-1)^{\sum_{i=1}^k \mathsf{w}_i}, \qquad \mathsf{w}_i := \mathsf{w}(\mathsf{v})_i.$$

Consequently,

$$\boldsymbol{A}_{\langle k\rangle} \cdot \boldsymbol{B}_{\langle l\rangle} \;=\; \sum_{\substack{1 \le v_1 < v_2 < \dots < v_k \le l \\ \mathsf{v}=(v_1, v_2, \dots, v_k)}} (-1)^{\sum_{i=1}^k \mathsf{w}_i \pm k} \dots$$

$$\dots \sum_{\pi \in \mathcal{S}(k)} sgn(\pi) \prod_{j=1}^{k} \left(\boldsymbol{a}_{k-(j-1)} \cdot \boldsymbol{b}_{\mathsf{v}_{\pi(j)}}\right) \left[\boldsymbol{B}_{\langle l\rangle} \setminus \bigcup_{r=1}^{k} \boldsymbol{b}_{\mathsf{v}_r}\right].$$

With the aid of equation (A.17) it can be seen that as long as the elements $v_1, v_2, \dots, v_k$ *of* v *are arranged in ascending order, a minimum of* $\sum_{i=1}^k \mathsf{v}_i - i$ *elementary transpositions of the vectors is necessary to reach setup* (A) *from setup* (B)*, and vice versa. In order to get rid of* w *in the previous formula, it is now being shown that* $(-1)^{\sum_{i=1}^k \mathsf{w}_i \pm k} = (-1)^{\sum_{i=1}^k \mathsf{v}_i - i}$ *is this minimum of transpositions. For this purpose,* w_i *can be substituted by* $\mathsf{v}_i - (i-1)$*, such that*

$$(-1)^{\sum_{i=1}^k \mathsf{w}_i \pm k} \;=\; (-1)^{\sum_{i=1}^k (\mathsf{v}_i - (i-1)) \pm k} \;=\; (-1)^{\sum_{i=1}^k \mathsf{v}_i - i}.$$

Self-evidently, the number of elementary transpositions can be related to a permutation by means of

$$(-1)^{\sum_{i=1}^k \mathsf{v}_i - i} \;=\; sgn(\sigma), \qquad \sigma \in \mathcal{S}(k, l-k),$$

[3] The bijection between v and w it is not yet stated - but it exists.

where $\sigma \in \mathcal{S}(k, l-k)$ denotes a (u,v)-shuffle, see definition 2.8 on page 54, with $\mathsf{v} = (\sigma(1), \sigma(2), \ldots, \sigma(k))$. Hence

$$\boldsymbol{A}_{\langle k\rangle} \cdot \boldsymbol{B}_{\langle l\rangle} \;=\; \sum_{\substack{\sigma\,\in\,\mathcal{S}(k,l-k)\\ \mathsf{v}:=(\sigma_1,\sigma_2,\ldots,\sigma_k)}} \operatorname{sgn}(\sigma) \left(\sum_{\pi\in\mathcal{S}(k)} \operatorname{sgn}(\pi) \prod_{j=1}^{k} \Big(\boldsymbol{a}_{k-(j-1)} \cdot \boldsymbol{b}_{\mathsf{v}_{\pi(j)}} \Big) \right) \Big[\boldsymbol{B}_{\langle l\rangle} \backslash \bigcup_{r=1}^{k} \boldsymbol{b}_{\mathsf{v}_r} \Big],$$

with the abbreviation $\sigma_i := \sigma(i)$, $1 \le i \le l$.

Finally, assume that k equals l. The outer sum consists of only one summand corresponding to $\mathsf{v} = (1, 2, \ldots, k)$, with $\operatorname{sgn}(\sigma) = +1$. The term $[\boldsymbol{B}_{\langle k\rangle} \backslash \bigcup_{r=1}^{k} \boldsymbol{b}_{\mathsf{v}_r}]$ takes on the value 1 and only

$$\boldsymbol{A}_{\langle k\rangle} \cdot \boldsymbol{B}_{\langle k\rangle} \;=\; \sum_{\pi\in\mathcal{S}(k)} \operatorname{sgn}(\pi) \prod_{j=1}^{k} \left(\boldsymbol{a}_{k-(j-1)} \cdot \boldsymbol{b}_{\pi(j)} \right), \qquad \mathsf{v}_{\pi(j)} = \pi(j),$$

is left over. If the subscription by means of v is just considered as a renaming scheme for the vectors $\{\boldsymbol{b}_{1\ldots k}\}$, it can be concluded that

$$\sum_{\pi\in\mathcal{S}(k)} \operatorname{sgn}(\pi) \prod_{j=1}^{k} \Big(\boldsymbol{a}_{k-(j-1)} \cdot \boldsymbol{b}_{\mathsf{v}_{\pi(j)}} \Big) \;=\; \boldsymbol{A}_{\langle k\rangle} \cdot (\boldsymbol{b}_{\mathsf{v}_1} \wedge \boldsymbol{b}_{\mathsf{v}_2} \wedge \ldots \wedge \boldsymbol{b}_{\mathsf{v}_k}),$$

as desired for proposition 2.8.

■

A.4 Additional Notes Tailored to CGA

There is a number of rules which are useful in the context of chapter 3. These are given here.

A.4.1 Commonly Occurring CGA Identities

$$\boldsymbol{I}\,\mathrm{e} \;=\; \overbrace{\mathrm{e}\,\boldsymbol{I}}^{\mathrm{e}\cdot\boldsymbol{I}} \;=\; \overbrace{\mathrm{e}\,\boldsymbol{I}_E}^{\mathrm{e}\wedge\boldsymbol{I}_E} \;=\; -\,\boldsymbol{I}_E\,\mathrm{e} \tag{A.19}$$

$$\boldsymbol{E}\,\boldsymbol{I} \;=\; \boldsymbol{I}\,\boldsymbol{E} \;=\; \boldsymbol{I}_E \tag{A.20}$$

The next three identities are also subject of figure 2.6 on page 63. In particular, when in its algebra $\mathbb{R}_3$, $\boldsymbol{I}_E$ behaves in the same way as $\boldsymbol{I}$; both square to minus one and both commute with all elements.

$$\boldsymbol{A}\,\boldsymbol{I} \;=\; \boldsymbol{A}\cdot\boldsymbol{I} \;=\; \boldsymbol{I}\cdot\boldsymbol{A} \;=\; \boldsymbol{I}\,\boldsymbol{A} \tag{A.21}$$

$$\boldsymbol{I}^{-1} \;=\; -\,\boldsymbol{I} \tag{A.22}$$

$$\boldsymbol{I}^2 \;=\; \boldsymbol{I}_E^2 \;=\; -1 \tag{A.23}$$

The geometric product of three vectors $\boldsymbol{a}, \boldsymbol{b}, \boldsymbol{c} \in \mathbb{R}^{p,q}$ amounts to

$$\boldsymbol{abc} \;=\; \boldsymbol{a}\wedge\boldsymbol{b}\wedge\boldsymbol{c} + (\boldsymbol{a}\cdot\boldsymbol{b})\boldsymbol{c} + (\boldsymbol{b}\cdot\boldsymbol{c})\boldsymbol{a} - (\boldsymbol{c}\cdot\boldsymbol{a})\boldsymbol{b}. \tag{A.24}$$

The following sandwich products are of certain importance

$$\boldsymbol{bxb} \;=\; 2(\boldsymbol{b}\cdot\boldsymbol{x})\boldsymbol{b} - \boldsymbol{b}^2\,\boldsymbol{x} \tag{A.25}$$

$$\boldsymbol{abxba} \;=\; \Big(4(\boldsymbol{b}\cdot\boldsymbol{x})(\boldsymbol{b}\cdot\boldsymbol{a}) - 2\boldsymbol{b}^2(\boldsymbol{a}\cdot\boldsymbol{x})\Big)\boldsymbol{a} - 2(\boldsymbol{b}\cdot\boldsymbol{x})\boldsymbol{b} + \boldsymbol{b}^2\boldsymbol{a}^2\boldsymbol{x} \tag{A.26}$$

Especially if $\boldsymbol{a}$ and $\boldsymbol{b}$ represent conformal points, it is

$$\boldsymbol{a}\,\boldsymbol{b}\,\boldsymbol{a} \;=\; 2\,(\boldsymbol{b}\cdot\boldsymbol{a})\boldsymbol{a} \tag{A.27}$$

$$\boldsymbol{a}\,\mathbf{e}\,\boldsymbol{a} \;=\; -\,2\,\boldsymbol{a} \tag{A.28}$$

$$\mathbf{e}\,\boldsymbol{a}\,\mathbf{e} \;\overset{!}{=}\; \mathbf{e}\;\mathbf{e}_o\,\mathbf{e} \;=\; -\,2\,\mathbf{e} \tag{A.29}$$

$$\mathbf{e}_o\,\mathbf{e}\;\mathbf{e}_o \;=\; -\,2\;\mathbf{e}_o \tag{A.30}$$

Making use of the notation introduced in section 3.1, it is

$$\|\vec{a}\wedge\vec{b}\| \;=\; \sqrt{\vec{a}^2\,\vec{b}^2 - (\vec{a}\cdot\vec{b})^2} \;=\; \|\vec{a}\|\;\|\vec{b}\|\;|\sin(\,\gamma\,)\,| \tag{A.31}$$

$$\vec{a}\times\vec{b} \;=\; (\vec{a}\wedge\vec{b})\,\boldsymbol{I}_E^{-1} \;=\; \vec{b}\cdot(\,\vec{a}\,\boldsymbol{I}_E\,), \tag{A.32}$$

and similarly

$$\vec{a}\times(\vec{b}\times\vec{c}) \;=\; \vec{a}\cdot(\vec{c}\wedge\vec{b}) \;=\; (\vec{a}\cdot\vec{c})\vec{b} - (\vec{a}\cdot\vec{b})\vec{c}.$$

Now let A be the 3×3-matrix holding the coefficients of $\vec{a}$, $\vec{b}$ and $\vec{c}$. Then the triple product corresponds to the (oriented) volume $\det(\mathsf{A})$ of the parallelepiped spanned by the vectors.

$$\vec{a}\cdot(\vec{b}\times\vec{c}) \;=\; (\vec{a}\wedge\vec{b}\wedge\vec{c})\boldsymbol{I}_E^{-1} \;=\; \det(\mathsf{A})\boldsymbol{I}_E\boldsymbol{I}_E^{-1} \;=\; \det(\mathsf{A})$$

Selecting Multivector Elements Algebraically

The following expression returns only those terms of a multivector $\boldsymbol{X}$ that belong to the Euclidean subalgebra $\mathbb{R}_3$, i.e. only those terms that do not involve $\mathbf{e}$, $\mathbf{e}_o$, $\mathbf{e}_+$, $\mathbf{e}_-$ or $\boldsymbol{E}$ elements

$$\boldsymbol{Y} \;=\; \boldsymbol{E}\cdot(\boldsymbol{E}\wedge\boldsymbol{X})\,. \tag{A.33}$$

Note that this is referred to as the *conformal split* in [76, 62].

Selecting only those parts of $\boldsymbol{X}$ that include an $\boldsymbol{E}$-component can be done by

$$\boldsymbol{Y} \;=\; \mathbf{e}_+\cdot(\mathbf{e}\cdot\boldsymbol{X})\;. \tag{A.34}$$

A.4.2 Commutator Products

Commutator Products Here some interesting commutator products are presented.

From the elucidations in section 2.3.3 it follows that $\boldsymbol{I}$ commutes with all elements in CGA; equation (A.35) shows some of the numerous possibilities and holds as well for the anti-commutator

$$(\boldsymbol{A}\,\boldsymbol{I})\underline{\times}\boldsymbol{B} \;=\; (\boldsymbol{A}\underline{\times}\boldsymbol{B})\,\boldsymbol{I} \;=\; \boldsymbol{I}\,(\boldsymbol{A}\underline{\times}\boldsymbol{B}) \;=\; (\boldsymbol{I}\,\boldsymbol{A})\underline{\times}\boldsymbol{B} \;=\; \boldsymbol{A}\underline{\times}(\boldsymbol{B}\,\boldsymbol{I}) \;=\; \dots \tag{A.35}$$

The subsequent equations hold for all $s \geq 2$

$$\boldsymbol{A}_{\langle 2\rangle}\underline{\times}\boldsymbol{B}_{\langle s\rangle} \;=\; \boldsymbol{a}_1 \wedge (\boldsymbol{a}_2 \cdot \boldsymbol{B}_{\langle s\rangle}) \;-\; \boldsymbol{a}_2 \wedge (\boldsymbol{a}_1 \cdot \boldsymbol{B}_{\langle s\rangle}) \tag{A.36}$$

$$\boldsymbol{A}_{\langle 2\rangle}\overline{\times}\boldsymbol{B}_{\langle s\rangle} \;=\; \boldsymbol{A}_{\langle 2\rangle} \cdot \boldsymbol{B}_{\langle s\rangle} \;+\; \boldsymbol{A}_{\langle 2\rangle} \wedge \boldsymbol{B}_{\langle s\rangle}. \tag{A.37}$$

Especially if the grade of $\boldsymbol{B}_{\langle s\rangle}$ is two, it may be seen that

$$\begin{aligned}\boldsymbol{A}_{\langle 2\rangle}\underline{\times}\boldsymbol{B}_{\langle 2\rangle} \;=\;& (\boldsymbol{a}_2 \cdot \boldsymbol{b}_1)(\boldsymbol{a}_1 \wedge \boldsymbol{b}_2) \;-\; (\boldsymbol{a}_2 \cdot \boldsymbol{b}_2)(\boldsymbol{a}_1 \wedge \boldsymbol{b}_1)\\ &+(\boldsymbol{a}_1 \cdot \boldsymbol{b}_2)(\boldsymbol{a}_2 \wedge \boldsymbol{b}_1) \;-\; (\boldsymbol{a}_1 \cdot \boldsymbol{b}_1)(\boldsymbol{a}_2 \wedge \boldsymbol{b}_2).\end{aligned}$$

$$\begin{aligned}\boldsymbol{A}_{\langle 3\rangle}\underline{\times}\boldsymbol{B}_{\langle 3\rangle} \;=\;& \boldsymbol{A}_{\langle 3\rangle} \wedge \boldsymbol{B}_{\langle 3\rangle} \;+\; \boldsymbol{a}_1 \wedge (\boldsymbol{a}_2 \cdot (\boldsymbol{a}_3 \cdot \boldsymbol{B}_{\langle 3\rangle}))\\ &-\underbrace{\boldsymbol{a}_2 \wedge (\boldsymbol{a}_1 \cdot (\boldsymbol{a}_3 \cdot \boldsymbol{B}_{\langle 3\rangle}))}_{\boldsymbol{a}_2\wedge((\boldsymbol{a}_1\wedge\boldsymbol{a}_3)\cdot\boldsymbol{B}_{\langle 3\rangle})} + \boldsymbol{a}_3 \wedge (\boldsymbol{a}_1 \cdot (\boldsymbol{a}_2 \cdot \boldsymbol{B}_{\langle 3\rangle})),\end{aligned} \tag{A.38}$$

where $\boldsymbol{A}_{\langle 3\rangle} \wedge \boldsymbol{B}_{\langle 3\rangle} \;=\; 0$ in CGA.

$$\begin{aligned}\boldsymbol{A}_{\langle 3\rangle}\overline{\times}\boldsymbol{B}_{\langle 3\rangle} \;=\;& \boldsymbol{A}_{\langle 3\rangle} \cdot \boldsymbol{B}_{\langle 3\rangle} \;+\; \boldsymbol{a}_1 \wedge \boldsymbol{a}_2 \wedge (\boldsymbol{a}_3 \cdot \boldsymbol{B}_{\langle 3\rangle})\\ &-\boldsymbol{a}_1 \wedge \boldsymbol{a}_3 \wedge (\boldsymbol{a}_2 \cdot \boldsymbol{B}_{\langle 3\rangle}) \;+\; \boldsymbol{a}_2 \wedge \boldsymbol{a}_3 \wedge (\boldsymbol{a}_1 \cdot \boldsymbol{B}_{\langle 3\rangle}).\end{aligned} \tag{A.39}$$

Other expressions can often be derived, e.g. with the help of equation (A.35) and equation (A.38)

$$\begin{aligned}\boldsymbol{A}_{\langle 3\rangle}\underline{\times}\boldsymbol{B}_{\langle 2\rangle} \;=\;& (\boldsymbol{A}_{\langle 3\rangle}\underline{\times}(\boldsymbol{B}_{\langle 2\rangle}\boldsymbol{I}))\,\boldsymbol{I}^{-1} \;=\; (\boldsymbol{A}_{\langle 3\rangle}\underline{\times}\boldsymbol{B}'_{\langle 3\rangle})\,\boldsymbol{I}^{-1}\\ =\;& \boldsymbol{A}_{\langle 3\rangle} \cdot \boldsymbol{B}_{\langle 2\rangle} + \boldsymbol{a}_1 \cdot (\boldsymbol{a}_2 \wedge \boldsymbol{a}_3 \wedge \boldsymbol{B}_{\langle 2\rangle})\\ &-\boldsymbol{a}_2 \cdot (\boldsymbol{a}_1 \wedge \boldsymbol{a}_3 \wedge \boldsymbol{B}_{\langle 2\rangle}) + \boldsymbol{a}_3 \cdot (\boldsymbol{a}_1 \wedge \boldsymbol{a}_2 \wedge \boldsymbol{B}_{\langle 2\rangle}),\end{aligned} \tag{A.40}$$

where it was used that

$$\begin{aligned}(\boldsymbol{a}_3 \wedge (\boldsymbol{a}_1 \cdot (\boldsymbol{a}_2 \cdot \boldsymbol{B}'_{\langle 3\rangle})))\,\boldsymbol{I}^{-1} \;=\;& (\boldsymbol{a}_3\underline{\times}(\boldsymbol{a}_1\underline{\times}(\boldsymbol{a}_2\overline{\times}\boldsymbol{B}'_{\langle 3\rangle})))\,\boldsymbol{I}^{-1}\\ =\;& \boldsymbol{a}_3\underline{\times}(\boldsymbol{a}_1\underline{\times}(\boldsymbol{a}_2\overline{\times}\boldsymbol{B}'_{\langle 3\rangle}\boldsymbol{I}^{-1}))\\ =\;& \boldsymbol{a}_3\underline{\times}(\boldsymbol{a}_1\underline{\times}(\boldsymbol{a}_2\overline{\times}\boldsymbol{B}_{\langle 2\rangle}))\\ =\;& \boldsymbol{a}_3 \cdot (\boldsymbol{a}_1 \wedge \boldsymbol{a}_2 \wedge \boldsymbol{B}_{\langle 2\rangle}).\end{aligned}$$

Appendix B

Abbreviations

BCH	Baker Campbell Hausdorff
CCD	charge coupled device
CGA	conformal geometric algebra
DOF	degrees of freedom
eIPNS	conformal points in an IPNS
eOPNS	conformal points in an OPNS
GA	geometric algebra
GH	Gauss-Helmert
IPNS	inner product null space
LS	least squares
LSA	least squares adjustment
MAP	maximum a posteriori
ML	maximum likelihood
MSE	mean square error
MVUE	unbiased minimum-variance estimator
OPNS	outer product null space
P3P	perspective 3-point problem
PCA	principal component analysis
PDF	probability density function
PNP	perspective N-point problem
RBM	rigid body motion
RMS	root mean square
SVD	singular value decomposition
TLS	total least squares

Appendix C

Notation

The following list of examples gives an overview of the mathematical symbols and the notation used in this text.

Symbols

n, p, q	Usually the dimension of the quadratic space $\mathbb{R}^{p,q}$, $n = p + q$, which underlies the geometric algebra $\mathbb{R}_{p,q}$
$\mathcal{N}$	The set $\mathcal{N} := \{1, 2, \ldots, n\}$
$\emptyset$	Empty set $\emptyset = \{\}$, $\quad \lvert\emptyset\rvert = 0$
$\mathbb{N}$	Natural numbers $\{1, 2, \ldots\}$
$\mathbb{N}_0$	Natural numbers including zero $\{0, 1, 2, \ldots\}$
$\mathbb{R}$, $\mathbb{C}$, $\mathbb{H}$	Real numbers, complex numbers and quaternions
$\mathbb{R}^{p,q}$	Quadratic space (vector space with associated scalar product, cf. page 238) over $\mathbb{R}$ of dimension $p + q = n$
$\mathbb{R}^n$	Euclidean vector space $\mathbb{R}^n = \bigoplus^n \mathbb{R}$, $\quad$ i.e. $p = n$, $q = 0$
I_u	A $u \times u$-identity matrix $\mathsf{I}_u \in \mathbb{R}^{u \times u}$
$\mathbb{R}_{p,q}$	Geometric algebra of $\mathbb{R}^{p,q}$ with dimension 2^n
$\mathbf{0}$	Vector with norm 0
$\boldsymbol{I}$	Pseudoscalar of the geometric algebra under consideration
a, α, A	Multipurpose elements: scalar numbers, functions or sets
$\mathbb{R}^{m_1 \times \ldots \times m_r}$	Space of multidimensional arrays over $\mathbb{R}$ of dimension $m_1 \times m_2 \times \ldots \times m_r$, being isomorphic to the tensor product $\mathbb{R}^{m_1} \bigotimes \mathbb{R}^{m_2} \bigotimes \ldots \bigotimes \mathbb{R}^{m_r}$
$\mathbb{R}^{m \times n}$	Space of matrices of dimension $m \times n$ over $\mathbb{R}$
a, A, $[\ldots]$	Vectors, matrices or generally any multidimensional arrays of numbers (tensor); specifically $[\mathsf{A}] := \mathsf{A}$
a^T, A^T	Transpose of a vector or a matrix
a	Column vector $\mathsf{a} = [a_1\ a_2\ \ldots\ a_m]^\mathsf{T} \in \mathbb{R}^m$
A	Matrix or tensor (generalized matrix concept)
$[\mathsf{A},\ \mathsf{B}]$	Horizontal concatenation of two matrices (commas may also be omitted in unambiguous cases)

$[\mathsf{A};\mathsf{B}]$	Vertical concatenation of two matrices
A_{ij}	Matrix element at the i^{th} row and j^{th} column - identical with $\mathsf{A}^i{}_j$, $\mathsf{A}_i{}^j$ or A^{ij}; similarly, $\mathsf{a} = [a_1;\ a_2;\ \ldots;\ a_m] \in \mathbb{R}^m \Rightarrow \mathsf{a}_i = \mathsf{a}^i = a_i$
$\mathsf{A}_{i_1 i_2 \ldots i_r}$	The element of an r-valence tensor that is indexed by the subscript $i_1 i_2 \ldots i_r$
$\mathsf{A}_i{}^j{}_k \mathsf{b}_j$	*Einstein summation convention*: summation over identical super- and subscript indices, i.e. $\mathsf{A}_i{}^j{}_k \mathsf{b}_j = \sum_j \mathsf{A}_{ijk}\mathsf{b}_j$
$\mathsf{a}_{\underline{i}}$, $\mathsf{A}_{\underline{i}}$	The i^{th} vector, matrix, tensor, etc. $\mathsf{A}_{\underline{i}}{}^j{}_{kl}$ is possible
$(\ldots)_{i_{z_1}\times\ldots\times i_{z_k}}$	Defines a tensor or a matrix, e.g. $\mathsf{B} := (\mathsf{A}_{i_1\ldots i_k})_{i_{z_1}\times\ldots\times i_{z_k}}$, where $\{z_{1\ldots k}\} := [1,k]_{\mathbb{Z}}$, it is $\mathsf{B}_{i_{z_1}\ldots i_{z_k}} = \mathsf{A}_{i_1\ldots i_k}$; specifically $(\mathsf{A}_{ij})_{j\times i} = \mathsf{A}^\mathsf{T}$
$[\![\ldots]\!]$	Defines a tensor or a matrix; $[\![\mathsf{A}_{i_1\ldots i_k}]\!] := (\mathsf{A}_{i_1\ldots i_k})_{i_1\times\ldots\times i_k} = \mathsf{A}$
$\mathsf{A}\|^{\mathsf{v}}$	Matrix A restricted to the columns determined by vector v
$\mathsf{A}\|_{\mathsf{v}}$	Matrix A restricted to the rows determined by vector v
$\mathrm{col}(\mathsf{A})$	Column space of the matrix A, e.g. $\mathsf{Aa} \in \mathrm{col}(\mathsf{A})$
$\mathrm{rank}(\mathsf{A})$	Rank of the matrix A
$\mathrm{diag}(\mathsf{A})$	Column vector of diagonal elements, i.e. $[\mathrm{diag}(\mathsf{A})]_i = \mathsf{A}_{ii}$; moreover $\mathrm{diag}(\mathrm{diag}(\mathsf{A})) = \mathsf{A}$
$\mathrm{vec}(\mathsf{A})$	Reshapes matrix A into a column vector
$\mathrm{tr}(\mathsf{A})$	Sum of diagonal elements of the matrix A, i.e. $\mathrm{tr}(\mathsf{A}) = \sum_i \mathsf{A}_{ii}$
$\mathbb{I}$	Set of arbitrary elements
$\mathbf{1}_{\mathbb{I}}(x)$	Characteristic/indicator function of the set $\mathbb{I}$
$\mathbb{u}$	Set $\mathbb{u} \subseteq \mathcal{N}$ to be used in basis blade notation $\mathbf{e}_{\mathbb{u}}$
$\|\mathbb{u}\|$	Number of elements in $\mathbb{u}$ and thus the grade of $\mathbf{e}_{\mathbb{u}}$
$I_{u/w}$	Set $I_{u/w} := \{(v_1, v_2, \ldots, v_u) \mid 1 \leq v_1 < v_2 < \ldots < v_u \leq w\}$
$\{A_{1\ldots k}\}$	The set $\{A_1, A_2, \ldots, A_k\}$
$[a,b]_{\mathbb{Z}}$	The set $\{a, a+1, \ldots, b\} \subset \mathbb{Z}$
$\mathcal{S}(k)$	Set of all permutations (automorphisms) of the (index) set $\{1, 2, \ldots, k\}$
$\mathcal{S}(u,v)$	Set of (u,v)-shuffles. It is $\mathcal{S}(u,v) \subseteq \mathcal{S}(u+v)$
$\mathrm{sgn}(\sigma)$	And $\sigma \in \mathcal{S}(k)\ :\ \mathrm{sgn}(\sigma) = +1\ (\mathrm{sgn}(\sigma) = -1)$ if σ is an even (odd) permutation of $\{1, 2, \ldots, k\}$
$\mathrm{sgn}(x)$	Sign of the real number $x \in \mathbb{R}$, i.e. $\mathrm{sgn}(x) = x/\|x\|$
$\underline{\times}$	Commutator, $A \underline{\times} B := \frac{1}{2}(AB - BA)$
$\overline{\times}$	Anti-commutator, $A \overline{\times} B := \frac{1}{2}(AB + BA)$
$\mathsf{e}_{\underline{i}}$	i^{th} canonical basis vector of $\mathbb{R}^n$
$\mathbf{e}_i$	i^{th} basis vector of $\mathbb{R}^{p,q} \subset \mathbb{R}_{p,q}$
$\mathbf{e}_{i_1 i_2 \ldots i_r}$	Basis blade $\mathbf{e}_{i_1}\mathbf{e}_{i_2}\ldots\mathbf{e}_{ir}$
$\mathbf{e}_{\mathbb{u}}$	Ordered basis blade $\mathbf{e}_{i_1}\mathbf{e}_{i_2}\ldots\mathbf{e}_{ir}$ with $i_1 < i_2 < \ldots < i_r$ and $\mathbb{u} = \{i_a \| 1 \leq a \leq r\} \subseteq \mathcal{N}$
$\mathbf{E}_i$	The i^{th} basis blade, $1 \leq i \leq 2^n$, of $\mathbb{R}_{p,q}$
$\vec{a}$	Vector from $\mathbb{R}^3 \subset \mathbb{R}_3$, i.e. $\vec{a} = a_1\mathbf{e}_1 + a_2\mathbf{e}_2 + a_3\mathbf{e}_3$
$\boldsymbol{a}$	Vector from $\mathbb{R}^{p,q} \subset \mathbb{R}_{p,q}$, i.e. $\boldsymbol{a} = a^i\mathbf{e}_i$
$\boldsymbol{a} *_{\boldsymbol{\varepsilon}} \boldsymbol{b}$	Euclidean (positive definite) scalar product of the vectors $\boldsymbol{a}$ and $\boldsymbol{b}$

$\boldsymbol{a} * \boldsymbol{b}$	Scalar product of the vectors $\boldsymbol{a}$ and $\boldsymbol{b}$, coincides with the inner product $\boldsymbol{a} \cdot \boldsymbol{b}$
$\perp$, $\parallel$	Indicates orthogonality and parallelism, respectively, regarding the inner product
$\perp_{\boldsymbol{\varepsilon}}$, $\parallel_{\boldsymbol{\varepsilon}}$	Indicates perpendicularity and parallelism, respectively, regarding the Euclidean scalar product '$*_{\boldsymbol{\varepsilon}}$'
$\boldsymbol{A}$	General multivector
$\boldsymbol{A}^*$	Dual of general multivector $\boldsymbol{A}$
$\widetilde{\boldsymbol{A}}$	Reverse of general multivector $\boldsymbol{A}$
$\boldsymbol{A}^\dagger$	Conjugate of general multivector $\boldsymbol{A}$
$\langle \boldsymbol{A} \rangle_r$	Grade-projection onto the grade-r components of $\boldsymbol{A}$
$\boldsymbol{A}_{[k]}$	A κ-vector
$\boldsymbol{A}_{\langle k \rangle}$	A blade of grade k, $\boldsymbol{A}_{\langle k \rangle} := \boldsymbol{a}_1 \wedge \boldsymbol{a}_2 \wedge \dots \boldsymbol{a}_k$
$\bigwedge\limits_{j=1}^{k} \boldsymbol{a}_j$	The k-blade $\bigwedge(\boldsymbol{a}_1, \boldsymbol{a}_2, \dots, \boldsymbol{a}_k) := \boldsymbol{a}_1 \wedge \boldsymbol{a}_2 \wedge \dots \wedge \boldsymbol{a}_k$
$[\boldsymbol{A}_{\langle k \rangle} \backslash \boldsymbol{a}_i]$	The $(k-1)$-blade $\boldsymbol{a}_1 \wedge \boldsymbol{a}_2 \wedge \dots \boldsymbol{a}_{i-1} \wedge \boldsymbol{a}_{i+1} \wedge \dots \wedge \boldsymbol{a}_k$
$\mathrm{span}\{\boldsymbol{a}_{1\dots k}\}$	Linear span of the vectors $\{\boldsymbol{a}_{1\dots k}\}$, $\mathrm{span}\{\boldsymbol{a}_{1\dots k}\} = \Bbbk\mathrm{er}(\bigwedge_{i=1}^{k} \boldsymbol{a}_i)$
$\Bbbk\mathrm{er}(\boldsymbol{A}_{\langle k \rangle})$	Outer product null space (OPNS) of the blade $\boldsymbol{A}_{\langle k \rangle}$
$\Bbbk\mathrm{er}^{\boldsymbol{*}}(\boldsymbol{A}_{\langle k \rangle})$	Inner product null space (IPNS) of the blade $\boldsymbol{A}_{\langle k \rangle}$
$\boldsymbol{A} \wedge \boldsymbol{B}$	Outer product of the multivectors $\boldsymbol{A}$ and $\boldsymbol{B}$
$\boldsymbol{A} \cdot \boldsymbol{B}$	Inner product of the multivectors $\boldsymbol{A}$ and $\boldsymbol{B}$
$\lVert \boldsymbol{A}_{\langle k \rangle} \rVert$	Magnitude of the k-blade $\boldsymbol{A}_{\langle k \rangle}$
$\boldsymbol{A} *_{\boldsymbol{\varepsilon}} \boldsymbol{B}$	Euclidean scalar product of the multivectors $\boldsymbol{A}$ and $\boldsymbol{B}$
$\boldsymbol{a} \cdot_{\boldsymbol{\varepsilon}} \boldsymbol{A}_{\langle k \rangle}$	Euclidean inner product
$\dim(\mathbb{A})$	Returns the dimension of a space, e.g. $\dim(\{\mathbf{0}\}) = 0$
$\mathbb{A} \oplus \mathbb{B}$	Outer sum of the vector sets $\mathbb{A}, \mathbb{B} \subseteq \mathbb{R}^{p,q}$
$\mathbb{A} \ominus \mathbb{B}$	Inner difference of the vector sets $\mathbb{A}, \mathbb{B} \subseteq \mathbb{R}^{p,q}$
$\mathbb{A} \ominus_{\boldsymbol{\varepsilon}} \mathbb{B}$	Inner difference (w.r.t. the Euclidean scalar product '$*_{\boldsymbol{\varepsilon}}$') of the vector sets $\mathbb{A}, \mathbb{B} \subseteq \mathbb{R}^{p,q}$
δ_{ij}	Kronecker delta
$\utilde{X}, \utilde{\mathsf{X}}$	Random variable, random vector
$\mathrm{E}(\utilde{X})$	Expectation of a random variable
$\mathrm{Var}(\utilde{X})$	Variance of a random variable
$\mathrm{Cov}(\utilde{X}, \utilde{Y})$	Covariance of the random variables $\utilde{X}$ and $\utilde{Y}$
$\Sigma_{\mathsf{xy}} \in \mathbb{R}^{r \times s}$	Covariance matrix for the random vectors $\utilde{\mathsf{X}} \in \mathbb{R}^r$ and $\utilde{\mathsf{Y}} \in \mathbb{R}^s$; specifically $[\Sigma_{\mathsf{xy}}]_{ij} := \mathrm{Cov}(\utilde{\mathsf{X}}_i, \utilde{\mathsf{Y}}_j)$

Bibliography

[1] S. J. Ahn. *Least Squares Orthogonal Distance Fitting of Curves and Surfaces in Space*. Volume 3151 of LNCS. Springer, Berlin, Heidelberg, 2004. Doctoral dissertation.

[2] D. G. Aliaga. Accurate catadioptric calibration for real-time pose estimation of room-size environments. In *8th International Conference on Computer Vision (ICCV)*, volume 1, pages 127–134, Vancouver, British Columbia, Canada, July 2001. IEEE Computer Society.

[3] P. Angles. Construction de revêtements du groupe conforme d'un espace vectoriel muni d'une ≪métrique≫ de type (p, q). *Annales de l'institut Henri Poincaré*, 33(1):33–51, 1980.

[4] A. Ansar and K. Daniilidis. Linear pose estimation from points or lines. In *7th European Conference on Computer Vision (ECCV)*, pages 282–296, Copenhagen, Denmark, 2002.

[5] K. S. Arun, T. S. Huang, and S. D. Blostein. Least-squares fitting of two 3-D point sets. *IEEE Transactions on Pattern Analysis and Machine Intelligence*, 9(5):698–700, 1987.

[6] M. F. Atiyah, R. Bott, and A. Shapiro. Clifford modules. *Topology*, 3:3–38, July 1964. Supplement 1.

[7] S. Baker and S. K. Nayar. A theory of catadioptric image formation. In *6th International Conference on Computer Vision (ICCV)*, pages 35–42, Bombay, India, January 1998. IEEE Computer Society.

[8] S. Baker and S. K. Nayar. A theory of single-viewpoint catadioptric image formation. *International Journal of Computer Vision*, 35:175–196, 1999.

[9] V. Banarer. *Struktureller Bias in neuronalen Netzen mittels Clifford-Algebren*. PhD thesis, Christian-Albrechts-University, Institute of Computer Science, Faculty of Engineering, Kiel, January 2004.

[10] J. P. Barreto and H. Araújo. Issues on the geometry of central catadioptric image formation. In *Conference on Computer Vision and Pattern Recognition (CVPR)*, volume 2, pages 422–427, Kauai, HI, USA, December 2001. IEEE Computer Society.

[11] E. Bayro-Corrochano and C. López-Franco. Omnidirectional vision: Unified model using conformal geometry. In Tomás Pajdla and Jiri Matas, editors, *Computer Vision - 8th European Conference on Computer Vision (ECCV), Part I*, volume 3021 of *LNCS*, pages 536–548, Prague, Czech Republic, May 2004. Springer, Berlin, Heidelberg.

[12] D. Betten and E. Montanucci. An elementary introduction to Lie groups. Technical Report Number 0312, Christian-Albrechts-University, Institute of Computer Science, Faculty of Engineering, Kiel, December 2003.

[13] M. J. Box. Bias in nonlinear estimation. *Journal of the Royal Statistical Society*, 33(2):171–202, 1971.

[14] S. Buchholz and G. Sommer. On averaging in Clifford groups. In H. Li, P.J. Olver, and G. Sommer, editors, *Computer Algebra and Geometric Algebra with Applications*, volume 3519 of *LNCS*, pages 229–238. 6th International Workshop IWMM 2004, Springer, Berlin, Heidelberg, 2005.

[15] R. Bunschoten and B. Kröse. Robust scene reconstruction from an omnidirectional vision system. *IEEE Transactions on Robotics and Automation*, 19(2):351–357, April 2003.

[16] S. R. Buss and J. P. Fillmore. Spherical averages and applications to spherical splines and interpolation. In *Commun. ACM*, volume 20, pages 95–126, New York, NY, USA, 2001. ACM Press.

[17] C. Cauchois, E. Brassart, L. Delahoche, and C. Drocourt. Spatial localization method with omnidirectional vision. In *11th International Conference on Advanced Robotics (ICAR)*, pages 287–292, Coimbra, Portugal, 2003. IEEE Computer Society.

[18] D. Claus and A. W. Fitzgibbon. A rational function lens distortion model for general cameras. In *Conference on Computer Vision and Pattern Recognition (CVPR)*, volume 1, pages 213–219, San Diego, CA, USA, June 2005. IEEE Computer Society.

[19] H. S. M. Coxeter and S. L. Greitzer. *Geometry Revisited*, chapter 2.1: The Power of a Point with Respect to a Circle, pages 27–31. Mathematical Association of America, Washington, DC, 1967.

[20] S. Derrien and K. Konolige. Approximating a single viewpoint in panoramic imaging devices. In *1st Workshop on Omnidirectional Vision (OMNIVIS)*, page 85, Hilton Head, SC, USA, 2000. IEEE Computer Society.

[21] L. Dorst. Honing geometric algebra for its use in the computer sciences. In Gerald Sommer, editor, *Geometric computing with Clifford algebras: theoretical foundations and applications in computer vision and robotics*, pages 127–151. Springer, Berlin, Heidelberg, 2001.

[22] L. Dorst. The representation of rigid body motions in the conformal model of geometric algebra. In *Human Motion - Understanding, Modelling, Capture, and Animation*, volume 36 of *Computational Imaging and Vision*, pages 507–529. Springer, Netherlands, 2008. Publication of the Universiteit van Amsterdam.

[23] L. Dorst, D. Fontijne, and S. Mann. *Geometric Algebra for Computer Science: An Object-Oriented Approach to Geometry.* The Morgan Kaufmann Series in Computer Graphics. Morgan Kaufmann Publishers Inc., San Francisco, CA, USA, 2007.

[24] E. B. Dynkin. On the representation by means of commutators of the series $\log(e^x e^y)$ for noncommutative x and y. *Matematicheskii Sbornik (N.S.)*, 25(67):155–162, 1949. In Russian.

[25] D. W. Eggert, A. Lorusso, and R. B. Fisher. Estimating 3-D rigid body transformations: a comparison of four major algorithms. *Machine Vision and Applications*, 9(5/6):272–290, 1997.

[26] J. Fabrizio, J.-P. Tarel, and R. Benosman. Calibration of panoramic catadioptric sensors made easier. In *3rd Workshop on Omnidirectional Vision (OMNIVIS)*, pages 45–52, Copenhagen, Denmark, 2002. IEEE Computer Society.

[27] O. Faugeras. *Three-Dimensional Computer Vision: A Geometric Viewpoint.* MIT Press, 1993.

[28] O. Faugeras. Stratification of three-dimensional vision, projective, affine and metric representations. *Journal of Optical Society of America*, 12(3):465–484, March 1995.

[29] M. Fiala and A. Basu. Panoramic stereo reconstruction using non-svp optics. In *16th International Conference on Pattern Recognition (ICPR)*, volume 4, pages 27–30, Quebec, Canada, August 2002. IEEE Computer Society.

[30] M. Fiala and A. Basu. Robot navigation using panoramic landmark tracking. In *15th International Conference on Vision Interface*, Calgary, Canada, May 2002. Society of Manufacturing Engineers (SME).

[31] M. A. Fischler and R. C. Bolles. Random sample consensus: A paradigm for model fitting with applications to image analysis and automated cartography. *Communications of the ACM*, 24(6):381–395, 1981.

[32] A. W. Fitzgibbon. Simultaneous linear estimation of multiple view geometry and lens distortion. In *Conference on Computer Vision and Pattern Recognition (CVPR)*, volume 1, pages 125–132, Kauai, HI, USA, December 2001. IEEE Computer Society.

[33] P. T. Fletcher, C. Lu, and S. C. Joshi. Statistics of shape via principal geodesic analysis on Lie groups. In *CVPR*, pages 95–101, 2003.

[34] W. Förstner. Choosing constraints in image triplets. In David Vernon, editor, *Computer Vision - 6th European Conference on Computer Vision (ECCV), Part II*, volume 1843 of *LNCS*, pages 669–684, Dublin, Ireland, June 2000. Springer, Berlin, Heidelberg.

[35] W. Förstner, A. Brunn, and S. Heuel. Statistically testing uncertain geometric relations. In G. Sommer, N. Krüger, and C. Perwass, editors, *Mustererkennung 2000*, Informatik Aktuell, pages 17–26, Springer, Berlin, Heidelberg, 2000.

[36] W. Förstner and B. Wrobel. Mathematical Concepts in Photogrammetry. In J. C. McGlone, E. M. Mikhail, J. Bethel, and J. Mullen, editors, *Manual of Photogrammetry*, chapter 2, pages 15–180. American Society of Photogrammetry and Remote Sensing (ASPRS), Bethesda MD, fifth edition, 2004.

[37] J. Gallier. *Geometric methods and applications for computer science and engeneering*. Texts in Applied Mathematics, Vol. 38. Springer, Berlin, Heidelberg, 2001.

[38] J. Gaspar, N. Winters, and J. Santos-Victor. Vision-based navigation and environmental representations with an omni-directional camera. *IEEE Transactions on Robotics and Automation*, 16(6):890–898, December 2000.

[39] C. F. Gauß. *Theoria Motus Coelestium*. Perthes und Besser, Hamburg, 1809.

[40] C. F. Gauß. *Theoria Combinationis Observationum Erroribus Minimis Obnoxiae*. Dieterich, Göttingen, 1823.

[41] C. Gebken, C. Perwass, and G. Sommer. Parameter estimation from uncertain data in geometric algebra. *Advances in Applied Clifford Algebras*, 18(3–4):647–664, September 2008. Birkhäuser Basel.

[42] C. Gebken and G. Sommer. Perspective pose estimation with geometric algebra. In Theodore Simos, George Maroulis, George Psihoyios, and Ch. Tsitouras, editors, *International Conference on Numerical Analysis and Applied Mathematics (ICNAAM-2007)*, volume 1046 of *AIP Conference Series*, pages 95–98, Corfu, Greece, September 2007. American Institute of Physics.

[43] C. Gebken and G. Sommer. Stochastically optimal epipole estimation in omnidirectional images with geometric algebra. In Bruce McDonald, Uwe Franke, Reinhard Klette, and Gerald Sommer, editors, *Robot Vision: Proceedings of Second International Workshop (RobVis 2008)*, volume 4931 of *LNCS*, pages 85–97, Auckland, New Zealand, February 2008. Springer, Berlin, Heidelberg.

[44] C. Gebken, A. Tolvanen, C. Perwass, and G. Sommer. Perspective pose estimation from uncertain omnidirectional image data. In *18th International Conference on Pattern Recognition (ICPR)*, volume 1, pages 793–796, Hong Kong, China, August 2006. IEEE Computer Society.

[45] C. Gebken, A. Tolvanen, and G. Sommer. Pose estimation from uncertain omnidirectional image data using line-plane correspondences. In Katrin Franke et al., editor, *Pattern Recognition: 28th DAGM-Symposium*, volume 4174 of *LNCS*, pages 587–596, Berlin, September 2006. Springer, Berlin, Heidelberg.

[46] C. Geyer and K. Daniilidis. Catadioptric camera calibration. In *7th International Conference on Computer Vision (ICCV)*, volume 1, pages 398–404, Kerkyra, Corfu, Greece, September 1999. IEEE Computer Society.

[47] C. Geyer and K. Daniilidis. Paracatadioptric camera calibration. *IEEE Transactions on Pattern Analysis and Machine Intelligence*, 24:398–404, 1999.

[48] C. Geyer and K. Daniilidis. Catadioptric projective geometry. *International Journal of Computer Vision*, 45(3):223–243, 2001.

[49] C. Geyer and K. Daniilidis. Structure and motion from uncalibrated catadioptric views. In *Conference on Computer Vision and Pattern Recognition (CVPR)*, volume 1, pages 279–286, Kauai, HI, USA, December 2001. IEEE Computer Society.

[50] C. Geyer and K. Daniilidis. Properties of the catadioptric fundamental matrix. In *7th European Conference on Computer Vision (ECCV), Copenhagen, Denmark*, pages 140–154, 2002.

[51] P. Gill and W. Murray. Algorithms for the solution of the nonlinear least-squares problem. *SIAM Journal on Numerical Analysis*, 15(5):977–992, October 1978.

[52] J. Gluckman and S. K. Nayar. Ego-motion and omnidirectional cameras. In *6th International Conference on Computer Vision (ICCV)*, pages 999–1005, Bombay, India, January 1998. IEEE Computer Society.

[53] T. Goedemé, M. Nuttin, T. Tuytelaars, and L. J. Van Gool. Omnidirectional vision based topological navigation. *International Journal of Computer Vision*, 74(3):219–236, August 2007.

[54] G. H. Golub and C. F. Van Loan. *Matrix Computations*. The Johns Hopkins University Press, Baltimore and London, third edition, 1989.

[55] C. Gramkow. On averaging rotations. *Journal of Mathematical Imaging and Vision*, 15(1–2):7–16, 2002.

[56] J. J. Gray. Olinde Rodrigues' paper of 1840 on transformation groups. In *Archive for History of Exact Sciences*, volume 21 of *4*, pages 375–385. Springer, Berlin, Heidelberg, December 1980.

[57] W. E. L. Grimson. *Object recognition by computer*. MIT Press, Cambridge, MA, 1990.

[58] R. M. Haralick, C.-N. Lee, K. Ottenberg, and M. Noelle. Review and analysis of solutions of the three point perspective pose estimation problem. *International Journal on Computer Vision*, 13(3):331–356, 1994.

[59] R. M. Haralick and L. G. Shapiro. *Computer and Robot Vision*, volume 1. Addison-Wesley Longman Publishing Co., Inc., Boston, MA, USA, 1991.

[60] F.R. Helmert. *Die Ausgleichsrechnung nach der Methode der kleinsten Quadrate*. Teubner, Leipzig, 1872.

[61] D. Hestenes. *Space-Time Algebra*. Gordon and Breach, New York, 1966. Doctoral dissertation.

[62] D. Hestenes. The design of linear algebra and geometry. *Acta Applicandae Mathematicae*, 23(1):65–93, April 1991. Springer Netherlands.

[63] D. Hestenes and G. Sobczyk. *Clifford Algebra to Geometric Calculus: A Unified Language for Mathematics and Physics*. Fundamental theories of physics. D. Reidel Publishing Company, Dordrecht, 1987. First publ. 1984.

[64] D. Hestenes and R. Ziegler. Projective geometry with Clifford algebra. *Acta Applicandae Mathematicae*, 23(1):25–63, April 1991. Springer Netherlands.

[65] S. Heuel. *Uncertain Projective Geometry*, volume 3008 of *LNCS*. Springer, Berlin, Heidelberg, 2004.

[66] B. K. P. Horn. Projective Geometry Considered Harmful, 1999. Available at http://www.ai.mit.edu/people/bkph/papers/harmful.pdf.

[67] S. Van Huffel and J. Vandewalle. The total least squares problem: Computational aspects and analysis. In *Frontier in Applied Mathematics*, volume 9. SIAM, Philadelphia, PA, 1991.

[68] B. Z. Iliev. On some generalizations of the Jacobi identity. I. *Bulletin de la Société des Sciences et des Lettres de Lodz, vol.42, No.21, Série: Recherches sur les Déformations*, 14(131):5–11, 1992.

[69] B. Z. Iliev. On some generalizations of the Jacobi identity. II. *Bulletin de la Société des Sciences et des Lettres de Lodz, vol.42, No.28, Série: Recherches sur les Déformations*, 14(138):93–102, 1992.

[70] A. Irle. *Wahrscheinlichkeitstheorie und Statistik*. B. G. Teubner GmbH, Stuttgart, Leipzig, Wiesbaden, 2001.

[71] G. Jang, S. Kim, and I. Kweon. Single camera catadioptric stereo system. In *6th Workshop on Omnidirectional Vision (OMNIVIS)*, Beijing, China, October 2005. IEEE Computer Society.

[72] K. Kanatani. Analysis of 3-D rotation fitting. *IEEE Transactions on Pattern Analysis and Machine Intelligence*, 16(1):543–549, January 1994.

[73] K. Kanatani. Statistical optimization and geometric inference in computer vision. *Philosophical Transactions of the Royal Society*, 356(1740):1303–1320, May 1998.

[74] K.-R. Koch. *Parameter Estimation and Hypothesis Testing in Linear Models.* Springer, Berlin, Heidelberg, 1997.

[75] H. Li and R. Hartley. A non-iterative method for correcting lens distortion from nine-point correspondences. In *6th Workshop on Omnidirectional Vision (OMNIVIS)*, Beijing, China, October 2005. IEEE Computer Society. Poster.

[76] H. Li, D. Hestenes, and A. Rockwood. Generalized homogeneous coordinates for computational geometry. In Gerald Sommer, editor, *Geometric computing with Clifford algebras: theoretical foundations and applications in computer vision and robotics*, pages 27–59. Springer, Berlin, Heidelberg, 2001.

[77] H. Li, D. Hestenes, and A. Rockwood. Spherical conformal geometry with geometric algebra. In Gerald Sommer, editor, *Geometric computing with Clifford algebras: theoretical foundations and applications in computer vision and robotics*, pages 61–75. Springer, Berlin, Heidelberg, 2001.

[78] H. Li, D. Hestenes, and A. Rockwood. A universal model for conformal geometries of Euclidean, spherical and double-hyperbolic spaces. In Gerald Sommer, editor, *Geometric computing with Clifford algebras: theoretical foundations and applications in computer vision and robotics*, pages 77–104. Springer, Berlin, Heidelberg, 2001.

[79] J. Liouville. *Extension au cas de trois dimensions de la question du tracé géographique*, chapter Notes de M. Liouville, pages 609–616. Bachelier, Paris, 5 edition, 1850. Appendix to the book 'Application de l'analyse à la géométrie' by Gaspard Monge.

[80] C. Lopez-Franco and E. Bayro-Corrochano. Omnidirectional vision and invariant theory for robot navigation using conformal geometric algebra. In *18th International Conference on Pattern Recognition (ICPR)*, volume 1, pages 570–573, Hong Kong, China, 2006. IEEE Computer Society.

[81] T. Mauthner, F. Fraundorfer, and H. Bischof. Region matching for omnidirectional images using virtual camera planes. In Ondřej Chum and Vojtěch Franc, editors, *11th Computer Vision Winter Workshop (CVWW)*, pages 93–98, Telč, Czech Republic, February 2006. Czech Society for Cybernetics and Informatics, Prague, Czech Republic.

[82] E. M. Mikhail and F. Ackermann. *Observations And Least Squares.* IEP-A Dun-Donnelley, New York, 1976.

[83] T. Nakamura, M. Oohara, T. Ogasawara, and H. Ishiguro. Fast self-localization method for mobile robots using multiple omnidirectional vision sensors. *Machine Vision and Applications*, 14(2):129–138, June 2003.

[84] S. K. Nayar and V. Peri. Folded catadioptric cameras. In *Conference on Computer Vision and Pattern Recognition (CVPR), Ft. Collins, CO, USA*, pages 2217–, 1999.

[85] T. Needham. *Visual Complex Analysis.* Clarendon Press, Oxford, 1997.

[86] D. Nistér and H. Stewénius. A minimal solution to the generalised 3-point pose problem. *Journal of Mathematical Imaging and Vision*, 27(1):67–79, January 2007.

[87] A. Paulino and H. Araújo. Pose estimation for central catadioptric systems: An analytical approach. In *16th International Conference on Pattern Recognition (ICPR)*, volume 3, pages 696–699, Quebec, Canada, August 2002. IEEE Computer Society.

[88] A. Pázman. *Nonlinear Statistical Models*. Kluwer Academic Publishers, Dordrecht, 1993.

[89] K. Pearson. On Lines and Planes of Closest Fit to Systems of Points in Space. *Philosophical Magazine*, 2(6):559–572, 1901.

[90] R. Penrose. Twistor algebra. *Journal of Mathematical Physics*, 8(2), February 1967. Publication of the American Institute of Physics.

[91] R. Penrose and W. Rindler. *Spinors and Space-time: Two-Spinor Calculus and Relativistic Fields*. Cambridge Monographs on Mathematical Physics. Cambridge University Press, UK, 1984.

[92] R. Penrose and W. Rindler. *Spinors and Space-time: Spinor and Twistor Methods in Space-time Geometry*. Cambridge Monographs on Mathematical Physics. Cambridge University Press, UK, 1986.

[93] C. Perwass. *Geometric Algebra with Applications in Engineering*, volume 4 of *Geometry and Computing*. Springer, Berlin, Heidelberg, 2009.

[94] C. Perwass, C. Gebken, and D. Grest. CLUCalc. http://www.clucalc.info/, 2006.

[95] C. Perwass, C. Gebken, and G. Sommer. Estimation of geometric entities and operators from uncertain data. In *27. Symposium für Mustererkennung, DAGM 2005, Wien, 29.8.-2.9.005*, number 3663 in LNCS. Springer, Berlin, Heidelberg, 2005.

[96] C. Perwass, C. Gebken, and G. Sommer. Geometry and kinematics with uncertain data. In A. Leonardis, H. Bischof, and A. Pinz, editors, *9th European Conference on Computer Vision (ECCV), Graz, Austria*, number 3951 in LNCS, pages 225–237. Springer, Berlin, Heidelberg, 2006.

[97] C. Perwass and D. Hildenbrand. Aspects of geometric algebra in Euclidean, projective and conformal space. Technical Report Number 0310, Christian-Albrechts-University, Institute of Computer Science, Faculty of Engineering, Kiel, September 2003.

[98] C. Perwass and G. Sommer. Numerical evaluation of versors with Clifford algebra. In Leo Dorst, Chris Doran, and Joan Lasenby, editors, *Applications of Geometric Algebra in Computer Science and Engineering*, pages 341–349. Birkhäuser Basel, 2002.

[99] C. Perwass and G. Sommer. The inversion camera model. In *28. Symposium für Mustererkennung, DAGM 2006, Berlin, 12.-14.09.2006*, number 4174 in LNCS, pages 647–656. Springer, Berlin, Heidelberg, 2006.

[100] A. J. Pope. Some pitfalls to be avoided in the iterative adjustment of nonlinear problems. In *38th annual meeting of the American Society of Photogrammetry*, Washington, D.C., USA, March 1972.

[101] L. Quan and Z.-D. Lan. Linear N-point camera pose determination. *IEEE Transactions on Pattern Analysis and Machine Intelligence*, 21(8):774–780, August 1999.

[102] B. Rosenhahn. *Pose Estimation Revisited*. PhD thesis, Inst. f. Informatik u. Prakt. Math. der Christian-Albrechts-Universität zu Kiel, 2003.

[103] B. Rosenhahn, C. Perwass, and G. Sommer. Pose estimation of 3d free-form contours. *Int. Journal of Computer Vision*, 62(3):267–289, 2005.

[104] B. Rosenhahn and G. Sommer. Pose estimation in conformal geometric algebra, part I: The stratification of mathematical spaces. *Journal of Mathematical Imaging and Vision*, 22:27–48, 2005.

[105] B. Rosenhahn and G. Sommer. Pose estimation in conformal geometric algebra, part I: The stratification of mathematical spaces, part II: Real-time pose estimation using extended feature concepts. *Journal of Mathematical Imaging and Vision*, 22:27–70, 2005.

[106] B. Rosenhahn and G. Sommer. Pose estimation in conformal geometric algebra, part II: Real-time pose estimation using extended feature concepts. *Journal of Mathematical Imaging and Vision*, 22:49–70, 2005.

[107] D. C. Royster. The origins of geometry. http://www.math.uncc.edu/∼droyster.

[108] G. Seber and C. J. Wild. Nonlinear regression. In *Wiley Series in Probability and Mathematical Statistics*. John Wiley & Sons, Inc., Hoboken, New Jersey, 2003.

[109] G. Sommer and C. Gebken. Robot vision in the language of geometric algebra. In Goro Obinata and Ashish Dutta, editors, *Vision Systems: Applications*, pages 459–486. IN-TECH Education and Publishing, Vienna, 2007.

[110] L. Spacek. A catadioptric sensor with multiple viewpoints. *Robotics and Autonomous Systems*, 51(1):3–15, February 2005.

[111] J. Steiner. Einige geometrische betrachtungen. *Journal für die reine und angewandte Mathematik*, (1):161–184, 1826.

[112] T. Svoboda, T. Pajdla, and V. Hlavác. Epipolar geometry of panoramic cameras. In *5th European Conference on Computer Vision (ECCV)*, volume 1406 of *LNCS*, pages 218–231, Freiburg, Germany, June 1998. Springer, Berlin, Heidelberg.

[113] R. Swaminathan, M. D. Grossberg, and S. K. Nayar. Caustics of catadioptric cameras. In *8th International Conference on Computer Vision*, volume 2, pages 2–9, Vancouver, BC, Canada, July 2001. IEEE Computer Society.

[114] R. Swaminathan, M. D. Grossberg, and S. K. Nayar. Non-single viewpoint catadioptric cameras: Geometry and analysis. *International Journal of Computer Vision*, 66(3):211–229, February 2006.

[115] P. Teunissen. Nonlinear least squares. In *Manuscripta geodaetica*, volume 15, pages 137–150. Springer, Berlin, Heidelberg, 1990.

[116] A. Tolvanen, C. Perwass, and G. Sommer. Projective model for central catadioptric cameras using Clifford algebra. In *27. Symposium für Mustererkennung, DAGM 2005, Wien, 29.8.-2.9.005*, volume 3663 of *LNCS*, pages 192–199. Springer, Berlin, Heidelberg, 2005.

[117] I. Tosic, I. Bogdanova, P. Frossard, and P. Vandergheynst. Multiresolution Motion Estimation for Omnidirectional Images. In *13th European. Signal Processing Conference (EUSIPCO)*, Antalya, Turkey, September 2005. EPFL, The European Association for Signal Processing (EURASIP).

[118] B. Vandeportaele, M. Cattoen, and P. Marthon. A fast detector of line images acquired by an uncalibrated paracatadioptric camera. In *18th International Conference on Pattern Recognition (ICPR)*, volume 3, pages 1042–1045, Hong Kong, China, August 2006. IEEE Computer Society.

[119] L. D. Weld. *Theory of errors and least squares, a textbook for college students and research workers.* New York, MacMillan, 1916.

[120] H. Wolf. Das geodätische Gauß-Helmert Modell und seine Eigenschaften. *Vermessungswesen*, 103:41–43, 1978.

[121] H. Wolf. The Helmert Block Method, its Origin and Development. In *Proceedings of the Second International Symposium on Problems Related to the Redefinition of North American Geodetic Networks*, pages 319–326. US Department of Commerce, Washington, 1978.

[122] B. Wrobel. Die ebene Blockausgleichung nach der Anblock-Methode. *Nachrichten aus dem öffentlichen Vermessungswesen Nordrhein-Westfalen*, pages 203–218, 1971.

[123] Y. Yagi. Omnidirectional sensing and its applications. *IEICE Transactions on Information and Systems*, E82-D(3):568–579, March 1999. INVITED SURVEY PAPER Surveys on Image Processing Technologies.

Index